Towards a full accounting and understanding of the energy levels in A = 16 – 44 nuclides

Freiburg im Breisgau

November 2019

Hartmut Röpke and Franz Glatz

Content

Part III

The energy levels of A = 38 - 44 nuclei and their underlying structure

Part IV

A Nilsson model interpretation of neutron rich isotopes of Mg, Na and Ne

Introductory remarks
or the attempt to bring some order into a bunch of notes written at very different times and under different aspects

A first step towards a theory of nuclear structure is the reproduction of the energy levels of nuclei. Experiment sets a limit at the excitation energy where the missing of levels can no longer be excluded. This limit must be found in a given nuclide for every value of level-spin, -parity, -isospin. A considerable contribution to a raising of this limit stems from work with the 7 MV single-stage Van de Graaff accelerator at Freiburg. Availability of sufficient running time made possible systematic work in the field of γ-ray spectroscopy.
Though the compiler of spectroscopic data in the A = 21 - 44 region, P. M. Endt *[1,2]* has already incorporated much of the information in his last compilations of 1990 and 1998 there is still a lot of work to do.
In the following we provide complete level schemes in the sense just defined for nuclides with small neutron excess and A = 16 - 44. Thus we are working our way through the nuclear s-d shell from ^{16}O to ^{40}Ca along the line of stability and cross the closure of the s-d shell for both protons and neutrons in ^{40}Ca. The closure for neutrons only is also considered in the case of the Mg isotopes.
The achieved level schemes are interpreted by combining several versions of the same model. In first approximation nucleons move independently of each other in a potential well which can have spherical symmetry or show quadrupol deformation with axial symmetry, the Nilsson approach. In the second step nucleons are divided into core nucleons and valence nucleons. The latter ones are distributed across a very limited number of orbits subject to a residual interaction. The interaction is given by a finite number of matrix elements. The most influential ones are obtained from a fit to experimental level energies while the less important ones may be derived from a nucleon-nucleon potential. A factor of merit of a model may be the ratio of level

energies that are accurately predicted to the number of levels used in the fit. We will show immediately that a factor of 20 can be reached.

In **Part I** we establish a system of roughly 1300 positive-parity levels in the $8 \leq N, Z \leq 20$ nuclei known as the s-d shell nuclei. The excitation energies of these levels are compared to the predictions of a shell model calculation in the spherical basis by Wildenthal *[3]*, known as the USD calculations. A – 16 nucleons are distributed without restrictions across the orbits of the N = 2 major shell, namely the $d_{5/2}$, $s_{1/2}$, $d_{3/2}$ orbits. The excellent quality of the USD calculations is known, but we can extend the comparison of experimental and predicted levels to energies in the region of the particle emission threshold where spectroscopy finds its end. Also we can identify with safety the positive-parity states which are not predicted by the USD model, the so called intruders.

In **Part II** we develop a Nilsson model with residual interaction for A = 16 - 31 nuclei. In the case of positive parity states there is an amazing overlap with the USD model. However the “intruders” are also predictable as are negative-parity states. In the case of the Magnesium isotopes with N – Z = 7 or 8 deformed character of the ground states is predictable with the implication that two particles carry the major quantum number N = 3. In the region from ^{34}S to ^{37}Ar the long-time predicted existence of oblate nuclear deformation is verified.

In **Part III** we turn to the complicated situation in the A = 36 - 44 region where multi-particle excitations from the orbits with major quantum number N = 2 into orbits with N = 3 occur. This happens in the frame of the spherical shell model and in the frame of the Nilsson model as well. It turns out that the excitation of a few particles is well described in the spherical model. The calculations which are due to Warburton *[4]*, allow, by the principle of exclusion the identification of multi-particle excitations. The latter ones are associated with deformed nuclear shapes. The situation will be described by a Nilsson model

with residual interaction for the A = 36 - 48 mass region in analogy to the A = 16 - 31 region. Last not least we have in A = 38 and A = 39 numerous experimental levels which are characterized by two or three particles in orbits with N = 3, not enough to generate deformation, but too many to be tractable in Warburton's shell model calculations. In this case we have revived the model of weak-coupling (between N = 2 and N = 3 nucleons) *[5]* with improved parameters (three in number). The hitherto unaccounted levels are successfully reproduced.

Part IV has developed from a rather casual glance (Part II section 10) at the nuclides ^{28}Mg and ^{30}Mg which exhibit deformation. In the course of events we saw the need for a systematic Nilsson model description of the neutron rich isotopes of Mg, Na, Ne. A simple explanation of what has been called the "island of inversion" is presented here.

References

1. P. M. Endt, Nucl. Phys. A 521, 1 (1990)
2. P. M. Endt, Nucl. Phys. A 633, 1 (1998)
3. B. H. Wildenthal in "Progress in Particle and Nuclear Physics", edited by D. H. Wilkinson (Plenum Press, New York 1984)
4. E. K. Warburton et al., Phys. Rev. C 41 (1147) 1990 and BNL report 40890 (1987)
5. R. Bansal, J. French, Phys. Lett. 11, 145 (1964)

Part I

Experimental level schemes of s-d shell nuclei compared to predictions of the USD-shell model

1. Introduction and Review

A set of roughly 1300 experimental $\pi = +$, $T \leq 3/2$ levels in A = 18 - 38 nuclei, among them 540 with first J^{π}, T assignments, are compared to shell model calculations in the unrestricted basis space of the nuclear s-d shell. About 120 $\pi = +$ „intruders“ from outside the s-d space are identified and understood (with aid of either the Nilsson or the weak-coupling model). They play a significant role only for A = 17 - 20 and 36 - 40.

The shell model calculations to which we refer were developed around 1984 by B. H. Wildenthal who communicated the resulting level schemes to us. Twenty years later an improved version of the same model was developed in a paper by B. A. Brown and W. A. Richter (Phys. Rev. C 74, 034315 (2006)), where a description of the methods employed can be found. However we have not been able at that time to get hold of the complete, but unpublished, set of level schemes. We obtained them only after finishing this manuscript and have refrained from welding them in. This is because the data are given in graphical form only and because they cover the realm below 10 MeV excitation energy only. Thus we stick to Wildenthal‘s first version, dubbed the USD calculations. They employ 63 empirically optimum matrix elements of the residual interaction which are assumed to have a $(18/A)^{0.3}$ mass dependence. In this way it was possible to use 440 experimental levels from various nuclei to obtain empirically the matrix elements. However data from the middle of the s-d shell were underrepresented for computational reasons and single particle energies were not varied but obtained otherwise. Both limitations are no longer present in the improved calculations of 2006 and the experimental situation had also improved considerably.

Thus at Freiburg we had completed γ-ray spectroscopy of ^{21}Ne, $^{25, 26}$Mg, ^{27}Al, ^{28}Si, ^{31}P, $^{32-34}$S, ^{35}Cl, ^{36}Ar and added to the already highly developed spectroscopy of ^{26}Al. In cooperation with B. H. Wildenthal it had been possible to compare not only level schemes to theory but also the γ-decays of ^{21}Ne, $^{25, 26}$Mg, ^{27}Al, ^{28}Si, and ^{32}S to theory, with good success. Prior to the USD calculations we had already finished work on ^{27}Mg, ^{29}Si, ^{30}Si. All A < 31 and the ^{32}S data have already entered the last compilation of A = 21 - 44 spectroscopic data by P. M. Endt (Nucl. Phys. A 521 and A 633, 1 (1990 and 1998)). The ^{31}P, ^{33}S, ^{34}S, ^{35}Cl data exist as theses at Freiburg (S. Fischer, A. Martinez, Th. Kern, J. Siefert authors) while the ^{36}Ar data were published after Endt's compilation (H. Röpke et al., Eur. Phys. J. 14, 159 (2002)). As yet unconsidered information on high spin states in ^{31}P and ^{34}S can be found in Phys. Rev. C 73, 024310 (2006) and C 71, 014316 (2005). Nuclides with neutron excess larger three are not subject of these notes but have been treated in detail by Brown and Richter.

Wildenthal and B. + R. have based their analysis exclusively on experimental levels which have definite J^{π}, T assignments in the opinion of the compiler who, in his own words, "must keep the record clean". Thus a large amount of information is left unused. As experimentalists who have generated much of the data, we try to improve the situation in the following compilation. Experimental levels characterized by an asterisk have a first J^{π}, T assignment. The justifications are given in (rather lengthy) separate notes (see p. 189). The comparison of experimental with USD energies terminates for every nuclide and separately every J^{π} at the excitation energy where the missing of an experimental level becomes feasible. A difference is made in the case of $J^{\pi} = 2^{+}$ and $J^{\pi} = 4^{+}$ states in ^{28}Si where spectroscopy was possible up to 14.5 MeV in excitation. The limiting energy of our comparison was set where the experimental level density prevents a level to level assignment. Above it is more reasonable to compare integral numbers of levels.

The 2_{18}^{+} state of USD, the highest one communicated to us, occurs at E_x = 13.8 MeV (Here we have already reduced the USD energy by 238 KeV which is the discrepancy of the experimental/theoretical binding energy of the ground state). Experimentally we have 27 levels. We have the choice of attributing the discrepancy to the presence of intruder states or to a compressure of the spectrum of $J^{\pi} = 2^{+}$ states at excitation energies above 11 MeV. The number of intruder states is probably small, say two or three states, as shown below. We discuss the alternative of compressure first.

Look at the depression of a state at energy E_x by a 2 ħω state. It is proportional to$1/(2\ \hbar\omega - E_x)$, with $2\ \hbar\omega = 2 \bullet 41\ \text{MeV}\ A^{-1/3} = 27$ MeV. The value of the denominator increases by roughly a factor of two in going from the yrast level at 1779 KeV to E_x = 13.8 MeV. The influence of the 2 ħω excitations on the 0 ħω states near the yrast line is absorbed in the empirical residual interaction but apparently not the growth with increasing level energy. In this way higher excited $J^{\pi} = 2^{+}$ states of 0 ħω origin have come down in energy and thus generate “compressure” of the spectrum. The effect is also noticeable in the case of the $J^{\pi} = 4^{+}$ states in ^{28}Si however nowhere else in the $N - Z \leq 3$ nuclei of the s-d shell. Simply experimental knowledge without gaps is not reaching high enough in energy.

While the discussed deficiency can be considered a principal one we have another specific deficiency in ^{28}Si. The binding energy (defined above as E_x − 238 KeV) of several states deviate from the USD predictions by 500 KeV or even more, three times the usual value. The deviations persist in the improved calculations of B + R so that the residual interaction can hardly be blamed. The reason must be sought in nuclear deformation. ^{28}Si is a deformed nucleus with oblate distortions at low energies while prolate distortions mix in above 6.7 MeV.

In Figs. 1, 2 we compare well founded rotational bands with USD predictions, where the 238 KeV correction just mentioned is already applied. Fig. 1 shows bands with oblate or, in a single case, marginal deformation. Fig. 2 shows bands of prolate distortion. The large deviations of theory from experiment are found for prolate bands and they are rather uniform within the band. Evidently we have close-by rotational bands which are not reproduced by the USD model and which depress the USD bands. A ready explanation is found in the Nilsson level scheme in Fig. 1 Part II (p. 100). The uppermost orbit which is occupied in the $K^{\pi} = 0_2^+$ band of (the present) Fig. 2 is the $\Omega^{\pi} = 1/2^+$ [211] orbit (Table 7, p. 167 in Part II) and the deformation is $\varepsilon = 0.37$. The distance to the first, $\Omega^{\pi} = 1/2^-$ [330] orbit derived from the f-p shell (N = 3) has shrunk to a mere 1 MeV. In the case of the $K^{\pi} = 0_3^+$ band of Fig. 2 it takes about 4 MeV to promote four particles into the first N = 3 orbit. Equally in the case of the $K^{\pi} = 0_4^+$ band it takes about 2 MeV to promote two particles into the first N = 3 orbit. Potential partners of the two expected $J^{\pi} = 0^+$ bandheads are rare and found only in the levels at 11142 KeV, J = 0 - 2 and 11388 KeV. Coming back to the proliferation of $J^{\pi} = 2^+$ states above 11 MeV compared to the USD model, the number of intruders is too small and compressure of the spectrum is the proper explanation.

Having clarified the few difficulties of the USD calculations we can state on the following pages excellent reproduction of about 1300 experimental levels. This is the most far reaching comparison. The number of reproduced levels surmounts the number of adjustable parameters by a factor of 20. As a valuable by-product we achieve clarity about the role of positive-parity intruder states (2, 4, 6 ħω excitations), roughly 100 in number. Thereafter the avenue is free to identify a set of about 700 negative parity states (1, 3, 5 ħω excitations). Their interpretation is possible and subject of other notes.

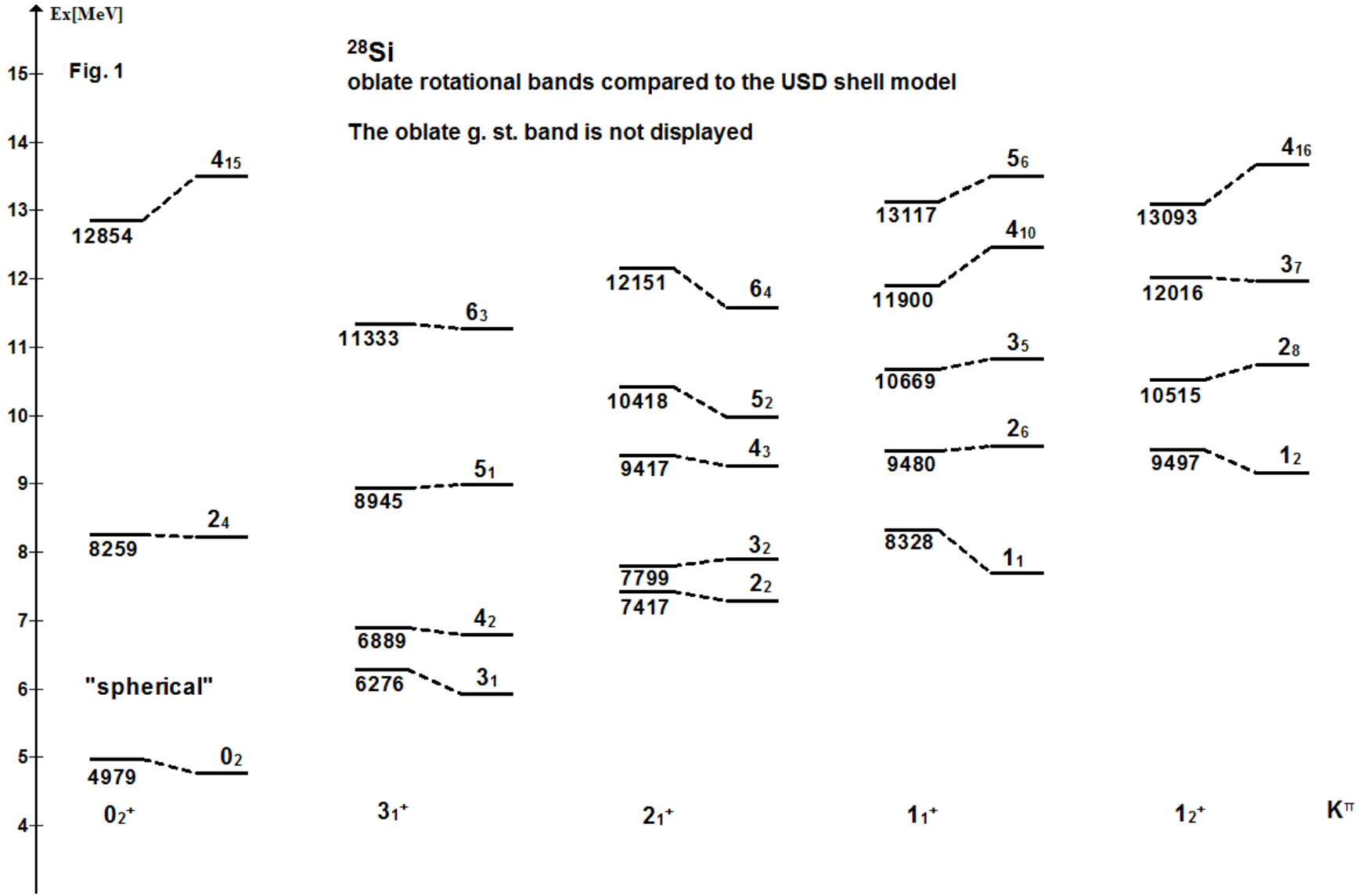
Ex[MeV]
Fig. 1
28Si
oblate rotational bands compared to the USD shell model
The oblate g. st. band is not displayed
15
14
13
12
11
10
9
8
7
6
5
4
4₁₅
12854
2₄
8259
"spherical"
0₂
4979
0₂⁺
6₃
11333
5₁
8945
4₂
6889
6276
3₁
3₁⁺
12151
6₄
10418
5₂
4₃
9417
3₂
7799
2₂
7417
2₁⁺
5₆
13117
4₁₀
11900
3₅
10669
2₆
9480
8328
1₁
1₁⁺
4₁₆
13093
3₇
12016
2₈
10515
9497
1₂
1₂⁺
Kᵖⁱ

Fig. 2

^{28}Si

prolate rotational bands compared to the USD shell model

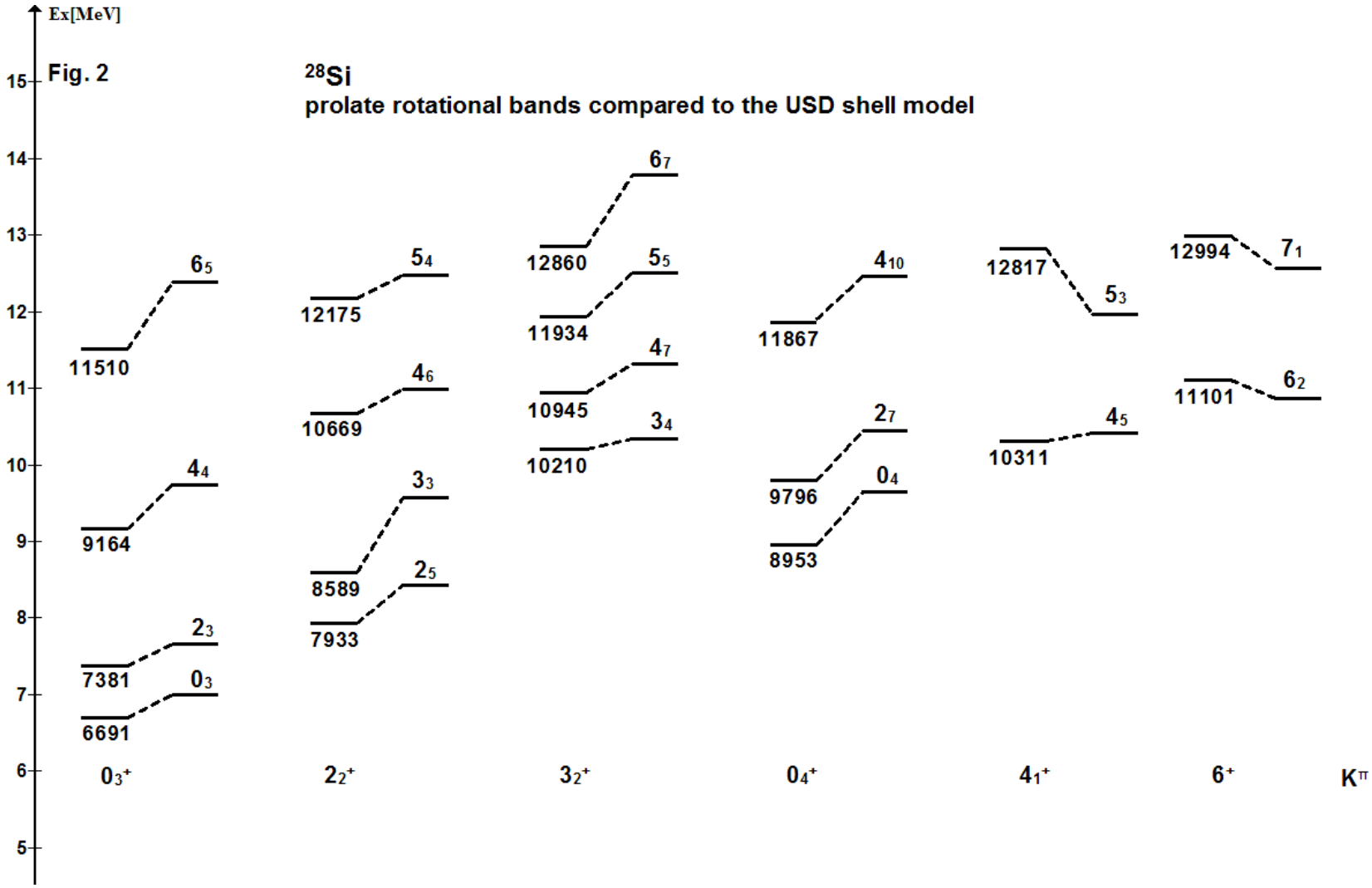

2. An updated comparison of experimental level energies with USD-shell model predictions

A,T	J^π	#	E_x[KeV]		Intruder States: E_x, J^π						
			SM	exp	2 ħω[a]			4 ħω[b]		6 ħω[c]	
					^{42}Sc, T = 0 ⊗ ^{36}Ar, T = 0			$K^\pi = 1^+$	J^π		J^π
38,0	1^+	1	635	459	3341	1^+		3978	1^+		
		2	1721	1698	3458	7^+					
		3	4153	3857	3668	3^+					
	2^+	1	3851	3431	3738	5^+					
	3^+	1	0	0							
38,1	0^+	1	0	0	^{42}Ca, T = 1 ⊗ ^{36}Ar, T = 0			$K^\pi = 0^+$		$K^\pi = 0$	
		2	6182	5974*	3377	0^+					
	1^+	1	5555	5552*	5594	2^+	$(2^+ \otimes 0^+)$	missing	0^+	4710	0^+
	2^+	1	2013	2168	6214	2^+	$(0^+ \otimes 2^+)$	3936	2^+	5157	2^+
		2	4489	4565*	6485	2^+	$(2^+ \otimes 2^+)$	5350	4^+	6053	
					6276	4^+		7288	6^+	7497	
					6408	6^+					
37,1/2	$1/2^+$	1	1586	1410	^{42}Ca, T = 1 ⊗ ^{35}Ar, T = 1/2			$K^\pi = 1/2^+$			
		2	4620	5120* ^{37}K	3937	$3/2^+$		3980	$1/2^+$		
	$3/2^+$	1	0	0	4318	$1/2^+$		4191	$3/2^+$		
		2	3529	3602	4743	$7/2^+$	$(2^+ \otimes 3/2^+)$	4573	$5/2^+$		
		3	5091	5091*	4799	$3/2^+$	$(2^+ \otimes 3/2^+)$				
	$5/2^+$	1	2884	2796	5102	$5/2^+$	$(2^+ \otimes 3/2^+)$				
		2	3112	3171	5130	$5/2^+$					
	$7/2^+$	1	2128	2217							
		2	4685	4624*							
37,3/2	$1/2^+$	1	1838	1726	^{42}Ca, T = 1 ⊗ ^{35}Cl, T = 1/2						
	$3/2^+$	1	0	0	3708	$3/2^+$					
		2	4107	4016							
	$5/2^+$	1	3265	3087							

A,T	J^π	#	E_x[KeV]		Intruder States: E_x, J^π						
			SM	exp	2 ħω[a]			4 ħω[b]		6 ħω[c]	
36,0	0^+	1	0	0	^{42}Ca, T = 1 ⊗ ^{34}Ar, T = 1			$K^\pi = 0^+$			
		2	4702	5194*	6632	0^+		4329	0^+		
					7137	2^+	$(2^+ \otimes 0^+)$	4951	2^+		
	1^+	1	7099	6866	7322	2^+	$(0^+ \otimes 2^+)$	6136	4^+		
	2^+	1	1927	1970	:			7766	6^+		
		2	4410	4440	9186	6^+		9929	8^+		
		3	7174	6730	^{42}Sc, T = 0 ⊗ ^{34}Cl, T = 0						
		4	8093	7180*	11902	10^+					
	3^+	1	7248	7140							
	4^+	1	4564	4414							
		2	6357	6356							
		3	8544	(8014)*							
	6^+	1	9696	9682*							
36,1	0^+	1	3354	3120	^{42}Ca, T = 1 ⊗ ^{34}Cl, T = 0						
	1^+	1	1201	1165	3941	3^+					
		2	1535	1601	^{42}Sc, T = 0 ⊗ ^{34}S, T = 1						
		3	2463	2676	5313	7^+					
		4	3613	3469	4521	1^+					
	2^+	1	0	0							
		2	2004	1959							
		3	2446	2492							
	3^+	1	805	788							
		2	2851	2864							
	4^+	1	3653	3830*							
35,1/2	$1/2^+$	1	1243	1219							
		2	4097	3967							
		3	4788	4839*	$1/2^+$, T = 1/2 ⊗ 0^+, T = 1						
					6649						
	$3/2^+$	1	0	0							
		2	2671	2694							
		3	3962	3918							
		4	4788	4839*							

A,T	J^{π}	#	E_x[KeV]		Intruder States: E_x, J^{π}						
			SM	exp	2 ħω[a)]			4 ħω[b)]		6 ħω[c)]	
35,1/2	$3/2^+$	5	5677	5526*	$3/2^+$, T = 1/2 ⊗ 0^+, T = 1						
cont'd					5838						
		6	6932	6779*							
	$5/2^+$	1	1780	1763							
		2	3145	3003							
		3	4595	4624							
		4	5535	5594*							
		5	5878	5727*							
		6	6394	6140*							
		7	7050	6946*							
	$7/2^+$	1	2778	2645							
		2	4405	4113							
		3	5120	4882*							
		4	6221	6145*							
		5	6883	6380*							
		6	8068	(7985)*							
	$9/2^+$	1	4196	3943							
		2	6695	6679*							
		3	7240	7217*							
	$11/2^+$	1	8181	7807*	$3/2^+$, T = 1/2 ⊗ 7^+, T = 0						
					8843	$17/2^+$					
					8787	$15/2^+$					
					7872	$13/2^+$					
35,3/2	$1/2^+$	1	1557	1572							
	$3/2^+$	1	0	0							
		2	2800	2939							
	$5/2^+$	1	2680	2717							
	$7/2^+$	1	3470	3597							

A,T	J^{π}	#	E_x[KeV]		Intruder States: E_x, J^{π}						
			SM	exp	2 ħω[a)]			4 ħω[b)]		6 ħω[c)]	
34,0	1^+	1	184	461							
		2	528	666							
		3	2389	2580							
		4	3117	3129							
		5	3748	3791*							
		6	4843	4971*							
		7	4978	4995*							
	2^+	1	1010	1230							
		2	1580	1887							
		3	4197	4148*							
		4	4894	4325*							
	3^+	1	0	146							
		2	1899	2181							
		3	2357	2611							
		4	3289	3334							
		5	3660	3964							
		6	4973	4695							
	4^+	1	2261	2376							
		2	3764	(3847)*							
		3	4708	5171*							
	5^+	1	3629	3646							
		2	4997	4824*	0^+, T = 0 ⊗ 7^+, T = 0						
					5315	7^+					
34,1	0^+	1	0	0	^{42}Ca, T = 1 ⊗ ^{32}S, T = 0						
		2	3905	3916							
		3	5172	5228							
					5847						
		4	7116	(7164)*							
		5	7919	8020*							
	1^+	1	3951	4074							
		2	5557	6318							
		3	7662	(7555)*							

A,T	J^{π}	#	E_x[KeV]		Intruder States: E_x, J^{π}						
			SM	exp	2 ħω[a]			4 ħω[b]		6 ħω[c]	
34,1	1^+	4	8172	8185*							
cont'd		5	8586	8657*							
		6	9103	(9246)*							
		7	9368	9478*							
		8	9947	9860*							
		9	10202	10170*							
		10	10639	10803*							
	2^+	1	2200	2127							
		2	3138	3304							
		3	4302	4115							
		4	4850	4890							
		5	6107	5998							
					6121						
		6	6683	6428							
		7	7072	6829 or 6848							
	3^+	1	4773	4877							
		2	6154	6174*							
			6969	6742							
	4^+	1	4896	4688							
		2	6819	6890*							
					7367						
	5^+	1	8823	8670*							
	6^+	1	9373	9307*							
					8507						
33,1/2	$1/2^+$	1	779	841							
		2	3863	4053							
		3	4286	4375							
		4	5561	5608*							
					5915		^{33}Cl*				
		5	6003	6254							
	$3/2^+$	1	0	0							

A,T	J^{π}	#	E_x[KeV]		Intruder States: E_x, J^{π}						
			SM	exp	2 ħω[a]			4 ħω[b]		6 ħω[c]	
33,1/2	$3/2^+$	2	2174	2312							
cont'd		3	3667	3935							
		4	4185	4421							
		5	4807	4939*							
		6	5075	5206*							
		7	5309	5620*							
	$5/2^+$	1	1895	1966							
		2	2839	2866							
		3	3899	3832							
		4	4697	4746							
		5	5145	5340*							
	$7/2^+$	1	2891	2969							
		2	3973	4094							
		3	5084	5279*							
		4	5306	5726*							
	$9/2^+$	1	4243	4048*							
		2	5966	6099*							
	$11/2^+$	1	6732	6611*							
		2	7372	7355*							
33,3/2	$1/2^+$	1	0	0							
		2	4242	(4047)*							
		3	5728	5674*							
	$3/2^+$	1	1531	1432							
		2	2646	2539							
		3	3606	3275							
		4	4997	4846*							
	$5/2^+$	1	1997	1848							
		2	3787	3490							
		3	3888	4194							
		4	5153	5050*							
	$7/2^+$	1	3949	3628							
		2	5905	(5816)*							
	$9/2^+$	1	5675	5549*							

A,T	J^{π}	#	E_x[KeV]		Intruder States: E_x, J^{π}						
			SM	exp	2 ħω[a)]			4 ħω[b)]		6 ħω[c)]	
32,0	0^+	1	0	0							
		2	3748	3778							
		3	7388	(7637)							
		4	8019	(7921)							
		5	8691	8507							
					9557						
		6	9180	9986							
		7	10877	10785							
								10457			
								11584			
								11607			
	1^+	1	4705	4695							
		2	7125	7190							
		3	9378	9290							
		4	9438	9950*							
		5	10084	10232							
	2^+	1	2148	2230							
		2	4353	4282							
		3	5490	5549							
		4	6695	6666							
		5	7563	7485							
		6	8284	8407							
		7	8647	8690							
		8	8922	8861							
		9	9483	9464							
		10	10108	10293*							
	3^+	1	5499	5413							
		2	7626	7350							
		3	8291	8281							
		4	9421	8746							
		5	10084	9920							
		6	10547	10221							

A,T	J^{π}	#	E_x[KeV]		Intruder States: E_x, J^{π}						
			SM	exp	2 ħω[a)]			4 ħω[b)]		6 ħω[c)]	
32,0											
cont'd	4^+	1	4698	4459							
		2	6265	6411							
		3	6866	6851							
		4	8131	8191							
		5	8990	7883							
		6	9427	9065							
		7	10303	10102							
		8	10743	11051							
	5^+	1	7634	7566							
		2	8918	9235							
		3	11117	10574							
		4	11721	11697							
	6^+	1	8854	8346							
		2	9636	9783							
32,1	0^+	1	260	513							
		2	4764	4432*	^{32}Cl						
	1^+	1	5	0							
		2	1048	1150							
		3	1965	2230							
		4	2722	2740							
		5	3967	3792							
		6	3976	4203							
		7	4689	4711							
		8	5614	5427*	^{32}Cl						
		9	5815	5869*	^{32}Cl						
		10	6145	6056*	^{32}Cl						
		11	6526	6532*	^{32}Cl						
		12	6859	6711*	^{32}Cl						
		13	7379	7307*	^{32}Cl						
		14	7543	7434*	^{32}Cl						
		15	7709	7580*	^{32}Cl						
		16	7918	7831*	^{32}Cl						
		17	8143	8127*	^{32}Cl						

A,T	J^{π}	#	E_x[KeV]		Intruder States: E_x, J^{π}						
			SM	exp	2 ħω[a]			4 ħω[b]		6 ħω[c]	
32,1											
cont'd	2^+	1	0	78							
		2	1135	1323							
		3	2036	2219							
		4	2602	2658							
		5	3518	3445							
		6	3587	3880							
	3^+	1	1528	1754							
		2	2224	2178							
		3	2916	3005							
		4	3592	3797							
		5	3909	3990							
		6	4217	4313							
		7	4674	4555							
		8	4730	4611							
	4^+	1	3168	3149							
		2	3727	4035							
	5^+	1	4977	4743							
					7420	7^+	0^+, T = 1 ⊗ 7^+, T = 0			Around this energy a 1^+ intruder state is also expected	
31,1/2	$1/2^+$	1	0	0							
		2	3310	3134							
		3	5084	5014							
		4	5536	5256							
		5	6531	6337							
		6	7346	7081*							
	$3/2^+$	1	1210	1266							
		2	3587	3506							
		3	4581	4261							
		4	4733	4594							
		5	5763	5559							
		6	6117	5988*							

A,T	J^{π}	#	E_x[KeV]		Intruder States: E_x, J^{π}						
			SM	exp	2 ħω[a]			4 ħω[b]		6 ħω[c]	
31,1/2	$3/2^+$	7	6586	6461*							
cont'd		8	7159	7313*							
		9	7621	7946*							
		10	8163	8208*							
	$5/2^+$	1	2275	2234							
		2	3297	3295							
		3	4344	4190							
		4	4866	4783							
		5	5321	5115							
		6	5968	5892*							
		7	6546	5672*							
		8	6801	6233*							
		9	7093	7163*							
		10	7641	7851*							
	$7/2^+$	1	3605	3415							
		2	4781	4634							
		3	5571	5529							
		4	5864	5773							
		5	6115	6048*							
		6	6753	6399*							
		7	7335	7083*							
		8	7961	7683*							
	$9/2^+$	1	5537	5343							
		2	5918	5892							
		3	6080	6080							
		4	7331	7118*							
		5	7725	unac-cessible yet							
		6	8315	8346							
		7	8891	8602							
		8	9004	9250							
		9	9518	9356							
		10	9593	9534							
	$11/2^+$	1	6843	6454							
		2	7673	7441							
		3	8263	8344							

A,T	J^{π}	#	E_x[KeV]		Intruder States: E_x, J^{π}						
			SM	exp	2 ħω[a]			4 ħω[b]		6 ħω[c]	
31,1/2	$13/2^+$	1	9231	9313							
cont'd		2	10478	10037							
					9600	$1/2^+$, T = 1/2 ⊗ 7^+, T = 0					
	$15/2^+$	1	12063	11734							
					10520	$1/2^+$ or $3/2^+$, T = 1/2 ⊗ 7^+, T = 0					
	$17/2^+$				11297	$3/2^+$, T = 1/2 ⊗ 7^+, T = 0					
31,3/2	$1/2^+$	1	815	752							
		2	4493	4720							
		3	5914	5282							
		4	6644	6776							
	$3/2^+$	1	0	0							
		2	2295	2317							
		3	3825	4259							
	$5/2^+$	1	1606	1695							
		2	2870	2789							
	$7/2^+$	1	3697	3876							
30,0	0^+	1	6289	6481?* $J^{\pi}=0^+,1^+$							
		2	7145	7931*							
	1^+	1	0	0							
		2	644	709							
		3	3131	3019							
		4	3737	3734							
		5	4931	4945							
		6	5896	5506*							
		7	6085	5702*							
		8	7085	6854*							
		9	7732	7493*							
		10	7972	7749*							
		11	8008	8095*							

A,T	J^{π}	#	E_x[KeV]		Intruder States: E_x, J^{π}						
			SM	exp	2 ħω[a]			4 ħω[b]		6 ħω[c]	
30,0	2^+	1	1491	1454							
cont'd		2	2461	2723							
		3	4113	3834							
		4	4358	4424							
		5	5471	not accessible							
		6	6652	6519*							
		7	7068	7203*							
		8	7701	7605*							
		9	8083	8023*							
	3^+	1	2061	1973							
		2	2510	2538							
		3	2973	2839							
		4	4285	3927							
		5	4862	4737							
		6	5574	5207							
		7	6166	5808							
		8	6310	6307*							
		9	7066	6873*							
		10	7263	7264*							
		11	7444	7560*							
		12	8028	7636*							
		13	8239	7921*							
		14	8469	8386*							
	4^+	1	4593	4298							
		2	5146	missing							
		3	5455	5595							
		4	6221	5934*							
		5	6643	(6978)*							
		6	7012	7370*							
		7	7766	7833*							
	5^+	1	4584	4343							
		2	5105	5232							

A,T	J^{π}	#	E_x[KeV]		Intruder States: E_x, J^{π}						
			SM	exp	2 ħω[a]			4 ħω[b]		6 ħω[c]	
30,0											
cont'd	5^+	3	5571	5714							
		4	6377	6181*							
		5	6575	6235*							
		6	6945	6607*							
	6^+	1	7120	6791*							
		2	7877	7345*							
	7^+				7199	7^+					
30,1	0^+	1	0	0							
		2	4085	3788							
		3	5525	5372							
		4	6763	6641							
		5	7551	7443							
					~7560	8214 in ^{30}P					
	0^+	6	8706	(8735)*							
		7	9081	(9035)*							
	1^+	1	4210	3767							
		2	7609	7668							
		3	8068	8290*							
		4	8528	(8799)*							
		5	8808	8942*							
		6	9090	9356*							
		7	9625	9768*							
		8	10001	10478*							
		9	10294	10669*							
	2^+	1	2310	2235							
		2	3550	3499							
		3	5048	4810							
		4	6205	5613							
		5	6520	6537							
		6	6967	6915							
		7	7307	7256*							
		8	7441	7634*							

A,T	J^π	#	E_x[KeV]		Intruder States: E_x, J^π						
			SM	exp	2 ħω[a)]			4 ħω[b)]		6 ħω[c)]	
30,1											
cont'd					8105						
	2^+	9	8115	7911*							
		10	8720	8673*							
		11	8872	8980*							
	3^+	1	4961	4831							
		2	5195	5231							
		3	7201	6865							
		4	7473	7079							
		5	8195	8330*							
		6	8757	8640*							
	4^+	1	5506	5280							
		2	5913	5950							
		3	6997	7225							
		4	8051	7810							
		5	8607	8190*							
		6	8696	8537*							
		7	8933	8684*							
		8	9321	9406*							
		9	9761	9475*							
		10	9932	9761*							
	5^+	1	7241	6999							
		2	8941	9131*							
		3	10032	9955*							
		4	10271	(10288)*							
		5	10749	(10991)*							
		6	10982	(11091)*							
		7	11401	11327)*							
		8	11539	(11348)*							
	6^+	1	9280	9371*							
		2	10485	(10420)*							
					10679						
		3	10966	10823*							
		4	11258	11417*							

A,T	J^π	#	E_x[KeV]		Intruder States: E_x, J^π						
			SM	exp	2 ħω[a]			4 ħω[b]		6 ħω[c]	
30,1	6^+	5	11671	(11493)*							
cont'd		6	11684	(12015)*							
		7	12186	12220*							
		8	12352	12524*							
	7^+	1	12098								
		2	12672	12912*							
		3	13113								
	8^+	1	13736	13330*							
29,1/2	$1/2^+$	1	0	0							
		2	4901	4840							
		3	6557	6695							
		4	6940	7057*							
		5	7536	7521*							
		6	8596	8528*							
		7	8881	8653*							
		8	9325	9596*							
	$3/2^+$	1	1394	1273							
		2	2630	2426							
		3	6155	5949							
		4	6267	6496*							
		5	6901	6715*							
		6	7179	7185*							
		7	7634	7892*							
		8	8268	8209*							
		9	8377	8418*							
		10	8562	8349*							
		11	8963	8854*							
		12	9203	9054*							
	$5/2^+$	1	2121	2028							
		2	3513	3067							
		3	4917	4895							
		4	6778	6522							
		5	6862	6710*							

A,T	J^{π}	#	E_x[KeV]		Intruder States: E_x, J^{π}						
			SM	exp	2 ħω[a)]			4 ħω[b)]		6 ħω[c)]	
29,1/2	$5/2^+$	6	7604	7197*							
cont'd		7	7669	7767*							
		8	7875	8104	in ^{29}P* = 8138 in ^{29}Si?						
	$7/2^+$	1	4410	4080							
		2	5219	5286							
		3	5881	5813							
		4	6389	6424							
		5	7391	6921*							
		6	7526	7072*							
		7	7878	7787*							
		8	8401	8161*							
		9	8841	8603*							
		10	9038	8815*							
		11	9227	9219*							
	$9/2^+$	1	4779	4741							
		2	5783	5652							
		3	6992	6616*							
		4	8055	7987*							
		5	8341	8331*							
		6	8895	8670*							
		7	9227	9157*							
		8	9551	9392*							
		9	9788	9765*							
	$11/2^+$	1	7308	7139*							
		2	8119	8173*							
		3	8830	8476*							
		4	9502	9326*							
		5	9603	9683*							
		6	10062	9952*							
		7	10400	10131*							
	$13/2^+$	1	8809	8641*							
		2	9880	9850*							

A,T	J^π	#	E_x[KeV]		Intruder States: E_x, J^π						
			SM	exp	2 ħω[a]			4 ħω[b]		6 ħω[c]	
29,1/2 cont'd	$13/2^+$	3	10542	10236 or 10444*	11_8 is contained: SM value is 10642						
		4	10921	10652 or 11111*	11_9 is contained: SM value is 11193						
		5	11920	11392*							
	15/2	1	11978	11697*							
		2	12389	12029*							
		3	13216	12960*							
29,3/2	$1/2^+$	1	1214	1398							
		2	3330	3433							
		3	4229	4057*							
	$3/2^+$	1	1959	2224							
		2	2735	2866							
		3	3577	3642							
		4	3976	3671*							
	$5/2^+$	1	0	0							
		2	2801	3062							
		3	3017	3184							
		4	3816	missing							
		5	4128	4220*							
		6	4501	4656*							
	$7/2^+$	1	1799	1754							
		2	3874	3935							
		3	4454	4403*							
	$9/2^+$	1	3381	3578							
	$11/2^+$	1	5944	5855*							
28,0	0^+	1	0	0							
		2	5011	4979							
		3	7239	6691							
		4	9879	8953							
		5	10359	(11142)*							
					(11388)						

A,T	J^{π}	#	E_x[KeV]		Intruder States: E_x, J^{π}						
			SM	exp	2 ħω[a]			4 ħω[b]		6 ħω[c]	
28,0	0^+	6	12167	12805*							
cont'd		7	12868	12977							
		8	13673	13236							
	1^+	1	7940	8328							
		2	9399	9497							
		3	10959	10725							
		4	11709	(10994)							
		5	12268	(11986)							
		6	12928	12715							
		7	13504	13190							
	2^+	1	1987	1779							
		2	7522	7417							
		3	7906	7381							
		4	8457	8259							
		5	8668	7933							
		6	9792	9480							
		7	10689	9796							
		8	10980	10515							
		9	11530	10806							
		10	11729	10953							
		11	12301	11148*							
		12	12519	11516*							
		13	12905	11657*							
		14	13118	12071*							
	3^+	1	6167	6276							
		2	8139	7799							
		3	9811	8589							
		4	10572	10210							
		5	11058	10669							
		6	11920	12295							
		7	12207	12016							
		8	12446	12635							
		9	12662	12866*							
		10	13070	13033*							
		11	13246	13558*							

A,T	J^{π}	#	E_x[KeV]		Intruder States: E_x, J^{π}						
			SM	exp	2 ħω[a]			4 ħω[b]		6 ħω[c]	
28,0											
cont'd	4^+	1	4568	4617							
		2	7037	6889							
		3	9493	9417							
		4	9978	9164							
		5	10660	10311							
		6	11233	10669							
		7	11552	10945							
		8	11886	11196							
		9	12162	11867							
		10	12697	11900*							
		11	12829	12241*							
		12	13183	12324*							
		13	13494	12474*							
		14	13516	12550*							
		15	13743	12854*							
		16	13908	13093*							
		17	14243	13360*							
		18	14557	13415*							
		19	14665	13667*							
	5^+	1	9232	8945							
		2	10222	10418							
		3	12202	12817							
		4	12723	12175							
		5	12751	11934							
		6	13733	13117							
		7	14023	13425							
		8	14298	14049							
		9	14348	14212							
		10	14455	14331							
		11	14898	14633							
	6^+	1	8459	8543							
		2	11104	11101							
		3	11513	11333							

A,T	J^{π}	#	E_x[KeV]		Intruder States: E_x, J^{π}						
			SM	exp	2 ħω[a]			4 ħω[b]		6 ħω[c]	
28,0	6^+	4	11819	12151							
cont'd		5	12629	11510							
		6	13595	13231*							
		7	14020	12860*							
		8	14083	13710*							
	7^+	1	12810	12994							
		2	14378	14245							
	8^+	1	14214	14643							
28,1	0^+	1	840	972							
		2	2895	3012							
		3	3449	3762*							
	1^+	1	1364	1373							
		2	1746	1620							
		3	2073	2202							
		4	3198	3105							
		5	3524	3542							
		6	3925	4115							
		7	4929	4846							
	2^+	1	0	30							
		2	1537	1623							
		3	2102	2138							
		4	2436	2485							
		5	3135	3347							
		6	3632	missing							
		7	3715	3936							
		8	4030	4245							
		9	4680	4761	^{28}Si						
		10	4967	4999							
		11	5083	5367	^{28}Si						
	3^+	1	142	0							
		2	977	1014							
		3	3061	2987							
		4	3249	3296							

A,T	J^{π}	#	E_x[KeV]		Intruder States: E_x, J^{π}						
			SM	exp	2 ħω[a)]			4 ħω[b)]		6 ħω[c)]	
28,1	3^+	5	3474	3671*							
cont'd		6	3598	3709*							
		7	3876	3901							
		8	4230	4597							
		9	4389	4498*							
		10	5049	4989*							
	4^+	1	2236	2272							
		2	2527	2656							
		3	3512	3601*							
		4	4357	4739*							
		5	4601	4462*							
		6	5034	4998	^{28}Si						
		7	5309	5593	^{28}Si						
		8	5549	5341	^{28}Si						
		9	5843	6030	^{28}Si						
	5^+	1	2653	2582							
		2	4295	4311	^{28}Si						
		3	4772	4927							
		4	5257	5362	^{28}Si						
		5	5445	6193	^{28}Si						
		6	5793	5917	^{28}Si						
	6^+	1	4531	4385							
		2	5825	5973							
		3	6673	6705							
	7^+				9821	0^+, T = 1 ⊗ 7^+, T = 0					
27,1/2	$1/2^+$	1	912	844							
		2	3709	3680							
		3	5603	5752							
		4	6787	6776*							
		5	7132	7071*							
	$3/2^+$	1	1264	1014							
		2	2780	2981							
		3	4027	3957							

A,T	J^{π}	#	E_x[KeV]		Intruder States: E_x, J^{π}						
			SM	exp	2 ħω[a]			4 ħω[b]		6 ħω[c]	
27,1/2	$3/2^+$	4	5776	5827*							
cont'd		5	6264	6081*							
		6	6949	6820*							
		7	7225	7280*							
		8	7515	7549*							
		9	7859	7677*							
		10	7955	8066*							
	$5/2^+$	1	0	0							
		2	2708	2735							
		3	4139	4410							
		4	4939	4812							
		5	5320	5552							
		6	5365	5247							
		7	6390	6115*							
		8	6684	6465							
		9	6714	6765							
		10	7300	7577*							
		11	7689	7721*							
	$7/2^+$	1	2326	2211							
		2	4665	4580							
		3	5519	5433							
		4	5948	5960							
		5	6188	6283							
		6	6467	6533							
		7	6920	6992*							
		8	7158	7679*							
		9	7258	7413*							
		10	7783	8037*							
	$9/2^+$	1	3025	3004							
		2	5292	5420							
		3	5887	5668							
		4	6523	6512							
		5	6718	6713							
		6	6898	7174							

A,T	J^{π}	#	E_x[KeV]		Intruder States: E_x, J^{π}						
			SM	exp	2 ħω[a]			4 ħω[b]		6 ħω[c]	
27,1/2	$9/2^+$	7	7462	(7226)*							
cont'd		6	6898	7174							
		7	7462	(7226)*							
		8	7667	7659*							
		9	8134	7805*							
	$11/2^+$	1	4584	4510							
		2	5400	5500							
		3	7504	6948*							
		4	7775	7400*							
		5	8339	7948*							
		6	8843	8396*							
	$13/2^+$	1	6746	7289*							
		2	7318	7442*							
		3	9006	8692*							
27,3/2	$1/2^+$	1	0	0							
		2	3249	3476							
		3	5017	5028							
		4	6055	5906?*							
		5	6276	(6380)*							
	$3/2^+$	1	895	985							
		2	3162	3491							
		3	3632	3786							
		4	5226	5422*							
		5	5404	5627*							
		6	5657	5764*							
		7	5887	5926*							
		8	6428	(6084)*							
		9	6648	6336*							
	$5/2^+$	1	1667	1698							
		2	1978	1940							
		3	4032	4150							
		4	4202	4553*							
		5	4719	4992*							

A,T	J^π	#	E_x[KeV]		Intruder States: E_x, J^π						
			SM	exp	2 ħω[a]			4 ħω[b]		6 ħω[c]	
27,3/2	$5/2^+$	6	5101	5172*							
cont'd		5	4719	4992*							
		6	5101	5172*							
		7	5454	5821*							
		8	6086	6125*							
		9	6483	(6508)*							
	$7/2^+$	1	3149	3109							
		2	3300	3427							
		3	4616	4776							
		4	5206	5412*							
		5	5481	5749*							
		6	5813	6009*							
	$9/2^+$	1	4152	3884							
		2	4360	4398*							
		3	5256	5296*							
		4	6017	(6312)*							
		5	6686	6651*							
		6	6753	6811*							
	$11/2^+$	1	6222	6161*							
		2	6581	6721*							
26,0	0^+	1	4698	5462							
		2	8092	> 8 MeV							
	1^+	1	818	1058							
		2	1737	1850							
		3	2004	2072							
		4	2899	2740							
		5	3685	3724							
		6	4938	5010							
		7	5154	5585							
		8	5668	5671							
					6198		$K^\pi=1^+$				
		9	5944	6270							
		10	6658	6874							

A,T	J^π	#	E_x[KeV]		Intruder States: E_x, J^π						
			SM	exp	2 ħω[a]			4 ħω[b]		6 ħω[c]	
26,0	1^+	11	6941	6936							
cont'd		12	7280	7198							
					7455		$K^\pi=0^+$				
		13	7633	7623*							
				7648	either $J^\pi = 1^+$, 2 ħω, or $J^\pi = 2^+$, 0 ħω						
		14	8122	7879*	safely s-d state						
	2^+	1	1326	1759							
		2	2588	2661							
		3	2749	2913							
		4	3923	3751							
		5	5288	5495							
		6	5453	5849							
		7	6003	6680							
		8	6149	6852							
					7001						
		9	6688	7093*							
		10	7114	7397*							
		11	7469	7558*							
		12	7527	7865*							
		13	7686	7648*	if $J^\pi = 2^+$, Endt quotes $1^+(2^+)$						
		14	8039	8008*							
	3^+	1	712	417							
		2	2121	2545							
		3	2325	2365							
		4	3069	3074							
		5	3357	3596							
		6	3655	3963							
		7	4103	3681							
		8	4380	4349							
		9	5014	4952							
		10	6241	5883							
		11	6589	6280							

A,T	J^{π}	#	E_x[KeV]		Intruder States: E_x, J^{π}						
			SM	exp	2 ħω[a]			4 ħω[b]		6 ħω[c]	
26,0	3^+	12	6697	6801							
cont'd		13	7128	7051							
		14	7194	7153							
		15	7450	7495							
		16	7883	7772							
		17	8020	7874							
	4^+	1	2303	2069							
		2	3309	3675							
		3	4052	4205							
		4	4721	4773							
		5	5211	5513							
		6	5348	5245							
		7	6031	6343							
		8	6667	unreachable (E_p = 300 KeV l = 2 resonance in ^{25}Mg(p, γ)							
		9	7265	7292							
		10	7402	7425							
		11	7557	7592							
		12	7651	7832							
	5^+	1	0	0							
		2	3422	3403							
		3	4481	4941							
		4	5533	5488							
		5	5579	5568							
		6	6069	6436							
		7	6321	6496							
		8	6448	6598							
		9	7017	7015							
		10	7167	7366							
		11	7291	7596							
	6^+	1	3334	3507							
		2	6176	6120							
		3	6520	6816							
		4	7479	missing							
		5	7940	7921							

A,T	J^{π}	#	E_x[KeV]		Intruder States: E_x, J^{π}						
			SM	exp	2 ħω[a)]			4 ħω[b)]		6 ħω[c)]	
26,0	7^+	1	3749	3922							
cont'd		2	6243	6496							
		3	7709	7.89	MeV* (α,d)						
		4	8871	8.94	MeV* (α,d)						
26,1	0^+	1	0	0							
		2	3681	3588							
		3	5204	4972							
		4	6062	6256							
					7428						
		5	8131	(7851)*							
		6	8645	(8399)*							
		7	10079								
	1^+	1	5833	5690							
		2	6798	6634							
		3	7721	7840*							
		4	8433	8577							
		5	9081	9239							
		6	9146	9560							
	2^+	1	1929	1809							
		2	3153	2938							
		3	4541	4332							
		4	5000	4834							
		5	5404	5291							
		6	6647	6744							
		7	6843	7099							
		8	7093	7371							
		9	7473	7816							
					8033*						
		10	8391	8532							
		11	8716	8863							
		12	9387	9281*							
	3^+	1	3921	3940							
		2	4511	4350							

A,T	J^{π}	#	E_x[KeV]		Intruder States: E_x, J^{π}						
			SM	exp	2 ħω[a]			4 ħω[b]		6 ħω[c]	
26,1	3^+	3	6268	6125							
cont'd		4	7282	7242							
		5	7602	7726							
		6	8005	8251							
		7	8404	8459							
		8	9115	(9291)*							
		9	9304	(9303)*							
		10	9576	9427*							
	4^+	1	4533	4319							
		2	4932	4900							
		3	5473	5474							
		4	6009	5716							
		5	6777	6621							
		6	7411	7773							
		7	7941	7677							
		8	8413	8706							
		9	8790	8930							
		10	8959	9261							
		11	9236	9371							
		12	9387	9579							
		13	9781	9814							
	5^+	1	7038	6978							
		2	7465	7395							
		3	8520	8670							
		4	8935	9065							
		5	9458	9471							
		6	9768	9542*							
	6^+	1	8194	8202							
		2	8428	8472							
		3	9034	9112							
		4	9724	9383							
		5	9957	9989							
					11,23 MeV, 2ħω; from (α,^{2}H) = 11191 or 11300 in (α, pγ)						
	7^+	1	9908	9829							

A,T	J^{π}	#	E_x[KeV]		Intruder States: E_x, J^{π}						
			SM	exp	2 ħω[a)]			4 ħω[b)]		6 ħω[c)]	
26,1	7^+	2	11038	11329*							
cont'd		3	11520	11570*							
		4	12130	12196*							
	8^+	1	11770	12479*							
25,1/2	$1/2^+$	1	743	586							
		2	2519	2564							
		3	5289	5475							
		4	6222	6777							
		5	7943	7964*							
		6	8231	8325*							
		7	8515	8363*							
	$3/2^+$	1	1200	975							
		2	2909	2801							
		3	4457	4359							
		4	5589	6169							
		5	6205	5748							
		6	6367	6363							
		7	6767	6570							
		8	7072	7088*							
		9	7614	7228*							
		10	8086	8142*							
		11	8303	(8245)*							
	$5/2^+$	1	0	0							
		2	2095	1965							
		3	3871	3908							
		4	4872	4722							
		5	5943	5862							
		6	5990	6082							
		7	6462	6839*							
		8	6798	6953*							
		9	7292	6914*							
		10	7494	7378*							
		11	7710	7505*							
		12	7741	7582*							
		13	8180	8312*							

A,T	J^{π}	#	E_x[KeV]		Intruder States: E_x, J^{π}						
			SM	exp	2 ħω[a)]			4 ħω[b)]			
25,1/2	$7/2^+$	1	1730	1612							
cont'd		2	2980	2738							
		3	5121	5012							
		4	5987	5744							
		5	6151	5978							
		6	6792	7181*							
		7	7135	7524*							
		8	7625	7961*							
		9	7757	7838*							
		10	7882	7633*							
		11	8167	8119*							
		12	8502	8267*							
		13	8732	8656*							
	$9/2^+$	1	3464	3405							
		2	3996	4060							
		3	4777	4711							
		4	6306	6433							
		5	6551	5972							
		6	6875	7185*							
		7	7380	7653*							
		8	8004	8076*							
		9	8442	8544*							
	$11/2^+$	1	5200	5251							
		2	5753	5534							
		3	6151	6041							
		4	7462	7493*							
		5	7973	7866*							
		6	8574	8551*							
		7	9003	9014*							
		8	9166	8530*							
		9	9634	9686*							
	$13/2^+$	1	5711	5462							
		2	7548	7551*							
		3	8026	8012*							
		4	8724	8811*							

A,T	J^{π}	#	E_x[KeV]		Intruder States: E_x, J^{π}						
			SM	exp	2 ħω[a)]			4 ħω[b)]			
25,1/2	$15/2^+$	1	9326	9652*							
cont'd		2	9699	9946*							
		3	10751	10653*							
		4	11124	11460*							
		5	11375	11486*							
		6	12190								
	$17/2^+$	1	10978	11004*			11410* $17/2^+$ or $15/2^+$				
		2	12266								
		3	12930	13332*							
25,3/2	$1/2^+$	1	1159	1069							
		2	4048	4289*							
	$3/2^+$	1	132	90							
		2	2130	2202							
	$5/2^+$	1	0	0							
		2	2843	2914							
	$7/2^+$	1	2730	2417							
	$9/2^+$	1	2542	2788							
24,0	0^+	1	0	0							
		2	7561	6432							
		3	9560	9305							
					10111	N = 1 → N = 2, two particle excitation					
		4	10679	10680							
					11457	N = 1 → N = 3, single particle excitation					
		5	12610	11727*							
		6	13317	13198*							
	1^+	1	7764	7747							
		2	9987	9827							
		3	11553	(11187)*							
		4	12601	(12181)*							

A,T	J^π	#	E_x[KeV]		Intruder States: E_x, J^π						
			SM	exp	2 ħω[a)]			4 ħω[b)]			
24,0	1^+	5	12966	12526*		Above 12 MeV up to two $J^\pi = 1^+$ intruders with $K^\pi = 0^+_o$ and 1^+ are feasible (see rotational model),just a consequence of the 11457 KeV 0^+ intruder					
cont'd		6	13463	12893*							
		7	13875	13630*							
	2^+	1	1509	1369							
		2	4122	4238							
		3	7442	7348							
		4	8941	8653							
		5	9876	9003*							
		6	10479	10360*							
		7	11109	10917*							
					11016	rotational excitation of the 10111, 0^+ intruder					
		8	11820	11453*							
		9	11956	11519*							
		10	12288	11964*							
		11	12799	11988*							
					12467	rotational excitation of the 11457, 0^+ intruder					
		12	13248	12577							
	3^+	1	5097	5236							
		2	9596	9456							
		3	10803	10581*							
		4	11223	10660*							
		5	11580	(11330)*							
		6	12347	12398*							
		7	12865	(12657)*							
		8	13082	(12731)*							
	4^+	1	4378	4123							
		2	5934	6010							
		3	8374	8437							
		4	9639	9298							
		5	11038	11217*							

A,T	J^{π}	#	E_x[KeV]		Intruder States: E_x, J^{π}						
			SM	exp	2 ħω[a)]			4 ħω[b)]			
24,0	4^+	6	11377	11695*							
cont'd		7	11746	12117*							
		8	12128	12161*							
		9	12432	12504*							
		10	12937	12972*							
	5^+	1	7883	7812							
		2	10565	10575							
		3	12296	(12128)*							
		4	12498	(12479)*							
		5	13100	(13178)*							
	6^+	1	8263	8113							
		2	9585	9528							
		3	11932	(11528)*							
		4	12140	12002*							
		5	12827	12861*							
		6	13372	13436*							
		7	14210	13852*							
		8	14312	14082*							
	7^+	1	12283	12344*							
		2	14276		>13.2 MeV						
	8^+	1	12088	11860*							
		2	13160	13210*							
		3	13948	14152*							
		4	15737	16300*							
		5	16551	16560*							
24,1	0^+	1	3329	3682							
	1^+	1	447	472							
		2	1091	1346							
		3	3210	3413							
		4	3599	3589							
		5	4489	(4621)*							
	2^+	1	587	563							
		2	1132	1341							

A,T	J^{π}	#	E_x[KeV]		Intruder States: E_x, J^{π}						
			SM	exp	2 ħω[a)]			4 ħω[b)]			
24,1	2^+	3	1603	1846							
cont'd		4	2825	2978							
		5	3357	3656							
		6	3999	3977							
		7	4481	4186*							
		8	4816	4208?*							
	3^+	1	1373	1344							
		2	1751	1885							
		3	2179	2513							
		4	2649	2904							
		5	3478	3628							
		6	3778	3896							
	4^+	1	0	0							
		2	2560	2562							
		3	2883	3217							
		4	3502	3534	From ^{24}Mg						
	5^+	1	1549	1512							
		2	3849	3943*							
		3	4130	(4459)*							
		4	4536	(4692)*							
		5	4665	(4891)*							
23,1/2	$1/2^+$	1	2324	2391							
		2	4311	4432							
		3	5976	6306*							
		4	7910	7734*							
		5	8254	8822*							
		6	9330	9253*							
		7	9714	9654*							
	$3/2^+$	1	0	0							
		2	2747	2982							
		3	5745	5766							
		4	6493	6736*							
		5	6832	6950*							
		6	7906	7872*							

A,T	J^{π}	#	E_x[KeV]		Intruder States: E_x, J^{π}						
			SM	exp	2 ħω[a)]			4 ħω[b)]			
23,1/2	$5/2^+$	1	412	440							
cont'd		2	3893	3915							
		3	5246	5377							
		4	5574	5741							
		5	6747	6868*							
		6	6836	7071*							
		7	6946	7132*							
		8	7910	7566*							
	$7/2^+$	1	2131	2076							
		2	4637	4775							
		3	5163	5929*							
		4	6499	6618*							
		5	7635	7390*							
		6	7633	7686*							
		7	7739	7834*							
		8	8197	7965*							
	$9/2^+$	1	2795	2704							
		2	5951	5778	From (d,α)						
		3	6180	6578*							
		4	7057	7185*							
		5	7602	7412*							
	$11/2^+$	1	5391	5533							
		2	6149	6117*							
		3	7156	7154*							
		4	7614	7980*							
	$13/2^+$	1	6259	6237*							
		2	7313	7267*							
	$15/2^+$	1	9001	9041*							
		2	9548	9802*							
23,3/2	$1/2^+$	1	992	1017							
		2	3494	3458*							
		3	5137	5491*							
		4	5487	5726*							

A,T	J^{π}	#	E_x[KeV]		Intruder States: E_x, J^{π}						
			SM	exp	2 ħω[a)]			4 ħω[b)]			
23,3/2	$3/2^+$	1	1768	1822							
cont'd		2	3238	3432							
		3	3778	3988*							
		4	4921	5036*							
		5	5434	5696*							
		6	6009	5740*							
	$5/2^+$	1	0	0							
		2	2184	2315							
		3	3826	4010*							
		4	5057								
	$7/2^+$	1	1759	1701							
		2	3605	3831*							
		3	4395	4436*							
	$9/2^+$	1	2516	2517							
		2	4197	4270*							
		3	4502	4754*							
	$11/2^+$	1	3931	3843*							
22,0	0^+	1	7595		7882*	sole	Possibility				
	1^+	1	390	583	4319	1^+	K = 1	6859	1^+	K = 0	
		2	2024	1937	5131	2^+	K = 1	7635	3^+	K = 0	
		3	3985	3944	5988	(3^+)	K = 1				
		4	5673	5739*	7278	4^+	K = 1				
	2^+	1	3155	3060							
		2	4175	4360							
		3	5208	5062*							
		4	5665	5603*							
	3^+	1	0	0							
		2	1766	1984							
		3	3138	2965							
		4	4474	4771							
		5	5575	(5318)*							
		6	5971	5700*							

A,T	J^{π}	#	E_x[KeV]		Intruder States: E_x, J^{π}						
			SM	exp	2 ħω[a)]			4 ħω[b)]			
22,0	3^+	7	7049	6997*							
cont'd		8	7272	7378*							
		9	7546	7514*							
	4^+	2	4983	5101							
		3	5652	5725*							
		4	6248								
		5	7050	7151*							
		6	7666	7572*							
	5^+	1	1563	1528							
		2	4353	4710							
		3	5378	5308*							
	6^+	1	3823	3707							
		2	7201								
		3	7991	8221*							
		4	8996	9137*							
		5	9404	9378*							
	7^+	1	4642	4524							
		2	7754	8610*							
		3	8849	9060*							
	8^+	1	8378	8572*							
	9^+	1	9680	9813*							
22,1	0^+	1	0	0							
		2	6343	6235							
					6900	0^+					
		3	7264	7341							
		4	8794	missing							
	1^+	1	5437	5329							
		2	6663	6854							
		3	8586	8561*							
		4	9192	9178*							
	2^+	1	1368	1275							
		2	4455	4457							
		3	5032	5363							

A,T	J^{π}	#	E_x[KeV]		Intruder States: E_x, J^{π}						
			SM	exp	2 ħω[a)]			4 ħω[b)]			
22,1	2^+	4	6179	6120							
cont'd		5	6573	6819							
		6	7804	7643							
					7921	2^+					
		7	8315	8134*							
		8	8464	8490*							
	3^+	1	5635	5641							
		2	6520	6636							
		3	7741	8162*							
		4	8435	8490*							
	4^+	1	3378	3358							
		2	5480	5524							
		3	6430	6345							
		4	6993	7344							
		5	8189	8077*							
		6	8725								
	5^+	1	7461	7423							
		2	8696	8900*							
		3	9143	9652*							
		4	10068	10654*							
		5	10667	10.76*	MeV						
	6^+	1	6396	6311							
		2	9219								
		3	9793								
		4	10270	10423*							
	7^+	1	10549								
		2	11481	11.48 *	MeV						
	8^+	1	10959	11032*							
21,1/2	$1/2^+$	1	2870	2796							
		2	5814	5993*							
		3	7042	7212*							
	$3/2^+$	1	0	0							
		2	4790	4689							

A,T	J^π	#	E_x[KeV]		Intruder States: E_x, J^π						
			SM	exp	2 ħω[a]			4 ħω[b]			
21,1/2	$3/2^+$	3	5782	5549							
cont'd					5822	$3/2^+$					
		4	6439	6609*							
		5	7560	7605	^{21}Na*						
		6	8309	8417	^{21}Na*						
	$5/2^+$	1	248	351							
		2	3731	3737							
		3	4576	4524							
					5775	$(5/2^+)$					
		4	7275	7017	^{21}Na*						
		5	7667	7840	^{21}Na*						
		6	8092	8135	^{21}Na*						
	$7/2^+$	1	1795	1746							
		2	5377	5628							
		3	6287	6175*							
		4	6975	7006*							
		5	7379	7360*							
	$9/2^+$	1	2813	2866							
		2	6134	6265*							
		3	6215	6640*							
		4	7774	8154*							
	$11/2^+$	1	4475	4432							
	$11/2^+$	2	8039	7981*							
	$13/2^+$	1	6180	6447*							
	$15/2^+$	1	9765	9862*							
	$17/2^+$	1	9735	9941*							
21,3/2	$1/2^+$	1	320	280							
	$3/2^+$	1	1853	1730							
	$5/2^+$	1	0	0							
		2	3681	3469*							
	$7/2^+$	1	3612	3638*							
		2	4427	4572*							
	$9/2^+$	1	1844	1755							

A,T	J^π	#	E_x[KeV]		Intruder States: E_x, J^π						
			SM	exp	2 ħω[a]			4 ħω[b]			
20,0	0^+	1	0	0							
		2	6756	6724							
								7191			
					8700						
					10950						
					11558		N = 1 → N = 3				
		3	11977	12436*							
		4	13829	13530*							
	1^+	1 2	12233 14444	} missing, however 2 ħω states at 9935,13171,13307 observed							
	2^+	1	1776	1634							
		2	7316	7424							
								7833			
					9000						
		3	10437	9483*							
					10584						
		4	10737	10843*							
					11320						
					11885		N = 1 → N = 3				
					12327						
		5	12954	12957*							
	3^+	1	10230	9873							
		2	11436	10917*							
					11653						
	4^+	1	4212	4248							
					8820						
								9031			
		2	9973	9940*							
		3	10676	10553*							
					10800						
		4	11752	11020*							
					12253						
					13048						
		5	13886	13341*							

A,T	J^{π}	#	E_x[KeV]		Intruder States: E_x, J^{π}						
			SM	exp	2 ħω[a)]			4 ħω[b)]			
20,0	4^+				13965		N = 1 → N = 3				
cont'd		6	14279	14270*							
		7	14988	14593*							
	5^+		These states are practically unaccessible experimentally (π = u)								
	6^+	1	8515	8777							
								12127			
					12865						
		2	12941	13105*							
		3	14550	14304*							
					14311						
		4	14894	14807*							
					15159						
					15346						
		5	16377	15970*							
	7^+		As with $J^{\pi} = 5^+$ these states are unaccessible experimentally								
	8^+	1	11591	11950							
		2	15896	15874*							
20,1	0^+	1	3490	3526							
	1^+	1	1048	1057							
		2	3348	3488							
					4082						
		3	4882	4312*							
	2^+	1	0	0							
		2	2095	2044							
		3	3361	3587*							
	3^+	1	598	656							
		2	2198	2195							
		3	2896	2966							
		4	3484	3590*							
	4^+	1	738	823							
		2	3800	3669*							
		5^+	1743	1824							
		6^+	4525	4510							
		7^+	4458	4590							

A,T	J^{π}	#	E_x[KeV]		Intruder States: E_x, J^{π}						
			SM	exp	2 ħω[a)]			4 ħω[b)]			
19,1/2	$1/2^+$	1	0	0							
					5938						
		2	6084	6250							
		3	7819	7364*							
	$3/2^+$	1	1698	1554							
					3908						
								5501			
					6497						
		2	6627	6528*							
		3	7728	7262*							
	$5/2^+$	1	99	197							
					4550						
		2	5155	5107							
					5535						
		3	6373	6282*							
								6.5 MeV, missing			
		4	7285	6838*							
		5	7565	8014*							
	$7/2^+$	1	4871	4377							
		2	5900	5465							
					6070						
		3	6297	6330*							
					6554						
								7560			
		4	9197	(9030)*							
		5	9329	(9509)*							
	$9/2^+$	1	2810	2780							
		2	6841	6592							
					7.5 MeV missing						
		3	7988	7929*							
	$11/2^+$	1	6729	6500							
		2	8069	7937							
	$13/2^+$	1	4789	4647							
		2	9886	10411							

A,T	J^{π}	#	E_x[KeV]		Intruder States: E_x, J^{π}						
			SM	exp	2 ħω[a)]			4 ħω[b)]			
19,3/2	$1/2^+$	1	1470	1472							
	$3/2^+$	1	294	96							
		2	3706	4109							
		3	5529	5455							
	$5/2^+$	1	0	0							
					3067						
		2	3169	3153							
		3	5011	5150							
	$7/2^+$	1	2061	2799							
	$9/2^+$	1	2479	2372							
18,0	1^+	1	0	0							
					1701						
		2	4108	3724							
					4360						
		3	6271	6108*or 6262							
	2^+	1	4087	3839							
	3^+	1	1153	937							
					3358						
		2	4288	4116							
								6485			
	4^+				5298						
		1	6557	6777*							
	5^+	1	1243	1121							
18,1	0^+	1	0	0							
					3634						
		2	4320	5336*							
	1^+		>10 MeV								
	2^+	1	2180	1982							
		2	4439	3921							
					5255						

A,T	J^{π}	#	E_x[KeV]		Intruder States: E_x, J^{π}						
			SM	exp	2 ħω[a)]			4 ħω[b)]			
18,1	2^+	3	9465	9361*							
cont'd	3^+	1	5726	5378							
	4^+	1	3782	3555							

a) For A = 26 - 38 we observe spherical 2p excitations from the s-d into the f-p shell. For A = 18 - 24 we observe deformed 2p excitations from the p into the s-d shell. An exceptional 2 ħω excitation is observed in ^{24}Mg by the promotion of one particle from the p into the f-p shell.

b) For A = 36 - 38 (and also ^{39}K and ^{40}Ca which are not displayed here) we observe deformed 4p excitations from the s-d into the f-p shell.
For A = 17 - 20 we have deformed 4p excitations from the p into the s-d shell.

c) In A = 38 (and also ^{40}Ca and ^{42}Ca which are not displayed here) we observe deformed 6p excitations from the s-d into the f-p shell.

Part II

Complete analysis of rotational structure between ^{16}O and A = 31 in terms of a Nilsson model with empirical residual interaction

1. Concept

We construct the deformed states of A = 16 - 31 nuclei by starting from the deformed 4p-4h configuration of ^{16}O as the core, adding A − 16 valence nucleons in the Nilsson orbits above the Fermi boarder, subject to an empirical residual interaction. The core is characterized by $\varepsilon \approx \delta \approx 0.5$. The downsloping deformation driving $1/2^+$ [220] orbit of Fig. 1 is occupied, the sphericity driving $1/2^-$ [101] orbit is empty. Between ^{16}O and ^{24}Mg orbits $1/2^-$ [101] and $3/2^+$ [211] get occupied and the deformations reduce to $\varepsilon \approx \delta = 0.3 - 0.4$. Starting with A = 25 (and ending with A = 31) we have a choice of filling the near degenerate orbits $5/2^+$ [202] or $1/2^+$ [211]. The latter choice maintains deformation and leads eventually to the $J^\pi = 0_3^+$ state of ^{28}Si at E_x = 6691 KeV. The former choice leads to a reduction of deformation by a factor of two, close to sphericity. The 4979 KeV, $J^\pi = 0_2^+$ state of ^{28}Si is the “bandhead”.

In addition to prolate deformations of normal and strongly reduced size, oblate distortions play a role for A = 27 - 31 and a new ordering (compare Table 4A, p. 93, Table 4B, p. 94) of the relevant Nilsson orbits must be found and new parameters of the residual interaction.

The present work uses a parametrization of the residual interaction by Brink and Kerman *[1].* The parameters and the single-particle energies must be taken from experiment, namely excitation and binding energies of bandheads. The B + K method includes automatically the rearrangement energies. The latter ones arise if the addition of valence nucleons is leading to a new equilibrium deformation ε. This is also true for the γ-degree of freedom so that deviations from axial symmetry are equally considered. The present analysis ex-

tends considerably the range of applicability of the Nilsson model in the s-d shell. It reveals a far reaching equivalence with the results of shell model calculations in the unrestricted s-d basis space *[2, 3]*. It provides in addition the remaining states (unnatural parity, multi-particle excitations across a major shell) which are (technically) not accessible to the shell model. The structure of the Nilsson model states is simple, requiring in general the participation of two orbits only.

The present analysis has become possible because we are safe, now (Part I), of the level schemes in s-d shell nuclei up to high excitation energies (up to the fiftieth state on the average). This is due to the advent of shell model calculations around 1984 *[2]* which maintained interest in spectroscopy for another 20 years. In addition results of the S. M. can substitute inaccessible data and, more important, serve as a check for completeness of information. In the section Data base (A = 16 - 30) we implement and extend our account of experimental levels with assigned J, π, T by about 230 levels. This is extremely useful for the following but pretty boring for a reader. Hence we have placed the chapter “Data base” at the end of these notes.

References

1. D. M. Brink, A. K. Kerman, Nucl. Phys. 12, 314 (1959)
2. B. H. Wildenthal in “Progress in Particle and Nuclear Physics”, edited by D. H. Wilkinson (Plenum Press, New York, 1984)
3. B. A. Brown, W. A. Richter, Phys. Rev. C 74, 034315 (2006)

2. Theoretical framework

The energy levels of A = 20 - 31 nuclei and several states in A = 16 - 19 nuclei are grouped in Figs. 2 - 30 into a system of all together 272 rotational bands. The bandhead energies are listed in Table 7, p. 167 and Table 8, p. 183. As with the spherical shell model we use part of the latter energies (about one third) to derive empirical single-particle energies of the Nilsson model and parameters, which specify the residual interaction. The remaining bandhead energies are subsequently reproduced, demonstrating the consistency of the analysis. The present treatment of the residual interaction is based on the work of Brink and Kerman (Nucl. Phys. 12, 314 (1959)) and is known to us due to the thesis of D. Pelte on the structure of ^{21}Ne (Freiburg 1965). The theory was successfully applied to s-d shell nuclei in connection with the phenomenon of high-K rotational bands (H. Röpke, Nucl. Phys. A 674, 95 (2000)).

The nuclear part of the total binding energy of a bandhead consists of a core energy, single-particle binding energies of valence nucleons and their interactions. The former two can be read directly from experimental data (Tables 1,2) while a treatment of the latter one needs explanation.

The interaction energy of two nucleons in Nilsson orbit i is

A_i, B_i, C_i for intermediate quantum numbers K', T' = 0,1; 0,0; $2\Omega_i$, 0 respectively. The interaction energy of four nucleons is

$S_i = 3A_i + B_i + 2C_i$

(We have used the notation T_i instead of S_i previously which could lead to confusion with isospin.)

The energy of three nucleons is 1/2 S_i.

The interaction of two sets of nucleons in orbits i and k is given by the operator

(1) $$V_{ik} = a_{i,k}\, n_i \bullet n_k + b_{ik}\, P_i \bullet P_k + 4c_{i,k}\, \vec{Ti} \bullet \vec{T}_k + 4\, d_{i,k}\, \vec{Q}_i \bullet \vec{Q}_k$$

with

n_i, n_k number of particles

P_i, P_k added normalized angular momentum projections $P_i = \sum \frac{\Omega\alpha}{|\Omega\alpha|}$

$\vec{T}_i$, $\vec{T}_k \rightarrow$ Isospin $\vec{T}_i = \sum \vec{t}_\alpha$

$\vec{Q}_i$, $\vec{Q}_k$ defined by $\vec{Q}_i = \sum \frac{\Omega\alpha}{|\Omega\alpha|} \vec{t}_\alpha$

In almost all cases it is sufficient to know the expectation values of $V_{i,k}$ only.

The $\vec{Q}_i \bullet \vec{Q}_k$ term yields vanishing contributions for either n_i or n_k = 0, 2, 4.

For $n_i = n_k$ = 1, 3 (particle-particle or hole-hole), the result agrees with that

of the operator $P_i P_k \vec{T}_i \bullet \vec{T}_k$

while a change of sign occurs for n_i = 1 n_k = 3 (particle-hole). This is kind of a Pandaya transform and it allows for instance to relate A = 22 energies to energies in A = 20 or A = 24.

A special situation occurs if we have an odd number of particles in two different orbits with however equal projection quantum number Ω. In this case a K = 0 rotational band with both even and odd values of J can be built.

The structure of the rotational wave function

(2) $\Psi = D_{MK}^J \chi_K + (-)^p D_{M-K}^J \chi_{-K}$

leads to a diagonal matrix element

$(-)^p < \chi_K|V|\chi_{-K}> \neq 0$ for K = 0

with $p = J - \frac{1}{2} \bullet m + \sum l_i$

m = Number of particles in altogether both orbits

$\sum l_i$ = Parity of the wave function

If this diagonal matrix element yields attraction for T = 0 states we have the situation that the lower lying branch of the rotational band has

$J^{\pi} = 0^{+}, 2^{+}, \ldots$

for A = 4n

$J^{\pi} = 1^{-}, 3^{-}, \ldots$

and

$J^{\pi} = 0^{-}, 2^{-}, \ldots$

for A = 4n + 2

$J^{\pi} = 1^{+}, 3^{+}, \ldots$

If the exchange term of this diagonal matrix element is dominating the direct term, repulsion is observed in the T = 1 states leading to reversed ordering. The proposed even-odd splitting is maintained without exception throughout this analysis.

Another complication arises if a single particle/hole in a Ω = 1/2 orbit is accompanied by two particles in another orbit, coupled to K', T' = 0, 1 or 0, 0. In the former case the decoupling factor remains unaffected, in the latter case it changes sign.

(The particle pair generates an overlap factor $(-)^{2*(-1/2)} < \chi_K | \chi_{-K} >$ with values ± 1).

This change of sign is observed once in the spectrum of ^{21}Ne.

The situation of three particles in two or three orbits coupled to T = 1/2 leads to the diagonalization of a 2 x 2 matrix, because two particles can couple to intermediate isospin T_{12} of 0 or 1 (Clever choice of the particle pair can lead to a good approximation with a single isospin value dominating). The isospin-dependent terms of (1) yield contributions of

(3) $-3(c_{12} + P_1 P_2 d_{12})$ for the diagonal matrix element with $T_{12} = 0$

$(c_{12} + P_1 P_2 d_{12}) - 2(c_{13} + P_1 P_3 d_{13}) - 2(c_{23} + P_1 P_2 d_{23})$ for $T_{12} = 1$

The non diagonal matrix element has the isospin-dependent contributions.

(4) $-\sqrt{3}\ (c_{13} + P_1 P_3 d_{13} - c_{23} - P_2 P_3 d_{23})$

(the matrix element is antisymmetric with respect to interchange of particles 1 and 2)

If a particle in orbit i is replaced by a hole the substitution $P_i \rightarrow -P_i$ becomes necessary. If particle 1 and 2 reside in the same orbit (coupled necessarily to $K_{12} = 0$) equation 4 reduces to $-\sqrt{3} \bullet 2d_{13}$. This result is cited in Brink and Kerman who seem to have missed the factor of 2. The empirical interaction includes to first order the rearrangement energy which is gained if the nucleus seeks a new equilibrium deformation under the influence of valence nucleons (H. Röpke, Eur. Phys. J. A 22, 213 (2004)).

If the core energies varies as

$E_c = E_c^0 + \alpha(\varepsilon - \varepsilon_0)^2/2$

and the single particle energy of orbit i as

$E_{b,i} = E_{0,i} + \beta_i(\varepsilon - \varepsilon_0)$

we gain $E_R = \sum(n_i \beta_i)^2 / \underbrace{1/6(\sum N + 3/2)\hbar\omega_0}_{= \alpha}$ where the sum runs over the core nucleons and $\hbar\omega_0 = 41\, A^{-1/3}$ MeV

The parameters A_i, B_i, C_i contain the amount $-\beta_i^2/\alpha$

the single particle energies $-\beta_i^2/2\alpha$ and the

parameter a_{ik} the contribution $-\beta_i \beta_k/\alpha$

which can have either sign so that the “monopole” interaction a_{ik} can be repulsive and in fact is in one case.

Equilibrium deformations can be calculated in the case of positive ε (for whatever reasons) using a renormalized Racavy expression (Nucl. Phys. 4, 375 (1957)).

$$\varepsilon = \underbrace{0.8 \bullet 3/2}_{\text{empirical}} \frac{\sum_p (3nz - N) - \sum_h (3nz - N)}{\sum_a (N + 3/2)}$$

where the sum runs over, respectively, particles, holes and all nucleons and with $[N, n_z, \Lambda]$ being the quantum numbers of orbits.

3. How to obtain the interaction

Coulomb interactions can be treated with sufficient accuracy (±100 KeV) and are tacitly included. It is noteworthy that the interaction energies of two protons depend practically on their principal quantum numbers only. Comparison of mirror analogues yields

E_c = 530 KeV $N_1 = N_2 = 2$

594 KeV $N_1 = N_2 = 1$

386 KeV $N_1 = 1, N_2 = 2$

The analysis uses excitation energies of bandheads. They contain a contribution

$\Delta E_x = (K - a\, \delta_{1/2, K})\, \hbar^2/2\Theta$

from zero point precession and, for K = 1/2, the decoupling effect.

Significant decoupling factors a occur for the orbits

$1/2^-_p$ [101] a = 1.7 in A = 17, 19; a = 0.8 in A = 23

$1/2^+_1$ [220] a = 2.5 in A = 15, 19; a = 1.8 in A = 23

$1/2^-_f$ [330] a = −3.2

and, on the oblate side (A = 27, 29)

$1/2^-_p$ [101] a = 1

$1/2^+_1$ [220] a = 1.7

Rotational constants vary between 120 and 400 KeV and can be deduced from the figures (2 - 30). Default values are 200, 160, 120 and 180 KeV for A = 17 - 23, 24 - 27, 28 - 30 and oblate bands.

The energy ΔE_x has to be subtracted before nuclear interactions are discussed.

Analysis of the nuclear interactions starts with the binding energies of a single neutron/proton or of a hole relative to the A = 4n parent ^{16}O, ^{20}Ne, ^{24}Mg, ^{28}Si, respectively. The heads of rotational bands with single particle/hole configuration are known from single-nucleon transfer except for the A = 17 states and the prolate A = 29 states because the parent is an excited

state (6049 KeV in ^{16}O, 6691 KeV in ^{28}Si). The A = 17, 29 states are, henceforth discussed separately. The neutron single particle/hole states and the deduced binding energies are given in Tables 1, 2. If the same single - particle/hole orbit i occurs in two different nuclei it is possible to deduce the interaction energies $4a_{ik}$ with those nucleons (in orbit k) which make up the difference between the two parent nuclei. Thus we obtain the a_{ik} interaction (Table 4A) between an $3/2_1^+$ [211] nucleon and, respectively, a $5/2^+$ [202], $1/2_2^+$ [211], $1/2_f^-$ [330], $1/2_3^+$ [200] nucleon from A = 21 and A = 25 in Table 1, the interaction with $1/2_p^-$ [101] and $1/2^+_1$ [220] from A = 23 and A = 19 in Table 2. The a_{ik} value for the pair $1/2_1^+$ [220] and $1/2_p^-$ [101] follows from the $K^\pi = 1/2^+$ states in ^{15}O and ^{19}Ne in Table 2.

The interaction between an $\Omega^\pi = 5/2^+$ [202] and an $\Omega^\pi = 1/2_2^+$ [211] nucleon is obtained by comparing the binding energies of the $(5/2^+)^2_{K=5}$ configurations in ^{26}Al and ^{30}P (Table 7, p. 177 and 181) relative to, respectively, ^{24}Mg g.st. and ^{28}Si, 6691 KeV state. They differ by $8a_{ik}$ plus Coulomb terms. The (prolate) $K^\pi = 5/2^+$ bandhead in ^{29}Si is subsequently predicted at $E_x = 6.14$ MeV and correlated with the experimental 6522 KeV state.

The interaction energy a_{ik} between a $1/2_1^+$ [220] and a $5/2^+$ [202] nucleon is deduced using the binding-energy relation for particle-hole configurations.

$E_{p-h} = E_p + E_h - E_{core} - n_p \bullet n_h\, a_{ik}$ + b, c, d terms

where the first three terms can be directly taken from experiment. Configurations with $n_h = 1$, $n_p = 1$ can be identified in A = 20 and A = 24, with $n_p = 2$ in A = 25 and $n_p = 3$ in A = 26 (see Table 7). The most error forgiving way of obtaining a_{ik} is the use of A = 24 data to deduce b_{ik}, c_{ik}, d_{ik} (see next paragraph) and, subsequently, use of the 3963 KeV, $J^\pi = K^\pi = 3^+$, T = 0 state of ^{26}Al (Table 7, p. 177) for the deduction of a_{ik} because $n_p = 3$ yields the best leaver. The resulting value of + 380 KeV is dominated by a large positive rearrangement energy $-\beta_i \beta_k/(1/6)\cdot\sum \hbar\omega(N + 3/2)$ (H. Röpke, Nucl. Phys, A 674, 95 (2000)) of 1.5 - 2 MeV which is due to the enormous slopes β of the

involved Nilsson orbits combined with opposite signs (Fig. 1). The nuclear part of a_{ik} is negative as expected.

The parameters b_{ik}, c_{ik}, d_{ik} describe the splitting of a $K = (\Omega_i \pm \Omega_k)$, T = 0, 1 multiplet generated by two particles/holes or a 1p-1h pair. Identification of these multiplets is the most challenging part of this work. The centroids of the multiplets (see Tables 5, 6) are however predictable since we know the single particle/hole energies already and the "monopole" interactions a_{ik}. Furthermore some multiplets or parts thereof (or their Pandaya transform) exist in different nuclides (A = 20, 22, 24). At the end we felt completely safe how to proceed. The b, c, d parameters which connect the very low-lying $1/2^+$ [220] and respectively $1/2^-_p$ [101] orbits with the higher-lying ones are obtained from A = 20 (Fig. 35) except for the combination $1/2_1^+$ [220] - $5/2^+$ [202] where a complete multiplet can be identified in A = 20, 24. The resulting b, c, d differ marginally but we have a slight preference of the A = 24 results (Fig. 39) because the latter ones are needed later on in A = 25, 26. The parameters b, c, d which connect the $3/2_1^+$ [211] orbit with the higher-lying ones are obtained from A = 24 (Fig. 39). The use of A = 22 data was avoided because of the higher level density and the large number of new J^π assignments which had to be performed for this mass. Conversely one can use the band structure of A = 22 in Fig. 37 as a consistency check which is very satisfying.

The b, c, d parameters connecting the $5/2^+$ [202] and $1/2_3^+$ [211] orbits with each other and the higher lying orbits are derived from the A = 26 system (Figs. 19, 20, 41), since it is very well investigated (H. Röpke and P. M. Endt, Nucl. Phys. A 632, 173 (1998)).

The case of oblate deformation is finally analyzed using data from ^{28}Si and A = 30 (Fig. 46). While it is possible to derive the parameters b, c, d the parameter a must remain undetermined. Single particle/hole energies have been deduced before (Tables 1, 2).

Now we come back to prolate deformation. The interaction energies $S_i = 3A_i + B_i + 2C_i$ of a nuclear quartet in orbit i must be known for the first four orbits outside the ^{16}O core. Experimental information is provided by A = 4n or A = 4n + 3 nuclei where the configurations $(\Omega^\pi)^4$ and $(\Omega^\pi)^3$ can be identified. We treat the first two orbits $1/2^-$ [101] and $3/2^+$ [211] together. Six bandheads with configuration $(1/2^-)^3$, $(3/2^+)^3$, $(1/2^-)^4$, $(3/2^+)^3$, $(1/2^-)^3(3/2^+)^4$, $(1/2^-)^4(3/2^+)^4$ = $^{19}F(110)$, $^{19}F(5501)$, $^{20}Ne(0)$, $^{23}Na(0)$, $^{23}Na(2640)$, $^{24}Mg(0)$ are used to predict two quartet energies, two single particle energies, the interaction a_{ik} already discussed before, and the binding energy of the ^{16}O core. In this way use of data from A = 16, 17 was avoided because the coexistence of spherical and deformed states in these nuclei could cause problems. The E_x of core - and single-particle states are

	$J^\pi = K^\pi$	exp[KeV]	theor[KeV]
^{16}O	0^+	6049	5492
^{17}O	$1/2^-$	3055	3629
	$3/2^+$	5869	4991

Thus the ^{17}O bandheads are safely identified which is not trivial. The ^{21}Ne g.st. with configuration $(1/2^-)^4(3/2^+)^1$ can be reproduced to within 40 KeV but the E_x of the 7191 KeV, $J^\pi = 0^+$ state of ^{20}Ne with configuration $(3/2^+)^4$ is predicted at 7995 KeV. We attribute this to mixing of the 7191 KeV level with the nearby 8700 KeV, 0^+ state with configuration$(1/2^-)^2(3/2^+)^2$. Both levels should thus be equal mixtures of the famous 4p-4h and 2p-2h $J^\pi = 0^+$states of ^{20}Ne.

Now we treat the remaining quantities.
The 6691 KeV, 0^+ state of ^{28}Si has the configuration $(1/2_2^+ [211])^4$ relative to ^{24}Mg while the ^{27}Al g.st. has $(5/2^+ [202])^3$ (See Lickert et al., Z. Physik A 331, 409 (1988) for proof of prolate deformation). These states serve to obtain S_i for the cited orbits. There is no $(5/2^+)^4$ configuration of prolate shape.

The decomposition of the aggregate quantity S_i into its constituents (A_i, B_i, C_i uses data from A = 18, 22, 26 for $\Omega^\pi = 1/2_p^-$, $3/2_1^+$, $5/2^+$ and $1/2_2^+$, respectively). The A = 26 system provides these quantities for the $1/2_3^+$ [200] orbit in addition while A = 30 provides the same data for oblate deformation. The calculation of S_i from its constituents introduces larger errors and serves as a plausibility check only.

4. Results

In Figs. 2 - 30 we try to order a sample of 1508 experimental levels from A = 16 - 31 nuclei (see Data base) into rotational bands. Another 378 levels can be added from the results of shell model calculations (Part I) for the complete s-d shell (^{16}O - ^{40}Ca). The reasoning is the following. The so-called USD calculations in the spherical basis infer complete occupancy of orbits with oscillator quantum number N = 0 and 1 while the N > 2 orbits are empty. In the deformed basis of the Nilsson model orbits maintain the quantum number N (neglect of major shell mixing). Thus with equal restrictions concerning N the Nilsson model will generate levels which form a subset of the USD levels. Outside this subset we have 373 levels of negative parity in Figs. 2 - 30 which requires an odd number of holes in N = 1 orbits or particles in N = 3 orbits. Furthermore there are 98 levels where the number of holes or particles is even. Together these levels, which had no comprehensive interpretation so far, amount to 25 percent of the investigated levels.

The bands of Figs. 2 - 30, 450 with prolate and 132 with oblate distortion are interpreted in Tables 7, 8. This is possible with aid of the single particle/hole energies of Tables 1, 2 and the residual interactions of Tables 3, 4A, and 4B. The orbits in Table 7 are given in short notation as in Table 4A. The notation is maintained in Table 8 (oblate deformation) but attention should be drawn to the inverted ordering of the $\Omega^{\pi} = 1/2_1^+$ and $1/2_2^+$ orbits. (This ensures orthogonality of wave functions for the $J^{\pi} = 0_{1\text{-}3}^+$ states of ^{28}Si). The vertical line in Tables 7, 8 indicates the Fermi boarder in the ground state of the nearest even-even nucleus as given in Tables 4A and 4B.

A summary of all rotational bands is given in Figs. 31 - 47 for every A between 16 and 31. We display bandhead energies and their K^{π} values. Isospins are given only if they deviate from the default values T = 0 or 2T = 1. At the bottom of the figures we repeat the assigned Nilsson model configurations of Tables 7, 8 in short notation. The present ordering of bands according to

occupation numbers of orbits yields the fastest insight into the structure of the investigated nucleus. The total of identified bands amounts to 582. The majority, 410 bands are also present in the USD-shell model calculations (Part I), 147 have negative parity and find a first systematic explanation here. The latter is also true for 25 positive-parity bands, most of them in the A = 16 - 20 region, which require excitations of two or four particles from an N = 1 into an N = 2 orbit. Compared to the USD-shell model we are able here to treat cross shell excitations. Also we have a simple structure of wave functions as discussed in the next section.

5. Construction principles of the Nilsson model

The construction principles of the Nilsson Model for A = 16 - 31 are very simple. The configurations with T = 0, 1/2, 1 are, in the overwhelming number of cases characterised by one or two active orbits (neither empty nor filled). Configurations with three active orbits occur at higher energies and only the energetically most favourable ones, appear. For T = 3 /2 they are more frequent, of course. The excitation mechanisms for T ≤ 1 are generally/occasionally.

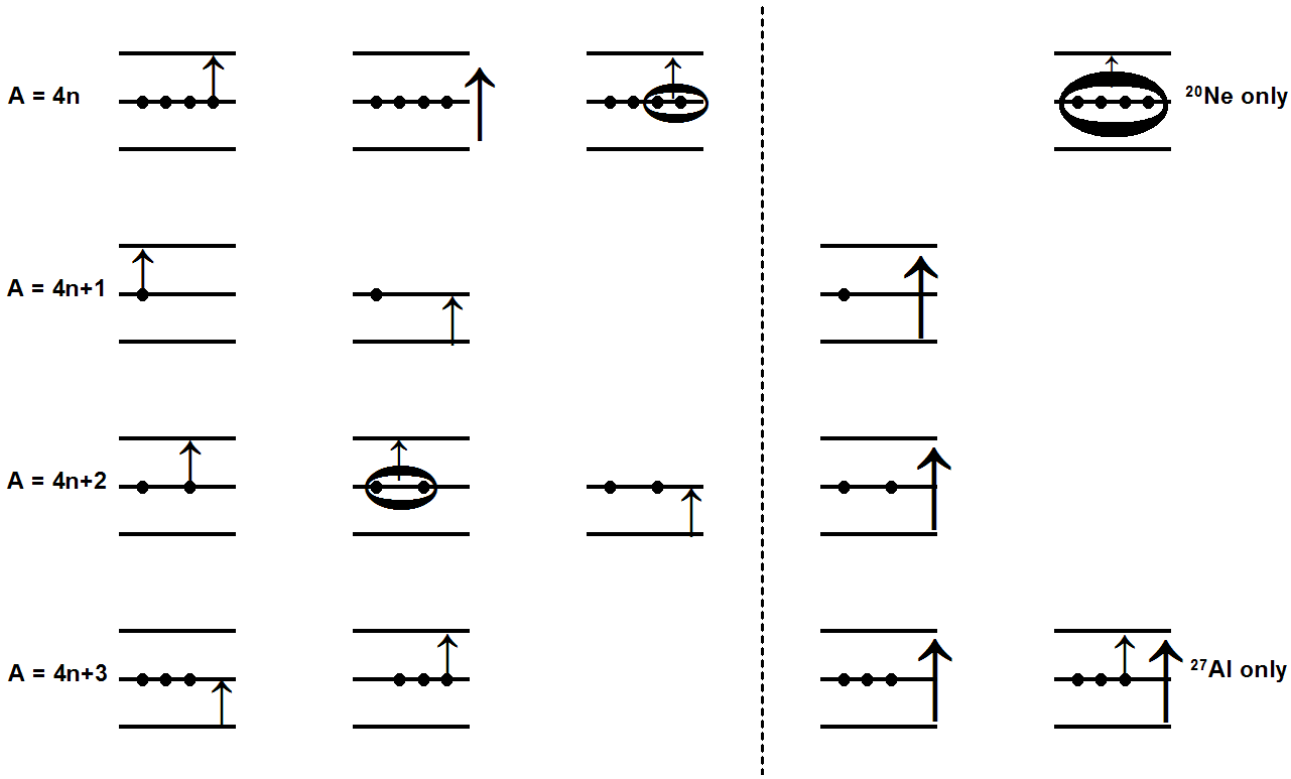

A = 4n

The T = 0, 1 excitations are 1p-1h states in general. The 2p-2h excitations are small in number and have the coupling schemes $K_p = K_h = 0$, $T_p = T_h = 1$, or $K_p = 2\Omega_p$, $K_h = 2\Omega_h$, $T_p = T_h = 0$.The first coupling leads to $K^\pi = 0^+$ states in ^{20}Ne, ^{24}Mg and ^{28}Si (prolate shape). The second coupling favours, in addition, the formation of states with maximum value of K. We have $K^\pi = 4^+, 4^+, 8^+, 6^+$ states in ^{16}O, ^{20}Ne, ^{24}Mg, ^{28}Si (prolate). The recoupling of either K_p, T_p or K_h, T_h to 0, 1 completes the spectrum of T = 1 states.

The 4p-4h excitation (necessarily with K^π, $T = 0^+$, 0) is important only in ^{20}Ne and due to the near degeneracy of the $1/2^-$ [101] and $3/2^+$ [211] orbits.

A = 4n + 1, T = 1/2

Almost all configurations have 1p or 2p-1h character. In the latter case we observe the bands with K_p, $T_p = 2\Omega_{p,0}$ very systematically. The bands with $K_p = 0$, $T_p = 0 + 1$ are equally observed. Usually the $T_p = 1$ coupling is dominating except for A = 21 where a case with dominating T = 0 coupling occurs (a consequence of the absence of a low-lying $K^\pi = 2^+$, T = 0 band in ^{20}Ne). Configurations with three active orbits occur in ^{25}Mg and ^{21}Ne because parents of favourably low energy are found in the first $K^\pi = 2^+$, T = 0 band of A = 24 and, respectively, the $K^\pi = 4^+$, T = 1 band of ^{22}Ne. (The parent energies are in turn favoured by small values of c_{ik} in Table 4A).

A = 4n + 2

These nuclei have the most simple structure. Two particles or two holes can be found in the same or different orbits. All residual interactions are comparable so that the spectrum is mainly determined by the single-particle energies. Configurations with three active orbits occur in A = 26 because ^{24}Mg constitutes an easy to excite core while ^{20}Ne is very rigid.

A = 4n + 3, T = 1/2

Compared to A = 4n + 1 we have to exchange the roles of particles and holes only. Thus we observe in first place (Tables 7, 8) the spectrum of 1h states, and second the 2h-1p states which are nothing else but three particles in two orbits each. As with A = 4n + 1 nuclei a few configurations with three active orbits are observed in ^{27}Al, ^{23}Na and ^{19}F. In the first case we couple three particles (equivalent to one hole) to the favourably low K^π, $T = 2^+$, 0 configuration of ^{24}Mg, in the second case it is just one hole. In the third case a hole is coupled to the first 2^+, 1 configuration of A = 20, equally favoured energe-

tically. A special situation is encountered in ^{27}Al where the J^{π}, T = 6^{+}, 0 and 5^{+}, 1 (prolate) configurations of ^{28}Si (Table 7) act as parents of high-K states in ^{27}Al which have emerged previously from an analysis of shell model B(E2)'s. (H. Röpke, Nucl. Phys. A 674, 95 (2000)).

6. Competition of nuclear shapes for A = 16 – 31

The present analysis allows to study, in the realm from doubly magic ^{16}O to A = 31, T = 1/2 and 3/2, the competition of three nuclear shapes.

1. Sphericity or small (ε ≤ 0.2) prolate deformations
2. Prolate distortion of normal size (ε > 0.2)
3. Oblate distortions

Spherical shape in the ground states is restricted to A = 16 - 18. Due to the extremely deformation driving character of the $\Omega^{\pi} = 1/2^{+}$, [220] orbit of Fig. 1 prolate distortion is already present in the ^{19}F ground state. However spherical states can still be traced at higher energies (Fig. 48). Starting with ^{20}Ne and terminating with ^{24}Mg spherical or marginally deformed prolate states occur at high energies only. Beginning with ^{25}Mg and terminating in ^{29}Si rotational bands with marginal prolate distortion slip in at energies around 5 MeV. These bands and their properties are

Nuclide	Bandhead E_x [KeV]	K^{π}	$\hbar^2/2\Theta$ [KeV]	ε(theoretical)
^{20}Ne	13530	0^+		0.1
^{24}Mg	13198	0^+		0.16
^{25}Mg	6777	$1/2^+$	455	0.21
^{26}Mg	4318	4^+	435	0.22
^{26}Al	3963	3^+	453	0.17
^{27}Al	0	$5/2^+$	338	0.23
^{28}Si	4979	0^+	394	0.18
^{29}Si	4840	$1/2^+$	400	0.20

The rotational constants $\hbar^2/2\Theta$ are experimental ones and exceed “normal” values $\hbar^2/2\Theta \leq 150$ KeV considerably, thus proving very small deformation.

The deformation parameter ε has been calculated using the following configuration of A − 16 nucleons.

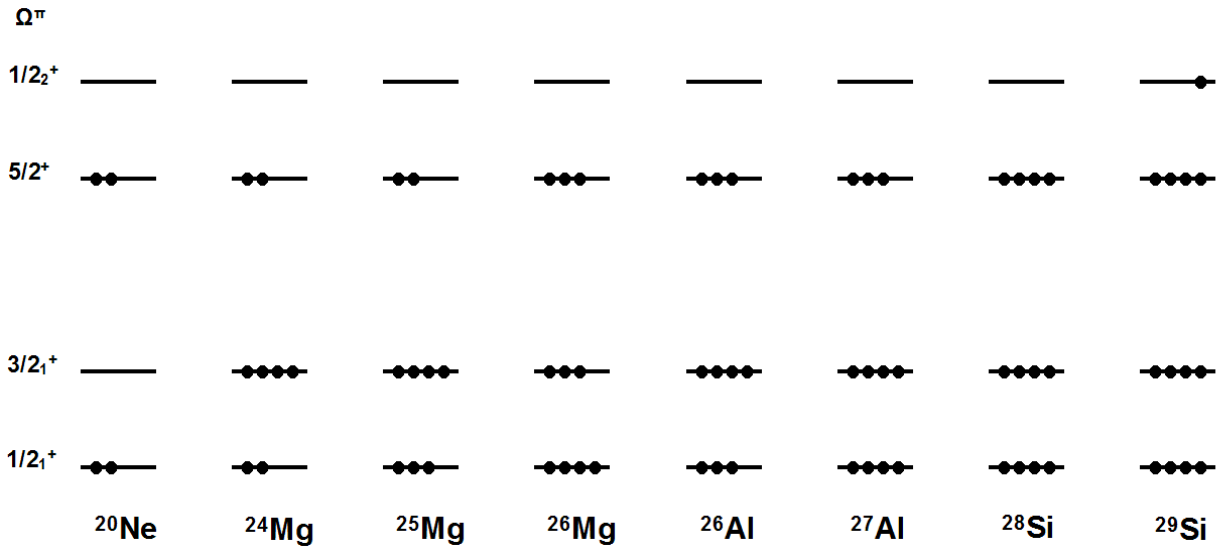

The small values of ε are due to the particles in the sphericity driving $\Omega^\pi = 5/2^+$ orbit supported for ^{20}Ne, ^{24}Mg, ^{25}Mg, ^{26}Al by holes in the deformation driving $\Omega^\pi = 1/2_1^+$ orbit.

We note in passing that the $J^\pi = 4^+$, T = 1 bandhead in A = 26 has been called a “condensate of particles into the $d_{5/2}$ subshell” in the USD-shell model calculations (Part I). The same can be said for the $J^\pi = 3^+$, T = 0 bandhead of A = 26. Both states have the configuration $d_{5/2}^{-2}$.

Levels of well developed prolate distortion have been observed previously between (and including) ^{16}O and ^{28}Si. The range is now extended to higher excitation energies and higher mass. In ^{31}P just one band can be localized still. From ^{19}F to A = 26 prolate deformation is already present in the ground states. Beginning with ^{27}Al the onset of well developed prolate distortion is moving up in energy by a few MeV. It is necessary for distortion to occupy the higher-lying, deformation favouring $\Omega^\pi = 1/2_2^+$ state prior to the lower-lying, sphericity driving $\Omega^\pi = 5/2^+$ orbit.

Levels with oblate distortion have been localized first in ^{29}Si and subsequently in ^{28}Si and ^{30}Si. The range is extended here to A = 27 and 31 while a new region will be found later (Chapter Oblate deformation in A = 28 - 36 and Figs. 50a - 52b).

In ^{28}Si, the middle of the s-d shell, we have to explain the presence of three different distortions. The next page offers an explanation which we have prepared in a different context.

7. A scheme of Nilsson orbits for ^{28}Si, inspired by Hartree-Fock calculations

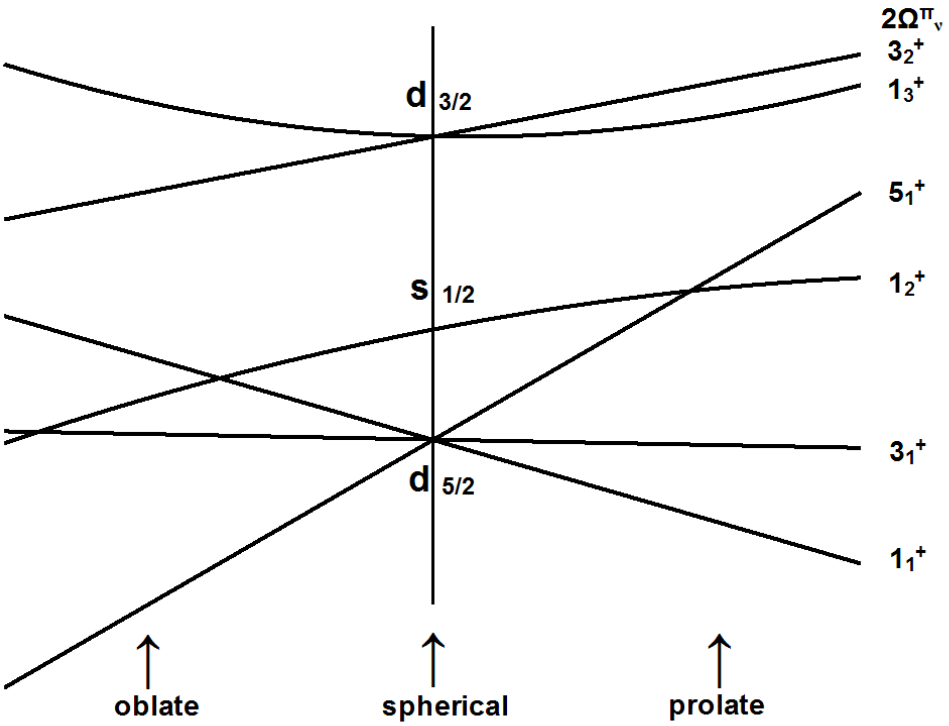

config.	oblate	spherical	prolate	shape unknown
	5_1^4	1_1^4	1_1^4	1_1^4
	3_1^4	3_1^4	3_1^4	1_2^4
	1_2^4	5_1^4	1_2^4	5_1^4
E_x[KeV]	0	4980	6691	≥ 12977

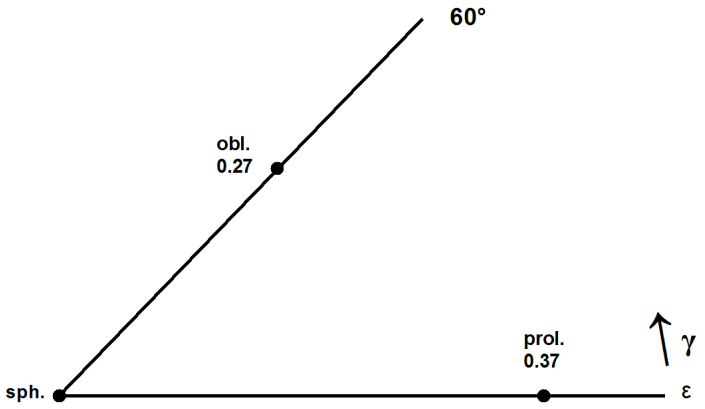

The first three configurations correspond to minima of the energy surface over the ε-γ plane. Does the fourth configuration yield a saddle point? Judging from the Nilsson model explanation of ^{28}Si we should observe three types of nuclear shape in ^{29}Si/^{27}Al by adding to/removing from ^{28}Si a single nucleon. This is born out by experiment.

Nuclid	Odd nucleon	shape	Exp. Bandhead [KeV]
	Ω^{π}		
^{29}Si	$1/2_1^+$	oblate	0
	$3/2_2^+$	oblate	1273
	$1/2_2^+$	almost spherical	4840
	$5/2^+$	prolate	6522
^{27}Al	$1/2_2^+$	oblate	843
	$3/2_1^+$	oblate	1013
	$5/2^+$	almost spherical	0
	$1/2_1^+$	prolate	3680

The enumeration of orbits with equal Ω^{π} is given on the preceding page.

8. Deformation alignment and large - K bands in A = 25 - 27

In 2000 we have investigated (Nucl. Phys. A 674, 95) the conspiracy of several nucleons in deformed s-d shell nuclei to add their angular momentum projections Ω_i to generate rotational bands of large K. The yrast line can thus be made up of bandheads with increasing values of K. If these states follow approximately a J(J+1) rule of excitation energies one can get the impression of a rotational band. The effect has got the name of “rotation around the symmetry axis”. In Fig. 49 we display such a situation for ^{25}Mg, ^{26}Al and ^{27}Al. The experimental states are amended by high-spin states obtained by the USD-shell model calculations in the unrestricted configuration space of the N = 2 major shell. The largest level spins obtained in this (spherical) basis are 25/2, 26/2, 27/2 for, respectively, ^{25}Mg, ^{26}Al and ^{27}Al. The classification of the yrast levels as members of a rotational band is given in Table 9. The K-quantum numbers are obtained from Figs. 17, 19, 21 and show an increase with increasing level spin. The angle Θ between spin and axis of deformation is extremely small as evidenced by the values of cos Θ.

The Nilsson model configurations underlying the K-assignments to levels are adopted from Table 7.

The building principle is as follows:

We start from the ^{20}Ne ground state configuration where the strongly deformation driving $\Omega^{\pi} = 1/2^{+}[220]$ orbit is fully occupied. Subsequently we add proton-neutron pairs with $K' = 2\ \Omega'_i$, $T' = 0$ and one odd nucleon if A = odd. All Nilsson orbits with major quantum number N = 2 must be considered. Thus we obtain maximum K-values K_M of 19/2, 22/2, 23/2 for ^{25}Mg, ^{26}Al, ^{27}Al, as shown in the drawing.

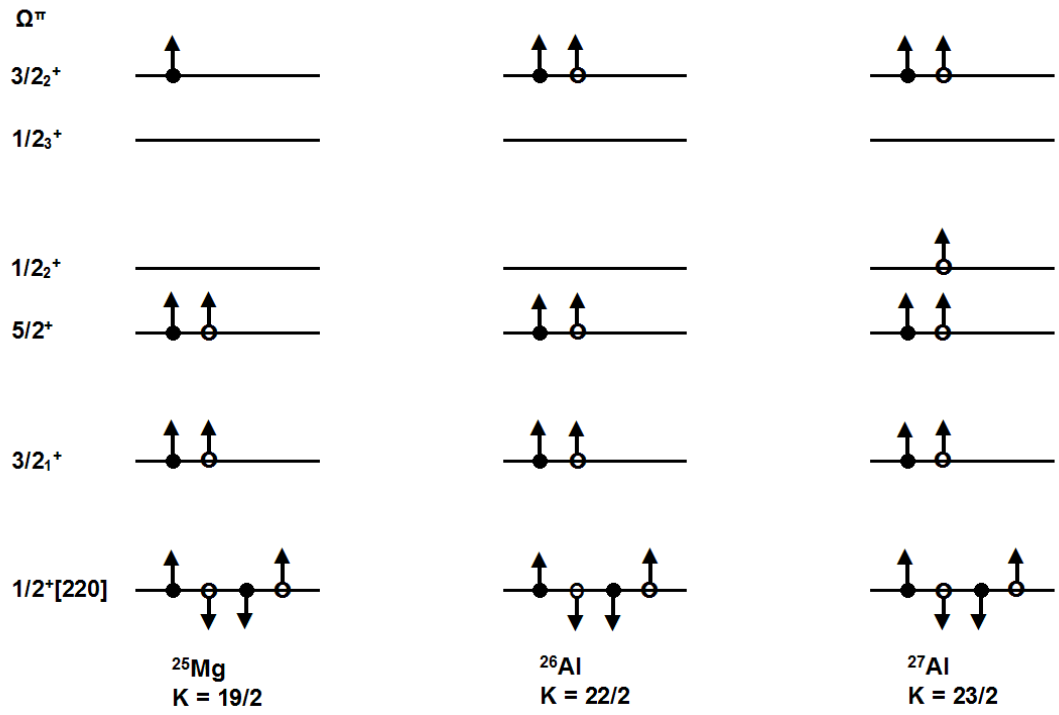

The expectation is born out by by experiment in the cases of ^{26}Al and ^{27}Al. In ^{25}Mg, however, the $J^{\pi} = 23/2^{+}$ yrast level (at $E_x = 20.6$ MeV) is too low to fit into a band with $K < 23/2$. Henceforth it must be a bandhead itself or spherical. A bandhead requires breaking of the ^{20}Ne core at the expense of deformation.

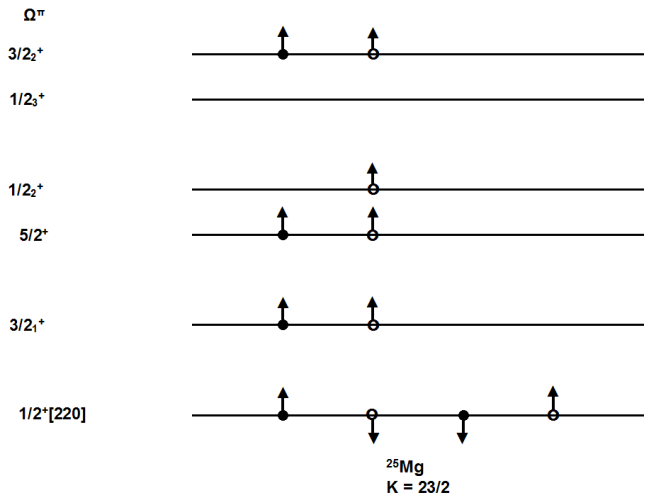

The calculated deformation parameter $\varepsilon = 0.11$ in Table 9 implies near sphericity. Sphericity can also be assumed for the levels of maximum spin in all three nuclei of Table 9. The quoted dimensionality d of the shell model basis states in Table 9 is just too small to generate substantial quadrupole moments.

9. Does hexadecupole deformation play a role in ^{28}Si?

Our analysis of ^{28}Si (Fig. 23) has revealed the existence of six $K^{\pi} = 4^{+}$ rotational bands in a narrow, 2 MeV, energy interval with bandheads at 10311, 12550, 11196, 11241, 12324 and 12474 KeV. The first two bands have prolate deformations, the others oblate ones. We could not believe in the existence at first but there are $J^{\pi} = 5^{+}$ levels at the proper distance and no $J^{\pi} = 3^{+}$ levels below. The Nilsson model wave functions must behave under rotation as $(Y_4^4 + Y_4^{-4}) = \sin^4\vartheta \cos 4\varphi$.

If the nuclear radius = $r_0 (\sum a_{l,m} Y_l^m)$ contains the same term we have a mechanism to bring $K^{\pi} = 4^{+}$ bands down. Equal curvature of intrinsic wave function and nuclear shape reduces kinetic energy. If we have an axially symmetric deformation as the basis

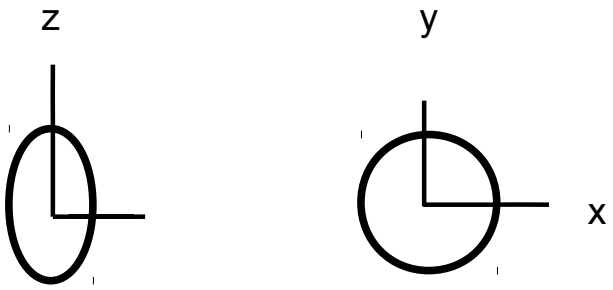

and add an $\sin^4\vartheta \cos 4\varphi$ term, the nuclear surface bulges out near z = 0

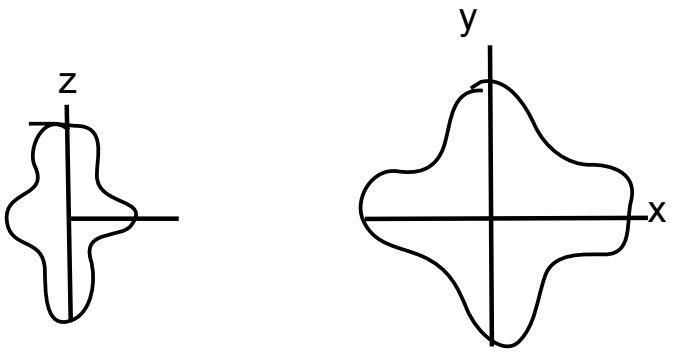

The questions then are:

Is the bulging out static or dynamic?

Where is the center of the hexadecupole strength whatever this means (theorists should care)?

In our wild imagination we see the afterglow of the generator coordinate method with seven α - particle like structures. The distance of the black α's from the x - y plane is decisive whether we have prolate or oblate shapes.

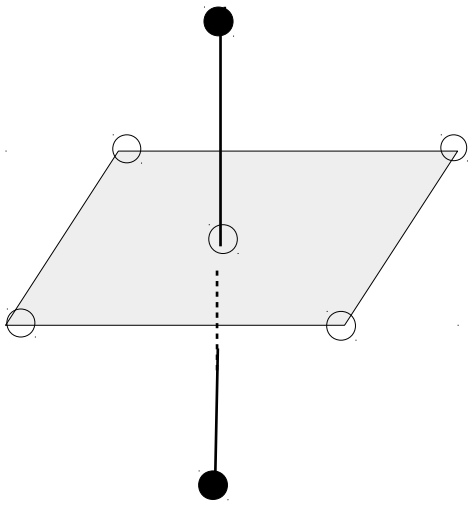

10. Prolate distortions in the Mg isotopes. Superseded by Part IV

The isotope ^{32}Mg should be characterized within the frame of the spherical shell model by a closed neutron shell (the N = 2 shell). The USD calculations, however, do not really reproduce the ground state energy. The explanation is given by 2 ħω excitations into the N = 3 major shell. This is possible at low excitation energy if the ground state of ^{30}Mg shows prolate distortion. In this case the last two neutrons of ^{32}Mg can go into the lowest, $\Omega^{\pi} = 1/2^{-}$, Nilsson orbit from the N = 3 shell yielding a deformed ground state. We repeat the level ordering from Fig. 1 for ε = 0.3 and show the occupation in ^{22}Mg. The $\Omega^{\pi} = 1/2_1^{+}$ orbit is strongly deformation driving and to a lesser extend the $\Omega^{\pi} = 3/2_1^{+}$ orbit. This results in ε = 0.38 as given in Table 7 for the identical situation in the mirror nucleus ^{22}Ne.

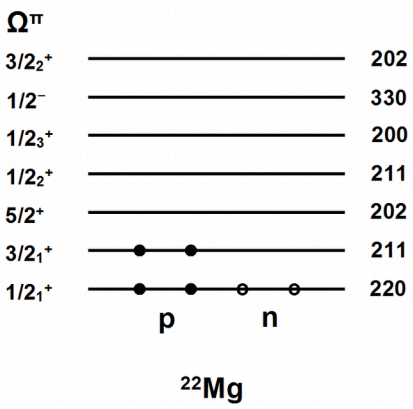

We can reach $^{24\text{-}30}$Mg from deformed ^{22}Mg by adding $K^{\pi} = 0^{+}$, T = 1 pairs of neutrons successively into orbits $\Omega^{\pi} = 3/2^{+}$, $5/2^{+}$, $1/2_2^{+}$, $1/2_3^{+}$. We have a safe indicator of whether this corresponds to reality. It is the one-proton excitation from the $\Omega^{\pi} = 3/2_1^{+}$ into the $\Omega^{\pi} = 5/2^{+}$ orbit which yields rotational bands with $K^{\pi} = 4^{+}$ and 1^{+}. The $K^{\pi} = 4^{+}$ band is unique and known already in ^{26}Mg, ^{24}Mg and ^{22}Ne (the mirror analogue of ^{22}Mg). In Fig. 50 we analyse the alleged rotational structure of ^{28}Mg and ^{30}Mg. If experimental levels are not available we use the highly precise (ΔE < 150 KeV) predictions of the USD-shell model. A $K^{\pi} = 0^{+}$ ground state band is present in both isotopes as is the characteristic $K^{\pi} = 4^{+}$ band. The $K^{\pi} = 0_2^{+}$ band, safe in ^{28}Mg and possibly in ^{30}Mg represents the two-proton excitation from the $\Omega^{\pi} = 3/2^{+}$ into the $\Omega^{\pi} = 5/2^{+}$ orbit, which is known in ^{26}Mg with a bandhead energy of 3589 KeV.

The bandhead excitation energies of the one-proton excitations in the Mg isotopes are

	$K^\pi = 4^+$	$K^\pi = 1^+$
^{22}Mg	5524 KeV	5329 KeV
^{26}Mg	4318 KeV	5691 KeV
^{28}Mg	5185 KeV	4561 KeV
^{30}Mg	5466 KeV	5242 KeV

In ^{24}Mg we do not have a pure proton excitation but a 50 : 50 mixture of proton and neutron excitation. The $K^\pi = 4^+$ and $K^\pi = 1^+$ bandheads occur at 8439 KeV and 7748 KeV.

Having verified ground state deformation in ^{30}Mg we can generate a deformed configuration in ^{32}Mg by placing a K^π, $T = 0^+$, 1 pair of neutrons into Nilsson orbit $\Omega^\pi = 1/2^-$ [330]. This orbit is not only energetically most favourable but leads to increased deformation (Fig. 1). We calculate a value $\varepsilon = 0.45$ of the deformation parameter which exceeds even $\varepsilon = 0.38$ obtained for the ground state band of ^{24}Mg (Table 7). The ground state and the 885 KeV, $J^\pi = 2^+$ state of ^{32}Mg are connected by a 15 W. u. E2 transition and are clearly members of a $K^\pi = 0^+$ rotational band. The excitation energy of the $J^\pi = 2^+$ states in the ground state bands of ^{32}Mg and ^{24}Mg, 885 KeV and 1368 KeV, point at equal deformation if a scaling law $\Theta \sim MR^2 \sim A^{5/3}$ is assumed.
The energy gain by deformation surmounts the energy gain by closure of the N = 2 shell for neutrons. We estimate the binding energy of the $K^\pi = 0^+$ bandhead in ^{32}Mg relative to the ^{24}Mg g.st. as − 53.8 ± 1.2 MeV. The uncertainty arises from missing values of the (less important) parameters a_{ik} and, respectively, c_{ik} in Table 4A. They were assumed to be − 700 KeV for a_{ik}

and + 700 KeV for c_{ik}. The USD-shell model generates a binding energy of − 50.14 KeV only. This would correspond to a first level of pure s-d character at E_x = 1.26 MeV. Possibly it has not been observed yet. Otherwise it would occur at $E_x \geq 2117$ KeV.

The strong deformation in the ^{32}Mg g.st. makes it possible to predict the Nilsson model configurations of levels in ^{31}Na and ^{31}Mg. In the case of ^{31}Na we must simply remove a $\Omega^\pi = 3/2^+$ [211] proton from ^{32}Mg. In the case of ^{31}Mg it is either a $\Omega^\pi = 1/2^-$ [330] or $\Omega^\pi = 1/2^+$ [200] neutron. This yields a $K^\pi = 3/2^+$ g.st. band in ^{31}Na and $K^\pi = 1/2^-$ and $K^\pi = 1/2^+$ bands in ^{31}Mg.

The $J^\pi = 3/2^-, 1/2^-, 7/2^-$ members of the first ^{31}Mg band (however not the $5/2^-$ member, which is lying higher due to the decoupling effect) can be reached by first-forbidden β-decay of ^{31}Na. The $J^\pi = 1/2^+, 3/2^+, 5/2^+$members of the second band can be reached by allowed β-decay. In addition there are the $J^\pi = 3/2^+$ and $5/2^+$ states of the pure s-d shell configuration which cannot be reached in β-decay (no two-particle transitions).

^{31}Mg has eight levels up to E_x = 1390 KeV followed by a 1 MeV gap. These eight levels are interpreted here with the aid of β-feeding and their γ-decay as follows:

Configuration	E_x[KeV]	J^π	log ft	J^π of final states in γ-decay
s-d	221	$3/2^+$	>6	$1/2^+$, $3/2^-$
	1029	$5/2^+$	>6	$3/2^+$
$K^\pi = 1/2^-$	51	$3/2^-$	5.3	$3/2^+$
	673	$1/2^-$	5.5	$1/2^+$, $3/2^-$, $3/2^+$
	945	$7/2^-$	6.2	$3/2^-$
$K^\pi = 1/2^+$	0	$1/2^+$	4.9	
	461	$3/2^+$		$3/2^+$
	1390	$5/2^+$		$3/2^+$

Please note:

The β-decay to the 945 KeV level is of the unique first-forbidden type and the subsequent γ-decay is an inband E2 decay.

The near degeneracy of three configurations is reproduced by theory. The binding energy of the lowest lying level relative to ^{24}Mg g.st. is

– 45.64 MeV for the s-d configuration according to USD

– 46.85 ± 1 MeV for the $K^{\pi} = 1/2^{+}$ band

– 45.5 ± 1 MeV for the $K^{\pi} = 1/2^{-}$ band

The experimental binding energy of the E_x = 221 KeV state is – 45.743 MeV in excellent agreement with the USD prediction.

11. Oblate deformation in A = 34 - 36
a detour to the upper s-d shell

Shell model calculations within the SU3 model are able to reproduce the deformed intrinsic states of nuclei at the beginning of the s-d shell. These are based on particle configurations and have prolate distortion. In the pure SU3 model without spin - orbit coupling each prolate particle configuration should be accompanied by an oblate hole configuration in the upper part of the s-d shell. Thus the rotational bands of ^{20}Ne, ^{21}Ne, ^{22}Ne, ^{22}Na should have partners of equal K^{π} in ^{36}Ar, ^{35}Cl, ^{34}S, ^{34}Cl. In ^{28}Si degeneracy of a $K^{\pi} = 0^{+}$ particle and a $K^{\pi} = 0^{+}$ hole band are predicted. The bandheads occur at 6691 KeV and 0 KeV. The large energy splitting is attributed to the spin-orbit coupling which is an essential ingredient also in the Nilsson model. Nevertheless some features of the SU3 model remain. The first two orbits with principal quantum number N = 2 have, for prolate deformation, $\Omega^{\pi} = 1/2^{+}$ and $3/2^{+}$. The same quantum numbers are “carried” by the two uppermost orbits for oblate deformation.

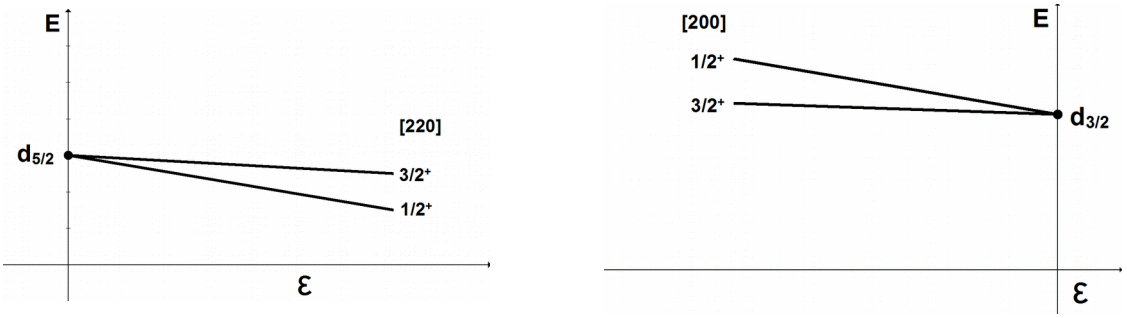

Thus starting from spherical ^{16}O we obtain prolate ^{20}Ne by adding four nucleons in the deformation driving $\Omega^{\pi} = 1/2^{+}[220]$ orbit. By the same token starting from spherical ^{40}Ca we obtain oblate ^{36}Ar by removing four particles from the sphericity driving $\Omega^{\pi} = 1/2^{+}[200]$ orbit. Thus a system of oblate hole bands can be constructed as follows.

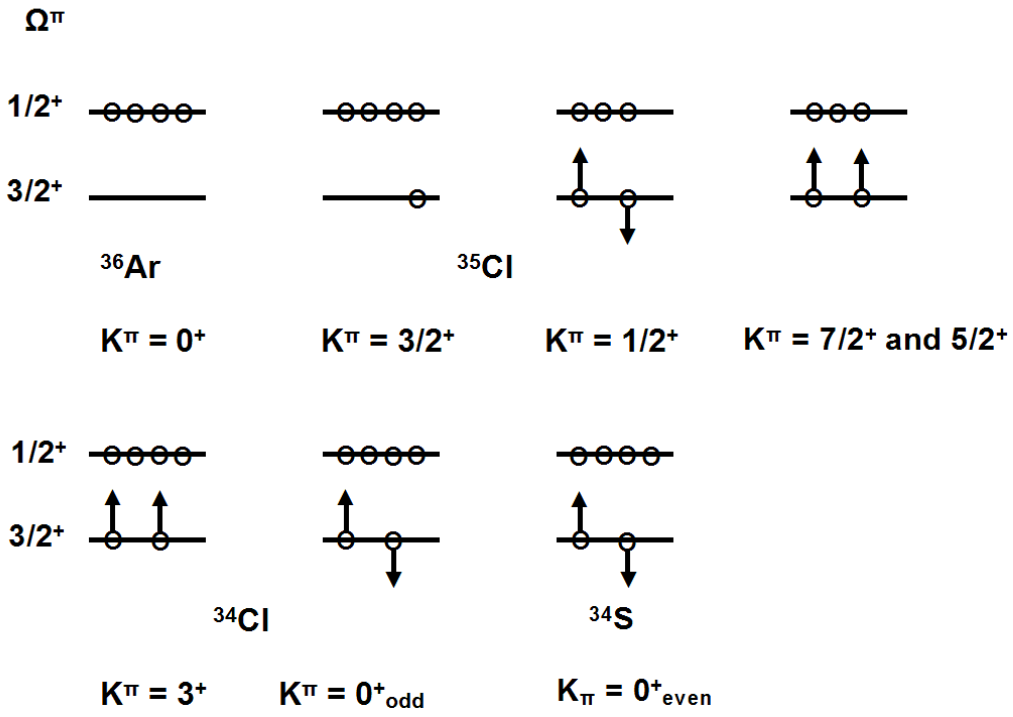

All constructed bands are present in Figs. 51, 52 (p. 164, p. 165) though the $K^{\pi} = 1/2^{+}$ band of ^{35}Cl cannot be called well developed. In ^{33}S and ^{32}S there is no evidence of rotational structure, probably because we have in ^{32}S g.st. closure of the $s_{1/2}$ subshell for ε = 0. The present analysis became feasible after identification of the proper $J^{\pi} = 6^{+}$ members of the ^{36}Ar and ^{34}S ground state bands (There are deeper lying intruders from the N = 3 shell). Helpful is also the achieved safety of the ^{35}Cl level scheme. The oblate deformation in the ground states of ^{34}S and ^{36}Ar can be enhanced by adding another nucleon in the $\Omega^{\pi} = 7/2^{-}$ orbit from the N = 3 shell which favours oblate deformations. The predictable $K^{\pi} = 7/2^{-}$ bands of ^{35}Cl and ^{37}Ar can be traced in Fig. 53 (p. 88) and even in ^{33}S this band seems to be present. In the cases of ^{36}Ar and ^{34}S the promotion of a single nucleon from a Nilsson orbit with N = 2 (the $\Omega^{\pi} = 1/2$ or $3/2^{+}$ orbits) into the $\Omega^{\pi} = 7/2^{-}$ orbit can equally lead to rotational bands of oblate type (Figs. 54, 55, p. 88, 89).

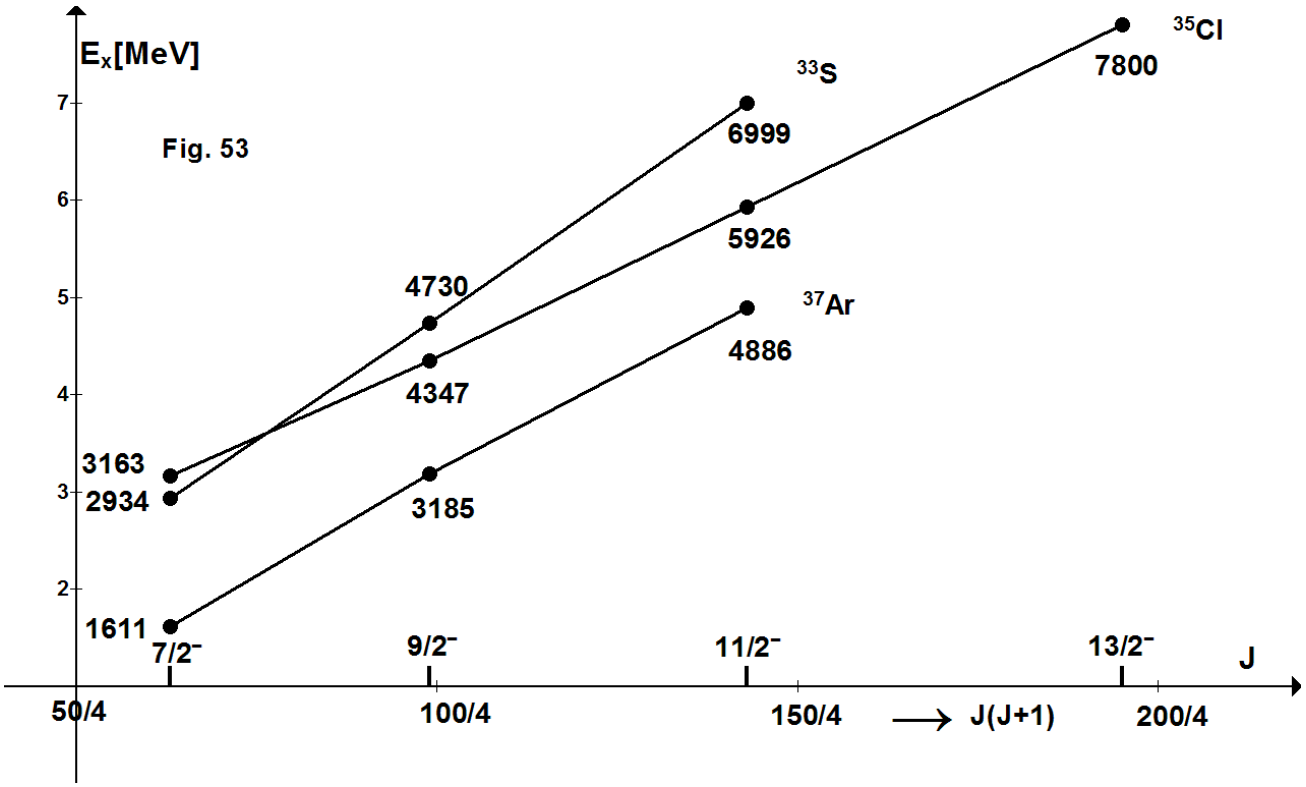
E_x[MeV]
Fig. 53
^{35}Cl
^{33}S
^{37}Ar
7800
6999
5926
4886
4730
4347
3185
3163
2934
1611
7/2⁻
9/2⁻
11/2⁻
13/2⁻
J
50/4
100/4
150/4
J(J+1)
200/4

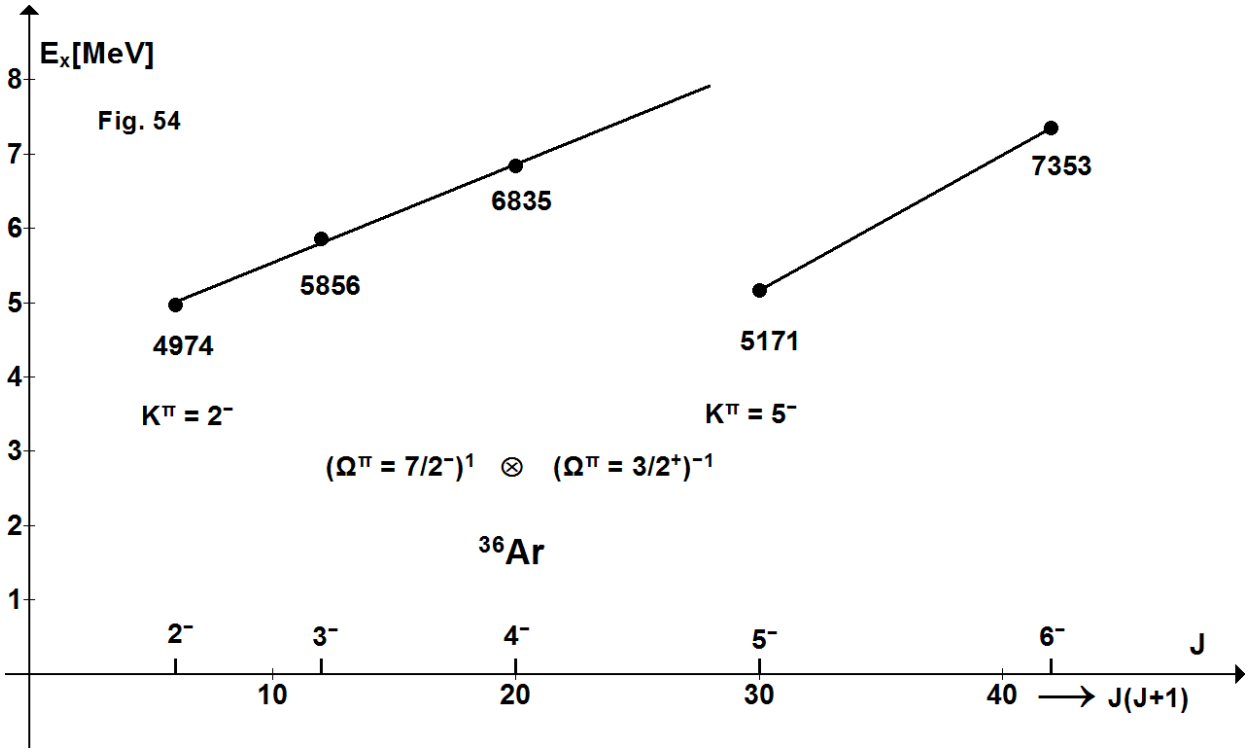
E_x[MeV]
Fig. 54
7353
6835
5856
4974
5171
$K^\pi = 2^-$
$K^\pi = 5^-$
$(\Omega^\pi = 7/2^-)^1 \otimes (\Omega^\pi = 3/2^+)^{-1}$
^{36}Ar
2⁻
3⁻
4⁻
5⁻
6⁻
J
10
20
30
40
J(J+1)

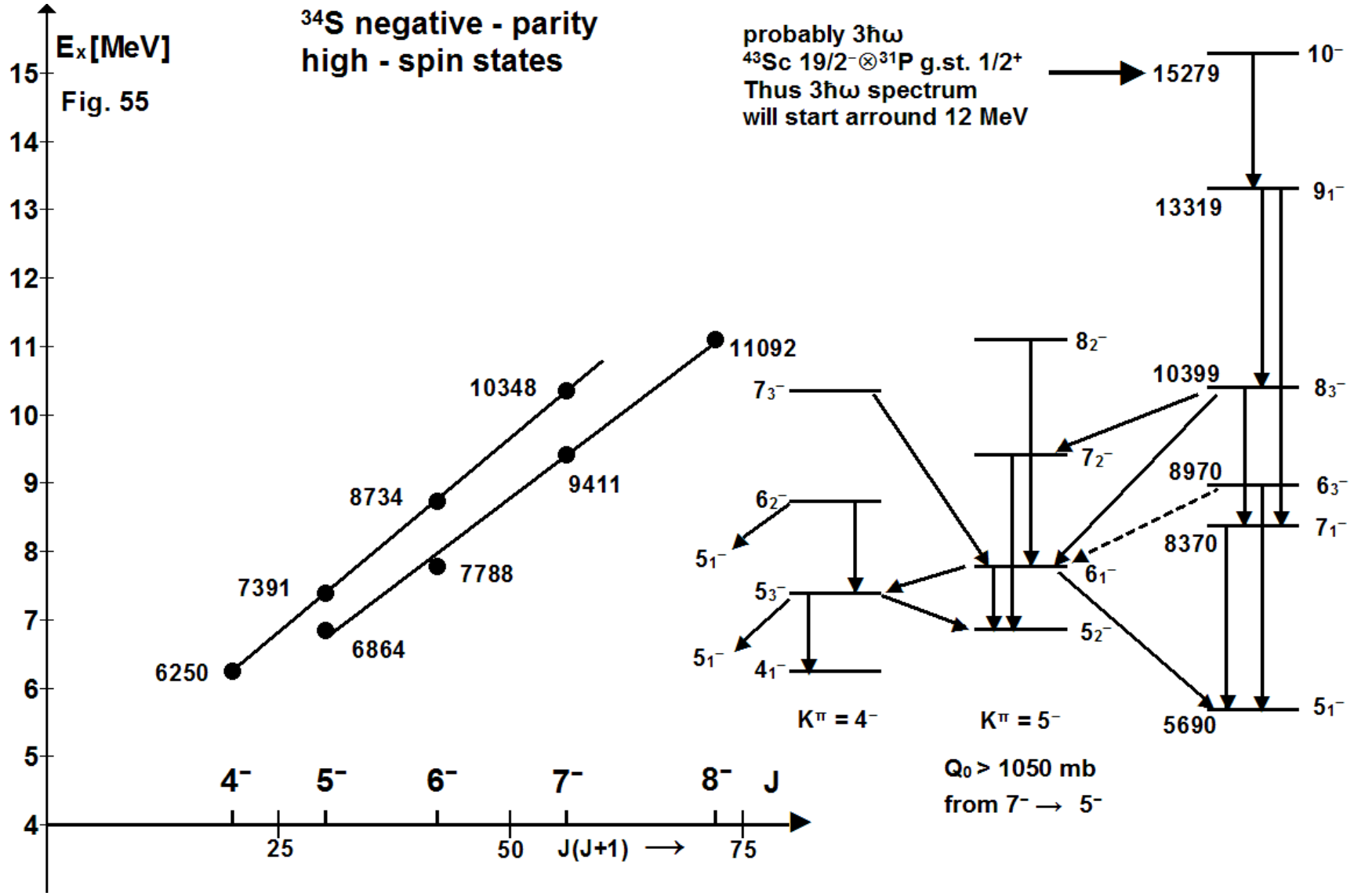
E_x [MeV]
Fig. 55
^{34}S negative - parity
high - spin states
probably 3ħω
^{43}Sc 19/2$^-$⊗^{31}P g.st. 1/2$^+$
Thus 3ħω spectrum
will start arround 12 MeV
15279
10$^-$
13319
9$_1^-$
10399
8$_3^-$
8970
6$_3^-$
8370
7$_1^-$
5690
5$_1^-$
11092
10348
8734
7391
6250
9411
7788
6864
7$_3^-$
8$_2^-$
7$_2^-$
6$_2^-$
6$_1^-$
5$_3^-$
5$_2^-$
5$_1^-$
4$_1^-$
5$_1^-$
Kπ = 4$^-$
Kπ = 5$^-$
Q_0 > 1050 mb
from 7$^-$ → 5$^-$
4$^-$ 5$^-$ 6$^-$ 7$^-$ 8$^-$ J
25 50 J(J+1) → 75
15 14 13 12 11 10 9 8 7 6 5 4

12.Tables

Table 1: **Neutron single-particle states and their binding energies**[a)]

State				Binding energy[KeV]			Corrections applied [KeV][b)]				
Nuclide	$2\Omega^{\pi}$	[N n_z Λ]	Ex[KeV]	exp[a)]	corrected	relative					
^{17}O	1_{p}^{-}	101	3055	−7137	−5766	0	−100	+340	n_z	+574	+557
	3_1^{+}	211	5085	−5107	−4944	822	−300			−94	+557
	1_2^{+}	211	8342	−1850	−1950	3816	−100				
^{21}Ne	3_1^{+}	211	0	−6761	−7061	0	−300				
	1_2^{+}	211	2794	−3967	−4067	2994	−100				
	5_1^{+}	202	3735	−3026	−3886	3175	−500		−360		
	1_f^{-}	330	5690	−1071	−1515	5546	−60	−384			
	1_3^{+}	200	5993	−768	−868	6193	−100				
^{25}Mg	5_1^{+}	202	0	−7331	−7831	0	−500				
	1_2^{+}	211	585	−6746	−6826	1005	−80				
	1_3^{+}	200	2564	−4767	−4847	2984	−80				
	1_f^{-}	330	4277	−3054	−3498	4333	−80	−384			
	3_2^{+}	202	6362	−969	1269	6568	−300				
^{29}Si	5_1^{+}	202	6522	−8642	−8942	0	−300				
	oblate										
	1^{+}	211	0	−8474	−8294	0					
	3^{+}	202	1273	−7201	−6744	1550					
	7^{-}	303	3624	−4850	−5375	2919					
	3^{-}		4935	−3539	−3659	4635					

a) relative to, respectively, ^{16}O(6049), ^{20}Ne g.st., ^{24}Mg g.st., ^{28}Si(6691), ^{28}Si g.st.

b) The corrections consider, from left to right,

zero point precession

decoupling effect

rotation – particle coupling

Mixing with spherical state in ^{17}O and ^{16}O

Table 2: **Neutron single-hole states and their binding energies**

State				Binding energy [KeV]
Nuclide	$2\Omega_v^{\pi}$	[N n_z Λ]	E_x[KeV]	exp. corrected
^{15}O	1_1^+	220	5186	−15637
^{19}Ne	1_1^+	220	0	−17148
	1_p^-	101	275	−17403
	3_p^-	101	(4556)[c)]	−21124
^{23}Mg	3_1^+	211	0	−16231
	1_p^-	101	2771	−19562
	1_1^+	220	4354	−21145
	3_p^-	101	5964	−22255
^{27}Si	1_2^+	211	3540	−13952[a)]
		oblate		
	1_1^+	211	781	−18175
	3_1^+	211	957	−17865
	1_p^-	101	4138	−20729
		ambigous		
	5_1^+	202	0	−16336[b)]
				−11356
				−9645

a) Relative to the 6690 KeV, 0_3^+ of ^{28}Si

b) Relative to, respectively, the 0, 4980, 6690 KeV states of ^{28}Si

c) Excitation energy from the mirror nucleus adopted

Table 3:

Parameters of the residual interaction

between particles in the same Nilsson orbit

Orbit		Parameters [KeV][a)]			
Ω^{π}	[N n_z Λ]	A	B	C	S = 3A + B + 2C
$1/2^-$	101	−2538	−3328	−5788	−23134[b)]
$3/2^+$	211	−2626	−2900	−3883	−18364[b)]
$5/2^+$	202	−2625	−2055	−4153	−18299[b)]
$1/2^+$	211	−1479	−2813	−3702	−14654[b)]
$1/2^+$	200	−2516	−3665	−4080	−19373[c)]
$1/2^-$	330	−3863	−3440	−6053	−27135[c)]
oblate					
$1/2^+$	211	−2537	−2865	−3394	−17264[c)]
$3/2^+$	202	−1846	−1729	−4015	−15297[c)]

a) A, B, C are the pairing energies for K, T = 0, 1: 0, 0; 2Ω, 0 couplings, respectively

b) obtained independently without use of A, B, C

c) calculated from A, B, C

Table 4A:

Parameters of the residual interaction

between particles in different Nilsson orbits (prolate deformation)

Orbit i		Orbit k		Parameters [KeV]			
Ω^{π}	[N n_z Λ]	Ω^{π}	[N n_z Λ]	a_{ik}	b_{ik}	c_{ik}	d_{ik}
$1/2^+$	220	$1/2^-$	101	−377	219	980	92
		$3/2^+$	211	−999	−676	−160	−82
		$5/2^+$	202	380	0	575	225
		$1/2^+$	211	−528	878	378	367
$1/2^-$	101	$3/2^+$	211	−539	−442	1151	−507
		$5/2^+$	202		170	1375	−400
$3/2^+$	211	$5/2^+$	202	−666	−672	748	−707
		$1/2^+$	211	−695	−512	1182	−441
		$1/2^+$	200	−994	−302	331	−16
		$1/2^-$	330	−495	−200	768	400
$5/2^+$	202	$1/2^+$	211	−423	119	647	296
		$1/2^+$	200		1011	824	375
		$1/2^-$	330		−1862	666	−348
		$3/2^+$	202		−739	295	−272
$1/2^+$	211	$1/2^+$	200		−541	749	239

Level ordering, qualitative

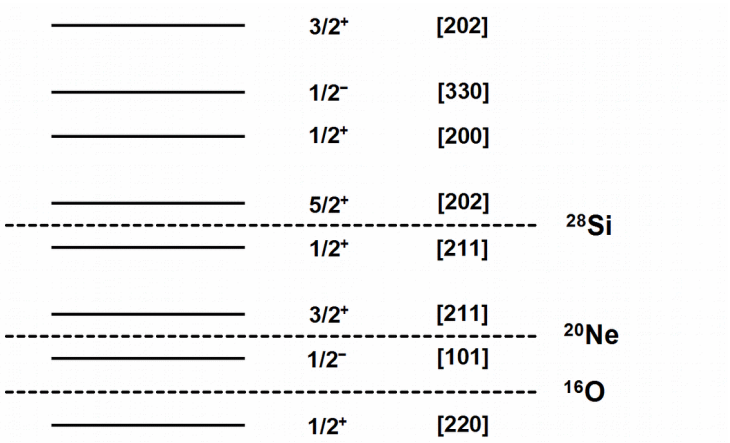

Table 4B:

Parameters of the residual interaction

between particles in different Nilsson orbits (oblate deformation)

Orbit i		Orbit k		Parameters [KeV]			
Ω^{π}	[N n_z Λ]	Ω^{π}	[N n_z Λ]	a_{ik}	b_{ik}	c_{ik}	d_{ik}
$1/2^+$	211	$1/2^+$	220		284	516	−439
		$3/2^+$	202		−249	502	146
		$7/2^-$	303		465	886	580
$3/2^+$	211	$1/2^+$	220		−659	529	38
		$3/2^+$	202		−222	344	−415
		$7/2^-$	303		−410	601	−283
$1/2^+$	220	$3/2^+$	202		−246	367	−3
		$7/2^-$	303		525	518	498
$3/2^+$	202	$7/2^-$	303		32	725	−44

Level ordering, qualitative

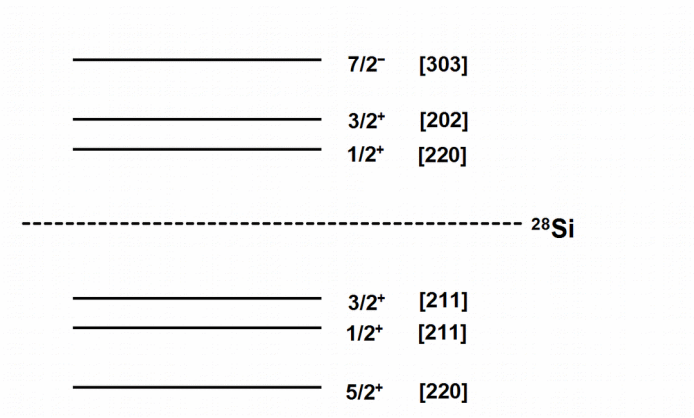

13. Caption to Tables 5, 6

A configuration with two particles/holes in different orbits gives rise to four bands with $K = \Omega_1 \pm \Omega_2$, $T = 0, 1$.

Let E_B stand for the binding energies of bandheads after removal of all influences of rotational motion (zero point precession, decoupling effect, strictly speaking but not always considered the corriolis coupling) and for $K = 0$ the J = even/odd splitting by means of

$$E_B = 1/2(E_B(0^+) + E_B(1^+) - 2\,\hbar^2/2\Theta)$$

The centroid of bandheads is defined by

$$E_B^C = 1/2[3/4\,E_B(\Omega_1 + \Omega_2, T = 1) + 1/4\,E_B(\Omega_1 + \Omega_2, T = 0) + 3/4\,E_B(\Omega_1 - \Omega_2, T = 1) + 1/4\,E_B(\Omega_1 - \Omega_2, T = 0)]$$

It is theoretically related to the binding energies of single-particle or single-hole states as given in the following examples

p - p state in ^{22}Na

$$E_B^C(^{22}\mathrm{Na}) = E_B(^{21}\mathrm{Na}, \Omega_1) + E_B(^{21}\mathrm{Ne}, \Omega_2) + a_{12}$$

h - h state in ^{22}Na

$$E_B^C(^{22}\mathrm{Na}) = E_B(^{23}\mathrm{Na}, \Omega_1) + E_B(^{19}\mathrm{Ne}, \Omega_2) - 3\,a_{12}$$

p - h state in ^{24}Mg

$$E_B(^{24}\mathrm{Mg}) = E_B(^{25}\mathrm{Mg}, \Omega_1) + E_B(^{23}\mathrm{Na}, \Omega_2) - a_{12}$$

The quantity $4a_{ik}$ is the interaction of a particle in orbit i with a fully occupied orbit k and corresponds to the monopole term in the spherical shell model.

Table 5: **Centroid energies of 1p-1h configurations in A = 4n nuclides**

Nuclide	Hole orbit		Particle orbit		Centroid energy [MeV]	
	Ω^{π}	$[Nn_z\Lambda]$	Ω^{π}	$[Nn_z\Lambda]$	predicted	observed
^{20}Ne	$1/2^+$	220	$3/2^+$	211	11.1	10.627
			$1/2^+$	211	13.5[a)]	13.495
			$5/2^+$	202	12.6	11.94
	$1/2^-$	101	$3/2^+$	211	10.7	9.984
			$5/2^+$	211	14.2[a)]	≥12.463
^{24}Mg	$3/2^+$	211	$1/2^+$	211	10.1	9.276
			$5/2^+$	202	9.4	9.299
			$1/2^+$	200	12.4	12.48
			$1/2^-$	330	13.2	~12.0
	$1/2^+$	220	$5/2^+$	202	12.5	11.312
	$1/2^-$	101	$5/2^+$	202	12.2[a)]	12.27
^{28}Si	$1/2^+$	211	$5/2^+$	202	12.3	11.859
^{28}Si oblate	$3/2^+$	211	$1/2^+$	220	10.7[a)]	9.189
			$3/2^+$	202	12.2[a)]	10.38
			$7/2^-$	303	13.6[a)]	11.66
	$1/2^+$	211	$1/2^+$	220	11.0[a)]	11.9
			$3/2^+$	202	12.5[a)]	12.17
			$7/2^-$	303	13.9[a)]	11.291

a) a_{ik} value unknown, assumed as − 700 KeV

Table 6: **Centroid energies of configurations with 2 particles/holes in different Nilsson orbits**

Nuclide	Particle/hole orbits				Centroid energy [MeV]	
	Ω_1^{π}	$[Nn_z\Lambda]_1$	Ω_2^{π}	$[Nn_z\Lambda]_2$	predicted	observed
^{18}F	$(1/2^+)^{-1}$	220	$(1/2^-)^{-1}$	101	6.3	6.1
^{22}Na	$3/2^+$	211	$1/2^+$	211	5.6	5.548
			$5/2^+$	202	6.1	5.68
			$1/2^-$	330	8.8	(8.4)
			$1/2^+$	200	9.1	8.78
	$5/2^+$	202	$1/2^+$	211	8.5	9.23
	$(3/2^+)^{-1}$	202	$(1/2^-)^{-1}$	220	6.5	5.56
			$(1/2^+)^{-1}$	220	7.2	7.070
			$(3/2^-)^{-1}$	101	~9.0[a)]	>8.2
^{26}Al	$5/2^+$	202	$1/2^+$	211	2.9	2.528
			$1/2^+$	200	5.1[a)]	5.787
			$1/2^-$	330	6.0[a)]	
			$3/2^+$	202	8.7[a),b)]	8.030
	$1/2^+$	211	$1/2^+$	200	6.1[a)]	5.420
			$1/2^-$	330	7.5[a)]	≥7.22
	$(5/2^+)^{-1}$	202	$(3/2^+)^{-1}$	211	4.9[a)]	5.085
			$(1/2^+)^{-1}$	220		7.13[c)]
^{30}P oblate	$1/2^+$	220	$3/2^+$	202	4.1[a)]	3.705
			$7/2^-$	303	5.4[a)]	6.149
	$3/2^+$	202	$7/2^-$	303	7.0[a)]	6.184
	$(1/2^+)^{-1}$	220	$(3/2^+)^{-1}$	211	7.7[a)]	6.961

a) assuming a value a_{ik} = − 700 KeV

b) The Ω^{π} = $3/2^+$ [202] single-particle band of ^{25}Mg is assumed to start at 6362 KeV

c) used to determine a_{ik} as +380 KeV

14. Figure captions

1 The Nilsson orbits of A = 22 (Fortune et al.)
The single particle energies of ^{17}O, ^{21}Ne, ^{25}Mg, ^{29}Si (prolate) in Table 1 agree with $\delta \sim 0.6; 0.4; 0.3; > 0.3$, respectively.

2 The excited states of ^{16}O. The 1p-1h and 2p-2h excitations of the deformed ^{16}O configuration are given. The classification as a n ħω excitation of the spherical ground state is added. Together with the omitted 1 ħω states which have no collective character one obtains a complete accounting of the T = 0 levels up to and including the 11097 KeV state.

3 Rotational states in ^{17}O. The spherical single-particle states are given in addition, making the level scheme complete.

4 Same as Fig. 7 - 30. The spherical 2p states are omitted otherwise the level scheme is complete.

5 Same as Fig. 7 - 30, including however spherical states. The level scheme is thus complete.

7 - 30
Decomposition of the energy levels of lowest isospin in A = 20-30 nuclei into rotational (like) bands. Experimental levels are characterized by the numerical value of E_x. Levels which are predicted by shell-model calculations in the s-d basis space are given without the numerical E_x. Levels of s-d character, whether identified or predicted, carry the SM enumeration as a subscript in their J^π. The dots …. separate the region where all existing or predicted levels are considered, from the region where completeness of information is no longer guaranteed.

31 - 47

Bandhead energies and K^{π} values of rotational bands for a given mass number. Isospins are indicated if they deviate from the default value T = 0 or, respectively, 2T = 1. The notations of N. M. configurations is explained in the foregoing Table caption.

48 The region of prolate ground state deformation in the s-d shell between A = 18 - 26 is characterised here by the difference in excitation energy between the first deformed and the first spherical state.

49 Structure of the yrast lines in ^{25}Mg, ^{26}Al and ^{27}Al in terms of deformed states with increasing value of the projection quantum number K. The plot of E_x versus J(J+1) shows that the impression of a rotational band can be generated, called “rotation around the symmetry axis”.

50a, 50b

The rotational bands of ^{28}Mg and ^{30}Mg as they are suggested by the USD-shell model calculations, where ever possible experimental proof is given.

51- 52

Positive-parity rotational bands of oblate deformation in the upper half of the s-d shell (A = 34 - 36)

53 - 55

(p. 88, 89) Negative-parity rotational bands of oblate deformation in the upper half of the s-d shell (A = 33 - 37)

15. Figures

Fig.1

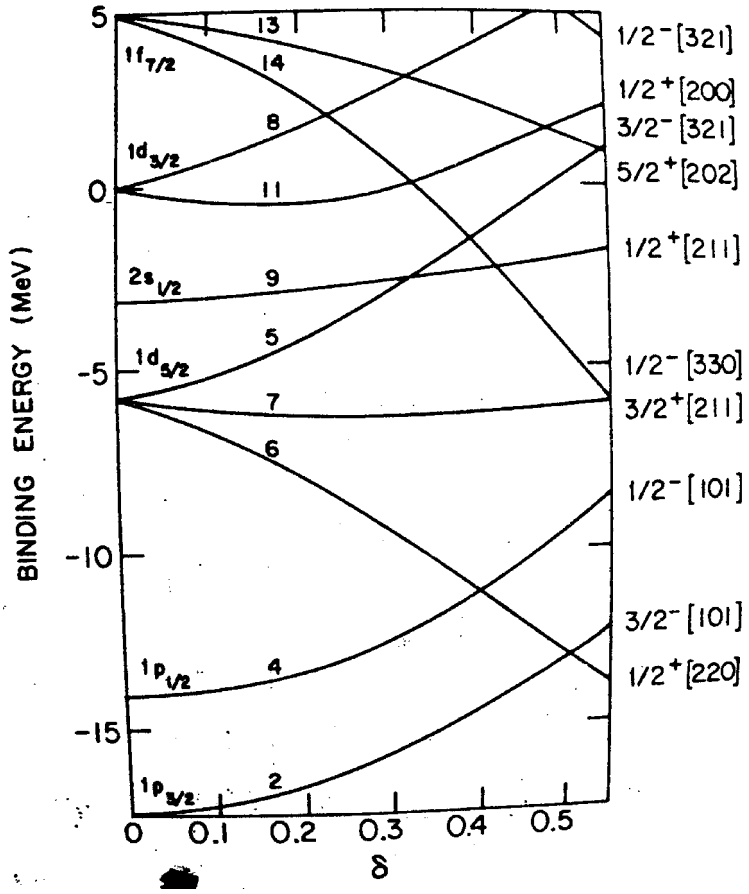

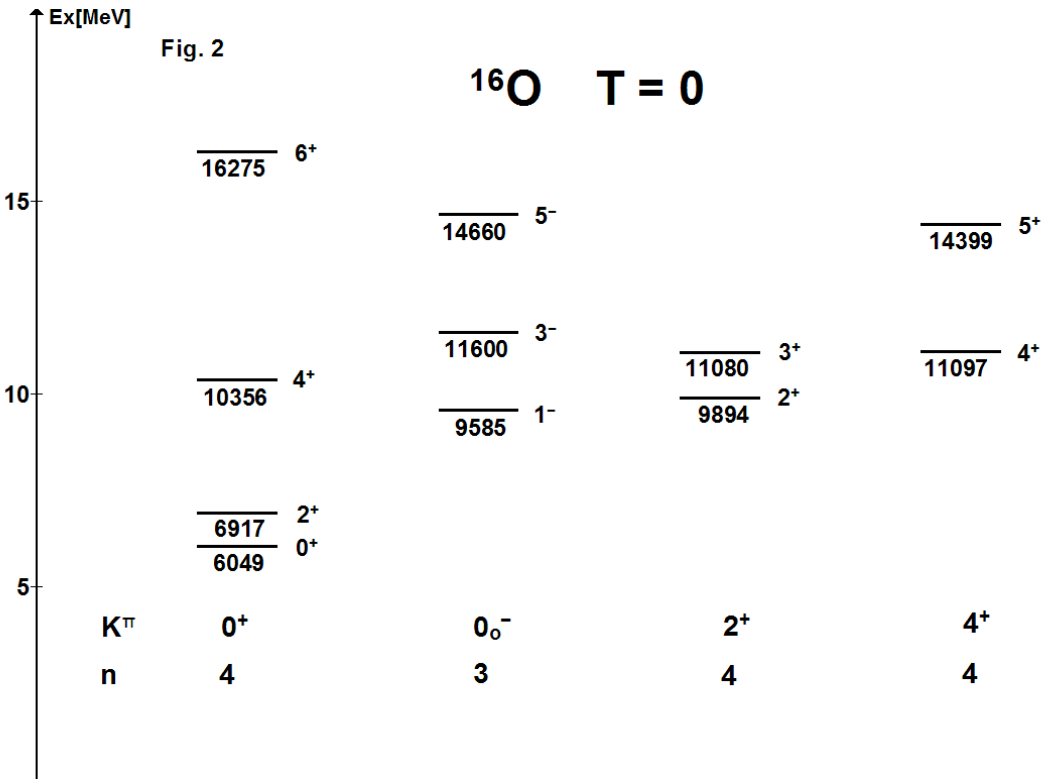
Ex[MeV]
Fig. 2
16O T = 0
15
10
5
16275
6+
14660
5−
14399
5+
11600
3−
11080
3+
11097
4+
10356
4+
9585
1−
9894
2+
6917
2+
6049
0+
Kπ
0+
0o−
2+
4+
n
4
3
4
4

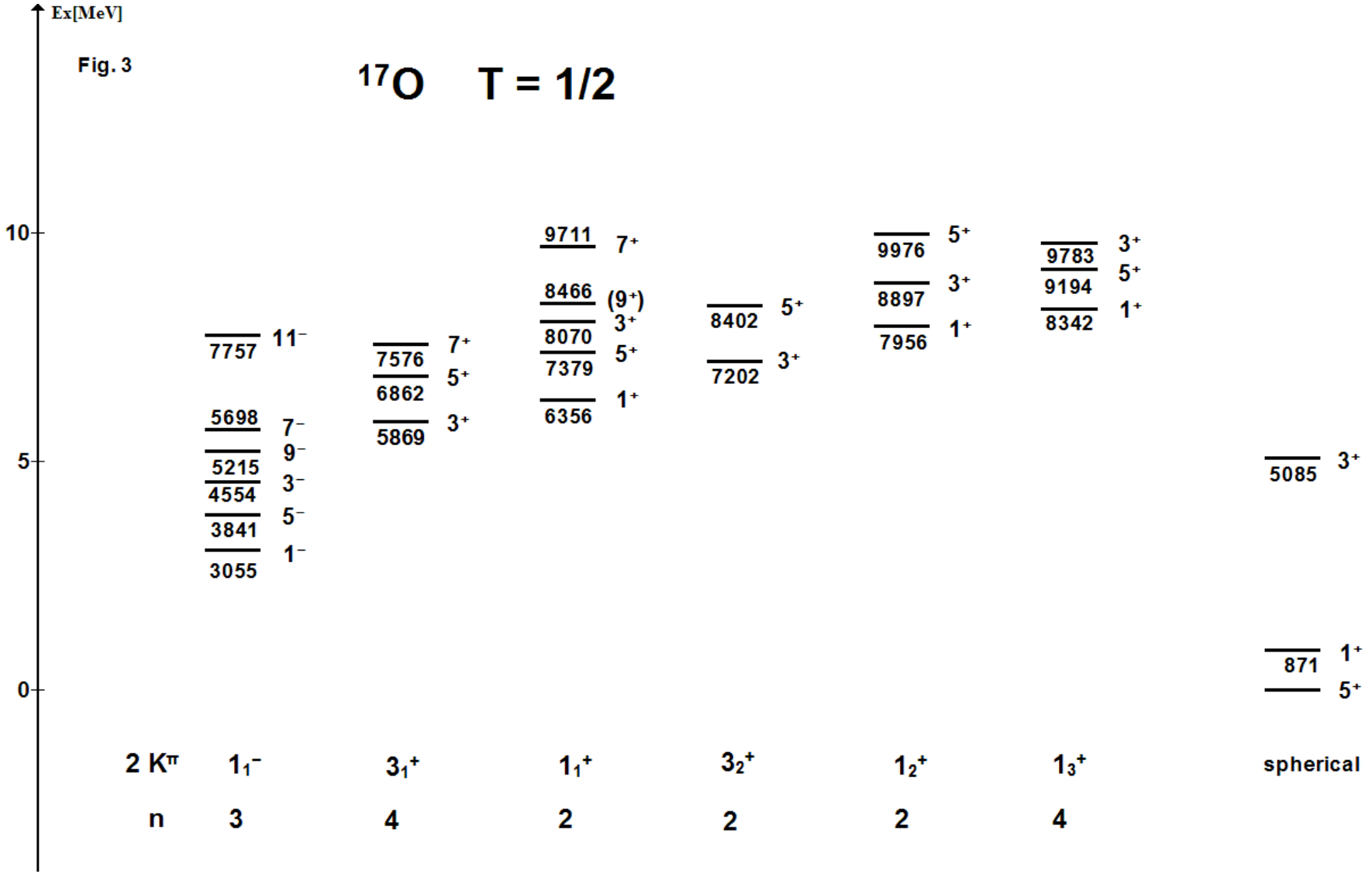
Ex[MeV]
Fig. 3
17O T = 1/2
10
5
0
11⁻ 7757
7⁻ 5698
9⁻
5215
3⁻ 4554
5⁻ 3841
1⁻ 3055
7⁺ 7576
5⁺ 6862
3⁺ 5869
9711 7⁺
8466 (9⁺)
3⁺ 8070
5⁺ 7379
1⁺ 6356
5⁺ 8402
3⁺ 7202
5⁺ 9976
3⁺ 8897
1⁺ 7956
3⁺ 9783
5⁺ 9194
1⁺ 8342
3⁺ 5085
1⁺ 871
5⁺
2 Kπ 1₁⁻ 3₁⁺ 1₁⁺ 3₂⁺ 1₂⁺ 1₃⁺ spherical
n 3 4 2 2 2 4

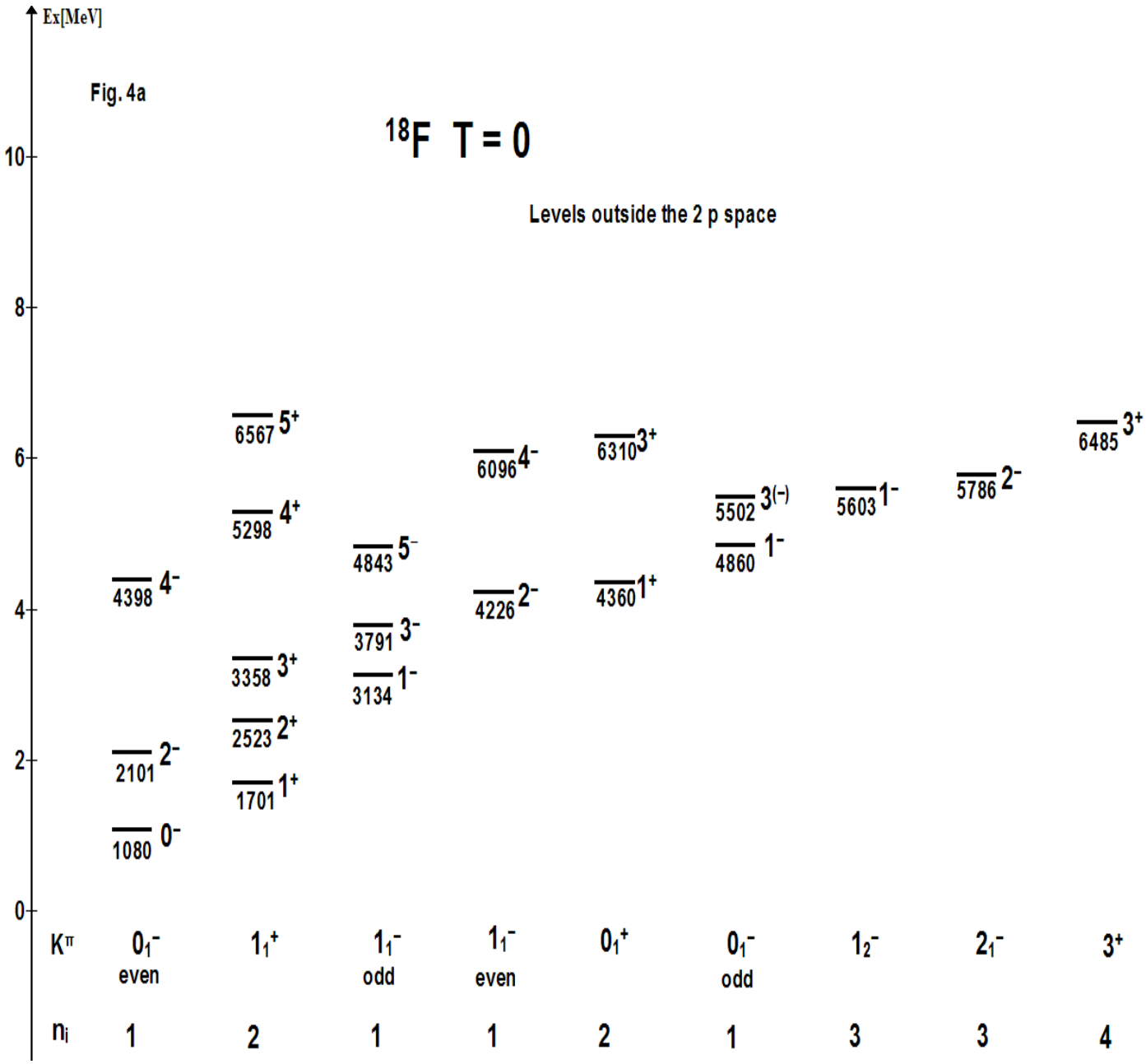
Ex[MeV]
Fig. 4a
^{18}F T = 0
Levels outside the 2 p space
10
8
6
4
2
0
6567 5+
5298 4+
4398 4-
3358 3+
2523 2+
2101 2-
1701 1+
1080 0-
4843 5-
3791 3-
3134 1-
6096 4-
6310 3+
4226 2-
4360 1+
5502 3(-)
4860 1-
5603 1-
5786 2-
6485 3+
Kπ
0$_1^-$ even
1$_1^+$
1$_1^-$ odd
1$_1^-$ even
0$_1^+$
0$_1^-$ odd
1$_2^-$
2$_1^-$
3+
ni
1
2
1
1
2
1
3
3
4

Fig. 4b

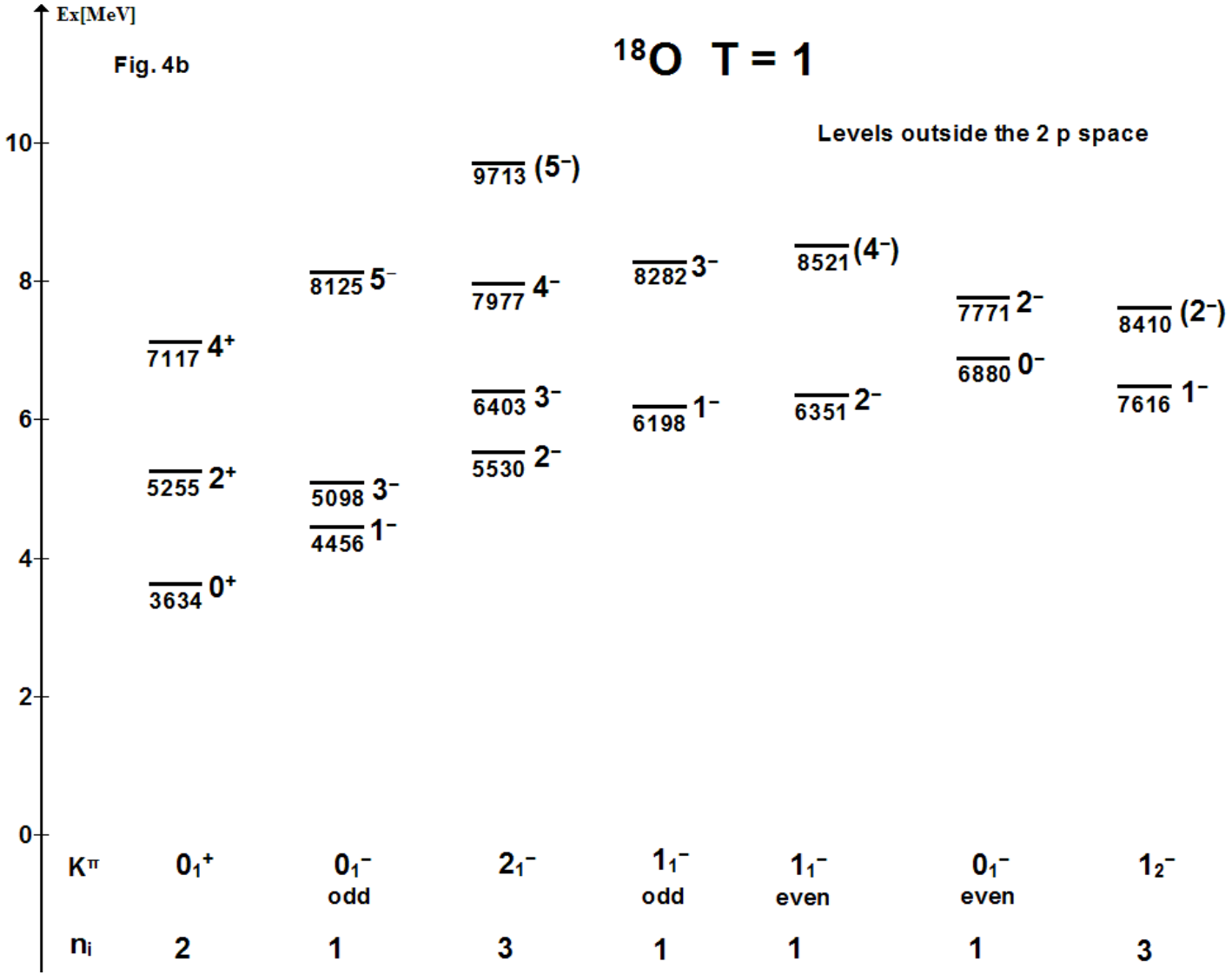
^{18}O T = 1
Levels outside the 2 p space
Ex[MeV]
10
8
6
4
2
0
9713 (5⁻)
8125 5⁻
7977 4⁻
8282 3⁻
8521 (4⁻)
7771 2⁻
8410 (2⁻)
7117 4⁺
6880 0⁻
6403 3⁻
6198 1⁻
6351 2⁻
7616 1⁻
5530 2⁻
5255 2⁺
5098 3⁻
4456 1⁻
3634 0⁺
Kᵖ
0₁⁺
0₁⁻ odd
2₁⁻
1₁⁻ odd
1₁⁻ even
0₁⁻ even
1₂⁻
nᵢ
2
1
3
1
1
1
3

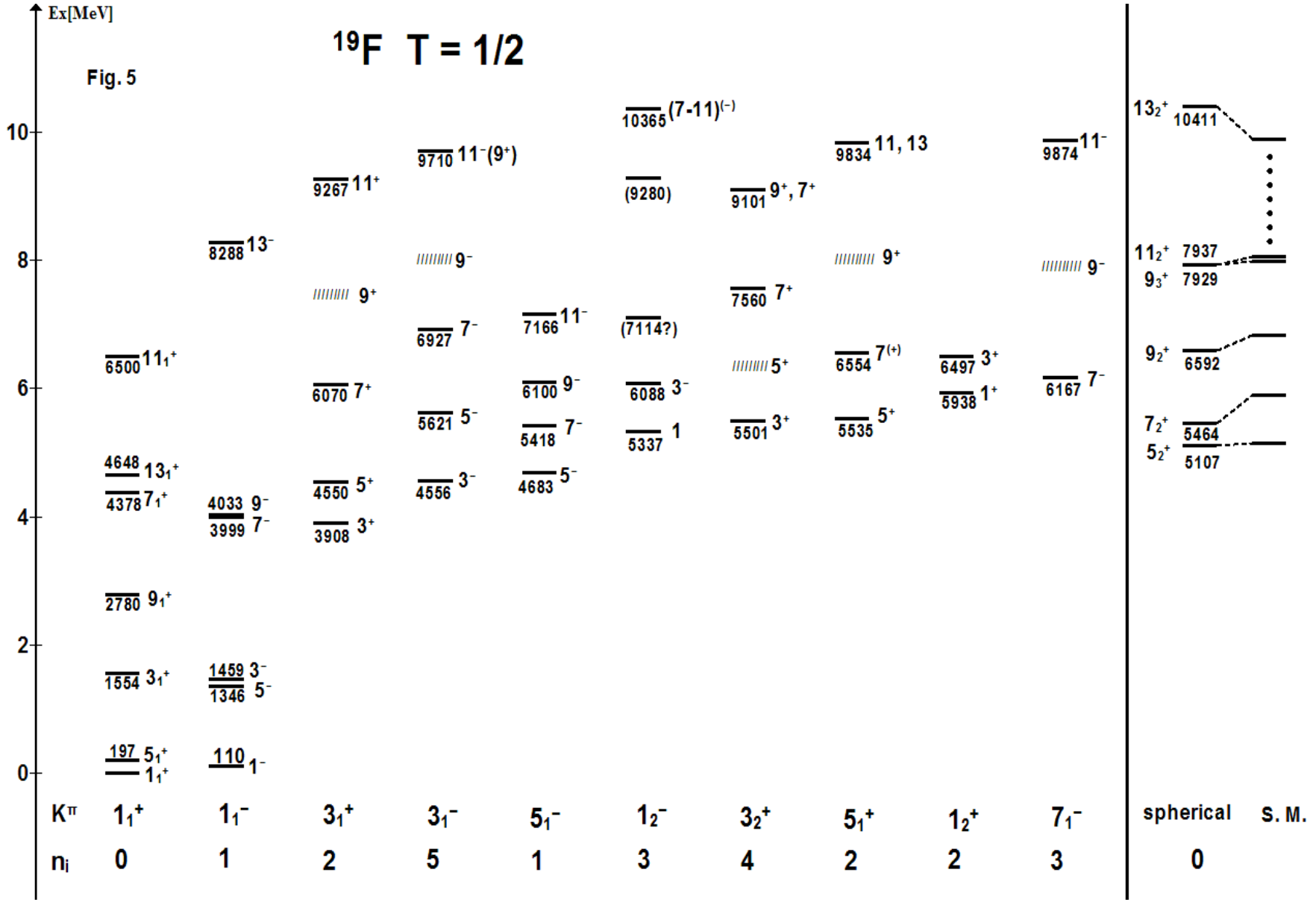
Ex[MeV]
^{19}F T = 1/2
Fig. 5
10
8
6
4
2
0
6500 11$_1^+$
4648 13$_1^+$
4378 7$_1^+$
2780 9$_1^+$
1554 3$_1^+$
197 5$_1^+$
1 1$_1^+$
8288 13$^-$
4033 9$^-$
3999 7$^-$
1459 3$^-$
1346 5$^-$
110 1$^-$
9267 11$^+$
9+
6070 7$^+$
4550 5$^+$
3908 3$^+$
9710 11$^-$(9$^+$)
9$^-$
6927 7$^-$
5621 5$^-$
4556 3$^-$
7166 11$^-$
6100 9$^-$
5418 7$^-$
4683 5$^-$
10365 (7-11)$^{(-)}$
(9280)
(7114?)
6088 3$^-$
5337 1
9101 9$^+$, 7$^+$
7560 7$^+$
5$^+$
5501 3$^+$
9834 11, 13
9+
6554 7$^{(+)}$
5535 5$^+$
6497 3$^+$
5938 1$^+$
9874 11$^-$
9$^-$
6167 7$^-$
K$^\pi$ 1$_1^+$ 1$_1^-$ 3$_1^+$ 3$_1^-$ 5$_1^-$ 1$_2^-$ 3$_2^+$ 5$_1^+$ 1$_2^+$ 7$_1^-$
n$_i$ 0 1 2 5 1 3 4 2 2 3
13$_2^+$ 10411
11$_2^+$ 7937
9$_3^+$ 7929
9$_2^+$ 6592
7$_2^+$ 5464
5$_2^+$ 5107
spherical S. M.
0

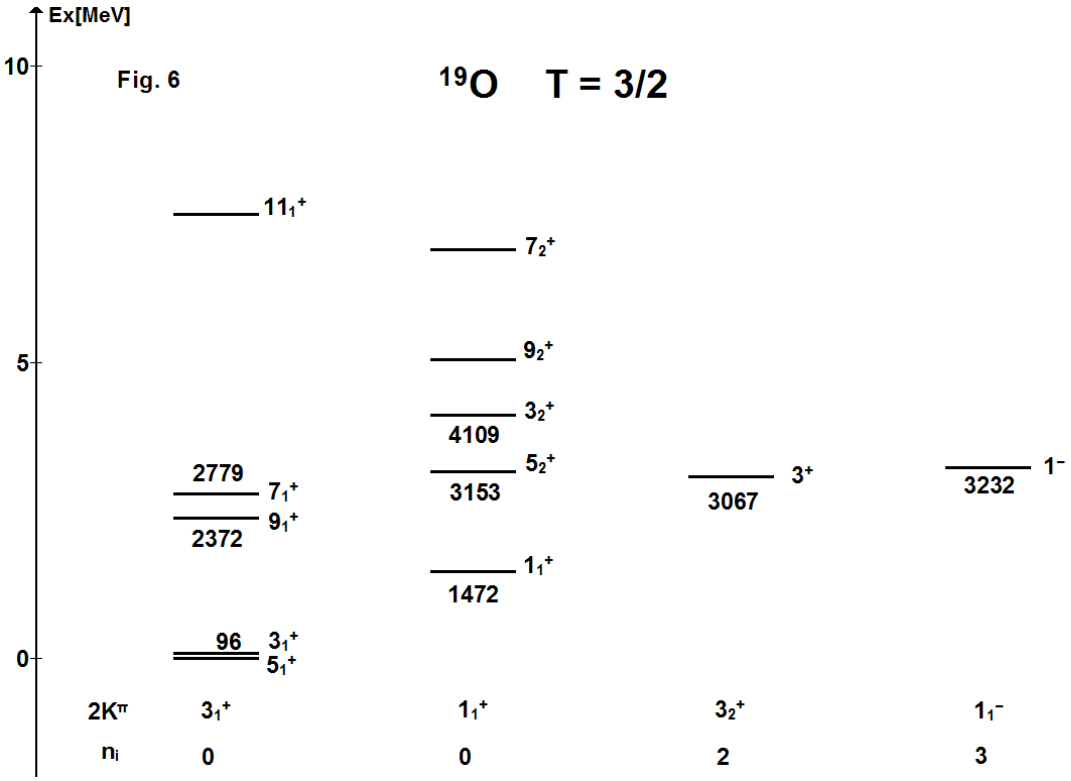
Ex[MeV]
10
5
0
Fig. 6
19O T = 3/2
11₁⁺
7₂⁺
9₂⁺
3₂⁺
4109
5₂⁺
3153
1₁⁺
1472
2779
7₁⁺
9₁⁺
2372
96
3₁⁺
5₁⁺
3⁺
3067
1⁻
3232
2Kπ
nᵢ
3₁⁺
0
1₁⁺
0
3₂⁺
2
1₁⁻
3

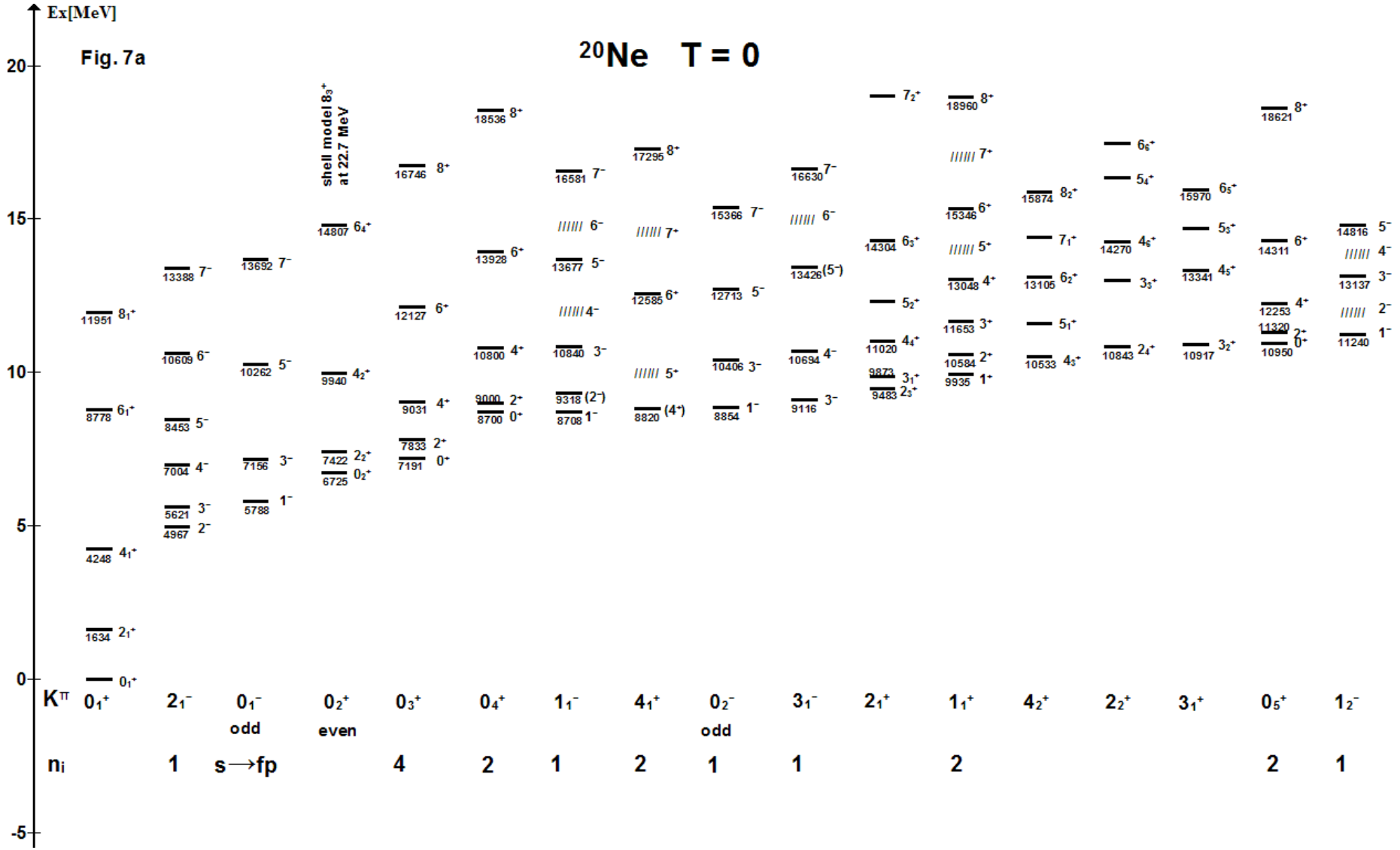
Ex[MeV]
Fig. 7a
20Ne T = 0
20
15
10
5
0
-5
shell model 8₃⁺ at 22.7 MeV
11951 8₁⁺
8778 6₁⁺
4248 4₁⁺
1634 2₁⁺
0 0₁⁺
13388 7⁻
10609 6⁻
8453 5⁻
7004 4⁻
5621 3⁻
4967 2⁻
13692 7⁻
10262 5⁻
7156 3⁻
5788 1⁻
14807 6₄⁺
9940 4₂⁺
7422 2₂⁺
6725 0₂⁺
16746 8⁺
12127 6⁺
9031 4⁺
7833 2⁺
7191 0⁺
18536 8⁺
13928 6⁺
10800 4⁺
9000 2⁺
8700 0⁺
16581 7⁻
13677 5⁻
10840 3⁻
9318 (2⁻)
8708 1⁻
17295 8⁺
12585 6⁺
8820 (4⁺)
15366 7⁻
12713 5⁻
10406 3⁻
8854 1⁻
16630 7⁻
13426 (5⁻)
10694 4⁻
9116 3⁻
14304 6₃⁺
11020 4₄⁺
9873 3₁⁺
9483 2₃⁺
18960 8⁺
15346 6⁺
13048 4⁺
11653 3⁺
10584 2⁺
9935 1⁺
15874 8₂⁺
13105 6₂⁺
10533 4₃⁺
14270 4₆⁺
10843 2₄⁺
15970 6₅⁺
13341 4₅⁺
10917 3₂⁺
18621 8⁺
14311 6⁺
12253 4⁺
11320 2⁺
10950 0⁺
14816 5⁻
13137 3⁻
11240 1⁻
Kᵀ
0₁⁺ 2₁⁻ 0₁⁻ 0₂⁺ 0₃⁺ 0₄⁺ 1₁⁻ 4₁⁺ 0₂⁻ 3₁⁻ 2₁⁺ 1₁⁺ 4₂⁺ 2₂⁺ 3₁⁺ 0₅⁺ 1₂⁻
odd
even
odd
nᵢ
1 s→fp 4 2 1 2 1 1 2 2 1

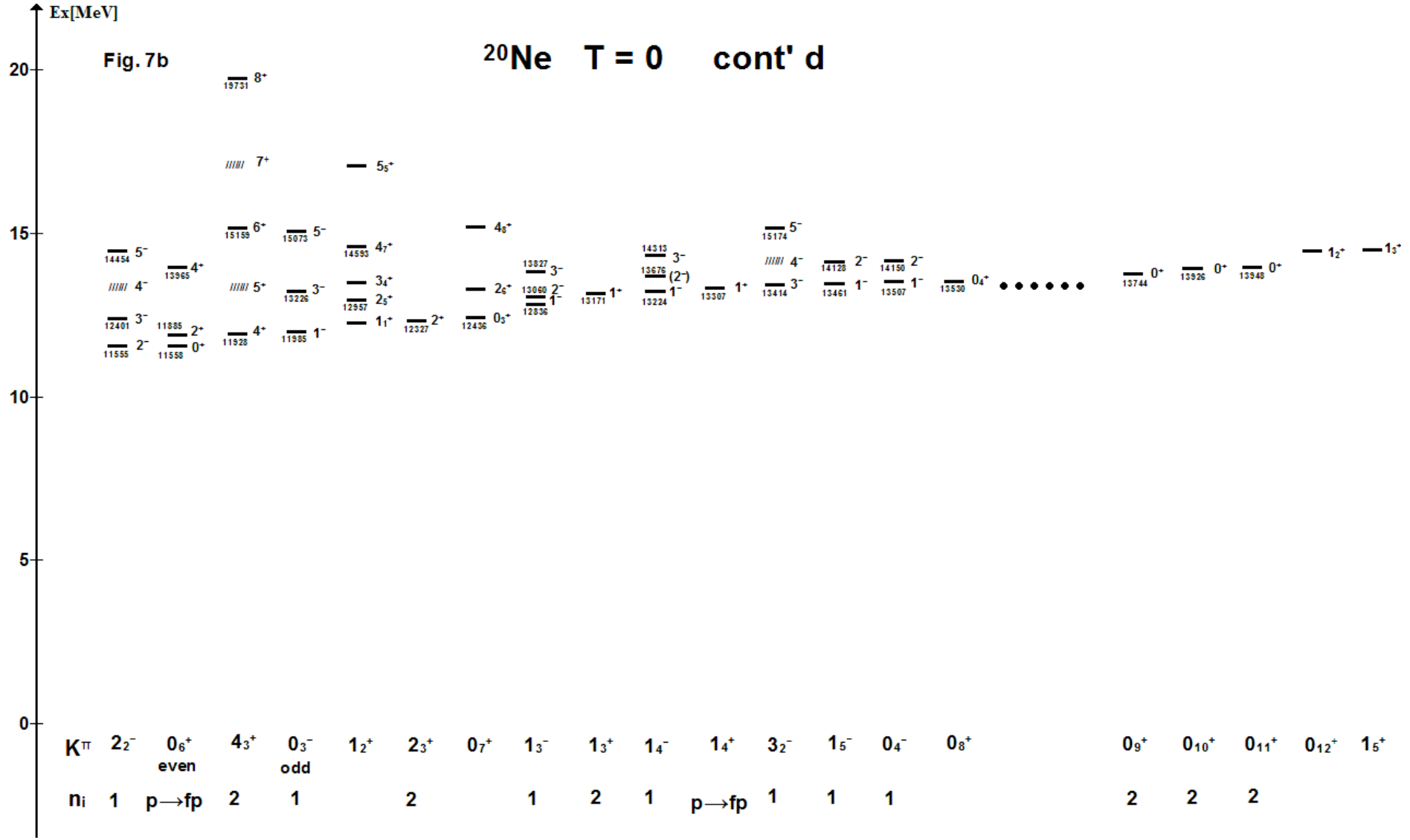
Ex[MeV]
Fig. 7b
20Ne T = 0 cont' d
20
15
10
5
0
19731 8+
15159 6+
15073 5−
14593 4+7
14454 5−
13965 4+
13226 3−
12957 3+4
12957 2+5
12401 3−
11885 2+
11928 4+
11985 1−
12957 1+1
11555 2−
11558 0+
12327 2+
12436 0+3
12436 4+8
12436 2+6
13827 3−
13060 2−
12836 1−
13171 1+
14313 3−
13676 (2−)
13224 1−
13307 1+
15174 5−
14128 2−
14150 2−
13461 1−
13507 1−
13530 0+4
13744 0+
13926 0+
13948 0+
1+2
1+3
Kπ 2−2 0+6 4+3 0−3 1+2 2+3 0+7 1−3 1+3 1−4 1+4 3−2 1−5 0−4 0+8 0+9 0+10 0+11 0+12 1+5
even
odd
ni 1 p→fp 2 1 2 1 2 1 p→fp 1 1 1 2 2 2

Fig. 8

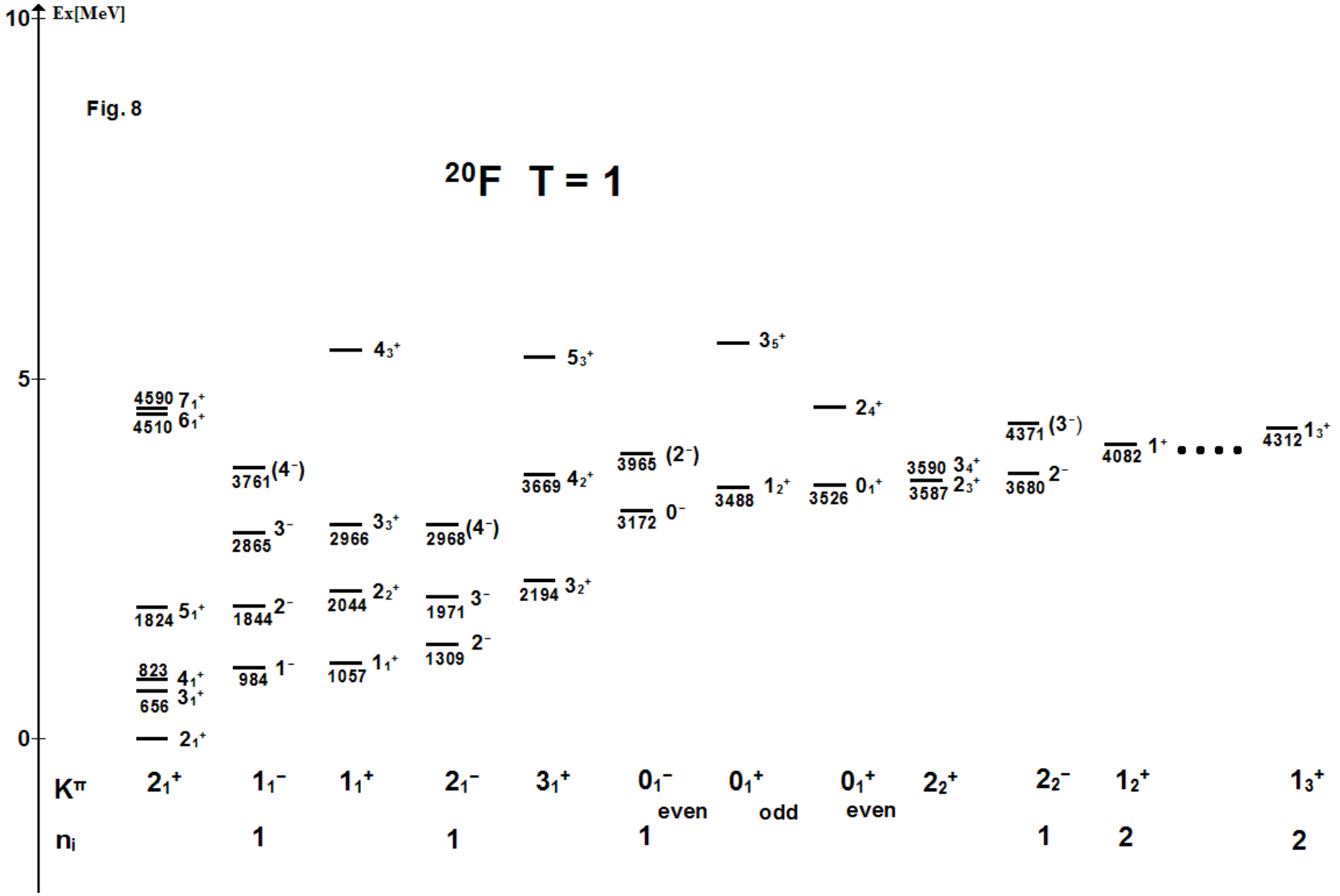
^{20}F T = 1
Ex[MeV]
10
5
0
4590 7$_1^+$
4510 6$_1^+$
4$_3^+$
5$_3^+$
3$_5^+$
2$_4^+$
3761 (4$^-$)
3669 4$_2^+$
3965 (2$^-$)
3172 0$^-$
3488 1$_2^+$
3526 0$_1^+$
4371 (3$^-$)
3680 2$^-$
4082 1$^+$
4312 1$_3^+$
2865 3$^-$
2966 3$_3^+$
2968 (4$^-$)
3590 3$_4^+$
3587 2$_3^+$
1824 5$_1^+$
1844 2$^-$
2044 2$_2^+$
1971 3$^-$
2194 3$_2^+$
823 4$_1^+$
656 3$_1^+$
984 1$^-$
1057 1$_1^+$
1309 2$^-$
2$_1^+$
K$^\pi$
2$_1^+$ 1$_1^-$ 1$_1^+$ 2$_1^-$ 3$_1^+$ 0$_1^-$ 0$_1^+$ 0$_1^+$ 2$_2^+$ 2$_2^-$ 1$_2^+$ 1$_3^+$
even odd even
n$_i$
1 1 1 1 2 2

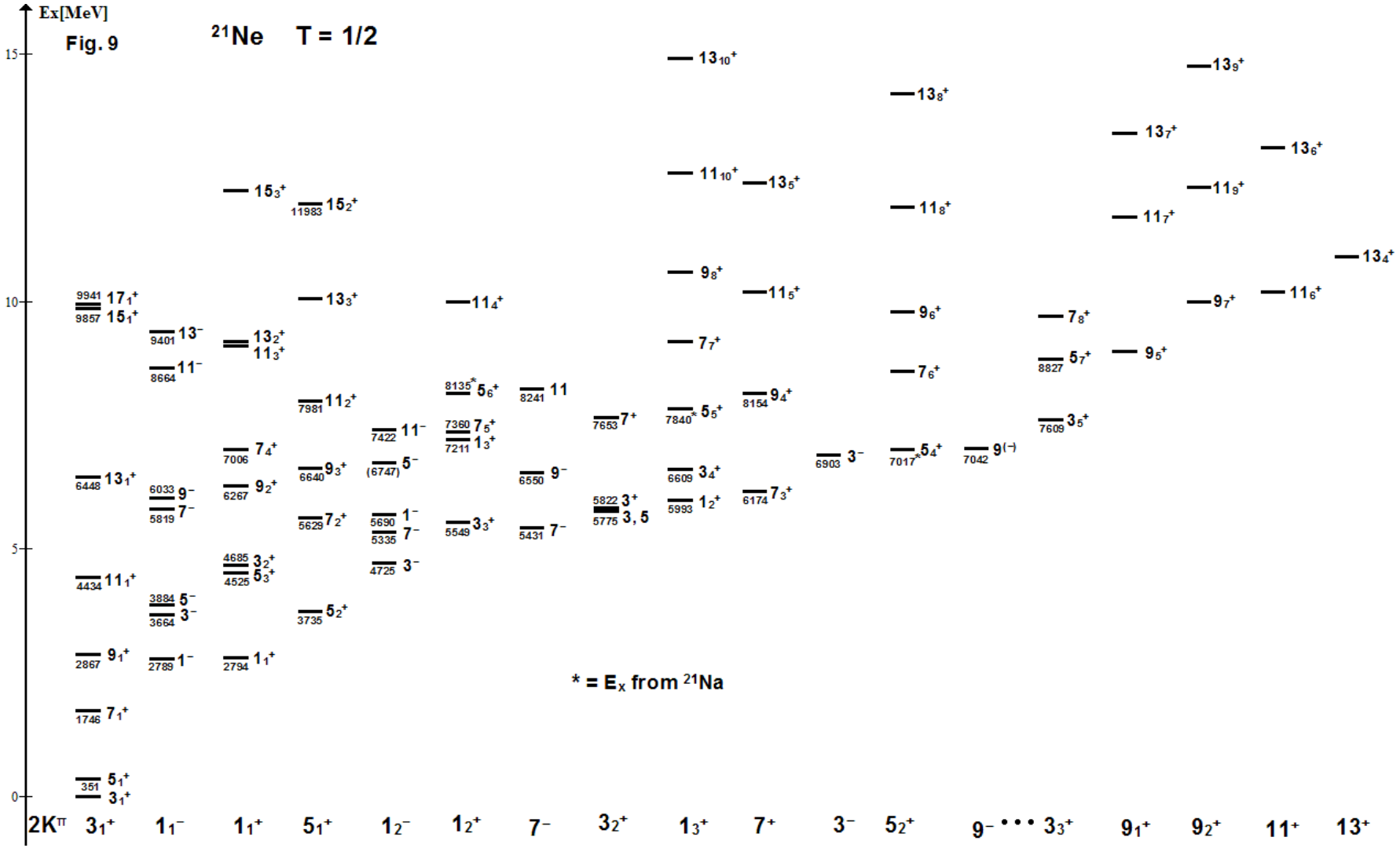
Ex[MeV]
Fig. 9
21Ne T = 1/2
15
10
5
0
9941 17₁⁺
9857 15₁⁺
13₁⁺ 6448
11₁⁺ 4434
9₁⁺ 2867
7₁⁺ 1746
5₁⁺ 351
3₁⁺
9401 13⁻
8664 11⁻
6033 9⁻
5819 7⁻
3884 5⁻
3664 3⁻
1⁻ 2789
15₃⁺
13₂⁺
11₃⁺
7₄⁺ 7006
9₂⁺ 6267
4685 3₂⁺
4525 5₃⁺
1₁⁺ 2794
11983 15₂⁺
13₃⁺
7981 11₂⁺
9₃⁺ 6640
7₂⁺ 5629
5₂⁺ 3735
7422 11⁻
(6747) 5⁻
5690 1⁻
5335 7⁻
3⁻ 4725
11₄⁺
8135* 5₆⁺
7360 7₅⁺
7211 1₃⁺
3₃⁺ 5549
11 8241
9⁻ 6550
7⁻ 5431
7653 7⁺
5822 3⁺
5775 3, 5
13₁₀⁺
11₁₀⁺
9₈⁺
7₇⁺
7840* 5₅⁺
6609 3₄⁺
5993 1₂⁺
13₅⁺
11₅⁺
8154 9₄⁺
6174 7₃⁺
3⁻ 6903
13₈⁺
11₈⁺
9₆⁺
7₆⁺
7017* 5₄⁺
9(⁻) 7042
7₈⁺
8827 5₇⁺
7609 3₅⁺
13₇⁺
9₅⁺
13₉⁺
11₉⁺
9₇⁺
13₆⁺
11₆⁺
13₄⁺
* = Eₓ from 21Na
2Kᵀ 3₁⁺ 1₁⁻ 1₁⁺ 5₁⁺ 1₂⁻ 1₂⁺ 7⁻ 3₂⁺ 1₃⁺ 7⁺ 3⁻ 5₂⁺ 9⁻ • • • 3₃⁺ 9₁⁺ 9₂⁺ 11⁺ 13⁺

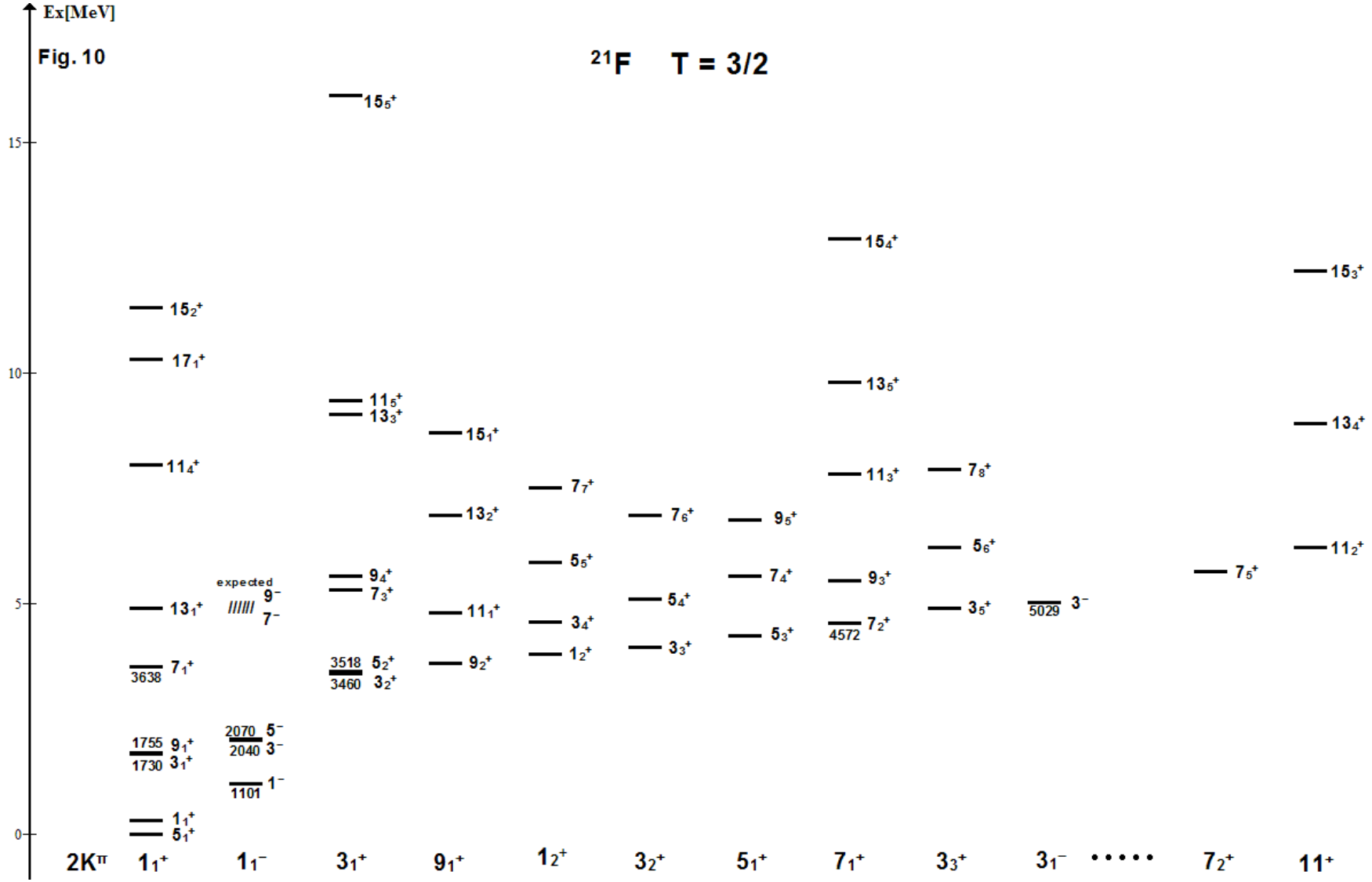
Ex[MeV]
Fig. 10
21F T = 3/2
15
10
5
0
15₅⁺
15₂⁺
17₁⁺
11₄⁺
11₅⁺
13₃⁺
15₁⁺
13₂⁺
7₇⁺
7₆⁺
9₅⁺
15₄⁺
13₅⁺
11₃⁺
7₈⁺
15₃⁺
13₄⁺
11₂⁺
5₆⁺
7₅⁺
13₁⁺
expected
9⁻
7⁻
9₄⁺
7₃⁺
5₅⁺
5₄⁺
7₄⁺
9₃⁺
3₅⁺
5029 3⁻
7₁⁺
3638
3518 5₂⁺
3460 3₂⁺
9₂⁺
11₁⁺
3₄⁺
1₂⁺
3₃⁺
5₃⁺
4572 7₂⁺
2070 5⁻
2040 3⁻
1755 9₁⁺
1730 3₁⁺
1101 1⁻
1₁⁺
5₁⁺
2Kπ
1₁⁺
1₁⁻
3₁⁺
9₁⁺
1₂⁺
3₂⁺
5₁⁺
7₁⁺
3₃⁺
3₁⁻
• • • • •
7₂⁺
11⁺

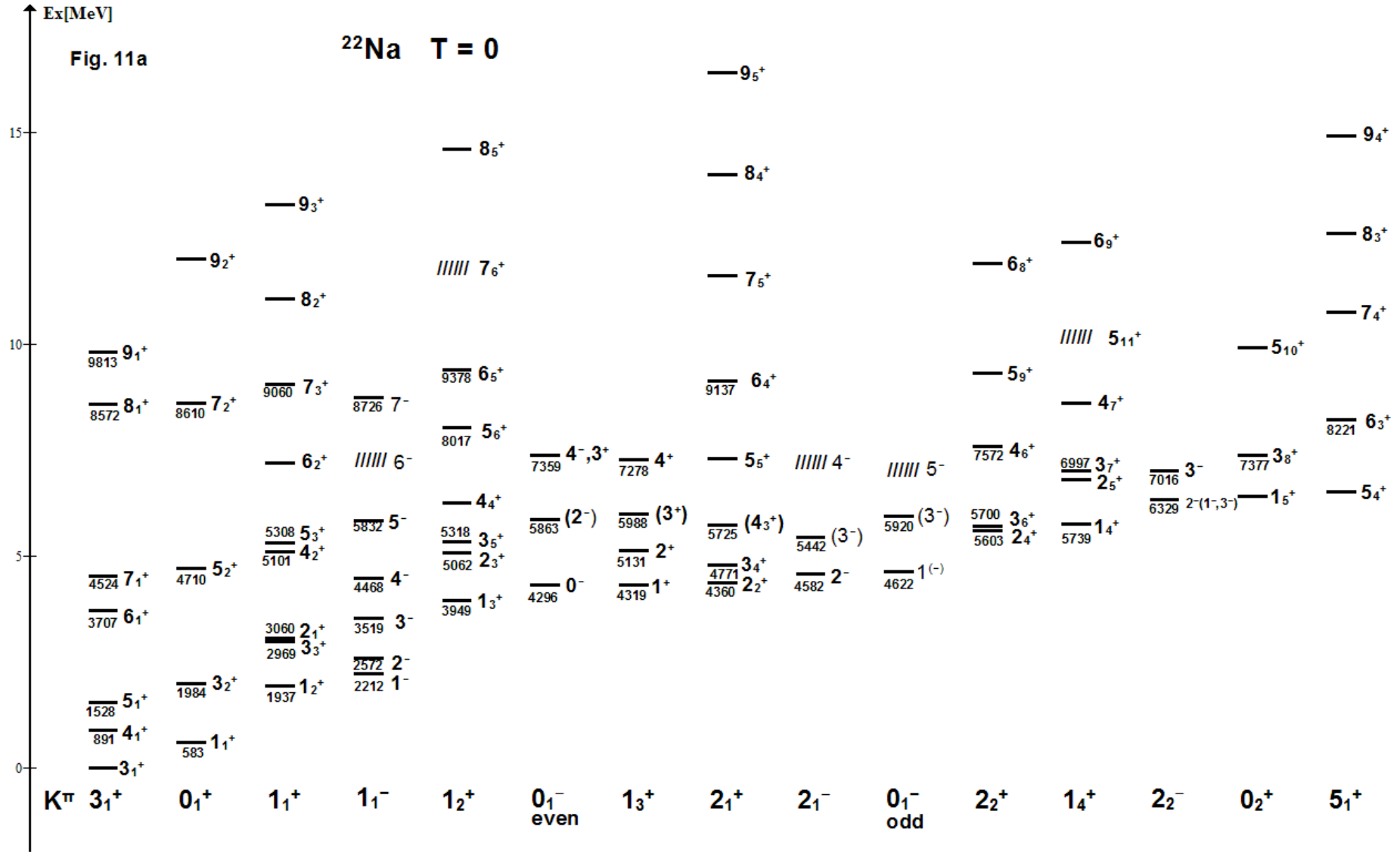
Ex[MeV]
Fig. 11a
22Na T = 0
15
10
5
0
9813 9₁⁺
8572 8₁⁺
4524 7₁⁺
3707 6₁⁺
1528 5₁⁺
891 4₁⁺
3₁⁺
9₂⁺
8610 7₂⁺
4710 5₂⁺
1984 3₂⁺
583 1₁⁺
9₃⁺
8₂⁺
9060 7₃⁺
6₂⁺
5308 5₃⁺
5101 4₂⁺
3060 2₁⁺
2969 3₃⁺
1937 1₂⁺
8726 7⁻
////// 6⁻
5832 5⁻
4468 4⁻
3519 3⁻
2572 2⁻
2212 1⁻
8₅⁺
////// 7₆⁺
9378 6₅⁺
8017 5₆⁺
4₄⁺
5318 3₅⁺
5062 2₃⁺
3949 1₃⁺
7359 4⁻,3⁺
5863 (2⁻)
4296 0⁻
7278 4⁺
5988 (3⁺)
5131 2⁺
4319 1⁺
9₅⁺
8₄⁺
7₅⁺
9137 6₄⁺
5₅⁺
5725 (4₃⁺)
4771 3₄⁺
4360 2₂⁺
////// 4⁻
5442 (3⁻)
4582 2⁻
////// 5⁻
5920 (3⁻)
4622 1⁽⁻⁾
6₈⁺
5₉⁺
7572 4₆⁺
5700 3₆⁺
5603 2₄⁺
6₉⁺
////// 5₁₁⁺
4₇⁺
6997 3₇⁺
2₅⁺
5739 1₄⁺
7016 3⁻
6329 2⁻(1⁻,3⁻)
5₁₀⁺
7377 3₈⁺
1₅⁺
9₄⁺
8₃⁺
7₄⁺
8221 6₃⁺
5₄⁺
Kπ 3₁⁺ 0₁⁺ 1₁⁺ 1₁⁻ 1₂⁺ 0₁⁻ even 1₃⁺ 2₁⁺ 2₁⁻ 0₁⁻ odd 2₂⁺ 1₄⁺ 2₂⁻ 0₂⁺ 5₁⁺

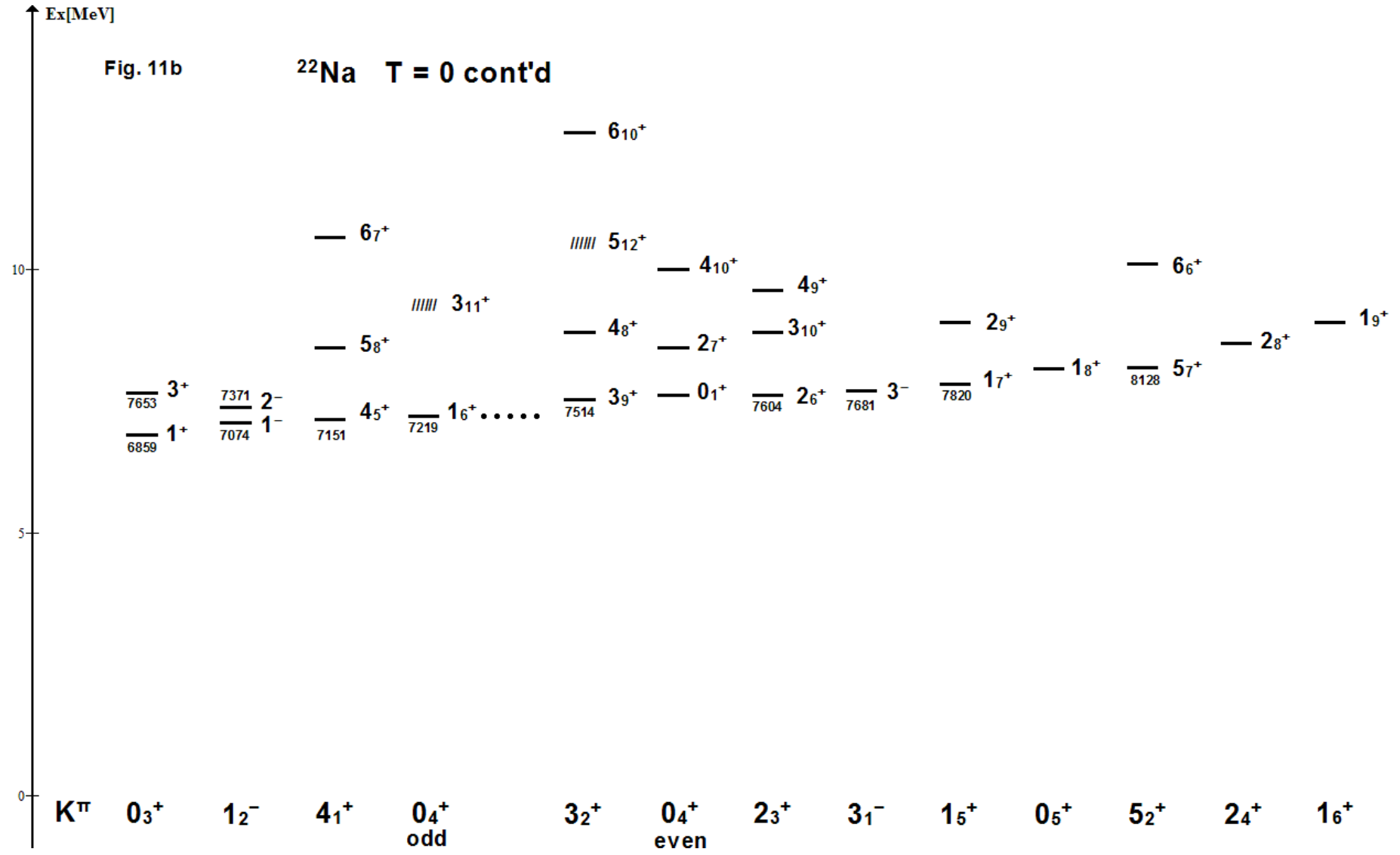
Ex[MeV]
Fig. 11b
22Na T = 0 cont'd
10
5
0
6 10+
6 7+
5 12+
4 10+
4 9+
6 6+
3 11+
4 8+
2 9+
2 8+
1 9+
5 8+
2 7+
3 10+
1 8+
5 7+
3+
7653
7371
2−
1+
6859
7074
1−
4 5+
7151
7219
1 6+
3 9+
7514
0 1+
2 6+
7604
3−
7681
1 7+
7820
8128
Kπ
0 3+
1 2−
4 1+
0 4+
odd
3 2+
0 4+
even
2 3+
3 1−
1 5+
0 5+
5 2+
2 4+
1 6+

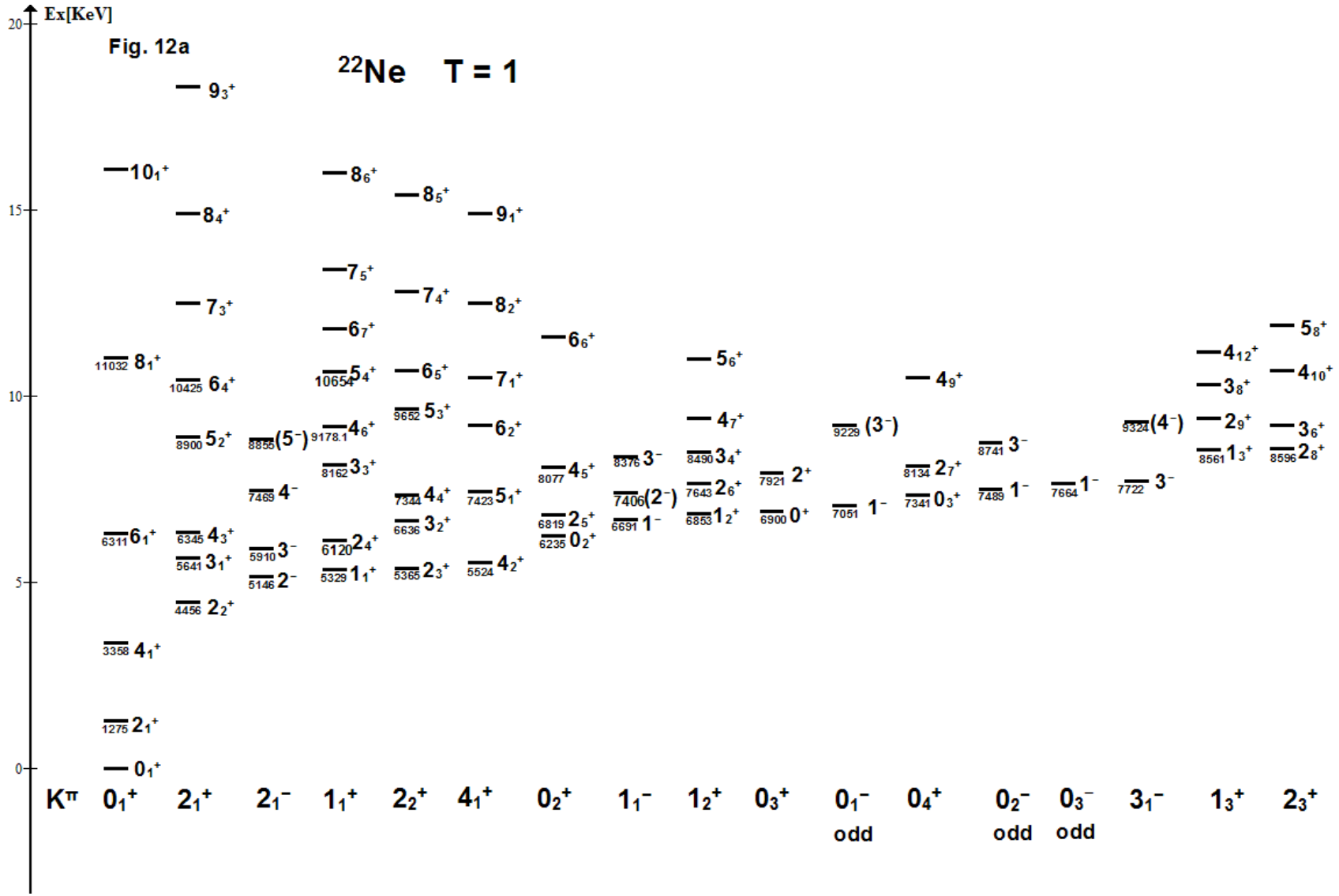
Ex[KeV]
Fig. 12a
22Ne T = 1
20
15
10
5
0
9 3+
10 1+
8 4+
7 3+
11032 8 1+
10425 6 4+
8900 5 2+
8855 (5−)
7469 4−
6311 6 1+
6345 4 3+
5641 3 1+
5910 3−
5146 2−
4456 2 2+
3358 4 1+
1275 2 1+
0 1+
8 6+
8 5+
9 1+
7 5+
7 4+
8 2+
6 7+
10654 5 4+
6 5+
9652 5 3+
9178.1 4 6+
8162 3 3+
7344 4 4+
7423 5 1+
6636 3 2+
6120 2 4+
5329 1 1+
5365 2 3+
5524 4 2+
6 6+
8077 4 5+
6819 2 5+
6235 0 2+
8376 3−
7406 (2−)
6691 1−
5 6+
4 7+
8490 3 4+
7643 2 6+
6853 1 2+
7921 2+
6900 0+
9229 (3−)
7051 1−
4 9+
8134 2 7+
7341 0 3+
8741 3−
7489 1−
7664 1−
9324 (4−)
7722 3−
4 12+
3 8+
2 9+
8561 1 3+
5 8+
4 10+
3 6+
8596 2 8+
Kπ
0 1+
2 1+
2 1−
1 1+
2 2+
4 1+
0 2+
1 1−
1 2+
0 3+
0 1−
odd
0 4+
0 2−
odd
0 3−
odd
3 1−
1 3+
2 3+

Fig. 12b

^{22}Ne T = 1 cont'd

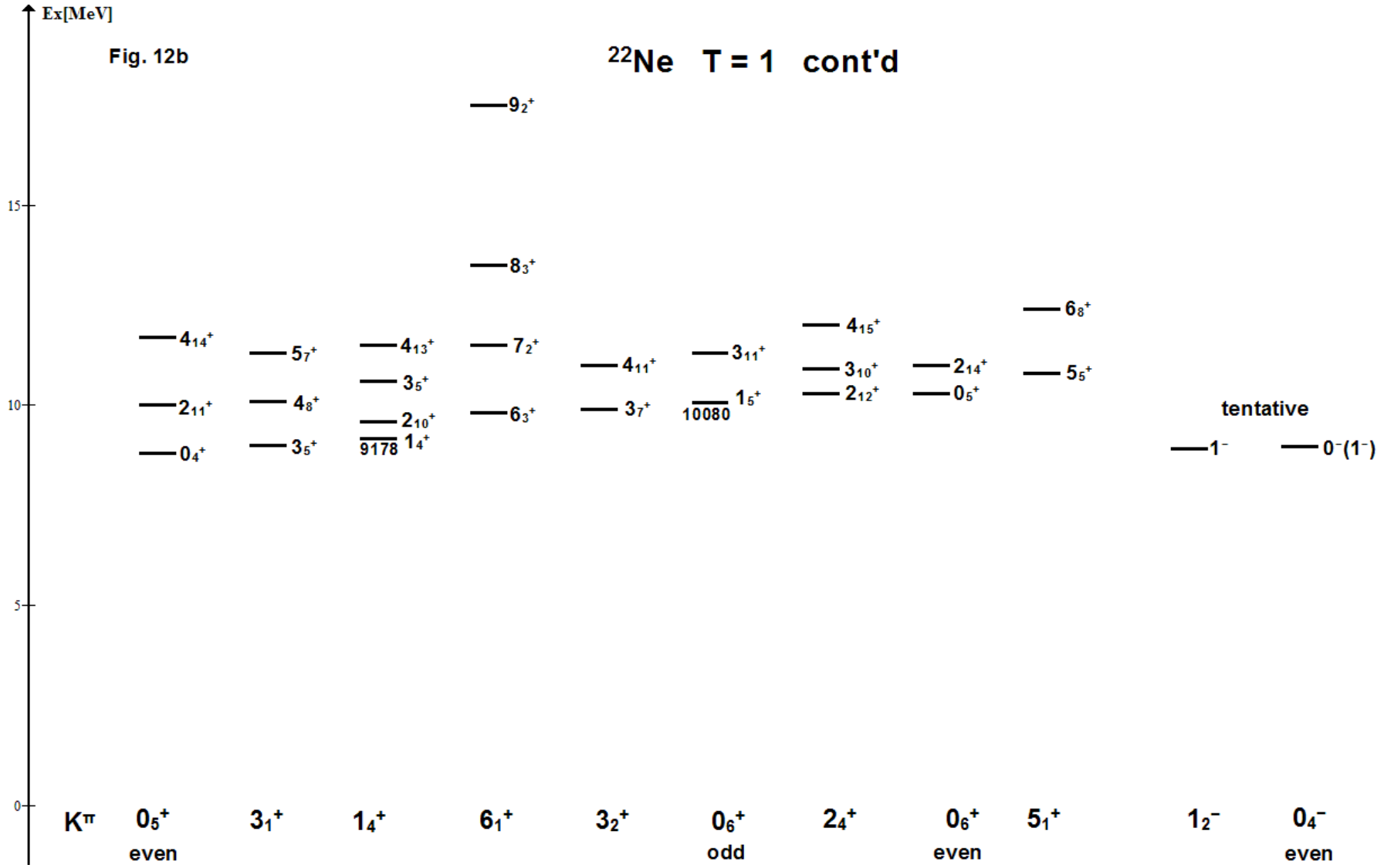

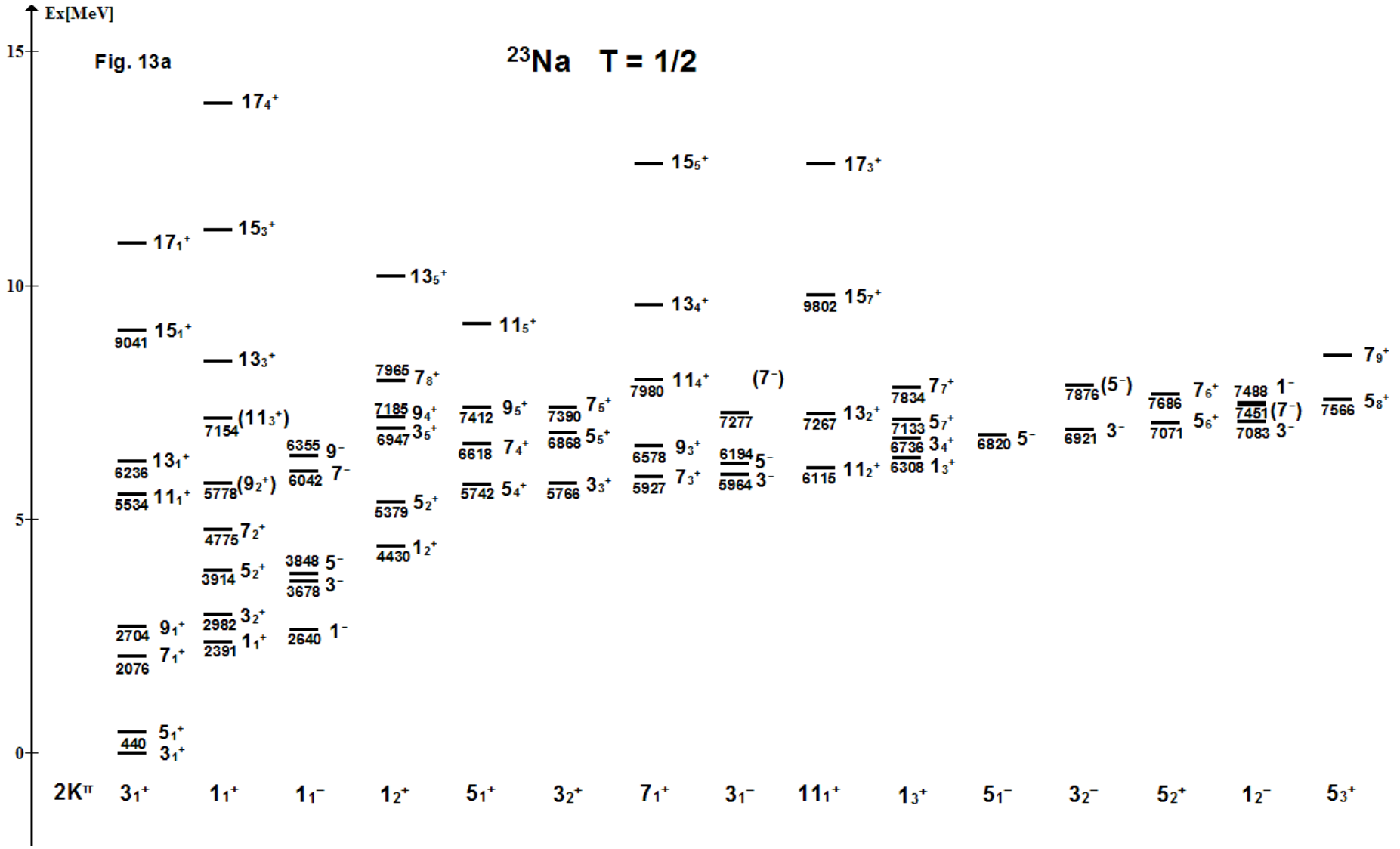
Ex[MeV]
Fig. 13a
^{23}Na T = 1/2
15
10
5
0
17_4^+
15_3^+
17_1^+
13_5^+
15_5^+
17_3^+
9041 15_1^+
13_3^+
11_5^+
13_4^+
9802 15_7^+
7_9^+
7965 7_8^+
7980 11_4^+
(7⁻)
7834 7_7^+
7876 (5⁻)
7686 7_6^+
7488 1⁻
7566 5_8^+
7154 (11_3^+)
7185 9_4^+
7412 9_5^+
7390 7_5^+
7277
7267 13_2^+
7451 (7⁻)
6947 3_5^+
6618 7_4^+
6868 5_5^+
6578 9_3^+
7133 5_7^+
7071 5_6^+
6355 9⁻
6236 13_1^+
6194 5⁻
6736 3_4^+
6820 5⁻
6921 3⁻
7083 3⁻
5778 (9_2^+)
6042 7⁻
5534 11_1^+
5379 5_2^+
5742 5_4^+
5766 3_3^+
5927 7_3^+
5964 3⁻
6115 11_2^+
6308 1_3^+
4775 7_2^+
4430 1_2^+
3914 5_2^+
3848 5⁻
3678 3⁻
2982 3_2^+
2704 9_1^+
2640 1⁻
2391 1_1^+
2076 7_1^+
440 5_1^+
3_1^+
2Kπ
3_1^+
1_1^+
1_1^-
1_2^+
5_1^+
3_2^+
7_1^+
3_1^-
11_1^+
1_3^+
5_1^-
3_2^-
5_2^+
1_2^-
5_3^+

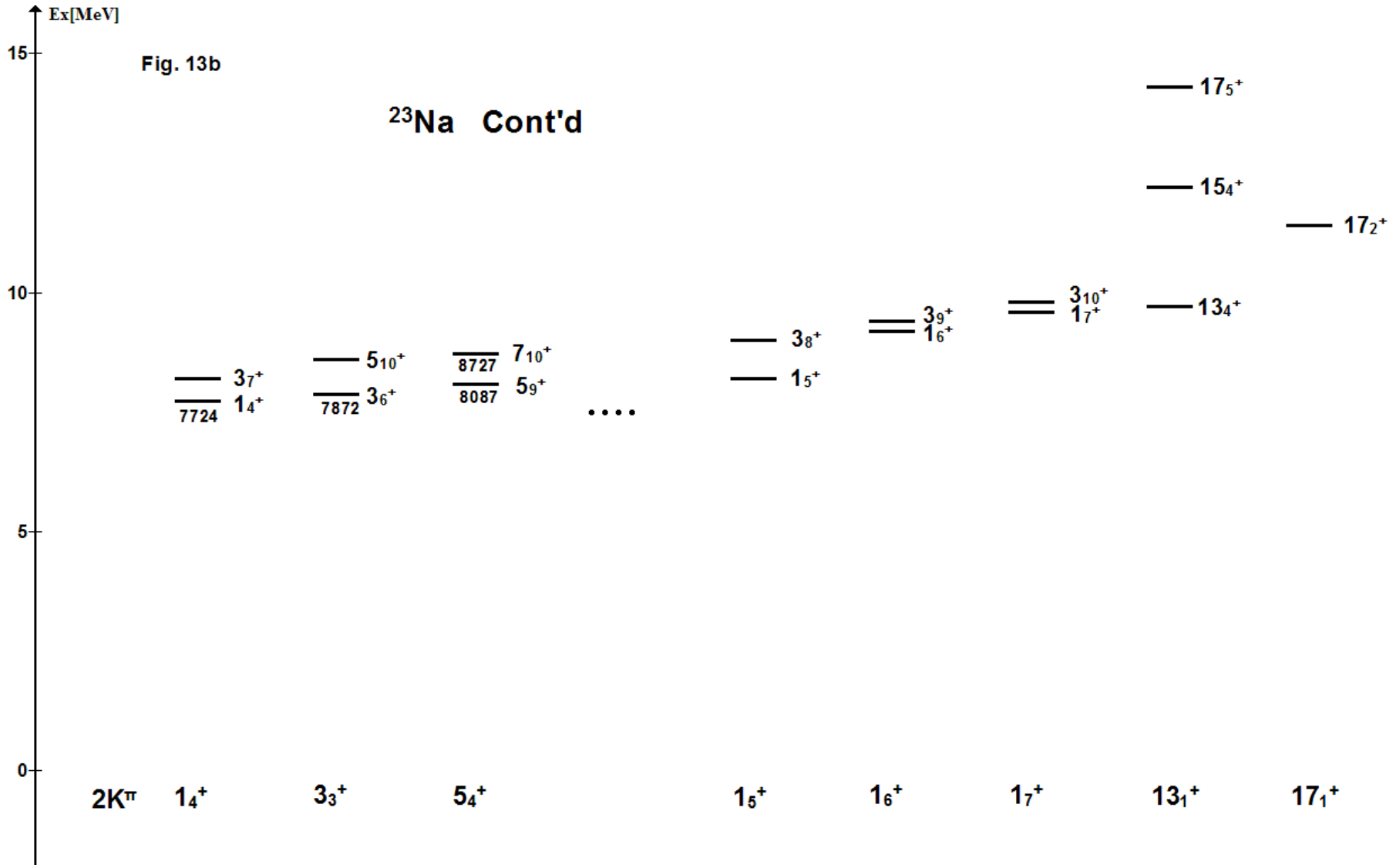
Ex[MeV]
15
10
5
0
Fig. 13b
23Na Cont'd
37+
14+
7724
510+
36+
7872
8727
710+
59+
8087
....
38+
15+
39+
16+
310+
17+
175+
154+
134+
172+
2Kπ
14+
33+
54+
15+
16+
17+
131+
171+

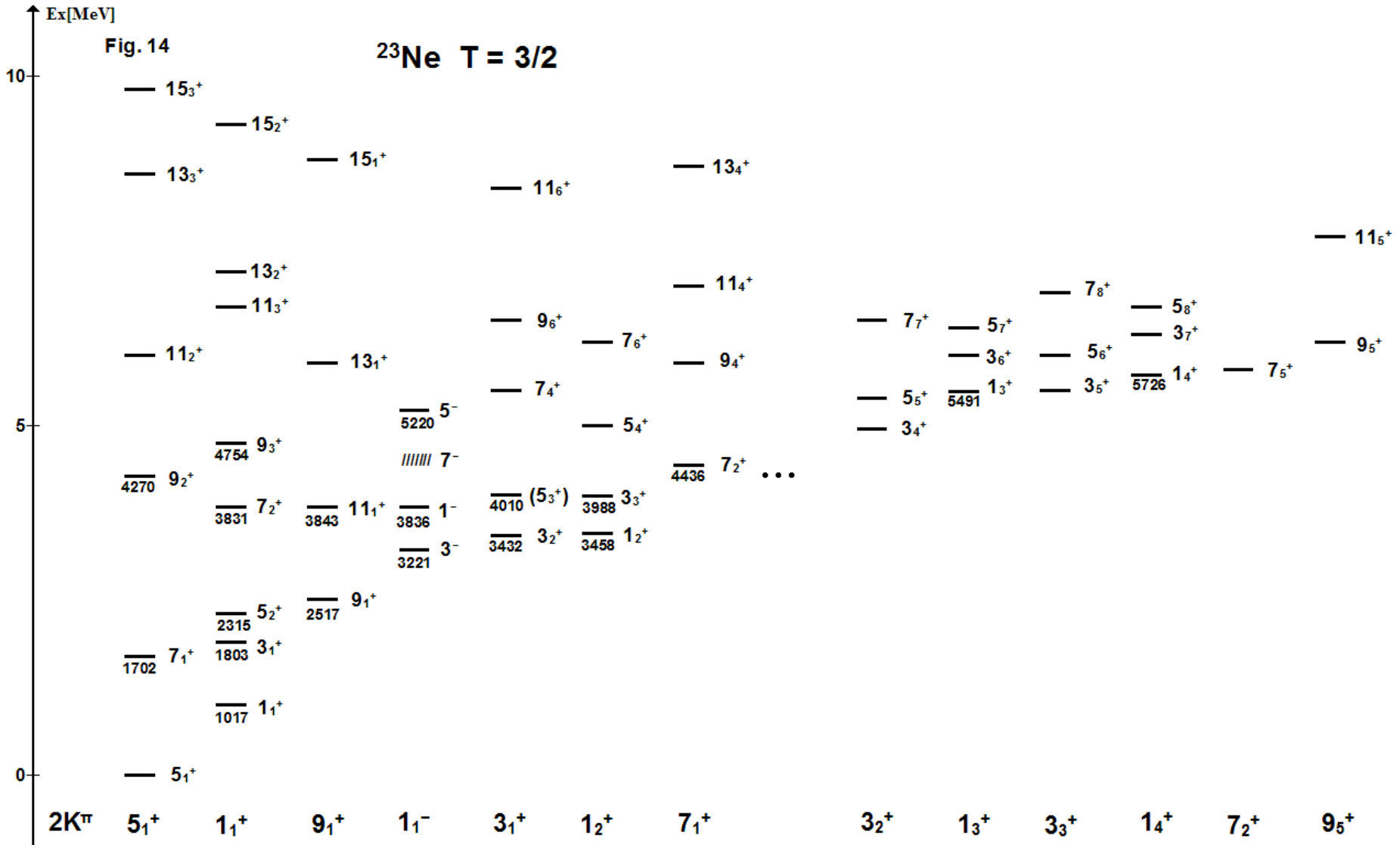
Ex[MeV]
Fig. 14
^{23}Ne T = 3/2
10
5
0
15_3^+
15_2^+
15_1^+
13_3^+
13_4^+
11_6^+
11_5^+
13_2^+
11_4^+
7_8^+
11_3^+
9_6^+
7_7^+
5_8^+
5_7^+
3_7^+
11_2^+
7_6^+
9_4^+
3_6^+
5_6^+
9_5^+
13_1^+
7_4^+
5_5^+
1_3^+
1_4^+
7_5^+
5_4^+
3_4^+
5_2^-
9_3^+
7^-
7_2^+
9_2^+
11_1^+
(5_3^+)
3_3^+
1^-
3_2^+
1_2^+
9_1^+
5_2^+
3_1^+
1_1^+
5_1^+
4754
4270
3831
3843
5220
3836
3221
4010
3432
3988
3458
4436
5491
5726
2315
1803
1017
2517
1702
2K$^\pi$
5_1^+
1_1^+
9_1^+
1_1^-
3_1^+
1_2^+
7_1^+
3_2^+
1_3^+
3_3^+
1_4^+
7_2^+
9_5^+

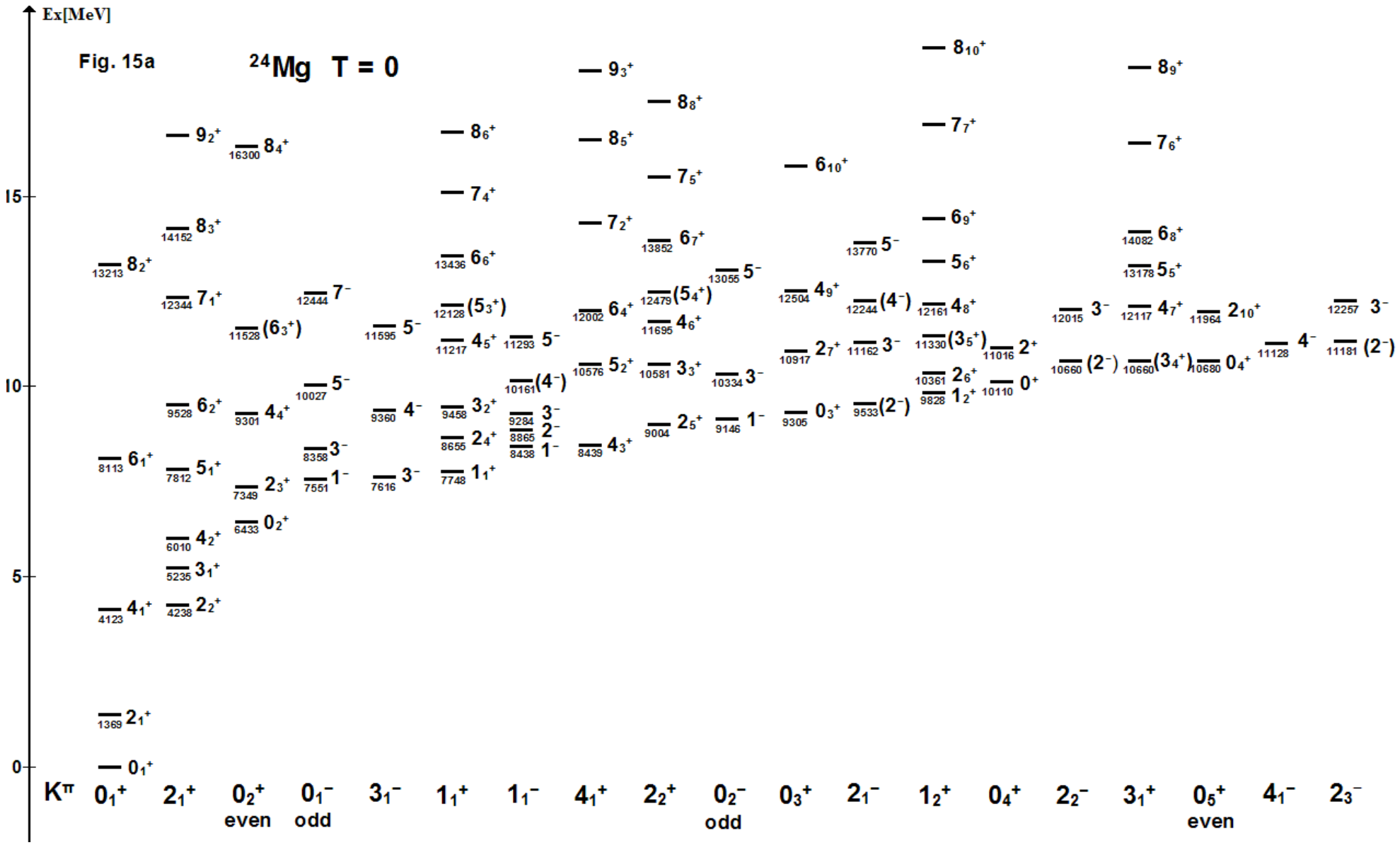
Ex[MeV]
Fig. 15a
24Mg T = 0
15
10
5
0
Kπ
0₁⁺
2₁⁺
0₂⁺ even
0₁⁻ odd
3₁⁻
1₁⁺
1₁⁻
4₁⁺
2₂⁺
0₂⁻ odd
0₃⁺
2₁⁻
1₂⁺
0₄⁺
2₂⁻
3₁⁺
0₅⁺ even
4₁⁻
2₃⁻
1369 2₁⁺
4123 4₁⁺
4238 2₂⁺
5235 3₁⁺
6010 4₂⁺
6433 0₂⁺
7349 2₃⁺
7616 3⁻
7748 1₁⁺
8113 6₁⁺
7812 5₁⁺
8358 3⁻
7551 1⁻
8439 4₃⁺
8438 1⁻
8865 2⁻
9284 3⁻
9458 3₂⁺
8655 2₄⁺
9360 4⁻
9528 6₂⁺
9301 4₄⁺
10027 5⁻
10161 (4⁻)
11293 5⁻
11217 4₅⁺
12128 (5₃⁺)
11595 5⁻
11528 (6₃⁺)
12444 7⁻
13213 8₂⁺
14152 8₃⁺
16300 8₄⁺
12344 7₁⁺
9528 6₂⁺
13436 6⁺
11217 4₅⁺
12128 (5₃⁺)
11595 5⁻
11528 (6₃⁺)
12444 7⁻
13436 6⁺
14152 8₃⁺
16300 8₄⁺
12344 7₁⁺
9528 6₂⁺
15 MeV
10 MeV
5 MeV
0 MeV

Fig. 15b

^{24}Mg T = 0 cont'd

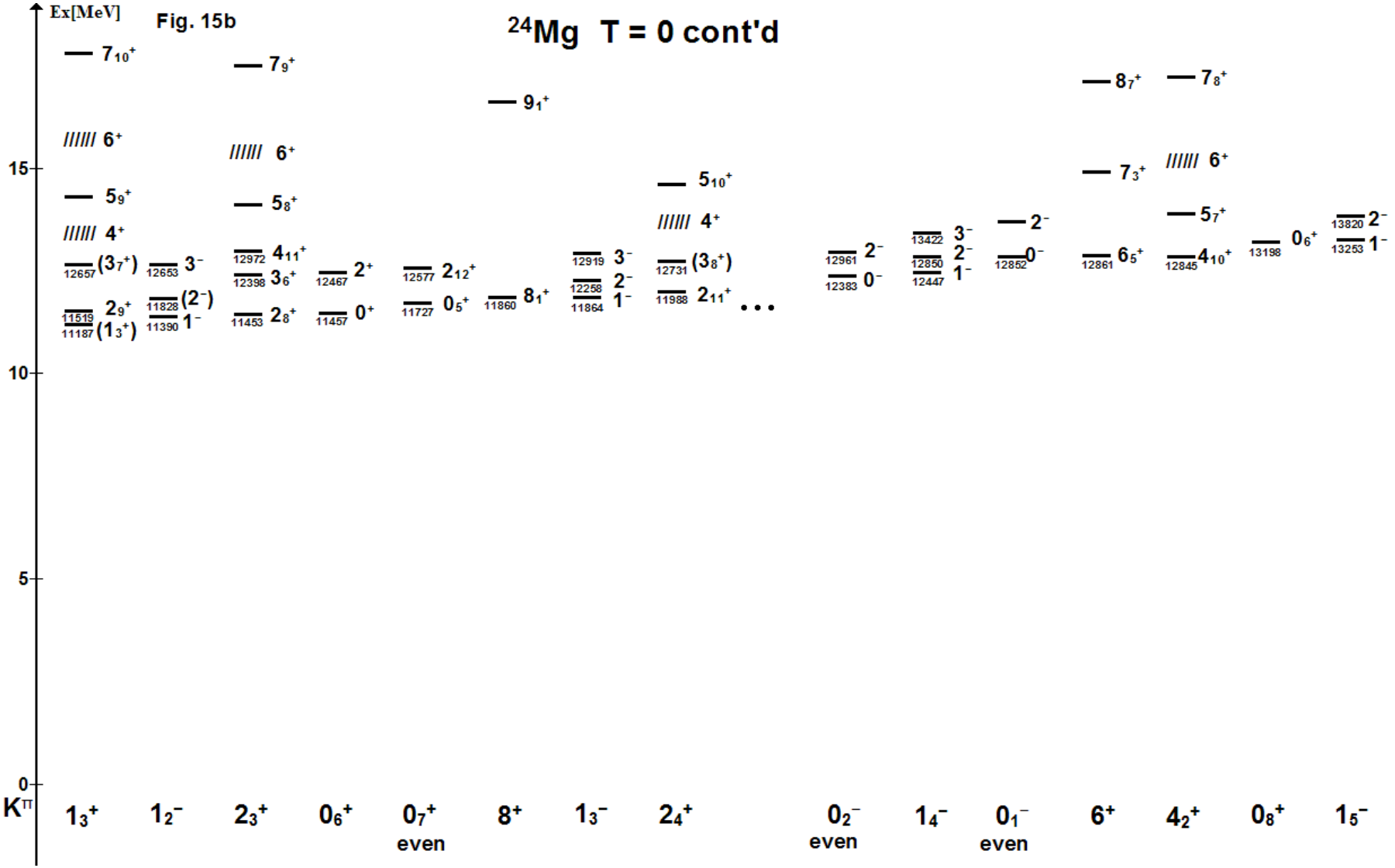

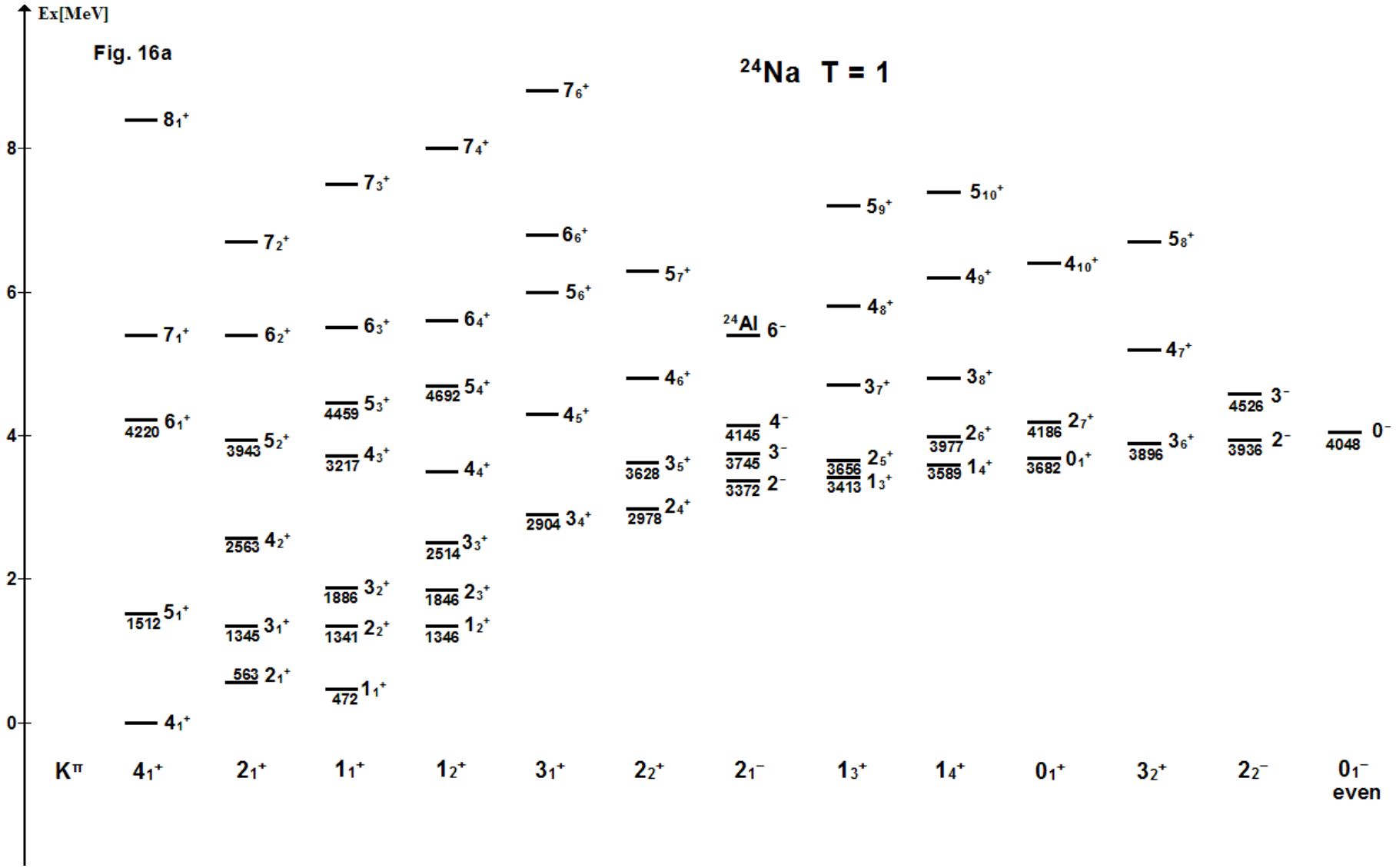
Ex[MeV]
Fig. 16a
^{24}Na T = 1
8
6
4
2
0
8_1^+
7_1^+
6_1^+ 4220
5_1^+ 1512
4_1^+
7_2^+
6_2^+
5_2^+ 3943
4_2^+ 2563
3_1^+ 1345
2_1^+ 563
1_1^+ 472
7_3^+
6_3^+
5_3^+ 4459
4_3^+ 3217
3_2^+ 1886
2_2^+ 1341
7_4^+
6_4^+
5_4^+ 4692
4_4^+
3_3^+ 2514
2_3^+ 1846
1_2^+ 1346
7_6^+
6_6^+
5_6^+
4_5^+
3_4^+ 2904
5_7^+
4_6^+
3_5^+ 3628
2_4^+ 2978
^{24}Al 6^-
4^- 4145
3^- 3745
2^- 3372
5_9^+
4_8^+
3_7^+
2_5^+ 3656
1_3^+ 3413
5_{10}^+
4_9^+
3_8^+
2_6^+ 3977
1_4^+ 3589
4_{10}^+
2_7^+ 4186
0_1^+ 3682
5_8^+
4_7^+
3_6^+ 3896
3^- 4526
2^- 3936
0^- 4048
K^π
4_1^+
2_1^+
1_1^+
1_2^+
3_1^+
2_2^+
2_1^-
1_3^+
1_4^+
0_1^+
3_2^+
2_2^-
0_1^- even

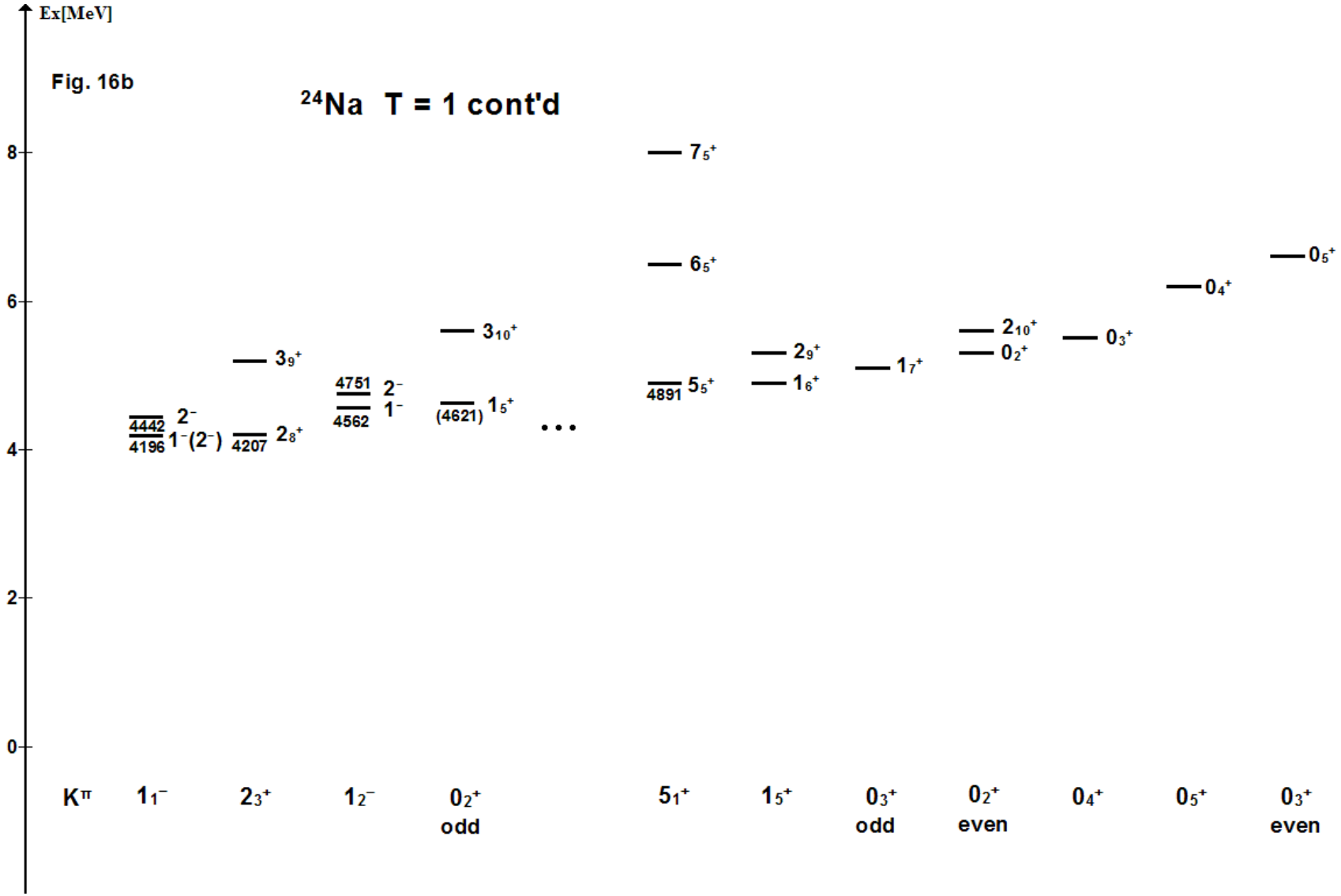
Ex[MeV]
Fig. 16b
^{24}Na T = 1 cont'd
8
6
4
2
0
7_{5}^{+}
6_{5}^{+}
3_{10}^{+}
3_{9}^{+}
4751
4562
2^{-}
1^{-}
4442
4196
2^{-}
$1^{-}(2^{-})$
4207
2_{8}^{+}
(4621)
1_{5}^{+}
4891
5_{5}^{+}
2_{9}^{+}
1_{6}^{+}
1_{7}^{+}
2_{10}^{+}
0_{2}^{+}
0_{3}^{+}
0_{4}^{+}
0_{5}^{+}
0_{5}^{+}
0_{4}^{+}
0_{3}^{+}
0_{2}^{+}
1_{5}^{+}
5_{1}^{+}
0_{2}^{+}
odd
1_{2}^{-}
2_{3}^{+}
1_{1}^{-}
K^{π}
odd
even
even

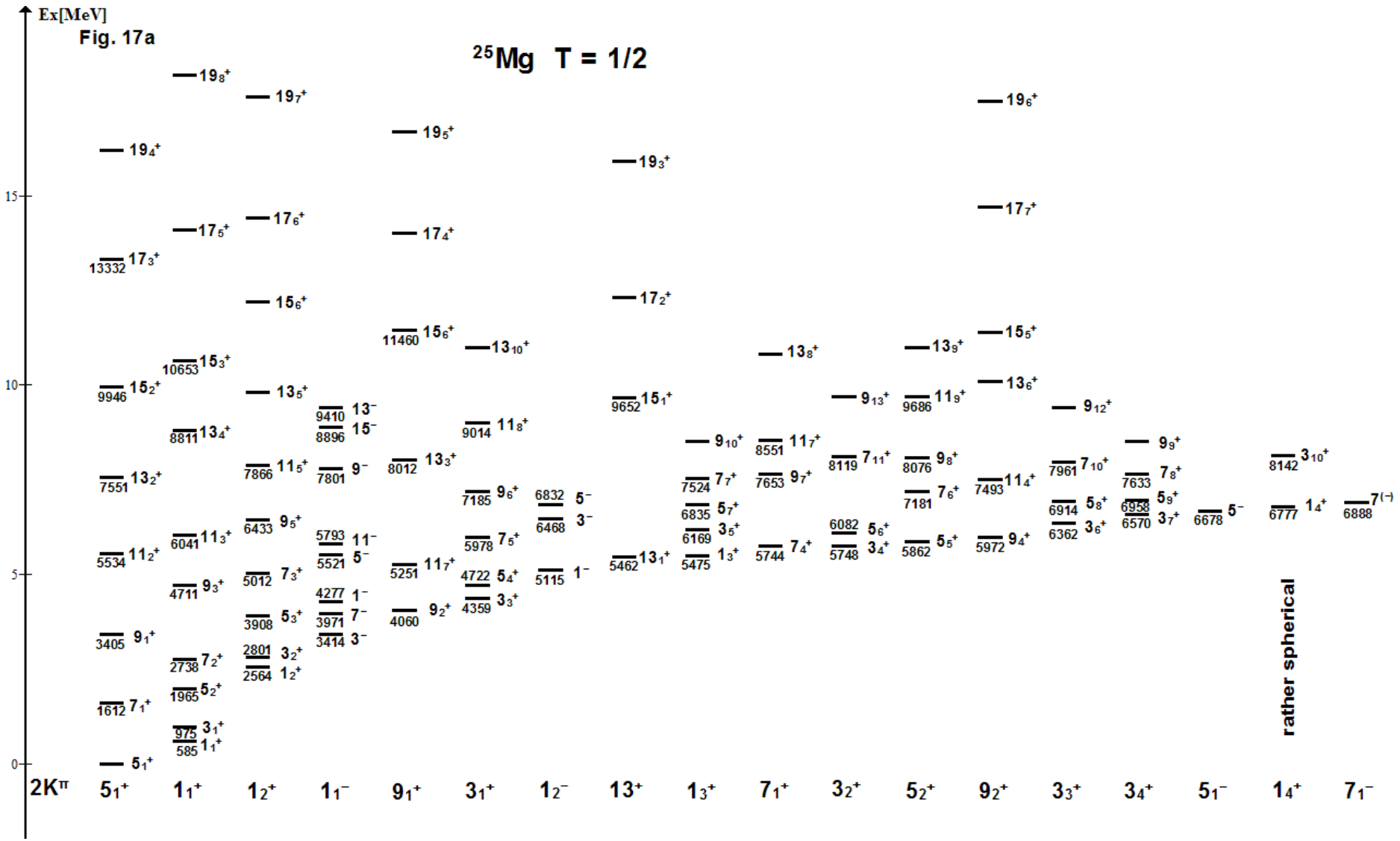
Ex[MeV]
Fig. 17a
25Mg T = 1/2
19 8+
19 7+
19 4+
19 5+
19 3+
19 6+
17 7+
17 6+
17 5+
17 4+
17 3+
17 2+
15 6+
15 5+
15 3+
15 2+
15 1+
13 10+
13 8+
13 9+
13 6+
13 3+
13 2+
13 1+
11 8+
11 7+
11 9+
11 4+
11 3+
11 2+
9 10+
9 13+
9 12+
9 9+
9 8+
9 7+
9 5+
9 4+
9 3+
9 2+
7 11+
7 10+
7 8+
7 7+
7 6+
7 5+
7 4+
7 2+
6 6+
6 5+
6 4+
5 11−
5 10−
5 9+
5 8+
5 7+
5 6+
5 5+
5 4+
5 3+
5 2+
5 1+
5 5−
4 10+
4 9+
4 7+
4 6+
4 5+
4 4+
4 3+
4 2+
4 1+
3 13−
3 11−
3 10−
3 9+
3 8+
3 7−
3 6+
3 5−
3 4+
3 3−
3 2+
2 15−
2 13−
2 11−
2 9−
2 7−
2 5−
2 3−
2 1−
1 7+
1 5+
1 3+
1 1+
0 9+
0 7+
0 5+
0 3+
0 1+
0 1−
0 (7−)
13332
9946
8811
7551
6041
5534
4711
3405
2738
1965
1612
975
585
10653
9410
8896
7866
7801
6433
5793
5521
5012
4277
3971
3908
3414
2801
2564
11460
8012
7185
5978
5251
4722
4359
4060
9014
6832
6468
5115
9652
5462
8551
7653
7524
6835
6169
5475
5744
8119
6082
5748
8076
7181
5862
9686
7493
5972
7961
6914
6362
7633
6958
6570
6678
8142
6777
6888
rather spherical
2Kπ
5 1+
1 1+
1 2+
1 1−
9 1+
3 1+
1 2−
13+
1 3+
7 1+
3 2+
5 2+
9 2+
3 3+
3 4+
5 1−
1 4+
7 1−

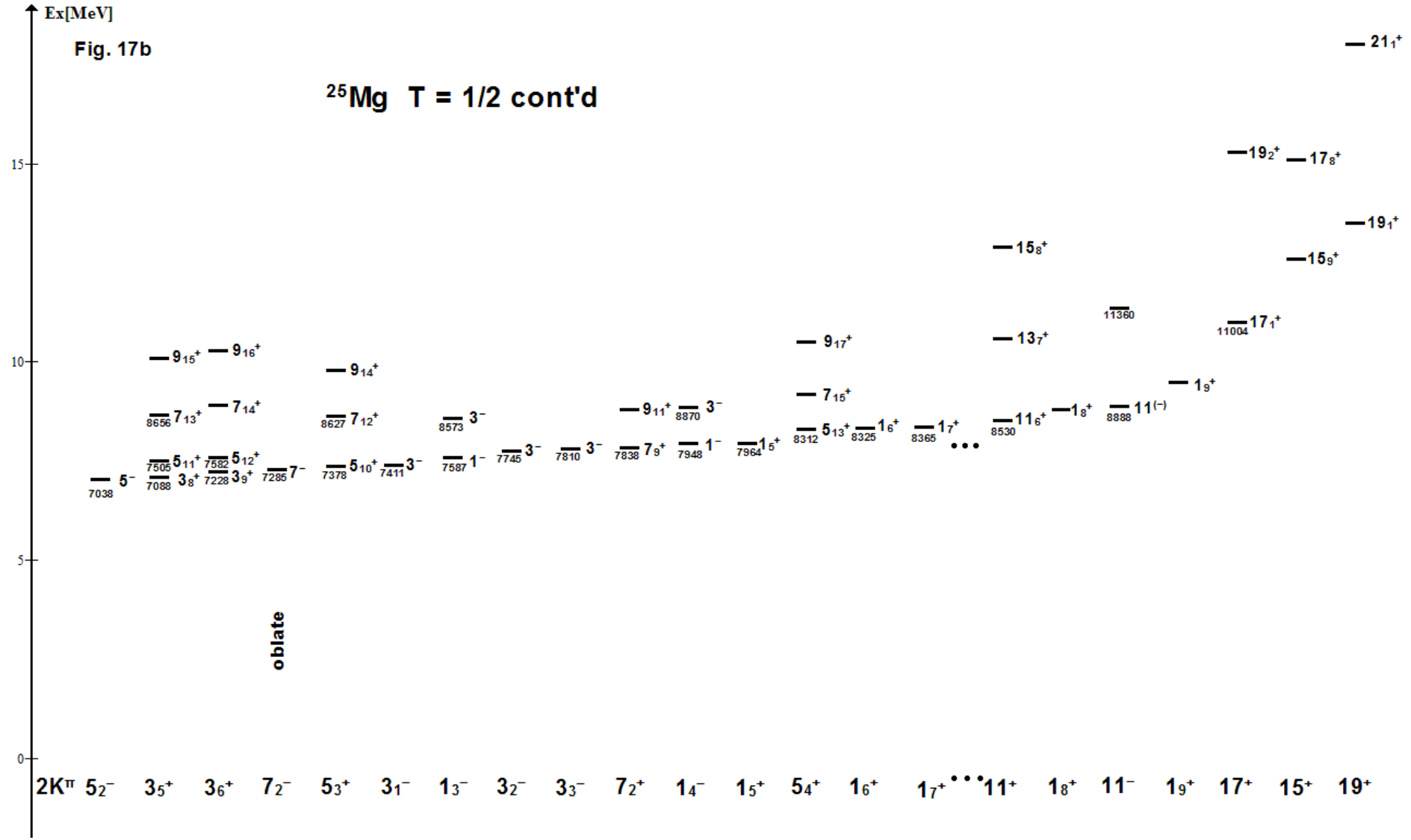
Ex[MeV]
Fig. 17b
25Mg T = 1/2 cont'd
15
10
5
0
oblate
2Kπ 5⁻ 3₅⁺ 3₆⁺ 7₂⁻ 5₃⁺ 3₁⁻ 1₃⁻ 3₂⁻ 3₃⁻ 7₂⁺ 1₄⁻ 1₅⁺ 5₄⁺ 1₆⁺ 1₇⁺ • • • 11⁺ 1₈⁺ 11⁻ 1₉⁺ 17⁺ 15⁺ 19⁺
7038 5⁻
7088 3₈⁺
7228 3₉⁺
7285 7⁻
7505 5₁₁⁺
7582 5₁₂⁺
8656 7₁₃⁺
7₁₄⁺
9₁₅⁺
9₁₆⁺
7378 5₁₀⁺
7411 3⁻
8627 7₁₂⁺
9₁₄⁺
7587 1⁻
8573 3⁻
7745 3⁻
7810 3⁻
7838 7₉⁺
7948 1⁻
8870 3⁻
9₁₁⁺
7964 1₅⁺
8312 5₁₃⁺
8325 1₆⁺
9₁₇⁺
7₁₅⁺
8365 1₇⁺
8530 11₆⁺
13₇⁺
15₈⁺
8888 11⁽⁻⁾
1₈⁺
11360
1₉⁺
11004 17₁⁺
19₂⁺
17₈⁺
15₉⁺
19₁⁺
21₁⁺

Fig. 18

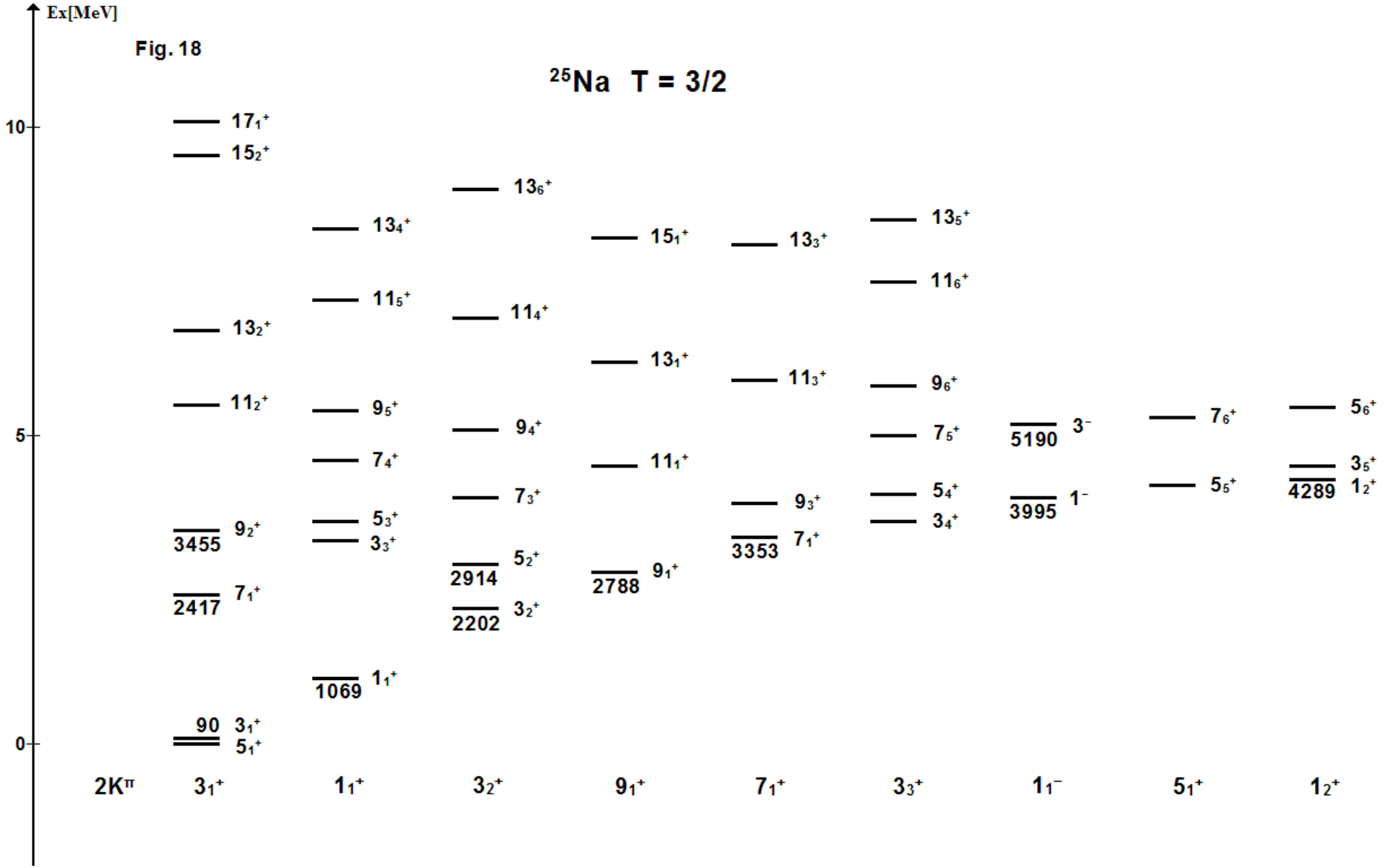
^{25}Na T = 3/2
Ex[MeV]
10
5
0
17_1^+
15_2^+
13_6^+
13_4^+
15_1^+
13_3^+
13_5^+
11_6^+
11_5^+
11_4^+
13_2^+
13_1^+
11_3^+
9_6^+
11_2^+
9_5^+
9_4^+
7_5^+
7_6^+
5_6^+
7_4^+
11_1^+
5_4^+
3455 9_2^+
5_3^+
7_3^+
9_3^+
3_4^+
5190 3^-
5_5^+
3_5^+
3_3^+
5_2^+
7_1^+
3995 1^-
4289 1_2^+
2914
3353
2417 7_1^+
2788 9_1^+
3_2^+
2202
1069 1_1^+
90 3_1^+
5_1^+
$2K^\pi$
3_1^+
1_1^+
3_2^+
9_1^+
7_1^+
3_3^+
1_1^-
5_1^+
1_2^+

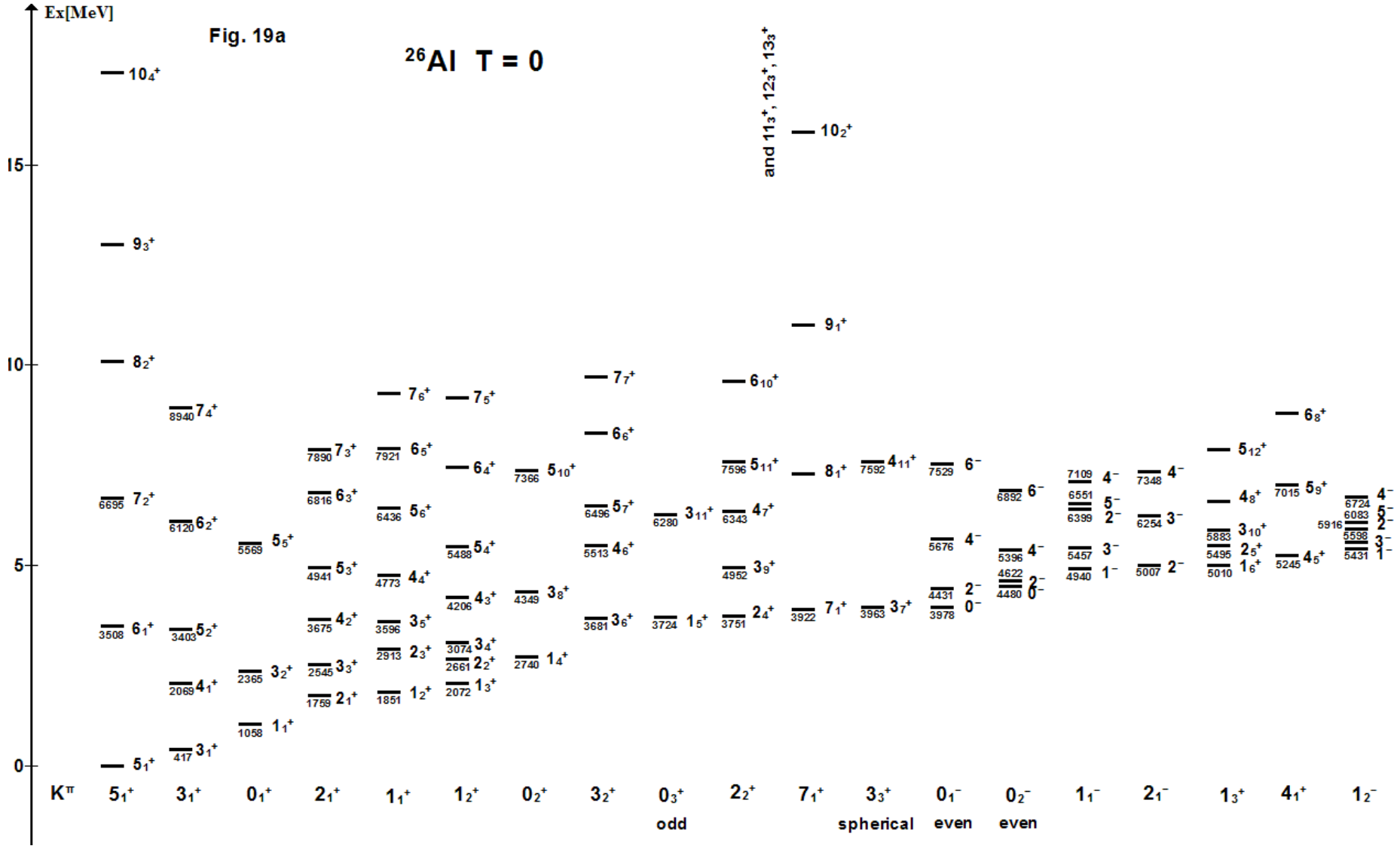
Ex[MeV]
Fig. 19a
^{26}Al T = 0
15
10
5
0
and $11_3^+, 12_3^+, 13_3^+$
10_4^+
9_3^+
8_2^+
7_4^+ 8940
7_2^+ 6695
6_2^+ 6120
5_5^+ 5569
5_3^+ 4941
4_2^+ 3675
3_3^+ 2545
2_1^+ 1759
6_1^+ 3508
5_2^+ 3403
4_1^+ 2069
3_2^+ 2365
3_1^+ 417
1_1^+ 1058
7_3^+ 7890
6_3^+ 6816
7_6^+
6_5^+ 7921
5_6^+ 6436
4_4^+ 4773
3_5^+ 3596
2_3^+ 2913
1_2^+ 1851
7_5^+
6_4^+
5_4^+ 5488
4_3^+ 4206
3_4^+ 3074
2_2^+ 2661
1_3^+ 2072
5_{10}^+ 7366
3_8^+ 4349
1_4^+ 2740
7_7^+
6_6^+
5_7^+ 6496
4_6^+ 5513
3_6^+ 3681
3_{11}^+ 6280
1_5^+ 3724
6_{10}^+
5_{11}^+ 7596
4_7^+ 6343
3_9^+ 4952
2_4^+ 3751
10_2^+
9_1^+
8_1^+
7_1^+ 3922
4_{11}^+ 7592
3_7^+ 3963
6
4_8^+ 5676
2_5^- 4431
0_4^- 3978
6_2^- 6892
4_3^- 5396
2_4^- 4622
0_3^- 4480
4_2^- 7109
5_3^- 6551
2_4^- 6399
3_3^- 5457
1_4^- 4940
4_3^- 7348
3_4^- 6254
2_3^- 5007
5_{12}^+
4_8^+
3_{10}^+ 5883
2_5^+ 5495
1_6^+ 5010
6_8^+
5_9^+ 7015
4_5^+ 5245
4_4^- 6724
5_4^- 6083
2_4^- 5916
3_4^- 5598
1_3^- 5431
K^π
5_1^+
3_1^+
0_1^+
2_1^+
1_1^+
1_2^+
0_2^+
3_2^+
0_3^+
odd
2_2^+
7_1^+
3_3^+
spherical
0_1^-
even
0_2^-
even
1_1^-
2_1^-
1_3^+
4_1^+
1_2^-

Fig. 19b

^{26}Al T = 0 cont'd

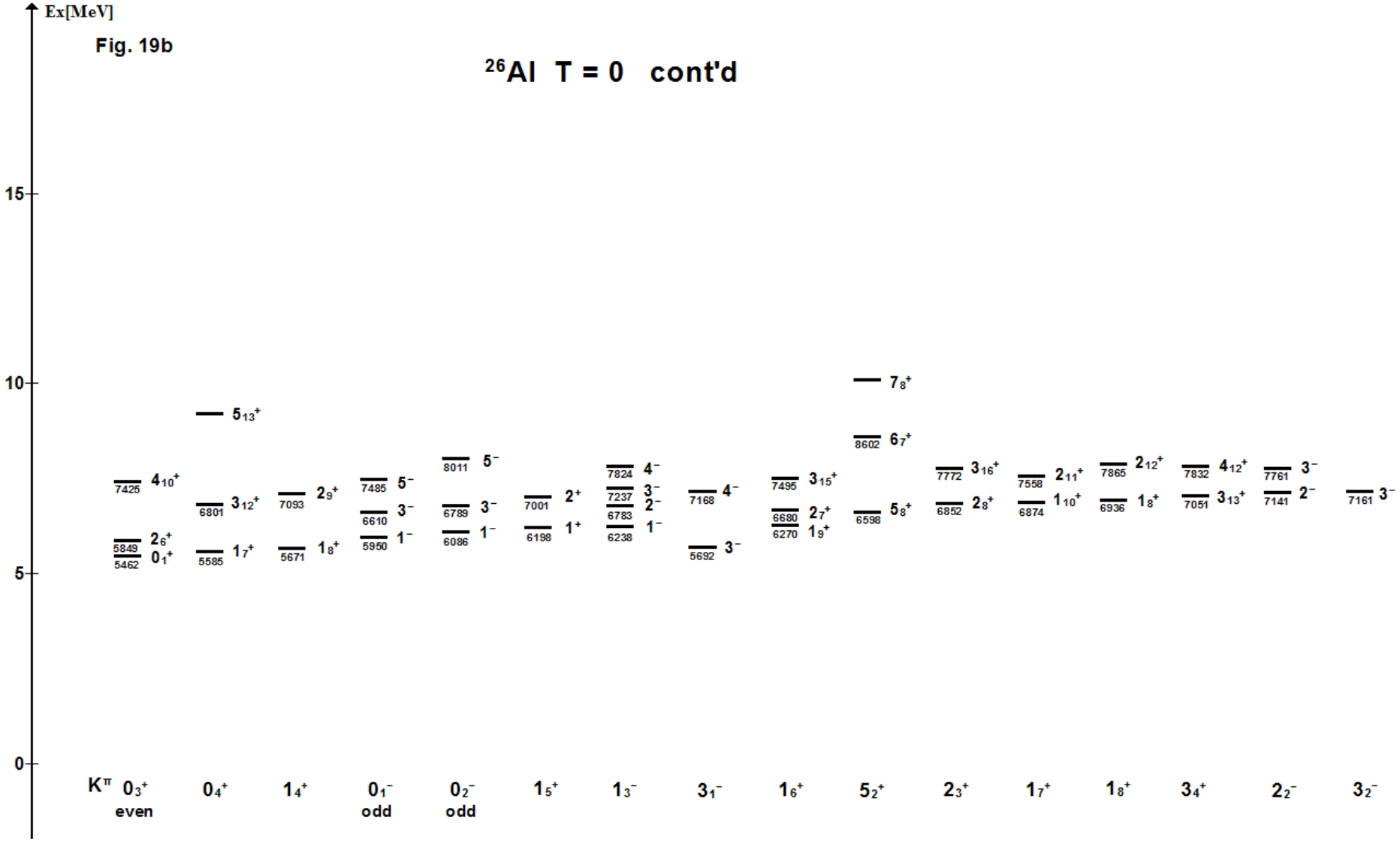

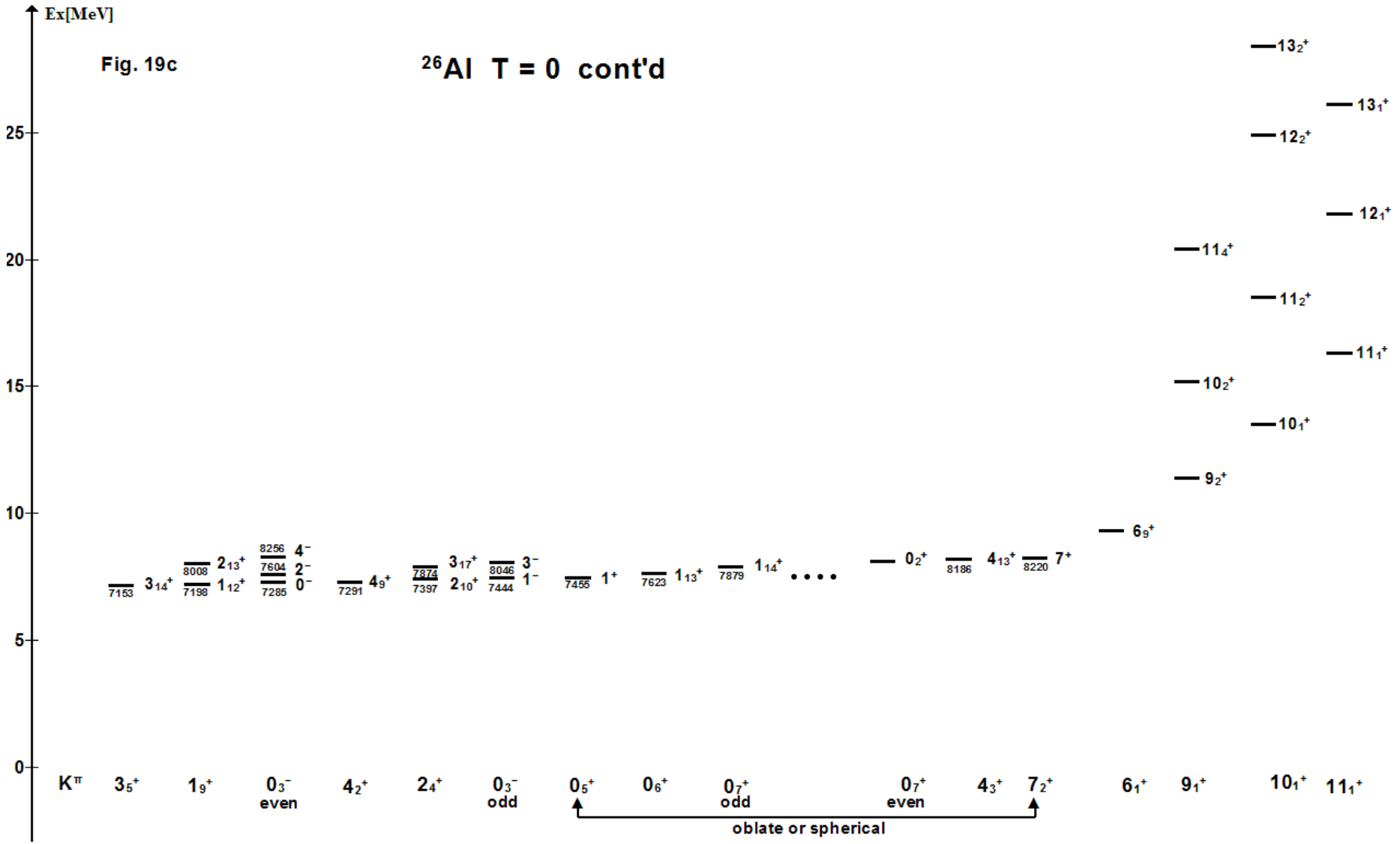
Ex[MeV]
Fig. 19c
^{26}Al T = 0 cont'd
25
20
15
10
5
0
13_2^+
13_1^+
12_2^+
12_1^+
11_4^+
11_2^+
11_1^+
10_2^+
10_1^+
9_2^+
6_9^+
0_2^+
4_{13}^+
7^+
1_{14}^+
1_{13}^+
1^+
3_{17}^+
2_{10}^+
3^-
1^-
4_9^+
3_{14}^+
2_{13}^+
1_{12}^+
4^-
2^-
0^-
7153
8008
7198
8256
7604
7285
7291
7874
7397
8046
7444
7455
7623
7879
8186
8220
K^π
3_5^+
1_9^+
0_3^- even
4_2^+
2_4^+
0_3^- odd
0_5^+
0_6^+
0_7^+ odd
0_7^+ even
4_3^+
7_2^+
6_1^+
9_1^+
10_1^+
11_1^+
oblate or spherical

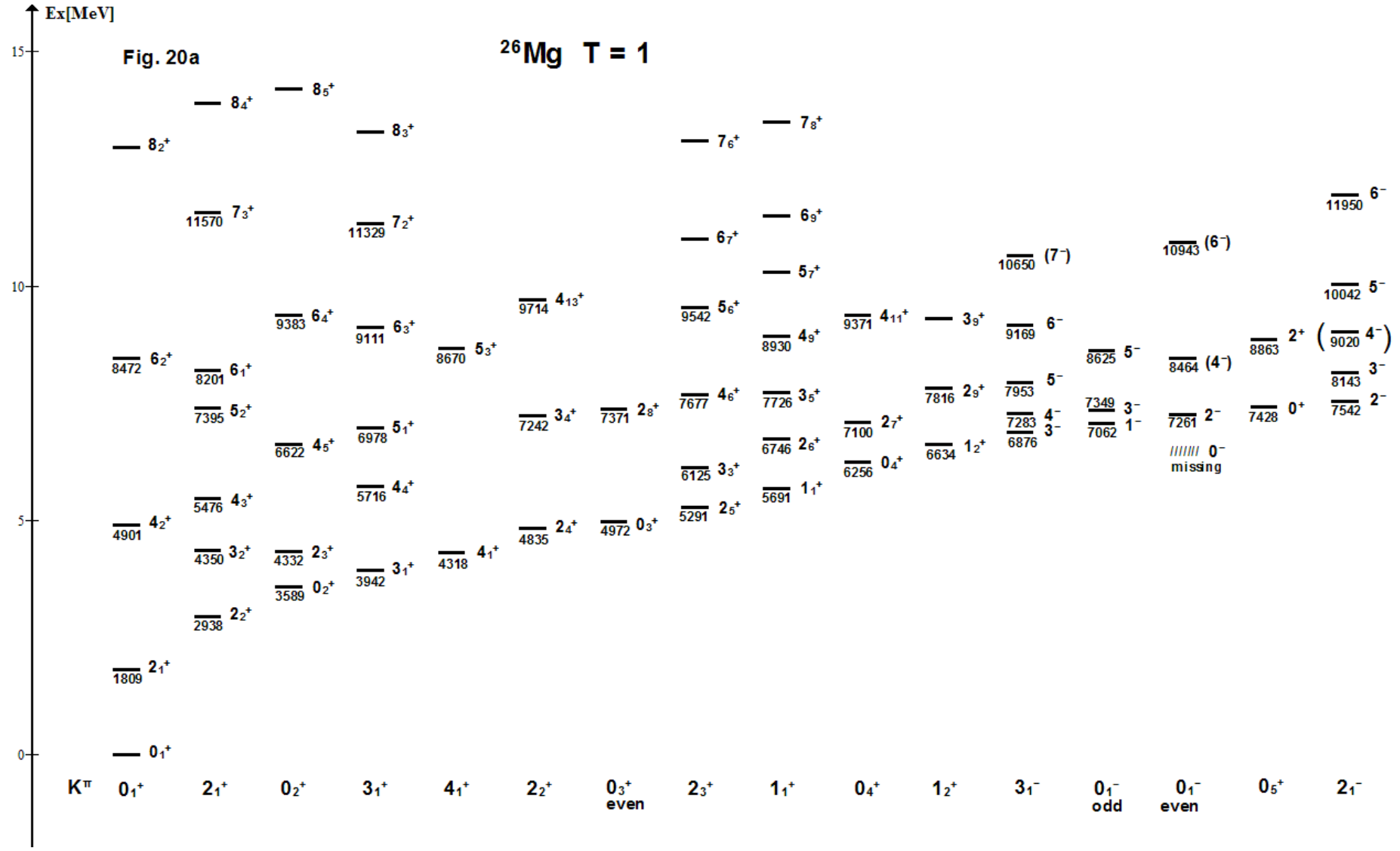
Ex[MeV]
Fig. 20a
^{26}Mg T = 1
15
10
5
0
K^π
0_1^+
2_1^+
0_2^+
3_1^+
4_1^+
2_2^+
0_3^+ even
2_3^+
1_1^+
0_4^+
1_2^+
3_1^-
0_1^- odd
0_1^- even
0_5^+
2_1^-
1809 2_1^+
4901 4_2^+
8472 6_2^+
11570 7_3^+
2938 2_2^+
4350 3_2^+
5476 4_3^+
7395 5_2^+
8201 6_1^+
3589 0_2^+
4332 2_3^+
6622 4_5^+
9383 6_4^+
3942 3_1^+
5716 4_4^+
6978 5_1^+
9111 6_3^+
11329 7_2^+
4318 4_1^+
8670 5_3^+
4835 2_4^+
7242 3_4^+
9714 4_{13}^+
4972 0_3^+
7371 2_8^+
5291 2_5^+
6125 3_3^+
7677 4_6^+
9542 5_6^+
6746 2_6^+
7726 3_5^+
8930 4_9^+
5691 1_1^+
6256 0_4^+
7100 2_7^+
9371 4_{11}^+
6634 1_2^+
7816 2_9^+
6876 3$^-$
7283 4$^-$
7953 5$^-$
9169 6$^-$
10650 (7$^-$)
7062 1$^-$
7349 3$^-$
8625 5$^-$
////// 0^- missing
7261 2$^-$
8464 (4$^-$)
10943 (6$^-$)
7428 0^+
8863 2^+
7542 2$^-$
8143 3$^-$
9020 (4$^-$)
10042 5$^-$
11950 6$^-$

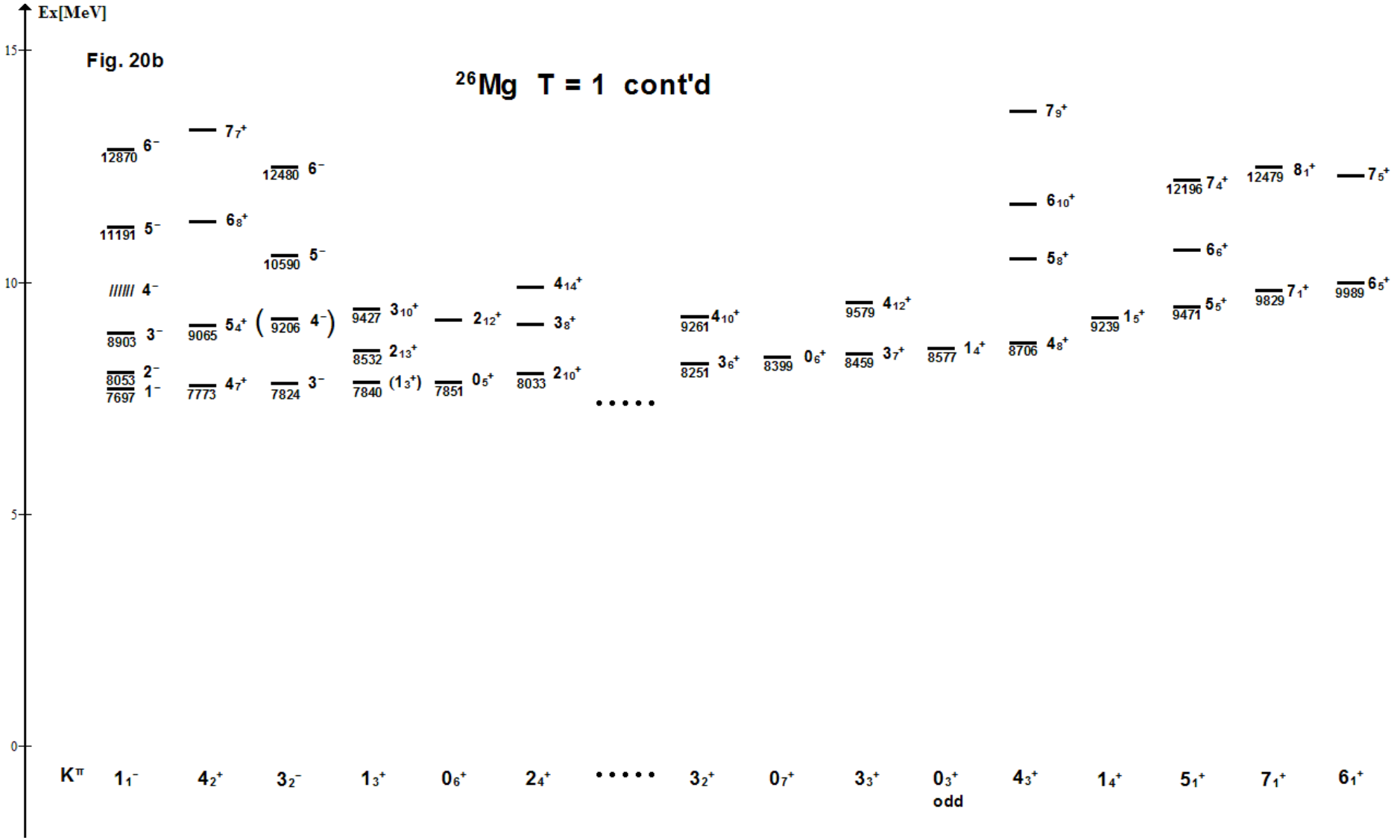
Ex[MeV]
Fig. 20b
^{26}Mg T = 1 cont'd
15
10
5
0
12870 6⁻
11191 5⁻
////// 4⁻
8903 3⁻
8053 2⁻
7697 1⁻
7⁺7
6⁺8
5⁺4
4⁺7
12480 6⁻
10590 5⁻
(9206 4⁻)
7824 3⁻
9427 3⁺10
8532 2⁺13
7840 (1⁺3)
2⁺12
0⁺5
7851
4⁺14
3⁺8
2⁺10
8033
9261 4⁺10
8251 3⁺6
8399 0⁺6
9579 4⁺12
8459 3⁺7
8577 1⁺4
7⁺9
6⁺10
5⁺8
8706 4⁺8
9239 1⁺5
12196 7⁺4
6⁺6
9471 5⁺5
12479 8⁺1
9829 7⁺1
7⁺5
9989 6⁺5
Kᵖ
1⁻1
4⁺2
3⁻2
1⁺3
0⁺6
2⁺4
3⁺2
0⁺7
3⁺3
0⁺3 odd
4⁺3
1⁺4
5⁺1
7⁺1
6⁺1

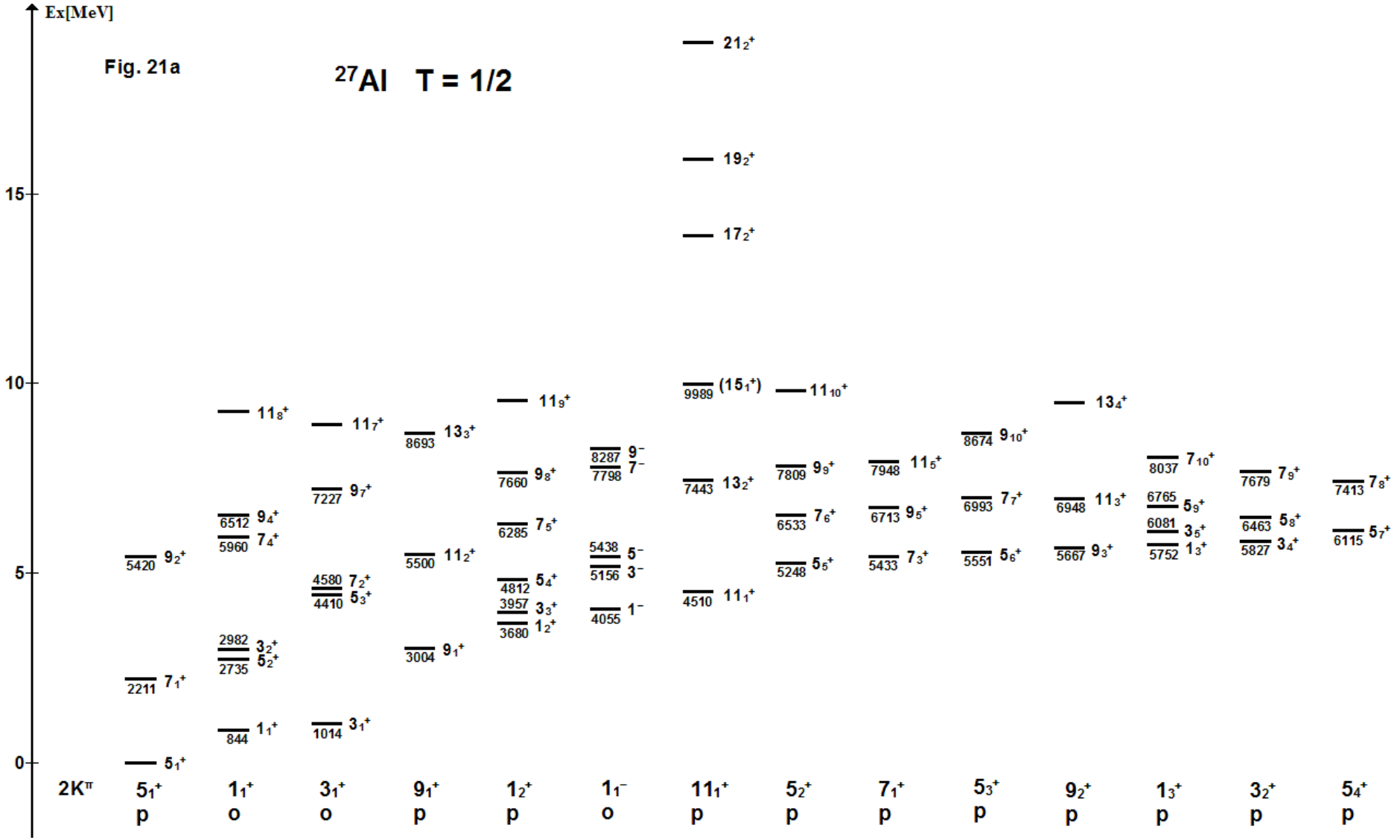
Ex[MeV]
Fig. 21a
^{27}Al T = 1/2
15
10
5
0
21_2^+
19_2^+
17_2^+
11_9^+
11_8^+
11_7^+
13_3^+
9_9^+
9_8^+
9_7^+
9_4^+
7_4^+
11_2^+
9_2^+
7_1^+
5_1^+
7_5^+
5_4^+
3_3^+
1_2^+
3_2^+
5_2^+
7_2^+
5_3^+
3_1^+
1_1^+
9_1^+
(15_1^+)
11_{10}^+
13_2^+
11_1^+
9_3^+
11_5^+
9_5^+
7_3^+
13_4^+
11_3^+
9_{10}^+
7_7^+
5_6^+
7_{10}^+
5_9^+
3_5^+
1_3^+
7_9^+
5_8^+
3_4^+
7_8^+
5_7^+
5_5^+
7_6^+
9_9^+
5^-
3^-
1^-
7^-
9^-
2K$^\pi$
5_1^+ p
1_1^+ o
3_1^+ o
9_1^+ p
1_2^+ p
1_1^- o
11_1^+ p
5_2^+ p
7_1^+ p
5_3^+ p
9_2^+ p
1_3^+ p
3_2^+ p
5_4^+ p

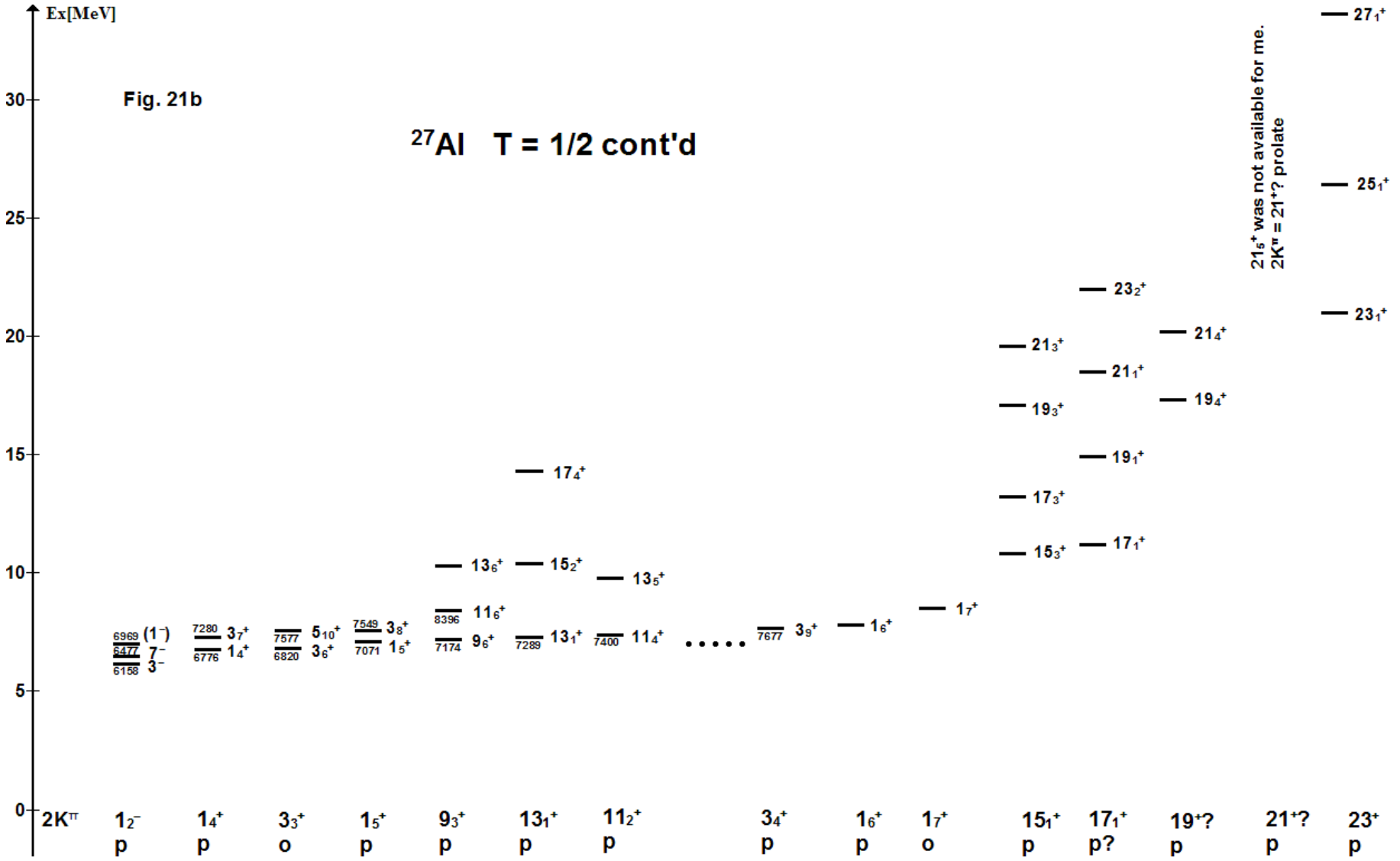
Ex[MeV]
Fig. 21b
27Al T = 1/2 cont'd
21₅⁺ was not available for me.
2Kᵀ = 21⁺? prolate
0
5
10
15
20
25
30
2Kᵀ
1₂⁻ p
1₄⁺ p
3₃⁺ o
1₅⁺ p
9₃⁺ p
13₁⁺ p
11₂⁺ p
3₄⁺ p
1₆⁺ p
1₇⁺ o
15₁⁺ p
17₁⁺ p?
19⁺? p
21⁺? p
23⁺ p
6969 (1⁻)
6477 7⁻
6158 3⁻
7280 3₇⁺
6776 1₄⁺
7577 5₁₀⁺
6820 3₆⁺
7549 3₈⁺
7071 1₅⁺
8396 11₆⁺
7174 9₆⁺
7289 13₁⁺
7400 11₄⁺
7677 3₉⁺
13₆⁺
15₂⁺
13₅⁺
17₄⁺
15₃⁺
17₃⁺
19₃⁺
21₃⁺
17₁⁺
19₁⁺
21₁⁺
23₂⁺
19₄⁺
21₄⁺
23₁⁺
25₁⁺
27₁⁺

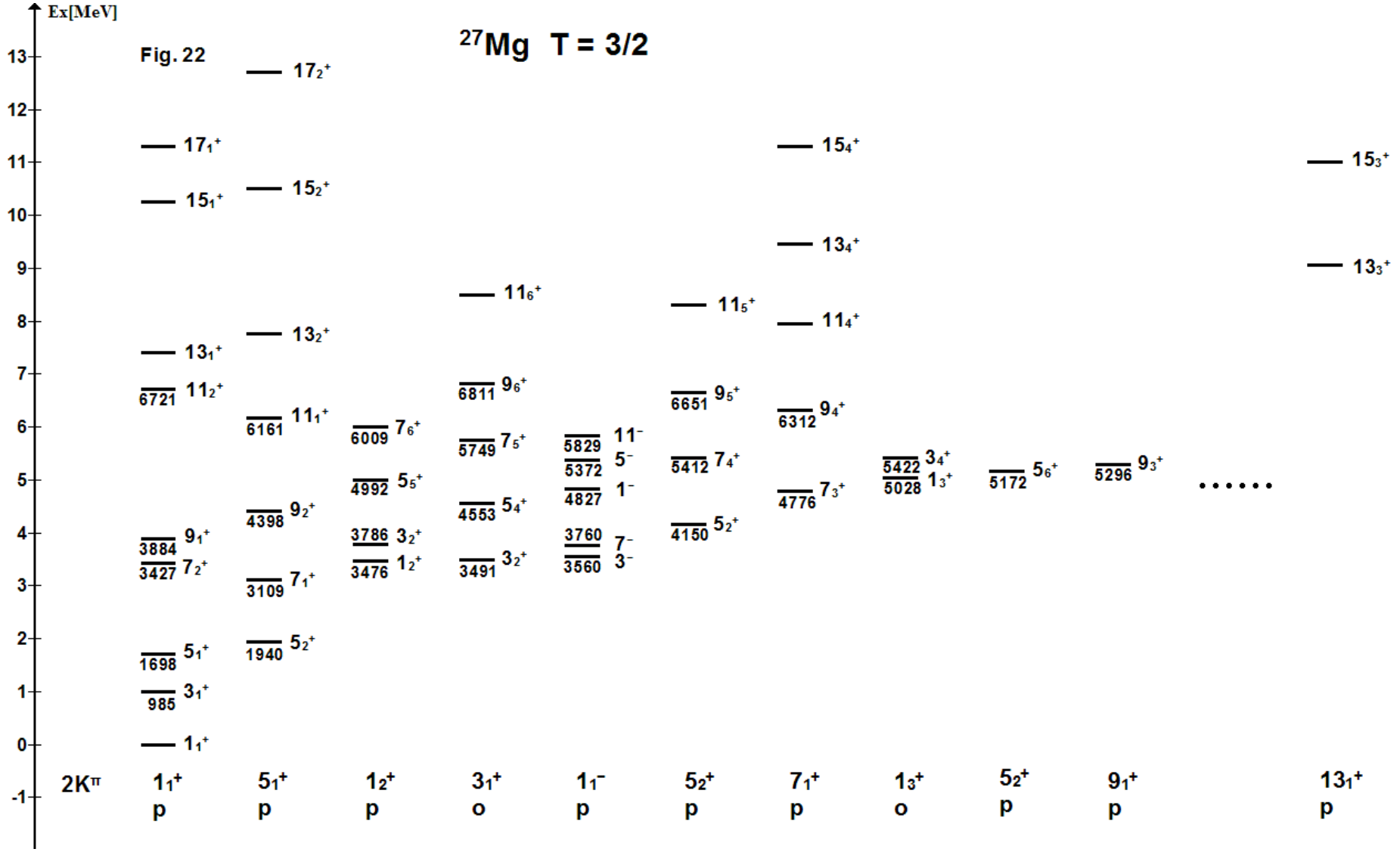
Ex[MeV]
Fig. 22
27Mg T = 3/2
13
12
11
10
9
8
7
6
5
4
3
2
1
0
-1
17₂⁺
17₁⁺
15₁⁺
15₂⁺
13₂⁺
13₁⁺
11₂⁺
6721
11₁⁺
6161
9₁⁺
3884
7₂⁺
3427
9₂⁺
4398
7₁⁺
3109
5₁⁺
1698
5₂⁺
1940
3₁⁺
985
1₁⁺
11₆⁺
9₆⁺
6811
7₅⁺
5749
5₄⁺
4553
3₂⁺
3491
11⁻
5829
5⁻
5372
1⁻
4827
3760
7⁻
3560
3⁻
11₅⁺
9₅⁺
6651
7₄⁺
5412
5₂⁺
4150
7₆⁺
6009
5₅⁺
4992
3₂⁺
3786
1₂⁺
3476
15₄⁺
13₄⁺
11₄⁺
9₄⁺
6312
7₃⁺
4776
3₄⁺
5422
1₃⁺
5028
5₆⁺
5172
9₃⁺
5296
15₃⁺
13₃⁺
2Kπ
1₁⁺ p
5₁⁺ p
1₂⁺ p
3₁⁺ o
1₁⁻ p
5₂⁺ p
7₁⁺ p
1₃⁺ o
5₂⁺ p
9₁⁺ p
13₁⁺ p

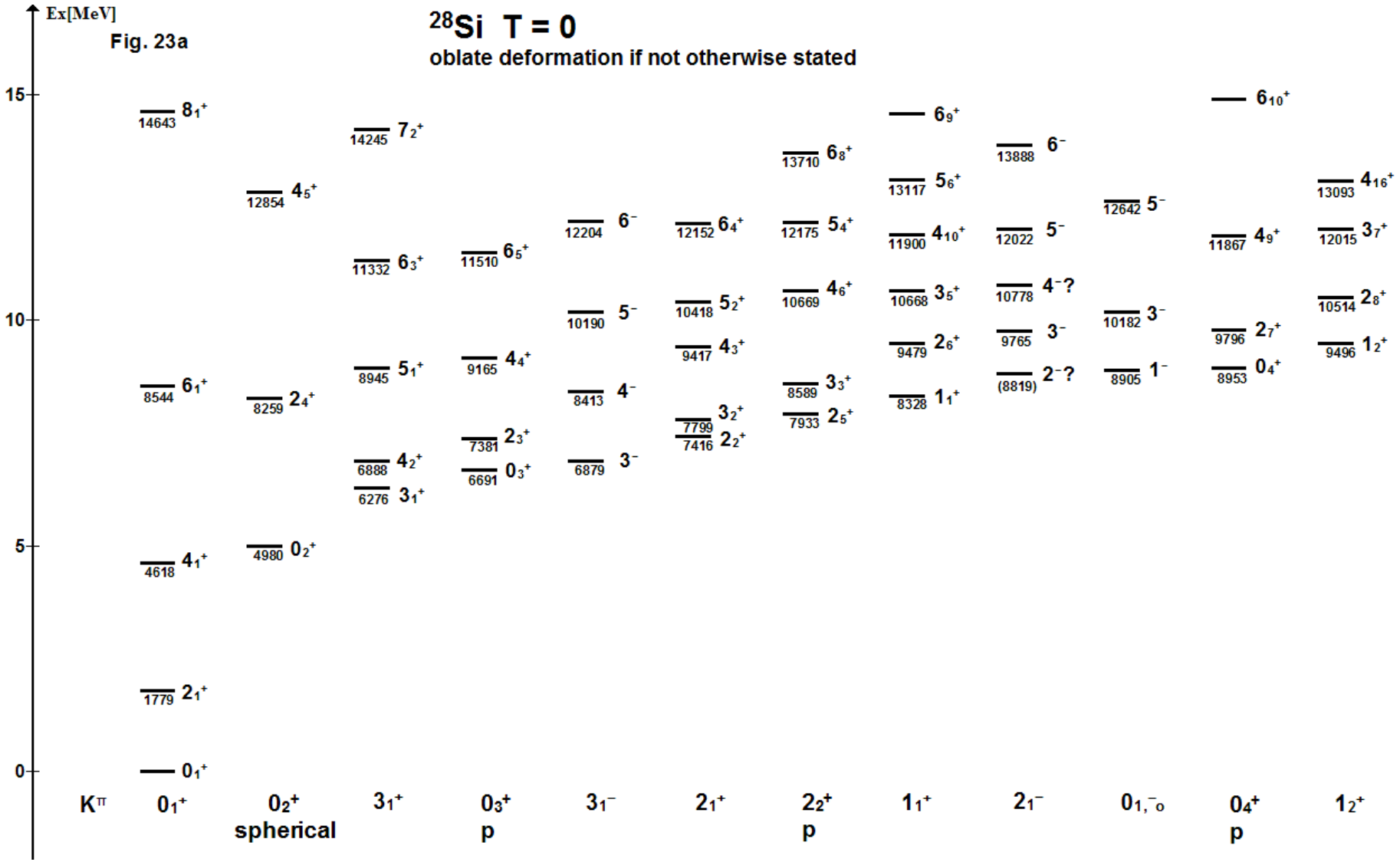
Ex[MeV]
Fig. 23a
28Si T = 0
oblate deformation if not otherwise stated
15
10
5
0
14643 8₁⁺
8544 6₁⁺
4618 4₁⁺
1779 2₁⁺
0 0₁⁺
12854 4₅⁺
8259 2₄⁺
4980 0₂⁺
14245 7₂⁺
11332 6₃⁺
8945 5₁⁺
6888 4₂⁺
6276 3₁⁺
11510 6₅⁺
9165 4₄⁺
7381 2₃⁺
6691 0₃⁺
12204 6⁻
10190 5⁻
8413 4⁻
6879 3⁻
12152 6₄⁺
10418 5₂⁺
9417 4₃⁺
7799 3₂⁺
7416 2₂⁺
13710 6₈⁺
12175 5₄⁺
10669 4₆⁺
8589 3₃⁺
7933 2₅⁺
13117 6₉⁺
11900 5₆⁺
10668 4₁₀⁺
9479 3₅⁺
8328 2₆⁺
1₁⁺
13888 6⁻
12022 5⁻
10778 4⁻?
9765 3⁻
(8819) 2⁻?
12642 5⁻
10182 3⁻
8905 1⁻
11867 6₁₀⁺
9796 4₉⁺
8953 2₇⁺
0₄⁺
13093 4₁₆⁺
12015 3₇⁺
10514 2₈⁺
9496 1₂⁺
Kᵖ
0₁⁺
0₂⁺
spherical
3₁⁺
0₃⁺
p
3₁⁻
2₁⁺
2₂⁺
p
1₁⁺
2₁⁻
0₁,⁻₀
0₄⁺
p
1₂⁺

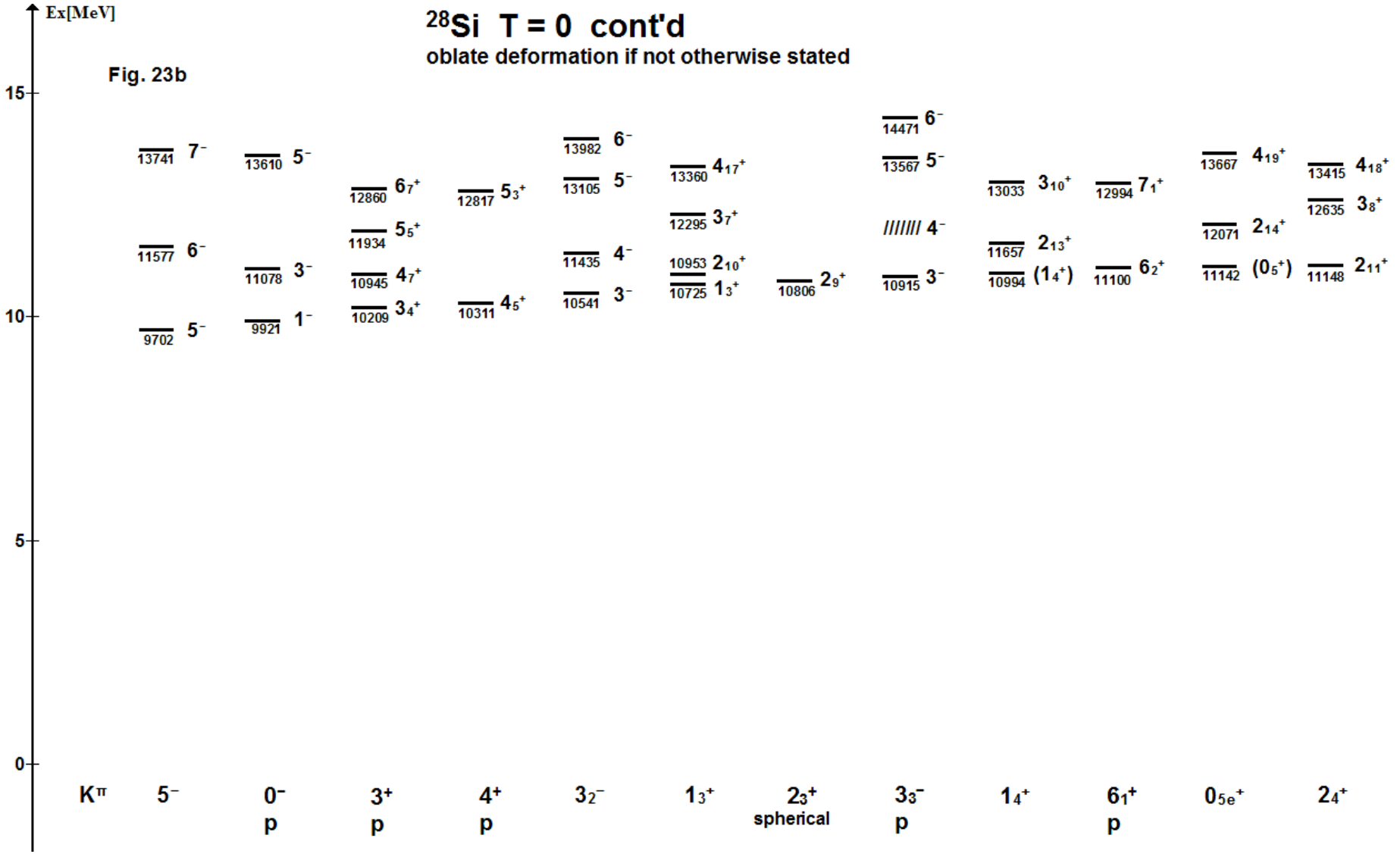
Ex[MeV]
28Si T = 0 cont'd
oblate deformation if not otherwise stated
Fig. 23b
15
10
5
0
13741 7⁻
11577 6⁻
9702 5⁻
13610 5⁻
11078 3⁻
9921 1⁻
12860 6₇⁺
11934 5₅⁺
10945 4₇⁺
10209 3₄⁺
12817 5₃⁺
10311 4₅⁺
13982 6⁻
13105 5⁻
11435 4⁻
10541 3⁻
13360 4₁₇⁺
12295 3₇⁺
10953 2₁₀⁺
10725 1₃⁺
10806 2₉⁺
14471 6⁻
13567 5⁻
////// 4⁻
10915 3⁻
13033 3₁₀⁺
11657 2₁₃⁺
10994 (1₄⁺)
12994 7₁⁺
11100 6₂⁺
13667 4₁₉⁺
12071 2₁₄⁺
11142 (0₅⁺)
13415 4₁₈⁺
12635 3₈⁺
11148 2₁₁⁺
Kπ
5⁻
0⁻ p
3⁺ p
4⁺ p
3₂⁻
1₃⁺
2₃⁺ spherical
3₃⁻ p
1₄⁺
6₁⁺ p
0₅e⁺
2₄⁺

^{28}Si T = 0 cont'd

oblate deformation if not otherwise stated

Fig. 23c

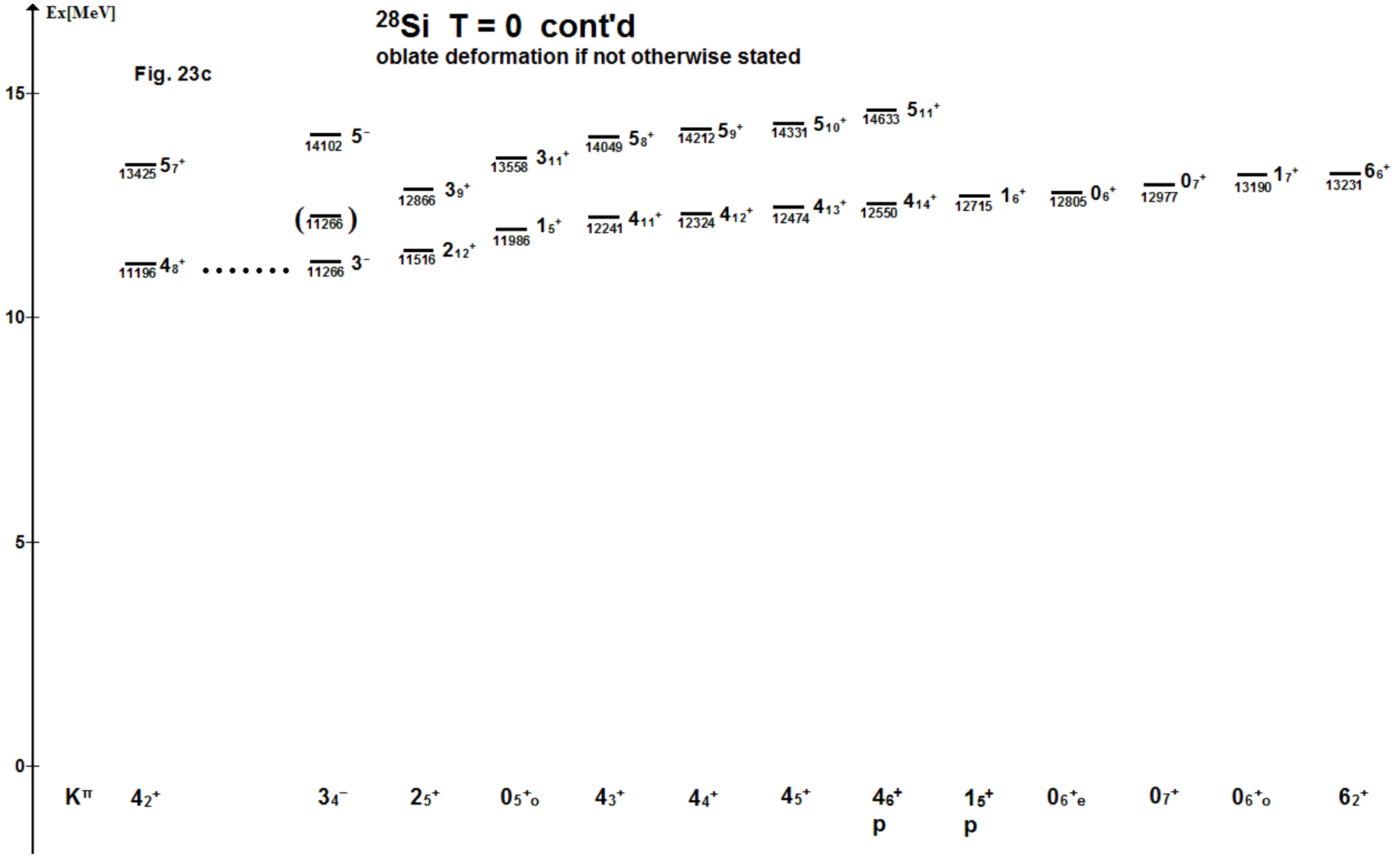

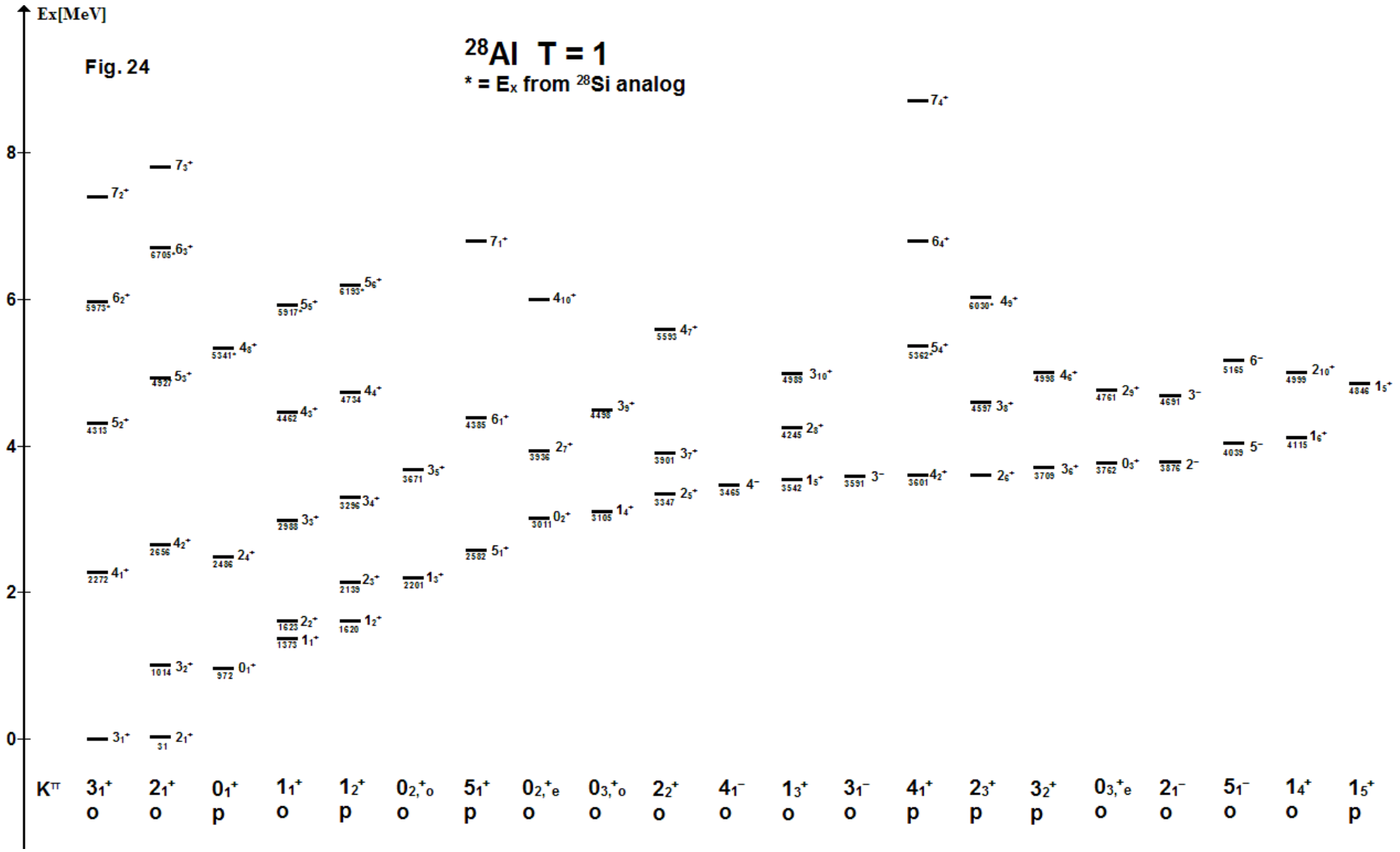
Ex[MeV]
Fig. 24
28Al T = 1
* = Ex from 28Si analog
8
6
4
2
0
Kπ
31+ o
21+ o
01+ p
11+ o
12+ p
02,+o o
51+ p
02,+e o
03,+o o
22+ o
41− o
13+ o
31− o
41+ p
23+ p
32+ p
03,+e o
21− o
51− o
14+ o
15+ p
7322+
6705 63+
5973* 62+
5927 55+
6195* 56+
5341* 48+
4927 53+
4313 52+
4462 43+
4734 44+
3671 35+
2656 42+
2496 24+
2272 41+
2988 33+
3296 34+
2139 23+
2201 13+
1625 22+
1373 11+
1620 12+
1014 32+
972 01+
31 21+
7191+
4385 61+
2582 51+
3936 27+
3011 02+
4498 39+
3105 14+
5593 47+
3901 37+
3347 25+
3465 4−
4589 310+
4245 28+
3542 15+
3591 3−
7241+
5362 54+
3601 42+
6030* 49+
4597 38+
2617+
4958 46+
3709 36+
4761 29+
3762 03+
4691 3−
3876 2−
5165 6−
4039 5−
4999 210+
4115 16+
4846 15+

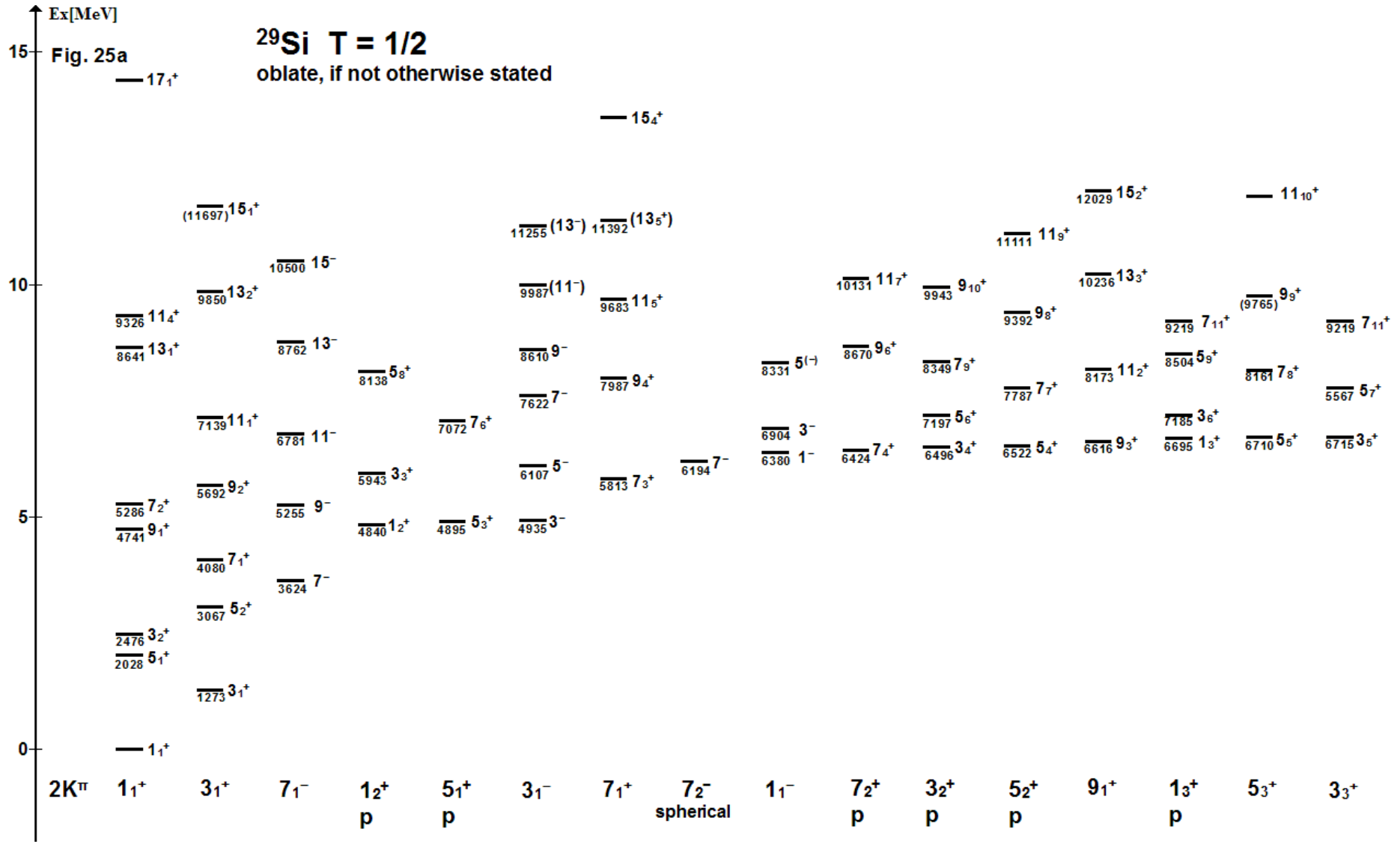
Ex[MeV]
Fig. 25a
29Si T = 1/2
oblate, if not otherwise stated
15
10
5
0
17 1+
15 4+
(11697) 15 1+
12029 15 2+
11 10+
10500 15−
11255 (13−)
11392 (13 5+)
11111 11 9+
10131 11 7+
10236 13 3+
9850 13 2+
9987 (11−)
9683 11 5+
9943 9 10+
9392 9 8+
(9765) 9 9+
9219 7 11+
9326 11 4+
8762 13−
8610 9−
8670 9 6+
8349 7 9+
8504 5 9+
8641 13 1+
8138 5 8+
7622 7−
7987 9 4+
7787 7 7+
8173 11 2+
8161 7 8+
7139 11 1+
7072 7 6+
8331 5(−)
7197 5 6+
7185 3 6+
5567 5 7+
6781 11−
6904 3−
6424 7 4+
6616 9 3+
6695 13+
6715 3 5+
5943 3 3+
6107 5−
6194 7−
6380 1−
6496 3 4+
6522 5 4+
6710 5 5+
5692 9 2+
5813 7 3+
5286 7 2+
5255 9−
4741 9 1+
4840 12+
4895 5 3+
4935 3−
4080 7 1+
3624 7−
3067 5 2+
2476 3 2+
2028 5 1+
1273 3 1+
1 1+
2Kπ
1 1+
3 1+
7 1−
1 2+
p
5 1+
p
3 1−
7 1+
7 2−
spherical
1 1−
7 2+
p
3 2+
p
5 2+
p
9 1+
1 3+
p
5 3+
3 3+

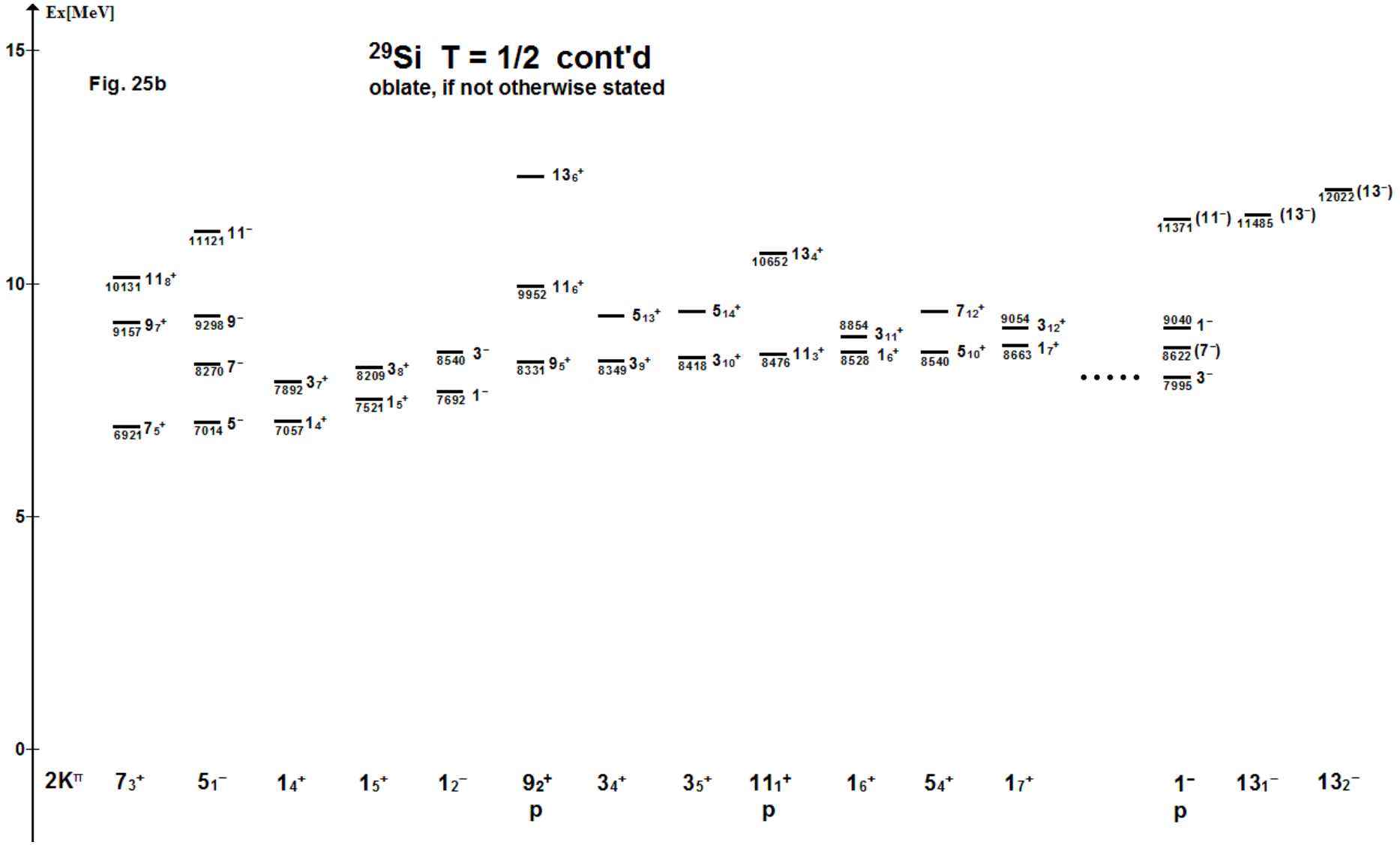
Ex[MeV]
15
10
5
0
29Si T = 1/2 cont'd
oblate, if not otherwise stated
Fig. 25b
10131 11 8+
9157 9 7+
6921 7 5+
11121 11−
9298 9−
8270 7−
7014 5−
7892 3 7+
7057 1 4+
8209 3 8+
7521 1 5+
8540 3−
7692 1−
13 6+
9952 11 6+
8331 9 5+
5 13+
8349 3 9+
5 14+
8418 3 10+
10652 13 4+
8476 11 3+
8854 3 11+
8528 1 6+
7 12+
8540 5 10+
9054 3 12+
8663 1 7+
11371 (11−)
11485 (13−)
12022 (13−)
9040 1−
8622 (7−)
7995 3−
2Kπ
7 3+
5 1−
1 4+
1 5+
1 2−
9 2+
p
3 4+
3 5+
11 1+
p
1 6+
5 4+
1 7+
1−
p
13 1−
13 2−

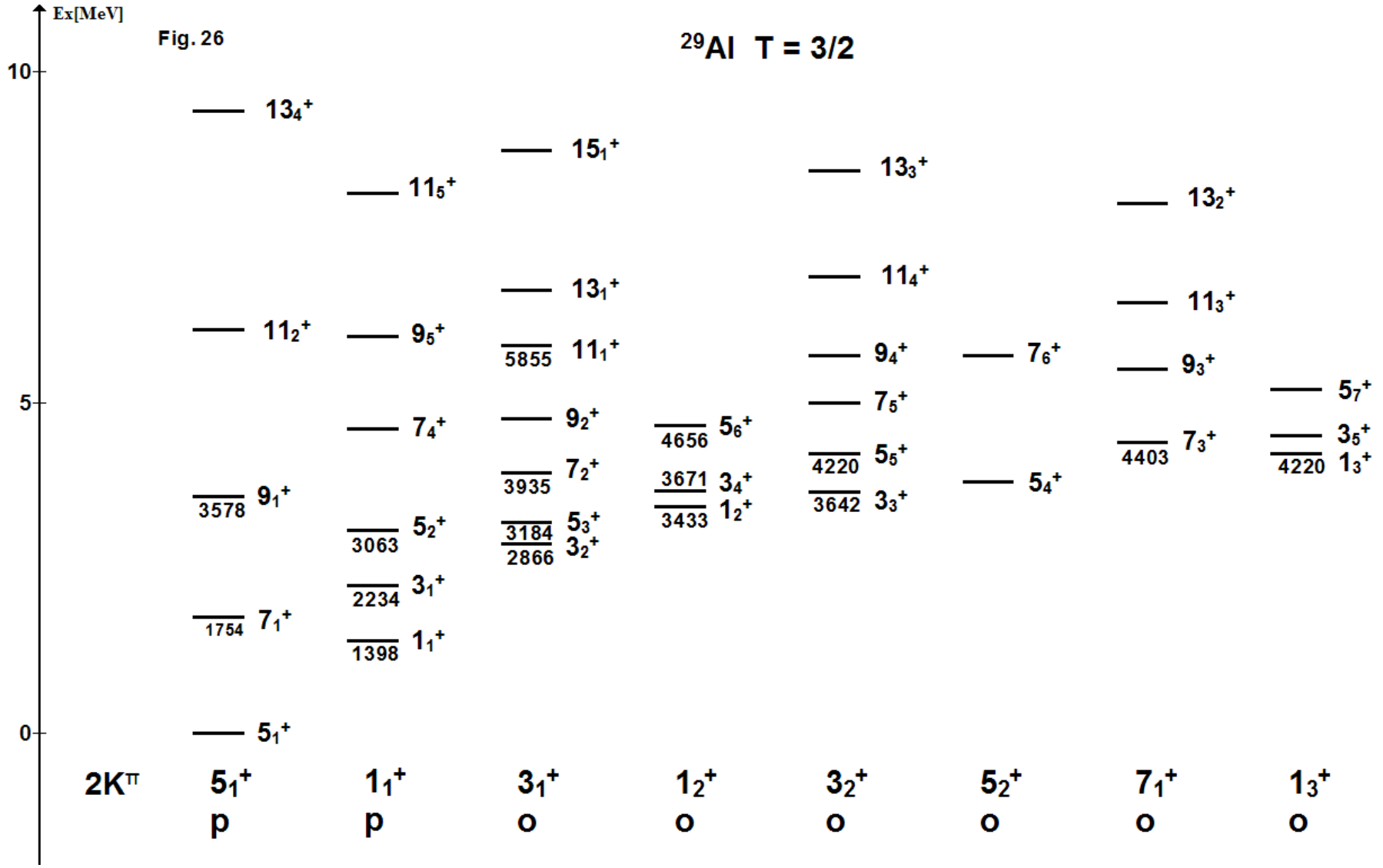
Ex[MeV]
Fig. 26
^{29}Al T = 3/2
10
5
0
13_4^+
11_5^+
15_1^+
13_3^+
13_2^+
11_2^+
9_5^+
13_1^+
11_4^+
11_3^+
9_4^+
7_6^+
9_3^+
5_7^+
7_5^+
7_4^+
9_2^+
5_6^+
3_5^+
9_1^+
3578
5_2^+
3063
7_2^+
3935
4656
5_5^+
4220
7_3^+
4403
4220
1_3^+
5_4^+
3_4^+
3671
5_3^+
3184
3_1^+
2234
7_1^+
1754
1_1^+
1398
3_2^+
2866
1_2^+
3433
3_3^+
3642
5_1^+
2K$^\pi$
5_1^+ p
1_1^+ p
3_1^+ o
1_2^+ o
3_2^+ o
5_2^+ o
7_1^+ o
1_3^+ o

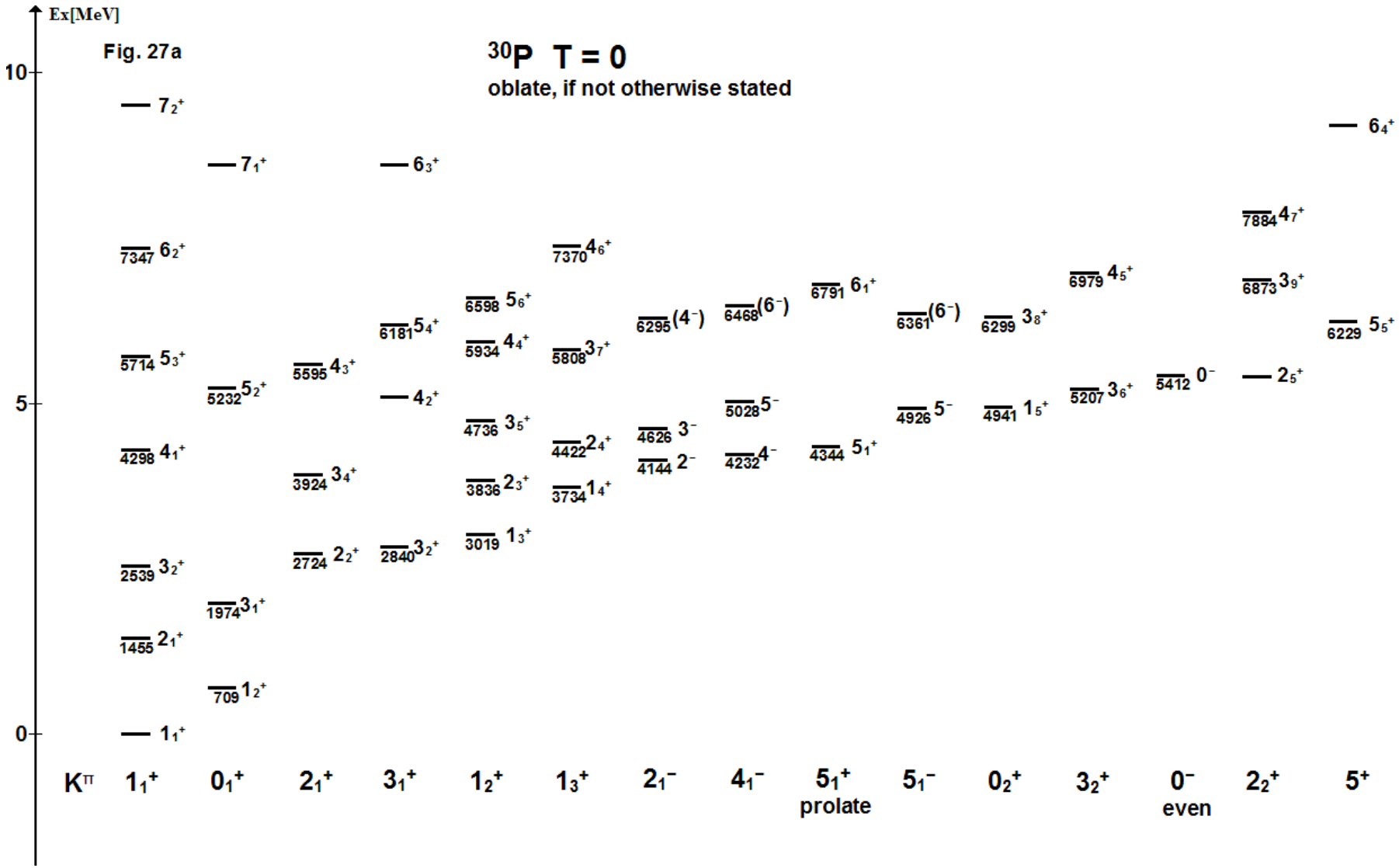
Ex[MeV]
Fig. 27a
30P T = 0
oblate, if not otherwise stated
10
5
0
7₂⁺
7₁⁺
6₃⁺
6₄⁺
7884 4₇⁺
7347 6₂⁺
7370 4₆⁺
6598 5₆⁺
6791 6₁⁺
6979 4₅⁺
6873 3₉⁺
6295 (4⁻)
6468 (6⁻)
6361 (6⁻)
6299 3₈⁺
6229 5₅⁺
5714 5₃⁺
5232 5₂⁺
5595 4₃⁺
6181 5₄⁺
5934 4₄⁺
5808 3₇⁺
5028 5⁻
5207 3₆⁺
5412 0⁻
2₅⁺
4298 4₁⁺
3924 3₄⁺
4736 3₅⁺
4422 2₄⁺
4626 3⁻
4926 5⁻
4941 1₅⁺
4232 4⁻
4344 5₁⁺
4144 2⁻
3836 2₃⁺
3734 1₄⁺
2539 3₂⁺
2724 2₂⁺
2840 3₂⁺
3019 1₃⁺
1974 3₁⁺
1455 2₁⁺
709 1₂⁺
1₁⁺
Kᵖⁱ
1₁⁺
0₁⁺
2₁⁺
3₁⁺
1₂⁺
1₃⁺
2₁⁻
4₁⁻
5₁⁺
prolate
5₁⁻
0₂⁺
3₂⁺
0⁻
even
2₂⁺
5⁺

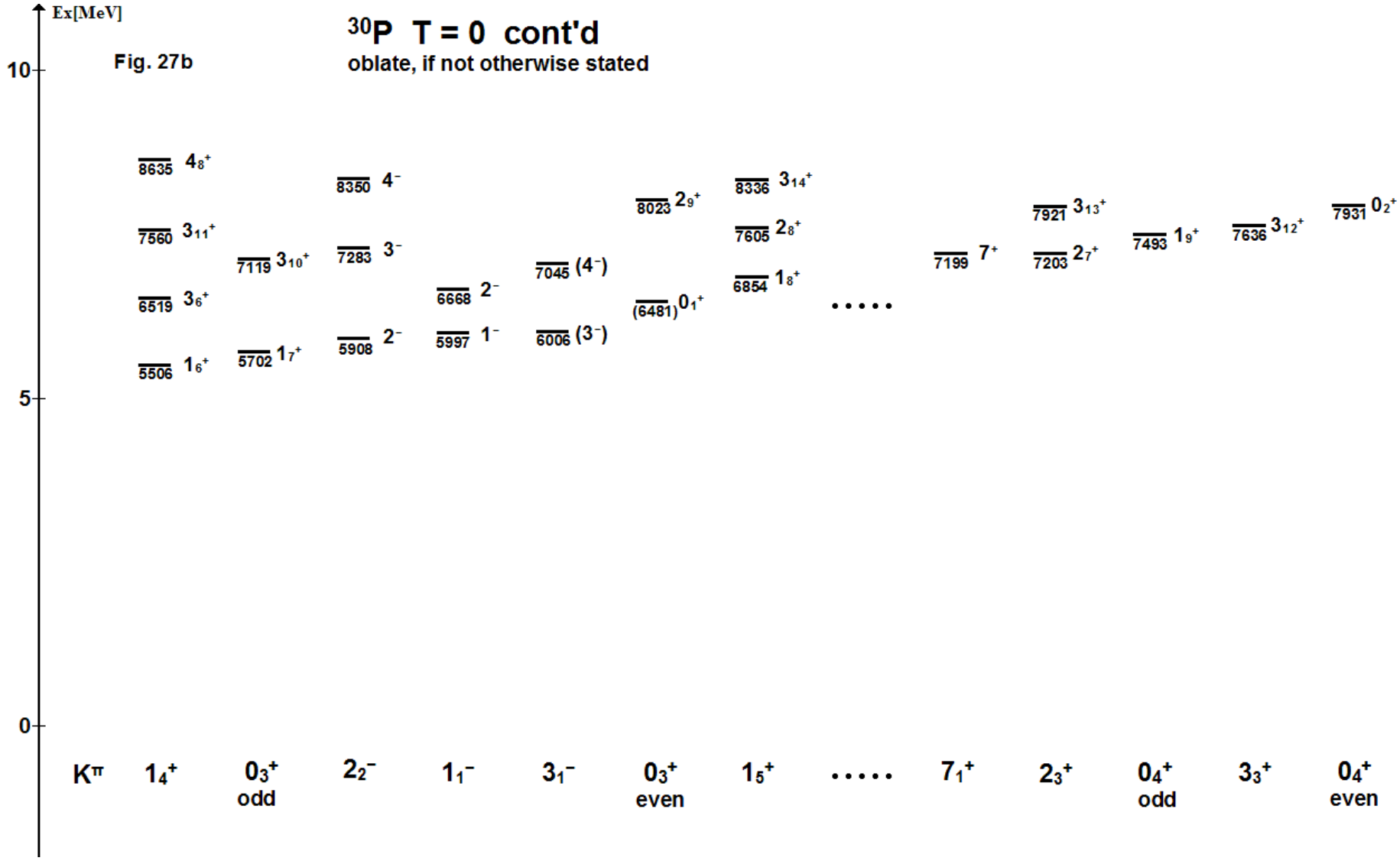
Ex[MeV]
30P T = 0 cont'd
Fig. 27b
oblate, if not otherwise stated
10
5
0
8635 4₈⁺
7560 3₁₁⁺
6519 3₆⁺
5506 1₆⁺
7119 3₁₀⁺
5702 1₇⁺
8350 4⁻
7283 3⁻
5908 2⁻
6668 2⁻
5997 1⁻
7045 (4⁻)
6006 (3⁻)
8023 2₉⁺
(6481) 0₁⁺
8336 3₁₄⁺
7605 2₈⁺
6854 1₈⁺
7199 7⁺
7921 3₁₃⁺
7203 2₇⁺
7493 1₉⁺
7636 3₁₂⁺
7931 0₂⁺
Kπ
1₄⁺
0₃⁺ odd
2₂⁻
1₁⁻
3₁⁻
0₃⁺ even
1₅⁺
7₁⁺
2₃⁺
0₄⁺ odd
3₃⁺
0₄⁺ even

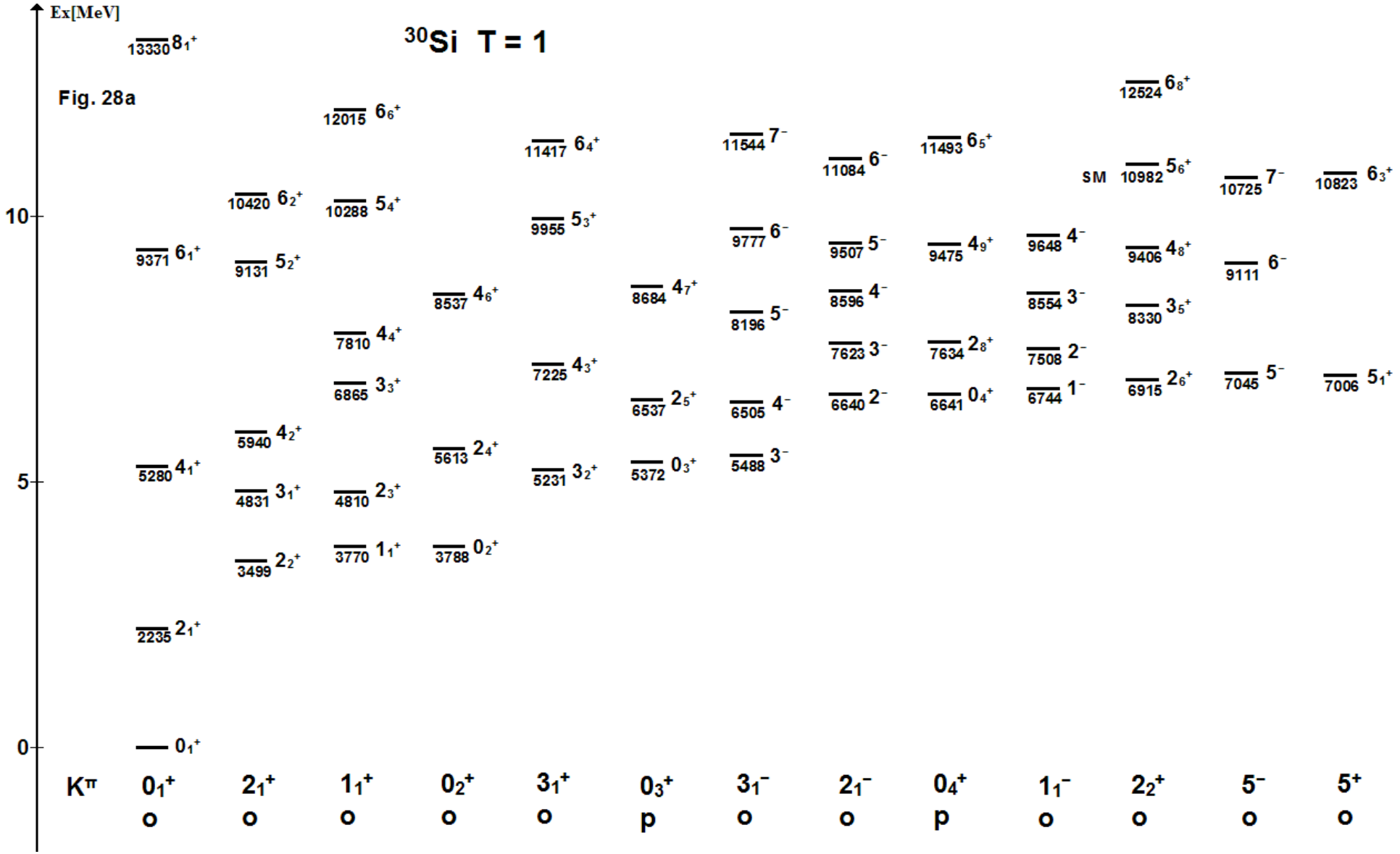
Ex[MeV]
^{30}Si T = 1
Fig. 28a
SM
13330 8$_1^+$
12524 6$_8^+$
12015 6$_6^+$
11544 7$^-$
11493 6$_5^+$
11417 6$_4^+$
11084 6$^-$
10982 5$_6^+$
10823 6$_3^+$
10725 7$^-$
10420 6$_2^+$
10288 5$_4^+$
9955 5$_3^+$
9777 6$^-$
9648 4$^-$
9507 5$^-$
9475 4$_9^+$
9406 4$_8^+$
9371 6$_1^+$
9131 5$_2^+$
9111 6$^-$
8684 4$_7^+$
8596 4$^-$
8554 3$^-$
8537 4$_6^+$
8330 3$_5^+$
8196 5$^-$
7810 4$_4^+$
7634 2$_8^+$
7623 3$^-$
7508 2$^-$
7225 4$_3^+$
7045 5$^-$
7006 5$_1^+$
6915 2$_6^+$
6865 3$_3^+$
6744 1$^-$
6641 0$_4^+$
6640 2$^-$
6537 2$_5^+$
6505 4$^-$
5613 2$_4^+$
5488 3$^-$
5372 0$_3^+$
5280 4$_1^+$
5231 3$_2^+$
4831 3$_1^+$
4810 2$_3^+$
3788 0$_2^+$
3770 1$_1^+$
3499 2$_2^+$
2235 2$_1^+$
0 0$_1^+$
10
5
0
K$^\pi$ 0$_1^+$ 2$_1^+$ 1$_1^+$ 0$_2^+$ 3$_1^+$ 0$_3^+$ 3$_1^-$ 2$_1^-$ 0$_4^+$ 1$_1^-$ 2$_2^+$ 5$^-$ 5$^+$
o o o o o p o o p o o o o

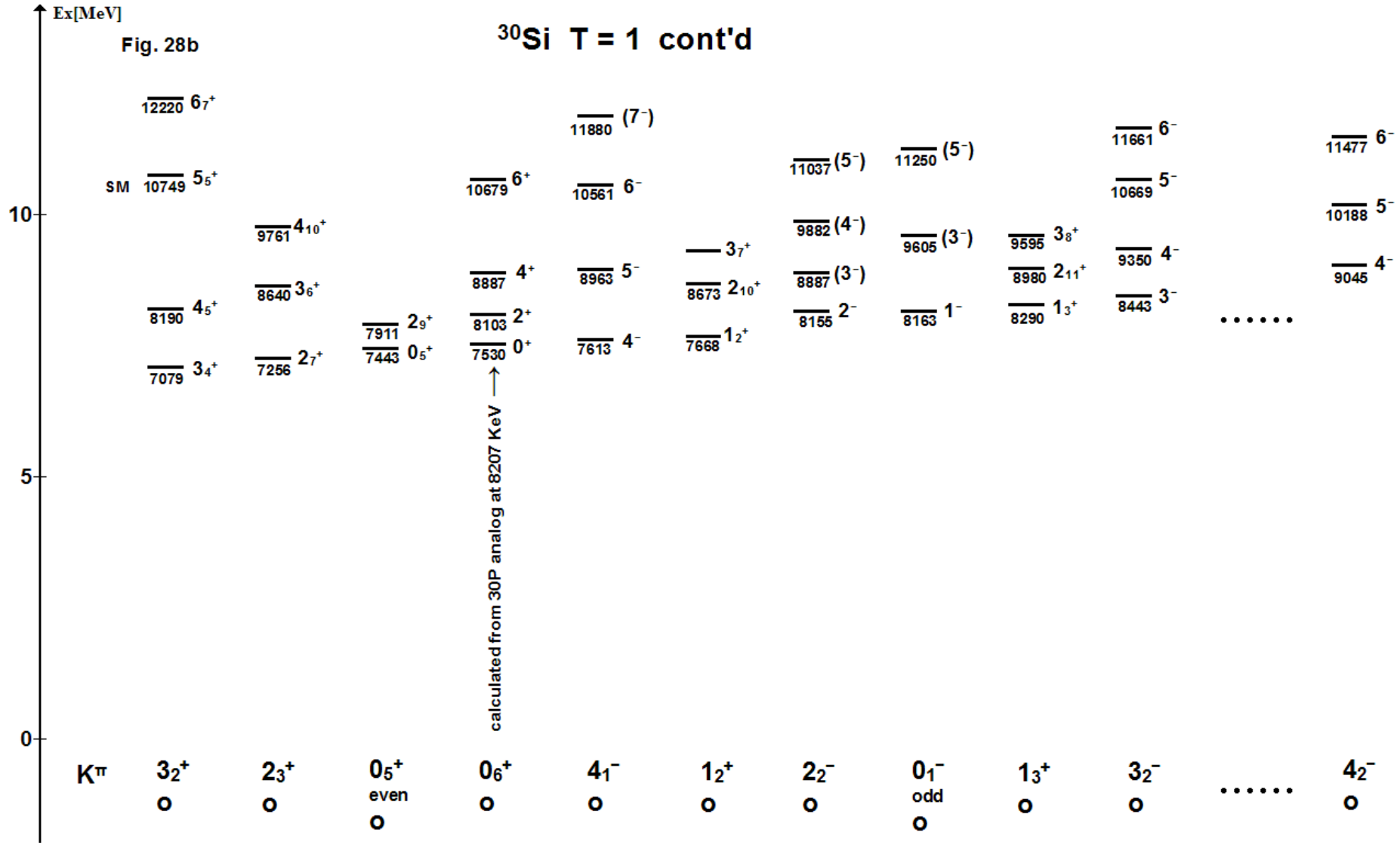
Ex[MeV]
Fig. 28b
30Si T = 1 cont'd
10
5
0
SM
12220 6⁷⁺
10749 5⁵⁺
8190 4⁵⁺
7079 3⁴⁺
9761 4¹⁰⁺
8640 3⁶⁺
7256 2⁷⁺
7911 2⁹⁺
7443 0⁵⁺
10679 6⁺
8887 4⁺
8103 2⁺
7530 0⁺
calculated from 30P analog at 8207 KeV
11880 (7⁻)
10561 6⁻
8963 5⁻
7613 4⁻
8673 2¹⁰⁺
7668 1²⁺
11037 (5⁻)
9882 (4⁻)
8887 (3⁻)
8155 2⁻
11250 (5⁻)
9605 (3⁻)
8163 1⁻
9595 3⁸⁺
8980 2¹¹⁺
8290 1³⁺
11661 6⁻
10669 5⁻
9350 4⁻
8443 3⁻
11477 6⁻
10188 5⁻
9045 4⁻
Kπ
3₂⁺
2₃⁺
0₅⁺ even
0₆⁺
4₁⁻
1₂⁺
2₂⁻
0₁⁻ odd
1₃⁺
3₂⁻
4₂⁻

Fig. 29

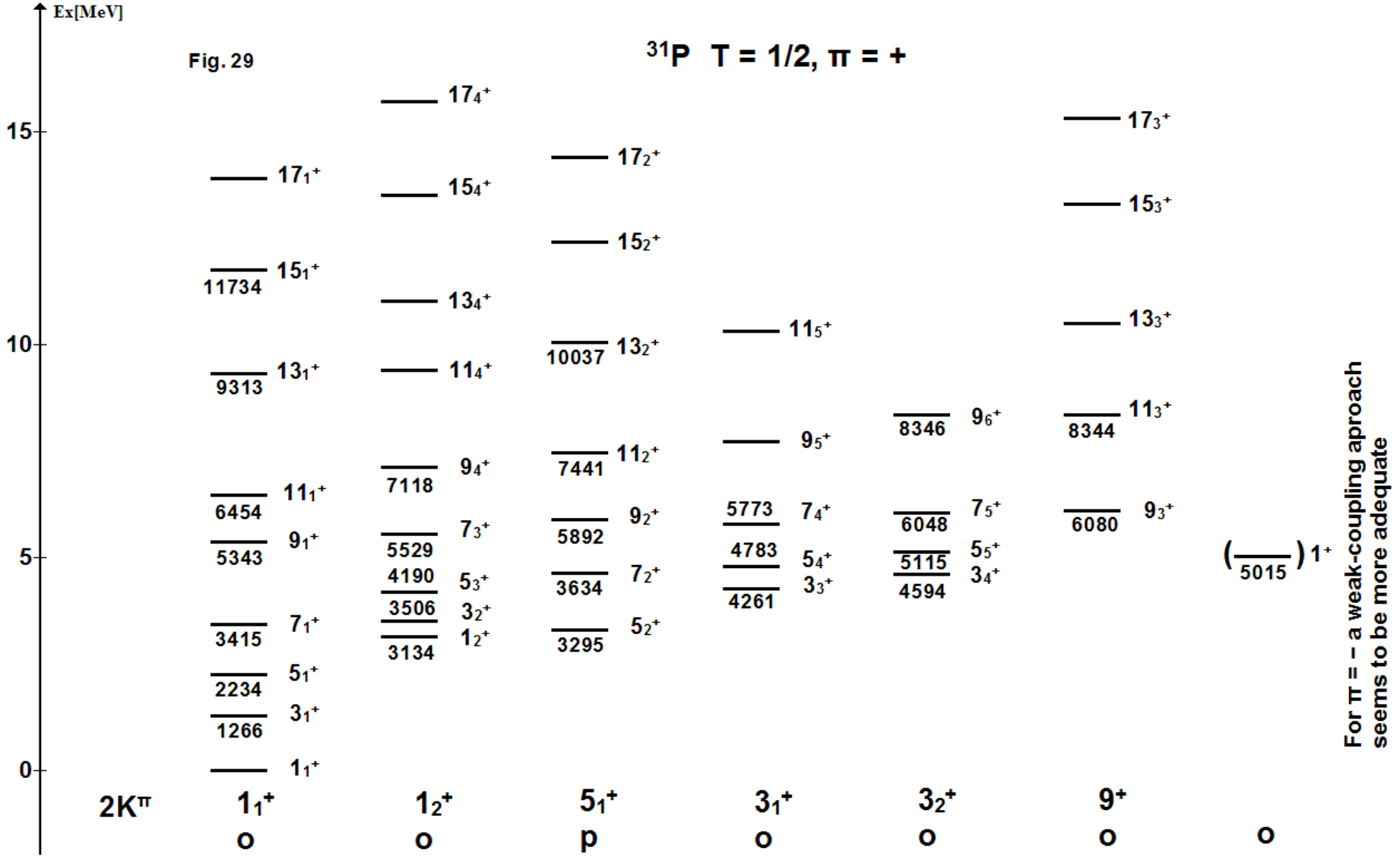
^{31}P T = 1/2, π = +
Ex[MeV]
15
10
5
0
17_4^+
17_1^+
15_4^+
15_1^+
11734
15_2^+
13_4^+
13_1^+
9313
11_4^+
17_2^+
17_3^+
15_3^+
13_3^+
10037
13_2^+
11_5^+
11_1^+
6454
9_4^+
7118
11_2^+
7441
9_5^+
8346
9_6^+
11_3^+
8344
9_1^+
5343
7_3^+
5529
9_2^+
5892
5773
7_4^+
6048
7_5^+
6080
9_3^+
4190
5_3^+
3506
3_2^+
7_1^+
3415
7_2^+
3634
4783
5_4^+
3_3^+
4261
5115
5_5^+
3_4^+
4594
5_1^+
2234
5_2^+
3295
3_1^+
1266
1_2^+
3134
1_1^+
(5015) 1^+
For π = – a weak-coupling aproach seems to be more adequate
2K$^\pi$
1_1^+ o
1_2^+ o
5_1^+ p
3_1^+ o
3_2^+ o
9^+ o
o

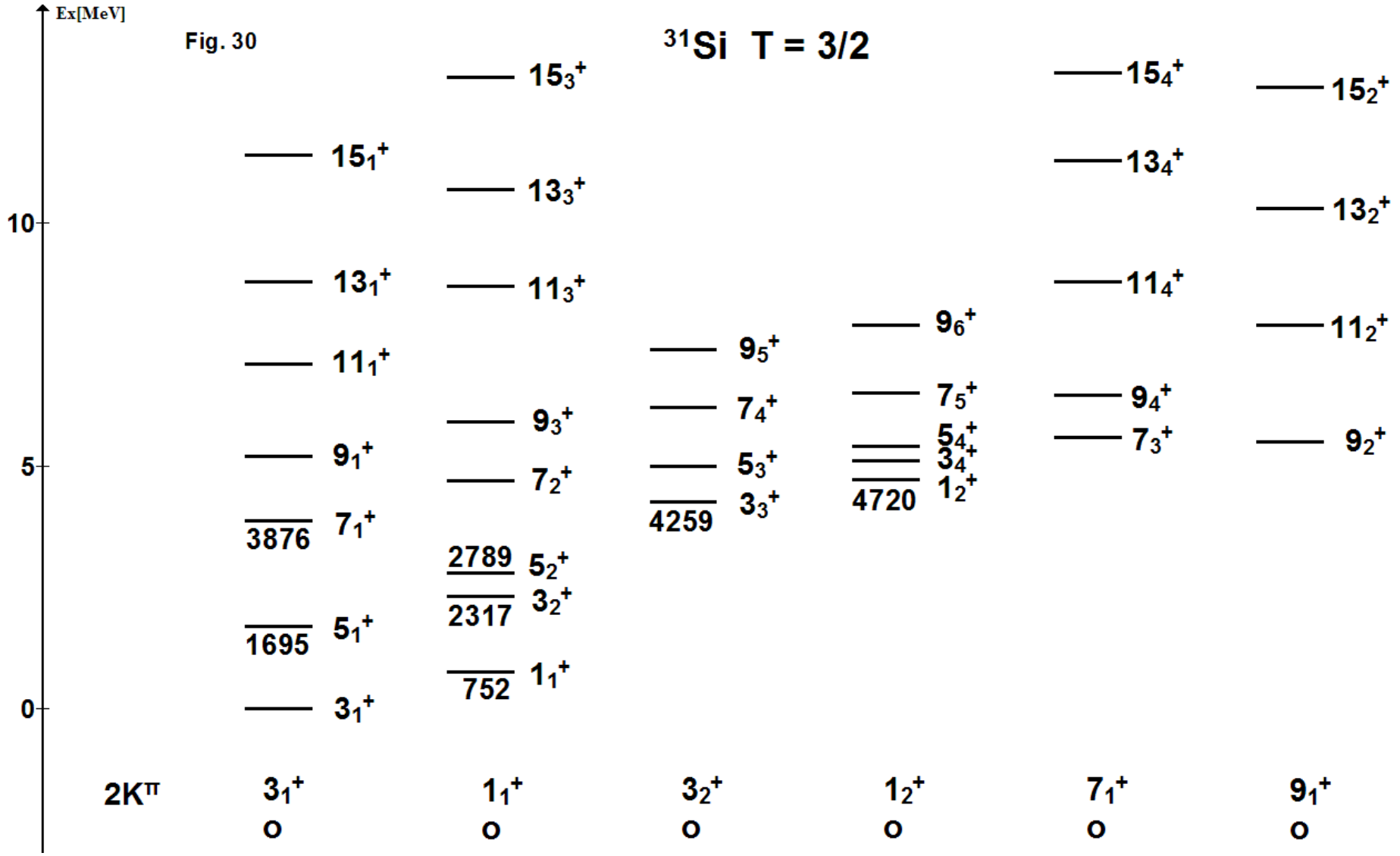
Ex[MeV]
Fig. 30
31Si T = 3/2
10
5
0
15₃⁺
15₁⁺
13₃⁺
13₁⁺
11₃⁺
11₁⁺
9₃⁺
9₁⁺
7₂⁺
3876
7₁⁺
2789
5₂⁺
2317
3₂⁺
1695
5₁⁺
752
1₁⁺
3₁⁺
9₆⁺
9₅⁺
7₅⁺
7₄⁺
5₄⁺
3₄⁺
5₃⁺
4720
1₂⁺
4259
3₃⁺
15₄⁺
15₂⁺
13₄⁺
13₂⁺
11₄⁺
11₂⁺
9₄⁺
7₃⁺
9₂⁺
2Kπ
3₁⁺
1₁⁺
3₂⁺
1₂⁺
7₁⁺
9₁⁺

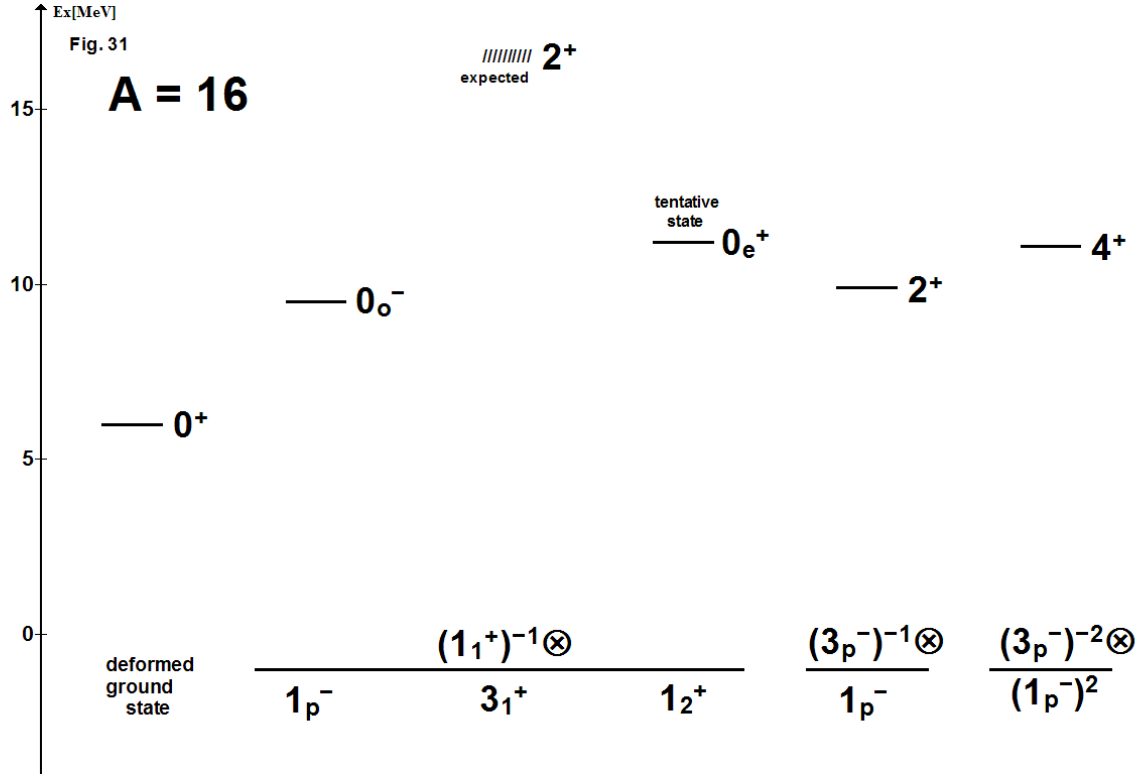
Ex[MeV]
Fig. 31
A = 16
15
10
5
0
2+
expected
tentative
state
0e+
4+
0o−
2+
0+
deformed
ground
state
(1₁+)−1⊗
1p−
3₁+
1₂+
(3p−)−1⊗
1p−
(3p−)−2⊗
(1p−)2

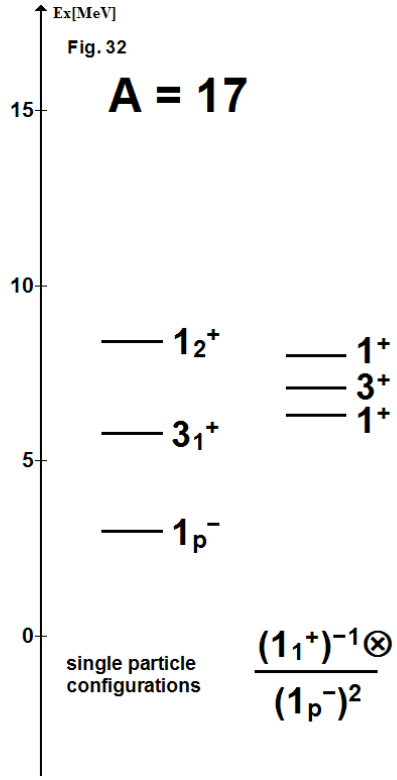
Ex[MeV]
Fig. 32
A = 17
15
10
5
0
1₂+
3₁+
1p−
1+
3+
1+
single particle
configurations
(1₁+)−1⊗
(1p−)2

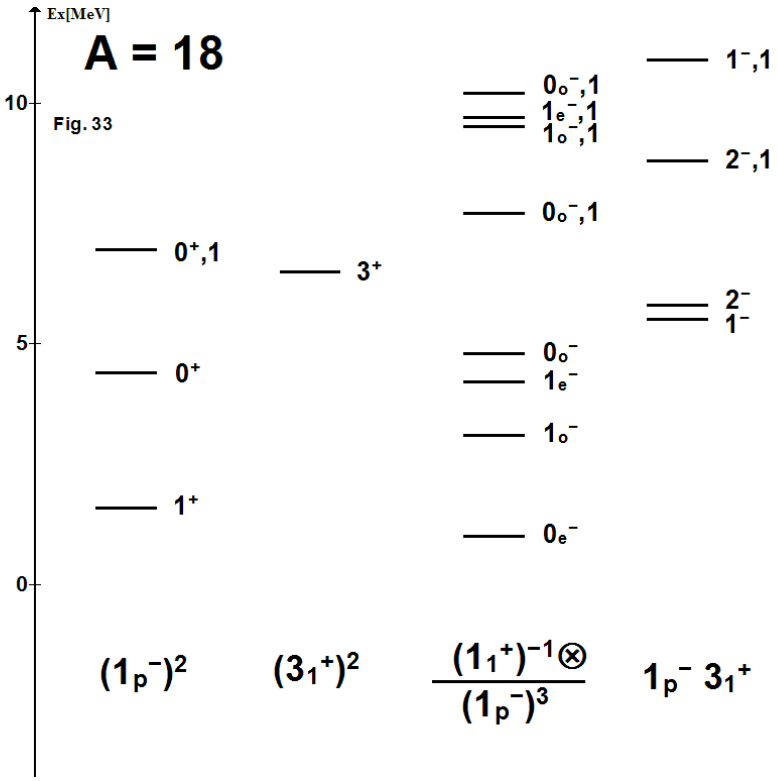
Ex[MeV]
A = 18
Fig. 33
10
5
0
0⁺,1
0⁺
1⁺
3⁺
0ₒ⁻,1
1ₑ⁻,1
1ₒ⁻,1
0ₒ⁻,1
0ₒ⁻
1ₑ⁻
1ₒ⁻
0ₑ⁻
1⁻,1
2⁻,1
2⁻
1⁻
(1p⁻)²
(31⁺)²
(11⁺)⁻¹⊗ / (1p⁻)³
1p⁻ 31⁺

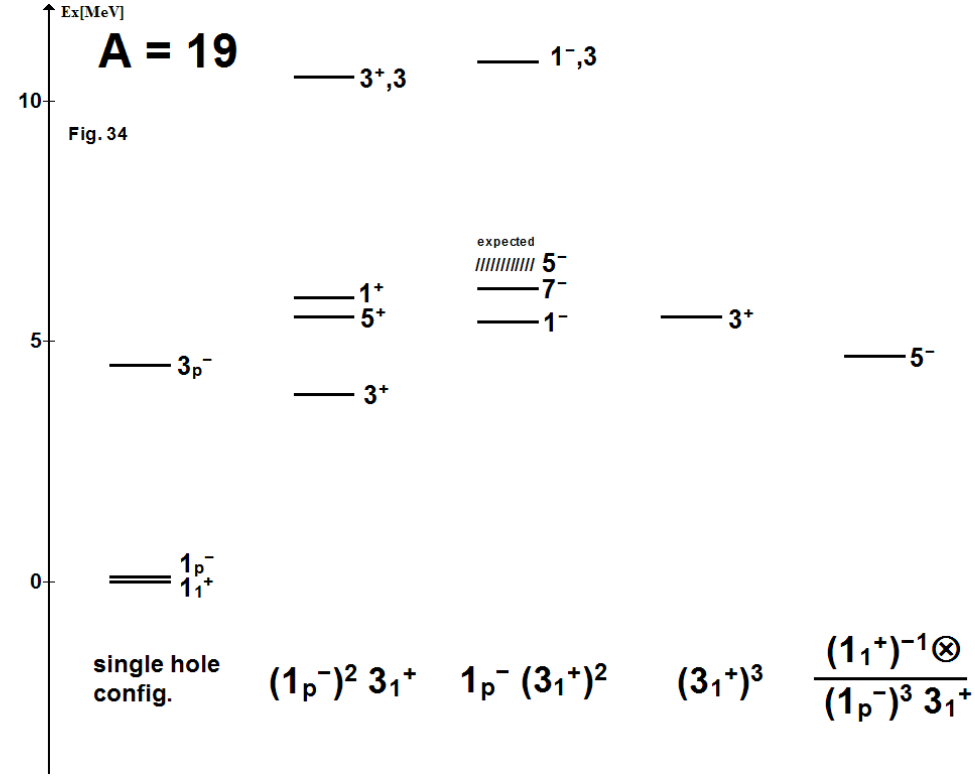
Ex[MeV]
A = 19
Fig. 34
10
5
0
3⁺,3
1⁻,3
expected
5⁻
7⁻
1⁻
1⁺
5⁺
3⁺
3p⁻
1p⁻
11⁺
3⁺
5⁻
single hole config.
(1p⁻)² 31⁺
1p⁻ (31⁺)²
(31⁺)³
(11⁺)⁻¹⊗ / (1p⁻)³ 31⁺

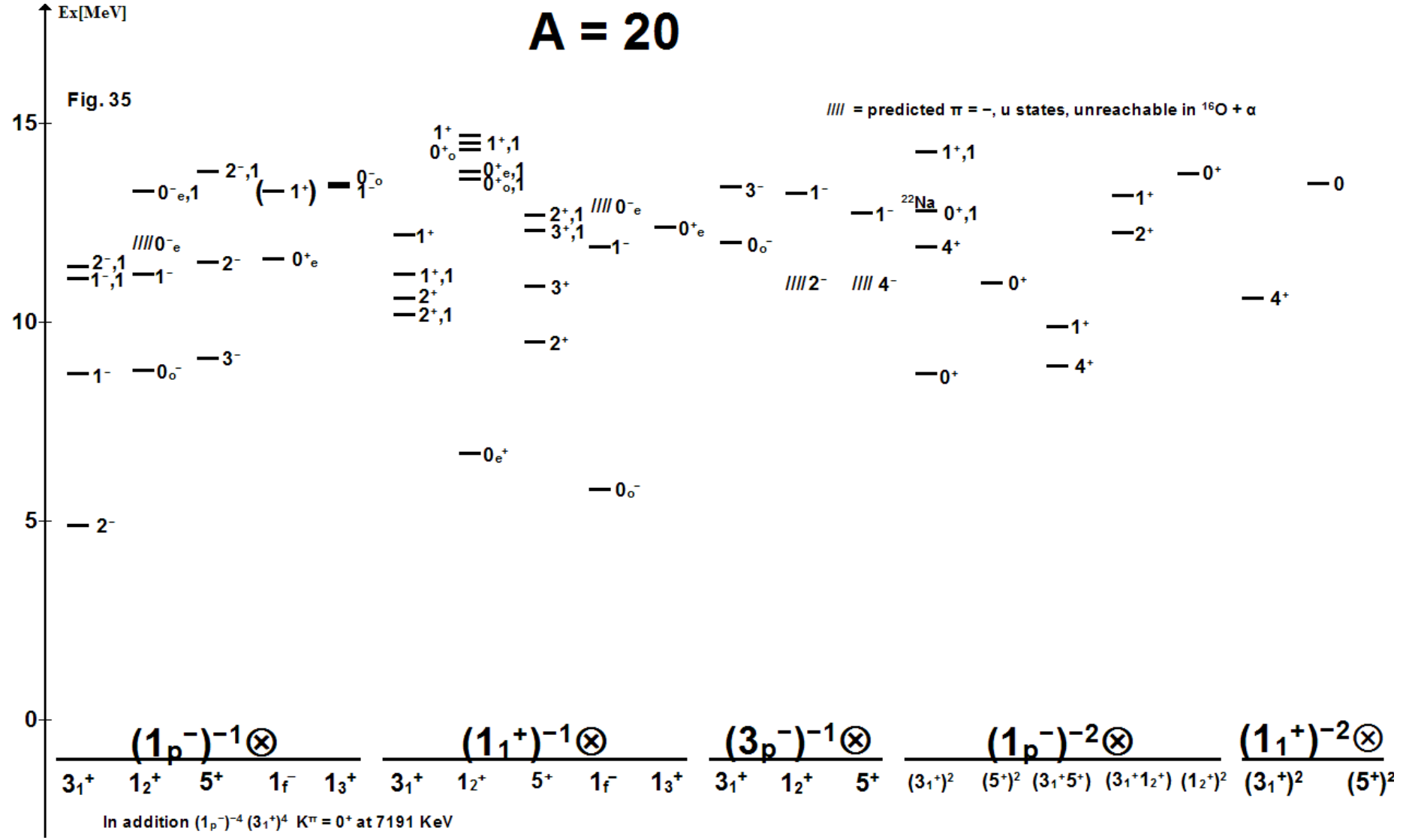
A = 20
Fig. 35
Ex[MeV]
//// = predicted π = −, u states, unreachable in ^{16}O + α
^{22}Na
15
10
5
0
$(1_p^-)^{-1}\otimes$
3_1^+ 1_2^+ 5^+ 1_f^- 1_3^+
$(1_1^+)^{-1}\otimes$
3_1^+ 1_2^+ 5^+ 1_f^- 1_3^+
$(3_p^-)^{-1}\otimes$
3_1^+ 1_2^+ 5^+
$(1_p^-)^{-2}\otimes$
$(3_1^+)^2$ $(5^+)^2$ $(3_1^+5^+)$ $(3_1^+1_2^+)$ $(1_2^+)^2$
$(1_1^+)^{-2}\otimes$
$(3_1^+)^2$ $(5^+)^2$
In addition $(1_p^-)^{-4}\,(3_1^+)^4$ $K^\pi = 0^+$ at 7191 KeV

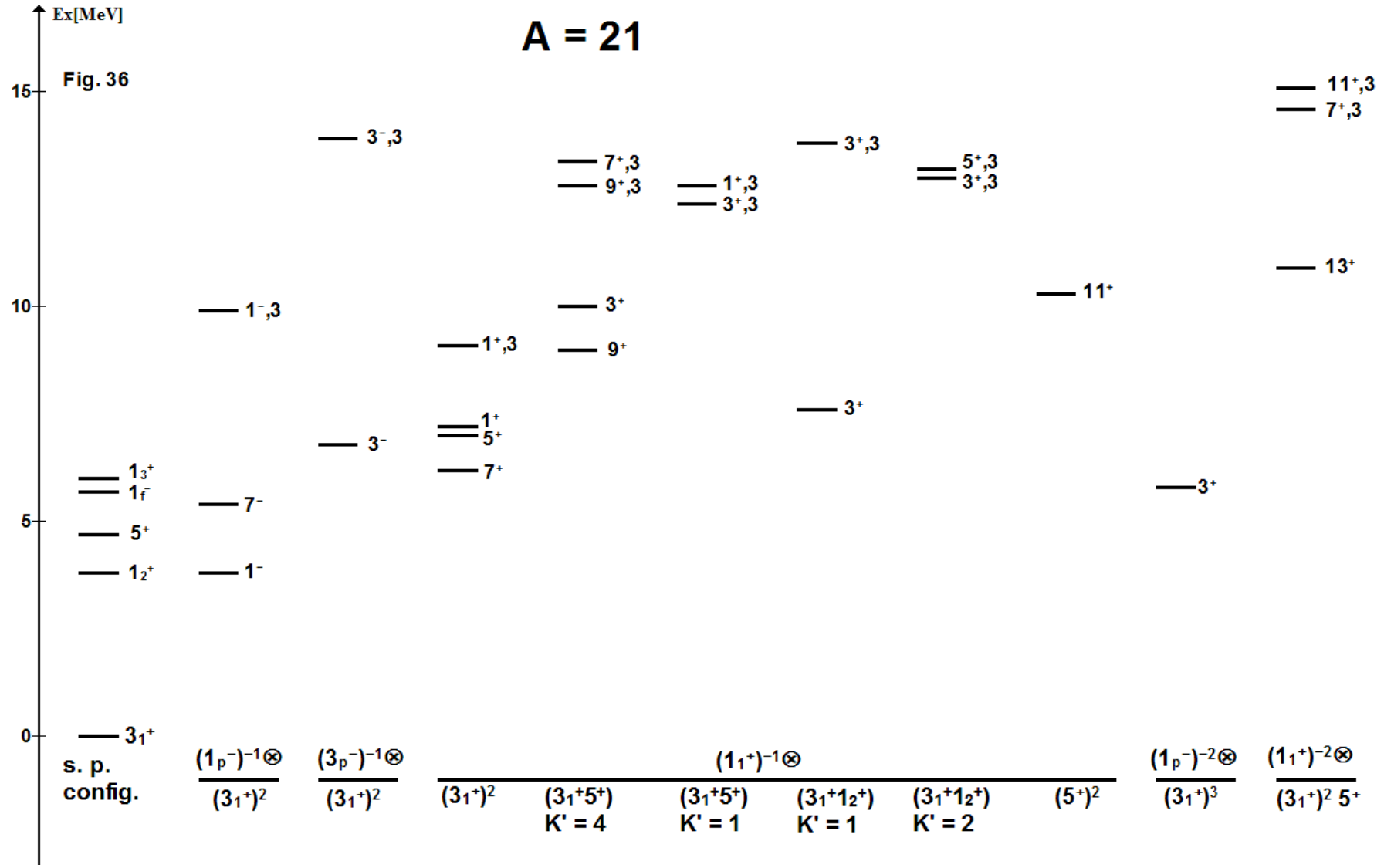
A = 21
Fig. 36
Ex[MeV]
15
10
5
0
3⁻,3
7⁺,3
9⁺,3
1⁺,3
3⁺,3
3⁺,3
5⁺,3
3⁺,3
11⁺,3
7⁺,3
13⁺
11⁺
1⁻,3
3⁺
1⁺,3
9⁺
3⁺
1⁺
5⁺
3⁻
7⁺
3⁺
1₃⁺
1f⁻
7⁻
5⁺
1₂⁺
1⁻
3₁⁺
s. p. config.
(1p⁻)⁻¹⊗ (3₁⁺)²
(3p⁻)⁻¹⊗ (3₁⁺)²
(1₁⁺)⁻¹⊗
(3₁⁺)²
(3₁⁺5⁺) K' = 4
(3₁⁺5⁺) K' = 1
(3₁⁺1₂⁺) K' = 1
(3₁⁺1₂⁺) K' = 2
(5⁺)²
(1p⁻)⁻²⊗ (3₁⁺)³
(1₁⁺)⁻²⊗ (3₁⁺)² 5⁺

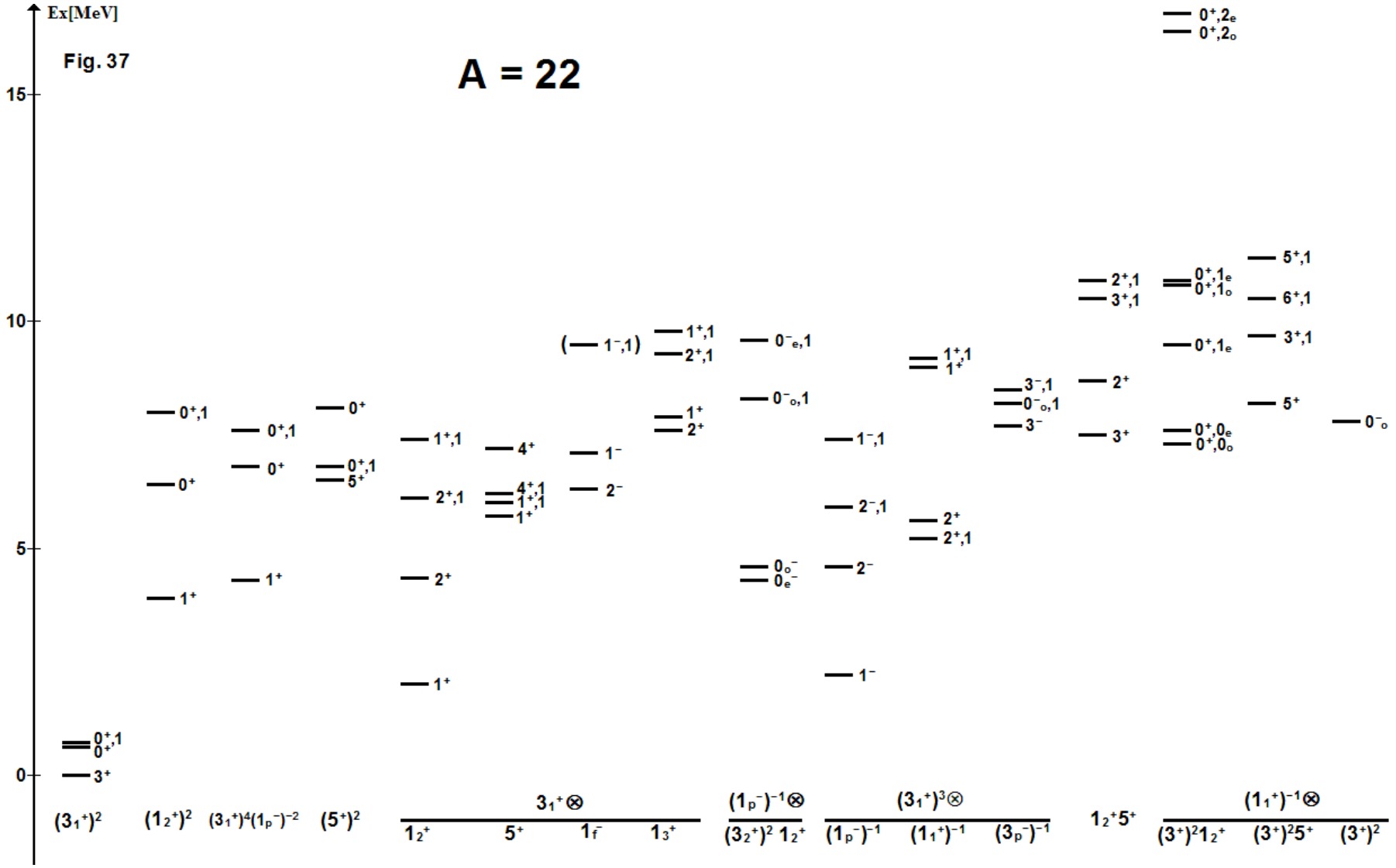
Ex[MeV]
Fig. 37
A = 22
15
10
5
0
0+,2e
0+,2o
5+,1
6+,1
3+,1
5+
0−o
2+,1
3+,1
0+,1e
0+,1o
0+,1e
2+
3+
0+,0e
0+,0o
3−,1
0−o,1
3−
1+,1
1+
2+
2+,1
1−,1
2−,1
2−
1−
0−e,1
0−o,1
0o−
0e−
(1−,1)
1+,1
2+,1
1+
2+
1+,1
4+
1−
2−
4+,1
1+,1
1+
2+,1
2+
1+
0+,1
5+
0+
0+,1
0+
1+
0+
0+,1
0+
1+
0+,1
0+
3+
0+,1
0+
3+
(31+)2
(12+)2
(31+)4(1p−)−2
(5+)2
31+⊗
12+
5+
1f−
13+
(1p−)−1⊗
(32+)2 12+
(31+)3⊗
(1p−)−1
(11+)−1
(3p−)−1
12+5+
(11+)−1⊗
(3+)212+
(3+)25+
(3+)2

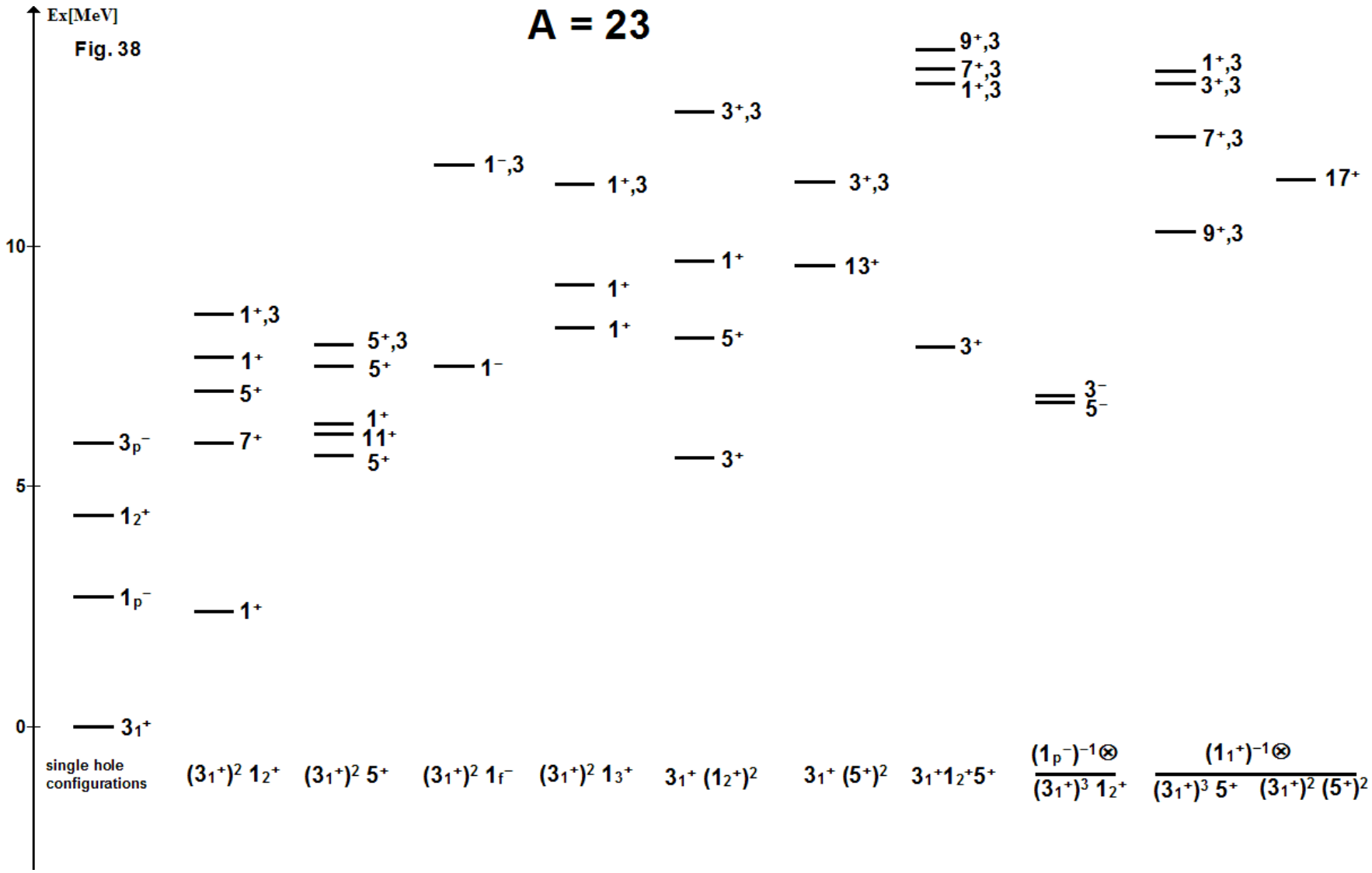
A = 23
Ex[MeV]
Fig. 38
10
5
0
3p−
12+
1p−
31+
1+,3
1+
5+
7+
1+
1+
11+
5+
5+,3
5+
1−,3
1−
1+,3
1+
1+
1+
5+
3+
3+,3
1+
13+
3+
9+,3
7+,3
1+,3
3+
3−
5−
1+,3
3+,3
7+,3
9+,3
17+
single hole configurations
(31+)2 12+
(31+)2 5+
(31+)2 1f−
(31+)2 13+
31+ (12+)2
31+ (5+)2
31+12+5+
(1p−)−1⊗ (31+)3 12+
(11+)−1⊗ (31+)3 5+ (31+)2 (5+)2

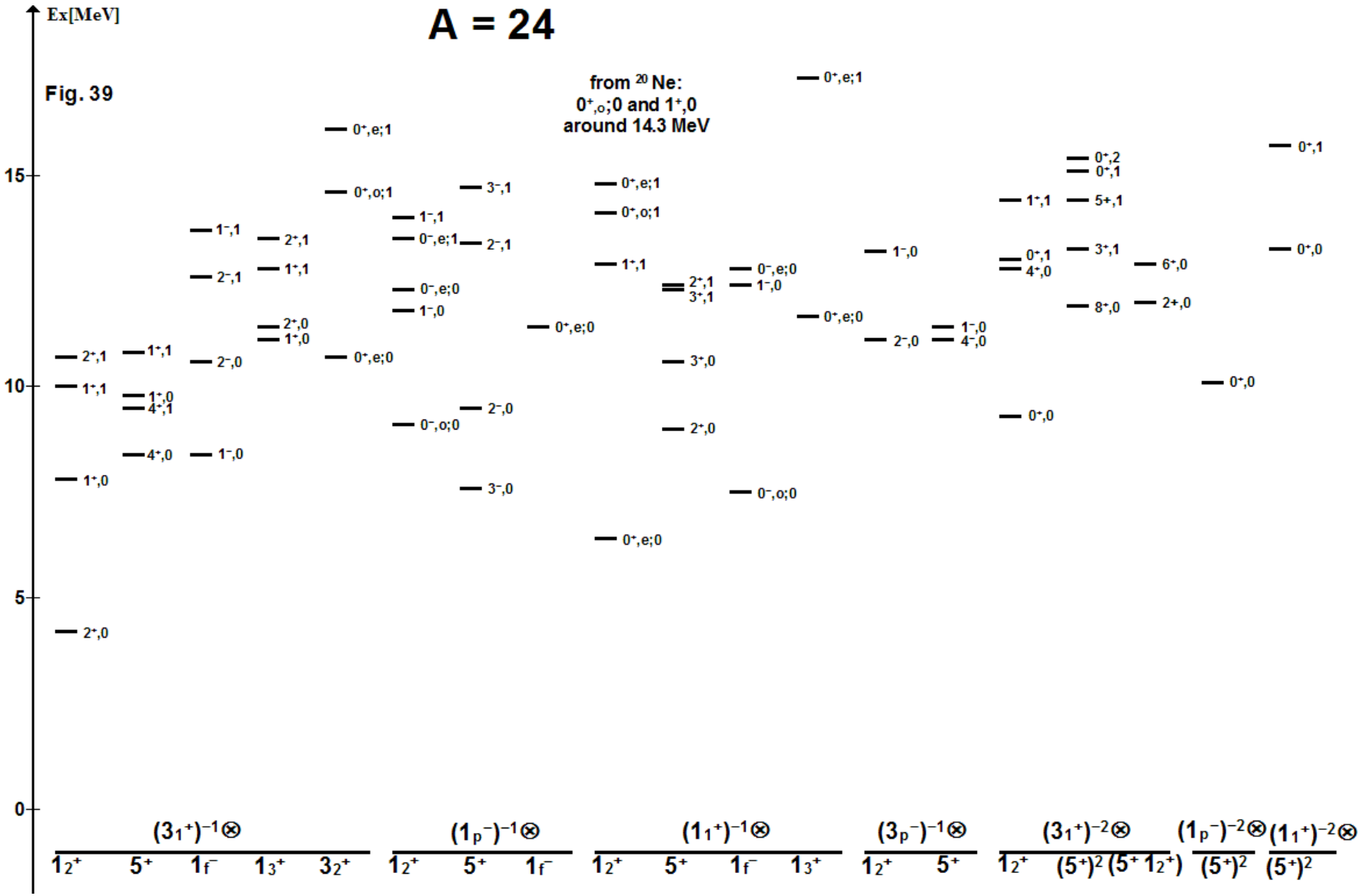
A = 24
Fig. 39
Ex[MeV]
15
10
5
0
from ^{20}Ne:
$0^+,o;0$ and $1^+,0$
around 14.3 MeV
$(3_1{}^+)^{-1}\otimes$
$1_{2}{}^+$ 5^+ $1_f{}^-$ $1_3{}^+$ $3_2{}^+$
$(1_p{}^-)^{-1}\otimes$
$1_{2}{}^+$ 5^+ $1_f{}^-$
$(1_1{}^+)^{-1}\otimes$
$1_{2}{}^+$ 5^+ $1_f{}^-$ $1_3{}^+$
$(3_p{}^-)^{-1}\otimes$
$1_{2}{}^+$ 5^+
$(3_1{}^+)^{-2}\otimes$
$1_{2}{}^+$ $(5^+)^2$ $(5^+\,1_2{}^+)$
$(1_p{}^-)^{-2}\otimes$ $(5^+)^2$
$(1_1{}^+)^{-2}\otimes$ $(5^+)^2$

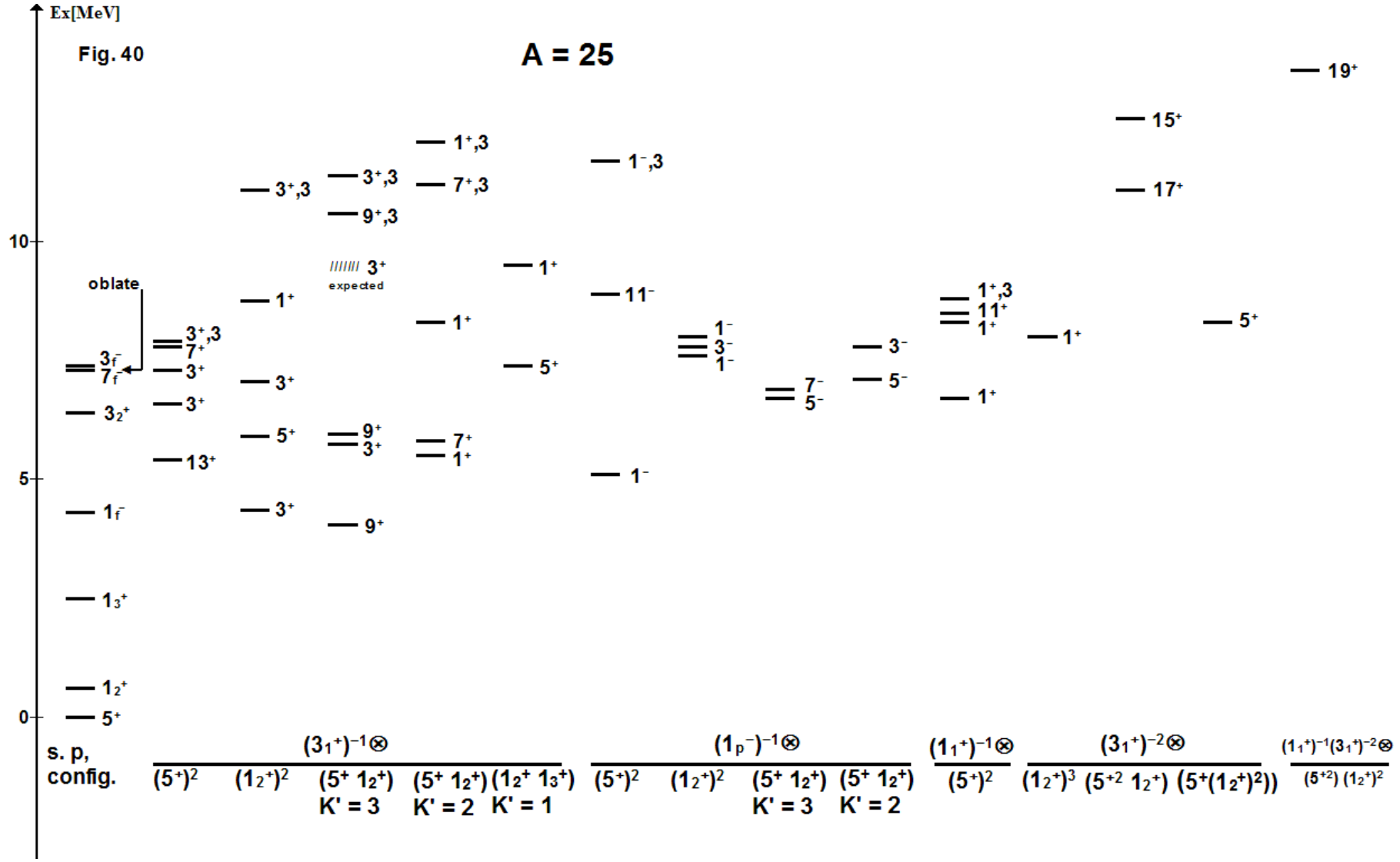
Ex[MeV]
Fig. 40
A = 25
10
5
0
oblate
3f⁻
7f⁻
3₂⁺
1f⁻
1₃⁺
1₂⁺
5⁺
3⁺,3
7⁺
3⁺
3⁺
13⁺
3⁺,3
1⁺
3⁺
5⁺
3⁺
3⁺,3
9⁺,3
////// 3⁺
expected
9⁺
3⁺
9⁺
1⁺,3
7⁺,3
1⁺
7⁺
1⁺
1⁺
5⁺
1⁻,3
11⁻
1⁻
1⁻
3⁻
1⁻
7⁻
5⁻
3⁻
5⁻
1⁺,3
11⁺
1⁺
1⁺
1⁺
15⁺
17⁺
5⁺
19⁺
s. p,
config.
(3₁⁺)⁻¹⊗
(5⁺)²
(1₂⁺)²
(5⁺ 1₂⁺) K' = 3
(5⁺ 1₂⁺) K' = 2
(1₂⁺ 1₃⁺) K' = 1
(1p⁻)⁻¹⊗
(5⁺)²
(1₂⁺)²
(5⁺ 1₂⁺) K' = 3
(5⁺ 1₂⁺) K' = 2
(1₁⁺)⁻¹⊗
(5⁺)²
(3₁⁺)⁻²⊗
(1₂⁺)³
(5⁺² 1₂⁺)
(5⁺(1₂⁺)²))
(1₁⁺)⁻¹(3₁⁺)⁻²⊗
(5⁺²) (1₂⁺)²

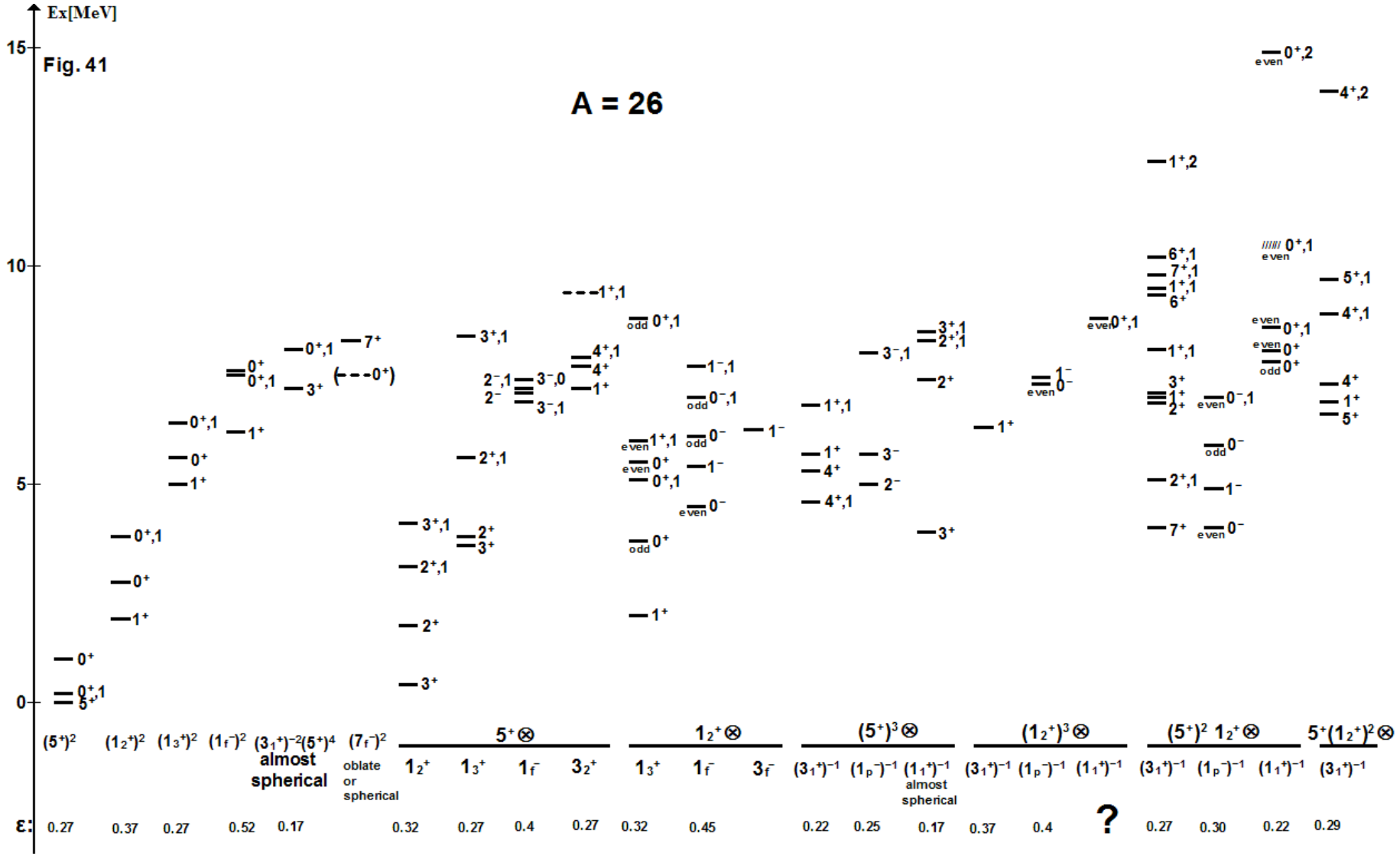
Ex[MeV]
Fig. 41
A = 26
15
10
5
0
ε:
(5⁺)²
(1₂⁺)²
(1₃⁺)²
(1f⁻)²
(3₁⁺)⁻²(5⁺)⁴
almost spherical
(7f⁻)²
oblate or spherical
5⁺⊗
1₂⁺
1₃⁺
1f⁻
3₂⁺
1₂⁺⊗
1₃⁺
1f⁻
3f⁻
(5⁺)³⊗
(3₁⁺)⁻¹
(1p⁻)⁻¹
(1₁⁺)⁻¹
almost spherical
(1₂⁺)³⊗
(3₁⁺)⁻¹
(1p⁻)⁻¹
(1₁⁺)⁻¹
?
(5⁺)² 1₂⁺⊗
(3₁⁺)⁻¹
(1p⁻)⁻¹
(1₁⁺)⁻¹
5⁺(1₂⁺)²⊗
(3₁⁺)⁻¹
0.27
0.37
0.27
0.52
0.17
0.32
0.27
0.4
0.27
0.32
0.45
0.22
0.25
0.17
0.37
0.4
0.27
0.30
0.22
0.29

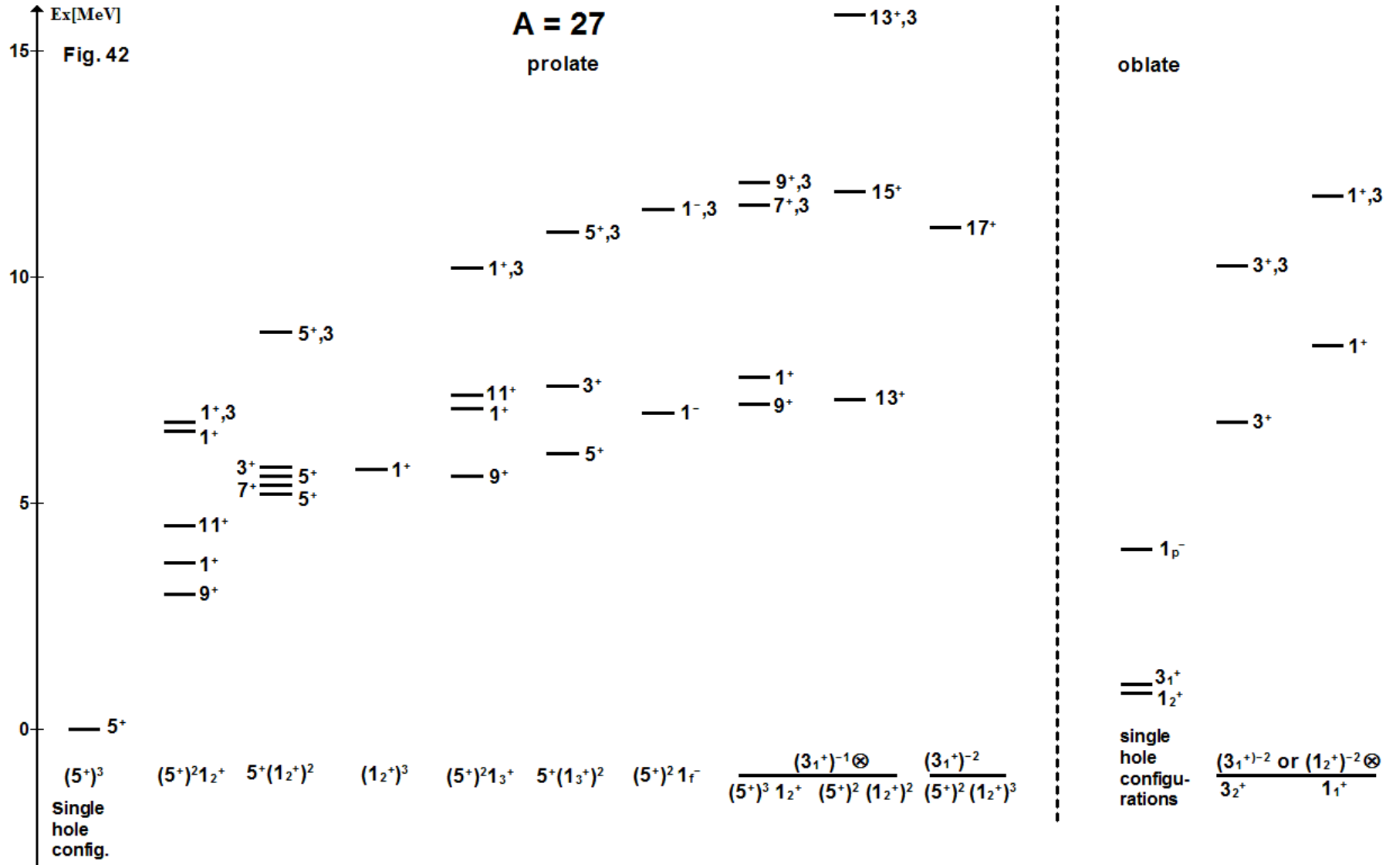
A = 27
Fig. 42
Ex[MeV]
prolate
oblate
15
10
5
0
5+
1+,3
1+
3+
5+
7+
5+
11+
1+
9+
5+,3
1+
1+,3
11+
1+
9+
3+
5+
5+,3
1-,3
1-
9+,3
7+,3
1+
9+
15+
13+
13+,3
17+
3+,3
3+
1+,3
1+
1p-
31+
12+
(5+)3
(5+)212+
5+(12+)2
(12+)3
(5+)213+
5+(13+)2
(5+)2 1f-
(31+)-1⊗
(5+)3 12+
(5+)2 (12+)2
(31+)-2
(5+)2 (12+)3
Single hole config.
single hole configu-rations
(31+)-2 or (12+)-2⊗
32+
11+

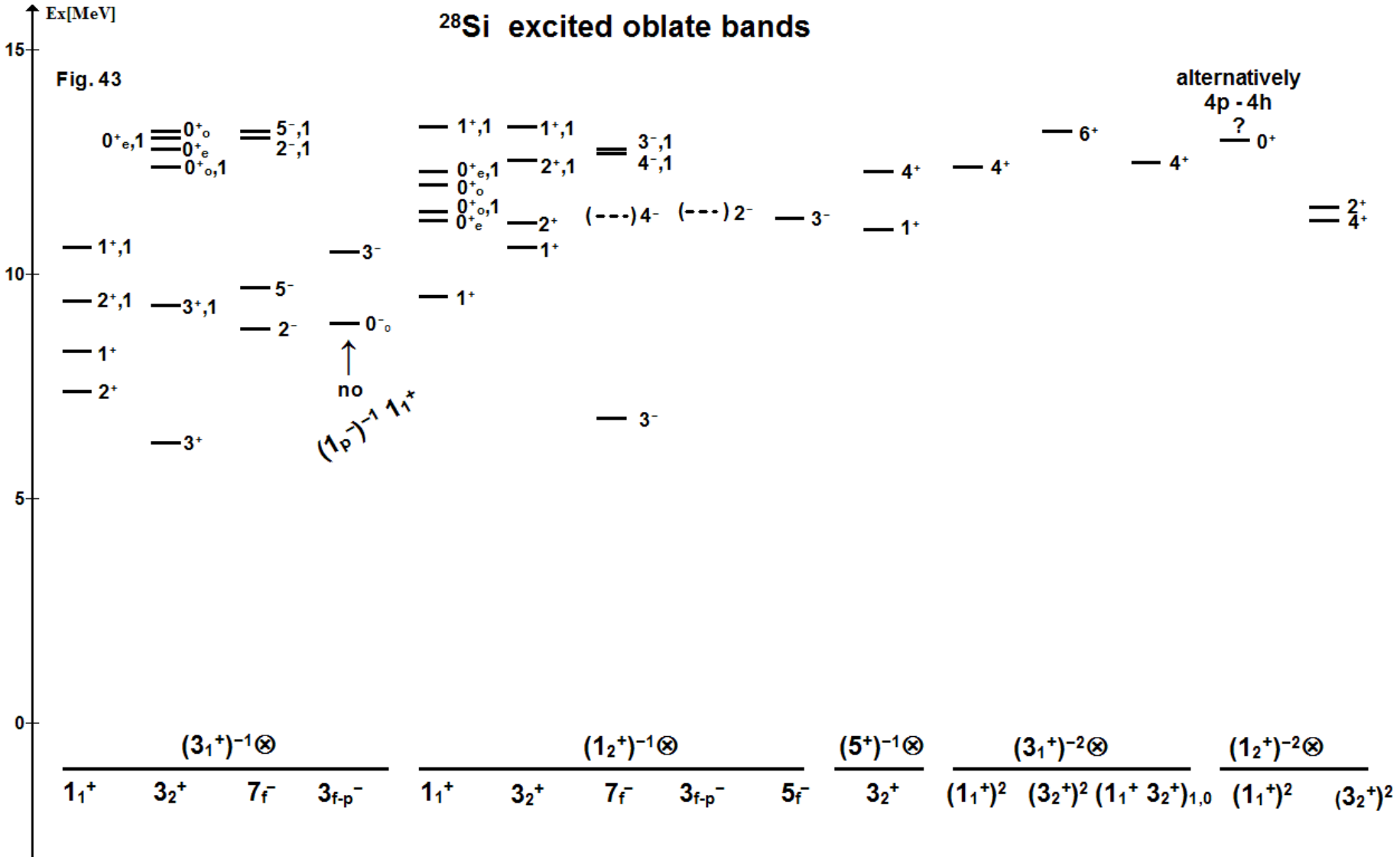
Ex[MeV]
28Si excited oblate bands
Fig. 43
15
10
5
0
alternatively
4p - 4h
?
no
(1p-1)-1 1+
(3₁⁺)⁻¹⊗
(1₂⁺)⁻¹⊗
(5⁺)⁻¹⊗
(3₁⁺)⁻²⊗
(1₂⁺)⁻²⊗
1₁⁺ 3₂⁺ 7f⁻ 3f-p⁻
1₁⁺ 3₂⁺ 7f⁻ 3f-p⁻ 5f⁻
3₂⁺
(1₁⁺)² (3₂⁺)² (1₁⁺ 3₂⁺)1,0
(1₁⁺)² (3₂⁺)²

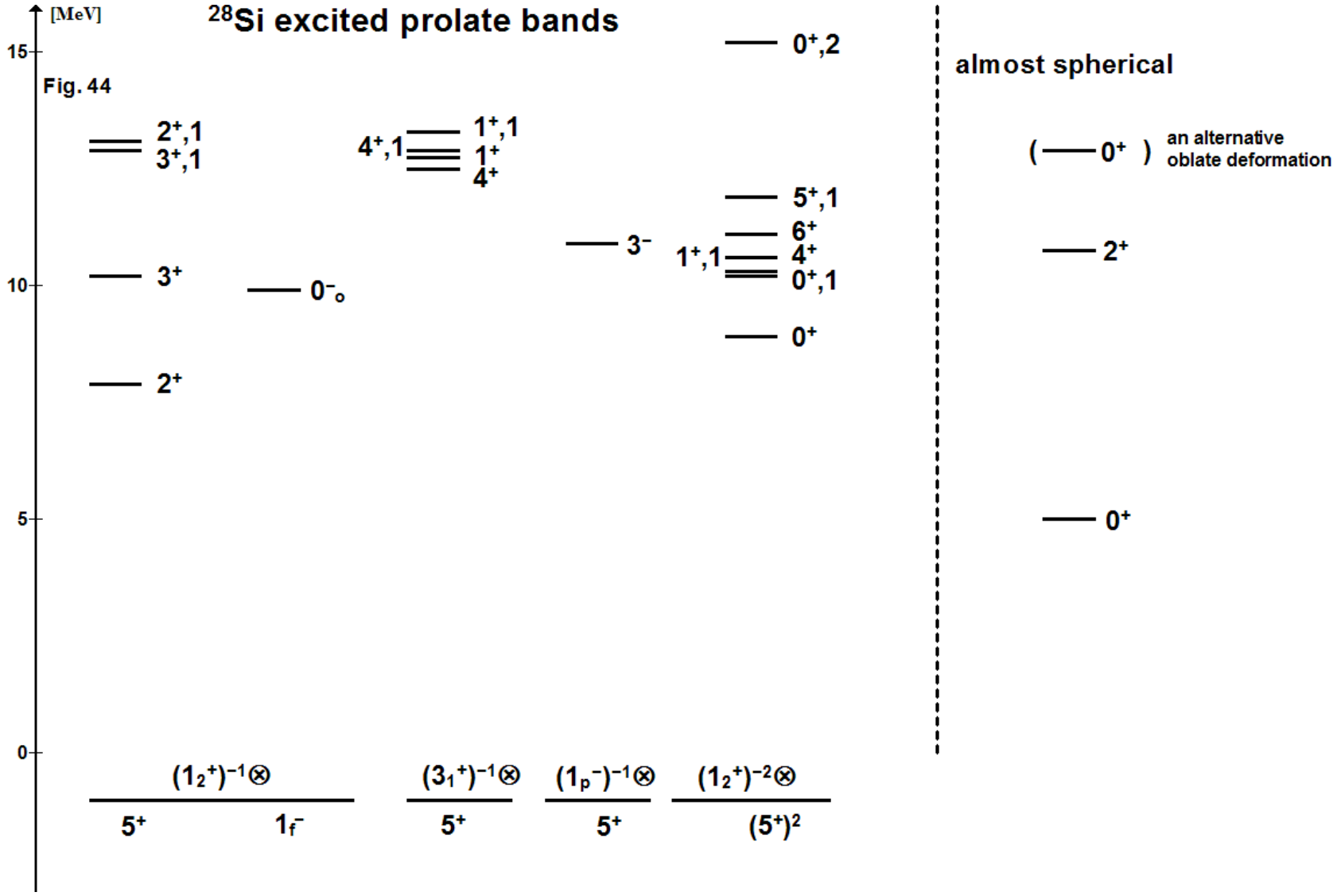
[MeV]
^{28}Si excited prolate bands
15
10
5
0
Fig. 44
$2^+,1$
$3^+,1$
3^+
2^+
0^-_o
$4^+,1$
$1^+,1$
1^+
4^+
3^-
$0^+,2$
$5^+,1$
6^+
$1^+,1$
4^+
$0^+,1$
0^+
$(1_2^+)^{-1}\otimes$
5^+ 1_f^-
$(3_1^+)^{-1}\otimes$
5^+
$(1_p^-)^{-1}\otimes$
5^+
$(1_2^+)^{-2}\otimes$
$(5^+)^2$
almost spherical
(0^+) an alternative oblate deformation
2^+
0^+

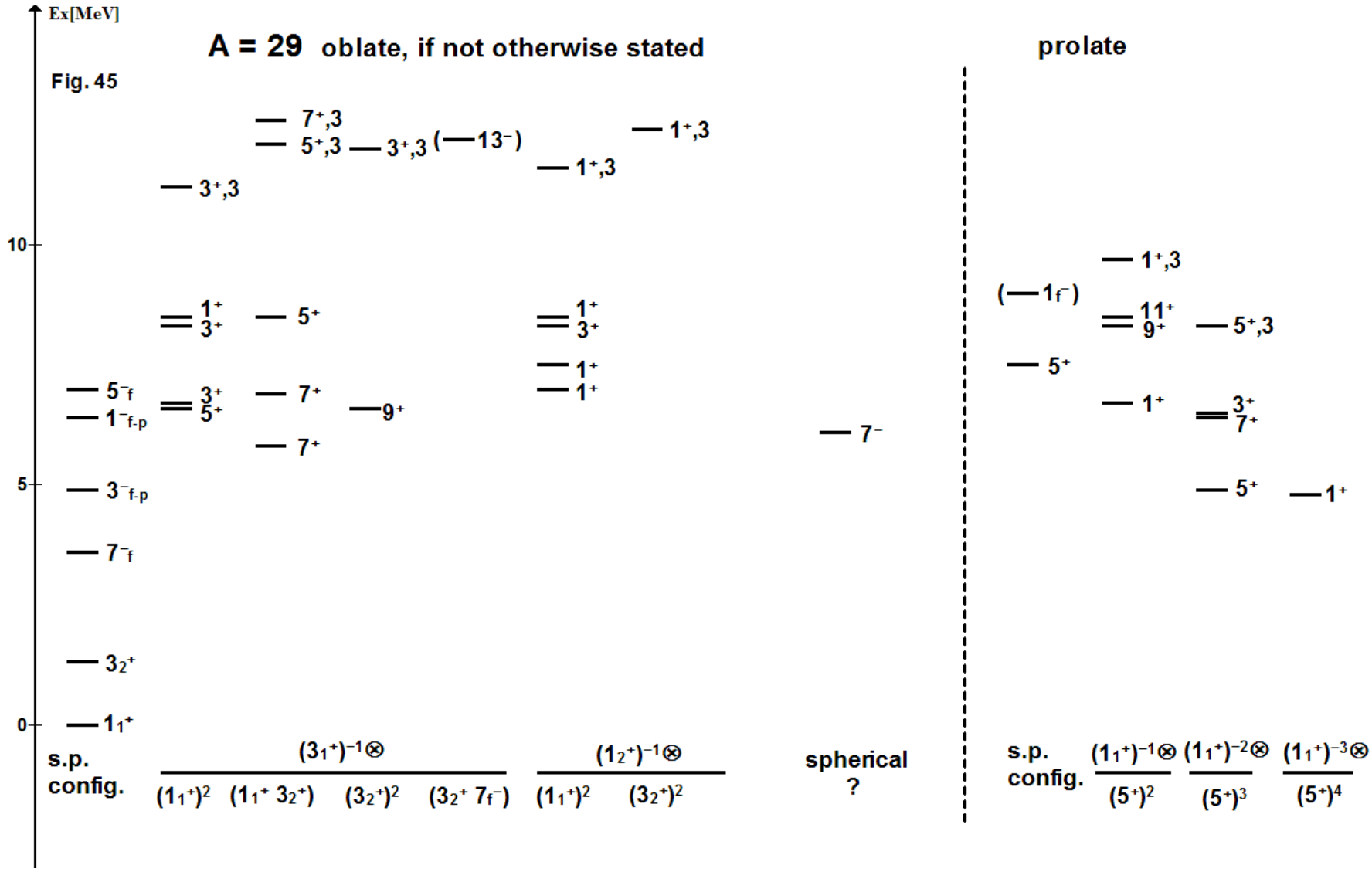
Ex[MeV]
A = 29 oblate, if not otherwise stated
prolate
Fig. 45
10
5
0
7+,3
5+,3
3+,3
(13−)
1+,3
3+,3
1+,3
1+
3+
5+
1+
3+
1+
1+
5−f
1−f-p
3+
5+
7+
9+
7+
7−
3−f-p
7−f
32+
11+
s.p. config.
(31+)−1⊗
(12+)−1⊗
spherical ?
(11+)2 (11+ 32+) (32+)2 (32+ 7f−)
(11+)2 (32+)2
(1f−)
1+,3
11+
9+
5+,3
5+
1+
3+
7+
5+
1+
s.p. config.
(11+)−1⊗
(11+)−2⊗
(11+)−3⊗
(5+)2
(5+)3
(5+)4

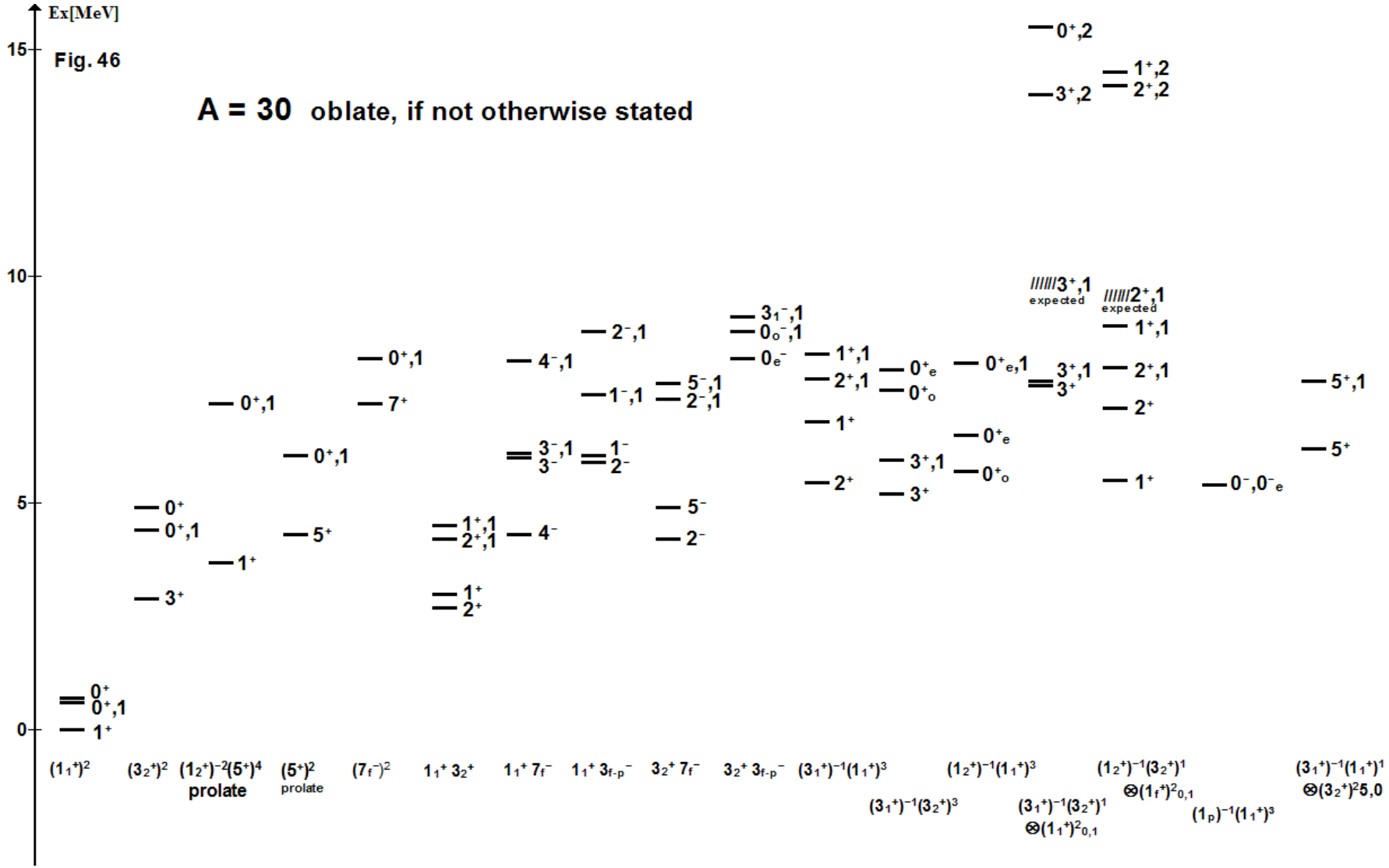
Ex[MeV]
Fig. 46
A = 30 oblate, if not otherwise stated
15
10
5
0
0+
0+,1
1+
0+
0+,1
3+
1+
0+,1
5+
0+,1
7+
4−,1
3−,1
3−
2−,1
1−,1
1−
2−
5−,1
2−,1
5−
2−
3₁−,1
0o−,1
0e−
1+,1
2+,1
1+
2+
0+e
0+o
3+,1
3+
0+e,1
0+e
0+o
0+,2
3+,2
1+,2
2+,2
////// 3+,1 expected
3+,1
3+
////// 2+,1 expected
1+,1
2+,1
2+
1+
0−,0−e
5+,1
5+
(1₁+)2
(3₂+)2
(1₂+)−2(5+)4 prolate
(5+)2 prolate
(7f−)2
1₁+ 3₂+
1₁+ 7f−
1₁+ 3f-p−
3₂+ 7f−
3₂+ 3f-p−
(3₁+)−1(1₁+)3
(3₁+)−1(3₂+)3
(1₂+)−1(1₁+)3
(3₁+)−1(3₂+)1 ⊗(1₁+)20,1
(1₂+)−1(3₂+)1 ⊗(1f+)20,1
(1p)−1(1₁+)3
(3₁+)−1(1₁+)1 ⊗(3₂+)25,0

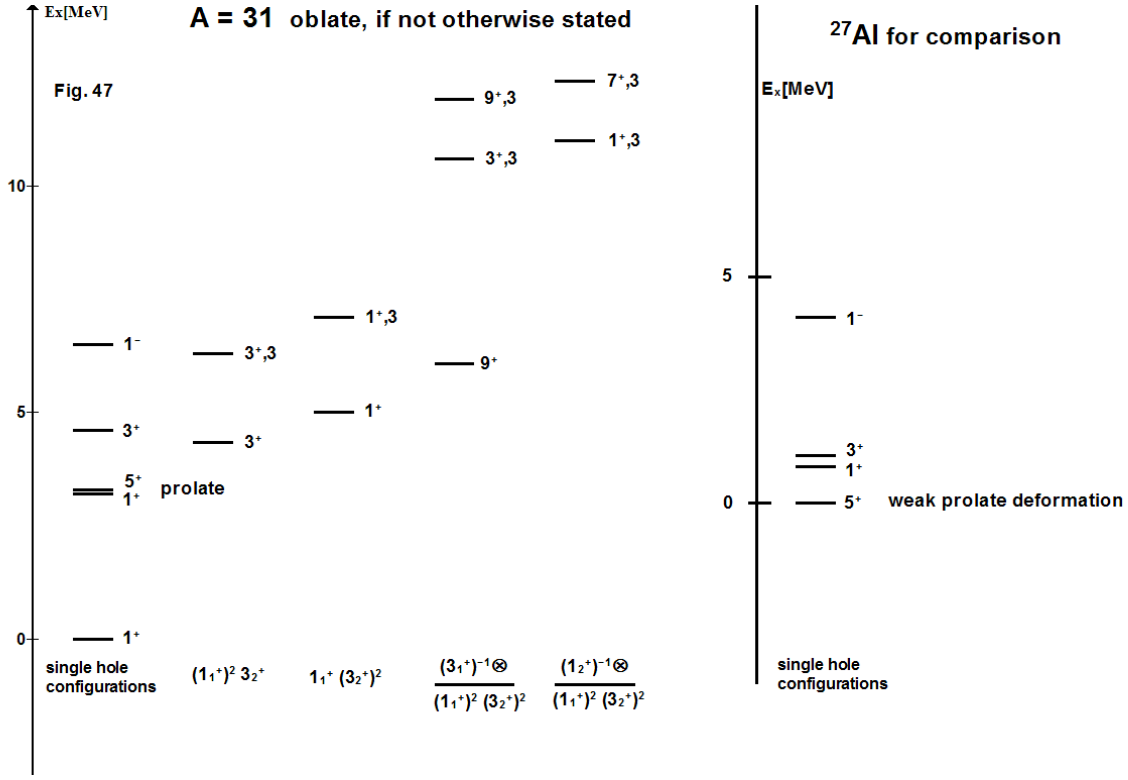

The $J^{\pi} = 1^-$ state in A = 31 is a p → s-d excitation, but its shape is unknown in contrast to ^{27}Al where oblate deformation is safe.

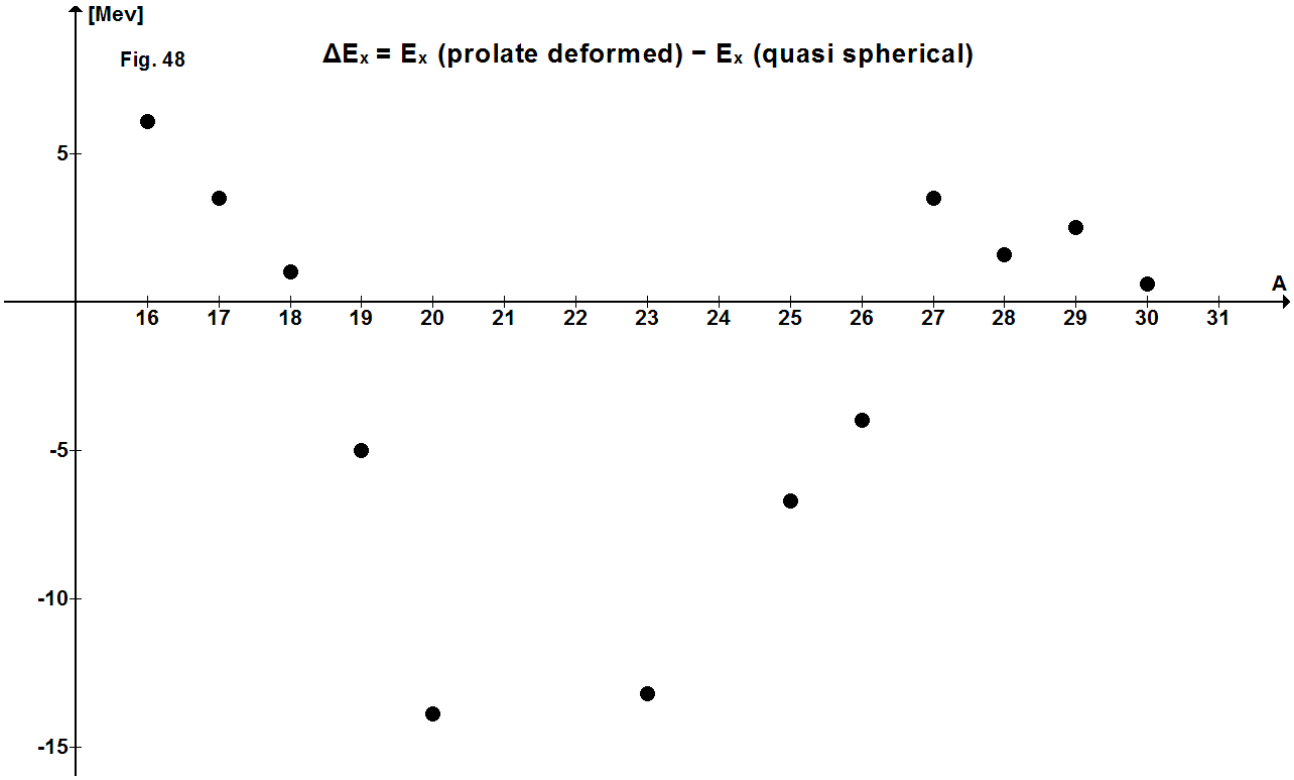
[Mev]
Fig. 48
ΔEx = Ex (prolate deformed) − Ex (quasi spherical)
5
-5
-10
-15
A
16
17
18
19
20
21
22
23
24
25
26
27
28
29
30
31

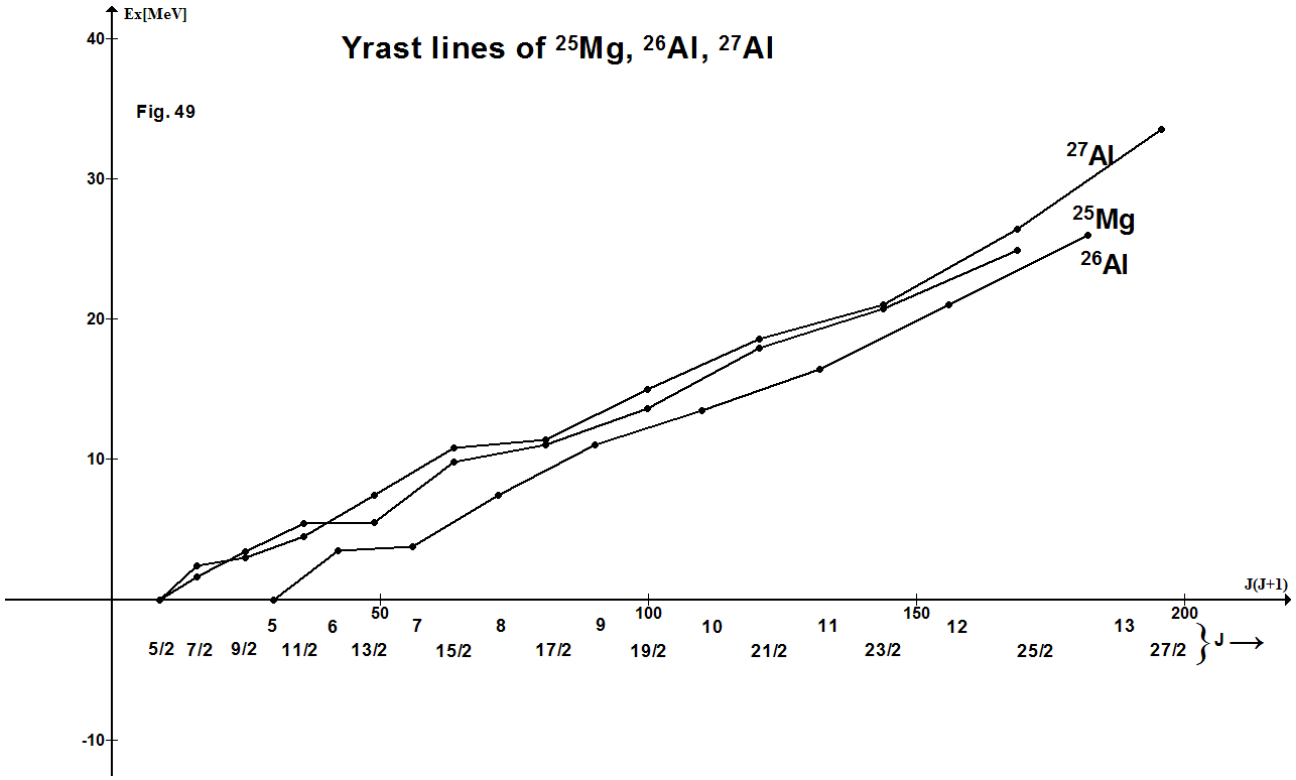
Ex[MeV]
Yrast lines of 25Mg, 26Al, 27Al
Fig. 49
27Al
25Mg
26Al
40
30
20
10
-10
J(J+1)
50
100
150
200
5
6
7
8
9
10
11
12
13
J
5/2
7/2
9/2
11/2
13/2
15/2
17/2
19/2
21/2
23/2
25/2
27/2

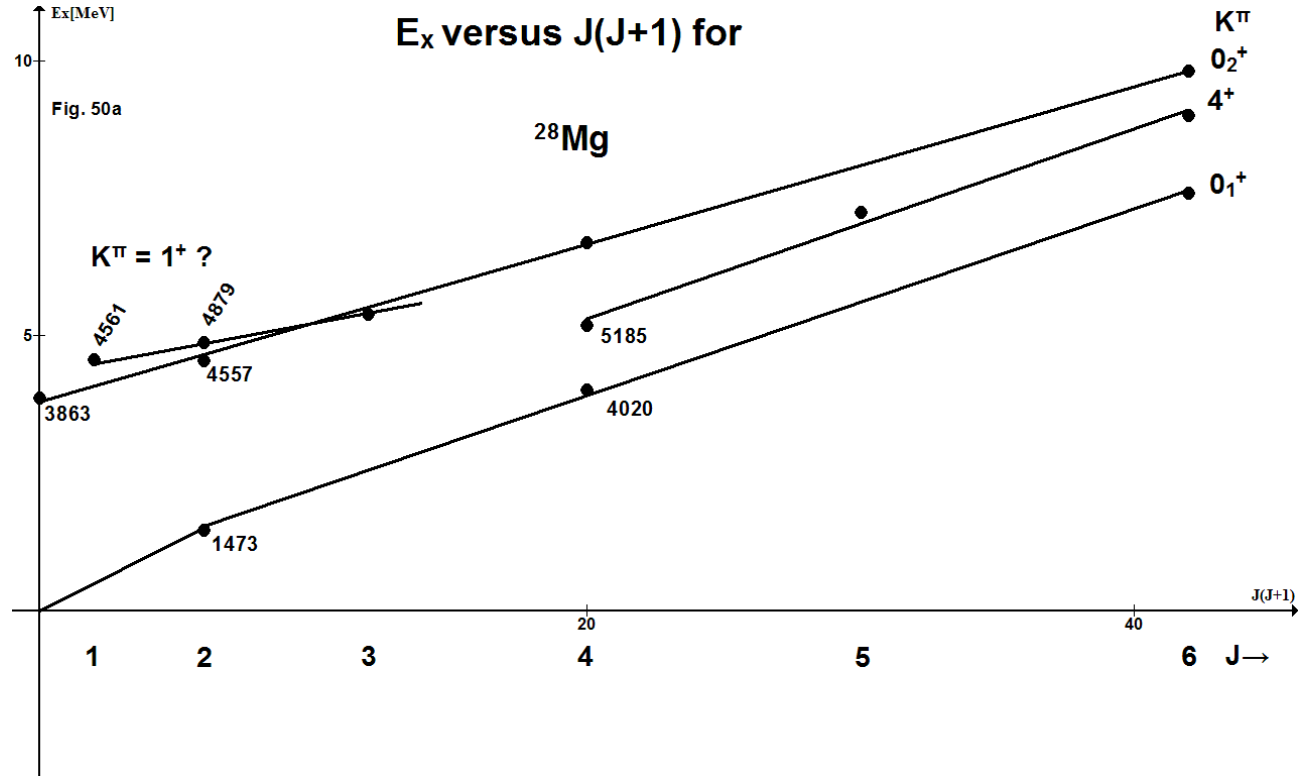
Ex[MeV]
10
5
Fig. 50a
E_x versus J(J+1) for
^{28}Mg
$K^\pi = 1^+$?
4561
4879
4557
3863
5185
4020
1473
K^π
0_2^+
4^+
0_1^+
J(J+1)
20
40
1
2
3
4
5
6
J→

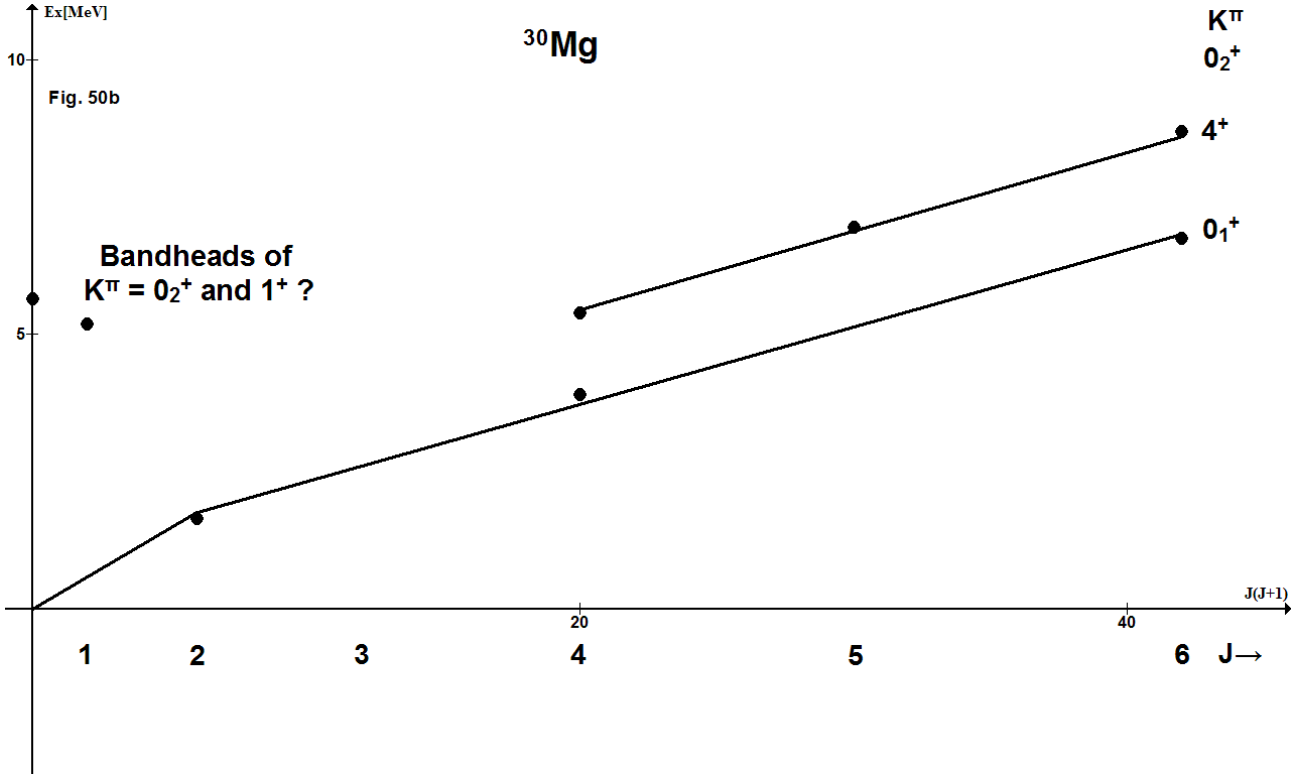
Ex[MeV]
10
5
Fig. 50b
^{30}Mg
Bandheads of
$K^\pi = 0_2^+$ and 1^+ ?
K^π
0_2^+
4^+
0_1^+
J(J+1)
20
40
1
2
3
4
5
6
J→

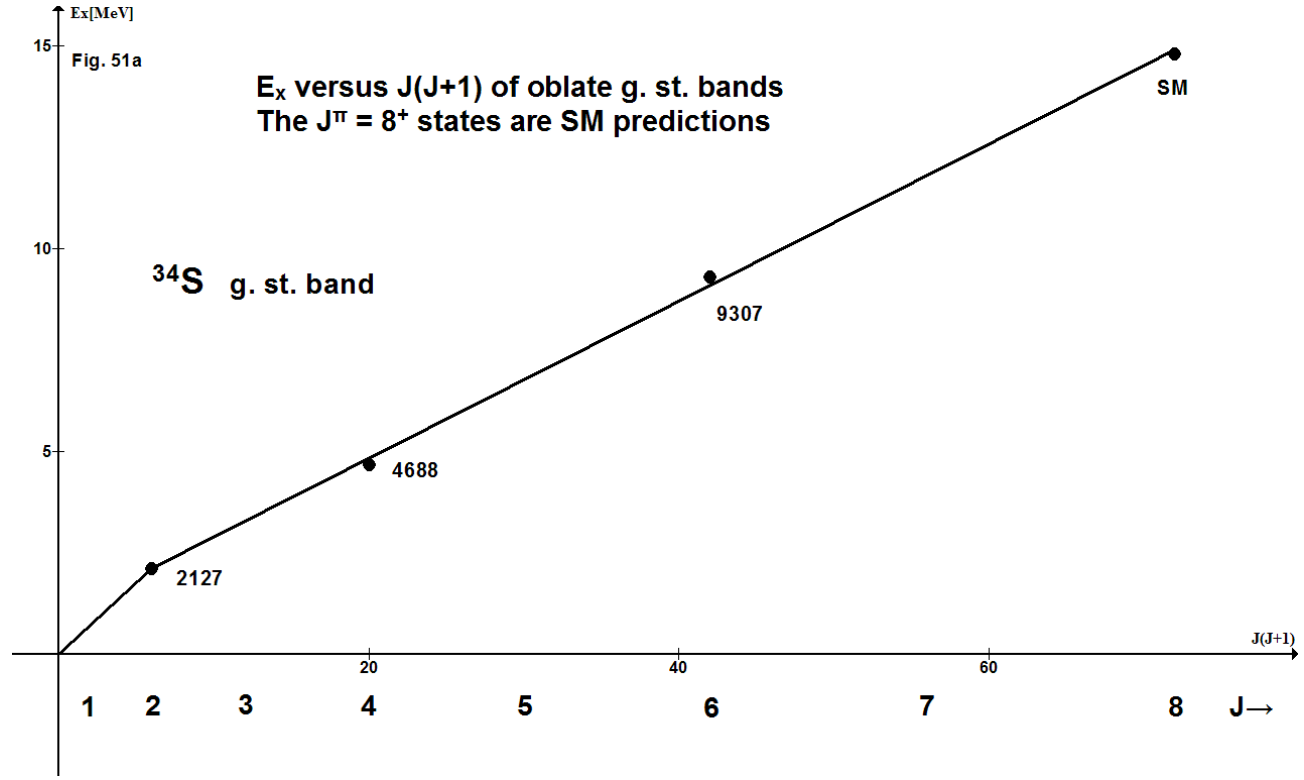
Ex[MeV]
Fig. 51a
E_x versus J(J+1) of oblate g. st. bands
The $J^\pi = 8^+$ states are SM predictions
SM
^{34}S g. st. band
9307
4688
2127
J(J+1)
15
10
5
20
40
60
1 2 3 4 5 6 7 8 J→

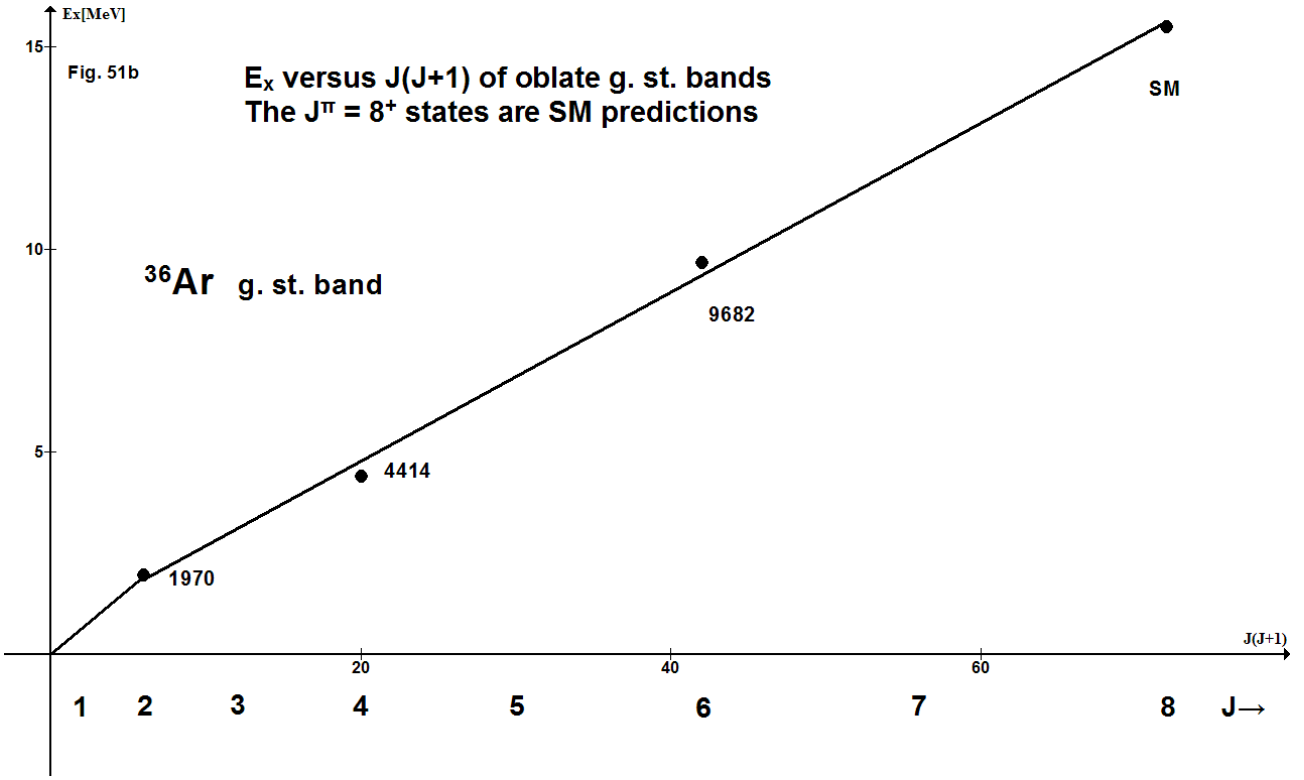
Ex[MeV]
Fig. 51b
E_x versus J(J+1) of oblate g. st. bands
The $J^\pi = 8^+$ states are SM predictions
SM
^{36}Ar g. st. band
9682
4414
1970
J(J+1)
15
10
5
20
40
60
1 2 3 4 5 6 7 8 J→

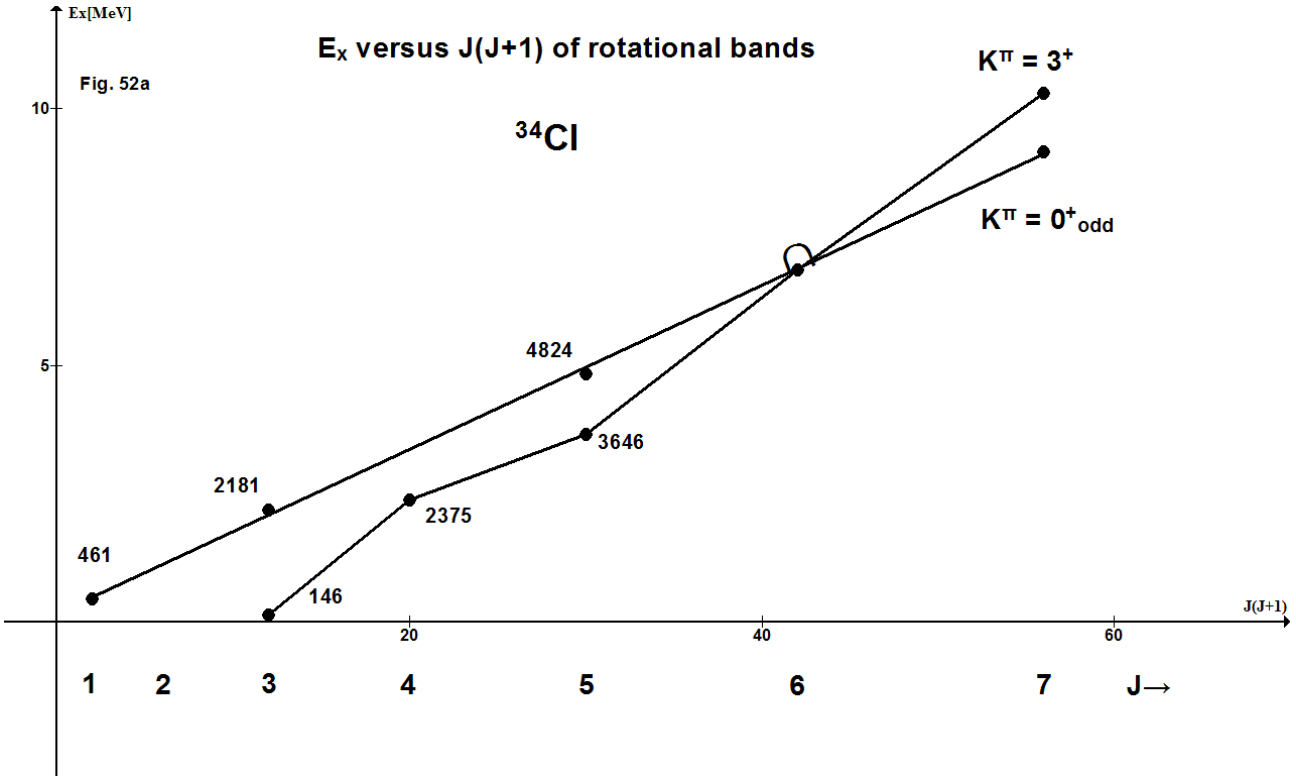
Ex[MeV]
Fig. 52a
E_x versus J(J+1) of rotational bands
^{34}Cl
$K^\pi = 3^+$
$K^\pi = 0^+_{odd}$
10
5
4824
3646
2181
2375
461
146
J(J+1)
20
40
60
1
2
3
4
5
6
7
J→

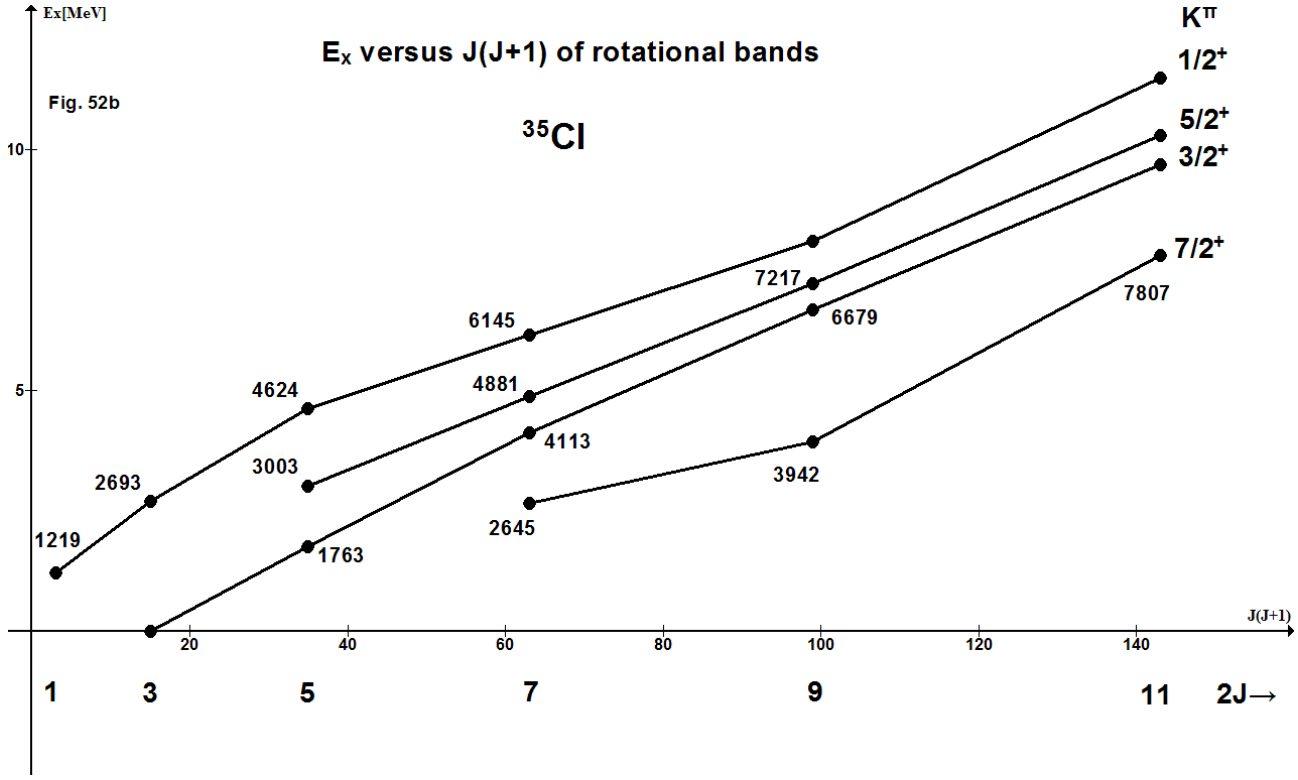
Ex[MeV]
Fig. 52b
E_x versus J(J+1) of rotational bands
^{35}Cl
K^π
$1/2^+$
$5/2^+$
$3/2^+$
$7/2^+$
10
5
7217
7807
6145
6679
4624
4881
4113
3003
3942
2693
2645
1219
1763
J(J+1)
20
40
60
80
100
120
140
1
3
5
7
9
11
2J→

16. Caption to Tables 7, 8

Notation: The Nilsson orbits are characterized by their values of $2\Omega^{\pi}$ and a label v with

v = f for orbits derived from the f-p shell of the spherical shell model

v = p for orbits from the p shell

v = 1, 2, 3 for orbits derived from, respectively, the $d_{5/2}$, $s_{1/2}$, $d_{3/2}$ orbits of the s-d shell

SM stands for a level predicted by the shell model but not yet identified experimentally

Occupancies of orbits are given relative to the ground state configurations of, respectively, ^{16}O, ^{20}Ne, ^{24}Mg, $^{28}Si_{prolate}$, $^{28}Si_{oblate}$.
The latter ones are

^{16}O $(3_p^-)^4\ (1_1^+)^4$

^{20}Ne $(3_p^-)^4\ (1_1^+)^4 (1_p^-)^4$

^{24}Mg $(3_p^-)^4\ (1_1^+)^4\ (1_p^-)^4\ (3_1^+)^4$

^{28}Si $(3_p^-)^4\ (1_1^+)^4\ (1_p^-)^4\ (3_1^+)^4\ (1_2^+)^4$

$^{28}Si_{oblate}$ $(3_p^-)^4\ (5^+)^4\ (1_p^-)^4\ (3_1^+)^4\ (1_2^+)^4$

Subscripts to bracketed occupation numbers indicate intermediate quantum numbers K', T'.

Table 7

Nilsson model configurations, band head energies and predicted quadrupole deformations of rotational bands with lowest isospin ($T = |T_z|$) and prolate deformation in A = 16 - 31

Nuclide		Number of holes/particles [a,b] in the Orbits [c] with $2\Omega_v^{\pi}$											Bandhead energy [MeV]		De-formation
A_z	T_z	3_p^-	1_1^+	1_p^-	3_1^+	1_2^+	5_1^+	1_f^-	1_3^+	3_2^+	3_f^-	K^{π} [d]	exp[e]	calc[f]	ε[g]
^{16}O	0											0^+	6.049		0.6
			−1	1								0^-_o	9.585		0.46
		−1		1								2^+	9.894		0.6
		−2		2								4^+	11.097		0.6
^{17}O	1/2			1								$1/2^-$	3.055	3.63	0.54
					1							$3/2^+$	5.869	4.99	0.58
			−1	2								$1/2^+$	6.356	8.14	0.40
			−1	$2_{1,0}$								$3/2^+$	7.202	~8.1	0.40
			−1	$2_{1,0}$								$1/2^+$	7.956	~8.1	0.40
						1						$1/2^+$	8.342	F	0.58
^{18}F	0		−1	3								0^-_e	1.080	F	0.35
			−1	3								0^-_o	4.860	F	0.35
				$2_{1,0}$								1^+	1.701	F	0.48
			−1	3								1^-_o	3.134	F	0.35
			−1	3								1^-_e	4.226	F	0.35
				$2_{0,0}$								0^+	4.360	F	0.48
				1	1							1^-	5.603	3.29	0.52
				1	1							2^-	5.786	4.57	0.52
					$2_{3,0}$							3^+	(6.485)	5.57	0.56
^{18}O	1			2								0^+	3.634	F	0.48
			−1	3								0^-_o	4.456	F	0.35
			−1	3								1^-_o	6.880	F	0.35
				1	1							2^-	5.530	7.1	0.52
			−1	3								1^-_o	6.196	F	0.35
			−1	3								0^-_e	6.351	F	0.35
				1	1							1^-	7.616	8.8	0.52

A_z	T_z	3_p^-	1_1^+	1_p^-	3_1^+	1_2^+	5_1^+	1_f^-	1_3^+	3_2^+	3_f^-	K^{π} [d]	exp[e]	calc[f]	ε[g]
^{19}F	**1/2**		−1	4								$1/2^+$	0.0	F	0.31
				3								$1/2^-$	0.110	F	0.43
				2	1							$3/2^+$	3.908	4.56	0.47
		−1		4								$3/2^-$	4.556		0.43
			−1	3	$1_{2,1}$							$5/2^-$	4.683	~5.	0.35
				1	2							$1/2^-$	5.337	4.8	0.51
					3							$3/2^+$	5.501	4.91	0.55
				$2_{1,0}$	1							$5/2^+$	5.535	5.23	0.47
				$2_{1,0}$	1							$1/2^+$	5.938	6.6	0.47
				1	$2_{3,0}$							$7/2^-$	6.167	8.12	0.51
^{19}O	**3/2**		−2	4	1							$1/2^+$	0.096	rather spherical	0.25
			−3	4	2							$1/2^+$	1.473		0.15
				2	1							$3/2^+$	3.067	3.93	0.47
				1	2							$1/2^-$	3.283	4.16	0.51
^{20}Ne	**0**											0^+	0.0	F	0.38
				−1	1							2^-	4.967	F	0.42
			−1					1				0^-_o	5.788	R	0.42
			−1					1				0^-_e	>10.5		0.42
			−1			1						0^+_e	6.725	F	0.31
			−1			1						0^+_o	14.444SM	F	0.31
				−4	4							0^+	7.191	F	0.53
				−2	2							0^+	8.700	7.89	0.46
				−1	1							1^-	8.708	F	0.42
				−2	1		$1_{4,1}$					4^+	8.820	~13.0	0.36
				−1		1						0^-_o	8.854	R	0.42
				−1		1						0^-_e	?		0.42
				−1			1					3^-	9.116	$R^{K)}$	0.35
			−1				1					2^+	9.483	$9.1^{K)}$	0.24
				−2	1		$1_{1,1}$					1^+	9.935	~12.8	0.36
			$-2_{1,0}$		$2_{3,0}$							4^+	10.553		0.24
			−1		1							2^+	10.843	F	0.31
			−1				1					3^+	10.917	$10.76^{K)}$	0.24
				−2			2					0^+	10.950	~12.4	0.32
				−1		1						1^-	11.240		0.42
				−1			1					2^-	11.555		0.35

A_z	T_z	3_p^-	1_1^+	1_p^-	3_1^+	1_2^+	5_1^+	1_f^-	1_3^+	3_2^+	3_f^-	K^{π} [d]	exp[e]	calc[f]	ε[g]
^{20}Ne	**0**	cont'd													
				−1					1			0^+_e	11.558		0.53
				$-2_{1,0}$	$2_{3,0}$							4^+	11.928	10.8	0.46
		−1			1							0^-_o	11.985		0.42
			−1		1							1^+	12.233SM		0.31
				−2	1	$1_{2,0}$						2^+	12.327	<15.8	0.46
			−1						1			0^+_e	12.436		0.23
		−1					1					1^-	12.836		0.35
				−2	1	$1_{1,0}$						1^+	13.171	<17.3	0.46
		−1				1						1^-	13.224		0.42
				−1				1				1^+	13.307		0.53
		−1			1							3^-	13.414		0.42
				−1					1			1^-	13.461	13.461	0.35
				−1					1			0^-_o	13.507	13.507	0.35
			−2				2					0^+	13.530	spherical	0.35
													:	:	
				−2		2						0^+	13.744	13.744	9.48
		−2			2							0^+	13.926	13.926	0.46
				−2	ambiguos			?	2			0^+	13.948	13.948	0.44
			−1			1						1^+	14.540SM	14.540SM	0.32
^{20}F	**1**		−1		1							2^+	0.0	F	0.31
				−1	1							1^-	0.984	F	0.42
			−1		1							1^+	1.057	F	0.31
				−1	1							2^-	1.309	F	0.42
			−1				1					3^+	2.194	2.16[K]	0.24
				−2	2							0^+	2.645 ^{20}Na	2.22	0.46
				−1		1						0^-_e	3.172		0.42
				−1		1						0^-_o	>4.082		0.42
			−1			1						0^+_o	3.488	F	0.31
			−1			1						0^+_e	3.526	F	0.31
			−1				1					2^+	3.587	3.54[K]	0.21
				−1			1					2^-	3.680	R	0.35
				$-2_{1,0}$	2							1^+	4.082	3.78	0.46
					.								:		
			−1			1						1^+	4.312	F	0.31

A_z	T_z	3_p^-	1_1^+	1_p^-	3_1^+	1_2^+	5_1^+	1_f^-	1_3^+	3_2^+	3_f^-	K^{π} [d]	exp[e]	calc[f]	ε[g]
^{21}Ne	**1/2**				1							$3/2^+$	0.0	F	0.38
				−1	2							$1/2^-$	2.789	3.56	0.42
						1						$1/2^+$	2.794	F	0.38
							1					$5/2^+$	3.735	F	0.31
								1				$1/2^-$	5.690[h]	F	0.48
			−1		$2_{0,0}$							$1/2^+$	7.211[h])	8.68	0.31
				−1	$2_{3,0}$							$7/2^-$	5.431	6.77	0.42
				−2	3							$3/2^+$	5.822[i]	6.76	0.45
									1			$1/2^+$	5.993	F	0.31
			−1		$2_{3,0}$							$7/2^+$	6.174	6.76	0.31
		−1			2							$3/2^-$	6.903		0.42
			−1		$2_{3,0}$							$5/2^+$	7.017 ^{21}Na	9.46	0.31
				−1	1		$1_{4,1}$					$9/2^-$	7.042	6.45	0.35
													: :		
			−1		1	$1_{1,0}$						$3/2^+$	7.609	~8.1	0.31
			−1				$2_{5,0}$					$9/2^+$	8.998 SM	~11.3	0.24
			−1		1		$1_{4,1}$					$9/2^+$	10.027 SM	~11.6	0.24
			−1				$2_{5,0}$					$11/2^+$	10.243 SM	~11.2	0.24
			$-2_{1,0}$		$2_{3,0}$		1					$13/2^+$	10.913 SM		0.18
^{21}F	**3/2**		−1		2							$1/2^+$	0.280	0.70	0.31
				−1	2							$1/2^-$	1.101	1.61	0.42
			−1		1		$1_{1,1}$					$3/2^+$	3.518	~4.6	0.25
			−1		1		$1_{4,1}$					$9/2^+$	3.962 SM	~3.6	0.25
			−1		1		$1_{1,1}$					$1/2^+$	3.938 SM	~3.6	0.25
			−1		1	$1_{2,1}$						$3/2^+$	4.097 SM	~3.7	0.25
			−1		1	$1_{2,1}$						$5/2^+$	4.270SM	~6.7	0.31
			−1		1		$1_{4,1}$					$7/2^+$	4.572	~5.1	0.25
			−1		1	$1_{1,1}$						$3/2^+$	4.892 SM	~3.7	0.31
					2							$3/2^-$	5.029		0.42
													: :		
			$-2_{1,0}$		2		1					$7/2^+$	5.720 SM		0.18
			−2		$2_{3,0}$		1					$11/2^+$	6.196 SM		0.18

A_z	T_z	3_p^-	1_1^+	1_p^-	3_1^+	1_2^+	5_1^+	1_f^-	1_3^+	3_2^+	3_f^-	K^{π} [d]	exp[e]	calc[f]	ε[g]
^{22}Na	**0**				$2_{3,0}$							3^+	0.0	F	0.38
					$2_{0,0}$							0^+	0.583	F	0.38
					1	1						1^+	1.973	2.1	0.38
				−1	3							1^-	2.212	1.26	0.41
						$2_{1,0}$						1^+	3.944	5.77	0.38
				−1	2	$1_{0,1}$						0^-_e	4.296	~4.3	0.39
				−1	2	$1_{0,1}$						0^-_o	4.622		0.39
				$-2_{1,0}$	4							1^+	4.319	3.23	0.45
					1	1						2^+	4.360	5.3	0.38
				−1	3							2^-	4.583	3.62	0.41
			−1		3							2^+	5.603	7.41	0.32
					1		1					1^+	5.739	5.45	0.32
					1			1				(2^-)	6.329		0.41
						$2_{0,0}$						0^+	6.413 SM	6.86	0.38
							$2_{5,0}$					5^+	6.454 SM	6.48	0.25
				$-2_{0,0}$	4							0^+	6.859	5.90	0.45
					1			1				1^-	7.074	F	0.43
					1		1					4^+	7.151	5.59	0.32
			−1		2	$1_{0,1}$						0^+_o	7.219	~8.7	0.32
			−1		2	$1_{0,1}$						0^+_e	7.585 SM	~8.9	0.32
						1	1					3^+	7.514	6.99	0.32
					1				1			2^+	7.604	7.66	0.32
		−1			3							3^-	7.681		0.41
					1				1			1^+	7.820	F	0.32
							$2_{0,0}$					0^+	8.059 SM	7.5	0.25
			−1		$2_{3,0}$		$1_{2,0}$					5^+	8.128	9.4	0.25
						1	1					2^+	8.600 SM	8.3	0.32
			−1		3							1^+	9.011 SM	9.1	0.32
^{22}Ne	**1**				2							0^+	0.0	F	0.38
			−1		3							2^+	4.456	5.77	0.32
				−1	3							2^-	5.146	5.54	0.41
					1		1					1^+	5.329	5.87	0.32
					1	1						2^+	5.365	4.73	0.38
					1		1					4^+	5.524	5.07	0.32
							2					0^+	6.235	6.36	0.25
				−1	3							1^-	6.691	7.24	0.41
					1	1						1^+	6.853	7.28	0.38

A_z	T_z	3_p^-	1_1^+	1_p^-	3_1^+	1_2^+	5_1^+	1_f^-	1_3^+	3_2^+	3_f^-	K^{π} [d]	exp[e]	calc[f]	ε[g]
^{22}Ne	**1**	cont'd													
				−2	4							0^+	6.900	5.63	0.45
			−1		2			$1_{0,0}$				0^-_o	7.051	6.8	0.41
			−1		2			$1_{0,0}$				0^-_e	≥8.976		0.41
						2						0^+	7.341	7.14	0.38
		−1			3							0^-_o	7.489		0.41
				−1	2	$1_{0,0}$						$0_2^-{}_o$	7.664		0.39
		−1			3							3^-	7.772		0.41
			−1		3							1^+	8,561	7.03	0.32
					1				1			2^+	8.596	8.27	0.32
			−1		2	$1_{0,0}$						0^+_e	8.794	7.3	0.31
					1			1				1^-_o	8.900	F	0.48
				−1	2	$1_{0,1}$						(0^-_e	8.976)	8.5	0.41
			−1		2		$1_{3,0}$					3^+	9.005 SM	10.9	0.25
					1				1			1^+	9.178	8.9	0.32
			−1		$2_{3,0}$		$1_{3,1}$					6^+	9.793 SM	11.7	0.25
						1	1					3^+	9.846 SM	9.5	0.32
						1	1					2^+	10.250 SM	8.6	0.32
			−1		2	$1_{0,1}$						0^+_o	10.080	12.2	0.31
			−1		2	$1_{0,1}$						0^+_e	10.247 SM	12.4	0.31
			−1		$2_{3,0}$		$1_{2,1}$					5^+	10.76	12.0	0.25
^{23}Na	**1/2**				3							$3/2^+$	0.0	0.09	0.34
					2	1						$1/2^+$	2.391	2.85	0.36
				−1	4							$1/2^-$	2.640	2.27	0.41
			−1		4							$1/2^+$	4.430	F	0.32
					2_{1+0}		1					$5/2^+$	5.742	7.2	0.32
					1	2						$3/2^+$	5.766	7.08	0.38
					$2_{3,0}$	1						$7/2^+$	5.927	6.55	0.38
		−1			4							$3/2^-$	5.964		0.41
					$2_{3,0}$		1					$11/2^+$	6.115	6.23	0.32
					$2_{3,0}$		1					$1/2^+$	6.308	7.56	0.32
				−1	3	$1_{2,0}$						$5/2^-$	6.820	~7.0	0.41
				−1	3	$1_{2,0}$						$3/2^-$	6.921	~7.0	0.41
					$2_{3,0}$	1						$5/2^+$	7.071	8.4	0.38
					2			1				$1/2^-$	7.488	~8.5	0.48
					$2_{0,0+1}$		1					$5/2^+$	7.566	8.02	0.32

A_z	T_z	3_p^-	1_1^+	1_p^-	3_1^+	1_2^+	5_1^+	1_f^-	1_3^+	3_2^+	3_f^-	K^{π} [d]	exp[e]	calc[f]	ε[g]
^{23}Na	**1/2**	cont'd													
					$2_{0,0}$	1						$1/2^+$	7.724	7.98	0.38
					1_1	1	$1_{1,1}$					$3/2^+$	7.872	8.8	0.32
					1	$2_{1,0}$						$5/2^+$	8.087	7.59	0.38
													: :		0.32
					2				1			$1/2^+$	8.254 SM	9.4	0.32
					$2_{0,0}$				1			$1/2^+$	9.253	10.4	0.32
					1	$2_{1,0}$						$1/2^+$	9.654	7.0	0.38
					1		$2_{5,0}$					$13/2^+$	9.667 SM	9.4	0.26
			−1		$2_{3,0}$		$2_{5,0}$					$17/2^+$	11.439 SM	~14.4	0.2
^{23}Ne	**3/2**				2		1					$5/2^+$	0.0	0.46	0.32
					2	1						$1/2^+$	1.017	2.53	0.38
			−1		3		1					$9/2^+$	2.519	5.3	0.32
					2			1				$1/2^-$	3.836	~5.3	0.48
					1		2					$3/2^+$	3.432	3.44	0.26
					2				1			$1/2^+$	3.458	3.47	0.32
			−1		3		1					$7/2^+$	4.436	7.1	0.32
													: :		
					1	2						$3/2^+$	4.921 SM	7.77	0.38
					1	1	1					$1/2^+$	5.491	6.62	0.32
			−1		3		1					$3/2^+$	5.606	~7.9	0.32
			−1		3		1					$1/2^+$	5.726	~7.2	0.32
					1	1	1					$7/2^+$	5.773 SM	7.13	0.32
					1	1						$9/2^+$	6.187 SM	5.96	0.32
^{24}Mg	**0**											0^+	0.0	F	0.38
					−1	1						2^+	4.238	F	0.38
			−1			1						0^+_e	6.433	7.8	0.32
			−1			1						0^+_o	≥12.6SM	15.5	0.32
			−1					1				0^-_o	7.555	7.82[l]	0.41
			−1					1				0^-_e	12.852		0.41
				−1			1					3^-	7.616	7.83[l]	0.35
					−1	1						1^+	7.748	F	0.38
					−1			1				1^-	8.438	F	0.46
					−1		1					4^+	8.439	F	0.32

A_z	T_z	3_p^-	1_1^+	1_p^-	3_1^+	1_2^+	5_1^+	1_f^-	1_3^+	3_2^+	3_f^-	K^{π} [d]	exp[e]	calc[f]	ε[g]
^{24}Mg	**0**	cont'd													
			−1				1					2^+	9.004	R	0.26
				−1		1						0^-_o	9.146	8.29[l]	0.41
				−1		1						0^-_e	12.383		0.41
					−2	2						0^+	9.305	8.2	0.38
				−1			1					2^-	9.533	7.52[l]	0.35
					−1		1					1^+	9.828	F	0.32
				−2			2					0^+	10.110	10.06	
			−1				1					3^+	10.660	R	0.26
					−1			1				2^-	10.660	F	0.46
					−1					1		0^+	10.680		0.32
		−1					1					4^-	11.128		0.35
		−1				1						2^-	11.181		0.41
					−1				1			1^+	11.187	F	0.32
		−1					1					1^-	11.390		0.35
					−1				1			2^+	11.453	F	0.32
				−1				1				0^+	11.457		0.49
			−1						1			0^+	11.727		0.26
					$-2_{3,0}$		$2_{5,0}$					8^+	11.860	11.88	0.26
				−1		1						1^-	11.864		0.41
					−2	1	$1_{2,1}$					2^+	11.988	13.33	0.36
													⋮		
			−1					1				1^-	12.447		0.41
					$-2_{3,0}$	$2_{1,0}$						4^+	12.845	12.13	0.38
					$-2_{3,0}$	1	$1_{3,0}$					6^+	12.861	12.92	0.36
			−2				2	spherical				0^+	13.198	10.92	0.16
		−1				1						1^-	13.253		0.41
^{24}Na	**1**				−1		1					4^+	0.0	F	0.32
					−1		1					1^+	0.472	F	0.32
					−1	1						2^+	0.563	F	0.38
					−1	1						1^+	1.346	F	0.38
			−1				1					3^+	2.904	R	0.26
			−1				1					2^+	2.978	F	0.32
					−1			1				2^-	3.372	F	0.46
					−1				1			1^+	3.413	F	0.32
			−1			1						1^+	3.589	6.07	0.38

A_z	T_z	3_p^-	1_1^+	1_p^-	3_1^+	1_2^+	5_1^+	1_f^-	1_3^+	3_2^+	3_f^-	K^{π} [d]	exp[e]	calc[f]	ε[g]
^{24}Na	**1**	cont'd													
					−2	2						0^+	3.682	3.41	0.38
					$-2_{3,0}$		2					3^+	3.896	5.41	0.26
				−1			1					2^-	3.936	2.65l)	0.35
				−1		1						0^-_e	4.048	3.36l)	0.41
				−1		1						0^-_o	>4.621		0.41
					−1			1				1^-	4.196	F	0.46
				−1		1						1^-	4.562		0.41
					−1				1			2^+	4.207	R	0.26
			−1			1						0^+_o	4.621	5.2	0.32
			−1			1						0^+_e	5.288 SM	5.04	0.32
													⋮		
					−2		$2_{5,0}$					5^+	4.891	5.46	
					−2	$2_{1,0}$						1^+	4.910 SM	6.14	0.32
					−1					1		0^+_o	5.082 SM		0.32
					−1					1		0^+_e	6.570 SM		0.32
					−2		2					0^+	5.562 SM	5.58	0.26
			−2				2					0^+	6.161 SM	4.6	0.16
				−1			1					3^-	4.7-5.2	F	0.35
^{25}Mg	**1/2**						1					$5/2^+$	0.0	F	0.32
						1						$1/2^+$	0.585	F	0.37
									1			$1/2^+$	2.564	F	0.32
					−1	1	$1_{3,0+1}$					$9/2^+$	4.060	5.16	0.32
								1				$1/2^-$	4.277[h])	F	0.46
					−1	2						$3/2^+$	4.359	4.81	0.37
				−1			2					$1/2^-$	5.116	~4.2	0.29
					−1		$2_{5,0}$					$13/2^+$	5.462	6.35	0.29
					−1	1	$1_{2,1(+0}$					$1/2^+$	5.475	6.05	0.32
					−1	1	$1_{2,1+0}$					$7/2^+$	5.744	5.17	0.32
					−1	1	$1_{3,0+1}$					$3/2^+$	5.748	6.51	0.32
					−1	$2_{1,0}$						$5/2^+$	5.862	7.04	0.37
					−1	1	$1_{3,0+1}$					$9/2^+$	5.972	7.6	0.32
										1		$3/2^+$	6.362		0.32
					−1		2					$3/2^+$	6.570	6.60	0.27
				−1		1	$1_{3,0}$					$5/2^-$	6.678		0.35
			−1				2					$1/2^+$	6.777	7.0	0.21

A_z	T_z	3_p^-	1_1^+	1_p^-	3_1^+	1_2^+	5_1^+	1_f^-	1_3^+	3_2^+	3_f^-	K^{π} [d]	exp[e]	calc[f]	ε[g]
^{25}Mg	**1/2**	cont'd													
				−1		1	$1_{3,0}$					$7/2^-$	6.888		0.36
				−1		1	$1_{2,0}$					$5/2^-$	7.038		0.36
					−1	$2_{0,0}$						$3/2^+$	7.088	~8.8	0.37
					−1		$2_{0,0}$					$3/2^+$	7.228	7.98	0.27
					−1	1			$1_{1,0}$			$5/2^+$	7.378	~8.2	0.32
											1	$3/2^-$	7.411		0.41
				−1		2						$1/2^-$	7.587		0.40
				−1		1	$1_{2,0}$					$5/2^-$	7.745		0.35
				−1		$2_{1,0}$						$3/2^-$	7.810		0.30
					−1		$2_{5,0}$					$7/2^+$	7.838	7.9	0.35
				−1		$2_{0,0}$						$1/2^-$	7.948		0.30
					−2	3						$1/2^+$	7.964	7.90	0.37
					−2	$2_{0,0}$	1					$5/2^+$	8.312	9.14	0.32
			−1				$2_{0,0}$					$1/2^+$	8.325	~10.3	0.21
					−1	1	$1_{2,0(+1)}$					$1/2^+$	8.365	8.56	0.35
													: :		
			−1				$2_{5,0}$					$11/2^+$	8.530	9.4	0.21
					−1	$2_{1,0}$						$1/2^+$	8.768SM	9.26	0.34
				−1			$2_{5,0}$					$11/2^-$	8.888	9.88	0.23
					−1	1			$1_{1,0}$			$1/2^+$	9.513SM	9.55	0.28
					$-2_{3,0}$	1	$2_{5,0}$					$17/2^+$	11.004	11.14	0.27
					$-2_{3,0}$	1	$2_{5,0}$					$15/2^+$	12.604SM	12.72	0.27
					$-2_{3,0}$		$2_{5,0}$			1		$19/2^+$	13.556SM		0.21
			−1		$-2_{3,0}$		$2_{5,0}$			$2_{3,0}$		$23/2^+$	20.613SM		0,11 spher-ical
^{25}Na	**3/2**				−1		2					$3/2^+$	0.09	0.26	0.27
			−1				2					$1/2^+$	1.069	2.1	0.21
					−1	1	$1_{3,1}$					$9/2^+$	2.781	4.25	0.32
					−1	2						$3/2^+$	3.796	4.7	0.37
					−1	1	$1_{2,1}$					$7/2^+$	3.533	3.34	0.32
					−1	1	$1_{3,1}$					$3/2^+$	3.623SM	4.73	0.32
							2					$1/2^-$	3.995	~4.54	0.29
					−2		3					$5/2^+$	4.227SM	4.02	0.21
					−1	1	$1_{2,1}$					$1/2^+$	4.289	3.53	0.32

A_z	T_z	3_p^-	1_1^+	1_p^-	3_1^+	1_2^+	5_1^+	1_f^-	1_3^+	3_2^+	3_f^-	K^{π} [d]	exp[e]	calc[f]	ε[g]
^{25}Na	**3/2**	cont'd													
													⋮		
		−1					2					$3/2^-$	5.690		0.30
^{26}Al	**0**						$2_{5,0}$					5^+	0.0	F	0.27
						1	1					3^+	0.417	F	0.32
							$2_{0,0}$					0^+	1.058	F	0.27
						1	1					2^+	1.759	F	0.32
						$2_{1,0}$						1^+	1.851	F	0.37
						1			1			1^+	2.072	F	0.32
						$2_{0,0}$						0^+	2.740	F	0.37
							1		1			3^+	3.681	F	0.27
						1			1			0^+_o	3.724	F	0.32
						1			1			0^+_e	5.462	F	0.32
							1		1			2^+	3.751	F	0.27
					−1	$1_{2,0}$	$2_{5,0}$					7^+	3.922	5.11	0.27
			−1				3					3^+	3.963	4.1	0.17
				−1		$1_{0,1}$	2					0^-_e	3.978	~4.3	0.30
				−1		$1_{0,1}$	2					0^-_o	5.950		0.30
						1		1				0^-_e	4.480		0.45
						1		1				0^-_o	6.086		0.45
				−1		$1_{1,1}$	2					1^-	4.940		0.30
				−1			3					2^-	5.007	3.8	0.25
									$2_{1,0}$			1^+	5.010	F	0.27
					−1		3					4^+	5.245	6.0	0.22
						1		1				1^-	5.431		0.45
					$-2_{0,0}$		4					0^+	5.585	6.4	0.17
					−1		3					1^+	5.671	5.3	0.22
				−1			3					3^-	5.692		0.25
								$2_{1,0}$				1^+	6.198		0.52
						1					1	1^-	6.238		0.39
					−1	3						1^+	6.270	4.80	0.4
					−1	$2_{1,0}$	$1_{4,0}$					5^+	6.598	9.9	0.29
					−1	1	$2_{0,0}$					2^+	6.852	5.5	0.27
					−1	$1_{1,1}$	2					1^+	6.874	7.9	0.27
					−1	2	$1_{1,1}$					1^+	6.936	6.3	0.29
					−1	$1_{2,0}$	$2_{5,0}$					3^+	7.051	6.3	0.27

A_z	T_z	3_p^-	1_1^+	1_p^-	3_1^+	1_2^+	5_1^+	1_f^-	1_3^+	3_2^+	3_f^-	K^{π} [d]	exp[e]	calc[f]	ε[g]
^{26}Al	**0**	cont'd													
							1	1				2^-	7.141		0.40
					$-2_{3,0}$		4					3^+	7.153	6.3	0.17
							1	1				3^-	7.161	F	0.40
							1			1		1^+	7.198		0.27
				−1		3						0^-_e	7.285		0.30
					−1	2	$1_{4,1}$					4^+	7.291	6.9	0.29
			−1				3					0^+	7.397	5.5	0.17
				−1		3						1^-	7.444		0.4
								$2_{0,0}$				0^+	7.623		0.52
			−1			$1_{0,1}$	2					0^+_o	7.879		
			−1			$1_{0,1}$	2					0^+_e	8.092 SM		0.22
													: :		
							1			1		4^+	8.186		0.29
			−1			3						0^+_e	8.855 SM		
					−1	$1_{1,0}$	$2_{5,0}$					6^+	9.388 SM	8.6	0.27
					$-2_{3,0}$	$2_{1,0}$	$2_{5,0}$					9^+	11.352 SM	13.2	0.27
					$-2_{3,0}$	1	$2_{5,0}$			1		10^+	13.550 SM		0.17
					$-2_{3,0}$		$2_{5,0}$			$2_{3,0}$		11^+	16.290 SM		0.13
^{26}Mg	**1**						2					0^+	0.0	F	0.27
						1	1					2^+	2.938	F	0.32
						2						0^+	3.589	F	0.37
						1	1					3^+	3.942	F	0.32
					−1		3					4^+	4.318	5.9	0.22
					−1	$1_{2,0}$	2					2^+	4.835	6.45	0.27
						1			1			0^+_e	4.972	F	0.32
												0^+_o	(8.577)	F	0.32
							1		1			2^+	5.291	F	0.27
						1			1			1^+	5.691	F	0.32
									2			0^+	6.256		0.27
					−1		3					1^+	6.634	6.1	0.22
							1	1				3^-	6.876	F	0.40
				−1		$1_{0,1}$	2					0^-_o	7.062		0.45
	Bandhead missing Ex ~6.8MeV			−1		$1_{0,1}$	2					0^-_e	7.261	$J^{\pi} = 2^-$	0.30
								2				0^+	7.428	6-7	0.52

A_z	T_z	3_p^-	1_1^+	1_p^-	3_1^+	1_2^+	5_1^+	1_f^-	1_3^+	3_2^+	3_f^-	K^{π} [d]	exp[e]	calc[f]	ε[g]
^{26}Mg	**1**	cont'd													
							1	1				2^-	7.542		0.40
						1		1				1^-	7.697		0.45
							1			1		4^+	7.773		0.29
				−1			3					3^-	7.824	8.2	0.25
					−1	$1_{1,0}$	2					1^+	7.840	8.4	0.27
					−2		4					0^+	7,851	6.4	0.17
			−1				3					2^+	8.033	8.3	0.17
													⋮ ⋮		
			−1			$1_{0,0}$	2					0^+_e	8.399	6.6	0.22
							1		1			3^+	8.251	F	0.27
			−1				3					3^+	8.459	6.2	0.17
					−1	2	$1_{4,1}$					4^+	8.706	9.8	0.29
					−1	$1_{1,1}$	2					1^+	9.239	9.3	0.29
					−1	$2_{1,0}$	$1_{4,1}$					5^+	9.471	10.97	0.29
					−1	$1_{2,1}$	$2_{5,0}$					7^+	9.829	10.6	0.27
					−1	$1_{1,1}$	$2_{5,0}$					6^+	9.989	10.8	0.27
^{27}Al	**1/2**						3					$5/2^+$	0.0	F	0.23
						1	$2_{5,0}$					$9/2^+$	3.004	5.24	0.27
						1	2					$1/2^+$	3.680	3.67	0.27
						1	$2_{5,0}$					$11/2^+$	4.510	5.97	0.27
						2	1					$5/2^+$	5.248	5.47	0.32
						$2_{1,0}$	1					$7/2^+$	5.433	6.7	0.32
						$2_{0,0}$	1					$5/2^+$	5.551	6.32	0.32
							$2_{5,0}$		1			$9/2^+$	5.667	~5.	0.23
						3						$1/2^+$	5.752	4.00	0.37
						$2_{1,0}$	1					$3/2^+$	5.827	5.82	0.32
							1		2			$5/2^+$	6.125	6.75	0.23
							2	1				$1/2^-$	6.996[h]	~8.4	0.35
						1	$2_{0,0}$					$1/2^+$	6.776	7.5	0.31
							2		1			$1/2^+$	7.071	~5.1	0.29
					−1	$1_{2,0}$	3					$9/2^+$	7.174	6.39	0.23
					−1	$2_{0,1+0}$	$2_{5,0}$					$13/2^+$	7.289	~10.	0.27
							$2_{5,0}$		1			$11/2^+$	7.400	~9.	0.23
													⋮ ⋮		

A_z	T_z	3_p^-	1_1^+	1_p^-	3_1^+	1_2^+	5_1^+	1_f^-	1_3^+	3_2^+	3_f^-	K^{π} [d]	exp[e]	calc[f]	ε[g]
^{27}Al	**1/2**	cont'd													
							1		$2_{1,0}$			$3/2^+$	7.677	~7.	0.23
					−1	$1_{2,0}$	3					$1/2^+$	7.792 SM	7.0	0.23
					−1	$2_{1,0}$	$2_{5,0}$					$15/2^+$	10.867 SM	12.8	0.27
					$-2_{3,0}$	3	$2_{5,0}$					$17/2^+$	11.212 SM	14.4	0.27
^{27}Mg	**3/2**					1	2					$1/2^+$	0.0	0.39	0.27
						2	1					$5/2^+$	1.940	2.96	0.32
							2		1			$1/2^+$	3.476	2.2	0.23
							2	1				$1/2^-$	4.827h)	~3.8	0.35
							1		2			$5/2^+$	4.150	5.62	0.23
					−1	$1_{1,1}$	3					$7/2^+$	4.776	6.79	0.23
					−1	$2_{1,0}$	2					$5/2^+$	5.172	7.23	0.27
					−1	$1_{2,1}$	3					$9/2^+$	5.296	6.49	0.23
					−1	2	$2_{5,0}$					$13/2^+$	9.062 SM	10.6	0.27
^{28}Si	**0**					−4	4	Near spherical				0^+	4.980		0.2
							vacuum					0^+	6.691	F	0.37
						−1	1					2^+	7.933	9.26	0.32
						−2	2					0^+	8.953	8.66	0.28
						−1		1				0^-_o	9.921		0.44
						−1	1					3^+	10.209	11.39	0.32
						$-2_{1,0}$	$-2_{5,0}$					4^+	10.311	10.09	0.28
				−1			1					3^-	10.915		0.35
						$-2_{1,0}$	$-2_{3,0}$					6^+	11.100	11.28	0.28
			−3				3	spherical				2^+	10.806		0.03
													: :		
					−1		1					4^+	12.550	16.1	0.23
					−1		1					1^+	12.715	17.5	0.23
^{28}Al	**1**					−2	2					0^+	0.972	1.93	0.28
						$-2_{1,0}$	2					1^+	1.620	2,42	0.28
						−2	$2_{5,0}$					5^+	2.582	3.59	0.28
					−1		1					4^+	3.601	7.8	0.32
						−1	1					2^+	3.632SM	3.7	0.32
						−1	1					3^+	3.709	3.48	0.32
					−1		1					1^+	4.846		

A_z	T_z	3_p^-	1_1^+	1_p^-	3_1^+	1_2^+	5_1^+	1_f^-	1_3^+	3_2^+	3_f^-	K^{π} [d]	exp[e]	calc[f]	ε[g]
^{29}Si	1/2					−3	4					$1/2^+$	4.840	5.38	0.2
						−2	3					$5/2^+$	4.895	4.72	0.23
						$-2_{1,0}$	3					$7/2^+$	6.424	5.49	0.23
						$-2_{1,0}$	3					$3/2^+$	6.496.	4.85	0.23
							1					$5/2^+$	6.522	6.14	0.32
						−1	2					$1/2^+$	6.695	5.17	0.28
								1				$1/2^-$	7995		0.44
						−1	$2_{5.0}$					$11/2^+$	8.476	8.2	ß.28
						−1	$2_{5,0}$					$9/2^+$	8.331	7.7	0.28
^{29}Al	3/2					−2	3					$5/2^+$	0.0	0.32	0.23
						−1	2					$1/2^+$	1.398	1.76	0.28
^{30}P	0						$2_{5,0}$					5^+	4.344	F	0.28
^{30}Si	1						2					0^+	5.372	4.18	0.28
						−2	4					0^+	6.642	5.57	0.20
^{31}P	1/2						3					$5/2^+$	3.295	3.1	0.24

a) holes in orbits below the Fermi boarder (vertical line) are characterized by negative occupation numbers so that $\mathbf{\Sigma u_p + \Sigma u_h = A \bmod 4}$

b) Particle/hole pairs in the same orbit must be specified by intermediate quantum numbers K', T' which are given as subscripts to the occupation numbers provided that they deviate from default values 0,1.

c) For complete identification of orbits see Fig. 1

d) The levels e, o stand for even or odd spin. An even-odd splitting is observed if two particles/holes reside in different orbits coupled to K = 0. A transfer of this splitting to K = 1 bands is possible via Corriolis coupling.

e) The label SM indicates a level predicted by the shell model, but not yet identified experimentally.

f) The letter F indicates use of the experimental energy in the process of fixing the parameters of Tables 3, 4A, the letter R indicates use for some additional predictions, see footnotes k

g) A theoretical estimate using 80 percent of the Racavy value. The renormalization ensures agreement with experimental data wherever available.

h) Level of lowest spin (rather than excitation energy) in a strongly decoupled band

I) Level of lowest spin (rather than excitation energy) in a perturbed band

k) Energy obtained from ^{24}Mg band of equal p-h character

l) Energy obtained from ^{20}Ne band of equal p-h character

Table 8

Nilsson model configurations and bandhead energies of the rotational bands with lowest isospin and oblate deformation in A = 26 - 31

Nuclide		Number of holes/particles in the orbits with $2\Omega_v^{\pi}$											Bandhead Energy [MeV]	
A_z	T_z	1_p^-	5_1^+	1_2^+	3_1^+	1_1^+	3_2^+	7_f^-	5_f^-	$3_{f\text{-}p}^-$	1_f^-	K^{π}	E_{exp}	E_{calc}
^{26}Al	0				−4			2				7^+	8.220	
					(−4			2				0^+	7.455)	
^{27}Al	1/2			−1								$1/2^+$	0.844	
					−1							$3/2^+$	1.014	
		−1										$1/2^-$	4.055	
					−2		1					$3/2^+$	6.820	
					−2	1						$1/2^+$	8.517	
^{27}Mg	3/2				−2		1					$3/2^+$	3.491	~3.4
					−2	1						$1/2^+$	5.028	~3.4
^{28}Si	0					vacuum						0^+	0.0	
					−1		1					3^+	6.276	
				−1				1				3^-	6.879	
					−1	1						2^+	7.416	
					−1	1						1^+	8.238	
					−1			1				2^-	8.819	
		−1				1						0^-_o	8.905	
		−1				1						0^-_e	≥11.142	
				−1		1						1^+	9.496	
					−1			1				5^-	9.702	
					−1					1		3^-	10.541	
				−1			1					1^+	10.725	
			−1				1					1^+	10.994	
				−1		1						0^+_e	11.142	
				−1		1						0^+_o	11.986	
				−1			1					2^+	11.148	
				$-2_{1,0}$			$2_{3,0}$					4^+	11.196	

A_z	T_z	1_p^-	5_1^+	1_2^+	3_1^+	1_1^+	3_2^+	7_f^-	5_f^-	$3_{f\text{-}p}^-$	1_f^-	K^π	E_{exp}	E_{calc}
^{28}Si	**0**	cont'd												
				−1					1			3^-	11.266	
			−1				1					4^+	12.241	
					$-2_{3,0}$	$2_{1,0}$						4^+	12.324	
					$-2_{3,0}$	$1\_\_\_\_1_{1,0}$						4^+	12.474	
					−1		1					0^+_e	12.805	
					−1		1					0^+_o	13.190	
				$-2_{1,0}$		$2_{1,0}$						0^+	12.977	
					$-2_{3,0}$		$2_{3,0}$					6^+	13.231	
^{28}Al	**1**				−1		1					3^+	0.0	
					−1	1						2^+	0.031	
					−1	1						1^+	1.373	
					−1		1					0^+_o	2.201	
					−1		1					0^+_e	3.011	
				−1		1						0^+_o	3.105	
				−1		1						0^+_e	3.762	
				−1			1					2^+	3.347	
				−1				1				4^-	3.465	
				−1		1						1^+	3.542	
				−1				1				3^-	3.591	
					−1			1				2^-	3.876	
					−1			1				5^-	4.033	
				−1			1					1^+	4.115	
^{29}Si	**1/2**					1						$1/2^+$	0.0	
							1					$3/2^+$	1.273	
								1				$7/2^-$	3.624	
										1		$3/2^-$	4.935	
					−1	1	$1_{2,1}$					$7/2^+$	5.813	6.3
				−4		4		1	spherical			$7/2^-$	6.194	
											1	$1/2^-$	6.380	
					−1		$2_{3,0}$					$9/2^+$	6.616	5.9
					−1	$2_{1,0}$						$5/2^+$	6.710	6.3
					−1	2						$3/2^+$	6.715	6.2
					−1	$1\_\_\_\_1_{2,0}$						$7/2^+$	6.921	7.3

A_z	T_z	1_p^-	5_1^+	1_2^+	3_1^+	1_1^+	3_2^+	7_f^-	5_f^-	$3_{f\text{-}p}^-$	1_f^-	K^π	E_{exp}	E_{calc}
^{29}Si	**1/2**	cont'd												
									1			$5/2^-$	7.014	
				−1		$2_{0,0}$						$1/2^+$	7.057	6.2
			−1	−1		2						$1/2^+$	7.521	7.0
		−1				$2_{0,1 \text{ or } 1,0}$						$1/2^-$	7.692	
					−1	$2_{0,0}$						$3/2^+$	8.349	8.4
				−1		$2_{1,0}$						$3/2^+$	8.418	8.3
					−1	$2_{1,0}$						$1/2^+$	8.528	8.9
					−1	1 ⊗	$1_{1,1}$					$5/2^+$	8.540	8.8
				−1		$2_{0,0}$						$1/2^+$	8.663	8.4
													⋮	
		possibly			−1		$1_{3,0+1}$	1				$13/2^-$	11.485	
		possibly			−1		$1_{3,1+0}$	1				$13/2^-$	12.222	
^{29}Al	**3/2**				−1	2						$3/2^+$	2.866	1.0
				−1		2						$1/2^+$	3.433	1.0
					−1		2					$3/2^+$	3.642	4.3
					−1	1 ⊗	$1_{1,1}$					$5/2^+$	3.816SM	3.0
				−1			2					$1/2^+$	4.220	4.7
					−1	1 ⊗	$1_{2,1}$					$7/2^+$	4.403	1.8
^{30}P	**0**					$2_{1,0}$						1^+	0.0	
						$2_{0,0}$						0^+	0.709	
						1	1					2^+	2.724	
							$2_{3,0}$					3^+	2.840	
						1	1					1^+	3.019	
				−2		4						1^+	3.734	
							1	1				2^-	4.144	
						1		1				4^-	4.232	
							1	1				5^-	4.926	
							$2_{0,0}$					0^+	4.941	
					−1		3					3^+	5.207	
		−1				3						0^-_e	5.411	
					−1	3						2^+	5.471SM	~6.
				−1 ⊗		2	$1_{1,1}$					1^+	5.506SM	

A_z	T_z	1_p^-	5_1^+	1_2^+	3_1^+	1_1^+	3_2^+	7_f^-	5_f^-	$3_{f\text{-}p}^-$	1_f^-	K^π	E_{exp}	E_{calc}
^{30}P	**0**	cont'd												
				−1		3						0^+_o	5.702	~4.8
				−1		3						0^+_e	(6.481)	
						1				1		2^-	5.908	
						1				1		1^-	5.997	
						1		1				3^-	6.006	
					−1	3						1^+	6.854	~7.4
					-1	$1_{2,0}$	$2_{3,0}$					5^+	6.229	
													:	
								$2_{7,0}$				7^+	7.199	
				−1		2	$1_{2,1}$					2^+	7.203	
					−1		3					0^+_o	7.493	
					−1		3					0^+_e	7.931	
					−1	2	$1_{3,1}$					3^+	7.636	
^{30}Si	**1**					2						0^+	0.0	
						1	1					2^+	3.499	
						1	1					1^+	3.770	
							2					0^+	3.788	
					−1		3					3^+	5.232	
						1		1				3^-	5.488	
							1	1				2^-	6.641	
						1				1		1^-	6.744	
					−1	3						2^+	6.914	~7.2
							1	1				5^-	7.044	
					−1	2	$1_{3,1}$					3^+	7.079	
				−1		2	$1_{2,1}$					2^+	7.256	
				−1		3						0^+_e	7.443	~8.
								2				0^+	7.530	
						1		1				4^-	7.613	
					−1	3						1^+	7.668	~8.8
						1				1		2^-	8.155	
		−1				3						0^-_o	8.163	
				−1		2	$1_{1,1}$					1^+	8.290	
							1			1		3^-	8.443	
					-1	$1_{2,1}$	$2_{3,0}$					5^+	7.001	
													:	

A_z	T_z	1_p^-	5_1^+	1_2^+	3_1^+	1_1^+	3_2^+	7_f^-	5_f^-	$3_{f\text{-}p}^-$	1_f^-	K^π	E_{exp}	E_{calc}
^{30}Si	**1**	cont'd												
							1		1			4^-	9.045	
^{31}P	**1/2**					3						$1/2^+$	0.0	
				−1		4						$1/2^+$	3.134	
					−1	4						$3/2^+$	4.594	
						2	1					$3/2^+$	4.261	
					−1	2	$2_{3,0}$					$9/2^+$	6.080	
^{31}Si	**3/2**					2	1					$3/2^+$	0.0	~0.9
						1	2					$1/2^+$	0.752	~2.2
					−1	2	2					$3/2^+$	4.259	
				−1		2	2					$1/2^+$	4.720	
					−1	2	$2_{3,0}$					$9/2^+$	5.580SM	~5.7
				−1		2	$2_{3,0}$					$7/2^+$	5.631SM	~8.6

Table 9

The high-K character of yrast states in ^{25}Mg, ^{26}Al and ^{27}Al

^{25}Mg						^{26}Al						^{27}Al					
E_x[MeV][a)]	$2J^\pi$	$2K^\pi$	cosΘ[b)]	ε	d[c)]	E_x[MeV]	$2J^\pi$	$2K^\pi$	cosΘ	ε	d	E_x[MeV]	$2J^\pi$	$2K^\pi$	cosΘ	ε	d
0.	5^+	5^+	0.84	0.32	3281	0.	10^+	10^+	0.91	0.27	2551	0.	5^+	5^+	0.84	0.23	5504
1.611	7^+	5^+	0.63	0.32	3444	3.508	12^+	10^+	0.77	0.27	1953	2.211	7^+	5^+	0.63	0.23	5860
3.405	9^+	5^+	0.50	0.32	3144	3.922	14^+	14^+	0.94	0.27	1403	3.003	9^+	9^+	0.90	0.27	5460
5.251	11^+	9^+	0.75	0.32	2544	7.3	16^+	14^+	0.76	0.27	850	4.509	11^+	11^+	0.92	0.27	4525
5.466	13^+	13^+	0.93	0.29	1839	11.0	18^+	14^+	0.74	0.27	483	7.289	13^+	13^+	0.93	0.27	3360
9.652	15^+	13^+	0.81	0.29	1181	13.5	20^+	20^+	0.95	0.17	216	10.8	15^+	15^+	0.94	0.27	2225
11.004	17^+	17^+	0.94	0.27	657	16.3	22^+	22^+	0.96	0.13	91	11.2	17^+	17^+	0.95	0.27	1308
13.6	19^+	19^+	0.95	0.21	315	21.1	24^+	22^+	0.84	0.13	24	14.9	19^+	17^+	0.85	0.27	666
18.0	21^+	19^+	0.86	0.21	123	26.1	26^+			0.13	6	18.4	21^+	17^+	0.77	0.27	290
20.6	23^+	(23^+)e)	0.96	0.11	37					0.13		21.0	23^+	23^+	0.96	0.18	101
25.0	25^+				8							26.4	25^+	23^+	0.88	0.18	26
												32.6	27^+			0.18	3

a) A one-digit accuracy characterizes a state predicted by the USD-shell model

b) Defined by cos Θ = K/ $\sqrt{J(J+1)}$

c) Dimension of the basis in the USD model

e) unsafe, see text

17. Data base (A = 16 - 30)

The analysis of parts I, II uses roughly 1500 experimental levels which are mainly from

Tilley et al.	Nucl. Phys.	A 636, 249 (1998)	A = 20
		A 595, 1 (1995)	A = 18 - 19
		A 564, 1 (1993)	A = 16 - 17
Endt	Nucl. Phys	A 521, 1 (1990)	A = 21 - 44
		A 633,1 (1998)	A = 21 - 44

Additional information is retrieved from

A. Hoffmann et al.	Z. Phys.	A 332, 289 (1989)	^{21}Ne
F. Heidinger et al.	Z. Phys.	A 338, 23 (1991)	^{25}Mg
H. Röpke and P.M.Endt	Nucl. Phys.	A 632, 173 (1998)	^{26}Al, ^{26}Mg
H. Röpke	Nucl. Phys.	A 674, 95 (2000)	^{27}Al
W. Brendler et al.	Z. Phys.	A 281, 75 (1977)	^{27}Mg
E. Bitterwolf et al.	Z. Phys.	A 298, 279 (1980)	^{30}Si

The standard compilations contain 3 levels which were considered dubious with, E_x (KeV)

6857 ^{21}Ne

7200 ^{26}Mg

8819 ^{29}Si

They are omitted as well as six other states which seem equally dubious to us.

6706 ^{20}Ne fed in β-decay with a branch of $3 \cdot 10^{-3}$ %

8820 ^{20}Ne l = 5 resonance in (α, α_0). Extremely difficult to accommodate in a Nilsson model. We prefer l = 4 resonance instead.

9196 ^{20}Ne Peak with "unusual" line shape in spectrum of β-delayed α's from ^{20}Ne. Interference effect rather than a state

2410 ^{21}F seen only in (d, τ) with l = 1 s = 0.04, not convincing

7122 ^{23}Na absent in all reactions except resonance fluorescence

5993/5997 ^{30}P $(0\text{-}2)^-/1^+$, T = 0/1. There is no 1^+, T = 1 state around. A single $J^\pi = 1^-$ state, formed with l = 1 .

A total of 21 levels have assignments/restrictions of quantum numbers which do not agree with our preferences.

Level		J^π or $2J^\pi$		
Nuclide	E_x[KeV]	previous	present	Our rationale
^{20}Ne	9935	1^+ π = u	2^-	Dominance of magnetic over electric dipole decay between T = 0 states
	15555	(3^+) π = u	2^-	Dominance of magnetic over electric dipole decay between T = 0 states
^{20}F	4312	0^+	1^+	Shell model demands a 1^+ level and excludes existence of a 0^+ below 7 MeV
^{21}Ne	5431	7^+	7^-	Alleged presence of a positive-parity mirror analog is abandoned. The β-delayed proton group could stem from p_1 rather than p_0 decay of ^{21}Na
^{19}F	7114	7^+, Γ_α = 32 KeV	(5^-)	l = 3 resonance in (α,α_0) rather than l = 4
	9280	7^+, 9^+	π = − (J = 7)	Exclusive γ-decay to π = − states
^{22}Na	5863	$(1, 2)^+$	2^-	l = 0+2 in transfer could be l = 1. While the spectrum of π = + states is under control, the 4296 KeV, 0^- state must be followed by a 2^- state.

Level		J^{π} or $2J^{\pi}$		
Nuclide	E_x[KeV]	previous	present	Our rationale
^{22}Na	6859	$(1 - 3)^-$	1^+	This E_p = 126 KeV resonance in (p, γ) should be s-wave in character ($J^{\pi} = 1^+$), 1_5^+, 6413 KeV.
^{22}Ne	8490	2^+	3^+	J = 3, 5 from (α,p γ) angular correlation 3_4^+, 8435 KeV
	9229	$(1, 2)^+$	3^-	Low energy γ-decay to $J^{\pi} = 1^-$ and 2^- states
	10751	5, π = u	5^+	Identification of this J = 5 level from (α,p γ) with an (α,γ) resonance is erroneous. 5_5^+, 10667 KeV
	11520	7, π = u	7^+	The combination of J = 7 from (α,p γ) and π = n from (t, p) is very doubtful. S. M. demands a 7_2^+ at 11481 KeV
^{23}Ne	2517	$(5, 7)^+$	9^+	The unique counterpart of the 9_1^+ shell-model state, predicted at 2516 KeV. The reported J^{π} rests on a pretty weak branch in β-decay.
^{24}Mg	9284	2^+	3^-	γ-decay to 4^+ speaks against 2^+. l = 2 from transfer not convincing. Proliferation of positive-parity states speaks for π = −
	11293	2^+, 3^-, 4^+ π = n	5^-	l = 1 assignment in transfer is not convincing because of insufficient resolution. γ-decay to 4^+ and 3^- speaks for $J^{\pi} = 5^-$
^{24}Na	3896	$(1 - 3)^-$	3^+	l = 1+3 from transfer could easily be l = 2 Shell model 3_6^+ is needed near 3778 KeV
^{25}Na	2788	$(3, 7)^+$	9^+	9_1^+ shell model state predicted at 2542 KeV. How trustworthy is an angular correlation in (t,α γ)?
^{27}Al	7227	9^-	9^+	Level has E_x and γ-decay of 9_7^+ SM state at 7462 KeV. π = + was excluded by an M2 contribution of a dicy feeding γ-ray in (p, γ)
^{27}Mg	4398	5^+	9^+	Reported J^{π} from feeding in (n,γ) is irrelevant because the γ-ray energy is wrong by 71 KeV. The J^{π} from Brendler is preferred.
	5422	3^-	3^+	The l = 1 assignment from (d, p) is questionable because of weak intensity. The 3_4^+ SM state is expected at 5226 KeV
^{30}P	5232	4^-	5^+	Feeding from 5^+, T = 1, decay to 3^+. The SM 5_2^+ is expected at 5105 KeV. A distinction between l = 3 and l = 4 in stripping is not beyond doubt.
^{30}Si	8190	2^+	4^+	A typical ambiguity in angular correlations $4^+ \rightarrow 2^+$ is mimiked by $2^+ \rightarrow 2^+$ with δ = − 2.0

Roughly 200 out of 1050 considered experimental states have restrictions of their quantum numbers only. In the following we use experimental facts which are considered weak arguments by the compilers, to arrive at a unique result or we use the predictions of the shell model. In this case we cite the J_ν^π and E_x of the SM. Another rationale which is frequently used is the alleged magnetic dipole character (MDC) of low-energy transitions to the higher-lying states of negative parity.

Level		J^π or $2J^\pi$		
Nuclide	E_x[KeV]	previous	present	Our rationale
^{19}F	5337	1	1^-	MDC
	7929	7^+, 9	9^+	9_3^+, 7988
	9267	11^+, 9^+	11^+	Rotational model
^{20}Ne	10694	4^-, 3^+	4^-	MDC
^{20}F	3171	0^-, 1^+	0^-	MDC
	3587	(2)	2^+	2_3^+, 3361
	3590	(3)	3^+	3_4^+, 3484
	3680	2	2^-	MDC
	3761	≥ 3	π = −	l = 3 in ^{18}O(τ,p)
	4371		π = −	MDC, (3^-) because of γ-decay to 3680 Kev, inband decay
^{21}Ne	6747		(5^-)	Rotational model, the sole candidate
	6550	9	9^-	Rotational model, the sole candidate
	8241	11	11^-	Rotational model, the sole candidate
	7042	9	(9^-)	Not s-d state, π = + Intruder impossible to explain
	6900	$(1, 3)^-$	3^-	J^π from mirror analog at 6879 KeV in ^{21}Na
^{21}F	1755	−	9^+	9_1^+,1844 Support from τ = 3.5 ps (E2→5_1^+)
	2070		5^-	Rotational model, the sole candidate
	3460	$(3, 5)^+$	3^+	3_2^+, 3512; 3460 → 1^+ speaks for 3^+

Level		J^{π} or $2J^{\pi}$		
Nuclide	E_x[KeV]	previous	present	Our rationale
^{21}F	3518	$(3, 5)^+$	5^+	5_2^+, 3681
	3638	–	7^+	7_2^+, 3612 (or 9_2^+, 3692) Decay to 1755 KeV
	4572		7^+	Decay to 5^+, 7^+; 7_2^+, 4427
^{22}Na	5131	–	2^+	Not s-d state. The 4319 KeV, 1^+ intruder state must be followed by a 2^+ state
	5308	–	5^+	Feeding from 7_3^+ state; 5_3^+, 5378 KeV
	5318	$(1, 3)^+$	3^+	3_5^+, 5575 KeV
	5442	$(2, 3)^-$	(3^-)	Rotational model
	5603	$(1, 2)^+$	2^+	2_4^+, 5665 KeV, No room in SM for 1^+
	5700	$0^+ - 4^+$	3^+	$\neq 4^+$ because of decay to 2^+, T = 1; 3_6^+, 3971 KeV
	5725	0 - 4	4^+	4_3^+, 5652 KeV
	5739	$(0, 1)^+$	1^+	1_4^+, 5673 KeV; $0^+ > 7.5$ MeV SM
	5863	$(1, 2)^+$	(2^-)	I = 0+2 in transfer could be I = 1, SM has no room for 1^+, 2^+ states
	5920		3^-	Rotational model, the sole candidate
	5988	2^+, 3^+	3^+	The third π = + state outside the s-d space; Rotational model requires 3^+.
	6329	$(0 - 3)^-$	(2^-)	Theoretical argument. There is an urgent need for a $K^{\pi} = 2^-$ bandhead and no other choice
	6433			4_4^+, 6268 KeV
	6523			1_5^+, 6413 KeV
	6580			5_4^+, 6454 KeV
	6636		**Correspond to**	2_5^+, 6785 KeV; hence all experimental levels have an explanation while two high - spin states have remained unobserved
	6668			4^-, K = 2, 6600 KeV
	6714			5^-, K = 0, 6900 KeV
	6981	High-spin		6^-, K = 1, 7200 KeV
				6_2^+, 7201 KeV
				5_5^+, 7290 KeV

T = 0 resonances of the ^{21}Ne(p, γ) reaction

Level		J^{π} or $2J^{\pi}$		
Nuclide	E_x[KeV]	previous	present	Our rationale
^{22}Na	6859		1^+	See page 191
	6998	3^+	3^+	
	7016	3	3^-	Decay to 2^-, T = 1
	7074	1^-, 2	1^-	Decay to 2^-, T = 1
	7151	$(3, 4)^+$	4^+	4_5^+, 7050 KeV; Decay to 4^+, T = 1
	7219	1^+, 2	1^+	1_6^+, 7054 KeV
	7278	4^+ - 6^+	4^+	I = 2 character of this low energy (p, γ) resonance (E_p = 566 KeV) is mandatory
	7359	3^+, 4^-	4^-	No room for 3^+ in SM while 4^- is badly needed by rotational model
	7371	2	2^-	MDC
	7377	$(2, 3)^+$	3^+	≠ 2^+ because of decay to 4^+, T = 1; 3_8^+, 7272 KeV
	7400	$(1, 2)^+$	1^-	π = − MDC, decay to 0^+ ≠ M2
	7422	2	2^-	MDC
	7514	3^+	3^+	3_9^+, 7546 KeV
	7604	$(1, 2)^+$	2^+	Two decays to 3^+ speak against J = 1, 2_8^+ 7221 KeV
	7635	2^+, 3	3^+	Decay to 4^+, T = 0 and 4^+ T = 1 speak against 2^+. Not a s-d state
	7682	2^+ - 4^+	3^-, 4^+	Suggested from decay, no room for 4^+ in SM and rotational model
	7800	1, 2^+	2^+	Decay to 3^+. Not a s-d state
	7820	1, 2^+	1^+	49% →0^+. 1_7^+, 7964 KeV
	8017	4, 5^+	5^+	T = 0 by decay to 4^+, T = 1. J = 5 by decay to 6^+; 5_6^+, 7908 KeV

Level		J^{π} or $2J^{\pi}$		
Nuclide	E_x[KeV]	previous	present	Our rationale
^{22}Na	8128		5^+	5_7^+, 8407 Level in (^{14}N, α), (τ, p) but not in (p, γ) $l_p \geq 4$ $J^{\pi} = 5^+, 6,...$
	8221	$4^+ - 6^+$	6^+	6_3^+, 7991 KeV
	8572	$5^+ - 8^+$	8^+	Decay properties of the 8_1^+ SM state at 8378 KeV
	8610	$3^+ - 7^+$	7^+	Decay properties of the 7_2^+ SM state at 7754 KeV
	8724	$0^- - 7^-$	7^-	Rotational model, inband decay to 5^-
	9060	$4^+ - 7^+$	7^+	Decay properties of the 7_3^+ SM state at 8849 KeV
	9813	$5^+ - 9^+$	9^+	Decay properties of the 9_1^+ SM state at 9681 KeV
^{22}Ne	6634	$(2, 3)^+$	3^+	3_2^+, 6520 KeV
	6900	$(0, 1)^+$	0^+	Analog of 7546 0, T = 1 in ^{22}Na Not a s-d state
	7344	$(3, 4)^+$	4^+	4_4^+, 6993 KeV
	7423	$(3, 5)^+$	5^+	5_1^+, 7264 KeV
	8162	3	3^+	3_3^+, 7741 KeV
	8490		3^+	See page 191
	8561	$(1, 2)^+$	1^+	1_3^+, 8586 KeV
	8855	4^+	5^-	Decay to 6^+ and 3^-
	8900	$(4, 5)^+$	5^+	Decay to 6^+, 5^+, 3^+ 6_2^+, 9219 KeV or 4_6^+, 8725 KeV would fit
	9229		3^-	See page 191
	9324	$1^- - 5^-$	4^-	100% → 7722, 3^-. Inband decay
	: :			
	10425	6, 8	6^+	6_4^+, 10425 KeV
	10654	5	5^+	5_4^+, 10068 KeV
	11130	6 - 8	6^+	6_6^+, 11655 KeV

Level		J^{π} or $2J^{\pi}$		
Nuclide	E_x[KeV]	previous	present	Our rationale
^{23}Na	5778	In (d, α)→ high spin	9^+	9_2^+, 5951 KeV
	6115	$(5^+ - 11^+)$	11^+	11_2^+, 6149 KeV
	6578	$(5, 9)^+$	9^+	Decay to 9^+; 9_3^+, 6180 KeV
	6618	$(5, 7)^+$	7^+	7_4^+, 6499 KeV
	6867	$(3, 5)^+$	5^+	5_5^+, 6747 KeV; ^{23}Mg 5^+ at 6899 KeV
	7070	$(3 - 7)^+$	5^+	5_6^+, 6836 KeV; ^{23}Mg 5^+ at 6984 KeV
	7122		Absent, see p. 116	
	7133	$(3, 5)^+$	5^+	5_7^+, 6946 KeV; ^{23}Mg 5^+ at 7146 KeV
	7154	in (d, α)	11^+	11_3^+, 7156 KeV
	7184	→ high spin	9^+	9_4^+, 7057 KeV
	7267		13^+	Decay to 11^+, 13^+; 13_2^+, 7313 KeV
	7277	5^-, 7	(7^-)	Rotational model, inband decay to 5^-
	7390	$1 - 7^+$	7^+	Decay to 9^+; 7_5^+, 7365 KeV
	7412	$5 - 9^+$	9^+	9_5^+, 7602 KeV
	7452	5^-, 7^-	7^-	Rotational model
	7488	$(1, 3)^-$	1^-	Decay to 1^-, 1^+ excludes 3^-
	7686	in (d, α)→ high spin	7^+	7_6^+, 7633 KeV
	7834	5^+, 7	$7(^+)$	Decay to 9^+; 7_7^+, 7739 KeV
	7876	5	5^-	MDC
	7965		7^+	Decay to 5^+, 7^+; 7_8^+, 8197 KeV
	7980		11^+	100% → 9^+ in ^{12}C(^{12}C,p γ), 11_4^+, 7614 KeV
	9041		15^+	Decay to 13^+,11^+; 15_1^+, 9001 KeV
	9802		15^+	Decay to 13^+,11^+; 15_2^+, 9548 KeV
^{23}Ne	2517		9^+	See p. 191
	3458	$(1 - 5)^+$	1^+	Decay to 1^+,3^+; 1_2^+, 3494 KeV
	3831	$(3 - 7)^+$	7^+	7_2^+, 3605 KeV
	3843		11^+	Decay to 2517 KeV; 11_1^+, 3931 KeV
	3988	$3^+(5^+)$	3^+	3_3^+, 3778 KeV
	4010		5^+	5_3^+, 3826 KeV, Decay to 5^+ is compatible

Level		J^{π} or $2J^{\pi}$		
Nuclide	E_x[KeV]	previous	present	Our rationale
^{23}Ne	4270		9^+	9_2^+, 4197 KeV. Absence in β-decay is compatible
	4436	$(3 - 7)^+$	7^+	Decay to 7^+,9^+; 7_3^+, 4395 KeV
	5220	$(5, 7)^-$	5^-	Weakness in stripping favours $f_{5/2}$ rather than $f_{7/2}$ transfer
^{24}Mg	7812	4^-, 5^+	5^+	5_1^+, 7883 KeV
	9284	2^+	3^-	See p. 191
	9299	$(3, 4)^-$	4^-	Rotational model
	9305	$0^+ - 2$	0^+	0_3^+, 9560 KeV the sole exp. candidate
	9458	$(2, 3)^+$	3^+	Two decays to 4^+; 3_2^+, 9596 KeV
	9533	2, 3	$(2)^-$	π = − from MDC, J from rotational model
	10161		4^-	Rotational model, sole exp. candidate J^{π} = $(0,1)^+$ in the compilation refers to the 11110 level (bad resolution)
	10581	3, 4^+	3^+	3_3^+, 10803 KeV; All 4^+ SM states > 500 KeV are known
	10659	$(1 - 3)^-$	3^-	Rotational model
	10660	$(3, 4)^+$	3^+	3_4^+, 11223 KeV
	11128		(4^-)	100% → 3_1^-
	11293		5^-	See p. 191
	11330	$2^+ - 4^+$	3^+	3_5^+,11580 KeV; Decay to 2^+ is compatible
	11595		5^-	Already known, errors in compilation
	11860	6^+, 7^-, 8^+	8^+	8_1^+, 12088 KeV
	12128	3 - 5	5^+	5_3^+,12296 KeV
	12344	π = N	7^+	7_1^+, 12283 KeV; Decay to 5_1^+ is compatible
	13213		8^+	8_2^+, 13160 KeV; Decay to 6_1^+ is compatible
^{24}Na	3896		3^+	See p. 191
	3936	$0^+ - 4^+$	2^-	$p_{1/2}$ hole; PRC 57,1256
	3944	$2^+ - 6^+$	5^+	5_2^+, 3943 KeV
	3977	1^-, 2^+	2^+	2_6^+, 3999 KeV
	4196	$(1, 2)^-$	$1^-(2^-)$	Rotational model
	4220		6^+	6_1^+, 3883 KeV; Decay to 4^+, 5^+ is compatible
	4621		1^+	1_5^+, 4485 KeV; 100% → 2^+

Level		J^{π} or $2J^{\pi}$		
Nuclide	E_x[KeV]	previous	present	Our rationale
^{24}Na	4692		5^+	5_4^+, 4536 KeV; 100%→ 4^+
	4891	3^+, 4^-, 5^+	5^+	5^+, 4665 KeV; 100% → 4^+
^{25}Na	2788	$(3, 7)^+$	9^+	See p. 191
	3353	$(3 - 7)^+$	7^+	7_2^+, 3019 KeV
^{27}Al	7227		9^+	See p. 191
	9989		15^+	86% → 8693 KeV, 13^+; Geesaman, private communication
	6996	$(1, 3)^-$	(1^-)	Rotational model
	7798	3 - 7	7^-	"Inband decay" to 5438, 5^-
^{27}Mg	4398		9^+	See above
	5172	$(3, 5)^+$	5^+	5_6^+, 5101 KeV
	5296	5, 7^+, 9	9^+	9_3^+, 5256 KeV; For J = 9 pure dipole decay to 9_1^+
	5412	5, 7	7^+	7_4^+, 5206 KeV; For J = 7 two decays by dipole radiation
	5422			See above
	5749	5, 7 ,9	7^+	7_5^+, 5481 KeV; pure dipole decay for J = 7
	6009	7, 9	7^+	7_6^+, 5813 KeV; pure dipole decay for J = 7
	6161	$7^+ - 11^+$	11^+	11_1^+, 6222 KeV; Stretched quadrupole decay to 7^+ verified by angular correlation
	6312	$3^+ - 9^+$	9^+	9_4^+, 6017 KeV
	6651		9^+	9_5^+, 6686 KeV; Decay to 7^+
	6721	$5^+ - 11^+$	11^+	11_2^+, 6581 KeV; unique candidate from γ-decay to 7^+, 9^+
	6811		9^+	9_6^+, 6753 KeV; Decay to 7^+
^{29}Al	3935	$(3, 7)^+$	7^+	7_2^+, 3874 KeV
^{30}Si	8330	Doublet?	4^+	Decay to 5^+ implies presence of a $J^{\pi} = 3^+$. 4… level; 4_5^+, 8607 KeV
	9131	$(4, 5)^+$	5^+	Angular correlation of decay to 3^+ compatible with stretched quadrupole transition; 5_2^+, 8941 KeV
	10288	$(4, 5)^+$	5^+	5_4^+, 10271 KeV
	10420	$(2 - 6)^+$	6^+	Exclusively to 4^+; 6_2^+, 10485 KeV
	10823	4, 5^+, 6^+	6^+	Angular correlation of decay to 4^+ compatible with stretched quadrupole transition; 6_3^+,10966 KeV

Level		J^{π} or $2J^{\pi}$		
Nuclide	E_x[KeV]	previous	present	Our rationale
^{30}Si	11417	6^+, 4^+	6^+	Angular correlation as with 10823 KeV; 6_4^+, 11258 KeV
	11493	3^+ - 6^+	6^+	6_5^+, 11671 KeV
	12015	4 - 6^+	6^+	6_6^+, 11684 KeV
	12220	5^-, 6^+	6^+	6_7^+, 12186 KeV
	12524	5^-, 6^+	6^+	6_8^+, 12352 KeV
	7634	1, 2^+	2^+	2_8^+, 7441 KeV
	7668	1^+, 2^+	1^+	1_2^+, 7609 KeV
	7623	2^+	3^-	Theoretical reasons. We have a surplus of 2^+ states (shell model) and a bad need of a 3^- state (Nilsson model). $J^{\pi} = 3^-$ has probably been excluded by an 8% branch for ground state decay which is not compelling

A series of levels above the 8190 KeV level can have $J^{\pi} = 4^+$ or lower spin. They are correlated here with the 4_6^+ - 4_{10}^+ and 3_6^+ - 3_8^+ levels of the shell model as follows

Level		J^{π} or $2J^{\pi}$		
Nuclide	E_x[KeV]	previous	present	Our rationale
^{30}Si	8537	3^+, 4^+		4_6^+, 8696 KeV
	8640	1^+, 2, 3, 4^+		3_6^+, 8757 KeV
	8684	2, 3, 4^+		4_7^+, 8933 KeV
	8887	0^+ - 4^+		
	9406	1^+ - 4^+		4_8^+, 9361 KeV
	9475	$1(^+)$ - 4^+		4_9^+, 9761 KeV
	9595	0^+ - 4^+		Feeding in thermal neutron capture speaks for $\pi = -$, together with γ-decay $J^{\pi} = 2^-$
	9576	1^+, 2, 3		3_8^+, 9562 KeV
	9605	2, 3, $4(^+)$		Decay to 3^- speaks for negative parity
	9761	2^+, 3, 4^+		4_{10}^+, 9932 KeV

The unassigned 8887 KeV level is the welcome and only candidate of a $J^{\pi} = 3^-$, $K^{\pi} = 2^-$ level

Level		J^{π} or $2J^{\pi}$		
Nuclide	E_x[KeV]	previous	present	Our rationale
^{30}P	5232		5^+	5^+ see further below
	5411	$0^-(2^-)$	$4^+ + 2^+$	Feeding from 5^+, T = 1 and strong decay to 2^+, T = 1 do not fit together. 4_2^+, 5146 KeV and 2_5^+, 5471 KeV are missing. It is also feasible to assign 5^+ to the high-spin part of the 5411 KeV doublet and 4^+ to the 5232 KeV state
	5506	1	1^+	1_6^+, 5896 KeV
	5714	$(5, 7)^+$	5^+	5_3^+, 5571 KeV
	5808	$(3, 5)^+$	3^+	3_7^+, 6166 KeV
	5934		4^+	Feeding from E_x = 6971 KeV level to which we shall assign J = 4, T = 0. Decay to 5^+ and 2^+, T = 1. The latter decay due to mixing of 5934 KeV with 6051 KeV, 4^+, T =1; 4_4^+, 6221 KeV
	5993	$(0 - 2)^-$		See p. 190
	6006	3	3^-	Feeding from 7045 KeV, π = − state
	6181	$(5 - 7)^+$	5^+	5_4^+, 6377 KeV; 6_1^+ far way at 7120 KeV
	6229	$(3, 5)^+$	5^+	This level is not resonant in the (p, γ) reaction (E_p ~ 660 KeV). L = 4 wave would in fact be suppressed. 5_5^+, 6575 KeV
	6295	High-spin	(4^-)	Rotational model. No room for π = + states
	6361	$(4 - 6)^-$	6^-	Extrapolation of π = − bands
	6468	$5^+, 6^-$	6^-	Extrapolation of π = − bands
	6519	$(1, 2)^+$	2^+	2_6^+, 6652 KeV
	6598	$(3, 5)^+$	5^+	3^+ unlikely, because level not a resonance in (p, γ) reaction in spite of E_p ~ 1 MeV. 5_6^+, 6945 KeV requires l_p = 4
	6668	$2^-, 3^+$	2^-	MDC
	6791	>5	6^+	6_1^+, 7120 KeV
	6979	$(3, 4)^+$	4^+	Very weak resonance in (p, γ) at $E_p \approx 1$ MeV. l = 4 more plausible than l = 2
	7045	$(2 - 4)^-$	4^-	"Inband" decay to 6006 KeV, J = 3
	7119	$1^+ - 3^+$	3^+	3_{10}^+, 7263 KeV
	7347	$(5 - 7)^+$	6^+	6_2^+, 7877 KeV
	7370		4^+	Not a (p, γ) resonance in spite of E_p ~ 1.8 MeV → $l_p \geq 4$; 4_6^+, 7012 KeV
	7884	$(3, 4)^+$	4^+	4_8^+, 7766 KeV

Part III

The energy levels of A = 38 - 44 nuclei and their underlying structure

1. Preface

The complete understanding of the energy levels of nuclei around doubly magic ^{40}Ca is a challenging task. This is due to multi-particle excitations from the s-d shell orbits (major quantum number N = 2) into the f-p shell (N = 3). We have interpreted the structure of A = 36 - 44 nuclides in a series of notes written for our own edification at very different times and in the order of growing enlightenment rather than systematics. Theoretical tools were introduced where they were needed first and are thus distributed across several chapters. Also the references to literature were incomplete. In this preface we try to remedy some of these defects.

The present notes are largely influenced by extensive spectroscopic work on the nuclides ^{38}Ar *[1, 2]*, ^{42}Ca *[2]* and ^{40}Ar *[3]* at Freiburg. Most of the results, but not all, are absorbed in the compilations of P. M. Endt *[4, 5]* which provide the data base in most cases.

On the theoretical side we have in first place shell model calculations by Warburton et al. *[6]* in the configuration space of an inert ^{16}O core (closed N = 0, 1 shells), A – 16 – x particles in the N = 2 shell and x particles in the N = 3 shell. Calculations were technically feasible if x acquires the minimum value xm which is allowed by the Pauli-Principle and for x = xm + 1. The xm values of ground states for various nuclides are

xm = 0 for ^{38}Ar, ^{38}K, ^{39}K, ^{40}Ca

1 ^{39}Ar, ^{40}K, ^{41}Ca

2 ^{40}Ar, ^{41}K, ^{42}Ca

3 ^{43}Sc, ^{43}Ca

4 ^{44}Ti, ^{44}V (= ^{44}Sc), ^{44}Ca

Energy levels generated by reordering of nucleons within the x = xm space are conventionally called 0 ħω excitations, those with x = xm + 1 are called 1 ħω excitations. Shell model calculations of n ħω excitations with n ≥ 2 were not possible technically. Hence we have developed a new version of the weak-coupling model *[7]* and of the Nilsson model with residual interaction *[8]*. All theoretical tools have in common that they use empirically optimum interaction energies that are derived from experimental level energies.

The weak-coupling model is a simplified version of the spherical shell model which has already been applied with good success in the ^{40}Ca region *[2]*. It is suited to explain configurations with n_p = 2 or 3 particles in the N = 3 shell and holes in the N = 2 shell. Level energies are obtained by coupling the experimental pure-particle and pure-hole energies derived from suitable nuclei using a particle-hole interaction which is reduced to a monopole (or spin averaged) interaction

$$V = a \bullet n_p \bullet n_h + 4b \bullet T_p \bullet T_h$$

This generates degenerate multiplets with fixed $\vec{T} = \vec{T}_p + \vec{T}_h$

but $|J_p - J_h| \leq J \leq J_p + J_h$.

We have decided that the safest way of obtaining parameters a and b is given by analysis of the 3 ħω excitations with both T = 1 and 0 in A = 38 where we know, today, complete J-multiplets and thus their centroids. Hence our analysis of ^{38}Ar contains a chapter “The weak-coupling model with emphasis on A = 38” (p. 232) where all details can be found.

The nuclear excitations with four or more particles in the N = 3 shell turn out to be connected with deformed shapes. They can be described by the Nilsson model with a residual interaction *[8]*. In 2004 we have started a programme *[9]* which will be improved and completed here. In our first assault we were not yet able to determine all of the parameters which specify the residual

interaction. However the way of arriving at them is described in detail. In the present notes the formalism is repeated in condensed form in Tables 1, 2 of our ^{40}Ca notes together with a new, complete set of parameters (p. 264, 265). The tricky way of arriving at them is discussed in the separate chapter “How to obtain the parameters of the Nilsson model for A = 36 - 48 “.

It turns out that in the realm A = 36 - 44 it is necessary to consider all p-h configurations which are compatible with A and the restriction of both n_p and n_h to values up to eight. This is demonstrated in notes starting at p. 213, where we have reanalysed the level spectra of A = 38 - 44 nuclei (The cases ^{36}Ar and ^{37}K have been treated in *[10, 9]* to which we refer.). The experimental level schemes are completely reproduced by the theoretical tools, which we have described. Vice versa theory does not predict additional facets of nuclear structure. The transition from the N = 2 to the N = 3 shell is thus completely under control.

2. How to obtain the parameters of the Nilsson model for A = 36 - 48

The model considers the distribution of A − 36 nucleons over three Nilsson orbits (as specified on p. 264 and displayed in the figure of p. 100) subject to a nuclear residual interaction which is specified by 24 parameters as outlined in Tables 1, 2 (p. 264, 265) of our ^{40}Ca notes. An additional three parameters, dubbed B_i, are calculable but due to an unfavourable error propagation they should also be taken from experiment. Anyway they play a negligible role. The Coulomb interaction can be considered as known and it is specified by six parameters which we have derived in 2004 from mirror analogs. The model is able to predict bandhead binding energies relative to the deformed 4329 KeV, $J^\pi = 0^+$ state of ^{36}Ar in more than 100 instances to an accuracy of 2 percent. The parameters of the nuclear residual interaction dubbed

$E_{B,i}$; A_i; C_i; S_i $\quad i = 1 - 3$

a_{ik}, b_{ik}, c_{ik}, d_{ik} $\quad i < k,\ k = 1 - 3$

were in part derived in 2004. Values of b_{ik}, d_{ik} are still missing and will be derived here. Also improvements are obtained in the other cases.

We begin with the latter ones. It is now possible to get along without using the first $K^\pi = 0^+$ bands of ^{44}Ti and ^{42}Ar for information. The ^{44}Ti band has a shaky deformation, in the case of ^{42}Ar, large neutron excess leads to unfavourable error propagation. As a replacement we have an expected third $K^\pi = 0^+$ band in ^{38}Ar and a safe identification of the 8p-8h, $K^\pi = 0^+$ band of ^{40}Ca.
In the following we determine the parameters E_{Bi}, a_{ik}, S_i, A_i, twelve in number by using 13 energies of band heads. Four of them are based on Nilsson configurations with a single nucleon outside fully occupied orbits. Nine band

heads have $K^{\pi} = 0^{+}$ and are based on configurations with either fully occupied orbits or a K, T = 0, 1 pair in addition. The model parameters were chosen as to match eleven band head energies and the difference between # 12 and # 13. The following experimental data were used.

Nuclide	K^{π}	E_x[KeV]	
^{37}K	$1/2^{+}$, $3/2^{-}$	3980, 4634	
^{41}Ca	$3/2^{-}$, $3/2^{+}$	2462, 3050	
^{38}Ar	0_1^{+}, 0_2^{+}, 0_3^{+}	3337, 4710, 6681	$0_2^{+} - 0_3^{+}$ difference fitted
^{40}Ca	0_1^{+}, 0_4^{+}, 0_5^{+}	3353, 7815, 8276	
^{42}Ca	0_1^{+}, 0_2^{+}	1837, 3300	
^{48}Cr	0_1^{+}	g.st.	

Next the parameters C_i can be read directly from the bandheads.

^{38}K	1^{+}	3978
^{42}Sc	3^{+}	2223
^{42}Sc	3^{+}	1846

Now we can turn to the parameters with double subscripts, namely b_{ik}, c_{ik}, d_{ik}. They describe the interactions of particles in two different orbits. Two pairs of K, T = 0, 1 particles coupled to T = 0, 1, 2 yield information on c_{ik}. An odd number of nucleons in both orbits, coupled to $K = |\Omega_1 \pm \Omega_2|$, T = 0, 1 yields information on b_{ik}, d_{ik}, c_{ik}. Thus we obtain c_{ik} for the pairs $\Omega_1^{\pi} = 1/2^{+}$, $\Omega_2^{\pi} = 3/2^{-}$ and $\Omega_1^{\pi} = 1/2^{+}$, $\Omega_2^{\pi} = 3/2^{+}$ from the $K^{\pi} = 0^{+}$, T = 2 bandheads of ^{40}Ar at 2121 KeV and 4470 KeV. The remaining parameters are obtained by combining information from two different nuclides (which was not yet available in our analysis of 2004).

The most difficult case is the combination of the $\Omega^{\pi} = 3/2^{-}$ with the $\Omega^{\pi} = 3/2^{+}$ orbit. Not only have all three parameters b_{ik}, c_{ik}, d_{ik} to be determined. Also K = 0 bands, which are possible here, have two branches with even and, respectively, odd spin. Fortunately the even-odd splitting turns out to be small for A = 4 n, T = 1 and A = 4 n + 2, T = 0 so that both branches are observable and the average value of bandhead energies can be adopted for the analysis. We have available the differences of bandhead energies

A = 42: $(K^{\pi}, T = 3^{-}, 1; E_x = 4761\ \text{KeV}) - (K^{\pi}, T = 3^{-}, 0; E_x = 1889\ \text{KeV})$
given by $4\ (c_{ik} + d_{ik})$

A = 44: $(K^{\pi}, T = 3^{-}, 1; E_x = (561 + 6958)\ \text{KeV}) - (K^{\pi}, T = 3^{-}, 0; E_x = 3175\ \text{KeV})$
given by $4\ (c_{ik} - d_{ik})$

Further there is the double - difference

^{44}Ti: $(K^{\pi}, T = 0^{-},1; E_x = ((68 + 146)/2 + 6598)\ \text{KeV}) - (K^{\pi}, T = 3^{-}, 1; E_x = 3175\ \text{KeV})$

minus

^{42}Sc: $(K^{\pi}, T = 3^{-}, 1; E_x = 4420\ \text{KeV}) - (K^{\pi}, T = 0^{-},1; E_x = (2297 + 2832)/2\ \text{KeV})$
given by $-4\ b_{ik}$

Note that the first T = 1 state in ^{44}Ti occurs at 6598 KeV while the ^{42}Sc g.st. has T = 1 already.
The resulting parameters are included in Table 2 of our ^{40}Ca notes (p. 265). Using these we conclude that the $K^{\pi}, T = 0^{-}_{odd}$, 1 bandhead of ^{42}Ca is depressed by 2168 KeV so that the J = even branch is pushed up by the same amount, giving a total even-odd splitting of 5.3 MeV.

Now we investigate the interaction of nucleons in the $\Omega^{\pi} = 3/2^{+}$ and $1/2^{+}$ orbits. Here the parameters b_{ik} and d_{ik} are still unknown. We match the energy of the $K^{\pi} = 2_1^{+}$ bandhead in ^{40}Ca at 5249 KeV and the bandhead differences of the $K^{\pi} = 2_2^{+}$ band in ^{42}Ca (E_x = 4761 KeV) and of the $K^{\pi} = 1^{+}$ band of ^{42}Sc (E_x = 1889 KeV).

In a final step we treat the interactions between the $\Omega^{\pi} = 1/2^{+}$ and $\Omega^{\pi} = 3/2^{-}$ nucleons. Again b_{ik} and d_{ik} must determined. In this case we have succeeded to find candidates of all bandheads with $K^{\pi} = 1^{-}, 2^{-}$; T = 0, 1 in both A = 38 and A = 40, namely

	K^{π}	E_x(KeV)
^{38}Ar T = 1	1^{-} 2^{-}	6948 7431
^{38}K T = 0	1^{-} 2^{-}	2828 3815
^{40}Ca T = 0	1^{-} 2^{-}	7113 6750
^{40}K T = 1	1^{-} 2^{-}	2807 3128

Thus we have a surplus of experimental data. Hence it is highly comforting that a correct ordering of bands according to $K = \left| \Omega_1 \pm \Omega_2 \right|$ can be achieved for both T = 0 and T = 1 in both A = 38 and A = 42. The parameters used are included in Table 2 (p. 265) of our ^{40}Ca notes.

3. The quest of octupole - vibrational bands around doubly magic ^{40}Ca

The excitation of an octupole phonon in an axially symmetric deformed even-even nucleus will generate rotational bands with $K^{\pi} = 0^{-}, 1^{-}, 2^{-}, 3^{-}$. The lowest bandhead excitation energy is expected for $K^{\pi} = 0^{-}$ because the curvature of the nuclear surface is minimized. According to Mottelson's textbook *[11]*, even spins are not present for $K^{\pi} = 0^{-}$, a conclusion probably drawn from the liquid drop model. Mottelson cites the case of well deformed ^{152}Sm, where the $K^{\pi} = 0^{-}$ band has its bandhead at the remarkably low energy of 963 KeV. The mass dependence of this energy should follow an $A^{-1/2}$ law, yielding 1926 KeV for ^{38}Ar. This energy must not be taken relative to the (spherical) g.st. but rather to the first $K^{\pi} = 0^{+}$ bandhead (at 3.4 MeV in this case).

In our analysis of A = 38 - 48 nuclei we could locate several negative-parity rotational bands all having $K^{\pi} = (0 - 3)^{-}$ as do octupole - bands. The data are summarized in Table 1. For every nuclide we have in the second row included excitation energies relative to the lowest lying $K^{\pi} = 0^{+}$ bandhead.

An alternative description of the situation which has a wider range of applicability is a version of the Nilsson model which we had developed already in 2004 *[9]* and improved in the preceding section. In this case (A − 36) nucleons are distributed across three orbits with $\Omega^{\pi} = 1/2^{+}, 3/2^{-}, 3/2^{+}$, subject to a residual interaction. The negative-parity bands which can thus be generated happen to have the same quantum numbers as the octupole bands, namely $K^{\pi} = 0^{-}, 1^{-}, 2^{-}, 3^{-}$. Both T = 0 and T = 1 are possible and the $K^{\pi} = 0^{-}$ band has two branches with, respectively, odd-spin and even-spin states. In odd-odd nuclei both branches can be traced, in even-even nuclei it is the odd-spin branch only (Table 1). On p. 206 we have already estimated that the even-

spin branch be higher in energy by 5.3 MeV, outside the investigated region of excitation.

The present Nilsson model approach is, however, not able to explain the very small excitation energies of $K^{\pi} = 0^-_{odd}$ and also of $K^{\pi} = 3^-$ bandheads in ^{38}Ar and ^{40}Ca relative to the first $K^{\pi} = 0^+$ bandhead. The data are

	K^{π}	E_x [KeV]	E_x [KeV]
		Exp.	N. M.
^{38}Ar	0^-_o 3^-	2308 2087	4252 4788
^{40}Ca	0^-_o 3^-	2551 3230	3032 4256

Hence the model of octupole - vibration with E_x around 2 MeV is superior in this respect. Thus we must assume a (coherent) interaction of the leading N. M. configuration with (numerous) higher lying configurations of equal K^{π}. The effect is particularly expressed for the $K^{\pi} = 3^-$ band of ^{38}Ar. Here the next configuration is extremely close (about 2.5 MeV) and due to the first orbit, with $\Omega^{\pi} = 5/2^-$ (see insert), which was not considered in the model.

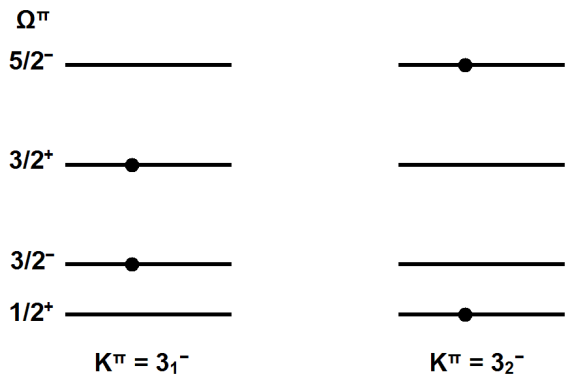

As a result the $K^{\pi} = 3^-$ bandhead occurs 220 KeV <u>below</u> the $K^{\pi} = 0^-_{odd}$ bandhead contrary to systematics in Table1. The normal value would be a few hundred KeV above.

A last item is the particularly small value of the rotational constant $\hbar^2/2\Theta$ in the $K^{\pi} = 0^-$ bands of even-even nuclei, as reported by Mottelson *[11]* for the

realm of heavy deformed nuclei and observed also here (Table 1). Mottelsons explanation in terms of Corrioliscoupling does not suite for observations in ^{42}Ca and ^{38}Ar. Here we have 6 or, respectively, 5 band members which faithfully follow the J(J+1) rule of excitation energies (p. 297, 243). Corrioliscoupling however, induces a $\sqrt{J(J+1)}$ dependence which is not noticeable.

We seek the explanation directly in the moment of inertia and propose, for $K^{\pi} = 0^{-}$, an extra term $\Delta\Theta$ so that

$$\Theta = \Theta_0 - (-)^J \Delta\Theta$$

The increase of Θ for J = odd must be accompanied by a decrease for J = even. Unfortunately we have no way of proving the latter consequence.

The origin of $\Delta\Theta$ must be found in a matrix element $\langle\psi_k^* \left| r^2 Y_2^0 \right| \psi_{-k}\rangle$ which can be different from zero only if k + 0 = − k. Hence k = 0.

Table 1

Negative - parity bands in A = 38 - 48[b)]

	$K^{\pi} = 0^{-}_{odd}$	
Nuclide	Band members, E_x[KeV] absolute / relative[a)]	$\hbar^2/2\Theta$[KeV]
^{38}Ar	5734, 6339, 7194, 8491, 10245 2308, 2913, 3768, 5065, 6819	50
^{40}Ca	5903, 6285, 7240, (8850) 2551, 2933, 3888, (5948)	46
^{40}Ar	4300, 4562, 5310, 6356 2179, 2491, 3189, 4235	39
^{42}Ca	3884, 4117, 4896, 6093, 7282, 9037 2047, 2280, 3059, 4256, 5445, 7100	40
^{44}Ti	3755, 4227 not clear	47
^{48}Ti	3653 } 3853, 4916, 6153, 7623 3703 not known	45
	$K^{\pi} = 3^{-}$	
^{38}Ar	5513, 6211, 7070, 8129, 9199,10455, 11630 2087, 2785, 3644, 4703, 5773, 7029, 8204	78
^{40}Ca	6582, 7114, 7769 3230, 3762, 4417	66
^{40}Ar	4929, 5675 2808, 3554	66
^{42}Ca	4420, 5188, 5775, 6542, (7758), 8512, 9760 2583, 3351, 3938, 4705, (5921), 6675, 7923	51
^{44}Ti	3176, 3645, 4061 not clear	49
^{46}Ti	3059, 3442, 3853, 4663, 5198, 6150 identical	51
^{48}Ti	3359, 3783, 4046, 4956, 5312, 6394, 6880 not known	45

Table 1 continued

	$K^{\pi} = 2^-$	
Nuclide	Band members, E_x[KeV] absolute / relative[a)]	$\hbar^2/2\Theta$[KeV]
^{38}Ar	7431, 8068, 8956, 10024, 11109 4054, 4691, 5579, 6647, 7732	102
^{40}Ca	6750, 7278, 7928, (8678) 3397, 3925, 4571, 5325	84
	$K^{\pi} = 1^-$	
^{38}Ar	6948, 7335, ? , ? , 9829, 10947[A] 3571, 3958, , , 6452, 7570	100
^{40}Ca	7113, 7532, 8188 3760, 4179, 4835	107

a) We cite experimental excitation energies and below energies relative to the first deformed state of the nuclide

b) The experimental data for ^{38}Ar*[1, 2]*, ^{40}Ar*[3]*, ^{42}Ca*[2]*, ^{48}Ti*[12]* are taken from work at Freiburg; all others from the literature*[4, 5]*

Bandheads [KeV] in odd-odd nuclei

Nuclide	K^{π}				
	0^-_e	0^-_o	3^-	2^-	1^-
^{46}V	1235	1200	1254		
^{44}Sc	146	68	531		
^{42}Sc	2269	2832	2726		2455
^{40}K		2290	3154	3128	2807
^{38}K				2828	3815

4. The T = 1 states of ^{38}K *[4, 5]*

The spectrum of energy levels at low excitation energy contains both T = 0 and T = 1 states. The first step is to recognize the T = 1 states by comparison with ^{38}Ar.

^{38}Ar		**^{38}K**		
E_x[KeV]	J^π	E_x[KeV]	J^π	comment
0	0^+	130	0^+	
2167	2^+	2402	2^+	
3377	0^+	(3347)		E_x from interpolation between ^{38}Ar and ^{38}Ca
(3423)		3701	$(0^+ - 4^+)$	0^+ and 2^+ states of $K^\pi = 0_1^+$ band, τ(3701) >1ps
3936	2^+	4214	2^+, 1	speaks for a 0^+ state, decaying to 2402 KeV, 2^+
3810	3^-	3933	2^-	π = u from (d, α) seems wrong
4480	4^-	4616		No γ-decay, speaks for high spin
4565	2^+	(4664)	2^+, 1	
4585	5^-	4704		Decay to 5_1^-, T= 0
4710	0^+	4723	$(0 - 3)^+$	
4876	3^-	5047	$(1 - 5)^-$	

There should be two $J^\pi = 0^+$ states around 3.4 MeV of, respectively, 2 ħω and 4 ħω character. They cannot be populated in ^{38}K by ^{40}Ca(d,α γ) at $\Theta_\alpha = 180°$. The 3701 KeV and also the 3347 KeV level, which we have introduced here, fulfill this requirement. The 3377, 3347 and 3057 KeV levels of, respectively, ^{38}Ar - ^{38}K - ^{38}Ca are of 2 ħω character, as evidenced by two-particle transfer. The 3701 KeV level of ^{38}K must thus be of 4 ħω origin as is the 3936 KeV, 2^+ level of ^{38}Ar and thereby the 4214 KeV, 2^+ level of ^{38}K. Thus we have the 2^+ - 0^+ spacing in the $K^\pi = 0^+$ band and can calculate the 0^+ bandhead in ^{38}Ar at E_x = 3423 ± 30 KeV. The uncertainty arises from the scatter of Coulomb -

energy differences. Note that γ-decay of the 3377 KeV state in ^{38}Ar has been investigated in the time of NaJ(Tl) detectors so that presence of a nearby 3423 KeV level could have easily been missed.

5. The T = 0 spectrum of ^{38}K levels

As with ^{38}Ar, T = 1 (see following chapter) we expect all n ħω excitations from the N = 2 into the N = 3 shell with n = 0 - 6. Detailed shell model calculations in the unrestricted N = 2 + 3 shell exist for n = 0, 1 *[6]*. Weak-coupling predictions of n = 2, 3 states can be made using the parameters derived for ^{38}Ar. All these states are spherical. Deformed states with n = 4 - 6 can be predicted by the Nilsson model and results are of value for establishing the Hamiltonian.

0 ħω states				1 ħω states			
SM		exp.		SM		exp.	
E_x[KeV]	J^π	E_x[KeV]	J^π	E_x[KeV]	J^π	E_x[KeV]	J^π
0	3^+	0	3^+	2300	3^-	2612	3^-
635	3^+	459	3^+	2413	4^-	2646	4^-
1721	1^+	1698	1^+	2922	2^-	2869	2^-
3581	2^+	3431	2^+	3409	5^-	3614	$(1 - 5)^-$ 100%→4_1^- a)
4143	1^+	3857	1^+	3805	6^-	3420	6^-
				3875	4^-	3687	$(2 - 4)^+$ Decay to 4^-,3^-,3^+
				3892	1^-	4174	$1, 2^+$
				4029	5^-	3840	$\pi = u$ 100%→4_1^- a)
				4078	2^-	4317	$1^+ - 5^+$
				4117	3^-	4394	$1^+ - 5^+$
				4462	0^-	4410	$0 - 3^+$ 100%→1_1^+ b)

a) First evidence that $\pi = u$ from $(\vec{d}, \alpha)$ is not always reliable
b) Interpretation as a deformed $K^\pi = 0^-$, $J^\pi = 0^-$ state is also feasible

2 ħω states				3 ħω states
Weak-coupl.		exp.		
E_x[KeV]	J^π	E_x[KeV]	J^π	The first weak-coupling multiplet
3615	1^+	2992	$1^{+a)}$	(with $J^\pi = 2^- - 5^-$) is expected at
3620	7^+	3458	7^+	5.1 MeV judging from the 3 ħω levels
				of high spin

a) $J^\pi = 0^-, 1^+$

$J^\pi = 0^-$ should first occur at 4.5 MeV

There remain to be interpreted the following levels up to and including 4410 KeV

E_x[KeV]	J^π	K^π	(J^π)	E_x[KeV]	J^π	K^π	(J^π)
2828	1^-	1^-	1^-	3341	1^+	0^+	1^+
3316	$1^+, 2^-, 3^+$	1^-	2^-	3668	3^+	0^+	3^+
3815	2^-	2^-	2^-	3978	1^+	1^+	1^+
4333	1 - 3	2^-	3^-	3738	$1^+ - 5^+$	3^+	3^+

We interpret them as 5 ħω and, respectively, 4 ħω states with K^π values as indicated.

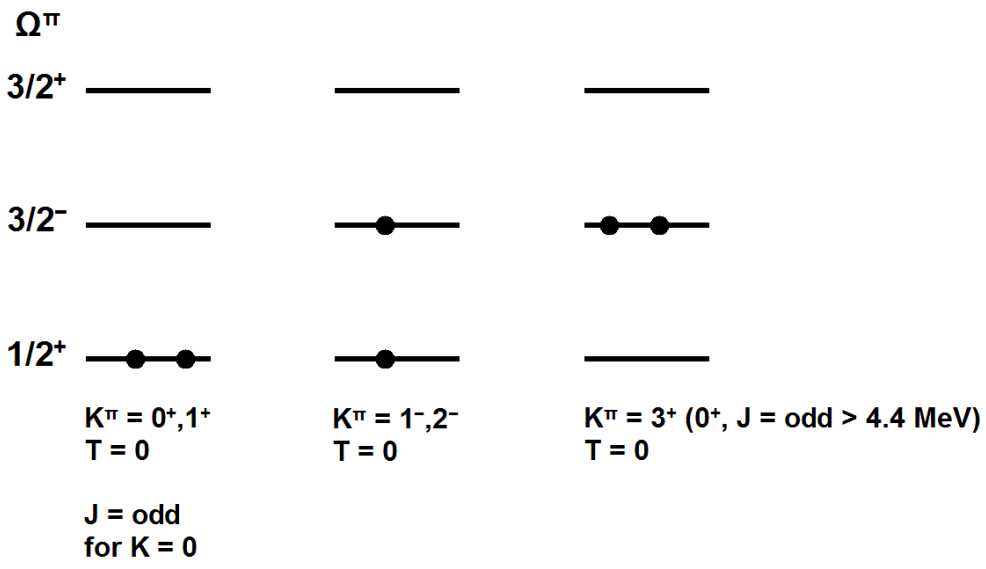

The configuration

is not observable because it cannot be expected below 4.5 MeV.

6. Complete analysis of the ^{38}Ar level scheme

The present analysis of ^{38}Ar (T = 1) is the last in a series of notes which elucidates the structure of A = 37 - 44 nuclei. It is the most challenging task because of the large amount of available data. Up to 8 MeV in excitation the level scheme is seemingly complete *[1]*, being comprised of 80 levels. Another 70 levels of high-spin (J = 5 - 11) up to E_x = 11.6 MeV have been observed at Freiburg around 1980 with the aid of the ^{35}Cl(α, p γ) reaction *[2]*. Twenty years later investigations with the ^{28}Si(^{16}O, α 2p γ) reaction have extended our knowledge of high spin states beyond 11.6 MeV excitation energy and suggested a few improvements in the foregoing ^{35}Cl(α, p γ) data. However when we prepared the present notes we did not have the paper of Rudolph et al. *[14]* nor its evaluation in the ENSDF file *[21]* at hand, yet. In order to avoid confusions we have not rewritten our notes but added necessary changes of experimental data at the end. They do not change the thread of our discussions. At the time of our investigations there was no hope to achieve a detailed understanding of the ^{38}Ar level scheme, especially since definite assignments of J^{π} quantum numbers were achieved only for yrast levels. However, according to the ideas developed in the preceding notes on A = 39 - 44 nuclei as summarized in the preface, it should be possible to unravel the complete level scheme of ^{38}Ar if all n-particle excitations from the N = 2 into the N = 3 major shell with n = 0 - 6 are properly taken into account. The (0 - 3) ħω excitations should be spherical in character and detailed shell model calculations are today available for n = 0 and n = 1 *[4-6]*. The n = 2, 3 excitations can be treated by the model of weak coupling of particles in the N = 3 and holes in the N = 2 major shell. The energy levels of the pure particle and pure hole configurations which are needed here can be completely identified from experimental data (see notes on A = 42, 43). The Nilsson model with residual interaction, developed in the preceding notes finally allows to treat

the (4 - 6) ħω excitations. In the following complete agreement between experiment and theory can be established step by step.

We start with the deformed states which have the character of (4 - 6) ħω excitations. In the present version of the Nilsson model *[9]* we must consider (Table 6) the distribution of two nucleons over the first three orbits above the Fermi level, having $\Omega^{\pi} = 1/2^{+}, 3/2^{-}, 3/2^{+}$. The K^{π} values of T = 1 configurations are $K^{\pi} = 0_1^{+}, 0_2^{+}, 0_3^{+}; 2^{+}, 1^{+}; 0^{-}, 3^{-}; 1^{-}, 2^{-}$.

The same configurations can be constructed in ^{42}Ca by either placing a K‘, T‘ = 0, 0 quartet of nucleons into the lowest empty orbit available or by replacing particles (occupation number n = 1) by holes (n = 3). The analogy to ^{42}Ca, which we had investigated already, suggests that we can observe in ^{38}Ar all $K^{\pi} = 0^{+}$ bands, the $K^{\pi} = 2^{+}$ and 3^{-} bands, and the J = odd branch of the $K^{\pi} = 0^{-}$ band. Contrary to expectation it will be possible even to locate the $K^{\pi} = 1^{-}$ and 2^{-} bands and there is some evidence that a second $K^{\pi} = 3^{-}$ band could come into play.

We begin with the positive parity bands or in other words the 4 ħω and 6 ħω excitations. The $K^{\pi} = 0_1^{+}$ band was located *[13]* at Freiburg in 1974 (Fig. 1) up to the $J^{\pi} = 8^{+}$ member at 9338 KeV. (It was erroneously assumed that the 3378 KeV, $J^{\pi} = 0^{+}$ state be the bandhead. The latter one is hitherto unobserved and predicted now at 3423 KeV with aid of information from ^{38}Ca and ^{38}K. Details are given in our ^{38}K notes). The $J^{\pi} = 10^{+}, 12^{+}$ members of the $K^{\pi} = 0_1^{+}$ band and the $J^{\pi} = 4^{+} - 12^{+}$ members of the $K^{\pi} = 0_2^{+}$ bands were observed about 25 years after our work *[14]*. The identification of the $J^{\pi} = 0^{+}, 2^{+}$ members of the $K^{\pi} = 0_2^{+}$ band in Fig. 1a is made by ourselves on the basis of suitable E_x and J^{π}.

The head of the predicted $K^{\pi} = 2^{+}$ band is identified here as the 6250 KeV, $J^{\pi} = 2^{+}$ state. The other band members are identified with aid of the J(J+1) rule and a suitable γ-decay which proceeds either within the band or to a level of

4 ħω character, namely a member of the $K^{\pi} = 0_1^+$ band. The highly excited 14119 KeV bandmember is obtained from the ENSDF Database *[21]*. (By the way, the $J^{\pi} = 9^+$ member of the band has escaped observation because reactions with heavy ion prefer the population of yrast levels.)

The predicted $K^{\pi} = 0_3^+$ band has its head in a 6681 KeV, J = 0 - 2 state because it shows a very unique decay to a 5734 KeV state which will immediately be identified as the head of the predicted $K^{\pi} = 0^-_{odd}$ band. The situation is in analogy to ^{42}Ca where the equally unique decay 4567 KeV; J^{π}, $K = 0^+$, 0 → 3885 KeV; J^{π}, $K = 1^-$, 0^-_{odd} has been observed. Assuming equal rotational constants in the $K^{\pi} = 0_3^+$ and 0_1^+ bands (because the involved $\Omega^{\pi} = 1/2^+$ and $3/2^+$ orbits have similar slopes) we can identify the 10443 KeV level as the J^{π}, $K = 6^+$, 0_3 state. The 7181 KeV, $J^{\pi} = 1, 2^+$ level is then the $J^{\pi} = 2^+$ band member on the basis of the J(J+1) rule. There remains to be assigned a 11087 KeV level which must be of 4 ħω character because of its γ-decay to the $J^{\pi} = 6^+$ member of the $K^{\pi} = 0_1^+$ band. We suggest a J^{π}, $K = 6^+$, 1 assignment in order to place the $K^{\pi} = 1^+$ band sufficiently high above the $K^{\pi} = 2^+$ band. Observations in A = 40, 42 suggest a 3 MeV difference which would about fit.

Now we turn to rotational bands of negative parity which constitute 5 ħω excitations. The presence of $K^{\pi} = 3^-$ and 0^-_{odd} rotational bands came into our mind only after we had identified such bands in ^{42}Ca and ^{40}Ar. The ^{38}Ar bands differ in structure from the ^{42}Ca bands only by the removal of a $\Omega^{\pi} = 1/2^+$ quartet of nucleons. The effect is easy to calculate and leads to predicted bandhead excitation energies in the 7.5 - 8.0 MeV region, uncomfortably high. Fortunately we scanned our old, 1979, data first. The ^{35}Cl(α, p γ) reaction at E_{α} = 16 MeV (our record high) had yielded a γ-cascade 11630 → 9199 → 8129→7070 KeV, ending in an established $J^{\pi} = 5^-$ state which was then considered the starting point of the 3 ħω excitations. Presence of 5 ħω excitations was beyond our imagination.

Now it is clear that we have observed the $J^{\pi} = 9^{-}, 7^{-}, 6^{-}, 5^{-}$ members of the $K^{\pi} = 3^{-}$ band. The mixing ratio of the $6^{-} \rightarrow 5^{-}$ transition is $\delta = -0.86^{+0.16}_{-0.7}$ indicating collectivity of the E2 part. The $J^{\pi} = 8^{-}$ member is found in a doublet (previous singlet) at 10455 KeV. A 10455 KeV^{A} level decays to the 8491 KeV; J^{π}, K = 7^{-}, 0 level discussed below, a 10455 KeV^{B} state to the 6408 KeV, 6^{+} level of 2 ħω character and the 7507 KeV, 7^{-} level of the 1 ħω character. Finally the $J^{\pi} = 3^{-}$ and 4^{-} members of the $K^{\pi} = 3^{-}$ band are found by the J(J+1) rule in the known 3^{-} and 4^{-} states at 5513 and 6211 KeV (Fig. 1b).

The $K^{\pi} = 0^{-}_{odd}$ band is traced as follows. A level at 10245 KeV decays by a γ-ray transition of remarkable low energy to an established $J^{\pi} = 7^{-}$ state at 8491 KeV. The interpretation as a $9^{-} \rightarrow 7^{-}$ inband transition is substantiated by an established $J^{\pi} = 1^{-}$ state at 5734 KeV. These three levels follow the J(J+1) rule very precisely with $\hbar^2/2\Theta$ = 50 KeV (Fig. 1b). Knowledge of the $K^{\pi} = 0^{-}_{odd}$ band in ^{42}Ca with $\hbar^2/2\Theta$ = 40 KeV leads to a prediction $\hbar^2/2\Theta$ = 47 KeV in ^{38}Ar (assuming a 1/2 MR² dependence). The missing $J^{\pi} = 3^{-}$ and 5^{-} states can be identified on the basis of the J(J+1) rule with the known 6339 KeV, $J^{\pi} = (1 - 3)^{-}$ and 7194 KeV, $J^{\pi} = (2^{-} - 5^{-})$ states. The unexpectedly low bandhead energies for the $K^{\pi} = 3^{-}$ and 0^{-}_{odd} bands will be discussed in our ^{40}Ca notes (Most likely we feel the influence of the octupole vibration in a deformed nucleus). There remain to be identified the predicted $K^{\pi} = 1^{-}$ and 2^{-} bands. A first hint was the observation (discussed below) that a 6948 KeV $J^{\pi} = 1^{-}$ state was not needed to complete the expected spectrum of 1 ħω and 3 ħω excitations, thus pointing at a 5 ħω character and thereby deformation. Subsequently we inspected the levels of high-spin which show γ-decay to final states which had already an assigned 5 ħω character. The inspected states (Fig. 2) must then have a 5 ħω character themselves or be generated by mixing of closely spaced levels of 3 ħω and 5 ħω character.

In first place we have the 9829 KeV and 10947^{A} KeV level of Figs. 1b and 2 which show suitable γ-decay to the 7070 KeV, $J^{\pi} = 5^{-}$ state. Together with the 6948 KeV, $J^{\pi} = 1^{-}$ state (Table 3B) they follow the J(J+1) rule for $K^{\pi} = 1^{-}$ with spin assignments of, respectively, 5^{-} and 6^{-}. Please note that the 10947 KeV level has turned out to be a doublet. The 10947^{B} KeV level shows decay to and feeding from high-spin states (Fig. 7) and has obtained *[14]* a $J^{\pi} = 9^{-}$ assignment.

Mixing of a deformed 5 ħω with 3 ħω states is observed twice (Fig. 2) in the cases of the 11630, 11452 KeV doublet and the 11109, 11068, 10890 KeV triplet. With some arbitrariness we have ordered the 11109 KeV and 11630 KeV levels into the spectrum of deformed 5 ħω states with assignments of, respectively, J^{π}, $K = 6^{-}$, 2 and 9^{-}, 3. As a consequence we assign $J^{\pi} = 9^{-}$ to the 11452 KeV level, $J^{\pi} = 6^{-}$ to the 11068 and 10890 KeV levels and order them (Fig. 7) into the spectrum of 3 ħω states.

The low-spin members of the $K^{\pi} = 1^{-}$, 2^{-} bands cannot be identified completely. However three levels at 8068, 7431 and 7335 KeV are available, which will not be needed later on to complete the expected spectrum of 1 ħω and 3 ħω states. The higher lying $J^{\pi} = 4^{-}$ and 3^{-} states of the $K^{\pi} = 1^{-}$ band are simply missing on experimental grounds.

Last not least we have to treat a 11163 KeV level in the $^{35}Cl(\alpha, p\,\gamma)$ reaction which has the remarkable property of showing four observably strong γ - ray transitions to final states of n = 1, 2, 4, 5 ħω character, namely 7507 KeV (7^{-}), 8077 KeV (7^{+}), 8124 KeV (5^{+}), 8491 KeV (7^{-}). We suspect a doublet, consisting of a deformed 11163^{A} KeV, 5 ħω state and a 11163^{B} KeV, $J^{\pi} = 7^{+}$, 2 ħω state with a 4 ħω wave function admixture from the 10274 KeV state of Fig. 1a. We tend to interpret the deformed 11163^{A} KeV level as the $J^{\pi} = 7^{-}$ member of a second $K^{\pi} = 3^{-}$ band just 2 MeV above the first one. In our discussion of the octupole bands (p. 209) we have already advertised such a band.

With the present identification of rotational bands as summarised in Table 6 we have treated the n ħω excitations with n = 4, 5, 6. It is an easy exercise to trace the 0 ħω excitations in the unrestricted basis space of the N = 2 major shell.

Here they are

J^{π}	Exp. [KeV]	SM [KeV][b]	
0_1^+	0	0	
2_1^+	2168	2013	
2_2^+	4565 + 5552[a]	4489	
1_1^+	5552	5555	
0_2^+	6476	6182	6280 in ^{38}Ca
4_1^+		8521	

a) Mixed 0 ħω and 2 ħω states, as shown by γ-decay

b) B. H. Wildenthal, private communication

Having obtained the n ħω excitations with n = 0, 4, 6 it should be possible to assign the remaining states of positive parity to the 2 ħω excitations which can be predicted by the weak-coupling model. The 2 ħω excitations of higher spin ($J \geq 4$) should show an observably strong γ-decay to other 2 ħω levels (or, by wave function admixture to 4 ħω levels) in spite of unfavourably low transition energies. The energetically favoured transition to levels of 1 ħω character are hindered because the leading $f_{7/2} \rightarrow d_{3/2}$ single particle transition cannot generate dipole decay. Equally dipole decay to 0 ħω states is not possible because of their low spin ($J \leq 2$). Fig. 3 shows all observed γ-decays to the previously established 2 ħω states at 6408 KeV (6^+), 8077 KeV (7^+), 8569 KeV (8^+) and to the lowest $J^{\pi} = 4^+$ states (all of which have already a definite spin-parity assignment). The J^{π} assignments to the other states except for the 7376 KeV level are the very logical interpretations of the γ-decay modes, supported by an ideal agreement with the predictions of the weak-coupling

model. The 7376 KeV level of Table 1 mixes with and has the J^{π} of the just established, deformed 7350 KeV, $J^{\pi} = 4^{+}$ level of Fig. 1a. This is evidenced by the common γ-decay to the deformed 6250 KeV, $J^{\pi} = 3^{+}$ state of Fig. 1a, a very unique decay.

The weak-coupling model which will be used now is developed in these notes in connection with 3 ħω excitations. For logical reasons they are treated subsequently. A switch to the chapter „The weak-coupling model with emphasis on A = 38" further below is thus advisable. Not only is the idea of the model developed but also are the free parameters determined from an analysis of the experimental spectrum of 3 ħω states. With this chapter in mind Table 1 is understandable. It yields the parameter-free prediction of the spectrum of 2 ħω states up to 9 MeV in excitation. The comparison with experiment is performed in Fig. 4. Some assignments of J^{π} to levels need discussion.

The model predicts four $J^{\pi} = 2^{+}$ states above 7 MeV which must be sought among ten $J^{\pi} = 1, 2^{+}$ states in the $6949 \leq E_x \leq 8391$ KeV region. Otherwise there would be an unexplainable proliferation of J = 1 levels. The distinction between J = 1 and $J^{\pi} = 2^{+}$ is made here by assuming that dipole decay of $J^{\pi} = 2^{+}$ states can compete with quadrupole decay to the ground state. With this reasoning we assign $J^{\pi} = 2^{+}$ to three states at 7370, 7702, 7856 KeV. Identification of the fourth $J^{\pi} = 2^{+}$ state is certainly ambiguous and our choice of E_x = 8233 KeV could be replaced by E_x = 7894 or 8391 KeV. Four levels at 7235, 7993, 8106 and 8181 KeV decay exclusively to the 2_1^{+} state at 2168 KeV. Since our accounting of $J^{\pi} = 2^{+}$ states is now complete and since there is no theoretical foundation of $J^{\pi} = 1^{+}$ states we have tentatively correlated these states with predicted $J^{\pi} = 3^{+}$ and 4^{+} states.

There remains to be discussed an exotic $J^{\pi} = 0^{+}$ state which arises from the isospin-coupling $T_p = 1$ ⓧ $T_h = 2$ (^{42}Ti ⓧ ^{36}S).

A coarse estimate of its excitation energy is 6 ± 1 MeV. It is feasible that an experimentally exotic state, the 7365 ± 2 KeV level of the compilation *[4]*, can be correlated with the predicted state. This level was not observable in the ^{35}Cl(α, p γ) reaction in spite of good statistics which points at very low spin.
At excitation energies above 9 MeV it is possible only for experimental reasons to identify the 2 ħω states with J ≥ 7 and some, however not all, J = 6 states. Table 2 yields the weak-coupling multiplets which contain such levels and the experimental levels which we assign to these multiplets on the basis of suitable excitation energies and γ-decay (Fig. 2).
The weak-coupling model of 2 ħω states works very well in the realm of high-spin and the largest deviation between experimental and theoretical E_x is observed for $J^\pi = 2^+$. The latter fact is not surprising because these 2 ħω states are imbedded in a system of two 0 ħω, three 4 ħω and one 6 ħω states.
At the present stage we have identified the positive-parity states and the deformed negative-parity states. The latter ones have 5 ħω character. The remaining states must have negative parity and either a 1 ħω or 3 ħω character. They are gathered in part A of Table 3. The limiting excitation energy of 10 MeV was reached at Freiburg by an extended measurement with the ^{35}Cl(α, p γ) reaction at E_α = 14 MeV *[1]*. Levels up to 11.6 MeV were observed in a brief experiment at E_α = 16 MeV *[2]* and the results are given further below.

The majority of levels in Table 3 had no J^π assignment up to now. In these cases we cite their modes of γ-decay as the experimental basis of J^π assignments. Theoretical guidance is obtained from shell model calculations of 1 ħω states as given in Table 4 and Fig. 6. At this stage presence and building principle of 3 ħω excitations becomes evident, providing the basis for

a successful weak-coupling model description. At the end a complete and intrinsically consistent classification of levels is obtained in Table 3.

We are now going into some details.

The 0_1^- state of the 1 ħω configuration, predicted (Table 4) at 6825 KeV is undoubtedly to be identified with the experimental 6846 KeV state because a 0^- level at this energy has no other decay mode available except to the 2_1^- state at 5084 KeV.

A $J^\pi = 1^-$ assignment to the 7234, 7894, 8391 KeV states of Table 3, part A and the 6948 KeV level of part B is safe because of their decay to $J^\pi = 0^+$ states. The alternatives $J^\pi = 1^+$ or 2^+ can be discarded because we believe to have all positive-parity states already. The number of $J^\pi = 1^-$ states in Table 3 amounts to seven, while the theoretical 1 ħω spectrum provides five only. The deformed 5 ħω states can account for one of the additional levels only (the 6948 KeV level), thus making the presence of one $J^\pi = 1^-$ level with 3 ħω character mandatory. This is of prime importance when the theory of 3 ħω states is discussed.

According to the weak-coupling model (which can reach beyond Warburtons calculations) we should have two $J^\pi = 7^-$, 1 ħω states in ^{38}Ar which are separated by the amount of 2464 KeV and connected by a strong M1 decay. They are generated by the coupling of a $f_{7/2}$ particle to the first two $J^\pi = 7/2^+$ states of ^{37}K. Experimentally we have the 7507 KeV, $J^\pi = 7_1^-$ state and two levels at 10135 and 10181 KeV which show the required γ-decay. They constitute an (intimately) mixed pair of (1+3) ħω states. With arbitrariness we order the 10135 KeV level into the spectrum of 1 ħω states and the 10181 KeV level into the 3 ħω spectrum. There is still another level at 9644 KeV, too low to be the $J^\pi = 7_2^-$, 1 ħω state, which decays to the 7505 KeV, 7_1^- state. This is just another $J^\pi = 7^-$, 3 ħω state which finds no way of γ-decay except by mixing with 1 ħω states (There are no 3 ħω → 1 ħω transitions).

Finally a level at 10557 KeV does also decay to the 7507 KeV, $J^{\pi} = 7_1^-$, 1 ħω state. It is most probably a 1 ħω state but $J^{\pi} = 7_3^-$, 8_1^-, 9_1^- assignments can be excluded because the energy is too low by at least 1.1 MeV (see Table 4). Hence a $J^{\pi} = 6^-$, 1 ħω assignment is the most probable one.

Table 3 contains 8 levels which show γ-decay to two different 5^- levels, however no decay to levels of lower spin. In view of the fact, that the spectrum of $J^{\pi} = 7^-$ level is already known we assign $J^{\pi} = 6^-$ to all these levels. Later on by theoretical considerations we saw the need for still another $J^{\pi} = 6^-$, 3 ħω state and have chosen the highest excited available candidate, the 9669 KeV level of Table 3.

Candidates of a $J^{\pi} = 5^-$ assignment are those levels which decay to a single 5^- state, however not to levels of lower spin. Further there are two states which decay to two $J^{\pi} = 5^-$ levels and a $J^{\pi} = 4^-$ state. (Remember that the 9669 KeV level has been taken out before and assigned $J^{\pi} = 6^-$).
In the case of $J^{\pi} = 4^-$ levels we need every candidate from Table 3 and take them all. Nevertheless the accounting of these states is no longer complete above 8.8 MeV.
All remaining states have $J^{\pi} = 2^-$, or 3^-, however there is no experimental handle to distinguish between the two possibilities. The problem must and will find a solution in theory.
Table 3 shows four cases where a pair of closely spaced levels show identical γ-decay to two or three final states with almost identical branching ratios. The phenomenon can be explained in two ways. In the first case we could have an equal mixture of two wave function components which themselves induce different γ-decays. It is, however, quite unlikely that a fulfillment of both conditions occurs several times. The alternative is presence of two wave function components of which only one is able to induce the observed γ-decays. The situation is always given here if a closely spaced 1 ħω and a

3 ħω state do interact. Gamma decay to 1 ħω states is not possible via the 3 ħω component. A variation of this mechanism which involves two components of 1 ħω character is observed in the case of the $J^{\pi} = 6^{-}$ pair of levels at 7617 KeV and 8215 KeV. The unperturbed states are generated by coupling of a $f_{7/2}$ particle to the closely spaced $J^{\pi} = 5/2_1^{+}$ and $5/2_2^{+}$ states of A = 37 (The 2750 KeV and 3239 KeV states in Table 37c of *[4])*. The $J^{\pi} = 5/2_2^{+}$ state shows a two - order of magnitude retardation of both γ- and proton-decay relative to the $J^{\pi} = 5/2_1^{+}$ state. Since the γ-decay of the ^{38}Ar pair of states is induced by the parents in A = 37 we have found the explanation of identical γ-decay.

The coupling mode $f_{7/2}$ ⓧ $5/2_1^{+}$ or $5/2_2^{+}$ can also generate a $J^{\pi} = 5^{-}$ pair of states in the vicinity of the $J^{\pi} = 6^{-}$ pair. The 7859/7899 KeV, $J^{\pi} = 5^{-}$ states show identical γ-decay to the 5_3^{-} state (Table 3), a decay mode which is not frequent in view of a very low transition energy of 1.2 MeV only. The double occurrence suggests that we have here the expected doublet. Contrary to the $J^{\pi} = 6^{-}$ doublet we can, however, not exclude mixing of states with 1 ħω and, respectively, 3 ħω character. For $J^{\pi} = 6^{-}$ this possibility could be excluded because the lowest lying $J^{\pi} = 6^{-}$ state of 3 ħω character is too high. It should occur in the vicinity of the 8972 KeV, $J^{\pi} = 7^{-}$ state of Table 3 and can in fact be identified with the 8789 KeV level of that table. The latter state decays to final states of 1 ħω and 5 ħω character. Hence we have here a 3 ħω state with admixtures from both the 1 ħω and the deformed 5 ħω configurations. The only source of the 5 ħω admixture lies in the deformed 8129 KeV, $J^{\pi} = 6^{-}$ state. Equal spin-parity can thus be assigned to the 8789 KeV level, in agreement with previous suggestions. Finally we have the situation that three levels with assumed $J^{\pi} = 6^{-}$ assignment at 9087, 9349 and 10101 KeV show identical γ-decay to the 5_1^{-} and 5_2^{-} levels of 1 ħω character. The 9349 KeV level has definitely 3 ħω character due to feeding from above (Fig. 7). The 9087 KeV level fits very well into the theoretical spectrum of 1 ħω states and

provides the source of γ-decay. The 10101 KeV level is still another 3 ħω state.

At the present stage we have available all the information which is needed for an experimental / theoretical comparison of the levels with 1 ħω character. The theoretical level scheme is available from Warburton‘s shell model calculations *[6]* in the unrestricted N = 2 + 3 major shells. The calculations extend to E_x = 8.2 MeV and comprise in addition the lowest lying J = 8 - 10 levels. The $J^{\pi} = 5^-, 6^-$ levels above 8.2 MeV are predicted here with use of the weak-coupling model placing the starting point of levels with $t_p = 1/2$, $t_h = 1/2$ configuration at 4.5 MeV. For $t_h = 3/2$ a starting point of 5.6 MeV is assumed.
In Table 4 we confront the theoretical 1 ħω spectrum with the experimental spectrum of both 1 ħω and 3 ħω states as given in part A of Table 3. It is very evident that we must introduce 3 ħω states in addition to those which were already identified before and which are marked by an asterisk. It appears that for every spin it is possible to trace the onset of 3 ħω excitations. This is due to the excellent predictive power of the theory in the case of 1 ħω excitations.

At excitation energies above 10 MeV, experimental work with heavy-ion induced reactions *[14]* and the ^{35}Cl(α, p γ) reaction at E_α = 16 MeV at Freiburg *[2]* emphasizes the 3 ħω excitations, because they provide the levels of higher spin. Fig. 7 yields the γ-decay of all levels from the ^{35}Cl(α, p γ) reaction which have not been identified yet as positive-parity states or deformed negative-parity states (of 5 ħω character) in other words the prospective 1 ħω and 3 ħω states. Two levels at 11651 KeV and 11997 KeV occur above the limiting excitation energy of 11.6 MeV in the ^{35}Cl(α, p γ) reaction and are adopted from the ENSDF Database *[21]*.

Two levels at 10315 KeV and 11434 KeV are of lesser interest because they decay to the 5_1^-, 4585 KeV level only. They could belong to the spectrum of 1 ħω states which is already incomplete above E_x = 10 MeV. These two states are omitted in Fig. 7 as is the 10315 KeV level which is very tentatively assigned in Fig. 6 to the spectrum of $J^\pi = 6^-$, 1 ħω states. The levels of Fig. 7 are thus completely of 3 ħω origin. The J^π assignments are obtained either earlier in this work or adopted from the ENSDF Database. Except are the levels at 11484 and 11078 KeV. In these cases we arrive at the proper assignments by comparing observed γ-decay to expectations born out by the weak-coupling model (Table 5) which is explained in the subsequent section.

Table 5 contains a $J^\pi = (8 - 11)^-$ multiplet with underlying configuration $19/2^-$, T = 1/2 ⓧ $3/2^+$, T = 1/2. Gamma decay of multiplet members can proceed only by isovector E2 transitions to members of a $J^\pi = (6 - 9)^-$ multiplet with configuration $15/2^-$, T = 3/2 ⓧ $3/2^+$, T = 1/2. The 11484 KeV and 11078 KeV states constitute the as yet unidentified $J^\pi = 9^-$ and $J^\pi = 8^-$ members of the first multiplet. The final states in their γ-decay are members of the second multiplet.

Two levels at 11651 and 11174 KeV with $J^\pi = 10^-$ and $J^\pi = 9^-$, respectively are ordered in Table 5 into a $J^\pi = (6 - 9)^-$, $15/2^-$, T = 1/2 ⓧ $3/2^+$, T = 1/2 multiplet. They should decay to two $J^\pi = (4 - 7)^-$ multiplets with configurations, $11/2^-$, T = 3/2 ⓧ $3/2^+$, T = 1/2 and $11/2^-$, T = 1/2 ⓧ $3/2^+$, T = 1/2. The established $J^\pi = 7^-$ states at 8972 and 9349 KeV belong to the two $J^\pi = (4 - 7)^-$ multiplets. Their γ-decay modes are identical, pointing at a mixture of the two $J^\pi = (4 - 7)^-$ configurations an effect which is not contained in the weak-coupling model.

Having completed the experimentally available spectrum of 3 ħω states in Table 3 and Fig. 7 a detailed discussion in terms of the weak-coupling model is to follow. A summary of results has been anticipated already in Fig. 7 by displaying the prediction of weak-coupling multiplets.

7. The weak-coupling model with emphasis on A = 38

The energy of configurations with n_p particles in the N = 3 major shell (among them k_p protons) and n_h holes (among them k_h proton-holes) is calculated using experimental binding energies of pure particle and pure hole configurations, for instance with $n_p = 3$, $n_h = 5$, $k_p = 1$, $k_h = 3$

$^{38}Ar = {}^{43}Sc + {}^{35}Cl - {}^{40}Ca$ ($- {}^{38}Ar$ g.st. if we want E_x instead of E_B).

In this expression we have a double counting of interactions their number being $n_p \bullet n_h$ or $k_p \bullet k_h$ in the case of the Coulomb interaction. These terms have to be subtracted and enter the theory as a residual interaction

$$V = - a\, n_p \bullet n_h + 4b\, t_p \bullet t_h + c\, k_p \bullet k_h$$

which has three constants a, b, c (other authors use b in place of 4b!). The Coulomb interaction can in fact be considered state independent. The other two terms base on the assumption that the interactions of particles in different major shells are <u>weak</u> so that it is sufficient to consider the monopole part only. As an acceptable price the weak-coupling model generates degenerate multiplets of levels with $\left| J_p - J_h \right| \le J \le J_p + J_h$.

The parameters of the residual interaction are deduced using experimental data from A = 38 only. We obtain c = −270 KeV using the binding energies of the first excited 0^+ states of ^{38}Ar and ^{38}Ca. The parameters a and b are obtained using the $J^\pi = (8 - 11)^-$ multiplets with T = 0 and T = 1. They are generated by coupling the $19/2^-$, T = 1/2 level of A = 43 with the $3/2^+$, T = 1/2 ground state of A = 35.

The interaction energies are

$$V = -15a + b + 3c \quad \text{for} \quad \begin{matrix} T=1 \\ -3b \quad T=0 \end{matrix}$$

The T = 1 multiplet has levels in ^{38}Ar at 11614 KeV (11^-), 11547 KeV (10^-) and 11484 KeV (9^-) which determine the (2J+1) weighted centroid rather accurately as 11555 KeV. The T = 0 multiplet has levels in ^{38}K at 8692 KeV (11^-), 8747 KeV (10^-) and 7396 KeV (9^-). Note that all spins are higher by one unit in Endt's compilation which is impossible because $J^\pi = 12^-$ cannot be reached at these energies. The ^{38}K centroid is rather accurately given as 8232 KeV, corresponding to 8102 in ^{38}Ar.

From the deduced centroids we derive a = − 268 KeV and 4b = 3451 KeV.

The lowest lying multiplet with $t_p = t_h = 1/2$ (and J = 2 - 5) in ^{38}Ar is predicted at E_x = 8432 KeV, the lowest multiplet with $t_p = 3/2$, $t_h = 1/2$ (and J = 2 - 5 again) at E_x = 7803 KeV.

This is in contrast to the prediction in 1980 *[2]*, which used the parameters of Kolota and Warburton (a = − 250 KeV, 4b = 2500 KeV, c = − 400 KeV) and led to inverted ordering (7540 and 8430 KeV). Actually we had anticipated this inversion when we tried to explain the number of $J^\pi = 1^-$ states.

The highest lying observable multiplet with $t_p = 3/2$, $t_h = 1/2$ which is also providing the level of highest spin for this isospin coupling has $J^\pi = (6 - 9)^-$, generated by $15/2^- \otimes 3/2^+$. The theoretical energy of 10481 KeV points at the well established 10174 KeV, 9^- state as the level of highest spin.

At the present stage we are able now to construct the experimental weak-coupling multiplets. They are given and compared to the theory in Table 5.

With a single exception we can trace all multiplets at least in the realm of high spin. At excitation energies above 10 MeV we observe high-spin states only, due to the kinematics of our ^{35}Cl(α, p γ) reaction. A 4 MeV proton cannot carry away the angular momentum of a 16 MeV α - particle, thus leaving the ^{38}Ar nucleus in a state of high spin. The experimental/weak coupling comparison of levels in Fig. 7 is complete to the highest energies for $J \geq 8$ states and complete up to 11 MeV for $J^{\pi} = 7^{-}, 6^{-}$ states. The spectrum of $J^{\pi} = 5^{-}$ states is complete to 10 MeV only.

With the successful reproduction of the 3 ħω states we have arrived at a complete understanding of the ^{38}Ar level scheme. The consideration of all n ħω excitations with n = 0 - 6 is necessary but also sufficient, thus confirming our introductory remarks.

8. Improvements of the ^{38}Ar level scheme

Our analysis of the ^{38}Ar level scheme was performed on the basis of our investigations with the ^{35}Cl(α, p γ) reaction in 1976 *[1]* and 1980 *[2]*. Subsequent work with the ^{28}Si(^{16}O, α 2p γ) *[14]* has added to our knowledge of high-spin states, their J^{π} assignments and γ-decay modes. Here we compare the new results with our ones, wherever there are differences.
In first place we have a doublet at 8124/8129 KeV with decay modes

previous		**present**	
8124 →	5350, 4^+	8124 →	5350, 4^+
	4585, 5^-	8126 →	4585, 5^-
	6674, 5^-		6674, 5^-
8129 →	7070, 5^-		7070, 5^-

There is agreement with *[14]* that $J^{\pi} = 6^-$ must be assigned to the 8126 KeV, formerly 8129 KeV level. Equally we agree that a 7070 → 4585 KeV transition has a mixing ratio around −0.5 for spin sequence 5 → 5. This fact remained unobserved in *[14]*. The reduced excitation energy of the former 8129 KeV leads to a 3 KeV reduction of E_x for the former 9199, 10029, 11068, 11109 and 11452 KeV levels. This is of no importance here except for the former 10029 KeV level which is identical now with the 10025 KeV, $J^{\pi} = 8^-$ level of *[14]*.This state should, however, not be mixed up with a closely spaced 10024 KeV level, which decays to the 7070 KeV, $J^{\pi} = 5^-$ state.
A 9928 → 8568 KeV transition of our previous work which would read 9930 → 8570 KeV today must be identical with a 9934 → 8570 KeV transition of *[14].* We have probably underestimated the excitation energy of the initial state because the latter one has a long lifetime so that its Dopplershift (measurement at $\Theta_\gamma = 0°$) is attenuated. (In fact we are dealing within the frame of

the weak coupling model with a $9^+ \rightarrow 8^+$ transition between configurations 7^+, $T = 0 \otimes 2^+$ $T = 1$ and 6^+, $T = 1 \otimes 2^+$, $T = 0$ which are not connectable by a one-body operator.)

In our previous work we observed two γ-rays of 1362 and 1959 KeV energy and interpreted them as the 11290 → 9928 KeV and 11298 → 9338 KeV transitions. With improved final state energies they read 11296 → 9934 KeV and 11298 → 9339 KeV. Rudolph et al. *[14]* observed the same transitions and assigned them to decay of a single, 11300 KeV level. The energy difference between the two γ-rays is, from both measurements, 597.3 ± 0.3 KeV. The energy difference of the final states is *[21]* 594.3 ± 0.8 ± 0.4 KeV. Hence our assumption of a doublet separated by 2 KeV, remains credible and moreover it makes sense. We have in Fig. 3 the $10_1^+ \rightarrow 9_1^+$ transition between two 2 ħω states and in Fig. 1a an $10^+ \rightarrow 8^+$ transition between two 4 ħω states, both members of the first $K^\pi = 0^+$ rotational band.

Table 1

The 2 ħω states of ^{38}Ar up to 9.014 MeV as predicted by the weak-coupling model using the same parameters as obtained for the 3 ħω states

The relevant particle states of A = 42 and hole states of A = 36

^{42}Ca		^{36}Ar	
E_x[KeV]	J^π, T	E_x[KeV]	J^π, T
0	0^+, 1	0	0^+, 0
1524	2^+, 1	1927	2^+, 0
2751	4^+, 1	4410	2_2^+,0
3190	6^+, 1	4564	4^+, 0
4452	2_2^+,1	6611	2^+, 1
5016	4_2^+,1	7337	3^+, 1
5380	5^+, 1	7710	1^+, 1

^{42}Sc	
616	7^+, 0

Predicted singlets[KeV] / assigned levels

2926	0^+	3377				
4450	2^+	5593	4853	2^+	6214	
5677	4^+	5974	7336	2^+	7702	
6116	6^+	6408	7490	4^+	6276	
7378	2^+	8233	6086	2^+	7370	(T = 1 ⊗ T = 1)
7942	4^+	7911	6812	3^+	7993	(T = 1 ⊗ T = 1)
8306	5^+	8650	7185	1^+		(T = 1 ⊗ T = 1)

The first multiplets[a)]

coupled states	J^π	centroid[KeV]	centroid	experimental levels[KeV]	
1524 ⊗ 1927	0 - 4	6377	7078	7060, 6852, 6485, 7235, 7376	In Order of
2751 ⊗ 1927	2 - 6	7604	7840	7856, 8311, 8106, 7539, 7663	increasing
3190 ⊗ 1927	4 - 8	8043	8510	8181, 8809, 8944, 8077, 8569	spin
1524 ⊗ 4564	2 - 6	9014	(8996)	8996(6^+) only	

a) Above 8 MeV we consider only multiplets which incorporate J ≥ 6 levels

Table 2

The ^{38} Ar states of 2 ħω character, high-spin and E_x > 9.014 MeV, predicted by the weak-coupling model

$E_x(J^\pi)$ of coupled states				Resulting		exp. multiplet members
Particle	⊗	Hole		J^π	Centroid	
616	(7^+)	6611	(2^+)	5 - 9	10153	9330(7^+), 9928(9^+)
5380	(5^+)	1927	(2^+)	3 - 7	10233	10112(7^+)
2751	(4^+)	4564	(4^+)	0 - 8	10241	10676(7^+), 10120 (8^+)
3190	(6^+)	4410	(2^+)	4 - 8	10526	11163(7^+)
3190	(6^+)	4564	(4^+)	2 - 10	10680	11379(7^+), 11495(8^+), 10634(9^+), 11290(10^+)
616	(7^+)	7337	(3^+)	4 - 10	10879	11428(7^+), 11543(8^+), 11199(9^+), 11620(10^+)
616	(7^+)	7710	(1^+)	6 - 8	11252	11595(7^+), 11608(8^+)

Two $J^\pi = 6^+$ levels at 10455^B and 10589 KeV can be assigned to any multiplet, except, for energetical reasons, the lowest and the highest lying one.

Table 3

The π = − states of ^{38}Ar up to 10 MeV and selected states above

A: The 1 ħω and 3 ħω states

(J^{π}, E_x [KeV], decay mode if J^{π} is still to be determined here)

0^-	1^-	2^-	3^-	4^-	5^-	6^-	7^-	8^-
6846→ 2_1^-	6354	5084	3810	4479	4585	7528→ 5_1^-,5_2^-	7507	
	6574	5858	4877	6042→ 3_1^-,4_1^-,5_1^-	5658	7667→ 5_2^-,5_3^-	*8972	
	6773	6824[A]	5825	6211	6674	8215→ 5_2^-,5_3^-	9644→ 7_1^-	11078→ 9644
	7234→ 0_1^+	6870→ 2_1^+,3_1^-	6496	6601	7485→ 5_2^-	8595→ 5_1^-,5_2^-	10135→ 7_1^-	
	7894→ 0_1^+	7101→ 2_1^+	6622	7495→ 3_1^-,4_1^-	*7859→ 5_3^-	*8789→ 5_3^-,5_D^-	10180→ 7_1^-	
	8391→ 0_1^+	7291→ 3_1^-	6904→ 2_1^+,2_2^+,4_1^-	7786→ 4_1^-,4_2^-	7899→ 5_3^-	9087→ 5_1^-,5_2^-		
		7452→ 2_1^+,3_2^-	7046→ 2_1^+,3_1^-,3_2^-	7828→ 3_1^-	8261→ 4_1^-,5_1^-,5_2^-	*9349→ 5_1^-,5_2^-		
			7128→ 2_1^+,3_1^-	8481→ 4_1^-,5_1^-	8417→ 5_2^-	9669→ 5_2^-		
			7684→ 2_1^+,3_1^-,3_2^-	*8520→ 4_1^-,5_1^-	8783→ 5_2^-			
			8311→ 2_1^+,3_1^-	8800→ 4_2^-	8828→ 5_1^-	*10101→ 5_1^-, 5_2^-		
			8668→ 2_1^+,3_2^-	9077→ 3_2^-	*8875→ 4_1^-,5_1^-, 5_2^-	10557→ 7_1^-		
				9170→ 4_1^-,5_1^-	9293→ 5_1^-			
					9374→ 5_1^-			
					9437→ 5_2^-			
					9460→ 5_1^-			
					9655→ 5_2^-			

B: The deformed 5 ħω states, just a reminder of the foregoing results

K^{π}	1^-	2^-	3^-	4^-	5^-	6^-	7^-	8^-
0^-_{odd}	5734		6339		7194		8491	
3^-			5513	6211	7070	8126	9196	10455[A]
2^-	6948→ 0_2^+,2_1^+	7335→ 2_1^+,3_1^-			10024→ 5_D^-	11109		
1^-		(7431→ 2_1^+)	8068→ 3_1^-,4_2^-	8956→ 5_1^-,5_D^-	9829	10947[A]		

The notation 5_D^- stands for the deformed $J^{\pi} = 5^-$, Ex = 7070 KeV state
The * indicates a 3 ħω character of the level. See text

Table 4

The experimental ^{38}Ar states of 1 ħω and 3 ħω character, as obtained in Table 3A, compared to the theoretical 1 ħω spectrum

J^{π}	0^-	1^-	2^-	3^-	4^-	5^-	6^-	7^-	8^-	9^-
E_x[KeV] exp/ theor	6846 / 6825	6354 / 6484	5084 / 5578	3810 / 4357	4479 / 4274	4585 / 4465	7528 / 6713	7507 / 7287	/ 11682	/ 12869
	/ 8400	6574 / 6861	5858 / 5877	4877 / 5030	6042 / 6030	5658 / 5685	7667 / 7296^{w}	8972*		
		6773 / 7036	6824^{A} / 6293	5825 / 5693	6211 / 6342	6674 / 6894	8215 / 7990			
		7234 / 7180	6870 / 7049	6496 / 5889	6601 / 6690	7485 / 7052	8595 / 8745^{w}	9349/		
		7894	7101	6622 / 6941	7495 / 7510	7859*	8789*	9644/		
		8391 / 8165	7291	6904 / 7175	7786 / 7722	7899 / 7684	9087 / 9124^{w}	10135 / 9124^{w}		
			7431 / 7508	7046	7828	8261 / 8192		10181/		
			/ 7851	7128	8481 / 8136	8417*	9669			
			/ 8157	7684 / 7562	8520*	8783 / 8427	10101*			
				8311 / 7767	8800 a)	8828 / 8745^{w}	10315 / 10465^{w}			
				8668 / 8250		8875*	10557 / 10623^{w}			
						9293 / 9124^{w}				
						9374				
						9437 / 9519^{w}				
						9460				
						9655 / 9674^{w}				
						/ 10465^{w}				
						/ 10623^{w}				

a) Weak-coupling predictions of 1 ħω states yield three levels already at 8100, 8433, 8745 KeV The experimental spectrum is no longer complete

***** A 3 ħω character of this level has been established previously

w Level predicted by the weak-coupling model

Table 5

The 3 ħω states of ^{38}Ar in terms of the weak-coupling model

Theoretical multiplets					**Theoretical centroids[KeV]**		**Experimental centroids [KeV]**		**Members of multiplets**
T_p	T_h	J^π_p	J^π_h	J^π	relative E_x	absolute E_x	relative E_x	absolute E_x	Members of multiplets
3/2	**1/2**	$7/2^-$	$3/2^+$	$(2\text{-}5)^-$	0	7803	0	7552	$7859(5^-)$, $7828(4^-)$, $7046(3^-)$, $7101(2^-)$
		$5/2^-$		$(1\text{-}4)^-$	372	8175	224	7776	$8520(4^-)$, $7128(3^-)$, $7291(2^-)$, $7894(1^-)$
		$3/2^-$		$(0\text{-}3)^-$	593	8396	Not identifiable - low spin and $E_x > 8$ MeV		
		$11/2^-$		$(4\text{-}7)^-$	1677	9480	1357	8909	$8972(7^-)$, $8789(6^-)$, $8875(5^-)$, $?(4^-)$
		$9/2^-$		$(3\text{-}6)^-$	2093	9896			
		$15/2^-$		$(6\text{-}9)^-$	2754	10557	2598	10150	$10174(9^-)$, $10025(8^-)$, $9644(7^-)$
		$7/2^-$	$5/2^+$	$(1\text{-}6)^-$	1750	9553	2549	≈ 10101	$10101(6^-)$
		$5/2^-$		$(0\text{-}5)^-$	2122	9925	1908	≈ 9460	$9460(5^-)$
		$11/2^-$		$(3\text{-}8)^-$	3427	11230	3208	≈ 10750	$11174(8^-)$, $10181(7^-)$, $10890(6^-)$
		$9/2^-$		$(2\text{-}7)^-$	3843	11646	3827	≈ 11379	$11068(6^-)$
		15/2		$(5\text{-}10)^-$	4584	12367	3420	≈ 10972	$11997(10^-)$, $10948(9^-)$
1/2	**1/2**	$7/2^-$	$3/2^+$	$(2\text{-}5)^-$	0	8431	0	≈ 8514	$8417(5^-)$, $?(4^-)$, $8668(3^-)$
		$11/2^-$		$(4\text{-}7)^-$	1677	10109	951	≈ 9465	$9349(7^-)$, $9669(6^-)$, $9374(5^-)$
		$15/2^-$		$(6\text{-}9)^-$	2987	11419	2911	≈ 11425	$11651(9^-)$, $11174(8^-)$
		$19/2^-$		$(8\text{-}11)^-$	3123	11558	3038	≈ 11552	$11614(11^-)$,$11547(10^-)$, $11484(9^-)$,$11078(8^-)$
		$17/2^-$		$(7\text{-}10)^-$	3700	12131	2838	≈ 11452	$11452(9^-)$
		$7/2^-$	$5/2^+$	$(1\text{-}6)^-$	1763	10195	} Not observed, Spin is too low in view of high E_x		
			$7/2^+$	$(0\text{-}7)^-$	2645	11077			
		$9/2^-$	$3/2^+$	$(3\text{-}6)^-$	2458	10897			

Table 6

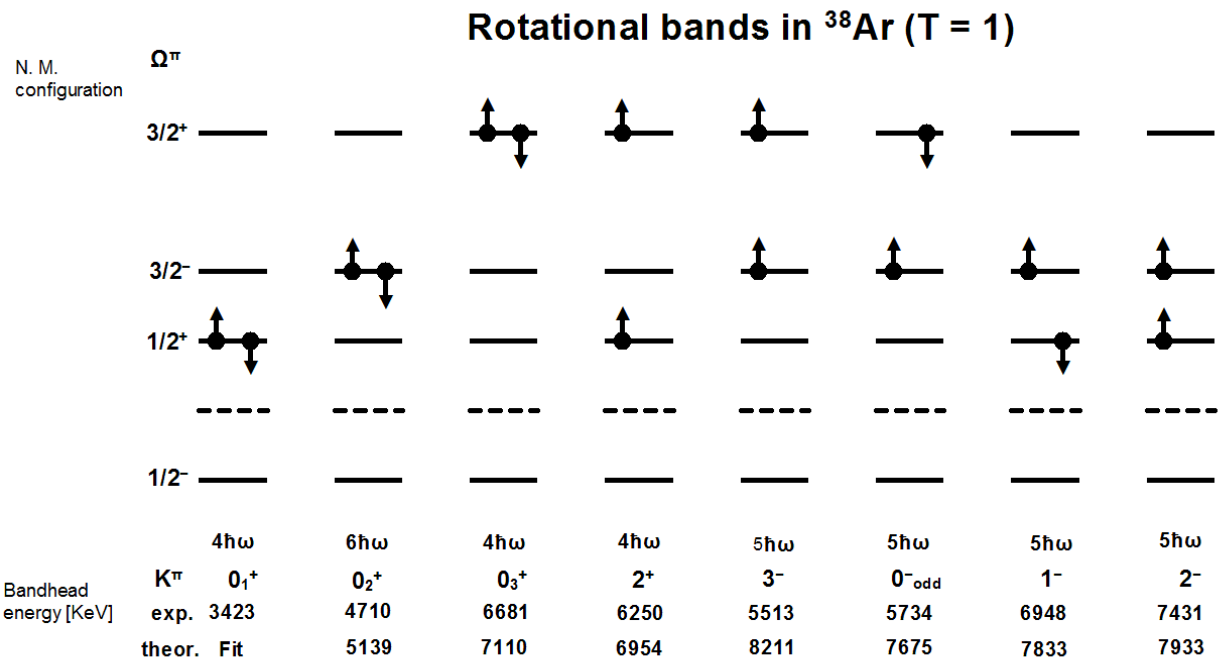
Rotational bands in ^{38}Ar (T = 1)
N. M. configuration
Ωπ
3/2+
3/2−
1/2+
1/2−
4ħω
6ħω
4ħω
4ħω
5ħω
5ħω
5ħω
5ħω
Kπ
0₁+
0₂+
0₃+
2+
3−
0−odd
1−
2−
Bandhead energy [KeV]
exp.
3423
4710
6681
6250
5513
5734
6948
7431
theor.
Fit
5139
7110
6954
8211
7675
7833
7933

Fig. 1a

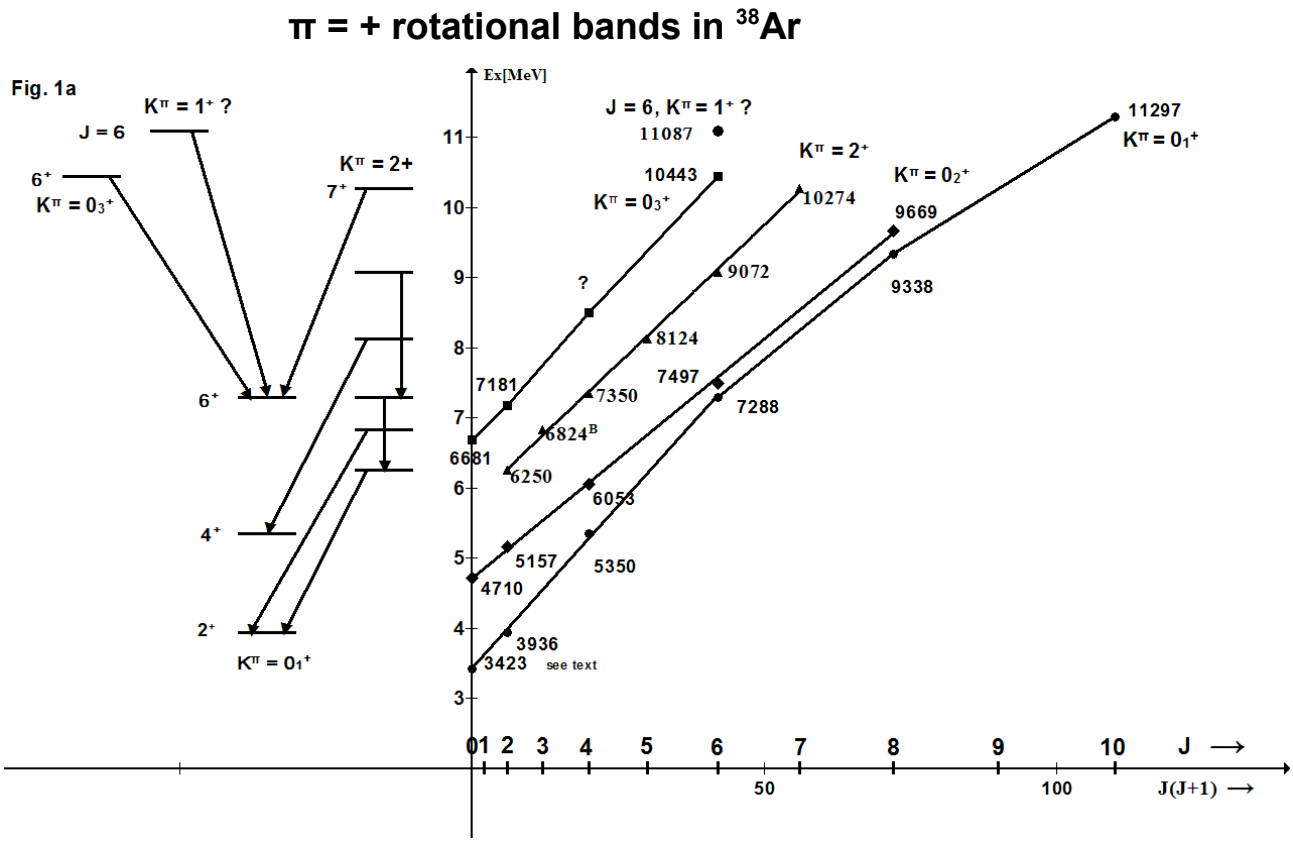
π = + rotational bands in 38Ar
Fig. 1a
Ex[MeV]
Kπ = 1+ ?
J = 6
6+
Kπ = 03+
Kπ = 2+
7+
6+
4+
2+
Kπ = 01+
J = 6, Kπ = 1+ ?
11087
10443
Kπ = 03+
?
7181
6681
6824B
Kπ = 2+
10274
9072
8124
7497
7350
6250
6053
5157
4710
5350
3936
3423 see text
Kπ = 02+
9669
9338
7288
11297
Kπ = 01+
J
J(J+1)

Fig. 1b

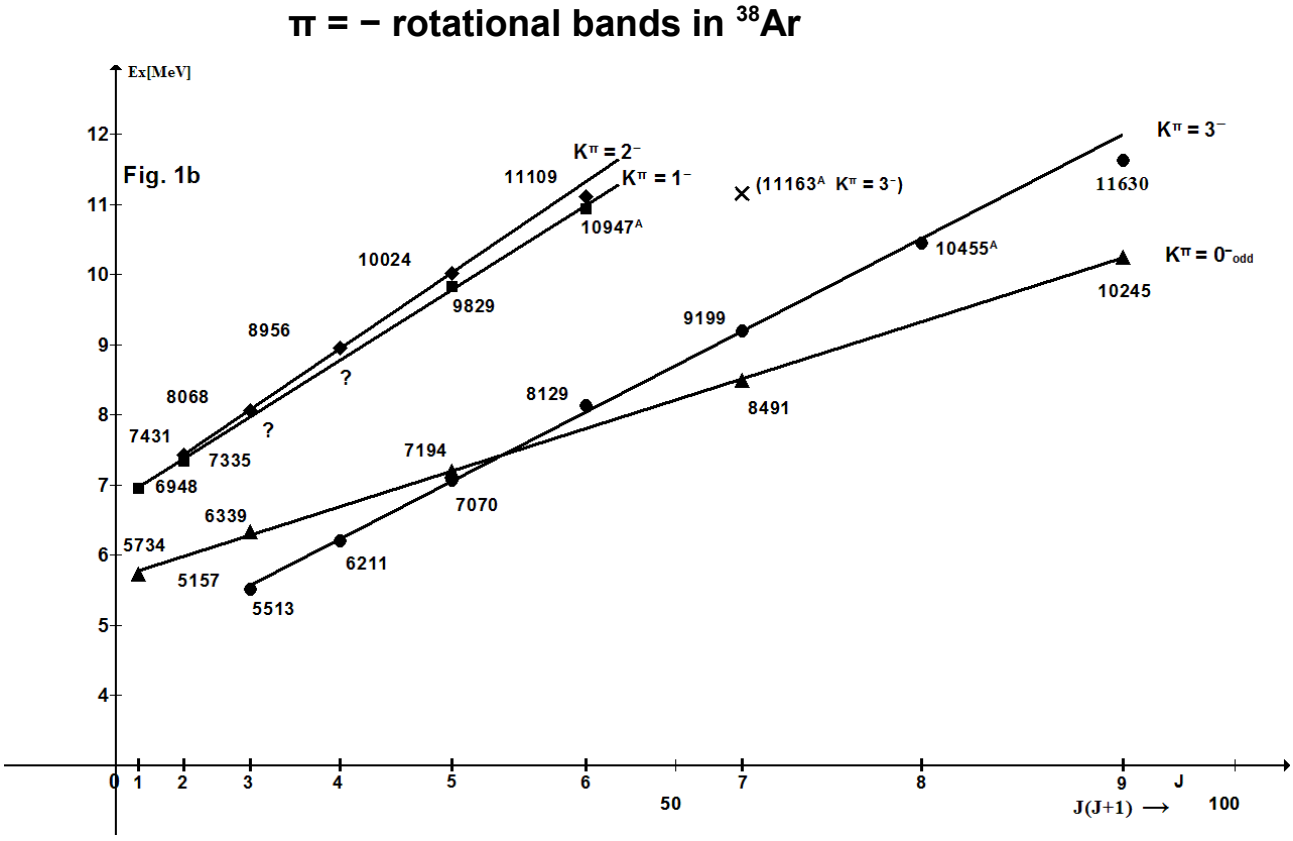
π = − rotational bands in 38Ar
Ex[MeV]
Fig. 1b
Kπ = 2−
11109
Kπ = 1−
10947A
(11163A Kπ = 3−)
Kπ = 3−
11630
10455A
Kπ = 0−odd
10245
10024
9829
8956
?
8068
?
7431
7335
6948
9199
8129
8491
7194
7070
6339
5734
5157
6211
5513
J
J(J+1)

Fig. 2

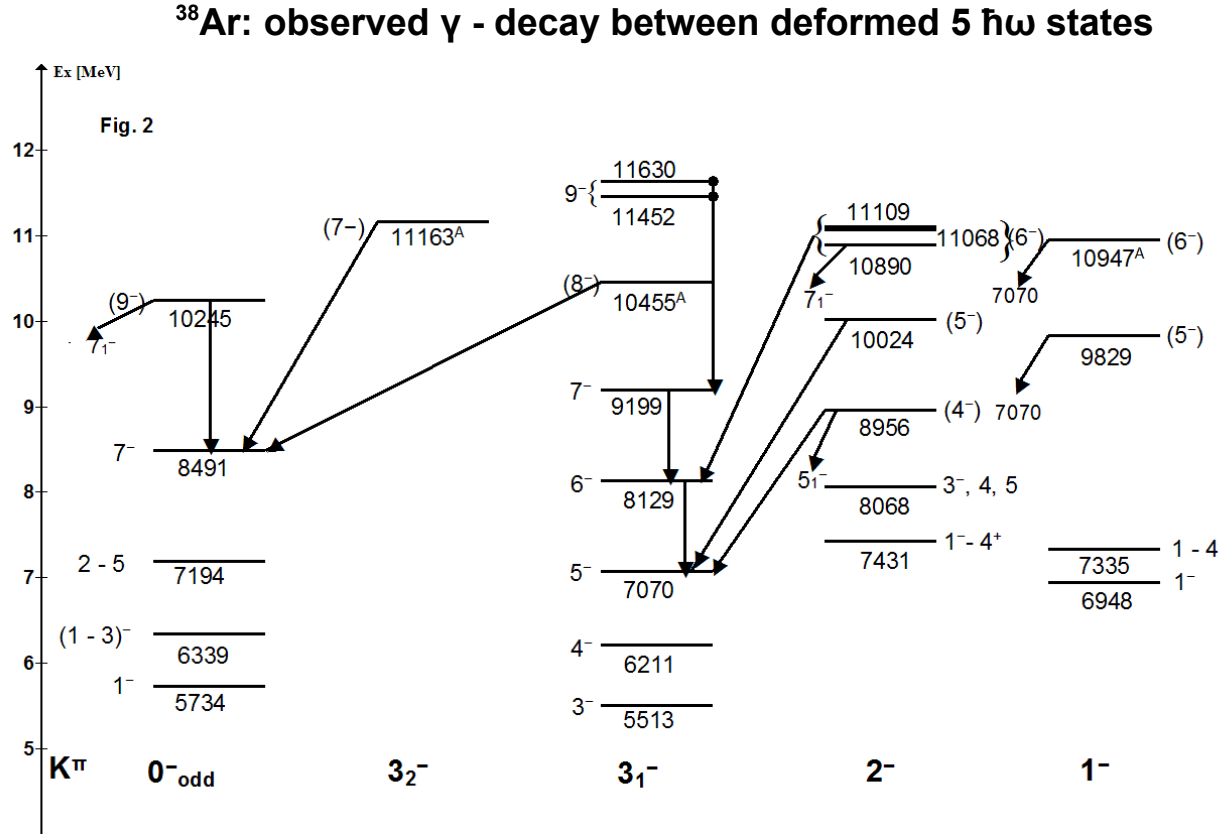
38Ar: observed γ - decay between deformed 5 ħω states
Ex [MeV]
Fig. 2
12
11
10
9
8
7
6
5
(9⁻)
10245
71⁻
7⁻
8491
2 - 5
7194
(1 - 3)⁻
6339
1⁻
5734
(7⁻)
11163A
(8⁻)
10455A
9⁻
11630
11452
7⁻
9199
6⁻
8129
5⁻
7070
4⁻
6211
3⁻
5513
11109
11068
10890
71⁻
(5⁻)
10024
(4⁻)
8956
51⁻
3⁻, 4, 5
8068
1⁻- 4⁺
7431
(6⁻)
7070
10947A
(6⁻)
(5⁻)
9829
7070
1 - 4
7335
1⁻
6948
Kπ
0⁻odd
32⁻
31⁻
2⁻
1⁻

Fig. 3

The interpretation of 2 ħω states from their decay and excitation energies

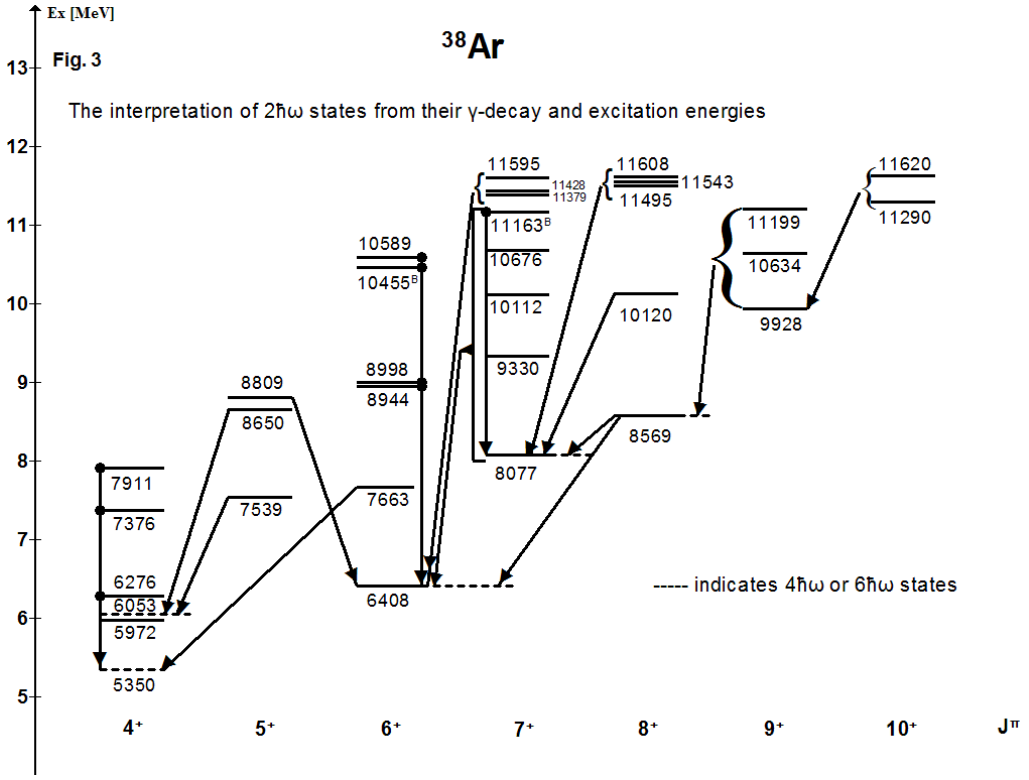

Fig. 4

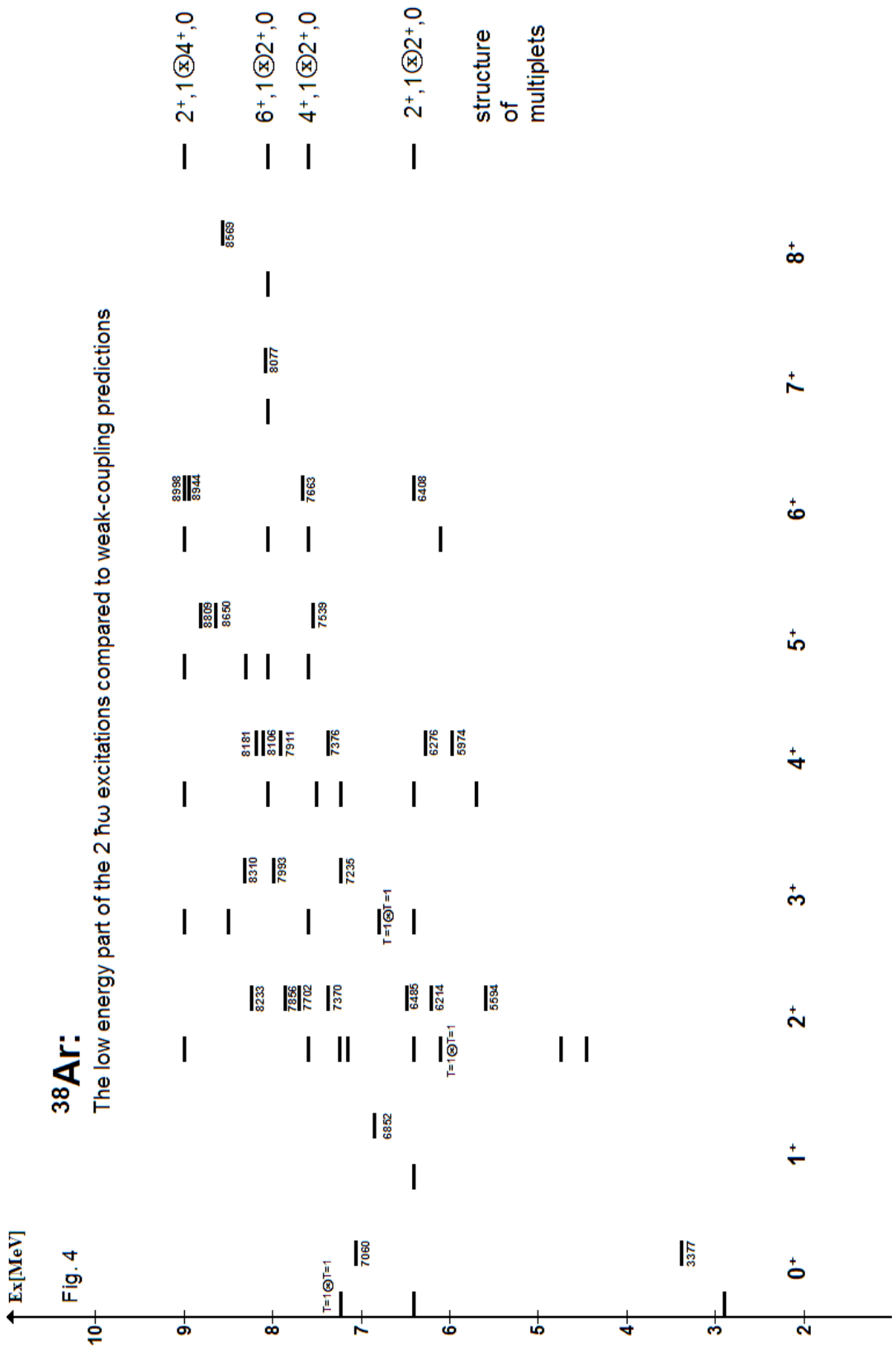
38Ar:
The low energy part of the 2 ħω excitations compared to weak-coupling predictions
Ex[MeV]
structure of multiplets
2+,1⊗4+,0
6+,1⊗2+,0
4+,1⊗2+,0
2+,1⊗2+,0
T=1⊗T=1
T=1⊗T=1
T=1⊗T=1
0+
1+
2+
3+
4+
5+
6+
7+
8+
10
9
8
7
6
5
4
3
2
7060
6852
8233
7856
7702
7370
8310
7933
7235
8181
8106
7911
7376
8998
8944
8809
8650
7539
7663
8569
8077
6485
6214
5594
6276
5974
6408
3377

Fig. 5

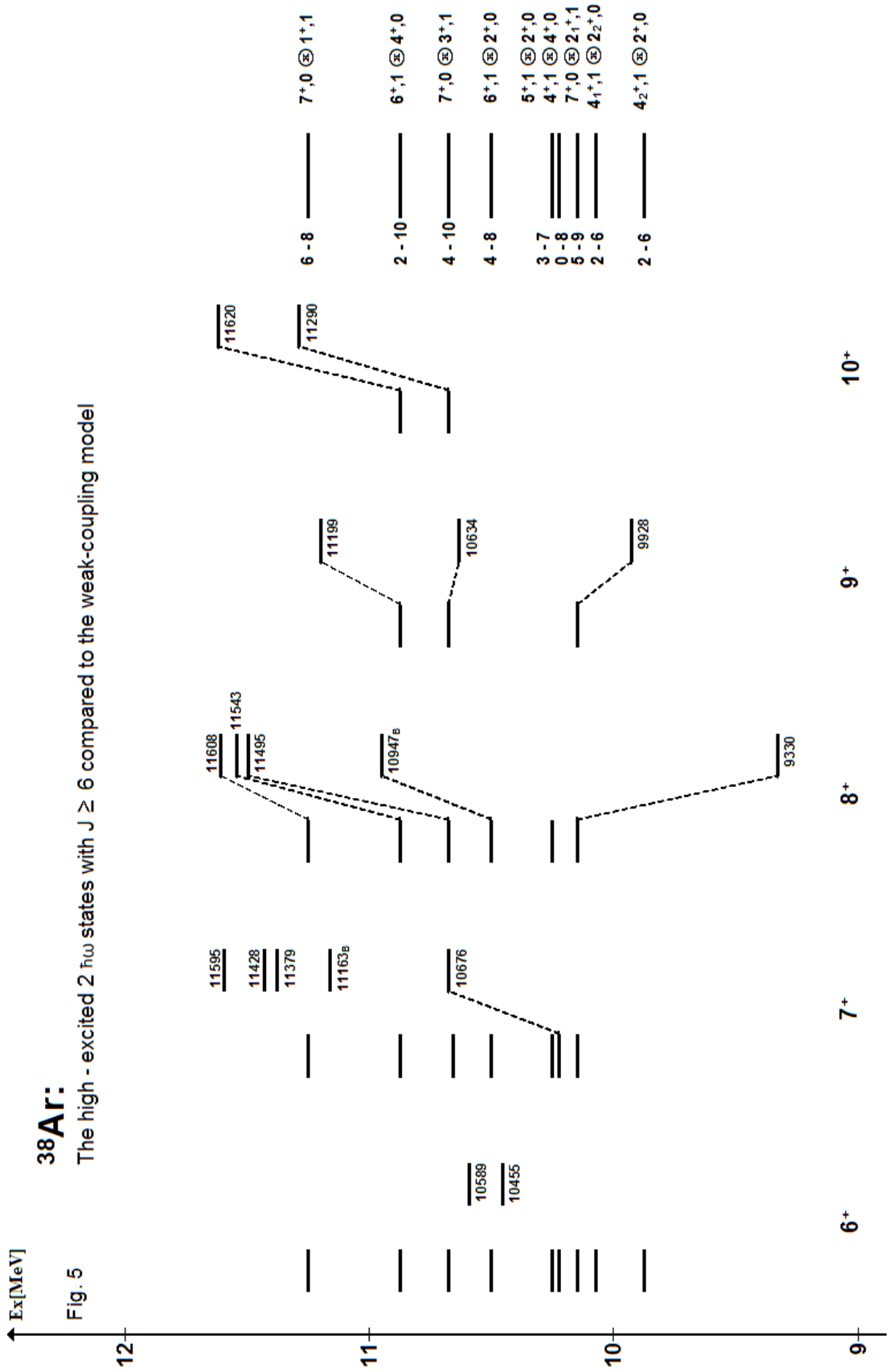
Ex[MeV]
Fig. 5
38Ar:
The high - excited 2 ħω states with J ≥ 6 compared to the weak-coupling model
12
11
10
9
6+
7+
8+
9+
10+
11595
11428
11379
11163B
10589
10455
10676
11608
11543
11495
10947B
9330
11199
10634
9928
11620
11290
6 - 8
2 - 10
4 - 10
4 - 8
3 - 7
0 - 8
5 - 9
2 - 6
2 - 6
7+,0 ⊗ 1+,1
6+,1 ⊗ 4+,0
7+,0 ⊗ 3+,1
6+,1 ⊗ 2+,0
5+,1 ⊗ 2+,0
4+,1 ⊗ 4+,0
7+,0 ⊗ 2+1,1
4+1,1 ⊗ 2+2,0
4+2,1 ⊗ 2+,0

Fig. 6

The 1 ħω excitations of ^{38}Ar

theoretical/experimental, repeated from Table 4 for a visual impression

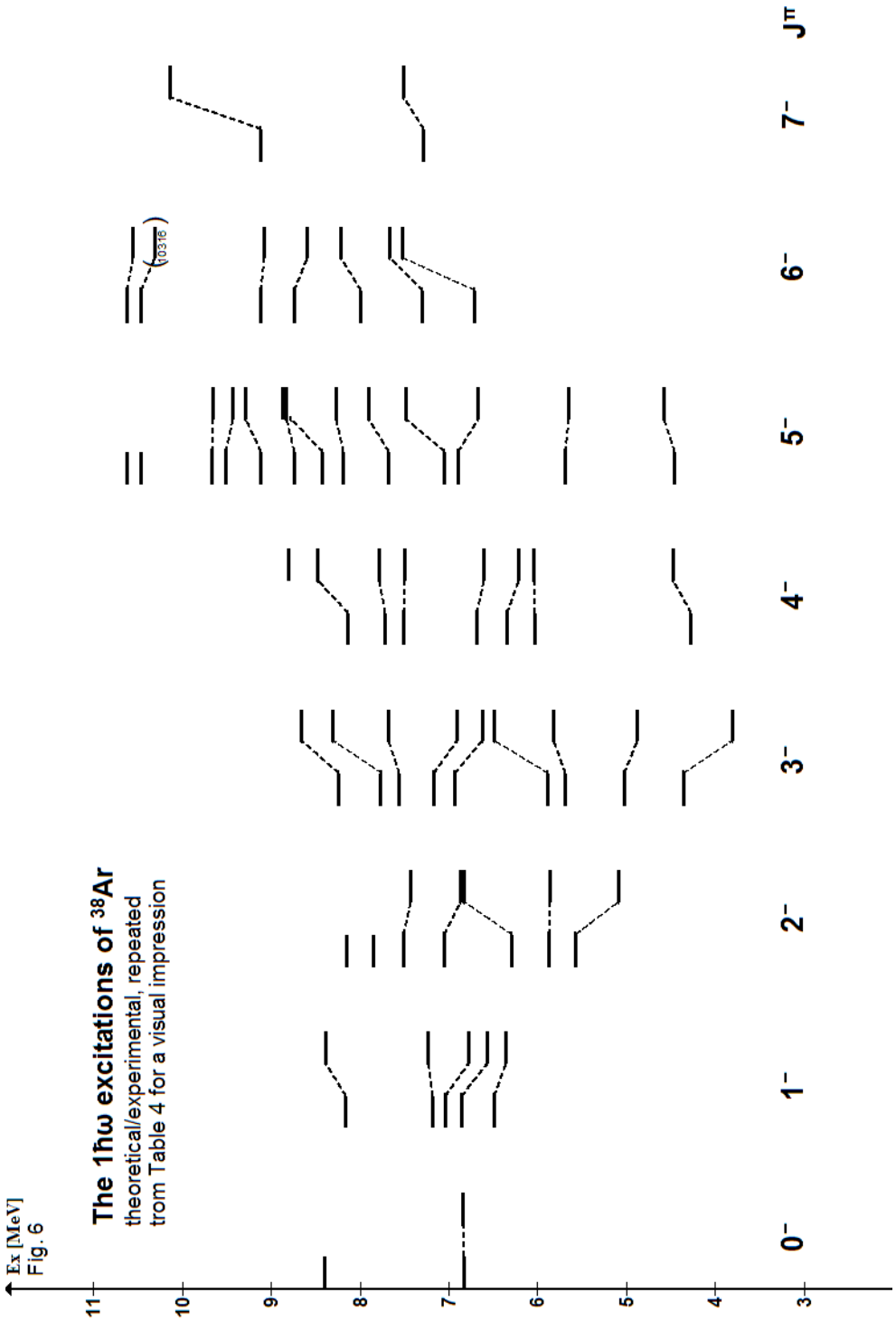

Fig. 7

3 ħω, J ≥ 5 states of ^{38}Ar and weak-coupling predictions

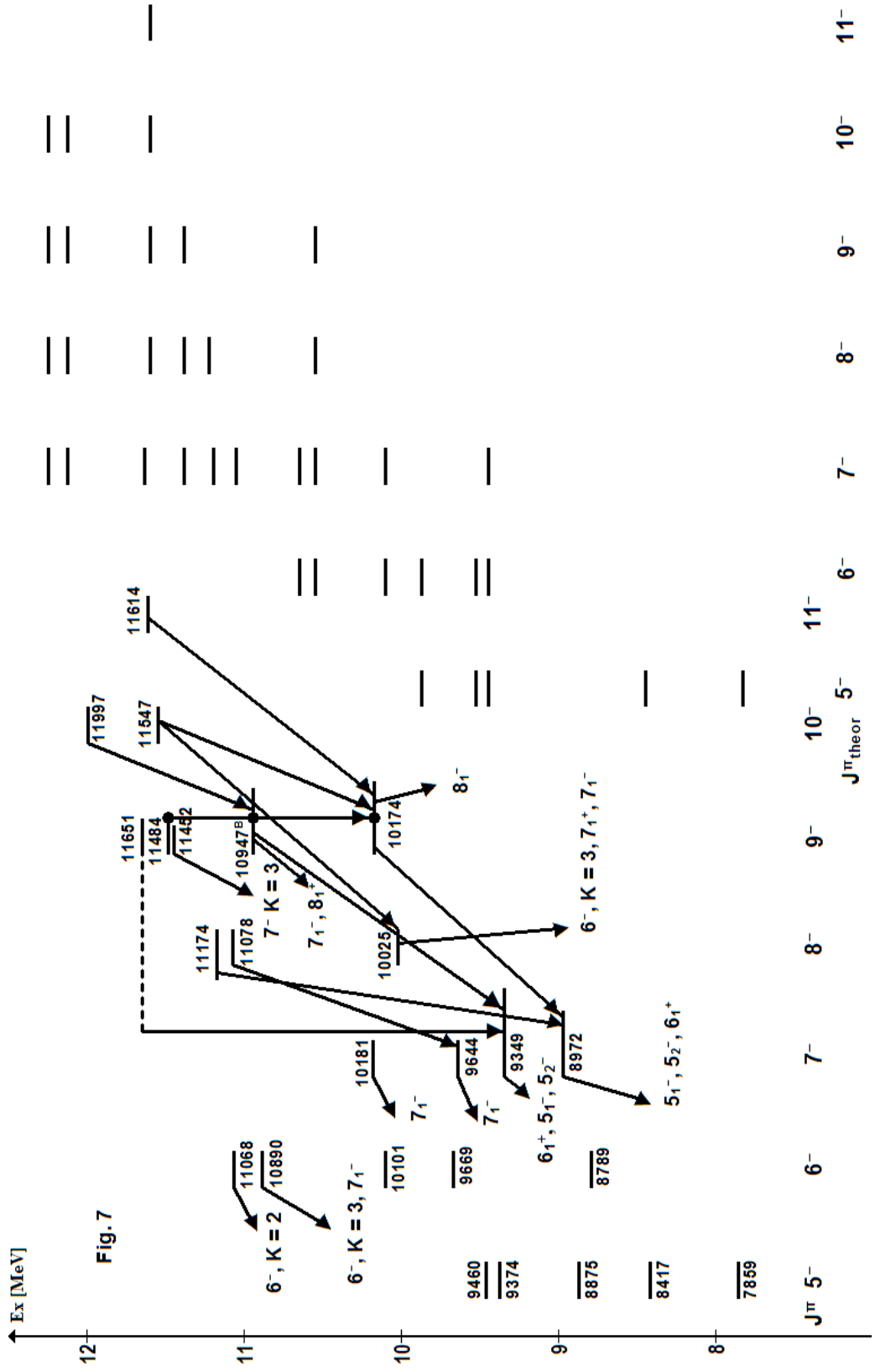

9. Decomposition of the ^{39}K level scheme in terms of n ħω excitations from n = 0 to n = 7

The excited states of doubly magic ^{40}Ca should be due to the excitation of n particles from the N = 2 into the N = 3 major shell. In 2004 we were able *[9]* to explain the complete level scheme up to 8 MeV by considering all excitations from n = 1 to n = 8. The n ≥ 4 excitations are connected with quadrupole deformation and found an explanation by a Nilsson model with residual interaction. In these notes we extend the analysis to the neighbouring nucleus ^{39}K. The expectation is a complete understanding in terms of all n ħω excitations from n = 1 to n = 7. (The n = 0 spectrum consists of a hole in one of the orbits $d_{3/2}$, $s_{1/2}$, $d_{5/2}$ of the N = 2 major shell and must be considered as given).
After a big leap to the end of our investigations it turns out that the expectation is completely fulfilled and that the spectrum of ^{39}K states up to the particle emission threshold is predictable without using ^{39}K data for adjustments.
The 1 ħω spectrum has been calculated by Warburton *[6]* considering all orbits of the N = 2 and N = 3 major shells. The results are given in the first column of Table 4. The spectrum of 2 ħω and 3 ħω excitations is predictable by the weak-coupling model as developed in our analysis of A = 38, T = 1 and 0. The predicted 2 ħω excitations are given in Table 1 and compared to experiment in Table 3. The 3 ħω excitations simply reflect the spectrum of ^{43}Sc. They are given in Table 4. The n ħω excitations with n = 4 - 7 are predicted in Table 2 using a Nilsson model Hamiltonian with residual interaction that is reported in our analysis of the A = 40 system.
The comparison with experiment necessitates a critical assessment of data in Endt‘s compilation *[4]*. This is done in Table 5. Up to the proton emission

threshold, where experimental information starts to have gaps, we are able to find the proper partner of every predicted level. Vice versa there is no surplus of experimental states.

Note in particular the beautiful $K^{\pi} = 3/2^{-}$ band, predicted in Table 4 and shown on p. 257. To our knowledge this band went unrecognised up to now. We lost the reference concerning these high-spin states. The data of appearance (in Phys. Rev. C) is later than 1998, the year of Endt's last compilation .

Table 1

Predicted 2 ħω excitations in ^{39}K

Parent states				^{39}K predicted		
^{42}Sc		^{37}Ar				
J^{π}, T	**E_x[KeV]**	**J^{π}, T**	**E_x[KeV]**	**E_x[KeV]**	**J^{π};**	**T**
0^+, 1	**0**	**$3/2^+$, 1/2**	**0**	**3197**	**$3/2^+$;**	**1/2**
2^+, 1	**1586**	**$3/2^+$, 1/2**	**0**	**4783**	**$1/2^+$ - $7/2^+$;**	**1/2**
7^+, 0	**616**	**$3/2^+$, 1/2**	**0**	**7264**	**$11/2^+$ - $17/2^+$;**	**1/2**
0^+, 1	**0**	**$1/2^+$, 1/2**	**1417**	**4614**	**$1/2^+$;**	**1/2**
2^+, 1	**1586**	**$1/2^+$, 1/2**	**1417**	**6200**	**$3/2^+$ - $5/2^+$;**	**1/2**

Table 2

Deformed intrinsic states of ^{39}K

Nilsson model configuration of the last 7 nucleons

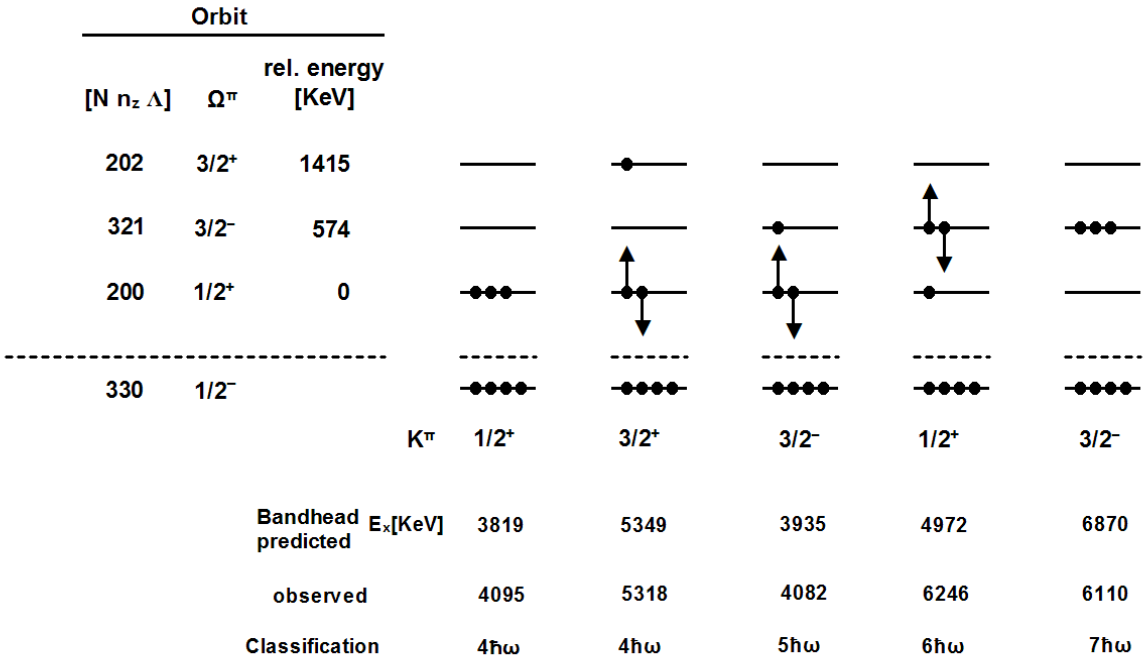

Table 3

^{39}K, positive parity - states

0 ħω		0	$3/2^+$		Theory
		2522	$1/2^+$		
		6356	$5/2^+$		
2 ħω	$3/2^+ \otimes 0^+,1$	3938	$3/2^+$		3197
	$1/2^+ \otimes 0^+,1$	4475	$1/2^+$	*	4614
	$3/2^+ \otimes 2^+,1$	5173[a)]	$1/2^+$		
		4930	$3/2^+$	Centroid 5556	4783
		5262	$5/2^+$		
		6186	$7/2^+$	*	
	$1/2^+ \otimes 2^+,1$	5711	$3/2^+$	Centroid 5846	6200
		5937	$5/2^+$		
	$3/2^+ \otimes 7^+,0$	(6192	$11/2^+$)	*	
		6434	$13/2^+$	Centroid 6800	7264
		6475	$15/2^+$		
		7776	$17/2^+$		
4 ħω	$K^\pi = 1/2^+$	4095	$1/2^+$		
		4514	$3/2^+$	*	
		4738	$5/2^+$		
		5788	$7/2^+$	*	
	$K^\pi = 3/2^+$	5318	$3/2^+$		
		5597	$5/2^+$		
		6042	$7/2^+$	*	
6 ħω	$K^\pi = 1/2^+$	6246	$1/2^+$		
		6331	$3/2^+$		

a) Member of a doublet

* J^π from Table 5

All level energies in KeV

Table 4

^{39}K, negative parity - states

1ħω			3ħω			5ħω $K^\pi = 3/2^-$		7ħω $K^\pi = 3/2^-$	
Shell model		exp.		exp.	theor.				
J^π	E_x	E_x	J^π			J^π	exp.	J^π	exp.
$7/2^-$	3028	2814							
$11/2^-$	4132	3944							
$9/2^-$	4183	3597							
$3/2^-$	4270	3019				$3/2^-$	4082		
$5/2^-$	4528	3883				$5/2^-$	4475 Doublet		
$7/2^-$	4623	5009	$7/2^-$	4126	4912	$7/2^-$	4678		
$9/2^-$	4790	4520				$9/2^-$	5166*		
$3/2^-$	5120	5826	$3/2^-$	5011*	6090				
$7/2^-$	5371	5501							
$7/2^-$	5425	5643							
$5/2^-$	5508	4737*							
$11/2^-$	5541	5354	$11/2^-$	5801*	6804	$11/2^-$	6005		
$13/2^-$	5613	5718							
$9/2^-$	5669	5164							
$7/2^-$	6010	5891							
$9/2^-$	6010	6396*							
$5/2^-$	6206	6093*							
								$3/2^-$	6110
			$9/2^-$	6247*	6795	and			
				and		$13/2^{(-)}$	7092		
			$15/2^-$	7141	7179	$15/2^-$	8008		
			$19/2^-$	8028	8035	$17/2^-$	?		
						$19/2^-$	10264		
						$21/2^-$	?		
						$23/2^-$	13009		
						$25/2^-$	?		
						$27/2^-$	16137		

J^π from Table 5

All level energies in KeV

Table 5 **Energy levels of ^{39}K**

E_x [KeV]	2 J$^\pi$ compilation	present	E_x [KeV]	2 J$^\pi$ compilation	present
0	3^+		5354	11^-	
2522	1^+		5501	7^-	
2814	7^-		5598	5^+	
3019	3^-		5643	7^-	
3597	9^-		5711	3^+	
3883	5^-		5718	13^-	
3938	3^+		5788	$(5, 7)^+$	7^+
3944	11^-		5801	7^-	11^-
4082	3^-		5826	$1^-, 3^-$	3^-
4095	1^+		5891	7^-	
4126	7^-		5938	5^+	
4475	$1^-, 3^-$	5^- plus 1^+	6005	11^-	
4514	5^+	3^+	6042	$(1 - 7)^+$	7^+
4520	9^-		6093	$(5, 7)^-$	5^-
4678	7^-		6110	$(1, 3)^-$	3^-
4737	$(5 - 9)^-$	5^-	6186	$(1^+ - 7^+)$	7^+
4738	5^+		6192	$(7^- - 13^-)$	11^+
4930	3^+		6246	1^+	
5009	7^-		6247	(5 - 9)	9^-
5011	$3, 5^-, 7^-$	3^-	6331		
5164	9^-		6356	5^+	
5166	$(5 - 9)^-$	9^-		^{38}Ar + p 6.38 MeV	
5173	decay to 3_1^+	1^+	6396	decay to 7_1^-, 7_2^-	9^-
5262	5^+		7092	$9, 13^+$	13^-?
5318	3^+				

10. Assessment of the ^{39}K level scheme

Table 5 (p. 255) gives the energy levels of ^{39}K and their assignments of J^{π} (isospin T = 1/2 is default) as compiled by P. M. Endt *[4, 5]* and the corrections which we introduce here.

The 4475 KeV level must be a doublet containing the $5/2^-$ member of the rotational band of Fig. 1. Gamma decay to the first $3/2^-$ level is compatible with the assumption but a competing decay to $1/2_1^+$ is at odds indicating doublet character of the state. Indeed it is inevitable that two hitherto unidentified $1/2^+$ states exist around this energy with weak-coupling configurations $1/2^+_h \otimes (0^+, T = 1)_p$ and $3/2^+_h \otimes (2^+, T = 1)_p$. We identify these states with the second member of the 4475 KeV multiplet and the 5173 KeV level of hitherto unknown J^{π}.

The reported $5/2^+$ assignment to the 4514 KeV level is connected with an unusually large, $\delta = 1 \pm 0.2$, mixing ratio of the principal γ-decay mode. The conclusion is drawn from a measurement of γ-ray angular distributions in the ^{36}Ar(α, p γ) reaction. For low spin the alignment coefficients α_2 and α_4 are not really predictable and α_4 is not even known in sign. Hence we feel justified to replace the unusual J^{π}, δ combination by the more conventional combination $J^{\pi} = 3/2^+$, δ around zero.

The 5801 KeV level has $J^{\pi} = 7/2^-$ but $11/2^-$ is excluded only because of a short lifetime of the state. This value is, however, controversial since the ^{36}Ar(α, p γ) reaction yields $\tau = 20 \pm 10$ fs while the ^{39}K(p, p' γ) reaction yields $\tau > 750$ fs. Hence we feel free to adopt an $11/2^-$ assignment, not only because such a state is needed, but also to avoid an undue proliferation of $7/2^-$ states.

The remaining J^{π} assignments of our own are all compatible with Endt's restrictions and theoretical predictions. Note especially that the assignment of

$11/2^+$ to the 6192 KeV level is justified though the level decays exclusively to π = - states. There are no final π = + levels of suitable spin available.
Last not least a level at 7092 KeV has $J^\pi = 9/2, 13/2^+$. The parity assignment rests on a measurement of a γ-ray polarisation, a difficult business. This level would perfectly fit (Fig. 1) into a negative-parity band, maybe wishful thinking.

Fig. 1

^{39}K $K^\pi = 3/2^-$ 5 ħω band

$\hbar^2/2\Theta$ = 62.8 KeV

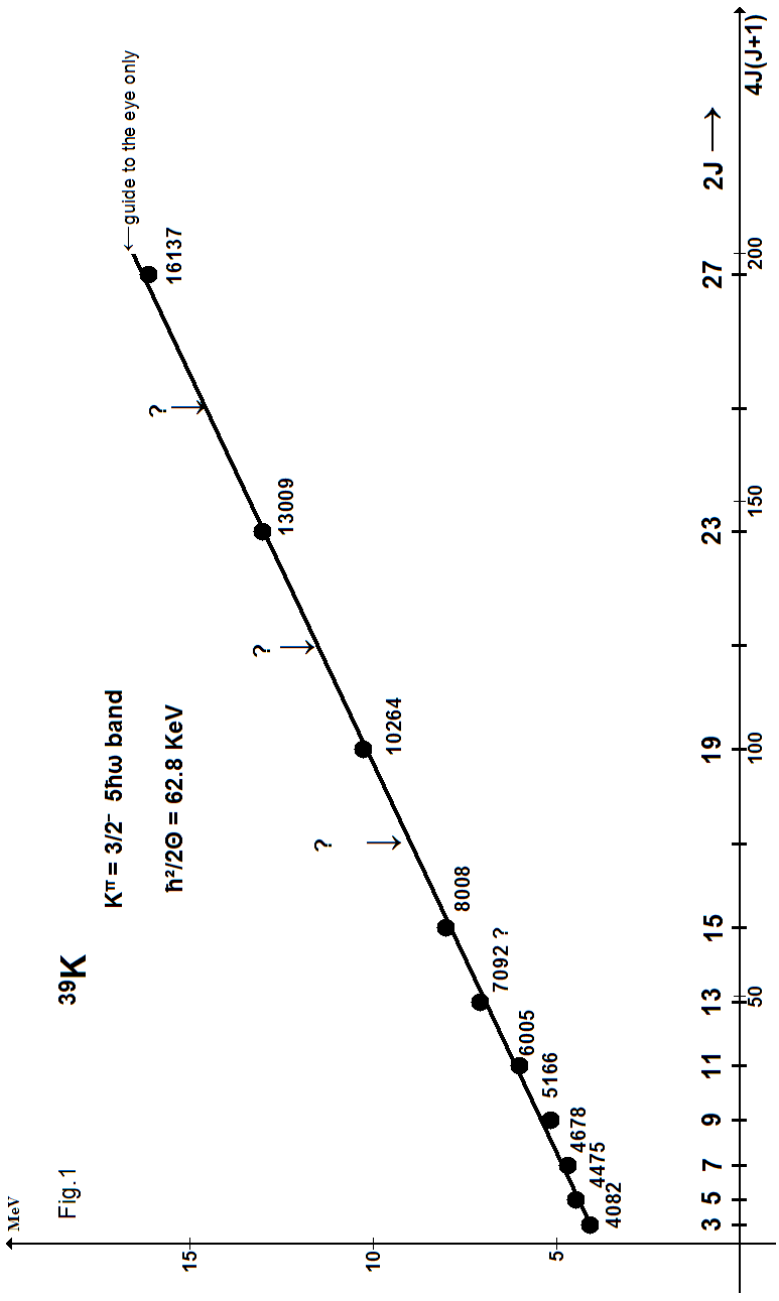

11. The structure of ^{40}Ca

A complete interpretation of the ^{40}Ca level scheme is possible up to 8439 KeV excitation energy and for the known J ≥ 6 levels above. The models employed are shell model calculations of 1 ħω excitations, performed by Warburton *[6]* in the untruncated space of the N = 2 + 3 major shells, and weak-coupling calculations of 2 ħω and 3 ħω excitations with parameters derived by ourselves for an interpretation of the A = 38 system. Nilsson model calculations with residual interaction in the parametrisation of Brink and Kerman *[8]* are used to describe the (5 - 8) ħω excitations. The parameters (Tables 1, 2) are derived from the energy levels of A = 36 - 48 nuclei.

To begin with we complete the experimental level scheme of Endt's compilation *[4]* and the more recent work on high-spin states by Ideguchi et al. *[17]*. The results are given in Table 3. Here we have made use of the strong retardation of E1 decay between T = 0 states in self-conjugate nuclei, which can either be supported or counteracted by the statistical factor E_γ^3. Thus for π = + states the forbiddeness of E1 decay is supported with the consequence that observably strong γ-decay leads to π = + final states only. The only exception occurs for J = 1 because the large energy of ground state decay enables an E1 character. Levels of negative parity can decay to final states of either parity but, with exception of $J^\pi = 1^-$, γ-decay to a final state of negative parity must have been observed.

In the following we give an interpretation of the first 59 levels up to and including the 8439 KeV state and of another 28 levels above. We start with the positive-parity states as they are listed in Fig. 1 and classified as 2, 4, 6, 8 ħω excitations. Spherical shape is assumed only for the 2 ħω excitations (and the 0 ħω g.st.). In principle we follow the paths of Gerace and Green *[16]* who interpreted the first five $J^\pi = 0^+$ states. In detail there are many changes and considerable extensions.

The 2 ħω states arise from weak-coupling of T‘ = 1 particle states in ^{42}Ca and T“ = 1 hole states in ^{38}Ca. Thus every level occurs three times with T = 0, 1, 2 and excitation energies which increase with T(T+1). The J^{π} values of the lowest lying states are, for every T : 0^+, 2_1^+, 2_2^+ with relative excitation energies of 0, 1.52, 2.17 MeV. The isospin triplets for $J^{\pi} = 2_1^+$ and 2_2^+ can be identified by combining information from ^{40}Ca, ^{40}K and ^{40}Ar. (See separate notes for ^{40}K and ^{40}Ar).

We obtain the following excitation energies [KeV] in ^{40}Ca

	$J^{\pi} = 2_1^+$	**$J^{\pi} = 2_2^+$**	**$J^{\pi} = 0^+$**
T = 0	7872	8091	?
T = 1	9564	10234 (7569 + 2575)	8018
T = 2	13449 (11988 + 1461)	15196 (11988 + 3208)	11988

Here we have assigned T = 1 character to the established 8018 KeV state of ^{40}Ca because Warburton‘s shell model calculations of ^{40}K predict a low lying 0^+ state at 717 KeV which is missing experimentally. The 8018 KeV state of ^{40}Ca could correspond to a ^{40}K level around 360 KeV. It could show E3 decay with an estimated lifetime of 10^{-2} s, almost an isomeric state. (Previously we had suggested *[9]* that the missing ^{40}K state be buried in the ^{39}K(d, p) reaction under the level at 800 KeV).

Fig. 2 shows a convincing energy dependence according to T(T+1) for the 2_1^+ and 2_2^+ states. If the same were true for the 0^+ level we would get an excitation energy of 6.1 MeV for this state. The experimental value of the 7301 KeV state, the only available one (Fig. 1), deviates considerably from expectation which must be attributed (see Gerace and Green) *[16]* to mixing with the 0 ħω ground state. The 2 ħω wave function component in the ground state must range in the 30% region (It would be highly interesting to compare with Gerace and Green, but we don‘t have the paper available). The 2 ħω

component of the g.st. is in turn responsible for the observed ground state decay of the 7872 and 8091 KeV, $J^{\pi} = 2^{+}$ states of the 2 ħω configuration. (The γ-decay of pure n ħω configurations has the selection rule $\Delta n = 0, \pm 1$ so that parity conserving decay proceeds within the same configuration only.)
The 7301 KeV, $J^{\pi} = 0^{+}$ level must seek another way of γ-decay (no $0 \rightarrow 0$ transitions). It mixes with the 7815 KeV level (a 4 ħω state) as suggested by an identical γ-decay to the 5249, $J^{\pi} = 2^{+}$ KeV state. The small energetic difference of the 7301 KeV and 7815 KeV levels even suggests that the unperturbed levels occur both around 7.5 MeV. This also explains the small energetic distance of the 7815 KeV level to the 7977 KeV level in Fig. 1.
The 7301 KeV, 2(+ 4) ħω state has an additional decay mode to the 5629 KeV, 2^{+} state which is small on absolute scale (5%) but significant on the scale of reduced E2 transition rates (5 W. u. for $0^{+} \rightarrow 2^{+}$ or 1 W. u. for $2^{+} \rightarrow 0^{+}$). The residual interaction, a two-body operator, has the selection rule $\Delta n = 0, \pm 2$ and henceforth it is impossible to assign an 8 ħω character to the 5629 KeV, 2^{+} state while 6(+ 4) ħω is possible. Previously in 2004 *[9]* we had assumed an 8 ħω character because of the reported quadrupole deformation $\varepsilon = 0.56 \pm 0.09$ of the well established $K^{\pi} = 0_2^{+}$ band. Today we have found the way of generating (Tables 1, 2) a low lying $K^{\pi} = 0_2^{+}$ band with 6 ħω configuration. The long-sought *[15]* $K^{\pi} = 0^{+}$ band with 8 ħω configuration is now easy to localize. The bandhead has no decay mode (even E1 decay to 7 ħω is energetically impossible) other than to the 5629 KeV level via mixing with the 6 ħω configuration. Thus we have exactly two candidates in Fig.1 at 8439 KeV and 8276 KeV. Our choice of the 8276 KeV level is arbitrary and probably the mixing of 6 ħω and 8 ħω configurations ranges around 50 : 50 due to the small energetic differences of the levels. The 6 ħω configuration gives rise to still another band, the $K^{\pi} = 2_3^{+}$ band of Fig.1 as suggested by the indicated γ-decay within the configuration.

All bands of Fig. 1 which have not been mentioned yet have, by the principle of exclusion, a 4 ħω character. This was already well established for the $K^\pi = 0_1^+$ and $K^\pi = 2_1^+$ bands. There are reasons to believe that the $K^\pi = 2_1^+$ band is generated by exciting a 1 phonon γ-vibration of the $K^\pi = 0_1^+$ band. Is it an accident that the energetic separation of roughly 2 MeV is observed once more in the case of the $K^\pi = 0_2^+$ and $K^\pi = 2_2^+$ bands of Fig. 1 which are certainly characterized by a larger deformation ($\varepsilon = 0.56 \pm 0.09$ versus $\varepsilon = 0.26 \pm 0.04$)?

Possibly we have a general instability of quadrupole deformation against the γ-degree of deformation or, in other language, triaxiality.

A Nilsson model interpretation of the positive parity bands in ^{40}Ca is possible (Table 4) using the Hamiltonian of Table 1, 2. It is assumed that four particles have to be distributed over three orbits. The occupation numbers are

4, 0, 0; 3, 1, 0; 2, 2, 0 and also 2, 1, 1

T‘=1 T“=1 T‘=1 T“=1

The last distribution becomes very important later, when negative-parity bands are discussed. The distributions with T‘ = T“ = 0 are not playing a role for $E_x < 10$ MeV. The same holds for $K^\pi = 1^+$ bands with 3, 1, 0 distribution which are pushed up in order to bring the alternative $K^\pi = 2^+$ band down.

The comparison with experiment is performed in Table 4. All predictable bands are present and the bandhead excitation energies which were not used for fixing the parameters of the Hamiltonian are in good agreement. For rotational bands which have an observed T = 1 and/or T = 2 version see notes on ^{40}K and ^{40}Ar (p. 273, p. 280).

The rotation-aligned band of Fig. 1 which is displayed in full size in Fig. 3 does also find an explanation in Table 4. The phenomenon of rotation alignment, which is well investigated in heavier nuclei, is connected with small

deformation and presence of large-j components in the Nilsson wave functions of valence nucleons. For light nuclei $f_{7/2}$ is large-j.
Small deformation arises from core-breaking. The promotion of a K‘, T‘ = 0,1 pair of particles from the strongly deformation driving $\Omega^{\pi} = 1/2^{-}$ into the less deformation driving $\Omega^{\pi} = 3/2^{-}$ orbit (Table 4) triggers rotation alignment. A promotion to the $\Omega^{\pi} = 3/2^{+}$ orbit would bring us back to the spherical 2 ħω states.

Now we turn to the interpretation of negative-parity states. They are made up of spherical 1 ħω and 3 ħω excitations and deformed 5 ħω excitations. Deformed 7 ħω excitations are certainly present, however above $E_x = 9$ MeV (so that the lowest 8 ħω state has no chance of E1 decay!). This can be deduced from the Nilsson model Hamiltonian of Tables 1, 2.
In Fig. 4 we interpret the spectrum of negative parity states. The 1 ħω states are predicted by the shell model calculations of Warburton *[6]*. The theoretical spectrum has a gap between $E_x = 8.5$ MeV and 10 MeV. Hence we are sure to have located all experimental 1 ħω states up to 8.5 MeV. The 8359 KeV, 0^{-} state shows exclusive decay to the 6950 KeV, 1^{-} state, but not to the 5903 KeV, 1^{-} state. The latter state is thus not member of the1 ħω configuration nor of the 3 ħω configuration, as detailed immediately.
The 3 ħω spectrum is generated by coupling the ^{37}Ca, $J^{\pi} = 3/2^{+}$ ground state successively to the $7/2^{-}$, $5/2^{-}$, $3/2^{-}$states of ^{43}Ca which have $E_x = 0$ KeV, 372 KeV, 593 KeV. This generates multiplets with $J^{\pi} = (2 - 5)^{-}$, $(1 - 4)^{-}$, $(0 - 3)^{-}$. The preference of the $t_p = t_h = 3/2$ over the $t_p = t_h = 1/2$ coupling was derived in A = 38 and amounts here to roughly 800 KeV. In Fig. 4 we see the 4^{-} and 3^{-} members of the first quartet and have available two levels at 8051 KeV and 8196 KeV of which we know nothing but their existence. Also observed is the 1^{-} member of the second quartet.

Another 13 levels must find an explanation as deformed 5 ħω states. A big stumbling block was the 5903 KeV, 1^- state. For almost 50 years it was considered *[15]* as a $K^\pi = 1^-$ state with a 3 ħω configuration. In 2004 we tried to improve the situation (no deformations for 3 ħω) by assigning a 5 ħω character, using a new ordering of Nilsson levels, but maintaining a $K^\pi = 1^-$ assignment.

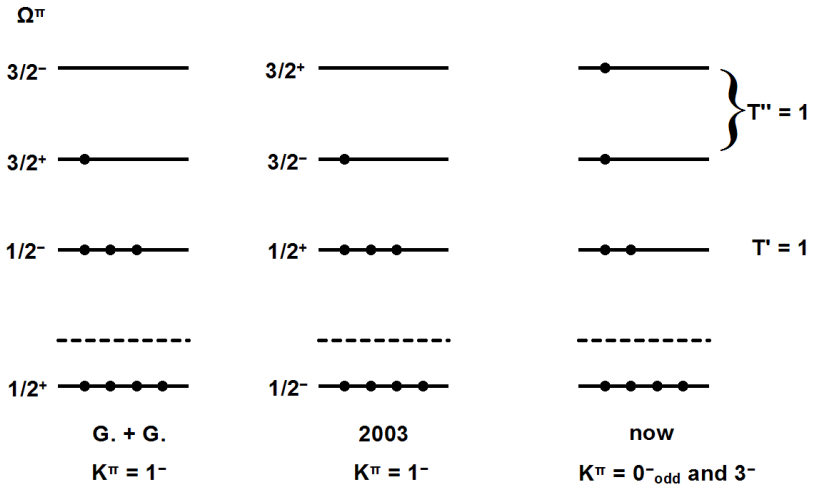

The present interpretation was not obvious and emerged after finding $K^\pi = 0^-_{odd}$ bands in ^{42}Ca, ^{40}Ar and ^{38}Ar and $K^\pi = 3^-$ bands in ^{38}Ar and ^{42}Ca (In ^{40}Ar $K^\pi = 3^-$ is probably too high to be located). Also an improved version of our Nilsson model Hamiltonian was able to explain the low excitation energy of the $K^\pi = 0^-_{odd}$ band. The complicated Nilsson model configuration is, last not least, confirmed by the existence of a T = 2 version in ^{40}Ar which is not possible otherwise. The remaining bands of Fig. 4 are straightforward to obtain. Fig. 5 demonstrates the fulfillment of the J(J+1) rule. The rotational constants $\hbar^2/2\Theta$ are also close to the situation in ^{38}Ar.

The interpretation of negative-parity states in ^{40}Ca seems to be very firm now. It is a different question whether we have observed here a complete set of one - octupole - phonon excitations of a deformed nucleus. We have discussed this possibility already (p. 208) separately. Here we compare the experimental results with the prediction of our version of the Nilsson model (Table 5). Certainly we have found the basic structure underlying the bands but there is room for improvement for the $K^\pi = 0^-_{odd}$ and 3^- bands of ^{40}Ca.

Table 1

Binding energies and interaction energies of nucleons in identical Nilsson orbits

Orbit			Neutron/Proton Binding energy [KeV]			Interaction energy [KeV]				
Ω^{π}	$[N\ n_z\ \Lambda]$		$E^{n}_{B,i}$	$E^{p}_{B,i}$		S_i	A_i	B_i	C_i	E_i
$1/2^{+}$	200		−9176	−2386		−13636	−3177	−3438	−2800	439
$3/2^{-}$	321		−8602	−2028		−10547	−2611	≈ −2260	−2490	422
$3/2^{+}$	202		−7761	−1187		−14635	−2322	≈ −2000	−4053	569

The interaction energy of two nucleons is A_i, B_i, C_i for K, T = 0, 1; 0, 0; 2Ω, 0. To be added, if necessary, is the Coulomb energy E_i. A quartet has the energy $S_i = (3\ A_i + B_i + 2\ C_i)$. Three nucleons have energy $1/2\ S_i$. The binding energies are calculated relative to the 4329 KeV level of ^{36}Ar.

Table 2

Parameters for the interaction

of nucleons in different Nilsson orbits for A = 38 - 48

Orbit i			Orbit k			Energies [KeV]				
Ω^{π}_i	$[N\ n_z\ \Lambda]_i$		Ω^{π}_k	$[N\ n_z\ \Lambda]_k$		a_{ik}	b_{ik}	c_{ik}	d_{ik}	e_{ik}
$3/2^+$	202		$1/2^+$	200		−257	−765	724	−765	294
$3/2^-$	321		$1/2^+$	200		−193	150	900	−100	328
$3/2^-$	321		$3/2^+$	202		−384	−415	706	−282	360

The nuclear part of the interaction between n_i nucleons in orbit i coupled to projection quantum number Ω_i and Isospin T_i with n_k nucleons in orbit k, having Ω_k, T_k is given as

$$V_{ik} = a_{ik}\ n_i \bullet n_k + b_{ik}\ P_i \bullet P_k + 4\ c_{ik}\ \vec{T}_i \bullet \vec{T}_k + 4\ d_{ik}\ \vec{Q}_i \bullet \vec{Q}_k$$

The quantity e_{ik} yields the coulomb interaction of two protons.
P_i and P_k are the added normalized angular momentum projections $\Omega_\alpha / |\Omega_\alpha|$ for orbit i or k.

$\vec{Q}_i$ and $\vec{Q}_k$ are the added values of $\Omega_\alpha / |\Omega_\alpha| \bullet \vec{t}_\alpha$. This term does not contribute, if either n_i or n_k is even, it behaves like $\vec{T}_i \bullet \vec{T}_k$ if $n_i = n_k = 1$ or 3 and changes sign if $n_i = 1$ (or 3) and $n_k = 3$(or 1).

Table 3

New J^{π} assignments to ^{40}Ca levels

E_x[KeV]	J^{π}		comment
	Endt	**present**	
(6422)	(2^+)		discarded
6931	3^-, 4^+	3^-	→ 3^-, 5^-, 4^- and 2^+(enabled by τ = 2 ps)
(6938)			discarded
7239	3^- - 5^-	5^- (4^-)	→ 3^-, 4^-, 5^-
7278	2^+, 3^+	3^-	→ 3^-, l = 2 from p, p' is then l = 3
7422		4^-	→ 3^- (100%)
7446	$(3,4)^+$	3^-	→ 2^+, 4^+ but also 4^-!! } Mixed 1ħω and 3ħω states a) b)
7623	2^- - 4^+	3^-	→ 2^+, 3^-, 4^-
7769	3 - 5^-	5^- (4^-)	→ 4^-, 3^-
8051			
8113	1	1^-	Theory does not yield a 1^+ state below 9.5 MeV
8134	2 - 4^+	3^+	→ 2^+ with low energy
8187	3 - 5^-	3^-	→ 3^- (100%)
8195			
8271	$(0 – 3)^-$	1^-	→ 1^-, 2^-
8323	1^-, 2^+	2^-	Mixing with 2^-, T = 1
8338	2^+ - 5^-	6^+	New data, Heavy ion reaction
8359	$(0\text{-}2)^-$	(0^-)	→ 1^- (100%), Decay within 1 ħω space!
.			
.			
.			
8764	3^-	4^+	→ 2^+, 3^+, 4^+ L = 3 in (p,t) is probably L = 4
8678	4^+	5^- (3^-)	→ 4^-, 3^- L = 4 in (p,t) is probably L = 3
			Later on 5^- K = 2 → 3^- K = 0

a) The 7623 KeV state has in addition an admixture of 5% at maximum from the 7694 KeV, 3^-, T = 1 state, inducing the decay to 3_1^-, T = 0.

b) It should be checked how the 7446 KeV → 5279 KeV, 3^- → 4^+ transition has entered the compilation.

Table 4

Nilsson model of π = + rotational bands in ^{40}Ca

The lowest lying T = 1 or, respectively, T = 2 states in ^{40}Ca occur at 7658 KeV and 11988 KeV

a) This level could be spherical, alternatively

Table 5

Negative - parity bands with T = 0, 1, 2 in, respectively, ^{40}Ca, ^{40}K and ^{40}Ar

Table 5

Negative - parity bands with T = 0, 1, 2 in, respectively, ^{40}Ca, ^{40}K and ^{40}Ar

K^{π}	0^-_{odd}	3^-	2^-	1^-	0^-_{even}
Bandhead E_x [KeV]					
^{40}Ca exp.	5903	6582	6750	7113	
^{40}Ca theor.	6385	7609	6872	7172	
^{40}K exp.	2290	3154	3128	2807	≈ 2800[c]
^{40}K theor.	1491[b]	2171	4499	3599	4630
^{40}Ar exp.	4300				
^{40}Ar theor.	3647[b]				
For comparison[a]					
^{38}Ar exp.	5734	5513	7431	6948	
^{38}Ar theor.	7188	7724	7933	7833	

a) the ^{38}Ar bands are generated by removing a K, T = 0, 1 pair from the $\Omega^{\pi} = 1/2^+$ orbit

b) Obtained by starting from the experimental T = 0 bandhead at 5903 KeV

c) Bandhead not observed. Value obtained from the 3229 KeV, 2^- state using the J(J+1) rule

Fig. 1

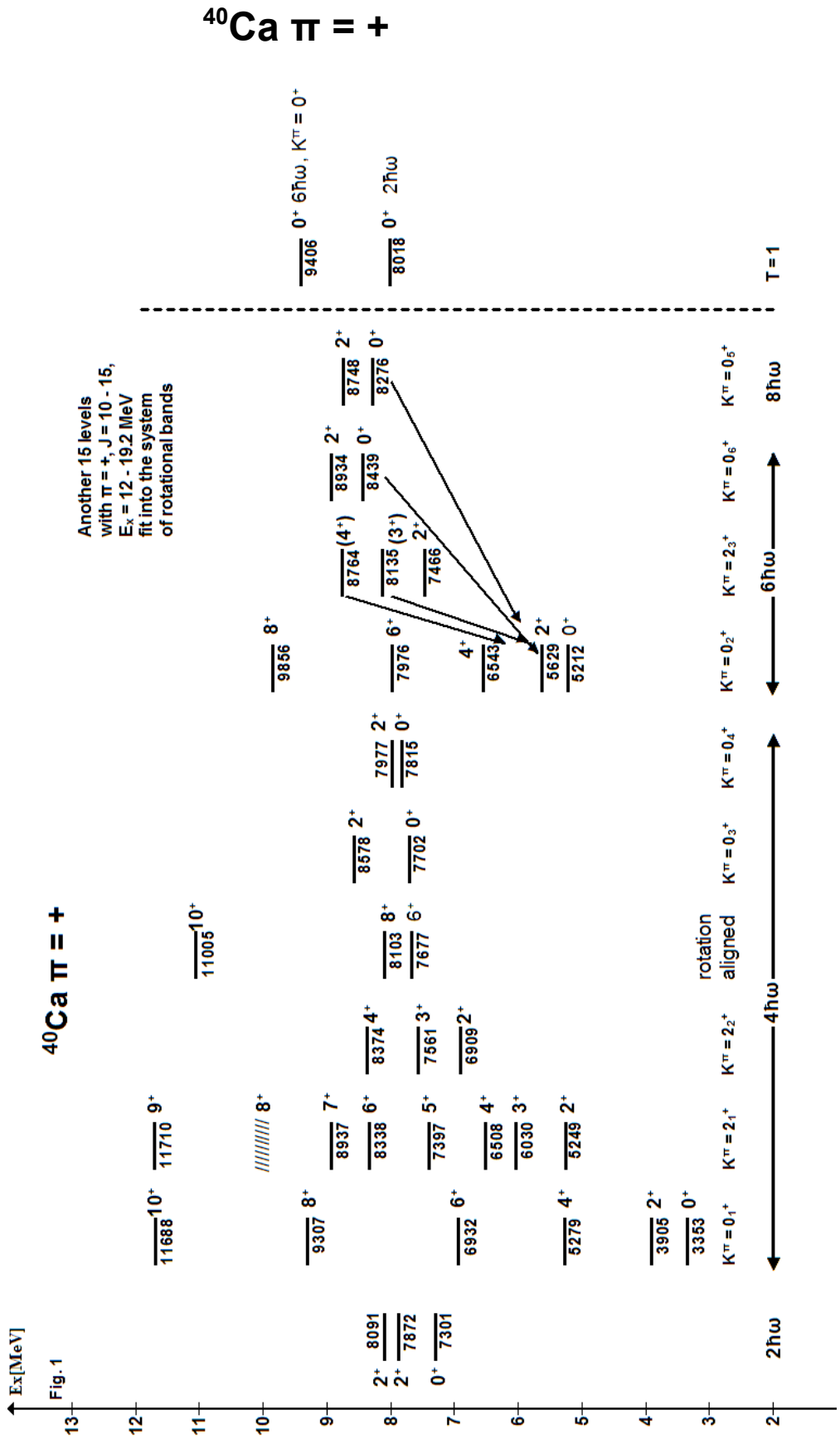
40Ca π = +
Another 15 levels
with π = +, J = 10 - 15,
Ex = 12 - 19.2 MeV
fit into the system
of rotational bands
0+ 6ħω, Kπ = 0+
0+ 2ħω
T = 1
8ħω
6ħω
4ħω
2ħω
rotation
aligned
Kπ = 01+
Kπ = 21+
Kπ = 22+
Kπ = 03+
Kπ = 04+
Kπ = 02+
Kπ = 23+
Kπ = 06+
Kπ = 05+
Ex[MeV]
Fig. 1

Fig. 2

The isospin dependence of E_x for 2 ħω states in ^{40}Ca

Numerical values on p. 259

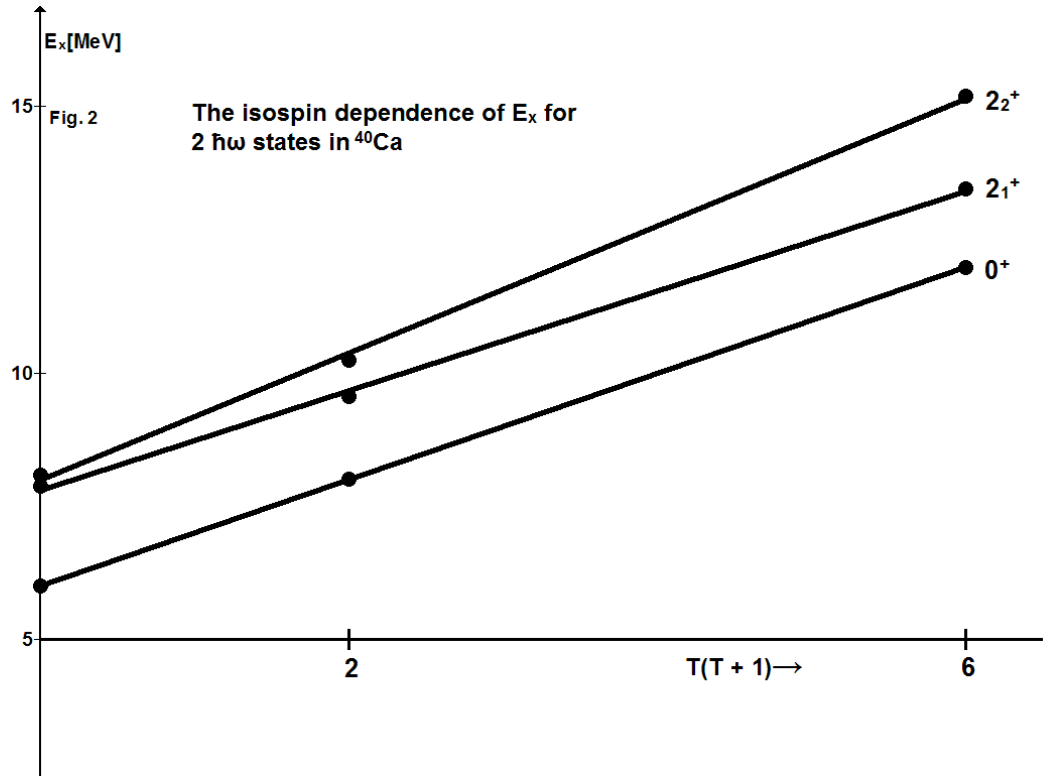

Fig. 3 **^{40}Ca rotation aligned band, deduced from *[17]***

The angular momentum of collective rotation is J – 6

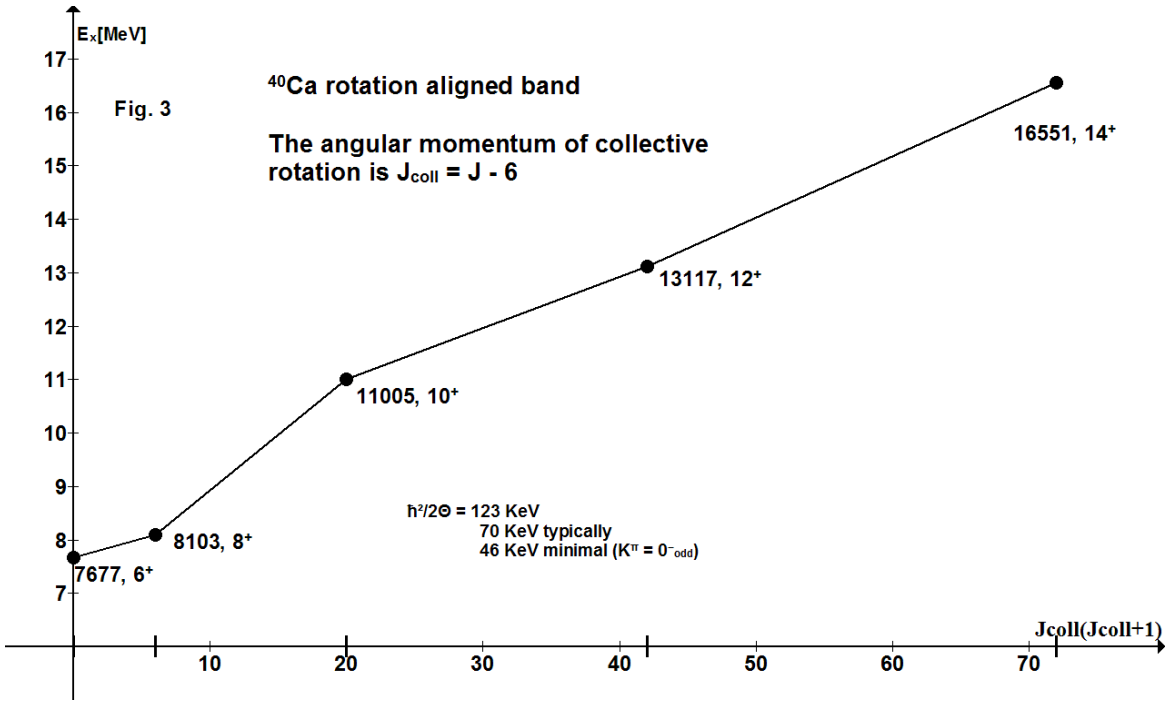

Fig. 4

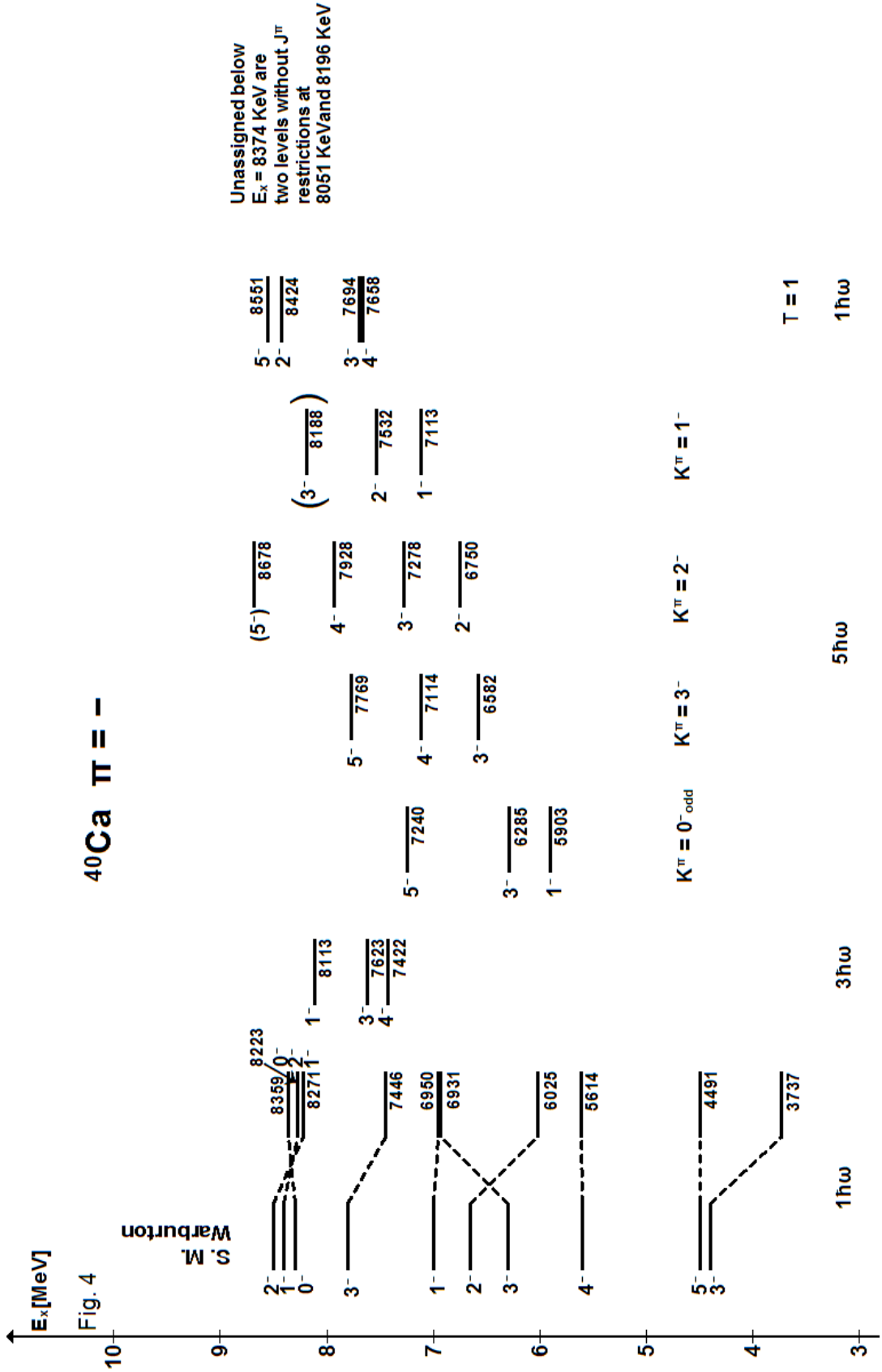
Fig. 4
S. M. Warburton
^{40}Ca π = −
E$_x$[MeV]
10
9
8
7
6
5
4
3
Unassigned below
E$_x$ = 8374 KeV are
two levels without Jπ
restrictions at
8051 KeVand 8196 KeV
T = 1
1ħω
3ħω
5ħω
Kπ = 0$^-_{odd}$
Kπ = 3$^-$
Kπ = 2$^-$
Kπ = 1$^-$
8223
8359
8271
8113
7623
7422
7446
6950
6931
6025
5614
4491
3737
7240
6285
5903
7769
7114
6582
8678
7928
7278
6750
8188
8551
8424
7694
7658
7532
7113

Fig. 5

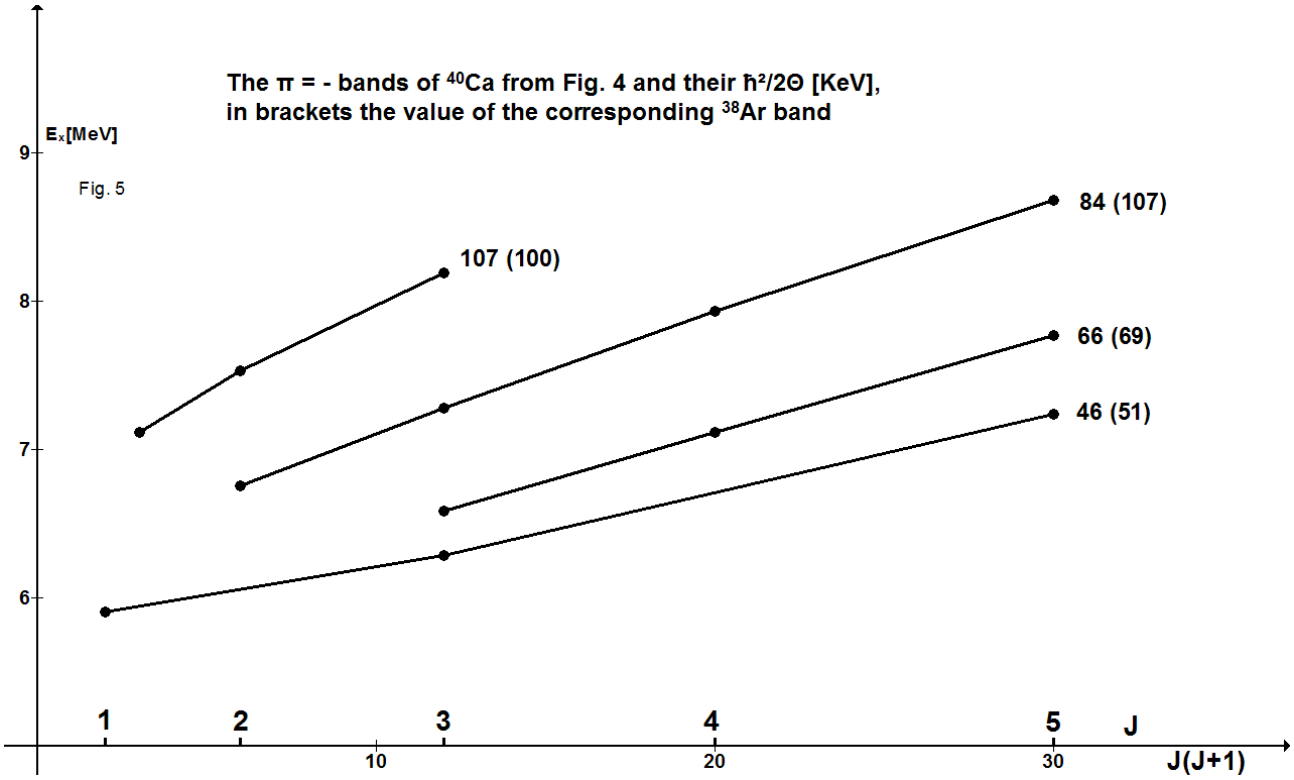
The π = - bands of 40Ca from Fig. 4 and their ħ²/2Θ [KeV],
in brackets the value of the corresponding 38Ar band
Ex[MeV]
Fig. 5
9
8
7
6
84 (107)
107 (100)
66 (69)
46 (51)
1
2
3
4
5
J
10
20
30
J(J+1)

12. The energy levels of ^{40}K for $E_x \leq 3869$ KeV

Endt‘s compilation *[4, 5]* lists 51 level, most of them having low - and frequently ambiguous - spin. However the spectrum of $J^\pi = 2^-$ is safer than all others and consists of 10 well established levels. We assume that this is the complete accounting, excluding $J^\pi = 2^-$ for other levels. (contrary to his statement Endt‘s $J^\pi = 2^-$ assignment to the 3869 KeV level is not safe, because natural parity is not excluded). As a first step we have critically reexamined the level scheme of Endt. The result is given in the following Table 1.
Our interpretation of the level begins with the 1 ħω and 2 ħω excitations of the ^{40}Ca ground state which are certainly spherical. They have been treated in Warburtons N = (2 + 3) shell model calculations *[6]*. The 1 ħω states were used to obtain parameters of the model. Hence we cite the underlying weak-coupling multiplets, instead, in Table 2. The 2 ħω spectrum was really predicted and showed a single flaw (Table 3). The first experimental 0^+ state was believed to occur at 1643 KeV, being high by one MeV. We had already (2004) reinterpreted this level as a deformed 6 ħω state. The true state was then believed to be hidden under the 800 KeV, first excited state. Today we have identified the analogue in ^{40}Ca at 8018 KeV corresponding to 360 ± 30 KeV in ^{40}K.
It was always clear that 1 ħω excitations alone cannot account for the spectrum of negative-parity states. The next series of states, 3 ħω excitations, were beyond Warburton‘s computational facilities, but the weak-coupling model (of $f_{7/2}$ particles and $d_{3/2}$ holes) proves to be very effective. There are two isospin coupling modes
$t_p = 3/2$ $t_h = 1/2$ yielding $J^\pi_{max} = 9^-$
$t_p = 1/2$ $t_h = 1/2$ yielding $J^\pi_{max} = 11^-$.

Our experience with ^{38}Ar tells us that we must consider the coupling of the first three ^{43}Ca states (J^{π} = 7/2^{-}, 5/2^{-}, 3/2^{-}) with the 3/2^{+} ground state of ^{37}K. Roughly one MeV above coupling of the 3/2^{+} g.st. of ^{37}Ar with the 7/2^{-} g.st. of ^{43}Sc should come into play. The presence of a 7472 KeV, J^{π} = 11^{-} state in ^{40}K suggests an onset of this coupling scheme at E_x = 3.3 MeV. The prediction agrees with experiment (Table 2).

There remains a set of 9 negative-parity states, proving the influence of deformed 5 ħω states. The T = 0 bands of ^{40}Ca with $J^{\pi} = 0^{-}_{odd}$, 1^{-}, 2^{-}, 3^{-} can also exist in the T = 1 mode and there is a fourth band for T = 1 only with Nilsson model configuration $K^{\pi} = 0^{-}$ even.

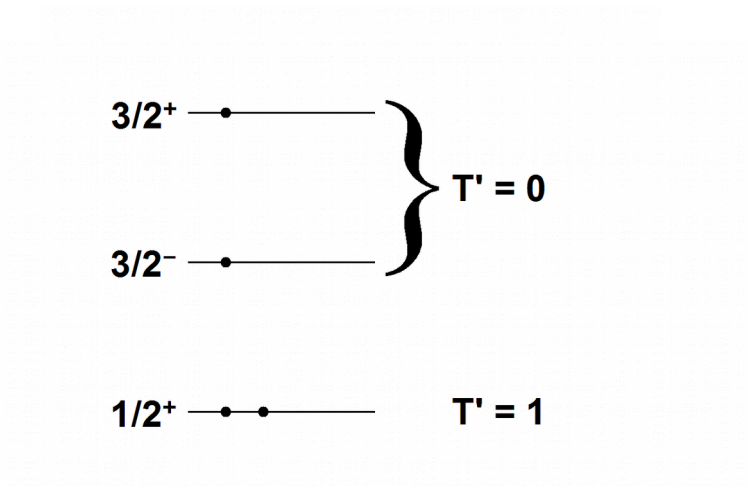

They account, together, for three $J^{\pi} = 2^{-}$ states which can even be depicted from the crowd of levels with equal J^{π}. Levels at 3028, 3128, 3229 KeV show decay to the 2290 KeV, $J^{\pi} = 1^{-}$ state. The latter state constitutes, quite evidently, the lowest lying 5 ħω state (with $J^{\pi} = 1^{-}$, $K^{\pi} = 0^{-}_{odd}$) as does the 5903 KeV state of ^{40}Ca for T = 0. With these corner stones and the J(J+1) rule we can establish the four bands of Table 2 except for a missing $J^{\pi} = 0^{-}$ state. The bandhead energies agree with expectation.

We have already touched the 1643 KeV, $J^{\pi} = 0^{+}$ state, believed to constitute the head of a $K^{\pi} = 0^{+}$ band of 6 ħω character. A $J^{\pi} = 4^{+}$, 5^{+} state is still available at 3100 KeV and could be the third band member, implying $\hbar^2/2\Theta$ = 73 KeV. This value appears very reasonable, placing the 2^{+} band member at 2154 KeV. The established pair of 2^{+} states at 1959 KeV and 2757 KeV are

believed to be mixed 2 ħω and 6 ħω states (though not by first order mechanism!).

The 4 ħω excitations play a marginal role because they result in $K^{\pi} = 0^{+}$, T = 0 excitations. The first T = 1 band, if there is any, will have $K^{\pi} = 1^{+}$ and occur at high energies. A 3821 KeV, 1^{+} state could agree with expectation. We would never have believed that the first fifty levels of ugly-looking ^{40}K can find a complete explanation, using proven concepts exclusively.

Table 1

^{40}K Critical version of Endt's 1990 compilation

E_x		J^{π}	Explanation
0		4_1^-	
30		3_1^-	
360	new	0_1^+	See p. 273, lifetime in the ms range expected
800		2_1^-	
891		5_1^-	
1643		0_2^+	
1959		2_1^+	
2047		2_2^-	
2070		3_2^-	
2104		1_1^-	
2260		3_1^+	
2290	}	1_2^-	π = + from l = 0 + 2. Could be a contaminated l = 1 transfer strong feeding in (n, γ) speaks for negative parity. J = 1 is safe
2291		3_3^-	
2397		4_2^-	
2419		2_3^-	
2542		7_1^+	
2576		2_2^+	
2626		0_1^-	
2730		1_1^+	π assumed by ourself
2746		3_4^-	2^- alternative excluded, proliferation of 2^- state
2757		2_3^+	

E_x		J^π	Explanation Table 1 cont'd
2786	}	3_5^-	J from (α, n γ). π = + from L = 4 in (α, d) not conclusive. There is no way of generating 3^+
2787		4_1^+	We trust in L = 4 from (α, d). 5^+ excluded by γ-decay. 3^+ excluded as above
2807		1_3^-	2^- alternatively excluded. proliferation of 2^- states
2879		6^+	
2951		5_2^-	Guess, based on 100% decay to 4_1^-. $J^\pi = 6^-$ has no theoretical foundation
2986		2_4^-	The alternative 3^+ assignment finds no theoretical foundation. Also feeding from J = 1
3028		2_5^-	
3100		4_2^+	The alternative 5^+ assignment is not completely excluded, but requires much fiddling
3110		1_2^+	2^+ would be possible
3128		2_6^-	
3146		1_4^-	π = − from analogue in ^{40}Ca
3154		3_6^-	2^- alternative excluded, no proliferation
3229		2_7^-	
3293		(4_3^-)	π = u, Absence in (n, γ), presence in (d, α) speak for higher spin. $J^\pi = 5^+, 6^-$ have no theoretical foundation
3368		3_7^-	2^- alternative excluded, no proliferation
3393		2_8^-	
3414		2_4^+	
3439		1_5^-	2^+ alternative implies E2 decay to 0^+
3448		5_1^+	3^+ remains a possibility
3486		2_9^-	
3557		$(3^-)_8$	$(1^- - 4^+)$
3599		2_{10}^-	
3630		3_9^-	
3663		4_3^+	3^+ remains a possibility
3717		0_2^-	$(0 - 3)^-$, but there are only a far chances for 0^-
3738		1_3^+	
3767		0_3^-	See 3717
3798		1_4^+	
3821		4_4^-	+ low spin (2^+?)
3840		1_5^+	Decay to both 0^+ and 2^+ speak against 1^- and 2^+
3869		3_{10}^-	2_{11}^- less likely

Table 2

The negative parity states of ^{40}K

1 ħω states								
$f_{7/2}^{1} \circledast d_{3/2}^{-1}$		$p_{3/2}^{1} \circledast d_{3/2}^{-1}$		$f_{7/2}^{1} \circledast s_{1/2}^{-1}$		$p_{3/2}^{1} \circledast s_{1/2}^{-1}$		
J^{π}	E_x [KeV]	J^{π}	E_x [KeV]	J^{π}	E_x [KeV]	J^{π}	E_x [KeV]	
2^-	800	0^-	2626	3^-	3869	1^-	(4221) ⟵ shell model prediction	
3^-	30	1^-	2104	4^-	3821	2^-	3486	
4^-	0	2^-	2047					
5^-	891	3^-	2070					

3 ħω states								
$T_p = 3/2, T_h = 1/2$						$T_p = 1/2, T_h = 1/2$		
$7/2^- \circledast 3/2^+$		$5/2^- \circledast 3/2^+$		$3/2^- \circledast 3/2^+$		$7/2^- \circledast 3/2^+$		
J^{π}	E_x [KeV]	J^{π}	E_x [KeV]	J^{π}	E_x [KeV]	J^{π}	E_x [KeV]	
2^-	2419	1^-	3146	0^-	(3717)	2^-	3599	
3^-	2291	2^-	2986	1^-	3439	3^-		
4^-	3397	3^-	2746	2^-	3393	4^-		
5^-	2951	4^-	3293	3^-	3630	5^-		

Table 2 cont'd

The negative parity states of ^{40}K

5 ħω states (rotational bands)									
$K^\pi = 0^-_{odd}$		**$K^\pi = 1^-$**		**$K^\pi = 2^-$**		**$K^\pi = 0^-_{even}$**		**$K^\pi = 3^-$**	
J^π	E_x [KeV]	J^π	E_x [KeV]	J^π	E_x [KeV]	J^π	E_x [KeV]	J^π	E_x [KeV]
1^-	2290	1^-	2807	2^-	3128	0^-	?	3^-	3154
3^-	2786	2^-	3028	3^-	3557	2^-	3229		
		3^-	3368						

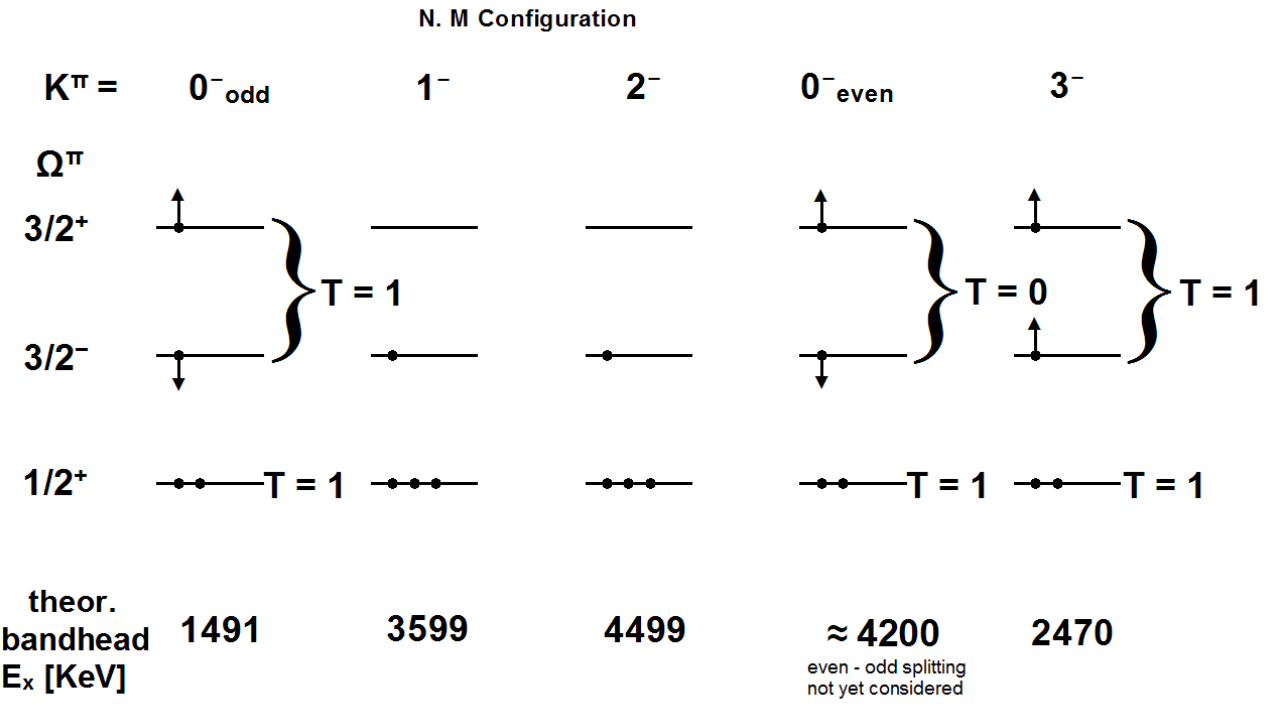

Table 3

The positive - parity states of ^{40}K

2 ħω states: shell model / experiment [KeV]

J^π	0^+	1^+	2^+	3^+	4^+	5^+	6^+	7^+
	717/360	2684/2730	1882/1959 ┐ 2576 ┘	2242/2260	2710/2787	3469/3448	3278/2879	3139/2542
	4820/	2970/3110		3486/	3799/3663	3764/	4178/	
		3290/3738	2762/2757	3961/	3858/			
		3621/3798	3315/3414					
		4307/	3830/3821					
			4378/					

6 ħω states: $K^\pi = 0^+$ theory/experiment [KeV]

J^π	0^+	1^+	2^+		3^+	4^+	5^+	6^+	7^+
	1154/1643		/ 1959 2576	} mixed		/ 3100			

4 ħω states: $K^\pi = 1^+$ theory/experiment [KeV]

J^π	0^+	1^+	2^+	3^+	4^+	5^+	6^+	7^+
		3731/3821						

13. The energy levels of ^{40}Ar

The T = 2 states of the A = 40 system can best be and have been investigated in ^{40}Ar *[3]*. In the following we characterize levels as either n ħω excitations of the ^{40}Ar g.st. or m_p - m_h excitations of the ^{40}Ca g.st.
The 0 ħω or 2p-2h spectrum is already rich and has been calculated by Warburton *[6]* in the untruncated space of the N = 2 + 3 major shells. In the left part of Fig. 3 it is compared with experiment. A 2 ħω or 4p-4h spectrum is absent in ^{40}Ar because it is confined to T = 0 states at our energies. The 4 ħω or 6p-6h configuration generates a $K^\pi = 0_1^+$ rotational band (Fig. 2) which has been observed at Freiburg in 1983 *[3]*. There are more positive-parity states outside the 0 ħω space around and it is possible to group them into a $K^\pi = 2^+$ and 0_2^+ band (Fig. 2). A level at 5654 KeV has the remarkable property of a 100% decay to the $J^\pi = 2^+$, $K^\pi = 0_1^+$ state. Possibly we have here the $J^\pi = 4^+$, $K^\pi = 0_2^+$ state.
The negative-parity states of the 1 ħω or 3p-3h configuration arise, within the framework of the weak-coupling model, from the isospin coupling schemes $T_p = 3/2$, $T_h = 1/2$ and $T_p = 1/2$, $T_h = 3/2$ with the first one being lower by 750 KeV. The third coupling scheme $T_p = T_h = 3/2$ is safely remote above 5.4 MeV in excitation. For each of the two important isospin coupling schemes we observe three members of the lowest lying, $7/2^- \otimes 3/2^+$, $J^\pi = (2 - 5)^-$ quartets while a $J^\pi = 1^-$ level at 4769 KeV belongs already to the next, $J^\pi = (1 - 4)^-$ quartet with $T_p = 3/2$, $T_h = 1/2$ expected 373 KeV above the first one.

The 3 ħω or 5p-5h spectrum should consist of rotational bands with $K^\pi = 0^-_{odd}$ and 3^-. These bands originate from known bands in ^{42}Ca by removal of a K‘, T‘ = 0, 1 pair of nucleons. In Fig. 1 we have identified the $K^\pi = 0^-_o$ band in

^{40}Ar by comparison with ^{42}Ca. Inband decay is observed between the 7^- and 5^- members.

The energetic spacing of the $K^\pi = 0_o^-$ and 3^- bands should be equal in ^{40}Ar and ^{42}Ca and also γ-decay should lead to corresponding states. Thus we can predict the $K^\pi = 3^-$ bandhead of ^{40}Ar at 4596 KeV and the decay should lead to the 2_1^+, 2_2^+, and 3_1^- states. The known 4929 KeV level, and only this level, meets both requirements. Equally we predict the second band member at 5724 KeV with γ-decay to 3_1^-. Again we have a suitable and sole candidate at 5675 KeV.

The theoretical understanding of the T = 2 rotational bands in A = 40 has already been given in Tables 4, 5 of our ^{40}Ca notes. We have exactly observed the bands which could be predicted by the applied Nilsson model Hamiltonian.

Rotational bands in ^{40}Ar

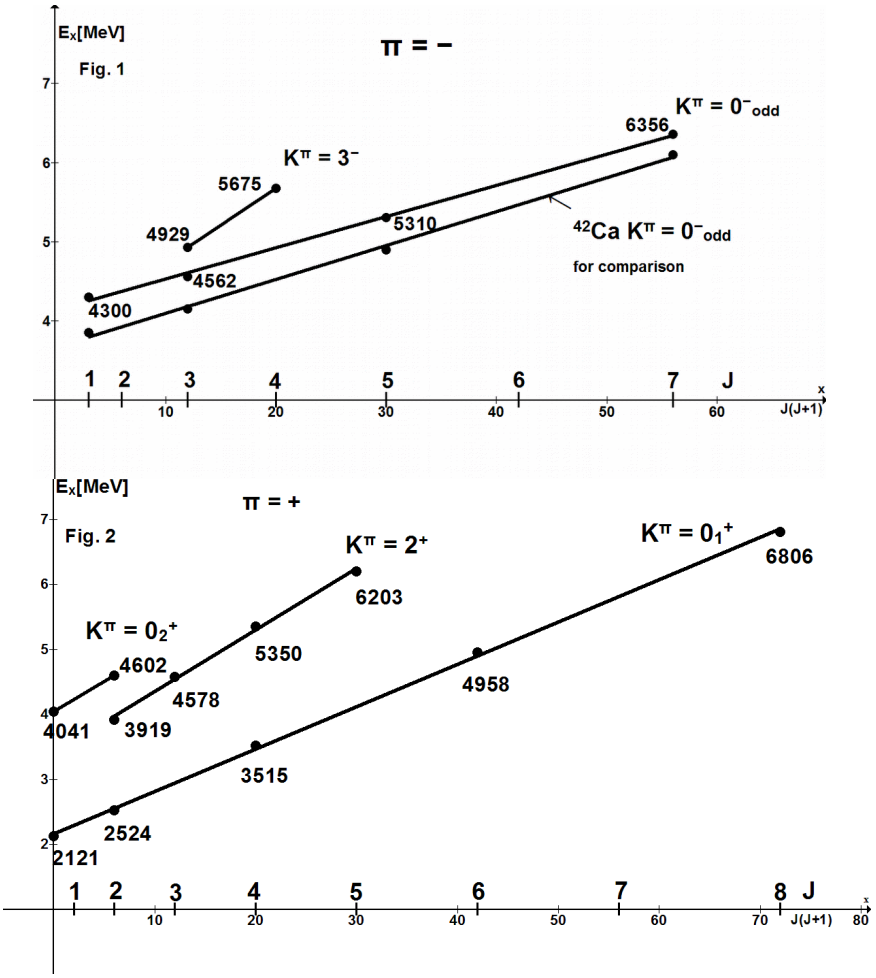

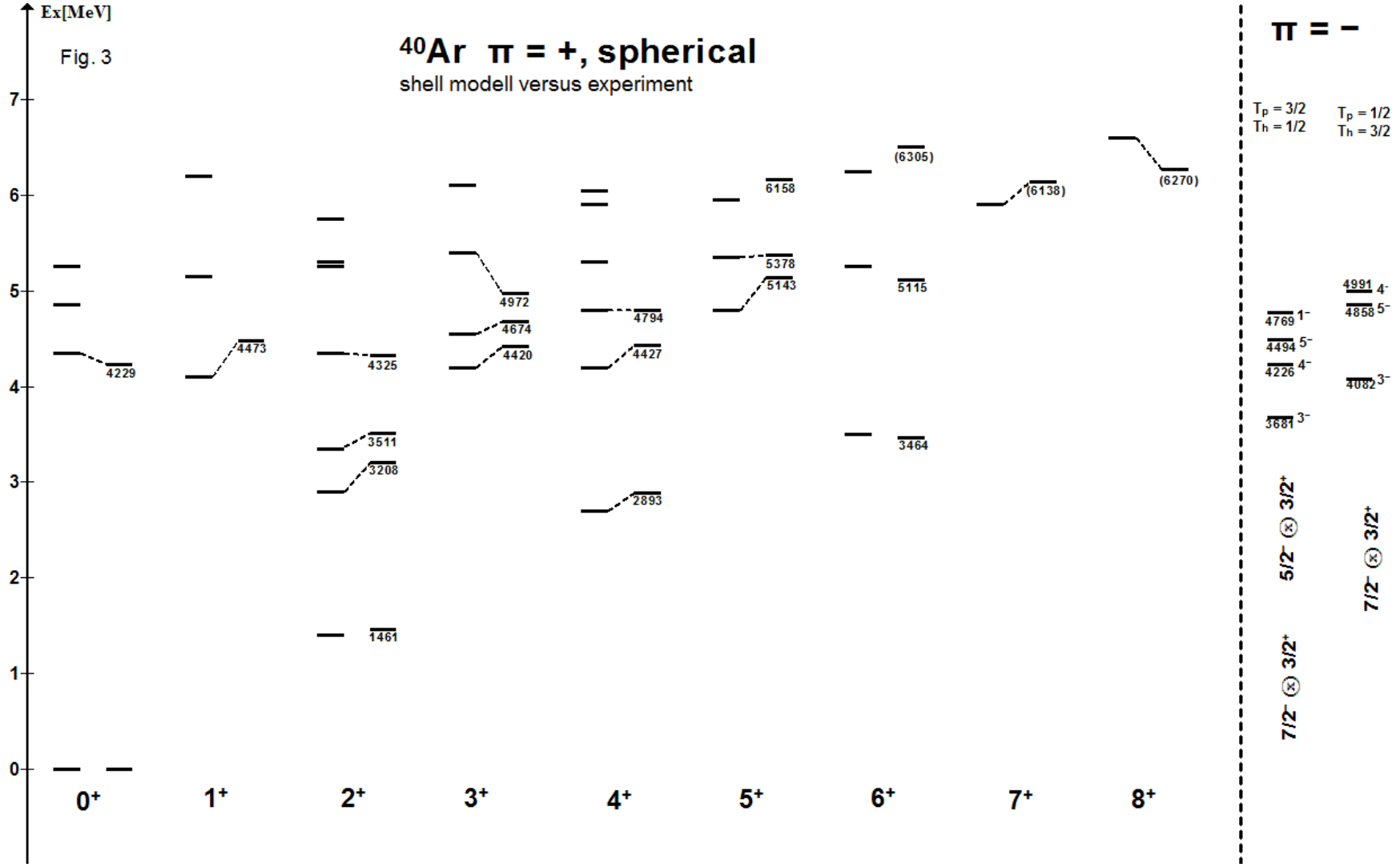
Ex[MeV]
Fig. 3
40Ar π = +, spherical
shell modell versus experiment
0
1
2
3
4
5
6
7
0+
1+
2+
3+
4+
5+
6+
7+
8+
4229
4473
4325
3511
3208
1461
4972
4674
4420
4794
4427
2893
6158
5378
5143
(6305)
5115
3464
(6138)
(6270)
π = −
Tp = 3/2
Th = 1/2
Tp = 1/2
Th = 3/2
4769 1−
4494 5−
4226 4−
3681 3−
4991 4−
4858 5−
4082 3−
5/2− ⊗ 3/2+
7/2− ⊗ 3/2+
7/2− ⊗ 3/2+

14. Decomposition of the ^{41}Ca / ^{41}Sc level scheme in terms of n ħω excitations with n = 0 - 7

In 2004 we were first able *[9]* to explain the complete level scheme of doubly magic ^{40}Ca up to 8 MeV in excitation by considering all n ħω excitations from n = 0 to n = 8. In other words the N = 2 major shell provides eight easy to excite particles (the $d_{3/2}$ particles) while the N = 3 major shell can easily accommodate up to eight particles. Hence one can reasonably expect that the spectrum of energy levels in the mirror nuclei ^{41}Ca and ^{41}Sc shows all n ħω excitations from n = 0 to n = 48 − A = 7. It can also be expected that the n ≥ 3 excitations result in deformed states. The latter ones should be predictable by the Nilsson model with a residual interaction while the n = 2 excitations reflect, at the beginning, the spectrum of the n = 0 excitations.
The level scheme of A = 41, T = 1/2 can be reliably constructed for J ≤ 9/2 by considering the information from ^{41}Ca and ^{41}Sc *[4, 5]*. Levels of higher spin are available in ^{41}Ca only (Table 1). The “trivial“ part of the spectrum, namely the n = 0 - 2 excitations are given in Fig. 1. The remaining levels are grouped in Fig. 2 into a system of rotational bands. Numerical values of level energies can be read from Table 1. The rotational bands are not perfect indicating some interaction with spherical states. The character of a band as a n ħω excitation is obtained in Table 2 by the Nilsson model using the assigned quantum numbers K^{π} and the bandhead energies.

The Nilsson model for A = 41 *[9]* considers the distribution of A − 36 = 5 nucleons over the first three orbits above the Fermi boarder. The latter ones are given in our ^{39}K notes. The analysis yields a complete agreement with experiment of the rotational bands up to 5 MeV except for the presence (last column of Table 2) of a core excited band which is outside our model. This $K^{\pi} = 1/2^{-}$ band which starts at 3614 KeV is, however, equal in structure as the

neighbouring $K^{\pi} = 1/2^{+}$ band with head at 3400 KeV. It is necessary only to exchange the roles of the orbits $\Omega^{\pi} = 1/2^{+}$ and $\Omega^{\pi} = 1/2^{-}$. The same situation has been encountered in ^{43}Ca. The only difference is the presence of an additional K, T = 0, 1 pair of nucleons in the $\Omega^{\pi} = 3/2^{+}$ orbit. The conclusion drawn in the case of ^{43}Ca, namely $\delta = 0.3$ or $\eta = 6$, is also applicable here.

The $K^{\pi} = 3/2^{+}$ band starting at 5095 KeV deserves interest. It originates from the second $K^{\pi} = 0^{+}$, T = 0 band of ^{40}Ca by adding just one $\Omega^{\pi} = 3/2^{+}$ nucleon. By the same token one should find a $K^{\pi} = 3/2^{+}$, T = 3/2 band in ^{41}K which has the $K^{\pi} = 0^{+}$, T = 1 band of ^{40}K, starting at 1643 KeV, as the parent. In Warburtons shell model calculation of ^{41}K, the 1559 KeV, $J^{\pi} = 3/2^{+}$ state has no room in the spectrum of 2p-1h states and is thus a prospective bandhead. The same holds for the 1593 KeV, $J^{\pi} = 1/2^{+}$ state which is then the head of a second, $K^{\pi} = 1/2^{+}$, T = 3/2 band in ^{41}K. The T = 3/2 bands occur of course in ^{41}Ca/^{41}Sc at higher excitation energies (by about 5819 KeV, the energy of the first T = 3/2 state) as shown in Table 2.

Table 1

The 2J ≤ 9, T = 1/2 levels of A = 41

^{41}Ca	^{41}Sc	SM	^{41}Ca	^{41}Sc	SM	^{41}Ca	^{41}Sc	SM	^{41}Ca	^{41}Sc	SM	^{41}Ca	^{41}Sc	SM	^{41}Ca	^{41}Sc	SM
1^+			3^+			5^+			7^+			9^+					
2669	2719	3648	2010	2095	2593	2605	2666	3696	2884	2882	3728	3201	3185	4207			
3400	3411	5 ħω	3050	3013	3 ħω	3494	3678	3 ħω	3613	3696	3 ħω	4448	4514	3 ħω			
3845	(3960)	3 ħω	3525	3652	5 ħω	3740	3780	5 ħω	3973		3 ħω	4970	4810	3 ħω			
5011	5023	5385	4184	4328a)	3 ħω	4094	4245	4897	4328	4328[a)]	5 ħω	5046	5036	5 ħω			
	5493	5856	4417	4502	4687	4730	4869	3 ħω	(5588)		4 986	5194		5 569			
5984			4728	4777	4866	4815	4947	5437	6036		5572	5750		6033			
			5095	5084	5 ħω	5283	5375	5 ħω			6199						
				5355		5411	5419				6876						
					6251			6341									
								6717									
1^-			3^-			5^-			7^-			9^-			11^-		
3614	3732	4 ħω	1942	1716	0 ħω	2574	2588	4 ħω	0	0	0 ħω	3676	-	4 ħω	4015		4 ħω
3944	3475	0 ħω	2462	2414	4 ħω	4278	(4440)	4 ħω	2959	2972	4 ħω	4341	-	4 ħω			
4752	4644	4 ħω	3730	3775	4 ħω	4878	4949	6 ħω		4022	2 ħω						
5072	5074		4603	4535	6 ħω	5520	5521	4 ħω		4030	4 ħω						
5078			5120	5143	4 ħω	5616	5650		5148	5011	4 ħω						
5451	5490		5370	5395		5648	5709		5349		6 ħω						
5704	5691		5468	5535	2 ħω	5801	5871	0 ħω(in part)									
5891	5705		5670	5755		5933											

a) Possibly a doublet, consisting of a $3/2^+$ state seen in β-decay of ^{41}Ti plus a g-wave resonance in ^{40}Ca(p, γ) which then has $J^\pi = 7/2^+$

Table 2

The Nilsson model configurations for A = 41

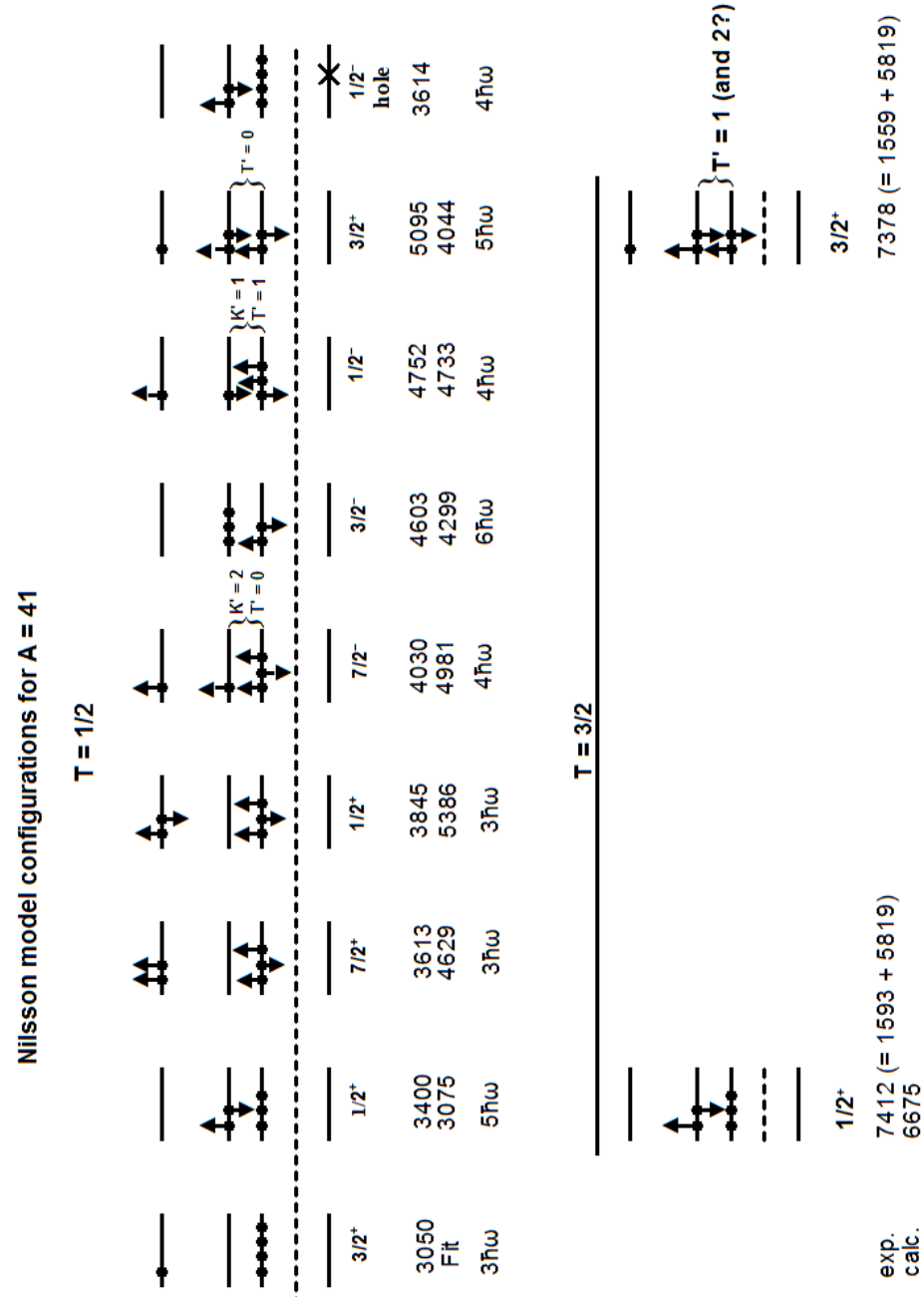

Fig. 1

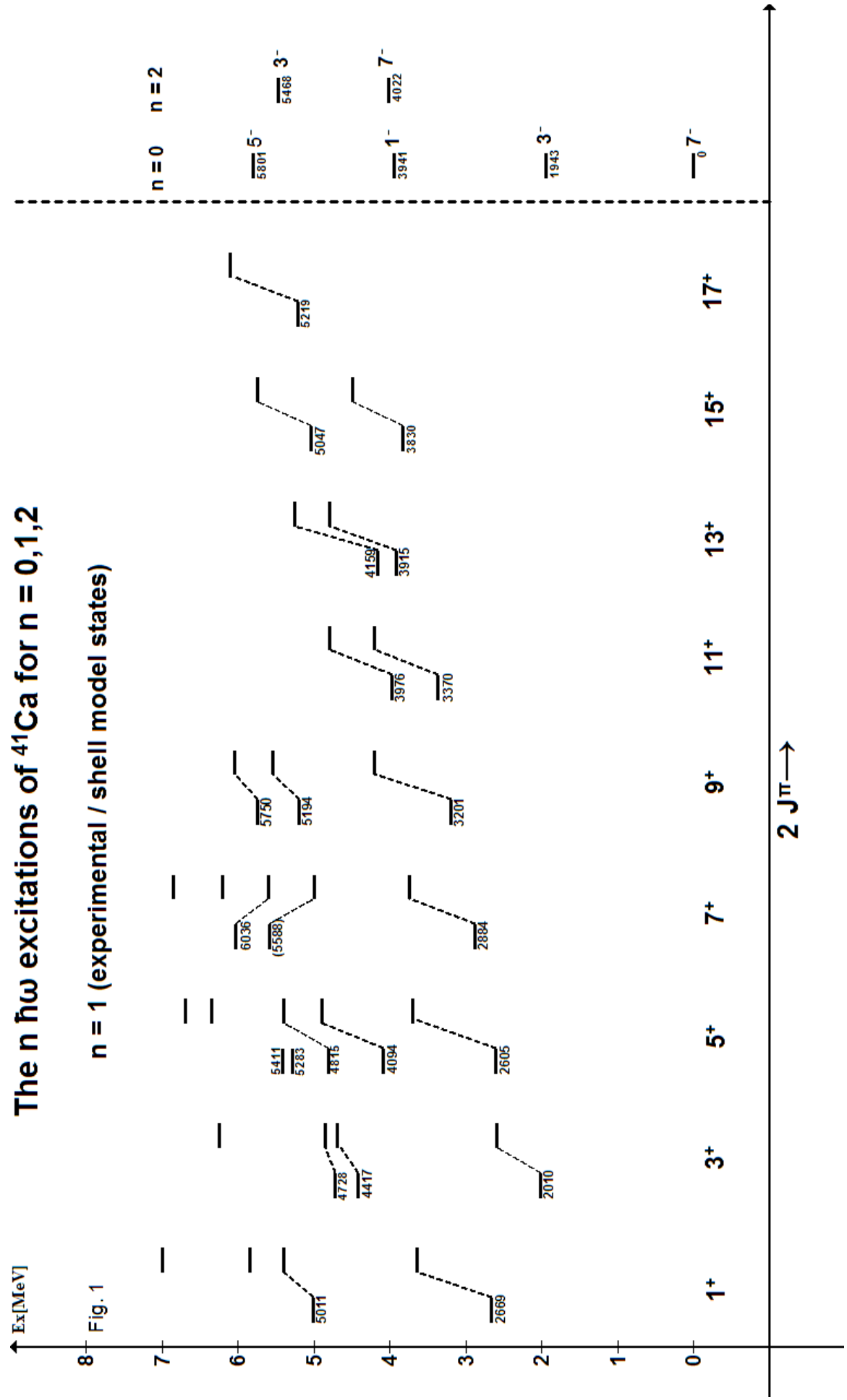
The n ħω excitations of 41Ca for n = 0,1,2
n = 1 (experimental / shell model states)
Ex[MeV]
2 Jπ⟶
n = 0
n = 2
1+
3+
5+
7+
9+
11+
13+
15+
17+
5011
2669
4728
4417
5411
5283
4815
4094
2605
6036
(5588)
5750
5194
2884
3201
3976
3370
4159
3915
5047
3830
5219
5801
5468
3941
4022
1943
0

Fig. 2

Rotational bands in ^{41}Ca

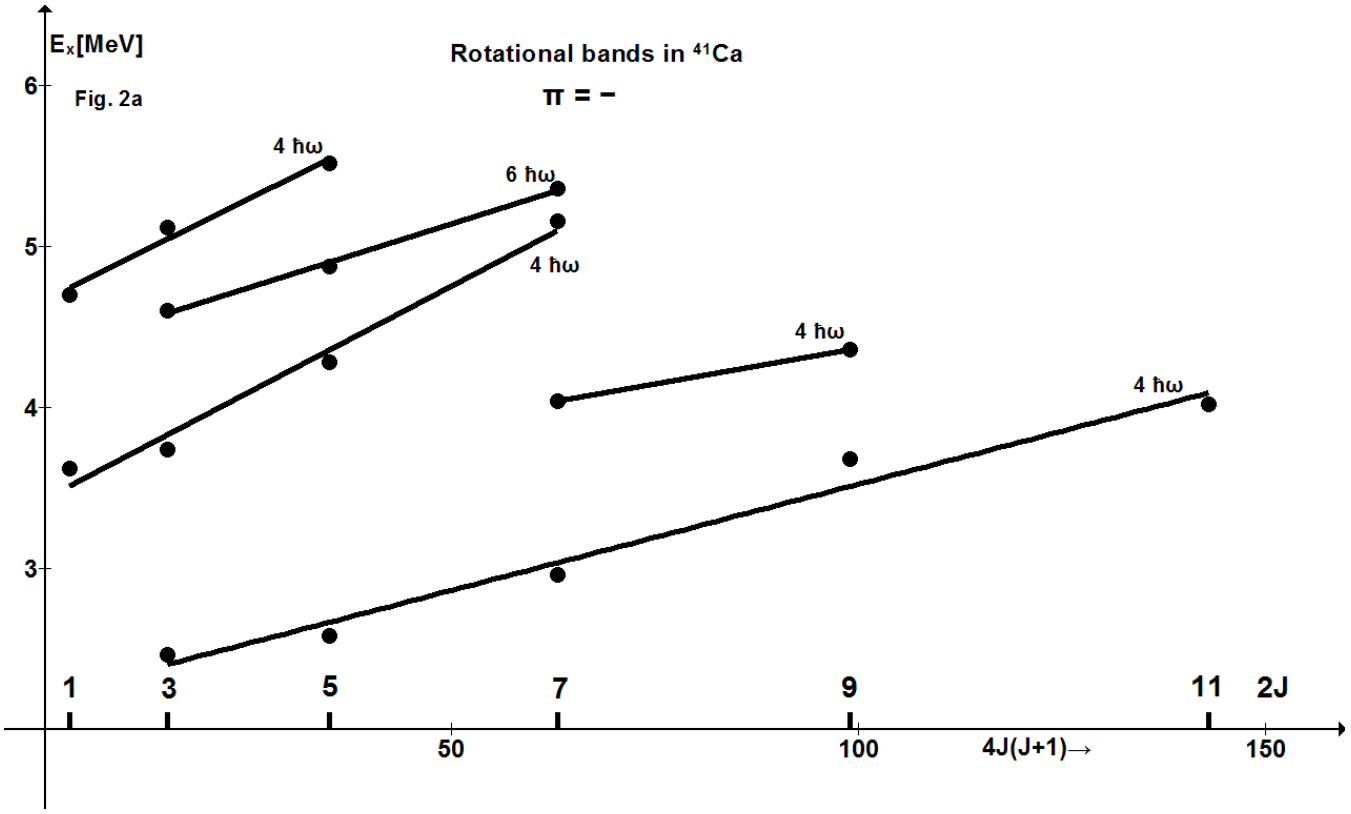

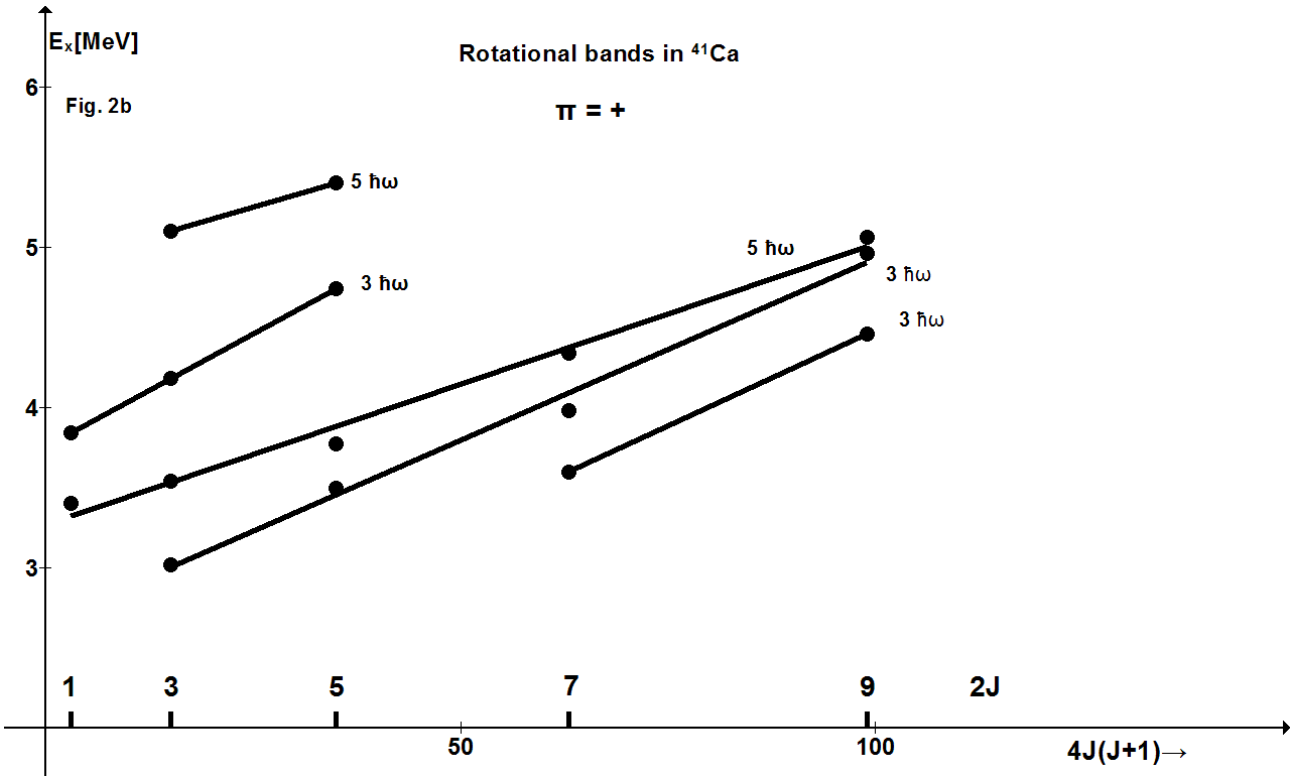

15. The energy levels of A = 42, T = 0 and T = 1

The energy levels of ^{42}Sc have T = 0 and T = 1 while a pure T = 1 spectrum can be observed in ^{42}Ca. The T = 1 levels in ^{42}Sc are observed at almost exactly the ^{42}Ca energies because the ground state of ^{42}Sc is the analogous state of the ^{42}Ca ground state. We start with the T = 1 spectrum as observed in ^{42}Ca.

According to the ideas developed for ^{41}Ca the spectrum of ^{42}Ca levels should be composed of all n ħω excitations of the ground states from n = 0, to n = 48 − A = 6. The n = 0, 1 excitations should be spherical and a shell model calculation in the combined (s-d) plus (f-p) space is available *[6]*. The n = 2 - 6 excitations should be deformed and thus be understandable in the frame of the Nilsson model with residual interaction.

The energy levels of ^{42}Ca are well investigated up to 6248 KeV *[4]* by a combination of γ-decay measurements with the ^{39}K(α, p γ) reaction and by particle transfer reactions. We accept in particular l = 1, 3 transfer in the ^{41}K(τ, d) and ^{41}Ca(d, p) reactions and L = 0 transfer in the ^{40}Ca(t, p) and ^{44}Ca(p, t) reactions. Between 6248 KeV and 10036 KeV, levels with higher spin (generally J ≥ 6) are known from the ^{39}K(α, p γ) reaction and heavy-ion induced reactions. In Tables 1, 2 we classify all $E_x \leq 6145$ KeV levels, altogether 81 levels, and 46 out of 53 high spin states above 6248 KeV, according to their quantum numbers J^π and their character as a n ħω excitation. The shell model energies of the (spherical) 0 ħω and 1 ħω excitations are also given. Unfortunately the calculations were not carried out to high enough energies, especially for $J^\pi = 3^-$ states. Weak-coupling estimates yield 10 to 11 $J^\pi = 3^-$ states below 6145 KeV, while level # 11 is reached at 5670 KeV already. Thus the experimental spectrum shows a slight compressure (indirect evidence of higher lying octupole vibration?).

16. The rotational bands of ^{42}Ca

Positive parity

Fig. 1 shows three $K^{\pi} = 0^{+}$ bands and gives indications of a fourth band. The bands #1, 2 have been discussed previously *[9,18]* and their band head energies were used to determine the parameters of a Nilsson model with residual interaction for A = 36 - 48. Bands # 3, 4 are predictable then.

Fig. 1 contains two $K^{\pi} = 2^{+}$ bands which are well established by the systematics of their γ-decay in Fig. 2. Another two bands with $K^{\pi} = 2^{+}$ seem to exist in ^{42}Ca in agreement with the Nilsson model prediction which allows a total of ten $K^{\pi} = 2^{+}$ bands.

Negative parity

Rotational bands of odd-parity in A = even nuclei beyond ^{40}Ca are feasibly only by coupling an odd number of $\Omega^{\pi} = 3/2^{+}$ holes with an odd number of $\Omega^{\pi} = 3/2^{-}$ particles, yielding $K^{\pi} = 3^{-}$ bands and $K^{\pi} = 0^{-}$ bands with a J = even and a J = odd branch. Such bands or parts thereof were known in ^{46}V, ^{44}Sc, possibly in ^{44}Ti *[9]* and were postulated for ^{42}Sc in order to explain the level density of negative parity states. Fig. 1 shows two sequences of negative parity states which, on the basis of the J(J+1) rule, seem to form $K^{\pi} = 3^{-}$ and 0^{-}_{odd} bands.

17. Nilsson model interpretation of rotational bands

The Nilsson model of A = 36 - 48 nuclei which we proposed in 2004 *[9]* explains the deformed intrinsic states by distributing A − 36 = 6 nucleons across three relevant orbits. This is shown in Fig. 3. The identification of K ≠ 0 bands made it necessary to improve the Hamiltonian of 2004 in one important aspect. The interaction between an odd number of nucleons in two orbits was not completely specified. Thus we resumed work on the A = 36 - 44 area and found just enough material to solve the problem. The structure of the Hamiltonian, which is due to Brink and Kerman *[8]*, is briefly outlined in our ^{40}Ca notes (p. 264, 265). A separate section (p. 204) describes the way of deducing the parameters of the Hamiltonian from experiment.

The nucleus ^{42}Ca turns out to be a friendly one. We are able to reproduce the observed bandhead energies and, for $K^{\pi} = 2^{+}$, the underlying isospin coupling schemes. A remarkable facet is the theoretical exclusion of $K^{\pi} = 1^{+}$ and $K^{\pi} = 1^{-}$, 2^{-}, 0^{-}_{even} bands in the experimentally accessible region $E_x < 6.2$ MeV. Many occupancies of Nilsson orbits can generate both T = 0 and T = 1 intrinsic states. The enumeration in Figs. 3, 5 serves for easy comparison.

18. The T = 0 spectrum of ^{42}Sc states

Having understood the T = 1 spectrum of A = 42 states it becomes feasible to completely untangle the T = 0 spectrum up to and including the 3323 KeV state and the states with J > 3 up to 4 MeV.

Table 3 presents the T = 1 states which have to be removed first and the 0 ħω and 1 ħω states which are believed to be spherical. The T = 1 states are compared to the ^{42}Ca analogs, the other states are easy to identify by single-particle transfer reactions. The first 1 ħω state (with $J^{\pi} = 3^{-}$) has no chance of γ-decay except to the 2_1^+, T = 1 state which is the unique feature of the 2297 KeV level. The „accepted“ ^{42}Sc level scheme of Endt‘s compilation has no room for the predicted 4_1^- and 5_1^- states of 1 ħω character, but two levels at 2510 KeV and 3196 KeV were discarded because they are observed only in the (α, d) reaction. The latter reaction emphasizes states of higher spin which in turn must decay by easy to miss γ-ray transitions of low energy. Finally an experimental level at 2650 KeV has J = 1, 2 from its γ-decay and constitutes the only candidate of the predicted 2_1^- state. Table 4 presents the deformed states of ^{42}Sc. They constitute the n ħω excitations with n = 2 - 6. The majority of bands has been proposed already in our first analysis of 2004 *[9]*. The $K^{\pi} = 0_2^+$ and $K^{\pi} = 1^-$ bands are introduced here to accommodate all levels which show γ-decay to the 0^+, T = 1 ground state. The inherent weakness of M2 and isovector E2 decay make a J = 1 assignment to three levels at E_x = 2269, 2455 and 2535 KeV mandatory. In 2004 only one level was explained. Also new is the proposed existence of the $K^{\pi} = 1_2^+$ and $K^{\pi} = 5^+$ bands. Five levels in the 2883 - 2964 KeV region of which we know nothing but their existence are arranged such that a J(J+1) dependence within bands is obtained (Fig. 4).The rotational bands with T = 1 (in ^{42}Ca) and T = 0 are intimately related and the T = 0 bands are exactly those which can be expected from the pre-

ceding analysis of the T = 1 part. In order to facilitate a comparison we have enumerated the different occupancies of orbits for T = 1 in Fig. 3 and applied the same enumeration for T = 0 in Fig. 5.

Table 1

^{42}Ca, π = + states, K^{π} assignments or shell model energies [c)]

J^{π}	0^+	1^+	2^+		3^+		4^+		5^+	
E_x[KeV]	K^{π}/SM	Neither observed nor expected (< 6 MeV)	E_x[KeV]	K^{π}/SM	E_x[KeV]	K^{π}/SM	E_x[KeV]	K^{π}/SM	E_x[KeV]	K^{π}/SM
0	0		1524	1592	3998	2_1^+	2751	2484	5210	2_1^+
1837	0_1^+		2423	0_1^+	5215	2_2^+	3253	0_1^+	5380	5226
3300	0_2^+		3393	2_1^+	5578	5047	4443	0_2^+	No data Round 6.3 MeV	2_2^+
4566	0_3^+		3654	0_2^+	5716[b)]	2_3^+	4505	2_1^+		
5345	0_4^+		4452	4161	5875	2_4^+	5016	4872	6817	2_3^+
5866[a)]	5716		4761	2_2^+			5472	0_3^+	7130	2_4^+
			4865	0_3^+			5601	2_2^+		
			5357	2_3^+			6113	2_3^+		
			5530	2^+						
			5866[a)]	0_4^+						

J^{π}	6^+	7^+		8^+		9^+		10^+	
E_x[KeV]	K^{π}/SM	E_x[KeV]	K^{π}/SM	E_x[KeV]	K^{π}/SM	E_x[KeV]	K^{π}/SM	E_x[KeV]	K^{π}/SM
3190	3176	6715	2_1^+	6635	0_1^+	8580	2_1^+	8847	0_1^+
4715	0_1^+	7838	2_2^+	7415	0_2^+			8950	0_2^+
5690	0_2^+	8517	2_3^+	7634	2_1^+				
5927	2_1^+			7940	0_3^+				
6675	0_3^+			8611	2_2^+				
6896	2_2^+								
7697	2_3^+								
7920	2_4^+								
8102	0_4^+								

a) Doublet, a $J^{\pi} = 0^+$ state from (t, p) and a $J^{\pi} = 1, 2^+$ state from (α, p γ)

b) The 5716 and 5726 KeV levels from (α, p γ), both decaying to $J^{\pi} = 4^+$ states, are assumed to constitute a single level

c) The table contains all $E_x \leq 6145$ KeV levels

Table 2

^{42}Ca, π = − states, exp. / SM (1 ħω)[a)]

J^π	0^-	1^-		2^-		3^-		4^-		5^-	
E_x[KeV]	SM	E_x[KeV]	SM	E_x[KeV]	SM	E_x[KeV]	SM	E_x[KeV]	SM	E_x[KeV]	SM
(5980)	6492	3884	3 ħω	4947	5217	3446	4299	3953	4131	4099	4298
		4232	5098	5075	5392	4048	4668	4355	5046	4896	3 ħω
		5624	5981	5393	5830	4117	3 ħω	5188	3 ħω	5439	5202
		5797	6102	(5491)	5947	4420	3 ħω	5320	5482	5775	3 ħω
		6180	6860 or 5 ħω	5820		4691	5005	5925	6168	6020	6071
				(6038)		4904	5302	5952		6248	6397
		ground state decay of all levels observed		(6104)		4971		6003			6817
						5158					7048
						5407	Absent in (α,pγ)				
						5510					
						5594					
						5665					
						5670					
						5769					
						5806					
						5993					
						6028					

J^π	6^-		7^-		8^-		9^-		10^-		11^-	
	E_x[KeV]	SM	E_x[KeV]	SM	E_x[KeV]	SM	E_x[KeV]	SM	E_x[KeV]	SM	E_x[KeV]	SM
	5492	5944	5743	5957	6408	7012	6553	6965	7368	8018	8296	9173
	6141	6326	6093	3 ħω	7345	7634	7282	3 ħω	8745	9904	9037	3 ħω
	6542	3 ħω	6145	6834	7801	8355	8083	7807				
	6746	6882	6585	7356	8060	8576		8490				
	6975	7762	7361	7863	8450	9068		8571				
	7542	7967	7758	3 ħω	8512	3 ħω	9206	9230				
			8365	8019	9376	9426	9760	3 ħω				
			8774	8402	(9842)							
					(10036)							

a) The Table contains all $E_x \leq 6145$ KeV levels and the observed $J \geq 6$ levels up to 10 MeV

Table 3

The "trivial" part of the ^{42}Sc level scheme

T = 1 states [KeV]				(f - p)² states that means 0 ħω states				(f - p)^3 states that means 1 ħω states		
^{42}Sc		^{42}Ca		^{42}Sc				^{42}Sc		
E_x	J^π	E_x		E_x	J^π	SM[c]		E_x [a]	J^π	SM[c]
0	0^+	0		611	1^+	477		2297	3^-	1963
1586	2^+	1524		617	7^+	561		2510	4^-	2086
1873	0^+	1837		1490	3^+	1296		2650	2^-	2589
2487	2^+	2424		1510	5^+	1312		3196	5^-	3003
2815	4^+	2752		3089	5^+	3364			1^-	3218
3242	6^+	3189		3392[b]	3^+	3668			2^-	3415
3281	0^+	3300		3933[b]	2^+	3992			6^-	3592
3223	4^+	3253			2^+	4161			5^-	3644
3321	2^+	3392		3687	1^+	4274			4^-	3645
	3^-	3447							0^-	3752
	2^+	3654							3^-	3934
	1^-	3885								
3933	4^-	3954								
4047	3^+	3999								

a) for identification see text

b) $J^\pi = (1 - 3)^+$

c) Ref. *[6]*

Table 4

The rotational bands with T = 0 in ^{42}Sc

Positive parity

K^π	3_1^+		1_1^+		$0_1^{+\,a)}$		3_2^+		$0_2^{+\,a)}$		1_2^+		5^+	
	E_x[KeV]	J^π	E_x [KeV]	J^π	E_x [KeV]	J^π	E_x[KeV]	J^π	E_x [KeV]	J^π	E_x[KeV]	J^π	E_x [KeV]	J^π
	1846	3^+	1889	1^+	2222	1^+	2223	2^+,3^+	2535	1	3866	1^+	3893	$(3\text{-}5)^+$
	2433	$(3\text{-}5)^+$	2188	2^+,3^+	2853	3^+	2587	c)	3166	$(3\text{-}5)^+$				
	2795	$(5\text{-}9)^+$	2389	3^+	3668	b)	2996	$(3\text{-}5)^+$						
	3719	$(5\text{-}7)^+$	2910	$(3\text{-}5)^+$			3600	$(5\text{-}7)^+$						

a) The $K^\pi = 0^+$ bands have members of odd spin only

b) γ-decay to $J^\pi = 3^+$ and 4^+ speak for $J^\pi = 5^+$

c) The sole γ-decay mode to $J^\pi = 3^+$ is compatible with $J^\pi = 4^+$

Negative parity [d)]

K^π	0^-_{odd}		1^-		3^-		0^-_{even}	
	E_x[KeV]	J^π	E_x[KeV]	J^π	E_x[KeV]	J^π	E_x[KeV]	J^π
	2269	1	2455	1	2726		2832	
	2883		2669					
			2964					

d) the basis for these assignments is discussed in the text. In addition see Fig. 4

Fig. 1

^{42}Ca Rotational bands

numerical values of E_x (for π = +) are given in the Tables

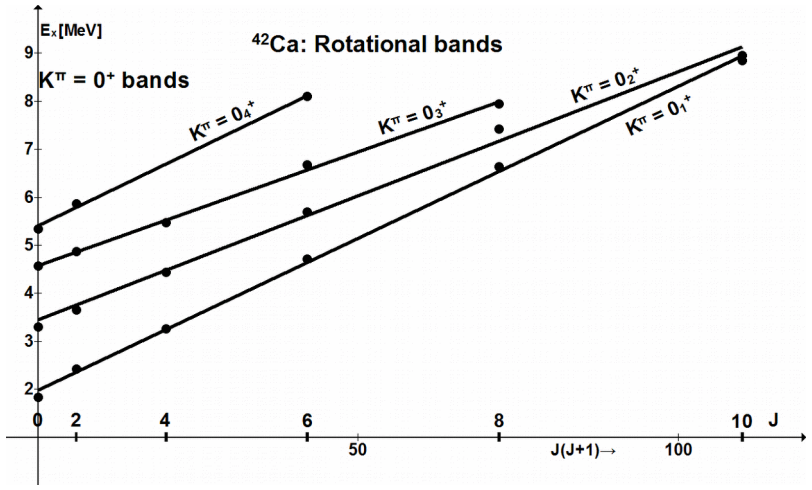

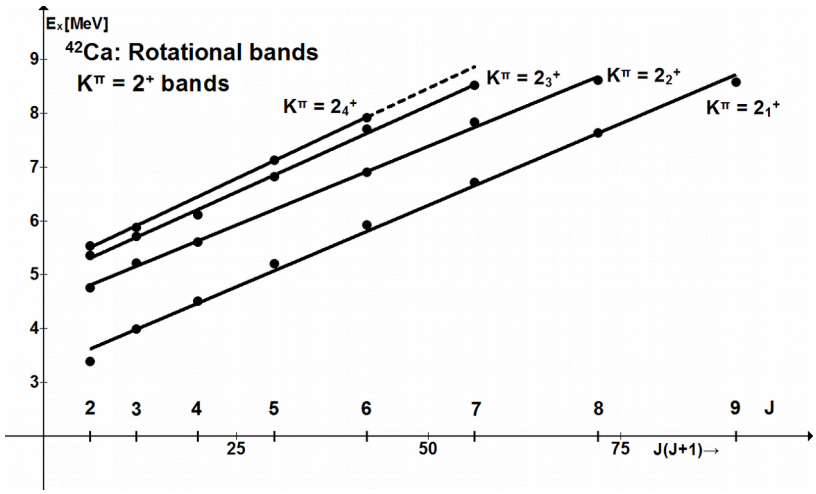

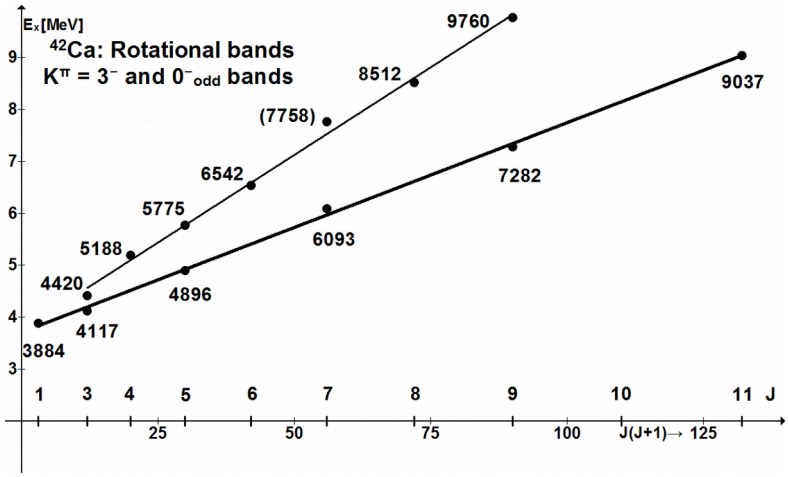

Fig. 2

γ - decay of the $K^{\pi} = 2_1^+$ and 2_2^+ bands in ^{42}Ca

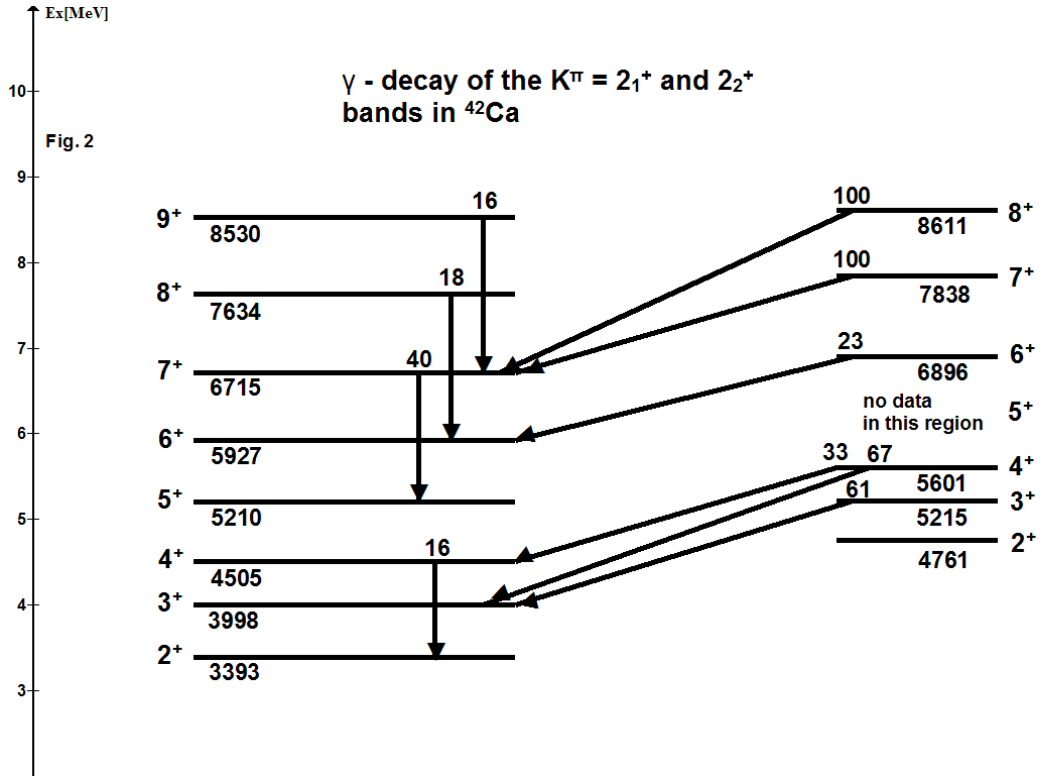

Fig. 3

The Nilsson model configurations of ^{42}Ca bands

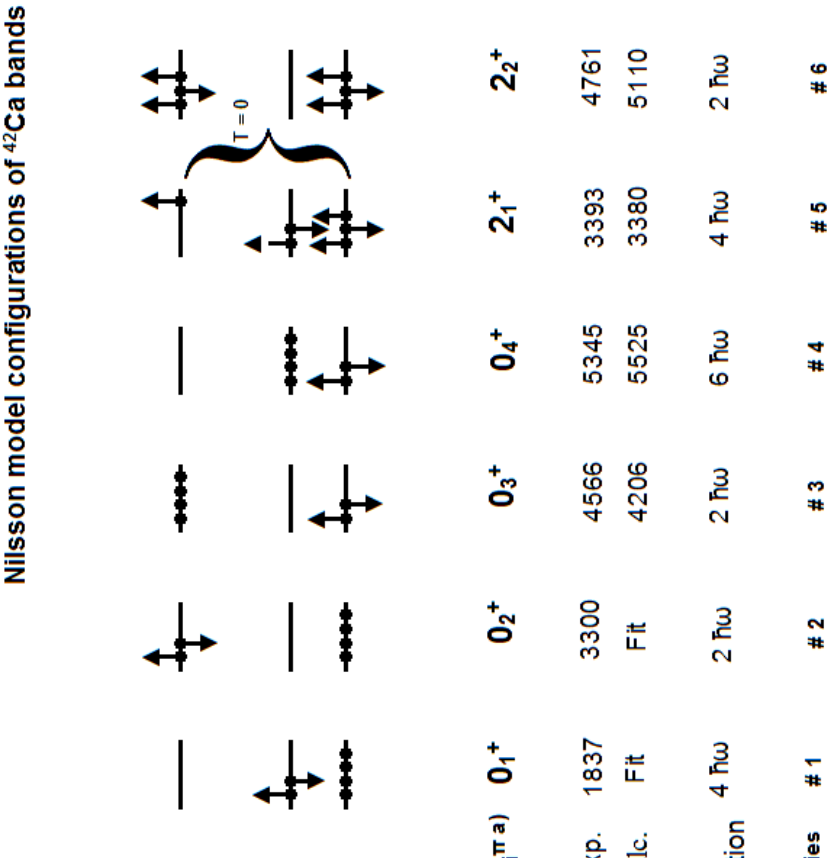

Fig. 3

a) The enumeration of bands with equal K^π follows the experimental data

b) the 0 ħω and 1 ħω excitations are spherical and contained in the tables

Fig. 4

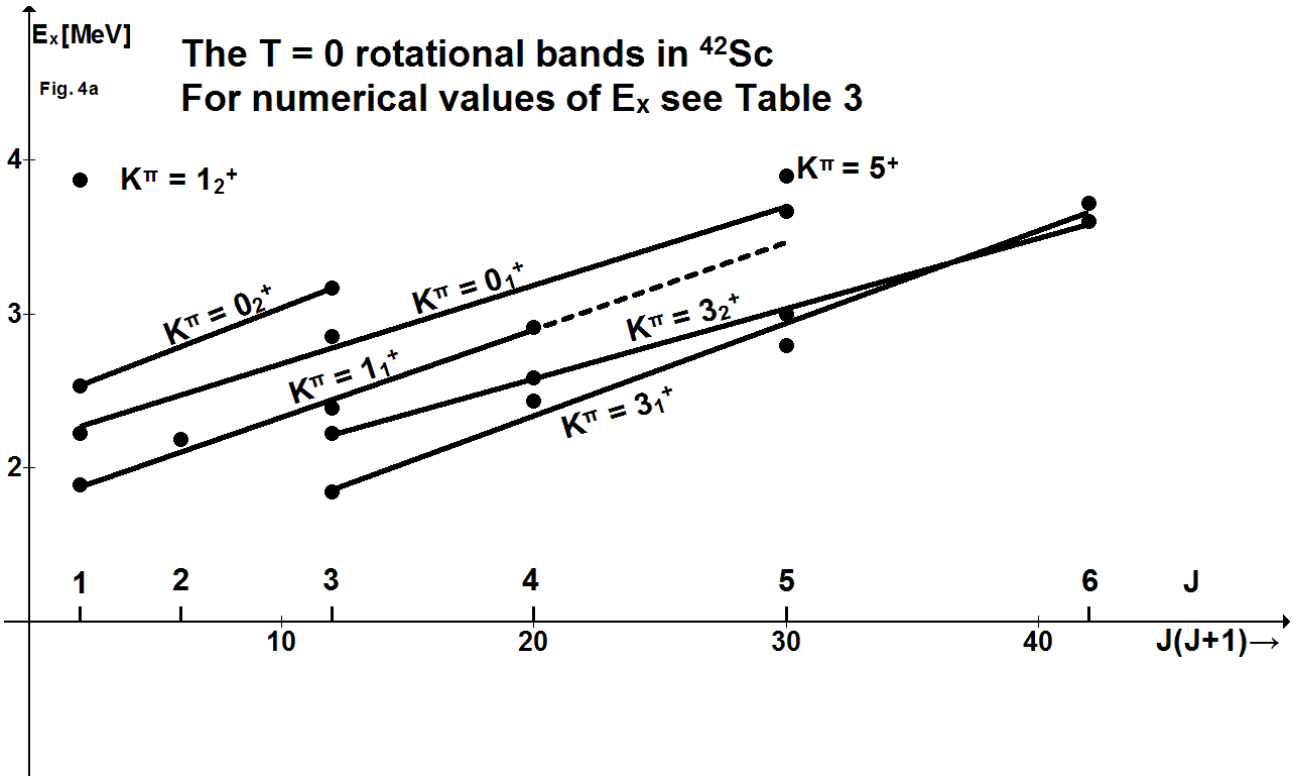
Ex[MeV]
Fig. 4a
The T = 0 rotational bands in 42Sc
For numerical values of Ex see Table 3
Kπ = 12+
Kπ = 5+
Kπ = 02+
Kπ = 01+
Kπ = 32+
Kπ = 11+
Kπ = 31+
4
3
2
1
2
3
4
5
6
J
10
20
30
40
J(J+1)→

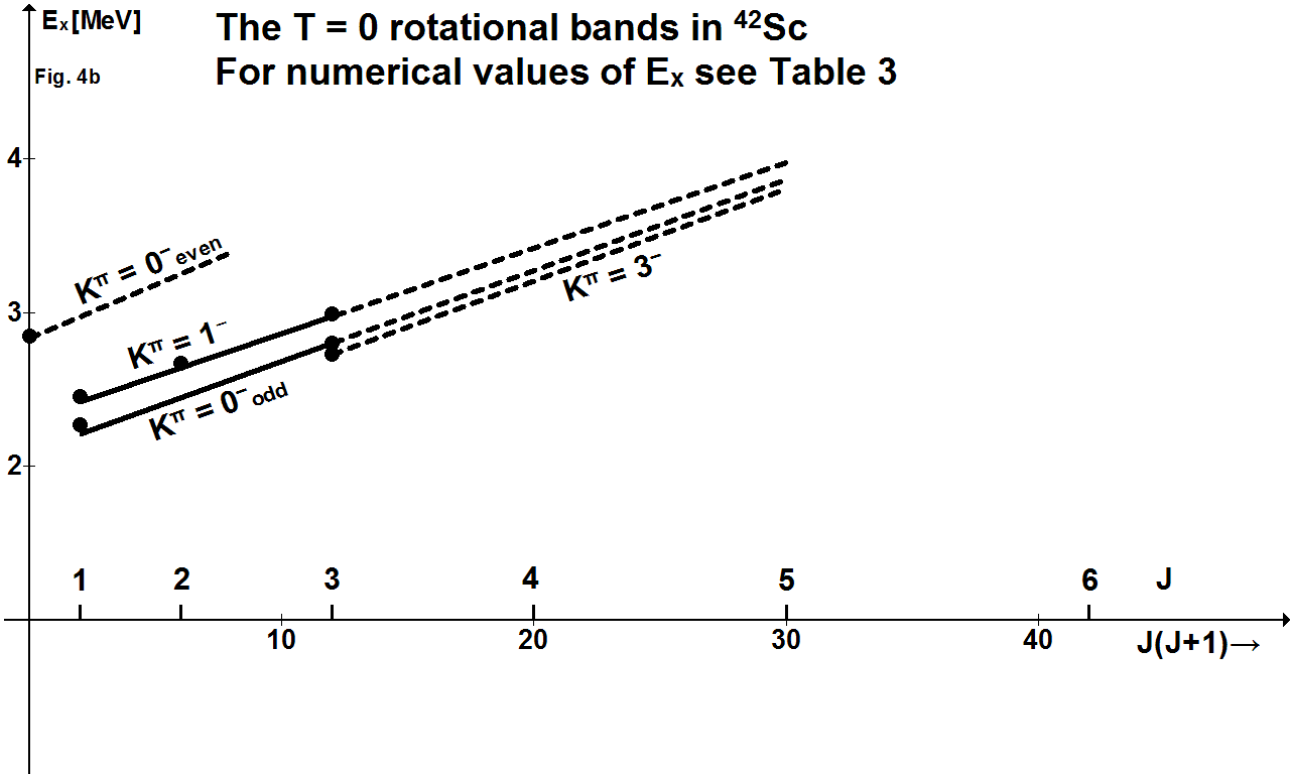
Ex[MeV]
Fig. 4b
The T = 0 rotational bands in 42Sc
For numerical values of Ex see Table 3
Kπ = 0− even
Kπ = 1−
Kπ = 0− odd
Kπ = 3−
4
3
2
1
2
3
4
5
6
J
10
20
30
40
J(J+1)→

Fig. 5

The Nilsson model configurations of ^{42}Sc, T = 0 bands

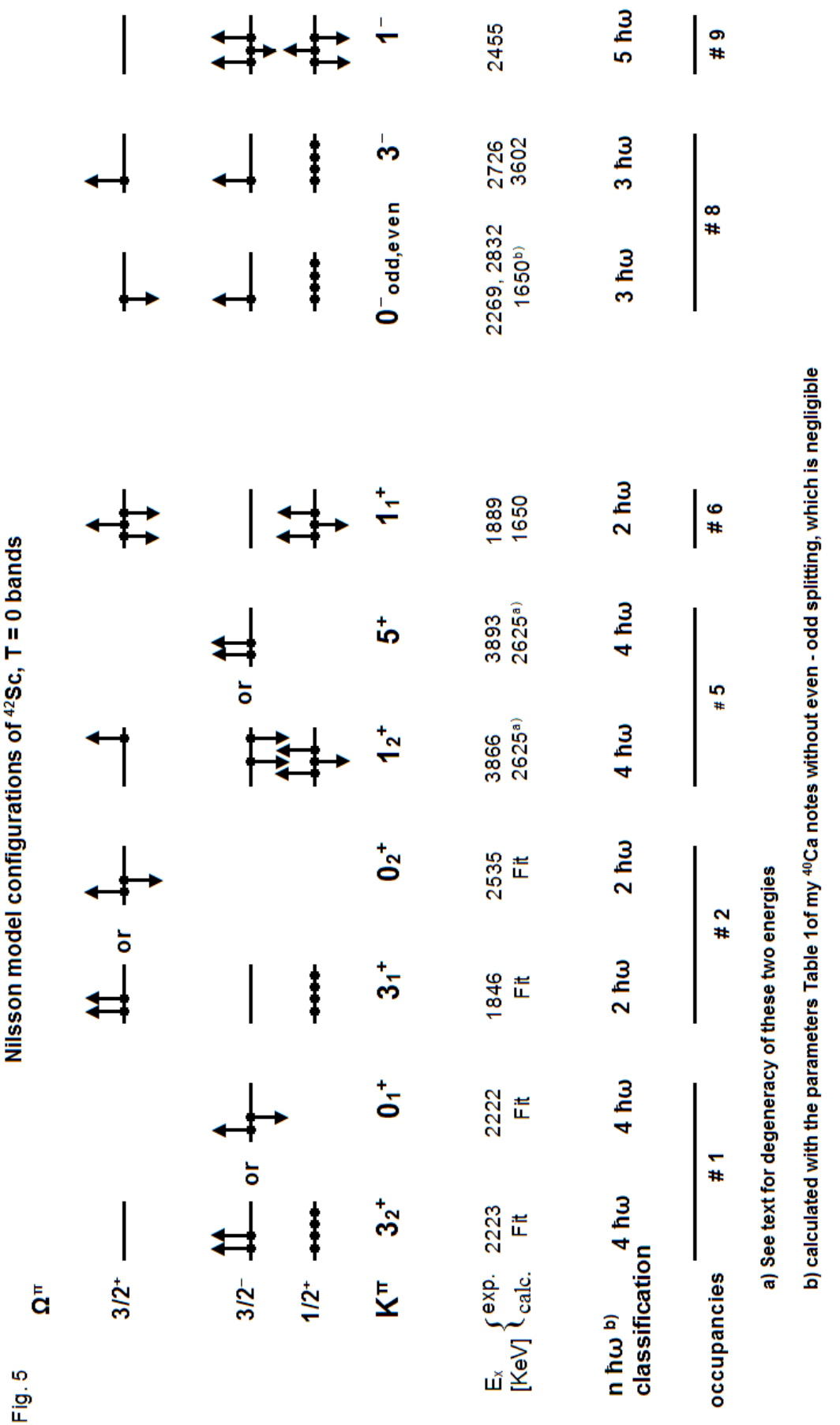

a) See text for degeneracy of these two energies

b) calculated with the parameters Table 1of my ^{40}Ca notes without even - odd splitting, which is negligible

19. Interpretation of the A = 43 level system

The interpretation of the T = 1/2 spectrum in ^{43}Sc and of the T = 3/2 spectrum in ^{43}Ca seemed to be straight forward because coexistence of spherical and deformed states is known since four decades. Rotational bands with $K^{\pi} = 3/2^{+}$ have been observed in both cases. Today we have a completely specified Nilsson model Hamiltonian which leads to a new view of the situation. However let us sort out spherical states at the beginning. Experimental results are obtained from Endt's compilation *[4, 5]* and the Appendix.

The 0 ħω or 3p spectrum of ^{43}Sc contains spherical states of negative parity and has been calculated by Warburton *[6]* in the untruncated space of the N = 2 + 3 major shells. It is compared to experiment in Table 1 and Fig. 1c.
The 1 ħω or 4p-1h spectrum has deformed states in general except for the lowest two states of the configuration ^{44}Sc g.st. $(2^{+}, T = 1) \otimes d_{3/2}^{-1}$. The 2114 KeV and 2140 KeV levels of Table 1 and Fig. 1 are thus generated. A T = 3/2 version exists in ^{43}Ca at 1957 KeV and 2273 KeV. The 4.3 MeV difference between the T = 3/2 and T = 1/2 states (in ^{43}Sc!) agrees with predictions of the weak-coupling model (see our A = 38 notes).

The deformed states of ^{43}Sc arise from the coupling of seven nucleons to a deformed ^{36}Ar core. The particles are distributed over three orbits with $\Omega^{\pi} = 1/2^{+}, 3/2^{-}, 3/2^{+}$. The K - quantum numbers of rotational bands are, with one exception, due to a single particle. Three particles contribute in the case of a $K^{\pi} = 9/2^{-}$ band only. Its bandhead is predicted at a low energy of 1472 KeV. This is also the only precise prediction. Otherwise, in the case of the $\Omega^{\pi} = 1/2^{+}, 3/2^{-}, 3/2^{+}$ bands we have clusters of 5 bands with equal K and different distributions of particles over three orbits and different isospin coupling-schemes.

The relevant occupation numbers are

4 3 0

4 2 1

T = 1 or 0

3 2 2

T = 1 or 0

It is possible to identify experimentally the two lowest lying bands of equal K (Table 1 and Fig. 1a, b). Last not least we discovered (by analogy to ^{25}Mg!) a $K^{\pi} = 1/2^{-}$ band in ^{43}Ca, which is due to an $\Omega^{\pi} = 1/2^{-}$ hole in the core. The occupation numbers are

-1 4 2 2

T = 1.

A T = 1/2 version of this band should exist in ^{43}Sc and a tentative identification of the first three band members is included in Table 1.

The equal K^{π} bands with $K^{\pi} = 1/2^{+}, 3/2^{-}, 3/2^{+}$ will show interaction which we were able to treat only between the 4 2 1 and the observed 4 2 1 configurations.

T = 1 T = 0

The observed 4 2 1 states get thus depressed by roughly 400 KeV.

T = 1

In Table 2 we summarize experimental results and compare them to the theory. The calculations predict in first place the binding energies of seven nucleons to the deformed 4329 KeV, 0^{+} state of ^{36}Ar. These range around 60

MeV, so that a 1 MeV deviation is corresponding to a relative error of 1.7 percent only. We noticed (Table 2) that the predicted first two bands of equal K^π are, for $K^\pi = 3/2^-$, $3/2^+$ and $1/2^+$, almost degenerate so that even a small interaction will lead to a 50:50 mixture of wave functions. Hence we compare average binding energies of the experimental bandheads to theory and in fact the error is reduced to 1 percent.

Information regarding the T = 3/2 spectrum of A = 43 comes from an analysis of the ^{43}Ca spectrum and is considered in the lower part of Table 2. The ^{43}Sc bandhead energies are obtained by adding the amount of 4240 KeV to the corresponding ^{43}Ca energy. The isospin-splitting of the T = 3/2 and T = 1/2 bandheads should be equal theoretically for $K^\pi = 3/2^-$ and $3/2^+$. The chosen ordering within the equal K^π bands is due to this demand, mainly.

The complete analysis of the ^{43}Ca level scheme is given in Figs. 2, 3 which are self-explaining. Only the $K^\pi = 1/2^-$ band of Fig. 2 needs explanation. This band is known in ^{25}Mg *[19]* and it is characterized by a large decoupling parameter a ≈ −3. The structure of the band as given in Table 2 is almost identical to that of the $K^\pi = 1/2_2^+$, T = 1/2 band in ^{43}Sc (Table 2). We need only exchange the roles of the $\Omega^\pi = 1/2^+$ and $1/2^-$ orbits and couple the total isospin to T = 3/2 instead of T = 1/2. As a feedback-loop presence of a $K^\pi = 1/2^-$ band in ^{43}Sc (T = 1/2) is almost mandatory and the first three prospective band members are included in the Table 1. The energetic difference between the $\Omega^\pi = 1/2^-$ orbit, just below the Fermi surface, and the $\Omega^\pi = 1/2^+$ orbit is certainly not bigger than 1 MeV, judging from the closeness of the $K^\pi = 1/2^-$ and $1/2^+$ bandheads. Degeneracy of these orbits is obtained in the Nilsson model for deformation δ = 0.3 or η = 6. Observation of the $K^\pi = 1/2^-$ band is thus no longer surprising.

20. A = 43 Appendix

Improved / corrected J^{π} assignments to A = 43 levels

A: ^{43}Sc

The reported J^{π} assignments *[4]* of $J^{\pi} = 3/2^{-}$ for $E_x = 2094$ KeV and $J^{\pi} = 9/2^{-}$ for $E_x = 2801$ KeV are changed into $1/2^{-}$ and, respectively, $9/2^{+}$. The γ-decay of the 2094 KeV level, obtained from the radiative capture reaction ^{42}Ca(p, γ) leads to the $3/2_1^{+}$, $3/2_1^{-}$, $5/2_1^{-}$, $1/2_1^{+}$, $3/2_2^{-}$ states but also to $5/2_1^{+}$ with 10 %. If the latter decay were futile, which is quite possible in radiative capture work, we would have the ideal partner of a safely predicted $J^{\pi} = 1/2^{-}$ state near 2 MeV.

The 2814 KeV, $J^{\pi} = 9/2$ level is the obvious member of a $K^{\pi} = 1/2^{+}$ band because its energy follows precisely the J(J+1) rule. In addition inband decay to the $7/2^{+}$ member of the band is present. The π = − assignment stems from an alleged L = 2 assignment in the (p, t) reaction. The latter reaction is really trustworthy for L = 0 only.

Doublet character can be inferred for the 3292 KeV level which decays to levels of widely differing J^{π}. One doublet level has $J^{\pi} = 3/2, 5/2, 7/2^{-}$. The other one has $J^{\pi} = 13/2^{+}$ and fits into the well known $K^{\pi} = 3/2_1^{+}$ band both from the J(J+1) rule and its inband decay to the 1931 KeV, $J^{\pi} = 9/2^{+}$ member of the band.

Equally the reported 3262 KeV, $J^{\pi} = 9/2^{-}$ state is a doublet. One level decays to the 1829 KeV, $11/2^{-}$ state and fits energetically into a $K^{\pi} = 3/2_2^{-}$ band. The other level, observed in β-decay of ^{43}Ti, has $J^{\pi} = (5/2 - 9/2)^{-}$. Finally a 2811 KeV, $J^{\pi} = 9/2$ level fits into a $K^{\pi} = 1/2^{+}$ band because inband decay to the 2106 KeV, $7/2^{+}$ band member is observed.

B: ^{43}Ca

The 2299 KeV level has $J^{\pi} = 7/2^{-}$, 9/2, $11/2^{-}$ on the basis of γ-decay and life-time. The Liverpool group measured angular distribution and polarization of the 2249 → 0 KeV transition with aid of the ^{40}Ar(α, n γ) reaction. They deduced $J^{\pi} = 9/2^{-}$ combined with an unusually large mixing ratio δ = 0.75 ± 0.12. Knowing the interplay between mixing ratio and experimentally undetermined alignment parameters we have the feeling that $J^{\pi} = 7/2^{-}$ combined with small δ would have been possible, also. Theory, which is now well developed, leaves no room for a $J = 9/2^{-}$ level at this energy.

Table 1

Decomposition of the ^{43}Sc level scheme[a)]

	0ħω states		Rotational bands									
J^π	**SM**	**Exp.**	**$K^\pi = 3/2_1^-$ (4 ħω)**			**$K^\pi = 3/2_2^-$ (2 ħω)**		**$K^\pi = 9/2_3^-$ (2 ħω)**		**$K^\pi = 1/2^-$ (core excited band, see ^{43}Ca)**	
$7/2^-$	0	0	$3/2^-$	472		1810		$9/2^-$	2335	$3/2^-$	2670
$3/2^-$	1378	1178	$5/2^-$	845		1962		$11/2^-$	2845?	$7/2^-$	2795
$11/2^-$	1976	1829	$7/2^-$	1408		2242				$1/2^-$	3198?
$9/2^-$	2144	2458	$9/2^-$	1882		2760					
$1/2^-$	2220	2094[e)]	$11/2^-$	2635		3262[b)]					
$5/2^-$	2340	2288	$13/2^-$	(3700)							
$15/2^-$	2995	2987									
$19/2^-$	3123	not calculated by Warburton									
$7/2^-$	3157	3292[b)]									
$13/2^-$	3414	3123									
$K^\pi = 3/2_1^+$ (3 ħω)			**$K^\pi = 1/2_1^+$ (1 ħω)**		**$K^\pi = 3/2_2^+$ (1 ħω)**			**$K^\pi = 1/2_2^+$ (3 ħω)**		**Not assigned, see text**	
$3/2^+$	152		$1/2^+$	855	$3/2^+$	2382		$1/2^+$	2650	π = +	2114
$5/2^+$	880		$3/2^+$	1158	$5/2^+$	2580		$3/2^+$	2861	π = +	2140
$7/2^+$	1337		$5/2^+$	1651	$7/2^+$	2840[c)]		$5/2^+$	(3160)		
$9/2^+$	1931		$7/2^+$	2106	$9/2^+$	3140					
$11/2^+$	2552		$9/2^+$	2811[d)]	$11/2^+$	3755[c)]					
$13/2^+$	3292[b)]										
$15/2^+$	4157										

a) all $E_x \leq 2861$ KeV levels are considered

b) member of a doublet

c) The $11/2^+ \rightarrow 9/2^+$ and $7/2^+ \rightarrow 3/2^+$ inband transitions have been observed

d) The $9/2^+ \rightarrow 7/2^+$ inband decay has been observed

π = − for the 2811 KeV level from (p, t) seems wrong

e) A 10% decay to 880 KeV, $5/2^+$ from (p, γ) is doubtful to us.

Table 2

The Nilsson model configurations of rotational bands in ^{43}Sc

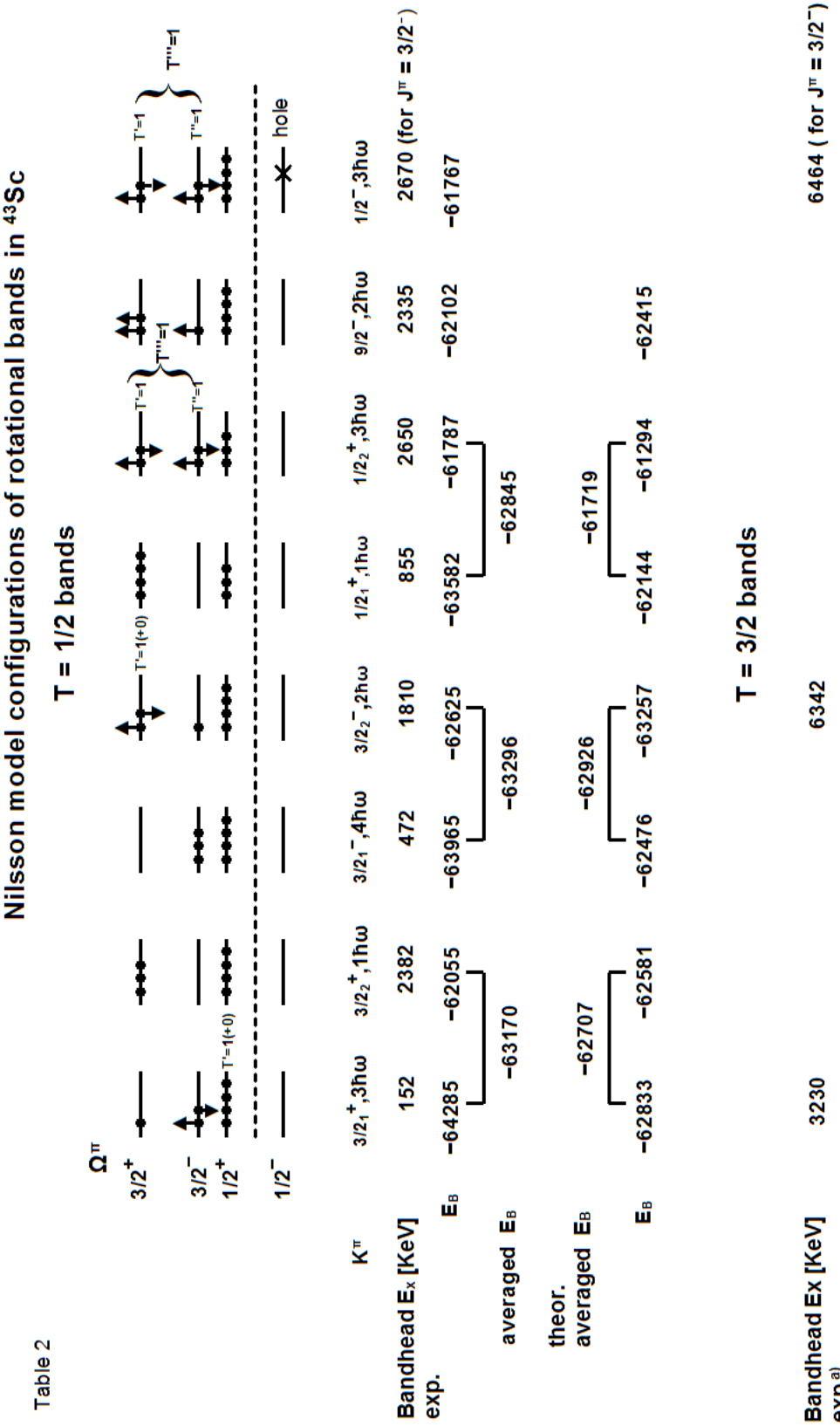

Fig. 1

^{43}Sc

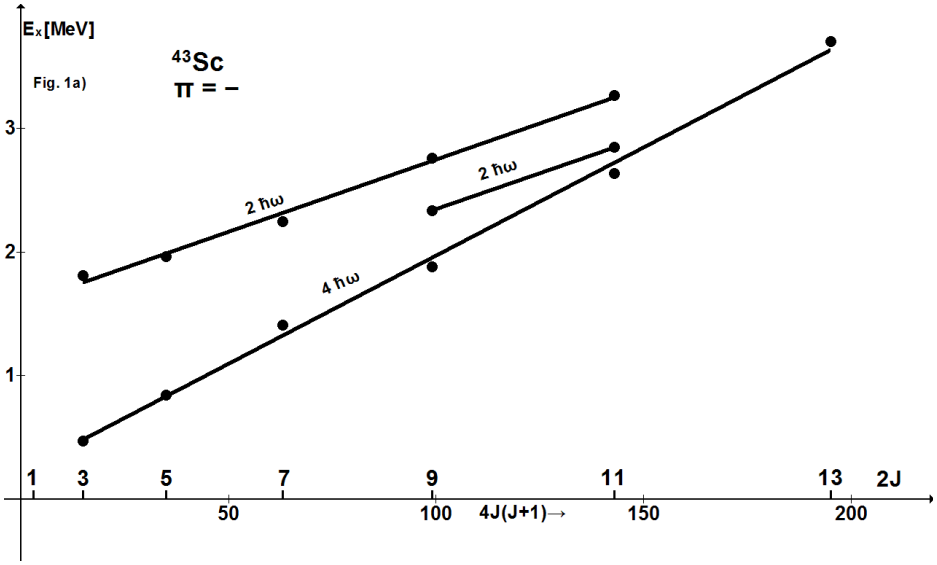
Ex[MeV]
Fig. 1a)
43Sc
π = –
2 ħω
2 ħω
4 ħω
1 3 5 7 9 11 13 2J
50 100 4J(J+1)→ 150 200

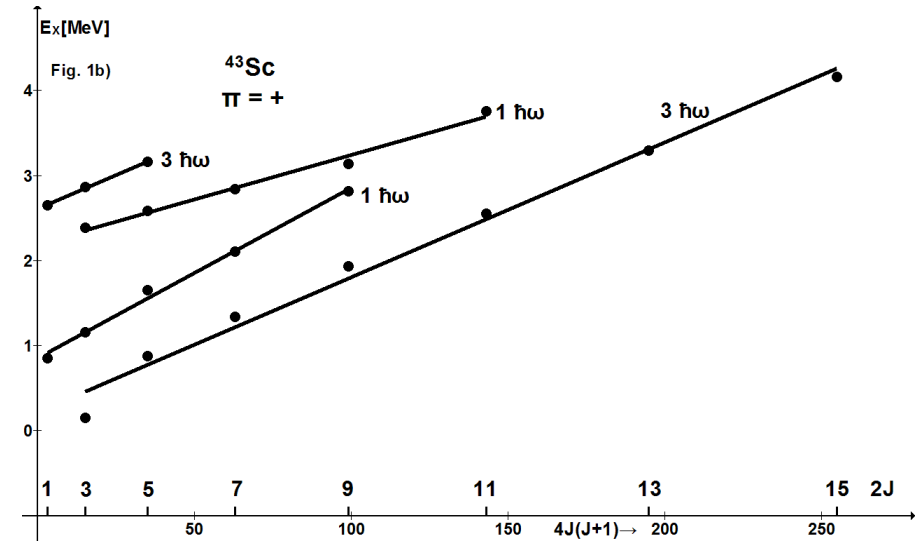
Ex[MeV]
Fig. 1b)
43Sc
π = +
3 ħω
1 ħω
1 ħω
3 ħω
1 3 5 7 9 11 13 15 2J
50 100 150 4J(J+1)→ 200 250

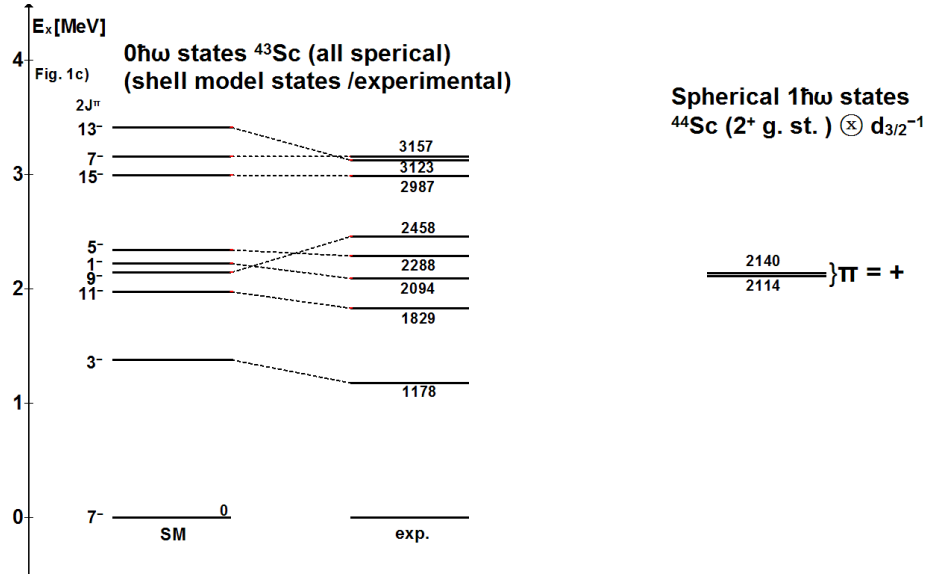
Ex[MeV]
Fig. 1c)
0ħω states 43Sc (all sperical)
(shell model states /experimental)
2Jπ
13⁻
7⁻
15⁻
5⁻
1⁻
9⁻
11⁻
3⁻
7⁻
3157
3123
2987
2458
2288
2094
1829
1178
0
SM
exp.
Spherical 1ħω states
44Sc (2⁺ g. st.) ⊗ d3/2⁻¹
2140
2114
}π = +

Fig. 2

The 3p or 0 ħω states of ^{43}Ca

compared to Warburton's shell model calculations

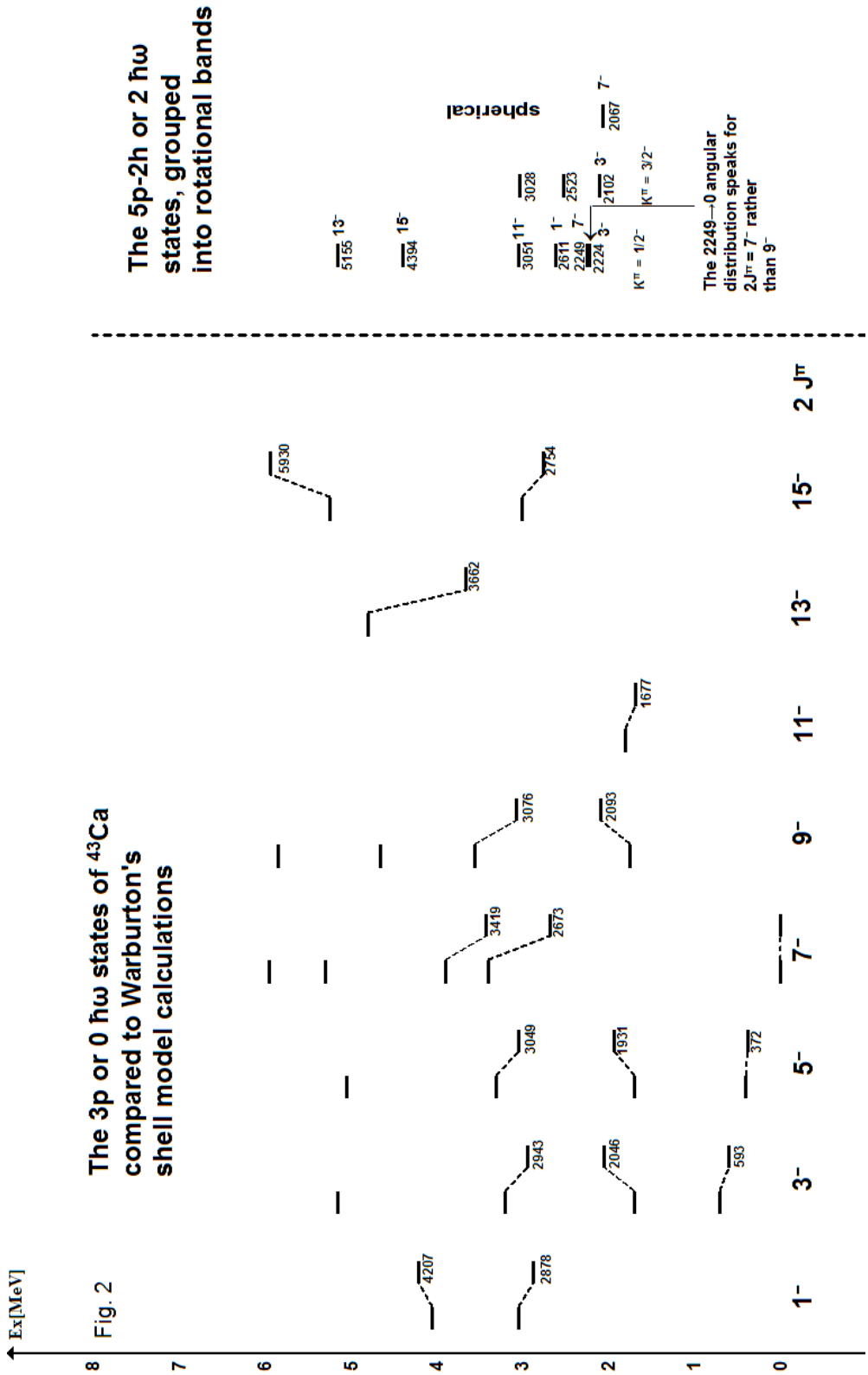

Fig.3

The 4p - 1h or 1 ħω states of ^{43}Ca

compared to Warburton's shell model calculations

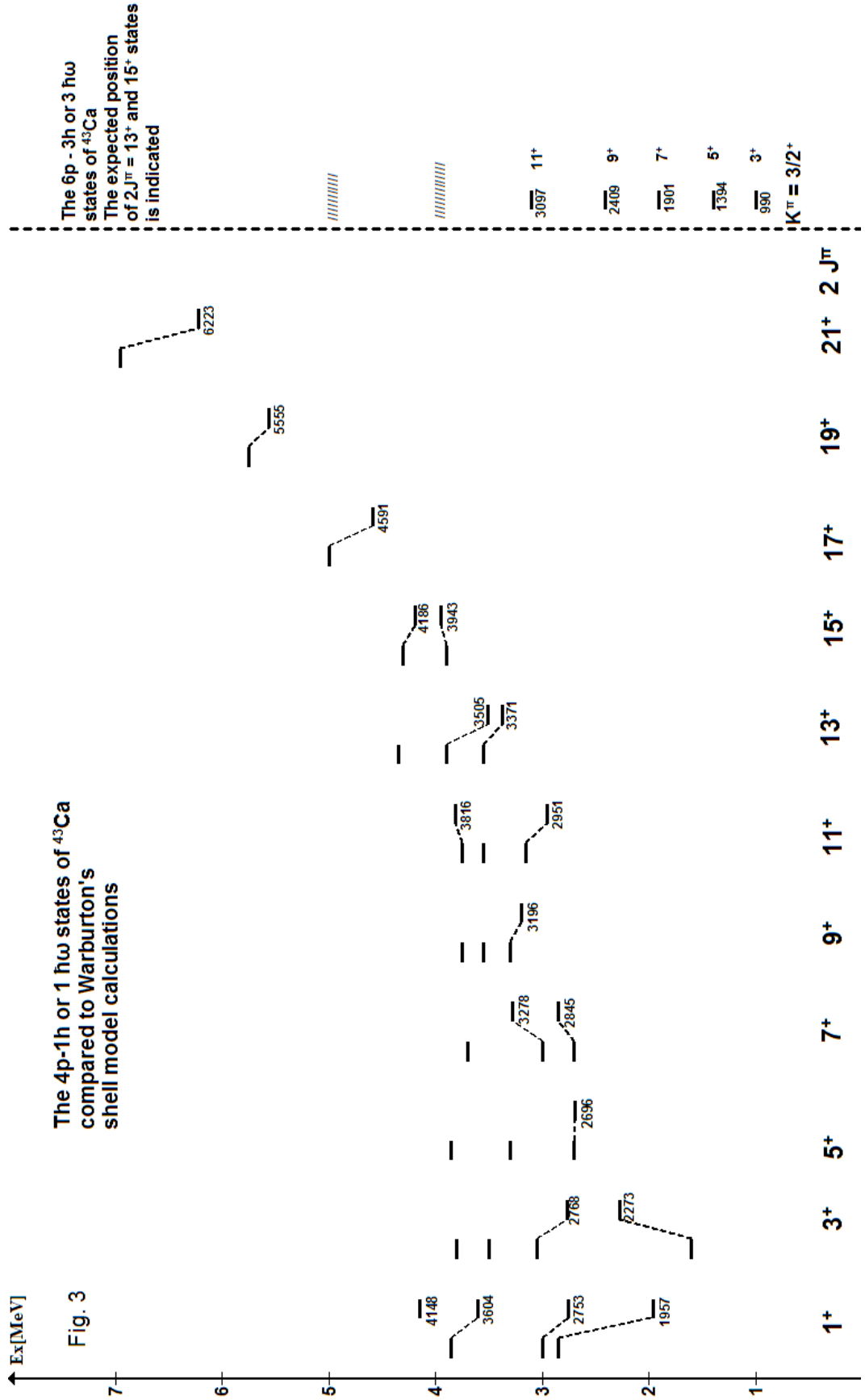

21. Decomposition of the ^{44}Ti level scheme

At the beginning we had little interest in ^{44}Ti because we had doubts concerning completeness of the experimental information *[4]*. The most important sources are α-particle transfer from ^{40}Ca with the (^{6}Li, d) reaction and feeding of ^{44}Ti levels from resonances of the ^{40}Ca(α, γ) reaction. The former reaction will miss levels of unnatural parity, the latter one high-spin states (say J > 4) because of low resonance-spin ($J^{\pi} = 0^{+}, 1^{-}, 2^{+}$). On the other hand 0 ħω excitations are theoretically under control due to shell model calculations in the complete $(f - p)^4$ basis space *[6]*. A comparison with experiment is given in the left part of Table 1. The level spectrum seems to contain already a rotational band (the $K^{\pi} = 0_1^{+}$ band which, however, gets shaky at $J^{\pi} = 6^{+}$ *[20]*) while the remaining states seem to be spherical. The overwhelming number of levels below 5 MeV is not explained and should constitute, in our concepts, rotational bands which are based on configurations with n = 1 - 4 holes in the N = 2 major shell and, accordingly, n = 5 - 8 particles in the N = 3 major shell. It turns out that all unexplained states can be ordered into bands. Vice versa it is evident that two levels of unnatural parity ($J^{\pi} = 4^{-}$ and 5^{+}) are missing. This is not embarrassing as explained above. In addition one $J^{\pi} = 5^{-}$ level, possibly two, are missing. On the other hand there is no convincing explanation of the 5210 KeV, $J^{\pi} = 4^{+}$ state. If, however, the L = 4 assignment in α - transfer to this state were misjudged by just one unit, we could have here a missing $J^{\pi} = 5^{-}$ state.

Table 1

Decomposition of the ^{44}Ti level scheme for $E_x \leq 5421$ KeV

$(f\text{-}p)^4$ states			Members of rotational bands (E_x[KeV], J^π)																					
J^π	E_x[KeV]			$K^\pi = o_2^+$			$K^\pi = 2_1^+$			$K^\pi = 2_2^+$			$K^\pi = o_4^+$			$K^\pi = o_3^+$			$K^\pi = 3_1^-$			$K^\pi = 0_{odd}^-$		$K^\pi = 3_2^-$	
	Exp.	SM																						
0^+	0	0	$K^\pi=0_1^+$	0^+	1904		2^+	2886		2^+	4792[a]		0^+	4840		0^+	4605		3^-	3175		1^-	3755	3^-	3942
2^+	1082	1441		2^+	2530		$3^+(2^+)$	3415		(3^+)	5421[b]					2^+	5055		4^-	3645		(3^-)	4227[b]	4^-	missing
4^+	2454	2598		4^+	3364		4^+	3980											5^-	4061			Possibly $J^\pi = 5^-$ at 5210, see text		
6^+	4015	3617		6^+	4499		5^+	missing											6^-	5148					
2^+	4116	3594																							
4^+	5305	4761																							
0^+	>5421	5065																							
possibly																									
4^+	5210	6107																							

a) Table 44.21 of compilation

b) The only level which fulfills the J(J+1) rule

Decomposition of the ^{44}Ti level scheme for $E_x \leq 5421$ KeV

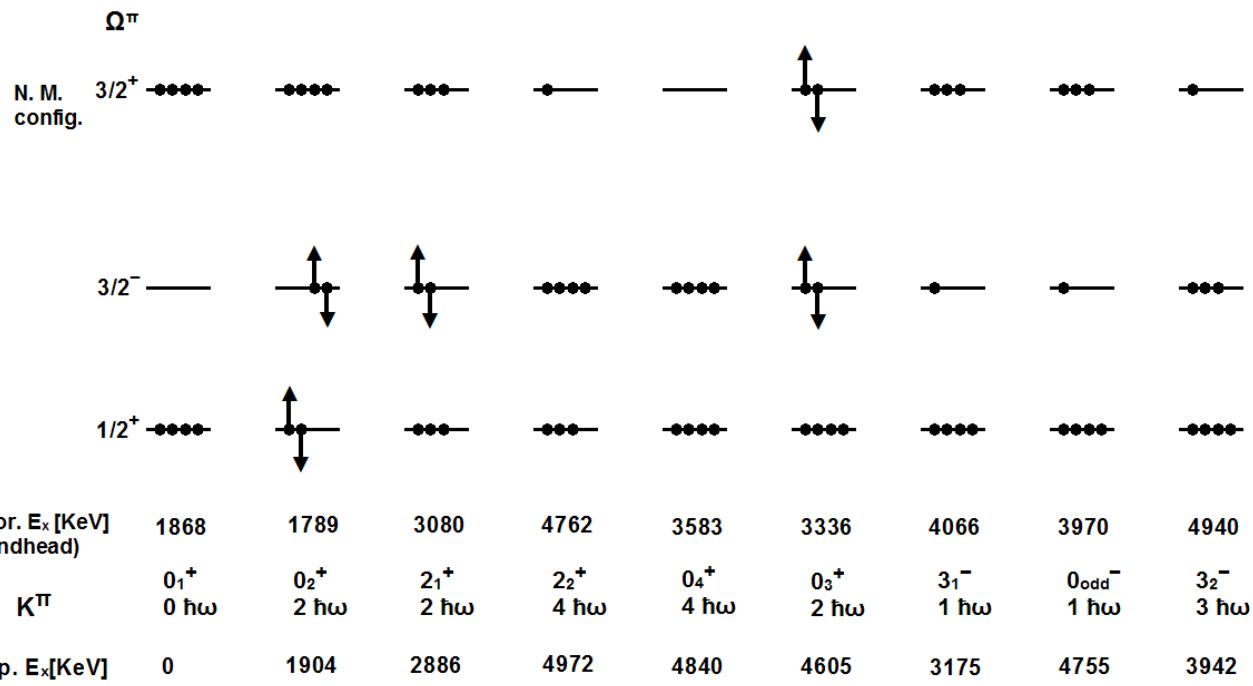

The lowest lying bands, as they are proposed in the upper part of Table 1 have, in our version of the Nilsson model, configurations with eight nucleons distributed across three orbits. They are displayed in the lower part of the table, together with the calculated bandhead energies, and compared to the experiment. The agreement is satisfactory except for the $K^{\pi} = 0^{+}$ bands, which were henceforth circumvented in establishing the Hamiltonian. The $K^{\pi} = 0^{+}$ configurations are due to orbit occupancies 4, 4, 0 and 4, 2, 2 which yield T = 0 states in the first case and T = 0, 1, 2 states in the second one. Hence evidence from ^{44}Sc and ^{44}Ca will turn out to be useful. Separate notes on these nuclei follow immediately. The naive expectation is that the first two $K^{\pi} = 0^{+}$ bandheads are based on a 4, 4, 0 distribution of nucleons. According to our calculations this is not the case for the second one. Also the binding energy of the first band, the g.st. band, is underestimated by 1.8 MeV (or 2.5 percent which sounds better!). In a plot of energy versus deformation ð the $K^{\pi} = 0^{+}$ bands must correspond to badly developed minima.

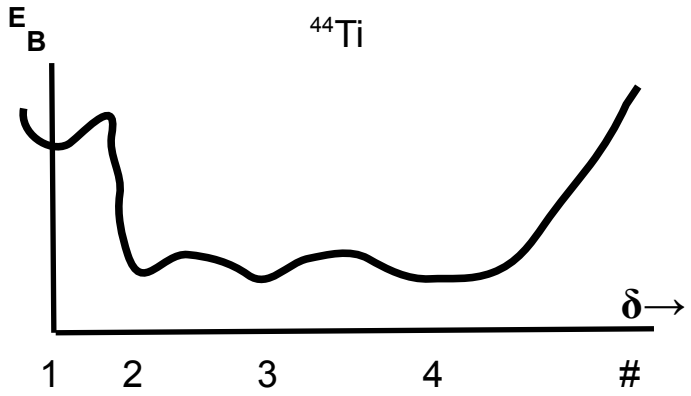

The number of particles in the N = 3 major shell amounts to four in the case of minima # 1, 2, to six in # 3 and eight in # 4. (The situation in #1, 2 is well described in Warburton's shell model calculation).

In ^{44}Sc (T = 1) and ^{44}Ca (T = 2) minima # 2, 4 are missing, in the case of # 2 because four particles in the N = 3 shell yield no deformation yet for T > 0, in the case of # 4 because T > 0 is not possible. Thus it is advisable to begin the discussion of $K^{\pi} = 0^{+}$ bands associated with minimum #3 and with the case of ^{44}Ca.

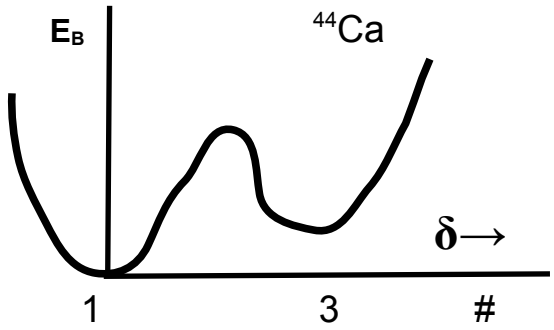

In separate notes which follow immediately we have located two $K^{\pi} = 0^{+}$ bands in ^{44}Ca with bandheads at E_x = 1883 KeV and 3580 KeV, corresponding to energies of 11113 KeV and 12810 KeV in ^{44}Ti. The second band differs from a ^{40}Ca, $K^{\pi} = 0^{+}$, T = 2 band with starting point at 14109 KeV only by the presence of a rather inert K', T' = 0, 1 quartet in the higher lying $\Omega^{\pi} = 3/2^{+}$ orbit (Fig.1). Hence the isospin splitting of the T = 2, 1, 0 triplet of bands in ^{40}Ca can be adopted for A = 44. As a consequence we predict the K^{π}, T = 0^{+},1 state in ^{44}Sc at 1405 KeV and identify it in Table 2 of our ^{44}Sc notes with the 1652 KeV state. The corresponding energy in ^{44}Ti is 8259 KeV. The K^{π}, T = 0^{+}, 0 bandhead is predicted at 3913 KeV in ^{44}Ti while the nearest experimental candidate occurs at 4605 KeV. If we assume that the latter state has been pushed up by 700 KeV due to interaction with the (experimental) 1940 KeV, $K^{\pi} = 0_2^{+}$ level then the unperturbed position of the latter level is E_x = 2.6 MeV. The leading configurations of the interacting states amount to roughly 75 percent in amplitude squared. The second $K^{\pi} = 0_2^{+}$ band in ^{44}Ti is thus connected with a 4, 2, 2 occupancy of orbits rather than 4, 4, 0.

The second T = 2 band with head at 11113 KeV in ^{44}Ti has its T = 0 partner in the experimental bandhead at 4840 KeV while the T = 1 partner is unknown. However the ^{44}Sc spectrum has possibly a candidate in the unsafe 829 KeV state in Table 44.12 of Endt's compilation *[4]*. The corresponding energy in ^{44}Ti is 7427 KeV and the triplet of $K^{\pi} = 0^{+}$, T = 0, 1, 2 bandheads shows a T(T+1) dependence of energies in Table 1. In the T = 0, 1, 2 triplet discussed before, the T = 1 part seems to deviate somewhat. We believe that the reason has something to do with the different symmetries of the isospin functions for T = 0, 2 and T = 1.

There remains the problem of the g.st. band where the present version of the Nilsson model underestimates the binding energy by 1.8 MeV. We seek the solution in the neighbouring ^{45}Ti. The g.st. has $J^{\pi} = 7/2^{-}$, indicating sphericity. With the Nilsson model we obtain a $K^{\pi} = 3/2^{-}$ rotational band at exactly the ground state energy. We do not have experimental data at hand but an old shell model calculation within an $(f_{7/2})^5$ space. The first three levels occur within 200 KeV and have, in order of ascending energy, $J^{\pi} = 7/2^{-}$, $3/2^{-}$, $5/2^{-}$. It appears that spherical and deformed states are degenerate so that considerable mixing and energy-shifts are possible. The spectrum of positive parity states is, on the other hand, completely rotational from the beginning.

Conclusion: Four or five particles in the N = 3 shell are not able to establish ground state deformation if they are not accompanied by holes in the N = 2 shell, preferably the $d_{3/2}$ subshell. The ^{44}Ti g.st. "band" is a hybrid which, however, is reproduced in Warburton's shell model calculation. The first well deformed ground state occurs in ^{46}Ti with six particles in the N = 3 shell.

Fig. 1

2p-2h excitations of the Nilsson model, relative to the lowest - energy configuration, in ^{44}Ti and ^{40}Ca

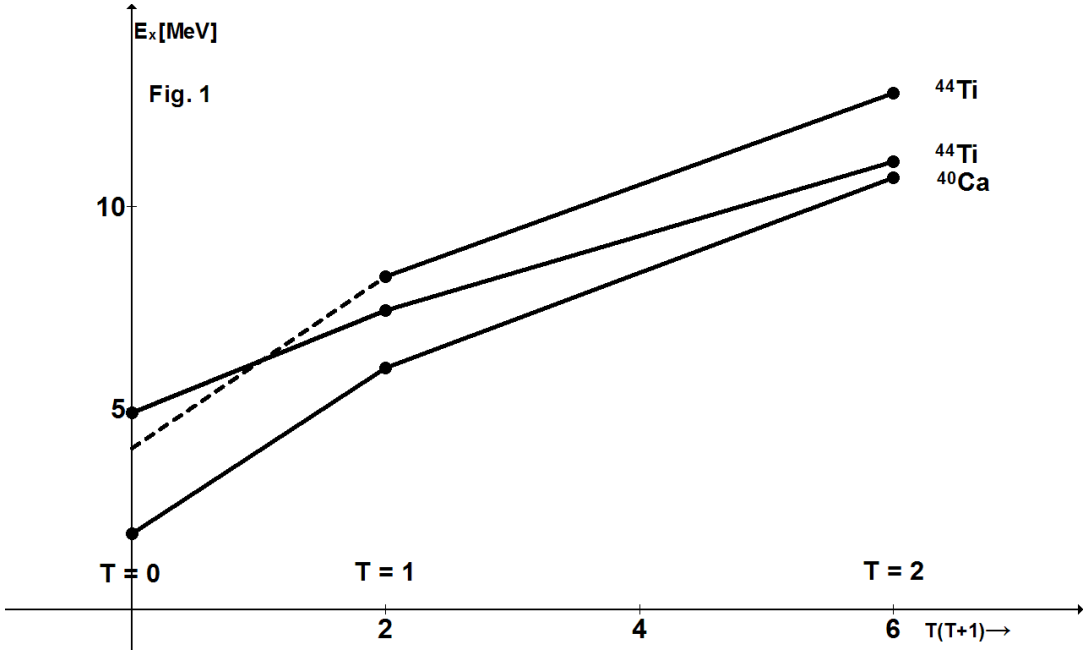

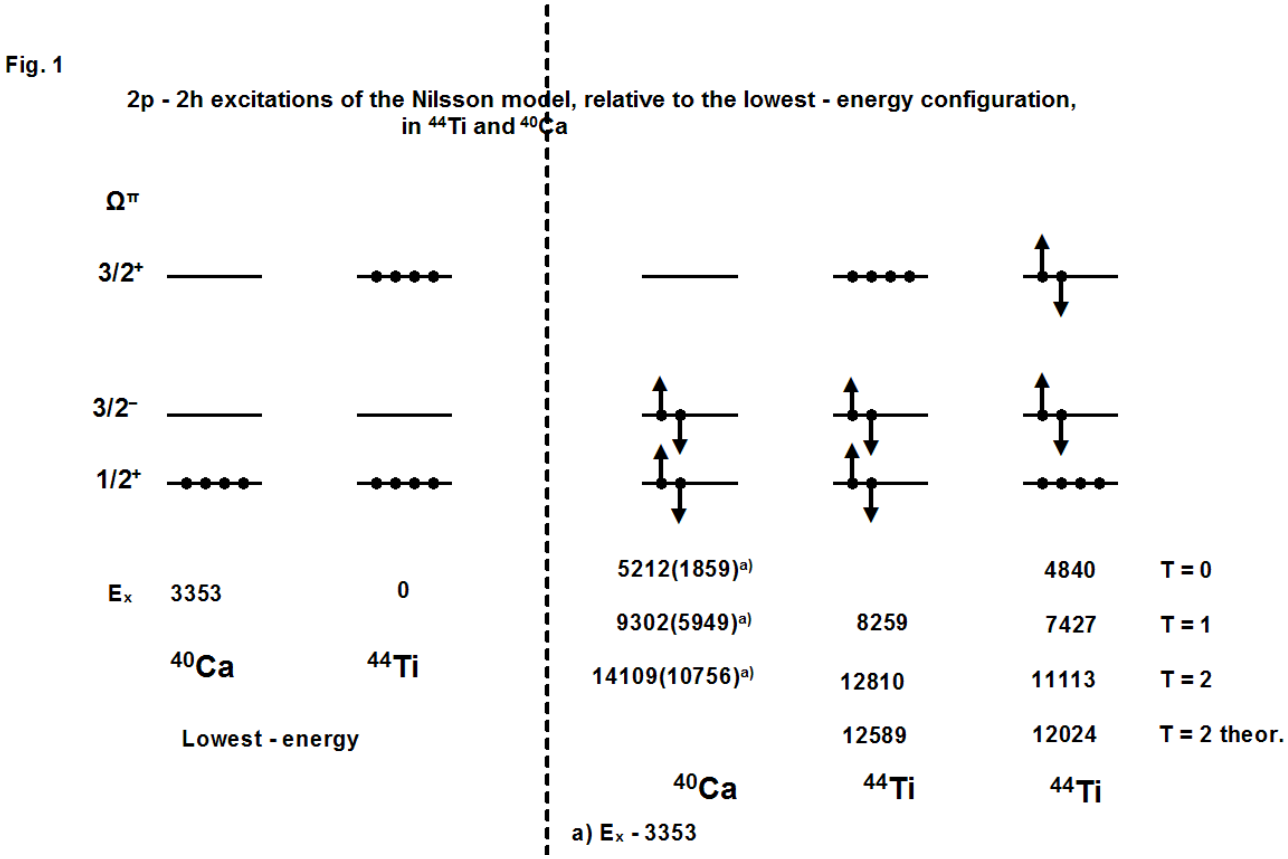

22. The level scheme of ^{44}Sc

In the ^{44}Sc g.st. and excited 0 ħω states we have four nucleons in the N = 3 major shell coupled to T = 1. The spectrum of these states has been calculated by Warburton *[6]* and it consists of spherical states. The spectrum of n ħω excitations with n > 0 on the other hand consists of deformed states. The underlying Nilsson model configurations are obtained by distributing eight nucleons across three orbits, coupled to T = 1. The possible occupancies of orbits are 4, 3, 1 and 4, 2, 2. The configurations which are relevant (according to our Hamiltonian) for E_x < 2 MeV are given in Table 1. With these predictions in mind it is possible to complete and interpret the experimental level scheme of Endt's compilation. This is done in Table 2 and Fig. 1 where the results of Table 2 with respect to deformed states are repeated in drawing. Two amendments to Endt's compilation are necessary. The (α, p) reaction in his Table 44.11e feeds high-spin states (J ≥ 4) only except for the 667 KeV, $J^\pi = 1^+$ state. We are obviously dealing with an unresolved doublet, with the second state having E_x = 674 KeV according to (α, p). Since we are in bad need of a very low lying $K^\pi = 2^+$ bandhead we perform a $J^\pi = 2^+$, $K^\pi = 2^+$ assignment to the second state. The prospective $J^\pi = 3^+$ and 4^+ members of the band can be located at the proper energies according to the J(J+1) rule and the $4^+ \rightarrow 2^+$ inband decay has been observed.
There is an unsafety as to the existence of a E_x = 829 KeV level which is mentioned in Table 44.12a however discarded in the master Table 44.11. Our analysis of ^{44}Ti, ^{44}Ca, and of the A = 40, T = 0, 1, 2 system suggests existence of a J^π, $K = 0^+$, 0 state around this energy. More on this topic in our ^{44}Ti notes (p. 315).

The experimental levels for $E_x \leq 1595$ KeV can be associated, completely, with theoretical ones. An explanation is also possible for the next two levels at

1648 KeV and 1651 KeV and of another five levels up to and including the 2031 KeV state. In the case of deformed states we notice a general tendency of the theory to predict bandheads roughly 1 MeV above the experimental one. This is not serious because actually we calculate a binding energy of around 70 MeV relative to an ^{36}Ar core. On the other hand relative bandhead energies for $K^{\pi} = 0_{1e}^{-}, 0_{1o}^{-}, 3^{-}$; T = 0, 1 are well reproduced which is trivial because they were used to specify the interaction of an odd number of nucleons in the $\Omega^{\pi} = 3/2^{+}$ and $3/2^{-}$ orbits. More details are given in separate notes concerning the interaction(p. 204).

Table 1

Nilsson model configurations of ^{44}Sc (T = 1) rotational bands

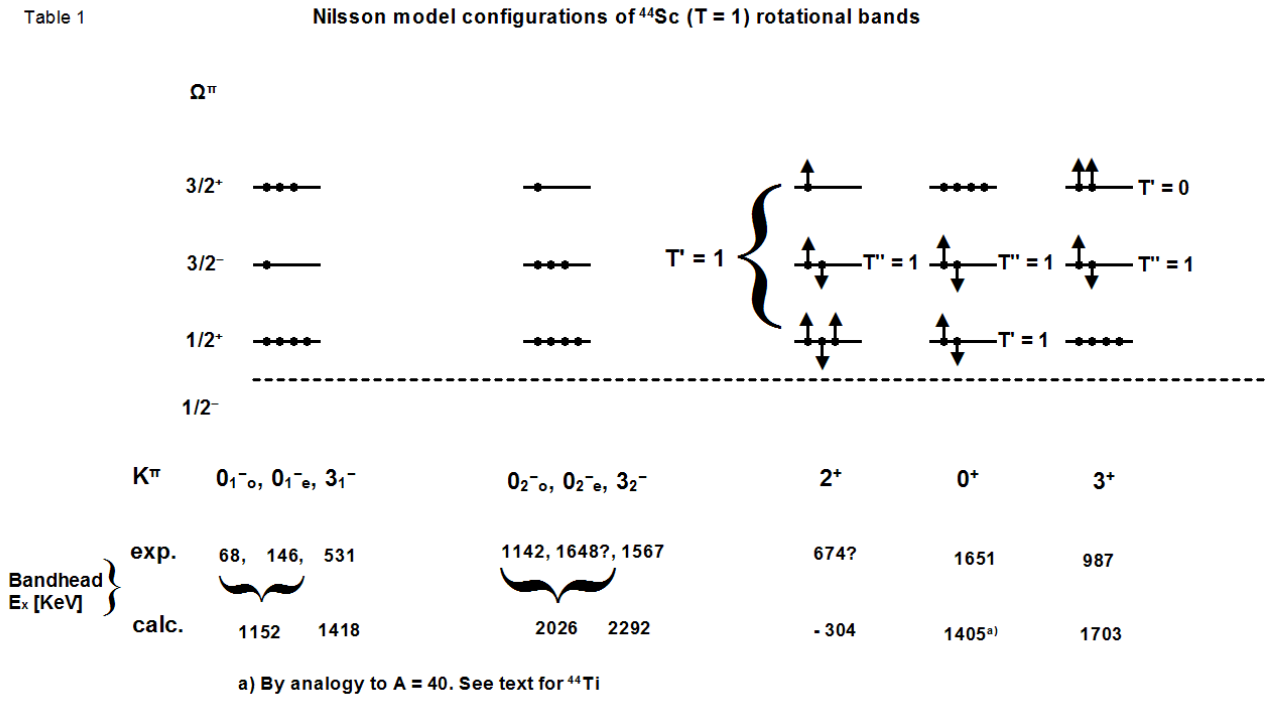

Table 2

The ^{44}Sc level scheme					
Level		J^{π}		K^{π} or shell model E_x [KeV]	
E_x[KeV]		Compilation	Present		
0		2^+		0	
68		1^-		0_1^-,o	
146		0^-		0_1^-,e	
235		2^-		0_1^-,e	
271		6^+		578	
350		4^+		438	
425		3^-		0_1^-,o	
531		3	3^-	3_1^-	
631		4^-		0_1^-,e	
667 674	}	1^+	1^+ 2^+	775 2^+	}
763		3^+		821	
968		$(5, 7)^+$	7^+	1326	
987		3^+		3_1^+	
1006		$3, 4^-$	4^-	3_1^-	
1050		$(3, 5)^+$	5^+	1242	
1142		$\pi = u$	(0^-)	0_2^-,e	
1186		3^+		2^+	
1197		$4^+, 5^-$	5^-	0_1^-,o	
1326		3^+		1337	
1427		2^-		0_2^-,e	
1507		$(2 - 5)^+$	3^+	3_2^+ ?	
1532		5^+		1577	
1567		3^-		3_2^-	
1595		$(2 - 5)^+$	4^+	3_1^+	
1648					Decay to 68 KeV, 1^-

The ^{44}Sc level scheme Cont'd					
Level		J^{π}		K^{π} or shell model E_x [KeV]	
E_x[KeV]		Compilation	Present		
1651					Decay to 0 KeV, 2^+
1681		$(4, 6)^-$	6^-	0_1^-,e	
1728			4^+	1955	Decay to 1050 KeV, 5^+
1768		3^+	4^+	2^+	Decay to 674 KeV, interpreted as $4^+ \rightarrow 2^+$ inband decay
…					
1986		$(3, 4)^-$	4^-	3_2^-	
2031		4^-		0_2^-,e	

Fig.1

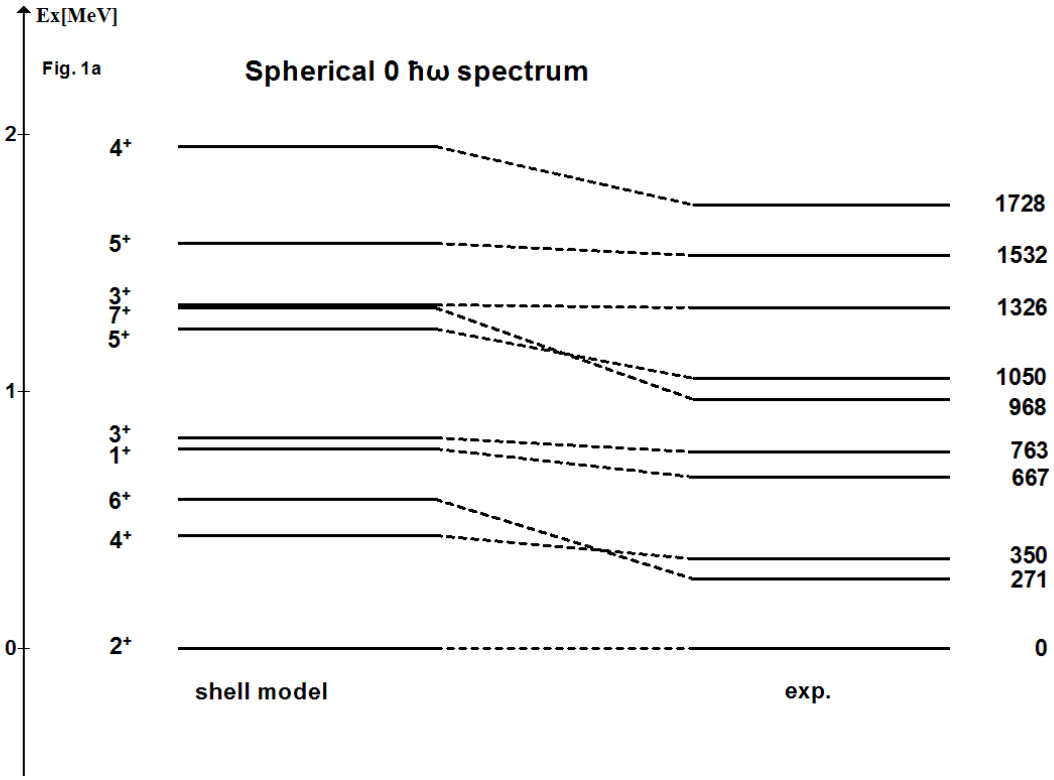

Fig.1 cont'd

^{44}Sc Rotational bands

(T = 1 throughout)

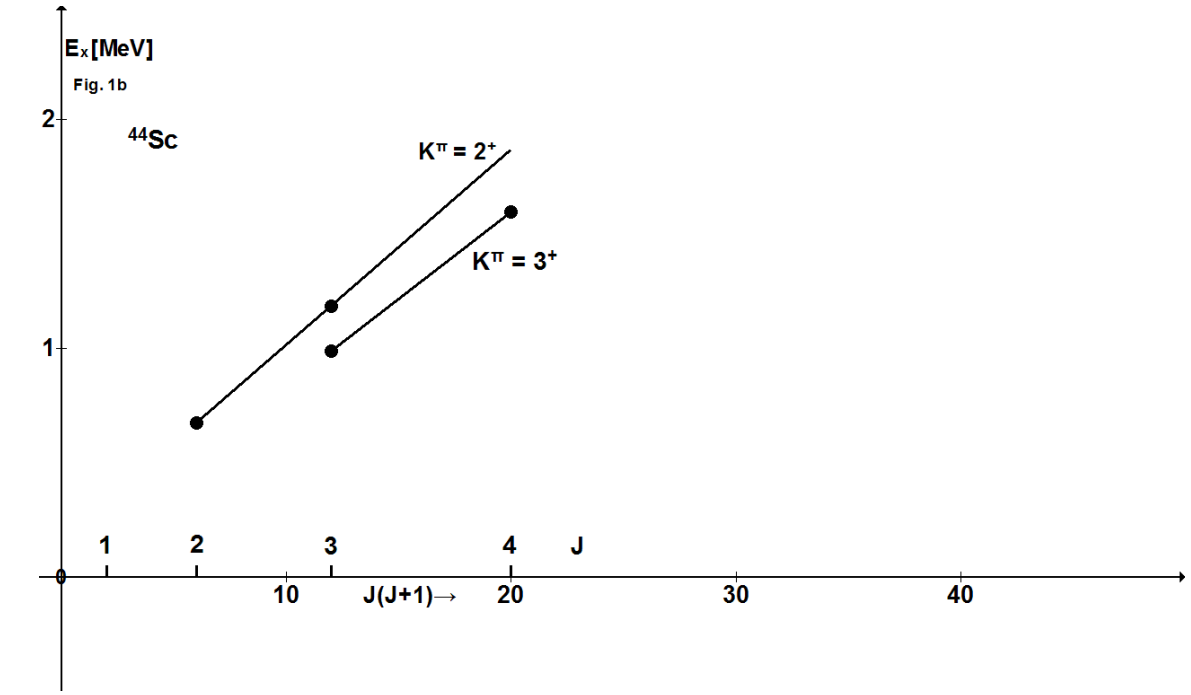

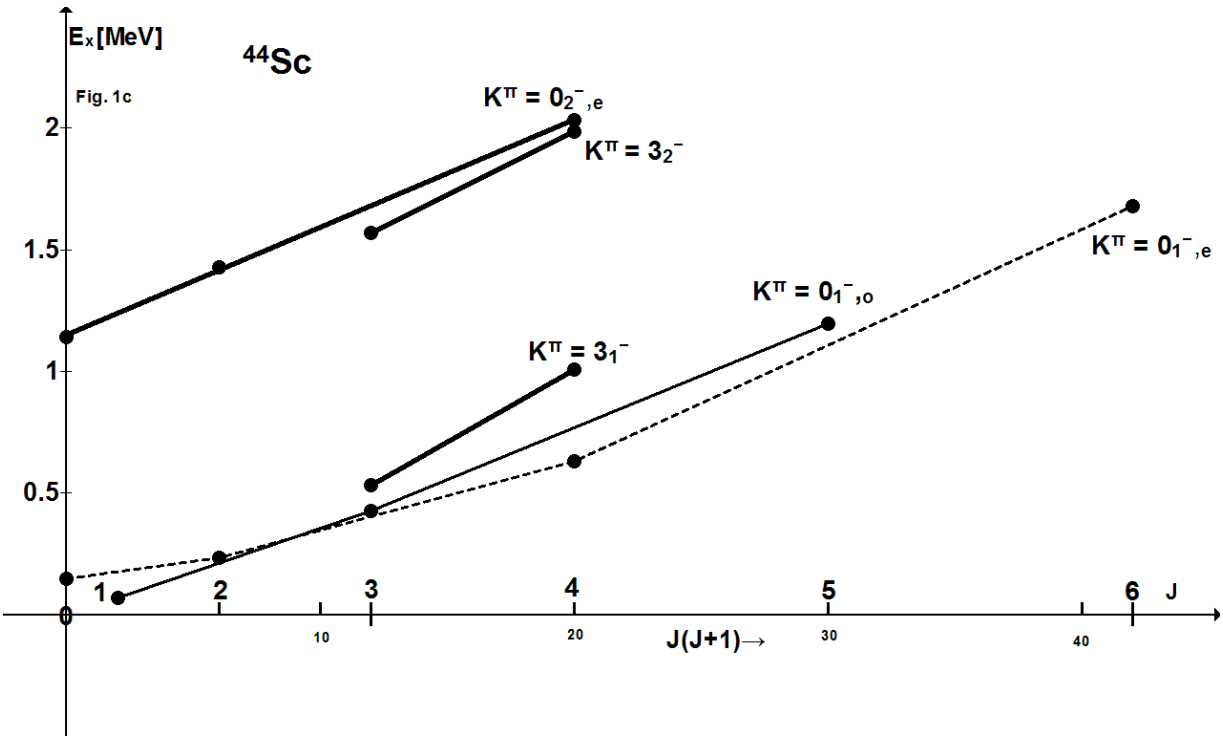

23. The energy levels of ^{44}Ca

The low lying levels of ^{44}Ca have isospin T = 2 and are of interest in connection with our analysis of ^{44}Ti which has T = 0 states for the first 6.6 MeV in excitation. The positive parity states of ^{44}Ca will arise in first place from a configuration with four particles in the (f-p) shell and they will be (near) spherical in nature. A shell model prediction of these states is available *[6]*. Negative-parity states will arise from the promotion of a single nucleon from the (s-d) into the (f-p) shell. The first states to be observed will inevitably belong to a $J^{\pi} = 2^{-} - 5^{-}$ quartet which is based on the coupling of an $f_{7/2}$ particle with a $d_{3/2}$ hole. The expectations are born out by experiment as shown in Fig. 1, except for a superfluous triplet of states, which apparently form a $K^{\pi} = 0^{+}$ rotational band, and a doublet which would equally form a $K^{\pi} = 0^{+}$ band. The bandheads at 1883 KeV and 3580 KeV have analogs in ^{44}Ti near 11113 KeV and 12810 KeV. The character of a known $J^{\pi} = 0^{+}$ state in ^{44}Ca at 5864 KeV (corresponding to 15197 KeV in ^{44}Ti) as belonging to or being outside the $(f\text{-}p)^4$ shell model space is not decided here. The shell model calculations provide a $J^{\pi} = 0_3^{+}$ state sufficiently close (Fig. 1). An interpretation of the proposed $K^{\pi} = 0^{+}$ rotational bands is given in our analysis of ^{44}Ti. The results in short are given in the insert.

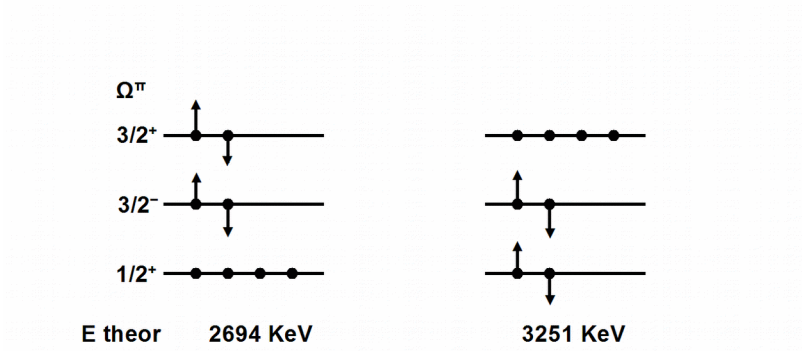

Fig. 1

The $E_x \leq 4260$ KeV levels of ^{44}Ca and the alleged 5^+ and 6^+ states above

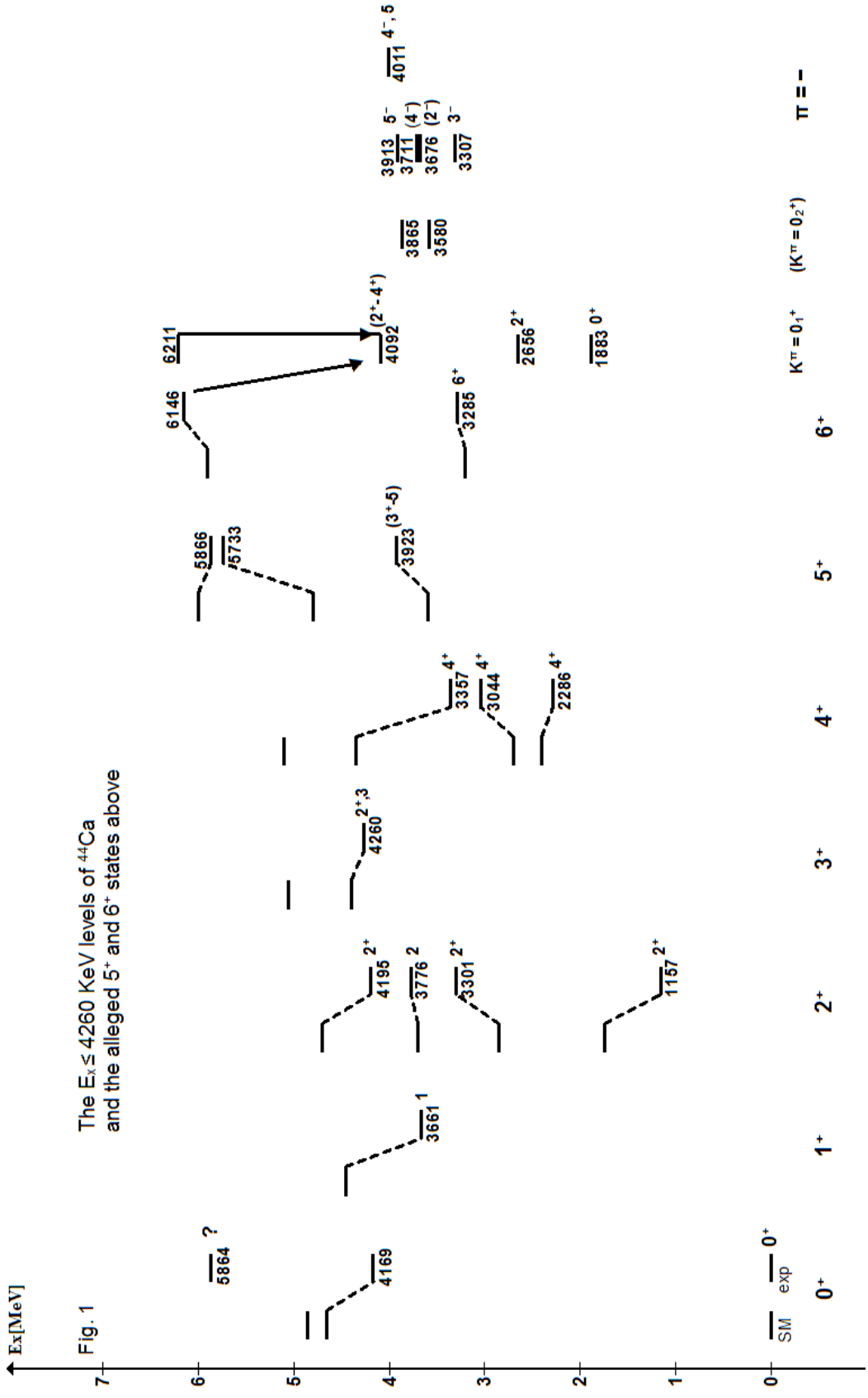

24. References for Part III

1. F. Glatz et al., Z. Physik A 278, 319 (1976)
2. Th. Kern et al., Z. Physik A 294, 51 (1980)
3. E. Bitterwolf et al., Z. Physik A 313, 123 (1983)
4. P. M. Endt, Nucl. Phys. A 521, 1 (1990)
5. P. M. Endt, Nucl. Phys. A 633, 1 (1998)
6. E. K. Warburton et al., Phys. Rev. C 41, 1147 (1990)
   and BNL report 40890 (1987)
7. R. Bansal, J. B. French, Phys. Lett. 11, 145 (1964)
8. D. M. Brink, A. K. Kerman, Nucl. Phys. 12, 314 (1959)
9. H. Röpke, Eur. Phys. J. A 22, 213 (2004)
10. H. Röpke et al., Eur. Phys. J. A 14, 159 (2002)
11. Mottelson Nuclear Structure Vol II, p. 577
12. F. Glatz et al., Z. Phys. A 293, 57 (1979)
13. P. Betz et al., Z. Phys. A 271, 195 (1974)
14. D. Rudolph et al., Phys. Rev. C 65, 034305-1 (2002)
15. W. J. Gerace, A. M. Green, Nucl. Phys. A 123, 241 (1969)
16. W. J. Gerace, A. M. Green, Nucl. Phys. A 93, 110 (1967)
17. Ideguchi et al., Phys. Rev. Lett. 87, 222501-1 (2001)
18. P. Betz et al., Z. Phys. A 276, 295 (1976)
19. F. Heidinger et al., Z. Phys. A 338, 23 (1991)
20. C. D. O' Leary et al., Phys Rev. C 61, 064314 (2000)
21. ENSDF: Evaluated Nuclear Structure Data File
    Brookhaven National Laboratory (2018)

Part IV

A Nilsson model interpretation of neutron rich isotopes of Mg, Na and Ne

1. Introduction

In Part II of our notes we have given a Nilsson model interpretation of s-d shell nuclei with neutron excess (N - Z) ≤ 3. Nuclides with larger excess were beyond our scope as experimentalists. Also they seemed less interesting because deformation of the nucleus is expected to decrease as neutron number approaches the value of 20. Here the orbits of the N = 2 major shell, the s-d shell, are completely occupied. Neutrons alone would make the nucleus spherical in its ground state. In the case of Ne, Na and Mg (Z = 10 - 12) however, protons reside in deformation driving orbits of the Nilsson model (Fig.1, p. 100 of Part II) so that some deformation might remain.

In the first part of these notes we will show that this is the case up to and including neutron number 18. Having proved this it is clear from the Nilsson model, that deformation will persist or even increase for larger neutron numbers. The reason is crossing of Nilsson orbits which emerge from the N = 3 major shell of the spherical shell model with orbits from the N = 2 shell. Thus in the configuration of minimum energy, N = 3 orbits can be occupied prior to the N = 2 orbits. The effect has got the name “inversion” and has been studied *[1]* in the frame of the spherical shell model where no level crossing is present. Nevertheless “inversion” emerges as a result of the residual interaction. The connection with nuclear deformation was also established by a calculation of quadrupole moments and transition rates which show enhancement. To our knowledge the alternative Nilsson model approach has not been persuaded systematically, yet.

2. Nuclides with less than 19 neutrons

The starting point of our analysis is the scheme of Nilsson orbits in Fig. 1, p. 100 of Part II which is repeated in Fig. 1 for deformation parameter ε = 0.33 which is adequate for ^{25}Mg. Rather than giving the usual quantum numbers [N n_z Λ] of the Nilsson orbits we give the more informative quantum numbers Ω^π and ($3n_z$ – N). The latter one indicates whether nucleons in this orbit drive the nuclide towards prolate deformation (positive value) or sphericity (negative value). Also given is the occupancy of orbits for the ground state of ^{24}Mg. By removing one or two protons from the $2\Omega_v^\pi = 3_1^+$ orbit we obtain the ground state configurations of ^{23}Na or ^{22}Ne. In all these cases we obtain a nuclide with healthy prolate deformation. Neutron rich isotopes can be generated by adding K', T' = 0, 1 pairs of neutrons or a single neutron into the orbits above the indicated Fermi boarder. The theoretical ordering of Nilsson orbits is confirmed experimentally by the heads of rotational bands in ^{25}Mg which have the configuration of a ^{24}Mg core plus a single nucleon. We have an almost identical situation in ^{21}Ne apart from the fact the ordering of the closely spaced $2\Omega_v^\pi = 1_3^+$ and 1^- orbits is inverted. This can happen at a slightly increased deformation (ε around 0.38) and can be expected because the ^{20}Ne g.st. is more deformed than the ^{24}Mg g.st. Also we have from ^{21}Ne the position of the $2\Omega_v^\pi = 3_1^+$ orbit. Up to 18 neutrons can be accommodated into the orbits below the $2\Omega_v^\pi = 1^-$ orbit so that inversion should not play a role yet. Instead a complete accounting of (positive parity) levels can be achieved by shell model calculations in the spherical s-d (N = 2) basis *[2]*. The accuracy is high, amounting to about 150 KeV. Hence a poor experimental knowledge of levels can be faithfully replaced by theoretical results. As explained before we wish to know whether the Nilsson model is disguised in these level schemes. The tool for doing this is in first place the J(J+1) rule of excitation energies. In Figs. 2 - 5 and 7 we give E_x versus J(J+1) plots

for the levels of the nuclides $^{28-30}$Mg, $^{26-29}$Na, $^{24-28}$Ne and, for later use, ^{29}Ne and ^{30}Na. For the ease of drawing error bars of level energies are omitted as well as the numerical values. The latter ones are given in Tables 1 - 5. In the case of even-even nuclei (Figs. 2a, 2b; 3a - 3c) presence of $K^\pi = 0^+$ ground state bands is immediately visible. The bandheads do not exactly follow the J(J+1) law. This can be attributed to "centrifugal stretching" of the nuclear shape. The bandhead does not rotate.

In the cases of even-odd nuclei (Figs. 4a - 4d; 5a, 5b) we observe several perturbations. Well known is the decoupling effect in K = 1/2 bands. The effect is directly noticeable in the ground state bands of ^{29}Mg and ^{27}Ne (Figs. 4d, 4b) where an odd neutron is residing the $2\Omega_v^\pi = 1_3^+$ orbit (Fig. 1). A large decoupling effect is also known for a configuration with an odd-particle in the $2\Omega_v^\pi = 1_1^+$ orbit (See ground state band of ^{19}F in Part II, Fig. 5, p. 105). This affects the ground state bands of the even-odd isotopes of Sodium which have $K^\pi = 3/2^+$ throughout. Corrioliscoupling between the $2\Omega_v^\pi = 1_1^+$ and 3_1^+ orbits of Fig. 1 is strong because both are derived from the same, $d_{5/2}$, orbit of the spherical shell model.

While this explanation might suffice for the A = 21, 23 and 25 isotopes of sodium which were already investigated in Part II, pages 110, 116, 125 (where we show the situation in ^{21}Ne rather than the mirror nucleus ^{21}Na), something else must have happened in ^{27}Na and ^{29}Na (Figs. 5a, 5b).

Within the Nilsson model we consider three angular momenta, collective rotation $\vec{R}$ of the $K^\pi = 0^+$ core and orbital angular momentum $\vec{l}$ and spin angular momentum $\vec{s}$ of the odd particle. If $\vec{l}$ aligns along $\vec{R}$ to yield intermediate angular momentum $\vec{J}'$ and if l = 2 than we get quantum number J' = 2, 4, 6….. If in addition $\vec{s}$ couples weakly to $\vec{J}'$ than presence of level-doublets with $J^\pi = 3/2^+, 5/2^+; 7/2^+, 9/2^+$; etc. is feasible. The doublet energies should have a R(R+1) dependence with R = 0, 2, 4, ….. We observe this in Fig. 6.

The effect of "centrifugal stretching", as it is known from normal $K^\pi = 0^+$ bands

in even-even nuclei is observable. In the cases of odd-odd nuclides ^{26}Na and ^{28}Na it seems fairly adventurous to claim presence of rotational bands. However if we count the number of levels with a given spin, we recognize that the Nilsson and the spherical shell model yield identical results (This is also true for ^{30}Na if we leave the $2\Omega_{\nu}^{\pi} = 1^{-}$ orbit, the intruder orbit, empty).

The K^{π} assignments to the rotational bands which we have proposed in Figs. 2 - 7 and Tables 1 - 5 find a ready explanation in Fig. 8. Here we construct the Nilsson model configurations of the ground states and the most elementary excitations. Intermediate quantum numbers K', T' are given where ever necessary. It is noteworthy that given $K^{\pi} = 4^{+}$ bands should be accompanied by $K^{\pi} = 1^{+}$ bands with equal occupancies of orbits but excitation energies higher by roughly 1.4 MeV (deduced from Table 8, see also p. 59 in Part II). Our analysis could not reach that far.

3. Nuclides with 19 or 20 neutrons

If we try to accommodate more than eighteen nucleons in the orbits of Fig. 1 we must occupy the $2\Omega_v^{\pi} = 1^-$ orbit (the intruder orbit) prior to the $2\Omega_v^{\pi} = 3_2^+$ orbit which is far away by roughly 2 MeV. In the case of twenty neutrons we have a K', T' = 0, 1 pair in the intruder orbit. In the case of nineteen neutrons the number can be one or two. (usually one speaks of 1 ħω or 2 ħω configurations). The configuration without neutrons in the intruder orbit (0 ħω configuration) is expected at higher energy.

The case of ^{31}Mg can serve for a demonstration since experimental information is rather complete. In Table 6 we have ordered the known levels according to their character as a n ħω excitation. The $K^{\pi} = 1/2_1^+$, $1/2_2^+$ and $5/2^+$ bands are just images of ^{29}Mg bands. We must just add a K', T' = 0, 1 pair of "spectator" neutrons into the intruder orbit. The configuration with just one neutron in the intruder orbit gives rise to a $K^{\pi} = 1/2^-$ rotational band with a large decoupling effect. The spin sequence of $3/2^-$,$7/2^-$, $1/2^-$, $5/2^-$ is well known from ^{25}Mg (p. 123 in Part II). The members of this band must be absent in allowed β-decay of ^{31}Na. The level at 673 KeV constitutes the first 0 ħω excitation, predicted *[1, 3]* in the first shell model calculation at $E_x = 700$ KeV with $J^{\pi} = 3/2^+$. The 3814 KeV level constitutes either the $J^{\pi} = 3/2_2^+$ or $J^{\pi} = 5/2_2^+$ state of 0 ħω character. Unsafe is the interpretation of the 2014 KeV level as a state of negative parity. Our argument is absence in allowed β-decay of ^{31}Na and γ-decay to the 221 KeV, $J^{\pi} = 3/2^-$ state.

At the present stage it has become evident that we are dealing with the phenomenon of shape coexistence in the isotopes of Mg (and possibly Na and Ne as well). For neutron number up to and including eighteen we have normal deformation ε_1 in the ground states and the excited states up to 5 MeV. For neutron numbers 19, 20 this deformation has practically vanished and near spherical states come first at $E_x = 673$ KeV in ^{31}Mg and, according to

USDA calculations by Brown and Richter *[3]*, at 2.7 MeV in ^{32}Mg. Instead a second type of levels with larger deformation ε_2 comes into play and provides the ground states. This new type of levels which arises from the occupation of the $2\Omega_\nu^\pi = 1^-$, intruder level of Fig. 1 should also be present in the Mg isotopes with A = 26 - 30. In the even-even isotopes we should observe $K^\pi = 0^+$ bands which are not contained in the USD shell model calculations *[2]* in the pure s-d model space. Racavy's renormalized formula (Part II, p. 62) predicts the following tendency for ε_1 and ε_2.

	^{26}Mg	^{28}Mg	^{30}Mg	^{32}Mg	^{34}Mg
ε_1	0.27	0.28	0.20	0.13	
ε_2	0.53	0.42	0.41	0.33	0.38

We have included a value of ε_2 for ^{34}Mg, assuming that the uppermost pair of neutrons goes into the $2\Omega_\nu^\pi = 3^-$ rather than 3_2^+ orbit of Fig. 1. For comparison we give the ground state deformation of ^{24}Mg as $\varepsilon = 0.38$.

The two values of deformation in ^{26}Mg differ by a factor of two. Hence an excited $K^\pi = 0^+$ rotational band with rotational constant $\hbar^2/2\Theta$ substantially smaller than 202 KeV, the value of the ground state band, must be sought. As it turns out all necessary data are already available in Parts I, II. We simply were not aware of the implications, yet.

The $J^\pi = 0^+$ bandhead is found in the 7428 KeV, $J^\pi = (0,1)^+$ state. In the mirror nucleus ^{26}Si we have the 7390 KeV, $J^\pi = (0^+)$ state (from L = 0 transfer in the ^{24}Mg(τ, n) reaction) and in ^{26}Al (where the T = 1 spectrum starts at 228 KeV) in the 7440 KeV, $J^\pi = 0(1, 2)$ T = 1 state *[4]*. The $J^\pi = 6^+$ band member is found in ^{26}Mg at 11320 KeV. This state is reached by an L = 6 transfer in the ^{24}Mg(α, ^{2}H) reaction *[5]* which proves its character as a two-particle excitation into the N = 3 major shell. The rotational constant can be calculated as $\hbar^2/2\Theta$ = 93 KeV and speaks for "superdeformation". It is also possible to identify the

$J^{\pi} = 2^{+}$ member of the band at E_x = 8033 KeV. (For more details see an add-on on Page 339).

As with ^{26}Mg we can identify the $J^{\pi} = 0^{+}$ head of the $K^{\pi} = 0^{+}$ "intruder" band in ^{28}Mg. From L = 0 transfer in the ^{26}Mg(t, p) reaction four $J^{\pi} = 0^{+}$ states are known *[4]* at E_x = 0 MeV, 3.86 MeV, 5.27 MeV and 5.7 MeV. The 5.27 MeV state is not predicted by the USD shell model calculations *[2]*.

The energy difference between the levels of lowest energy with deformation ε_2 and ε_1 is

	^{26}Mg	^{28}Mg	^{30}Mg	^{32}Mg	^{34}Mg
ΔE [KeV]	7428	5270	(1320)	−671	−2300

and goes almost parabolic with A. The ^{30}Mg value stems from the Nilsson model calculation given further below. The ^{32}Mg and ^{34}Mg values are adopted from the shell model calculations of *[1]*.The smooth A-dependence of ΔE is, in our opinion, in support of shape coexistence.

At the present stage we have gained information which enables us to implement our Nilsson model Hamiltonian of Part II, Tables 3, 4A, p. 92 and p. 93. The residual interaction depends (among others) from the interaction energies A_i of K', T' = 0, 1 neutron pairs in the identical orbit and of the interaction energies between n_i neutrons in orbit i with n_k neutrons in orbit k. This interaction energy is given by $n_i \bullet n_k (a_{ik} + c_{ik})$. The a_{ik} term yields the isospin independent contribution, usually negative, the c_{ik} term the isospin dependent part, usually positive. In Table 7 we have summarized the experimental data which serve to obtain missing interactions. The results are given in Table 8 which is an update of Table 4A, p. 93 in Part II.

We obtain the pairing energy A_i of the "intruder" orbit with principal quantum number N = 3, the $2\Omega\nu^{\pi} = 1^{-}$ orbit of Fig. 1, as 3863 KeV. It surmounts the values obtained previously for N = 2 orbits by at least 1.3 MeV.

Thus it becomes possible that a 2 ħω character must not only be assigned to the ground states of the Mg, Na and Ne isotopes with 20 but also to those with 19 neutrons while 0 ħω levels are safely remote. One could have expected a 1 ħω character of the ground state if single particle energies were considered only.

The final analysis with inclusion of the residual interaction is given in Table 9. Here we have calculated the binding energies of the lowest lying states with 2 ħω and 1 ħω character for the Mg, Na and Ne isotopes with 18, 19, 20 neutrons. We cannot calculate the energies of 0 ħω excitations but USD shell model calculations *[3]* yield very reliable values. Also given are experimental ground-state binding energies *[4, 6, 7]*. The Nilsson model predicts 2 ħω character for the ground states of the isotopes with 19 and 20 neutrons. In the isotopes with neutron number 19 we can predict 1 ħω excitations starting at E_x = 470 KeV and 40 KeV for, respectively, the even-odd nuclides ^{31}Mg and ^{29}Ne. They constitute the $J^\pi = 3/2^-$ members of a decoupled $K^\pi = 1/2^-$ band. This has already been confirmed experimentally for ^{31}Mg (Table 6). In the case of ^{29}Ne this level provides already the ground state *[6]* followed within 200 KeV by the $J^\pi = 3/2^+$ and $J^\pi = 1/2^+$ members of a decoupled $K^\pi = 1/2^+$ band of 2 ħω character. Apart from the inversion of bands the situation in ^{29}Ne is completely analogous to ^{31}Mg. We must simply remove a K', T' = 0, 1 pair of protons from ^{31}Mg to generate ^{29}Ne.

In the case of odd-odd ^{30}Na we have decidedly a 2 ħω character of the ground state, which could be the head of either a $K^\pi = 2^+$ or 1^+ rotational band. These arise (Fig. 1) from coupling an $2\Omega_v^\pi = 3_1^+$ proton to a $2\Omega_v^\pi = 1_3^+$ neutron. The values of $(b_{ik} - c_{ik})$ from Table 8 favour the $K^\pi = 2^+$ band energetically by 572 KeV. The experimental ground state spin is in fact J = 2.

In the isotopes with neutron number 18 we have a 0 ħω character of the ground state. However, we are not able to completely generate the experimental binding energy of the ^{28}Ne g.st. The amount of 1.7 MeV is missing.

If we had calculated the ^{29}Ne and ^{30}Ne energies relative to the experimental g.st. energy of ^{28}Ne, then good agreement would have been achieved.

4. Nuclides with more than twenty 20 neutrons

The successful Nilsson model interpretation of the Mg isotopes up to and including the neutron number 20 inspires an extension to larger neutron numbers. The ground state configuration of ^{33}Mg must be that of a deformed, $K^\pi = 0^+$ core plus a neutron in either of the closely spaced (Fig. 1) orbits with $2\Omega_\nu^\pi = 3_2^+$ or $2\Omega_\nu^\pi = 3^-$. The Nilsson model diagram of Fig. 1 in Part II, p. 100 predicts a crossing of these orbits around $\varepsilon = 0.34$. The $K^\pi = 3/2^+$ and $K^\pi = 3/2^-$ bands associated with these orbits start at $E_x = 6362$ KeV and $E_x = 7441$ KeV in ^{25}Mg but in reversed ordering at $E_x = 2462$ KeV and $E_x = 3050$ KeV in ^{41}Ca (Part II, Fig. 17a, p. 176, p. 124 and Part III, Table 2, p. 286). Thus the theoretical situation for ^{33}Mg is open. The most recent experimental information *[7]* is a $J^\pi = 3/2^-$ assignment to the ground state.

Hence the $2\Omega_\nu^\pi = 3/2^+$ orbit remains empty. The same is true if we add another neutron to form the ^{34}Mg g.st. Because of the deformation driving character of the $2\Omega_\nu^\pi = 3^-$ orbit the deformation parameter ε increases from $\varepsilon = 0.33$ in ^{32}Mg to $\varepsilon = 0.38$ in ^{34}Mg. The $J^\pi = 3/2^-$ assignment to the ^{33}Mg ground state also clarifies the situation in ^{32}Na which is obtained by removing a $2\Omega_\nu^\pi = 3_1^+$ proton. There should be a ground state band with either $K^\pi = 0^-$ or 3^-. The early shell model predictions of *[1]* can be interpreted in a way that the $J^\pi = 0^-$ and $J^\pi = 2^-$ even-spin members of the first band occur at excitation energies of 0 KeV and 329 KeV, the $J^\pi = 3^-$ and $J^\pi = 4^-$ members of the second band at 73 KeV and 424 KeV. The same prediction for positive-parity states can be interpreted in terms of a $K^\pi = 0^+$ band with its $J^\pi = 0^+$ and 2^+ states at $E_x = 487$ KeV and $E_x = 711$ KeV and its $J^\pi = 1^+$ and $J^\pi = 3^+$ members at $E_x = 750$ KeV and $E_x = 895$ KeV.

The recovery of deformation in the ^{34}Mg g.st. can be the reason for still another orbit crossing in the case of ^{35}Mg. The $2\Omega^\pi = 5^-$ orbit, derived from the $f_{7/2}$ shell model state (no more given in Fig. 1, p. 100 of Part II) will cross our

$2\Omega_v^{\pi} = 3_2^+$ orbit around ε = 0.47. The experimental information for ^{35}Mg is still scanty. However there exists a Monte-Carlo shell model calculation in the (s-d − f-p) space *[8]*. The authors predict levels up to 1130 KeV excitation energy and give the wave function contents in terms of n ħω excitations. We notice that they have generated a Nilsson model spectrum with four rotational bands. The E_x [KeV], $2J^{\pi}$ of levels are

$2K^{\pi}$:	5^- (2 ħω)	1^- (2 ħω)	3^+ (1 ħω)	3^- (0+2 ħω)
	0, 5^-	30, 3^-	360, 3^+	790, 3^-
	766, 7^-	350, 7^-	810, 5^+	1130, 5^-
		400, 1^-		

An interpretation of the alleged bands is given in the subsequent drawing, where the distributions of neutrons are displayed.

Fig. 10

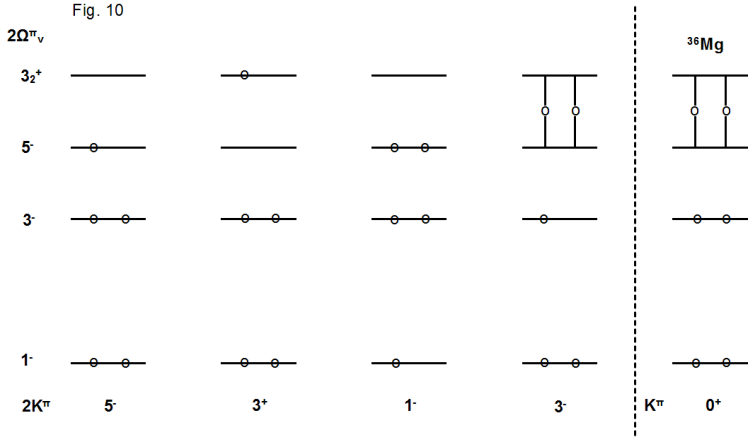

The proposed interpretation of the $2K^{\pi} = 1^-$ band is not without an alternative, as detailed below. It explains, however, the large decoupling effect. The sequence of levels with $2J^{\pi} = 3^-$, 7^- and 1^- is known from ^{25}Mg (Fig. 17A, p.123 in Part II).

In the case of the $2K^{\pi} = 3^-$ band we have an equal probability of finding a neutron pair in the $2\Omega_v^{\pi} = 5^-$ and 3_2^+ orbits. This follows from the shell model

calculations of *[8]*. Similar calculations for ^{36}Mg *[9]* yield a $K^{\pi} = 0^{+}$ ground state band with the same mixing of orbits.

We come back to the $2K^{\pi} = 1^{-}$ band. Rather than having a hole in the $2\Omega_{\nu}^{\pi} = 1^{-}$ orbit of our drawing we could have a particle in the $2\Omega^{\pi} = 1^{-}$ [321] orbit which originates from the $2p_{3/2}$ shell-model state. This orbit becomes just visible in Fig. 1, p. 100 of Part II. If not in ^{35}Mg, this orbit will be of importance for the ^{40}Mg g.st. Due to its deformation driving character it will get occupied prior to the sphericity driving $2\Omega^{\pi} = 7^{-}$ orbit which originates from the $1f_{7/2}$ shell model state.

5. Conclusion

The Nilsson model with empirical residual interaction does not only work for nuclei near the line of stability but also for the neutron-rich isotopes of Ne, Na, and Mg (Z = 10-12). These nuclei are deformed due to the protons which reside in deformation driving orbits. The diagram of Nilsson orbit shows several level crossings which give rise to shape coexistance. All what is known experimentally can thus be explained.

The Nilsson model phenomenology is contained in shell model calculations which start from a spherical basis. For neutron number up to and including 18 the s-d shell basis space is sufficient. At larger neutron numbers the (f-p) space must be included. The advantage of the shell model is its more general character. It is not restricted to deformed nuclei. The advantage of the Nilsson model is its simplicity, giving immediate insight into the underlying physics.

6. An add-on concerning ^{26}Mg

In the supplement to his compilation *[4]* P. M. Endt has identified (Table 26K) the 7428 KeV, $J^{\pi} = (0,1)^{+}$ state with the theoretical $J^{\pi} = 1_3^{+}$ state, predicted at 7721 KeV by shell model calculations in the unrestricted s-d basis space *[2]*. We have instead given good reasons that we are dealing with a $J^{\pi} = 0^{+}$ state from outside this space. It would be very satisfying if a replacement of the then missing $J^{\pi} = 1_3^{+}$ state could be found. There is a single possibility. A E_x = 7840 KeV level shows an awkward γ-decay to the $J^{\pi} = 2_1^{+}$, 2_2^{+}, 0_2^{+} and 4_1^{+} levels. We suspect a doublet consisting of the $J^{\pi} = 1_3^{+}$ level and a level of higher spin. The $J^{\pi} = 1_3^{+}$ level is responsible for decay to the $J^{\pi} = 0_2^{+}$ state, the level of higher spin for decay to the $J^{\pi} = 4_1^{+}$ state.

The $J^{\pi} = 1_3^{+}$, T = 1 state is known in ^{26}Al and occurs 7652 KeV above the lowest lying T = 1 state (at E_x = 228 KeV). A $J^{\pi} = 3^{-}$ state at E_x = 8131 KeV occurs 7903 KeV above the lowest lying T = 1 state. This level could be the analogue of the level with higher spin in the 7840 KeV doublet of ^{26}Mg.

By giving up the idea of a single level at 7840 KeV, which necessarily would have had a $J^{\pi} = 2^{+}$ assignment, we could improve our understanding of levels with this spin-parity. The levels with s-d configuration #9 and #10, predicted *[2]* at E_x = 7473 KeV and 8391 KeV occur at E_x = 7816 KeV and 8532 KeV. In between we have the 8033 KeV, $J^{\pi} = 2^{+}$ level which is member of the $K^{\pi} = 0^{+}$ “intruder” band.

7. References for Part IV

1. E. K. Warburton et al., Phys. Rev. C 41, 1147 (1990)
2. B. H. Wildenthal in “Progress in Particle and Nuclear Physics”, edited by D. H. Wilkinson, Plenum Press New York (1984)
3. B. A. Brown, W. A. Richter, Phys. Rev. C 74, 034315 (2006)
4. P. M. Endt, Nucl. Phys. A 521, 1 (1990) and A 633, 1 (1998)
5. De Meijer et al., Phys. Rev. C16, 2442 (1977)
6. ENSDF: Evaluated Nuclear Structure Data File, Brookhaven National Lab (2018)
7. XUNDL: eXperimental Unevaluated Nuclear Data List, Brookhaven National Lab (2018)
8. A. Gade et al., Phys. Rev. C 83, 044305 (2011)
9. A. Gade et al.,Phys. Rev. Lett. 99, 072502 (2007)

Table 1

Rotational model interpretation of USD shell model states in neutron-rich even - A Ne isotopes

J^π	E_x [KeV]				
	^{24}Ne				
	$K^\pi = 0_1^+$	$K^\pi = 2^+$	$K^\pi = 3^+$	$K^\pi = 0_2^+$	
0^+	0			4764*	
1^+	–			–	
2^+	1981*	3867*		5339	
3^+	–	4568	5472	–	
4^+	3962*	5645	5941	7394	
5^+	–	6690	7646	–	
6^+	7898	8532	9935	10144	
7^+	–	9770	11127	–	
8^+	11665	12638	13133	14830	
	^{26}Ne				
	$K^\pi = 0_1^+$	$K^\pi = 2^+$	$K^\pi = 4^+$	$K^\pi = 0_2^+$	
0^+	0			3812	
1^+	–			4356	
2^+	2011	3448		4717	
3^+	–	5120		6056	
4^+	3662	7023	5143	7637	
5^+	–	8230	7519	8497	
6^+	6501	10160	8831	n. a.	
	^{28}Ne				
	$K^\pi = 0_1^+$	$K^\pi = 2_1^+$	$K^\pi = 4^+$	$K^\pi = 2_2^+$	$K^\pi = 1^+$
0^+	0				
1^+	–				5391
2^+	1785	3678		4300	6202
3^+	–	5106		5837	7039
4^+	3300	6868	5182	6979	7821
5^+	–	9700	6304	8655	
6^+	6270	n. a.	9050		

*) = experimental instead of USD value

n. a. = not available

Table 2

Rotational model interpretation of USD shell model states in neutron-rich odd - A Ne isotopes

$2J^{\pi}$	E_x [KeV]					
	^{25}Ne					
	$2K^{\pi} = 1_1^+$	$2K^{\pi} = 5_1^+$	$2K^{\pi} = 3^+$	$2K^{\pi} = 9^+$	$2K^{\pi} = 1_2^+$	$2K^{\pi} = 5_2^+$
1^+	0				4678	
3^+	1687		2987		4593	
5^+	2971	1779	4226		5573	4648
7^+	4249	3638	4692		6205	6175
9^+	6382	5034	6750	3593	n. a.	n. a.
11^+	n. a.	6445	–	5727		
13^+			8539	7490		
15^+			10945	9359		
	^{27}Ne					
	$2K^{\pi} = 1_1^+$	$K^{\pi} = 5^+$	$K^{\pi} = 3^+$	$K^{\pi} = 9^+$	$2K^{\pi} = 1_2^+$	
1^+	868				2763	
3^+	0		2538		3371	
5^+	2170	2582	3264		4578	
7^+	2017	4253	4662		5092	
9^+	4129	5552	n. a.	4392		
11^+	3344	n. a.	n. a.	n. a.		
13^+	6846	n. a.	n.a.	8275		
	^{29}Ne					
	$2K^{\pi} = 3^+$	$2K^{\pi} = 1^+$	$2K^{\pi} = 7^+$			
1^+		1669				
3^+	0	3006				
5^+	2088	4155				
7^+	3647	5198	2023			
9^+	5813	n. a.	2779			
11^+	(9546)	n. a.	3859			

n. a. = not available

Table 3

Rotational model interpretation of USD shell model states in neutron-rich even - A Na isotopes

J^{π}	E_x [KeV]							
	^{26}Na							
	$K^{\pi} = 2^+$	$K^{\pi} = 1_1^+$	$K^{\pi} = 1_2^+$	$K^{\pi} = 4^+$	$K^{\pi} = 0^+$		$K^{\pi} = 1_3^+$	
0^+					1600			
1^+		0	1531			2271	2720	
2^+	187	413	1844		2166		2954	
3^+	182	1429	2796			3576	3709	
4^+	1652	1829	3365	2933	3905		4205	
5^+	2458	3006	4766	4961		5111	5530	
6^+	4578	4924	n. a.	5743	n. a.		n. a.	
	^{28}Na							
	$K^{\pi} = 2_1^+$	$K^{\pi} = 1_1^+$	$K^{\pi} = 2_2^+$	$K^{\pi} = 0^+$		$K^{\pi} = 1_2^+$	$K^{\pi} = 1_3^+$	$K^{\pi} = 4^+$
0^+				1460				
1^+		92			1658	2258	2795	
2^+	0	1030	1537	2091		2968	n. a.	
3^+	505	978	2261		3234	3862	n. a.	
4^+	698	3186	3499	4197		n. a.	n. a.	3760
5^+	2875	3544	4434		n. a.	n. a.	n. a.	
6^+	3251	5874	6373	n. a.		n. a.	n. a.	
	^{30}Na							
	$K^{\pi} = 2^+$	$K^{\pi} = 0^+$		$K^{\pi} = 3^+$	$K^{\pi} = 1_1^+$	$K^{\pi} = 4^+$	$K^{\pi} = 1_2^+$	
0^+		301						
1^+			66		2511		3251	
2^+	0	1979			2802		3450	
3^+	1604		2961	200	3605		n. a.	
4^+	3561	5224		651	n. a.	4048	n. a.	
5^+	4751		6880	2736	n. a.	5577	n. a.	
6^+	7550	n. a.		3215	n. a.	7738	n. a.	

n. a. = not available

Table 4

Rotational model interpretation of USD shell model states in neutron-rich odd - A Na isotopes

$2J^{\pi}$	E_x [KeV]					
	^{27}Na					
	$2K^{\pi} = 3_1^+$	$2K^{\pi} = 1_1^+$	$2K^{\pi} = 3_2^+$			
1^+		1630				
3^+	14	3643	3121			
5^+	0	2671	3571			
7^+	2091	n. a.	4136			
9^+	2197	3675	5180			
11^+	5845	n. a.	6133			
13^+	5339		7271			
15^+	9335		9617			
17+	9750		12134			
	^{29}Na					
	$2K^{\pi} = 3^+$	$K^{\pi} = 1^+$	$K^{\pi} = 7^+$			
1^+		1962				
3^+	137					
5^+	0					
7^+	2871		3111			
9^+	2093		4042			
11^+	5476		6757			
13^+	5391		7562			
15^+	10141		11679			
17+	11102		n. a.			

n. a. = not available

Table 5

Rotational model interpretation of USD shell model states in neutron-rich Mg isotopes

J^π	E_x [KeV]								
	^{28}Mg								
	$K^\pi = 0_1^+$	$K^\pi = 0_2^+$	$K^\pi = 4^+$	$K^\pi = 1_1^+$	$K^\pi = 2_1^+$	$K^\pi = 1_2^+$	$K^\pi = 2_2^+$	$K^\pi = 0_3^+$	$K^\pi = 0_4^+$
0^+	0	3863*						6187	6856
1^+	–	–		4561*		5193		–	–
2^+	1473*	4557*		4879*	5469*	5673*	6758	7330	7420
3^+	–	–		5582	6402	6742	7059	–	–
4^+	4020*	6790*	5186	6964	7318	7542	8133	8348	8480
5^+	–	–	7311	8180	8917	9288			
6^+	7715	9885	9043	10050	10458	10759			
7^+	–	–	11259	11283	12334	12671			
8^+	11628	12415	13633	14879	n. a.				
	^{30}Mg								
	$K^\pi = 0_1^+$	$= 2_1^+$	$K^\pi = 4^+$	$K^\pi = 2_2^+$	$K^\pi = 1^+$	$K^\pi = 2_3^+$	$K^\pi = 0_2^+$	$K^\pi = 0_3^+$	
0^+	0						5710	6597	
1^+	–				5242		–	–	
2^+	1463*	3467		4803	6495	5193	6147	7315	
3^+	–	4693		6500	7450	7268			
4^+	3961	6325	5466	n. a.	n. a.	n. a.	7125		
5^+	–	8376	7001	9418	9539				
6^+	6760	10343	8714				9553		
7^+	–	12606	11560						
8^+	11508	n. a.	13530						
	^{29}Mg								
$2J^\pi$	$2K^\pi = 1_1^+$	$2K^\pi = 3^+$	$2K^\pi = 1_2^+$	$2K^\pi = 5^+$	$2K^\pi = 9^+$		Add on:	$2K^\pi = 1^-$	
1^+	54*		2438					1096	3^-
3^+	0	2614*	3227					1430	7^-
5^+	1640*	3223*	3974	3532					
7^+	2106	4147.	4869	4624					
9^+	4071	5532	n. a.	5850	4183				
11^+	4618	7351	n. a.	7115	6081				
13^+	7017	8735	n. a.	9219	8261				

*) = experimental instead of USD value

n. a. = not available

Table 6

Interpretation of the known ^{31}Mg levels

2 ħω states						
E_x[KeV]	K^π	J^π		log ft	Theor. E_x[KeV]	
		present	NDS	$^{31}Na \rightarrow ^{31}Mg$	Nilsson	USD
0	$1/2_1^+$	$3/2^+$	$(1/2)^+$	4.9	Fit	
51	$1/2_1^+$	$1/2^+$	$(3/2)^+$	5.6		
945	$1/2_1^+$	$5/2^+$	$(5/2)^+$	6.3		
1154	$1/2_1^+$	$7/2^+$	$(7/2)^+$			
2244	$1/2_2^+$	$5/2^+$ b)	$1/2^+$,$3/2^+$, $5/2^+$	4.7	1758 + 800 a)	
3760	$5/2^+$	$5/2^+$ b)	$1/2^+$,$3/2^+$, $5/2^+$	5.4	4192	
1 ħω states						
221	$1/2^-$	$3/2^-$	$(3/2^-)$			
461	$1/2^-$	$7/2^-$	$(3/2^-)$			
1029	$1/2^-$	$1/2^-$	$1/2^- 7/2^-$		471 + 400 a)	
1390	$1/2^-$	$5/2^-$				
2014	$(3/2^-)$	$(3/2^-)$				
0 ħω states spherical						
673		$3/2^+$	$(3/2)^+$	5.5		700
3814		$3/2^+$, $5/2^+$	$1/2^+$,$3/2^+$, $5/2^+$	5.3		3906 or 3933

a) influence of the decoupling effect and zero point precession

b) The levels at 2244 KeV and 3760 KeV have three γ-decay modes in common and hence equal J^π.

Table 7

Nilsson model configurations of the uppermost neutrons, experimental binding energies relative to ^{24}Mg ground state and calculated deformation parameters of levels in Mg isotopes which are used for specify the residual interaction

N. M. config. [a]	Level [c]				Deformation	
$(2\Omega_i^{\pi})^n$	E_x[KeV]		E_B[KeV] [d]		$\varepsilon(0\hbar\omega)$[b]	$\varepsilon(2\hbar\omega)$
	^{26}Mg					
$(5_1^+)^2$	0		−18423		0.27	
$(1_1^+)^2$	3589		−14834			
$(1_2^+)^2$	6256		−12167			
$(1^-)^2$	7428		−10995			0.53
	^{28}Mg					
$(1_1^+)^2$	0		−33371		0.28	
$(1_2^+)^2$	3863		−29508			
$(1^-)^2$	5270		−28101			0.42
	^{29}Mg					
$(1^-)^2$ $(1_2^+)^1$	0		−37152			0.42
	^{30}Mg					
$(1_2^+)^2$	0		−43563		0,20	
$(1^-)^2$	–					0.41
	^{32}Mg					
$(1^-)^2$	0		−51428			0.33
$(3_2^+)^2$	–				0.13	

a) The notation follows Fig. 1

b) In addition ε = 0.38 for the ^{24}Mg g. st.

c) All levels are heads of rotational bands

d) Relative to ^{24}Mg g.st.

Table 8

Parameters of the residual interaction energy between particles in different Nilsson orbits. An update of Table 4A, p. 93 in Part II

Orbit i			Orbit k			Parameters [KeV]				
Ω^{π}	[N n_z Λ]		Ω^{π}	[N n_z Λ]		a_{ik}	b_{ik}	c_{ik}	d_{ik}	(a_{ik} + ci_k)
$1/2^+$	220		$1/2^-$	101		−377	219	980	92	603
			$3/2^+$	211		−999	−676	−160	−82	−1159
			$5/2^+$	202		380	0	575	225	955
			$1/2^+$	211		−528	878	378	367	−150
$1/2^-$	101		$3/2^+$	211		−539	−442	1151	−507	612
			$5/2^+$	202			170	1375	−400	
$3/2^+$	211		$5/2^+$	202		−986	−583	152	−117	−834
			$1/2^+$	211		−666	−672	748	−707	82
			$1/2^+$	200		−994	−302	331	−16	−663
			$1/2^-$	330		−495	−200	768	400	273
$5/2^+$	202		$1/2^+$	211		−423	119	647	296	−29a)
			$1/2^+$	200		−554	1011	824	375	270
			$1/2^-$	330		−337	−1862	666	−348	329
			$3/2^+$	202			−739	295	−272	
$1/2^+$	211		$1/2^+$	200		−526	−541	749	239	223
			$1/2^-$	330						203
$1/2^+$	200		$1/2^-$	330						251

a) We prefer this value, obtained directly, rather than 224 KeV obtained by adding a_{ik} and c_{ik}

Table 9

Binding energies of the lowest-lying 0, 1, 2 ħω states in neutron rich isotopes of Ne, Na and Mg

Nuclide		E_B[MeV] [a]					
		Nilsson model				g.st.	
		2 ħω	1 ħω	0 ħω		Exp.	S.M.[b]
^{28}Ne		−43.56		−44.82		−46.52	−46.3
^{29}Ne		−44.26	−44.22			−47.17	−45.78
^{30}Ne		−47.48				−50.36	−47.66
^{29}Na		−36.54		−35.82		−36.25	−37.02
^{30}Na		−39.62	−37.9			−38.6	−37.63
^{31}Na		−43.3				−43.03	−40.59
^{30}Mg		−42.24		−43.78		−43.56	−43.3
^{31}Mg		Fit	−45.5			−45.97	−45.27
^{32}Mg		Fit				−51.42	−49.1

a) Relative to, respectively, ^{20}Ne, ^{23}Na and ^{24}Mg ground state

b) S. M. stands for the spherical shell model with nucleons in the N = 2 shell only

Fig. 1

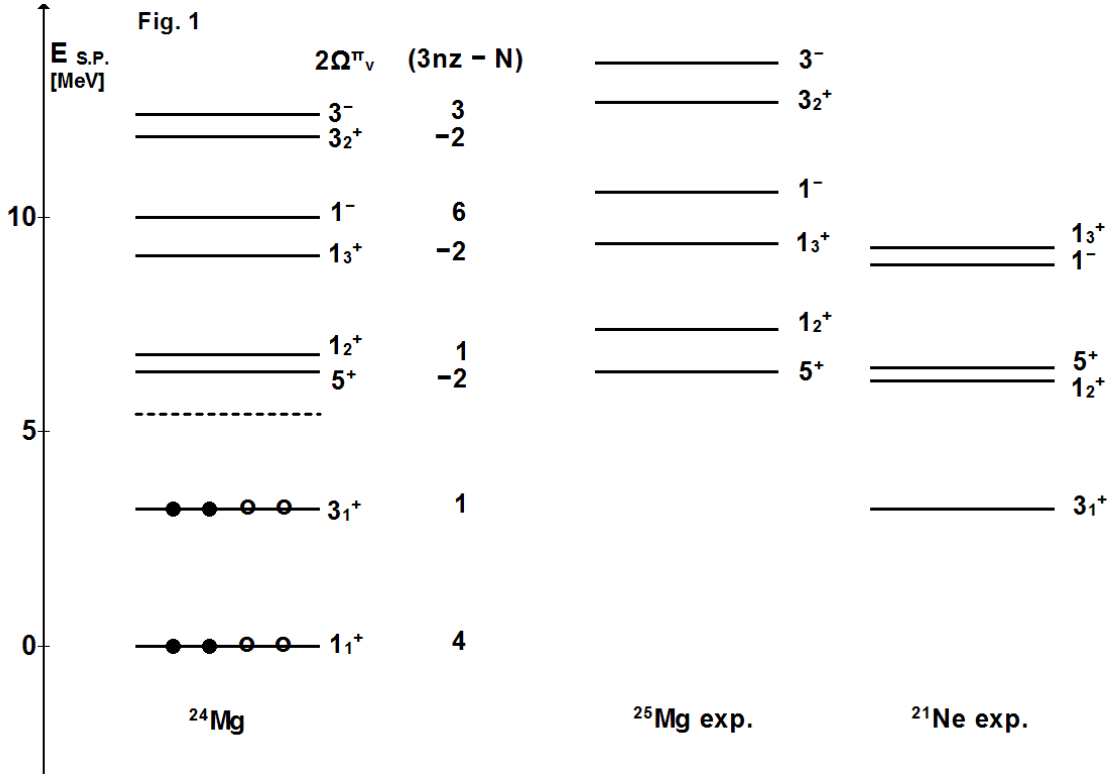
E S.P. [MeV]
2Ω^π_ν
(3nz − N)
10
5
0
3⁻
3₂⁺
1⁻
1₃⁺
1₂⁺
5⁺
3₁⁺
1₁⁺
3
−2
6
−2
1
−2
1
4
24Mg
25Mg exp.
21Ne exp.

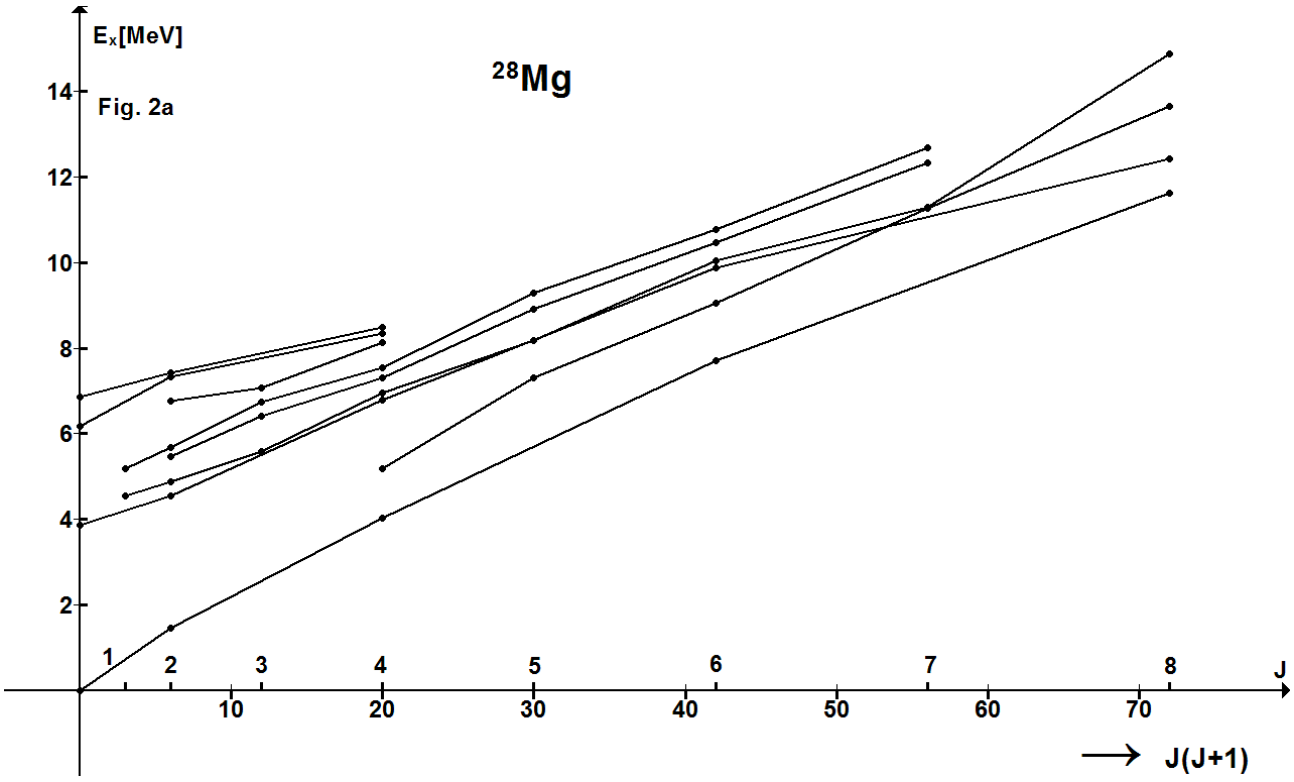
Ex[MeV]
28Mg
Fig. 2a
14
12
10
8
6
4
2
1
2
3
4
5
6
7
8
J
10
20
30
40
50
60
70
J(J+1)

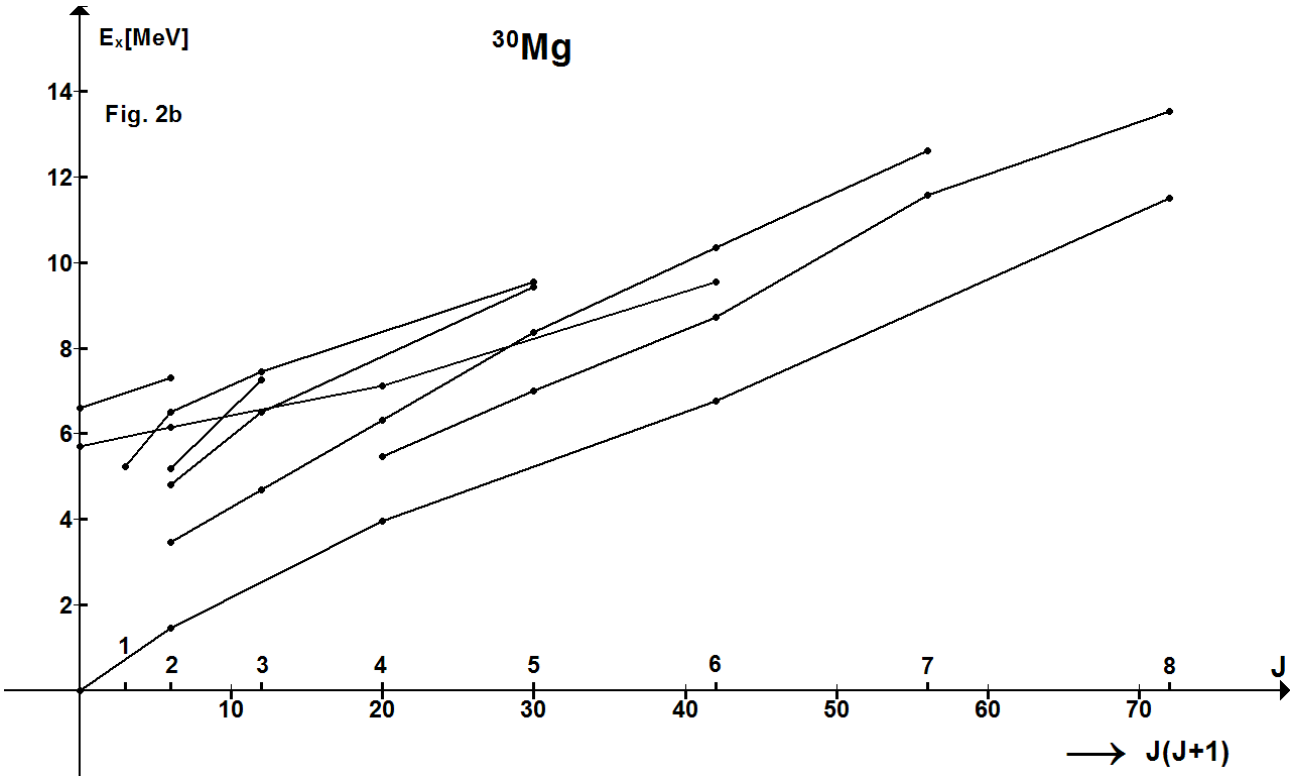
Ex[MeV]
30Mg
Fig. 2b
14
12
10
8
6
4
2
1
2
3
4
5
6
7
8
J
10
20
30
40
50
60
70
J(J+1)

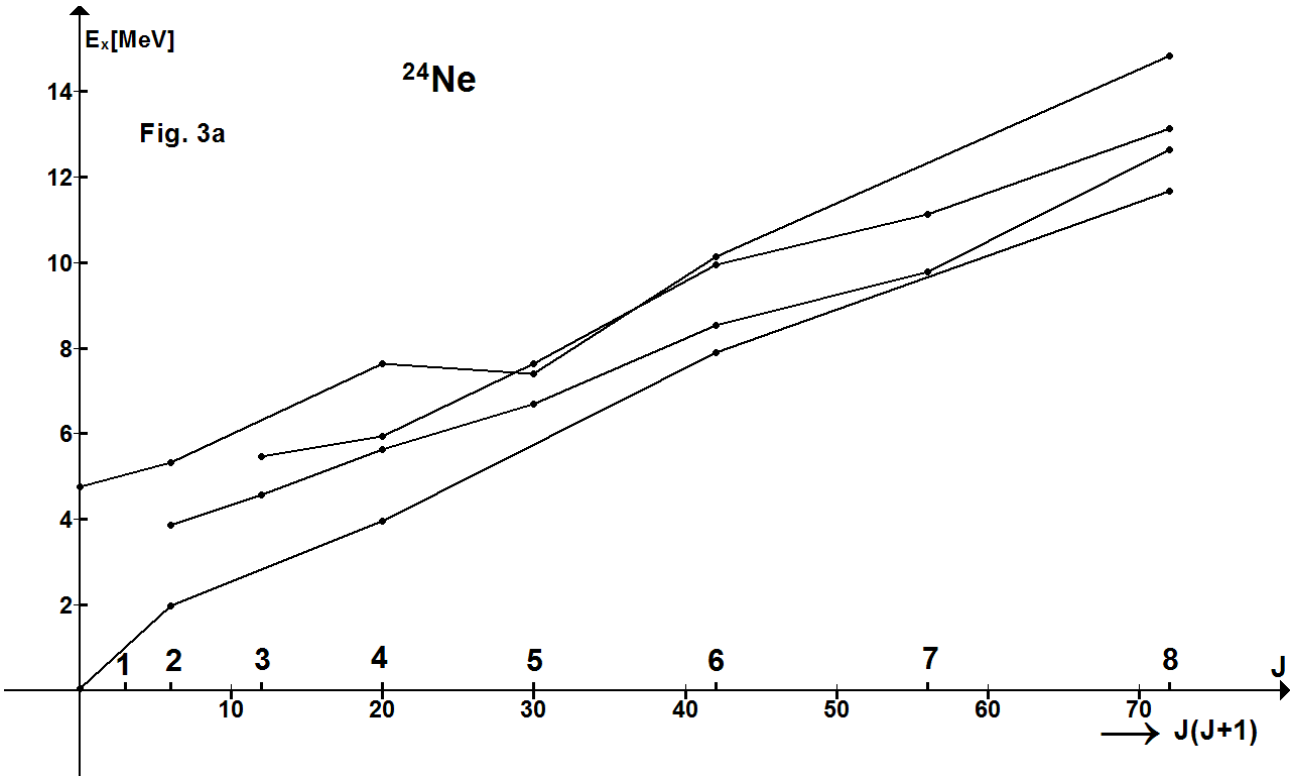
E_x[MeV]
^{24}Ne
Fig. 3a
14
12
10
8
6
4
2
1
2
3
4
5
6
7
8
J
10
20
30
40
50
60
70
J(J+1)

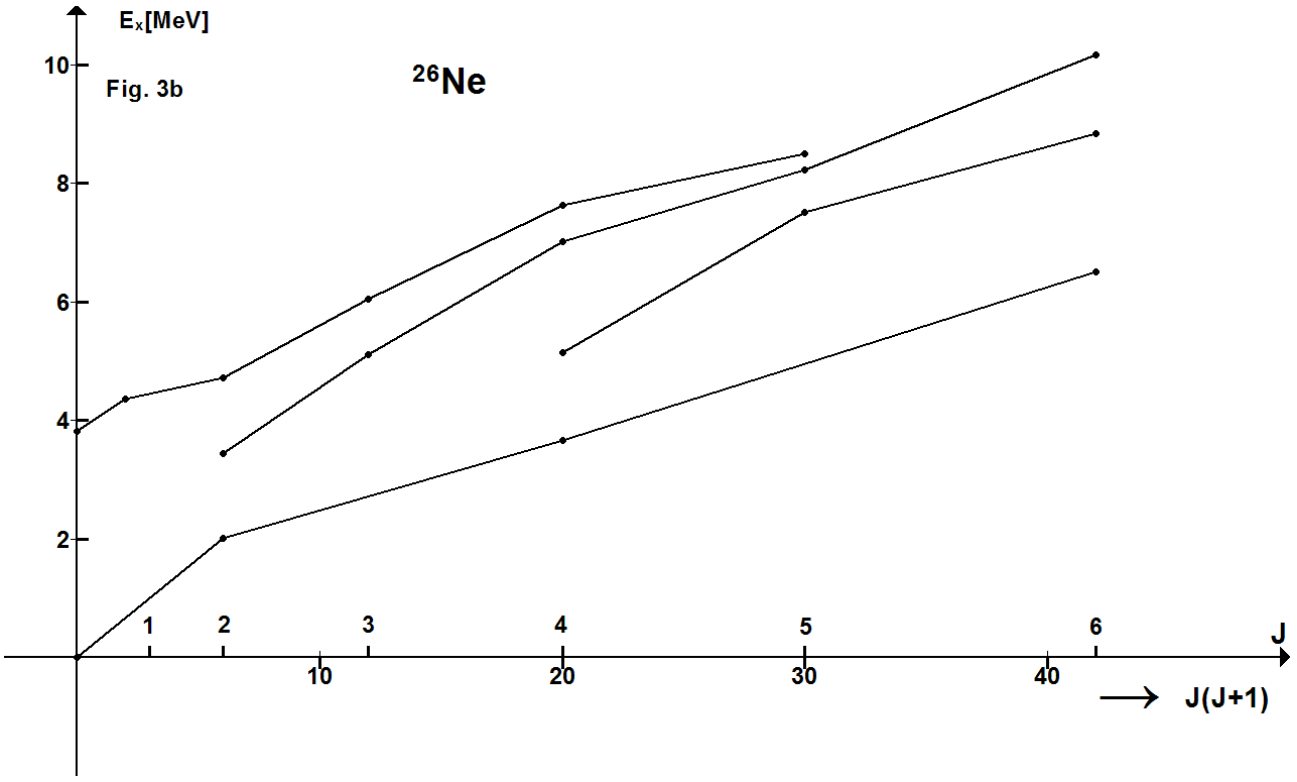
E_x[MeV]
Fig. 3b
^{26}Ne
10
8
6
4
2
1
2
3
4
5
6
J
10
20
30
40
J(J+1)

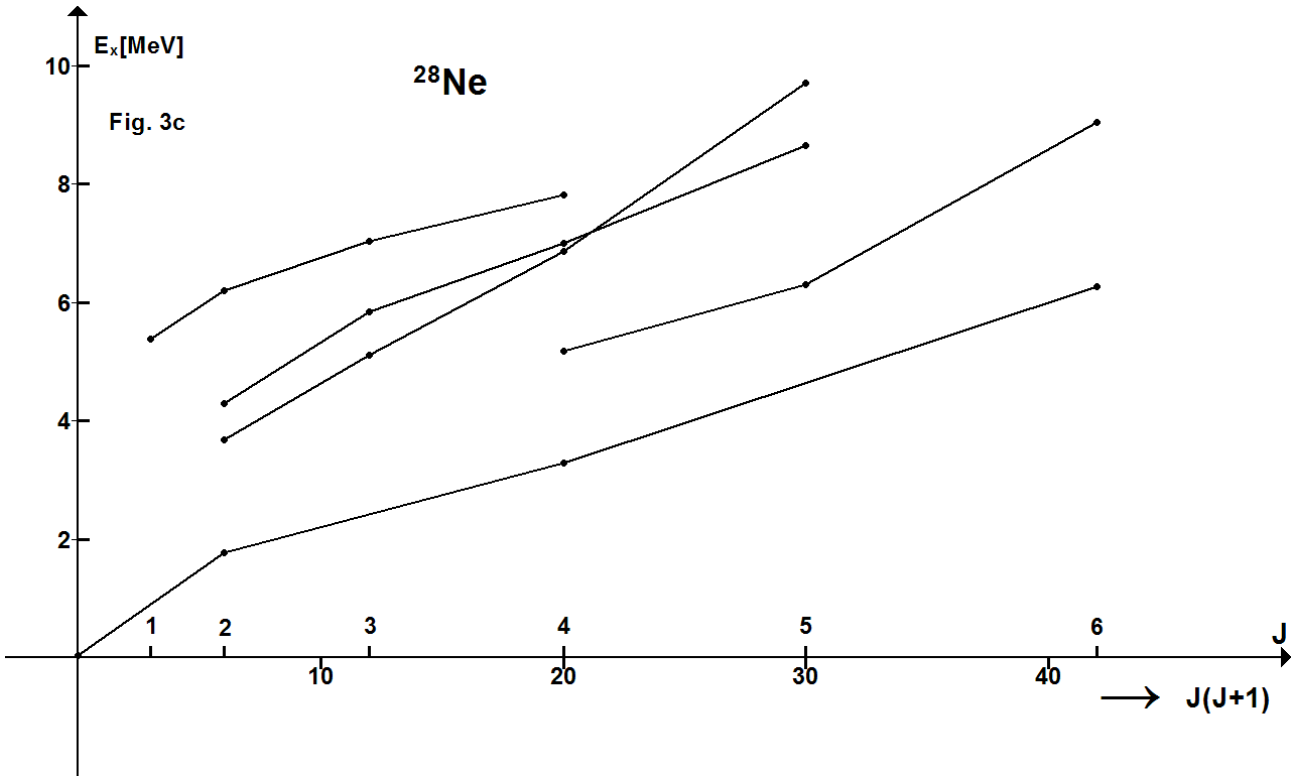
E_x[MeV]
^{28}Ne
Fig. 3c
10
8
6
4
2
1
2
3
4
5
6
J
10
20
30
40
J(J+1)

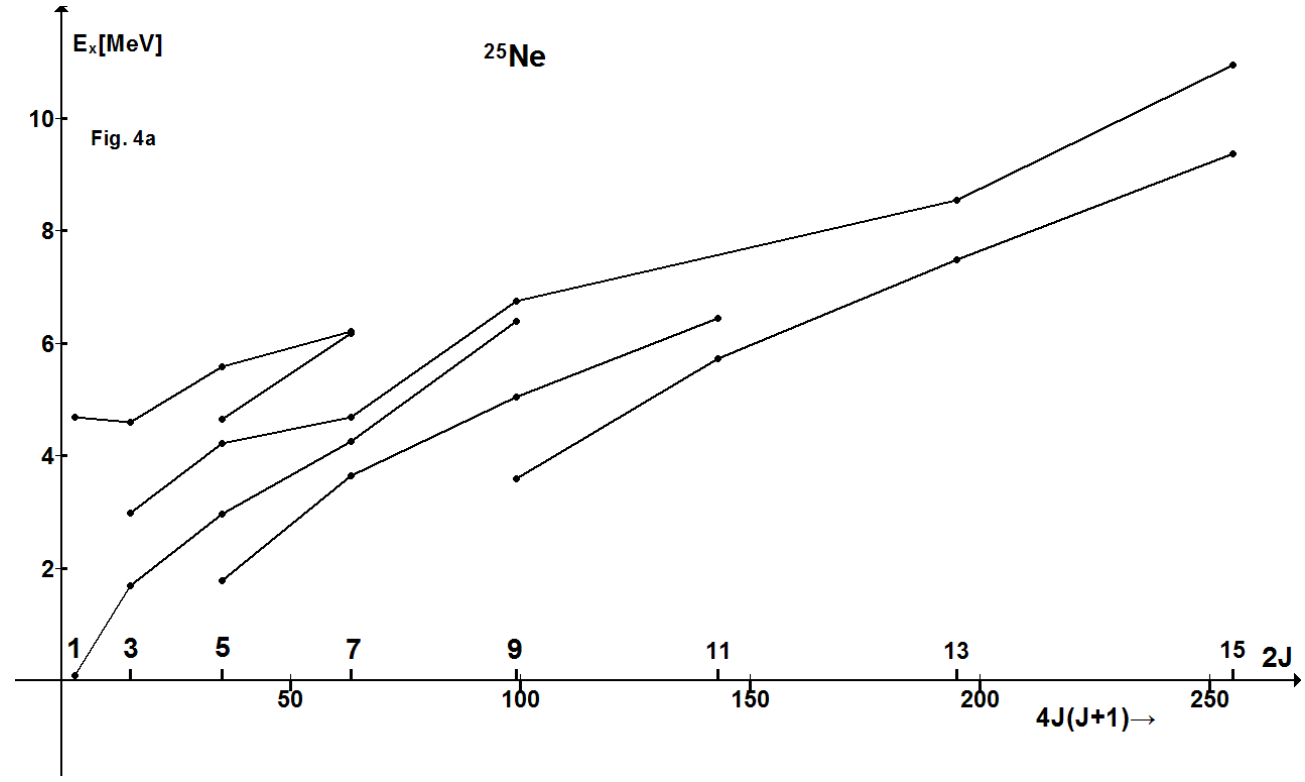
E_x[MeV]
^{25}Ne
Fig. 4a
10
8
6
4
2
1
3
5
7
9
11
13
15
2J
50
100
150
200
250
4J(J+1)→

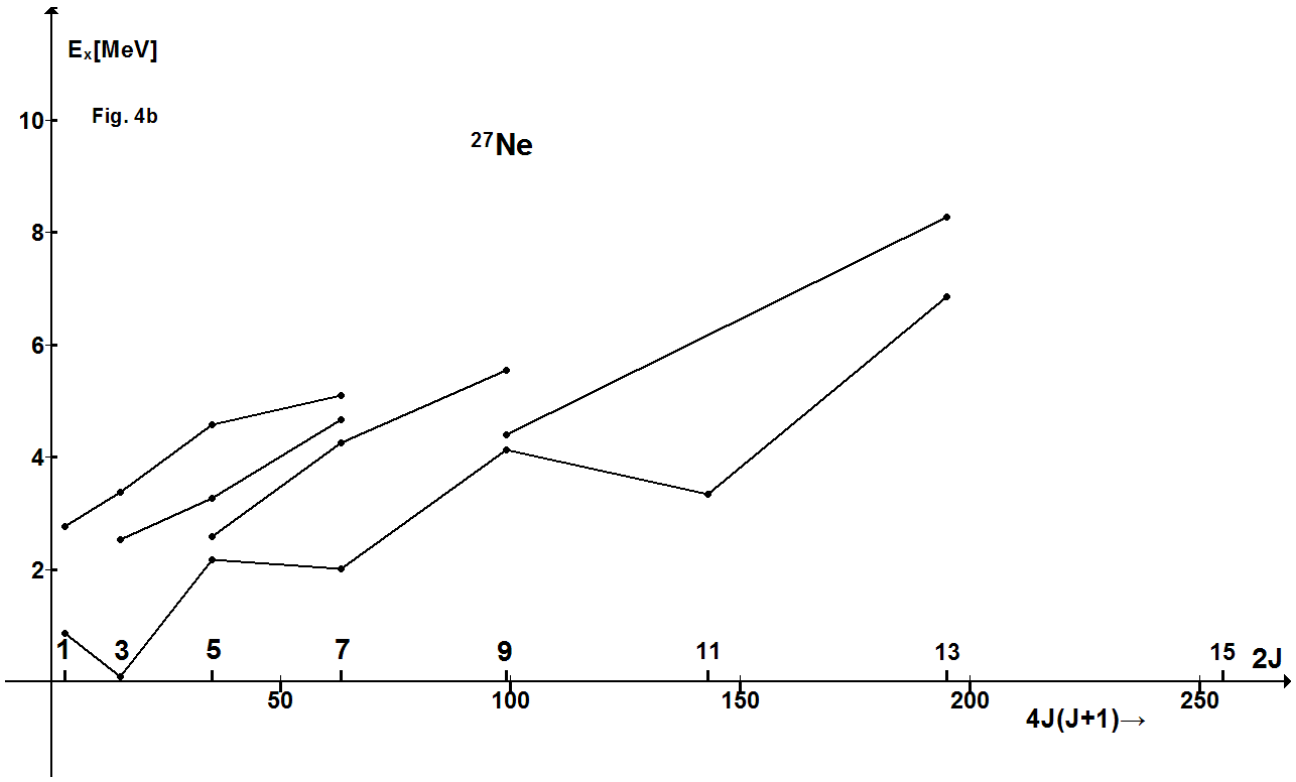
E_x[MeV]
Fig. 4b
^{27}Ne
10
8
6
4
2
1
3
5
7
9
11
13
15
2J
50
100
150
200
250
4J(J+1)→

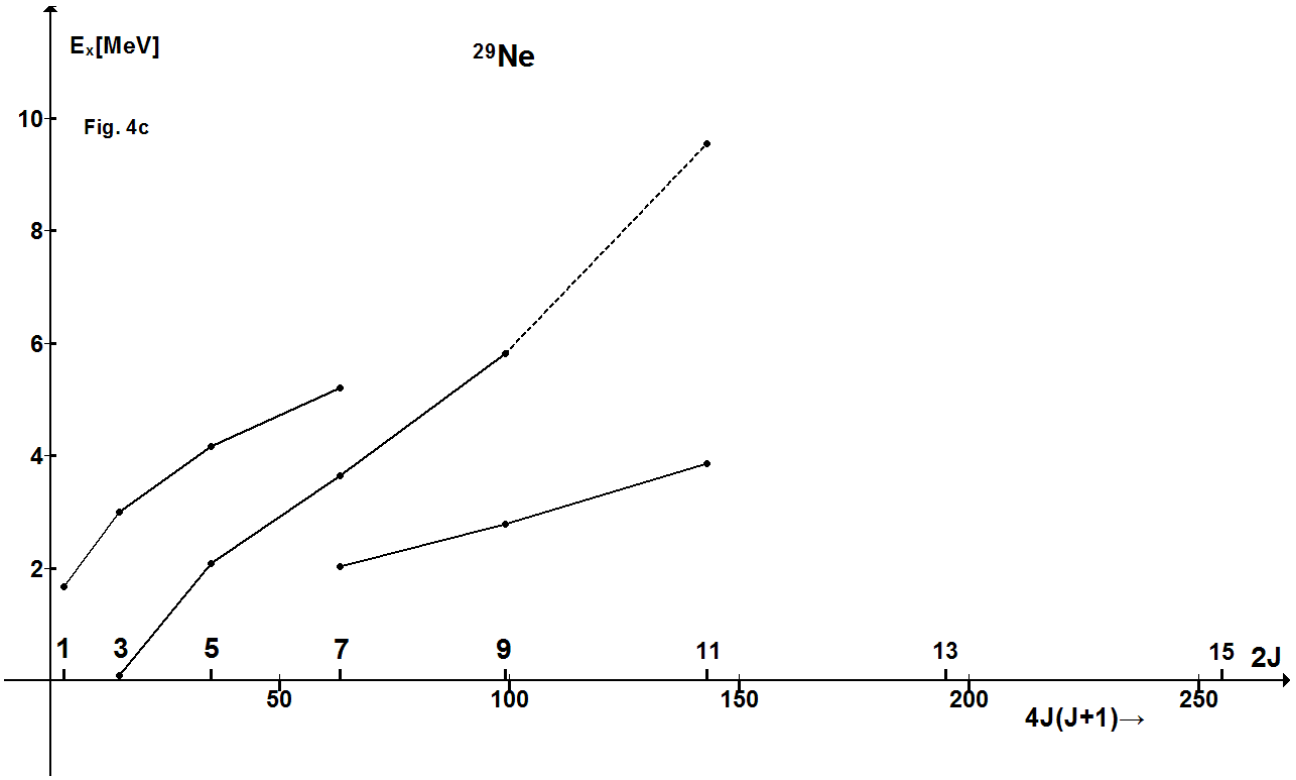
Ex[MeV]
29Ne
Fig. 4c
10
8
6
4
2
1
3
5
7
9
11
13
15
2J
50
100
150
200
250
4J(J+1)→

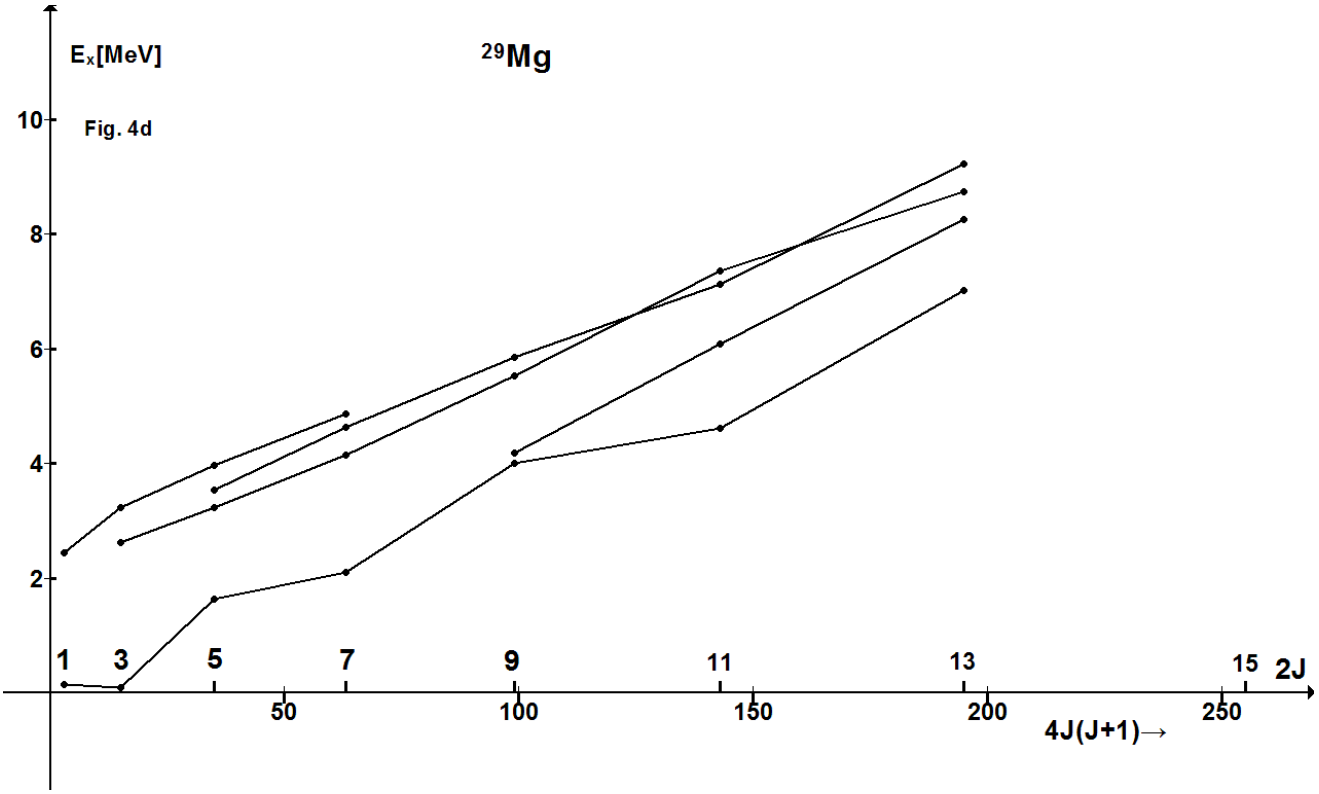
Ex[MeV]
29Mg
Fig. 4d
10
8
6
4
2
1
3
5
7
9
11
13
15
2J
50
100
150
200
250
4J(J+1)→

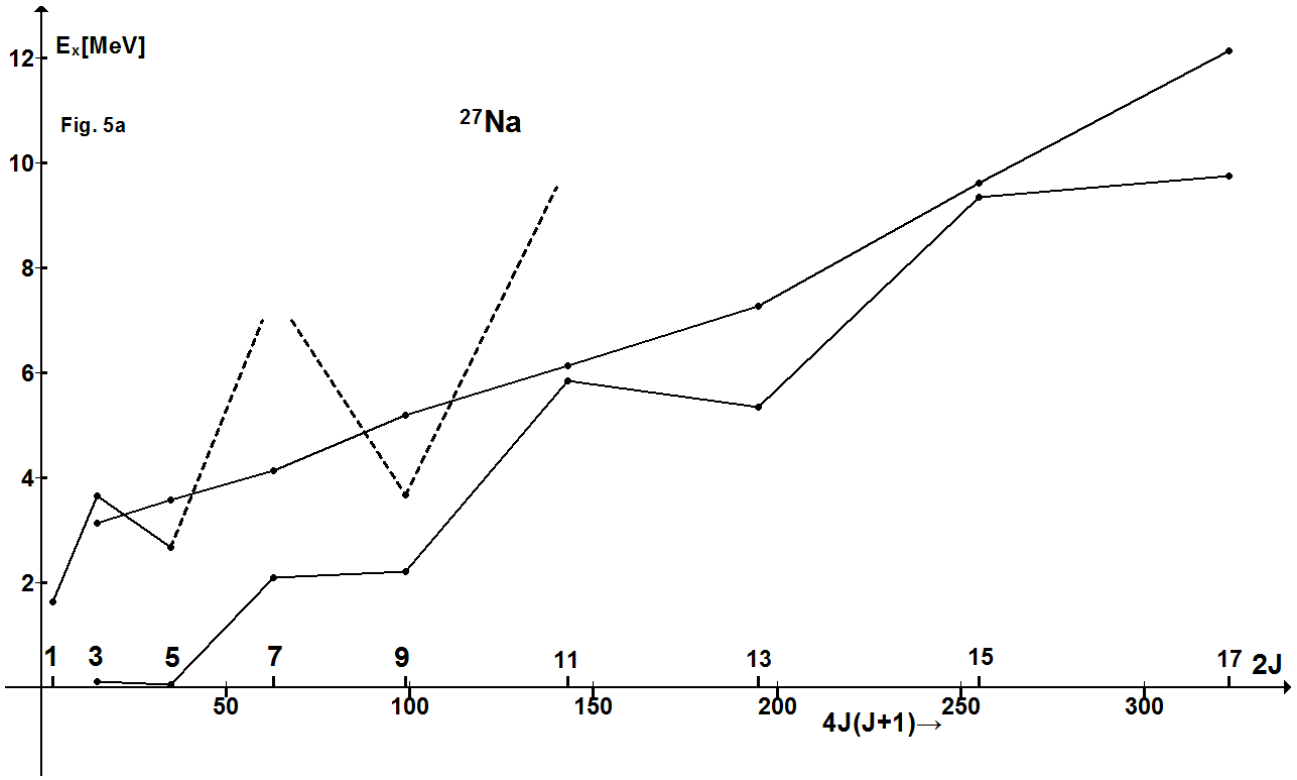
Ex[MeV]
Fig. 5a
27Na
12
10
8
6
4
2
1
3
5
7
9
11
13
15
17
2J
50
100
150
200
250
300
4J(J+1)→

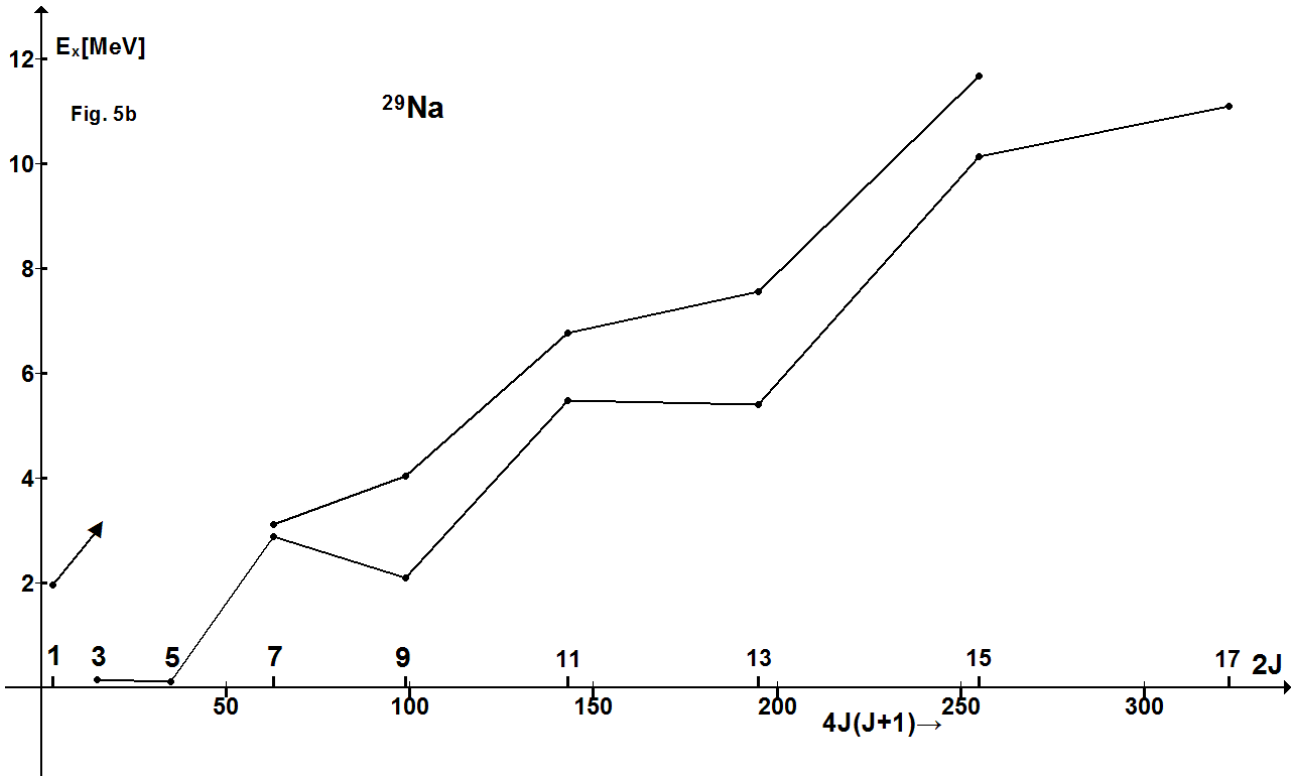
Ex[MeV]
Fig. 5b
29Na
12
10
8
6
4
2
1
3
5
7
9
11
13
15
17
2J
50
100
150
200
250
300
4J(J+1)→

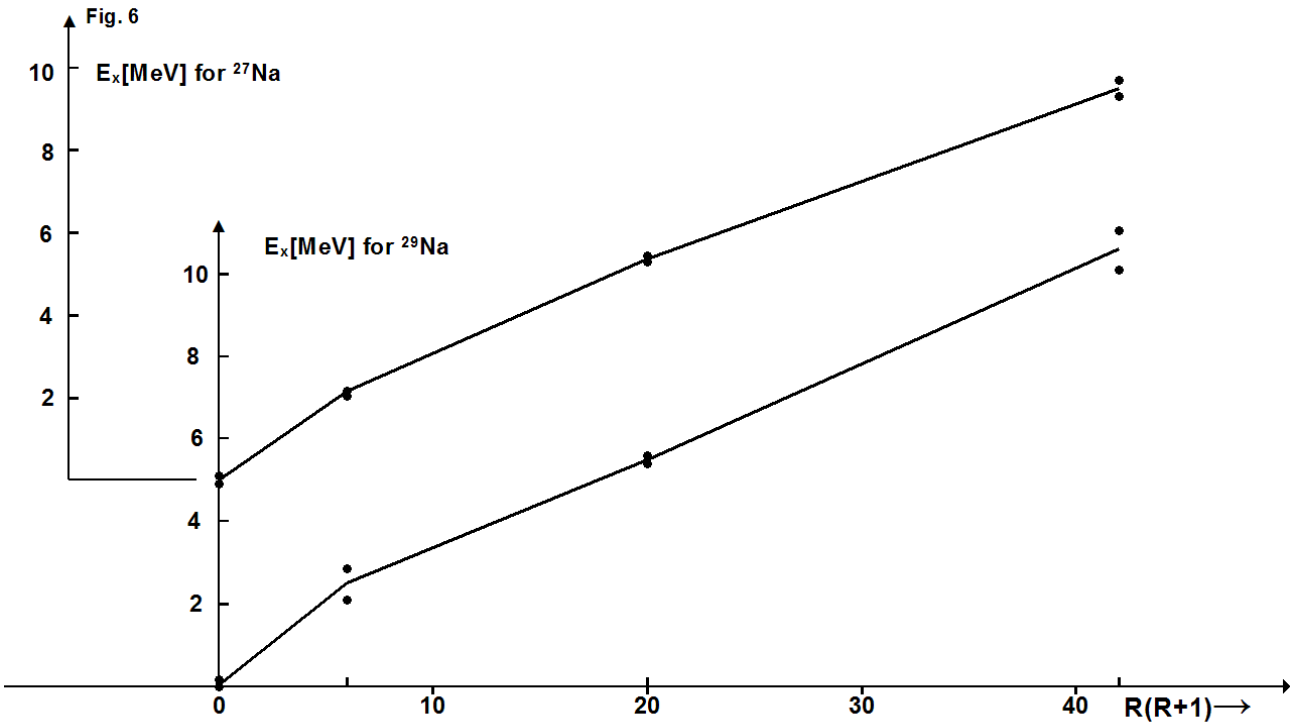
Fig. 6
E_x[MeV] for ^{27}Na
E_x[MeV] for ^{29}Na
10
8
6
4
2
0
10
20
30
40
R(R+1)⟶

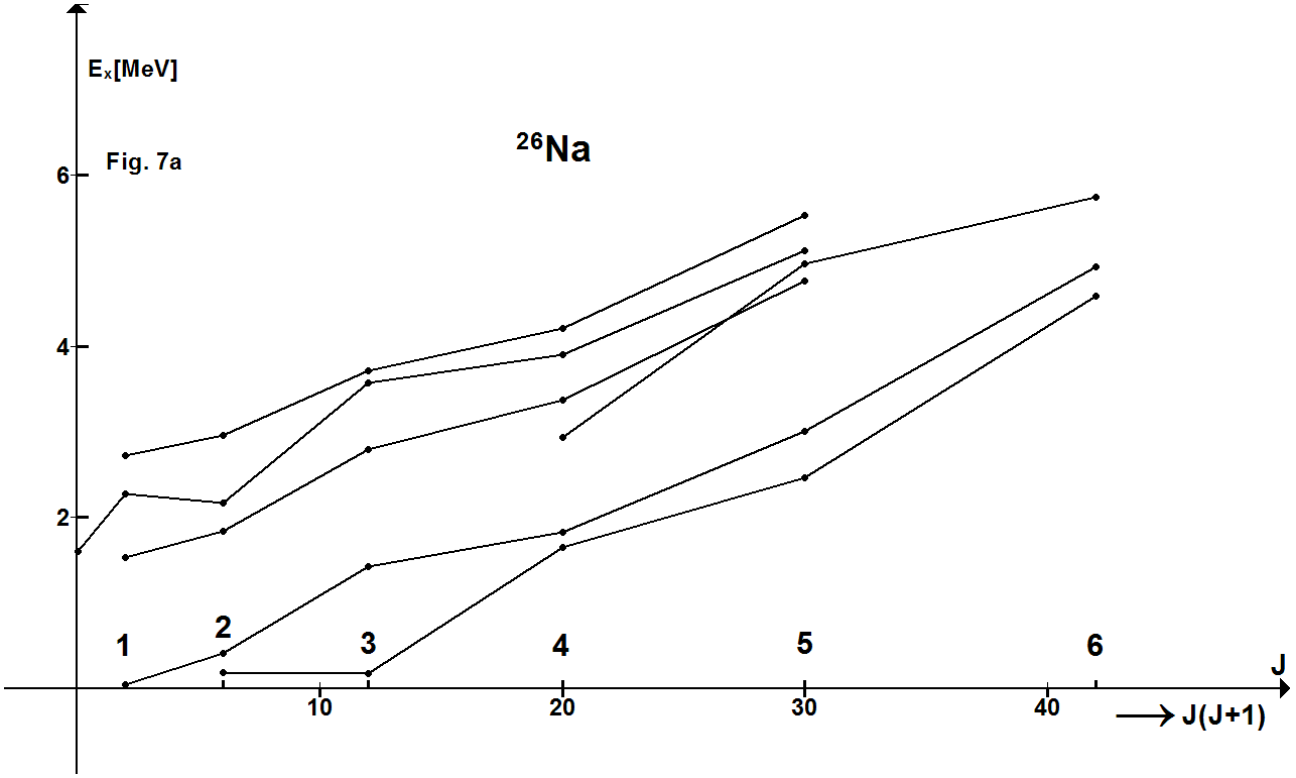
E_x[MeV]
Fig. 7a
^{26}Na
6
4
2
1
2
3
4
5
6
J
10
20
30
40
J(J+1)

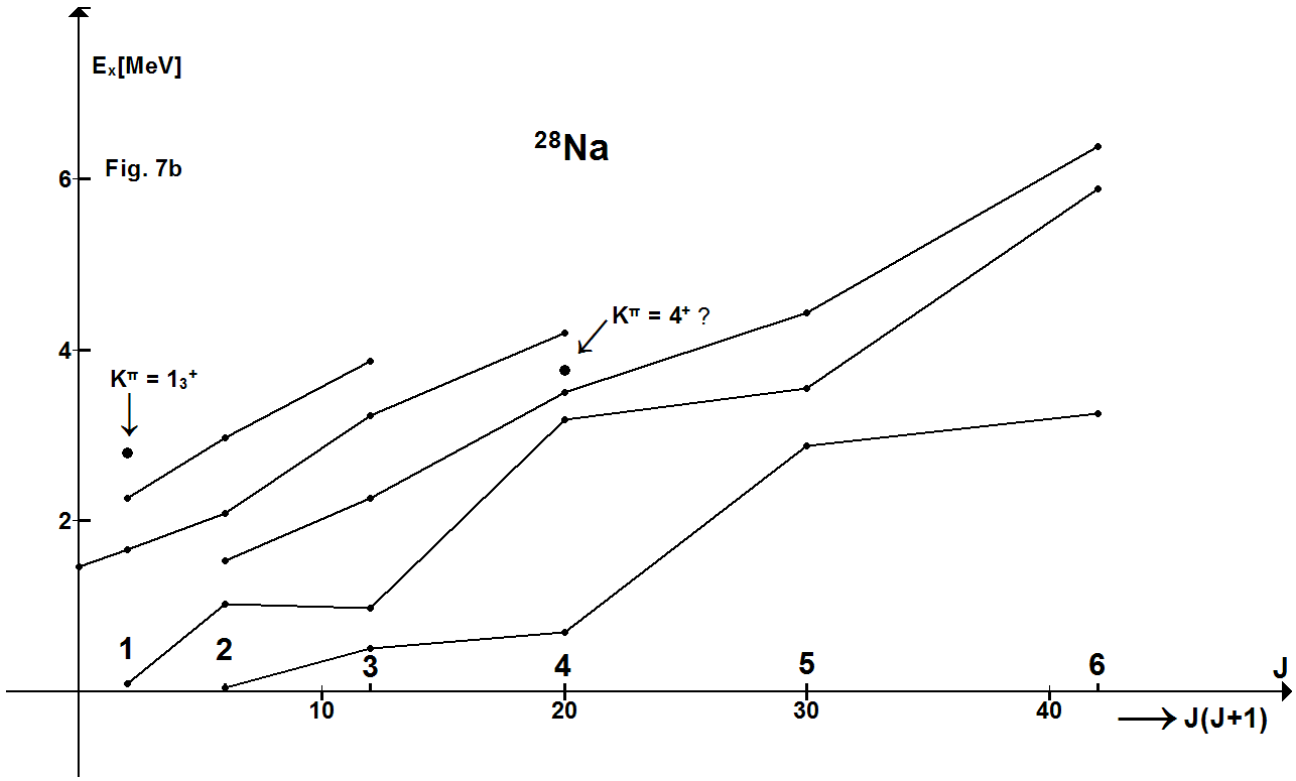
E_x[MeV]
Fig. 7b
^{28}Na
6
4
2
$K^\pi = 1_3^+$
$K^\pi = 4^+$?
1
2
3
4
5
6
J
10
20
30
40
J(J+1)

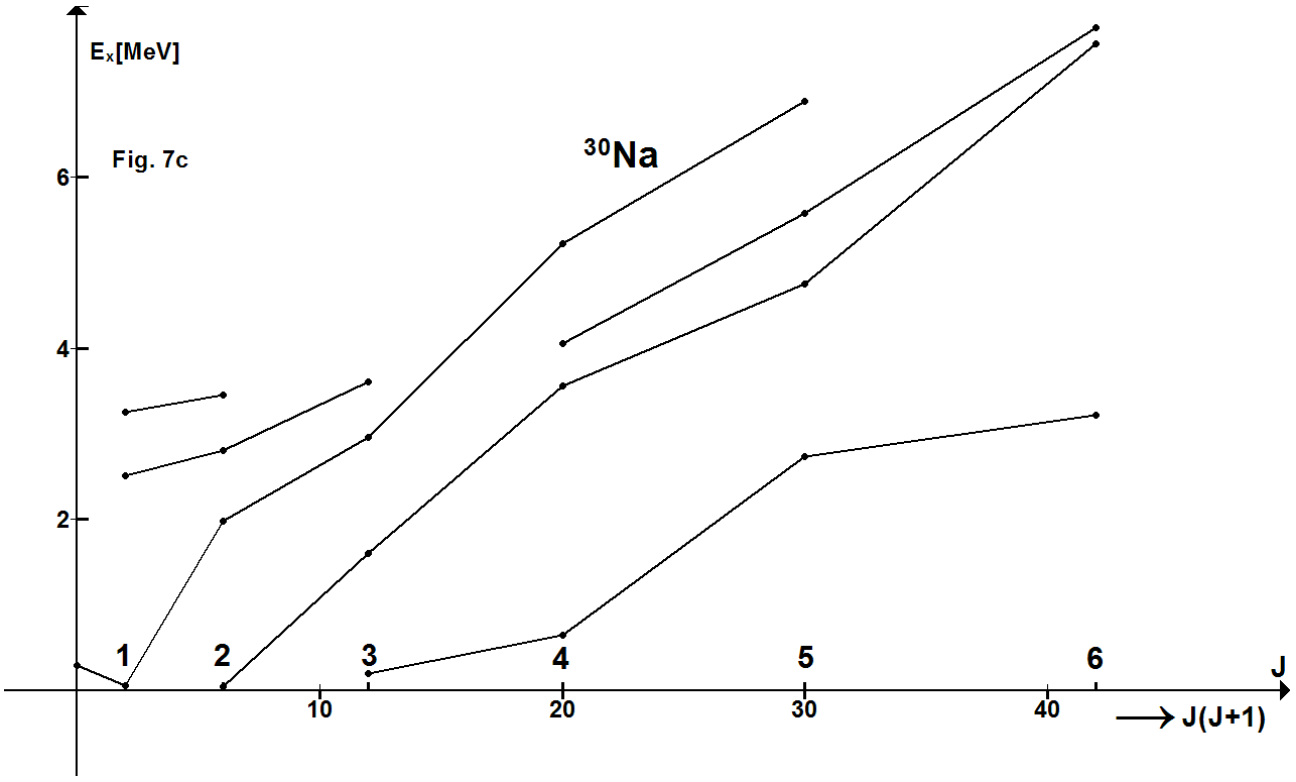
Ex[MeV]
Fig. 7c
30Na
6
4
2
1
2
3
4
5
6
J
10
20
30
40
J(J+1)

Fig. 8a

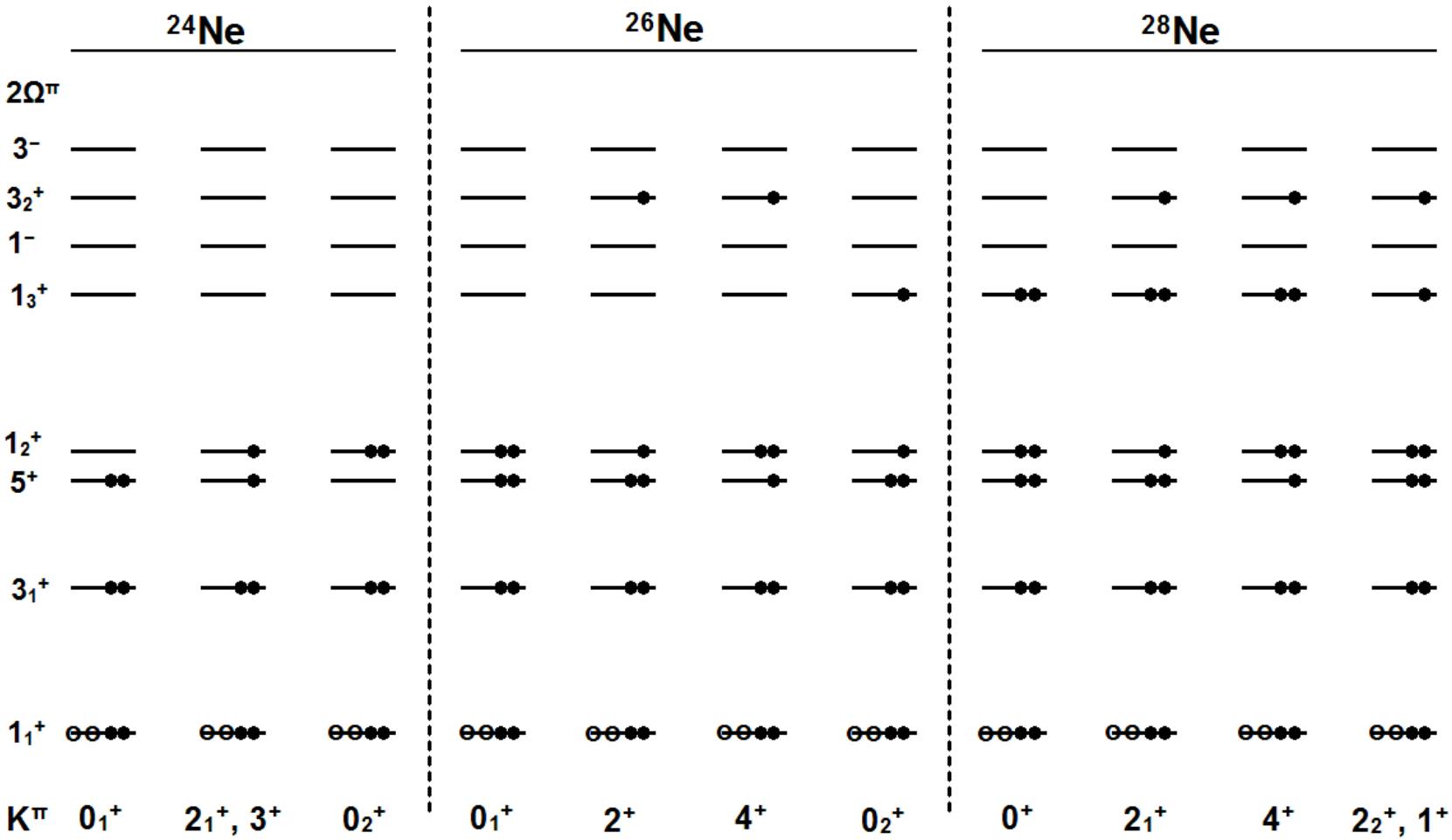
24Ne
26Ne
28Ne
2Ω^π
3^−
3_2^+
1^−
1_3^+
1_2^+
5^+
3_1^+
1_1^+
K^π
0_1^+
2_1^+, 3^+
0_2^+
0_1^+
2^+
4^+
0_2^+
0^+
2_1^+
4^+
2_2^+, 1^+

Fig. 8b1

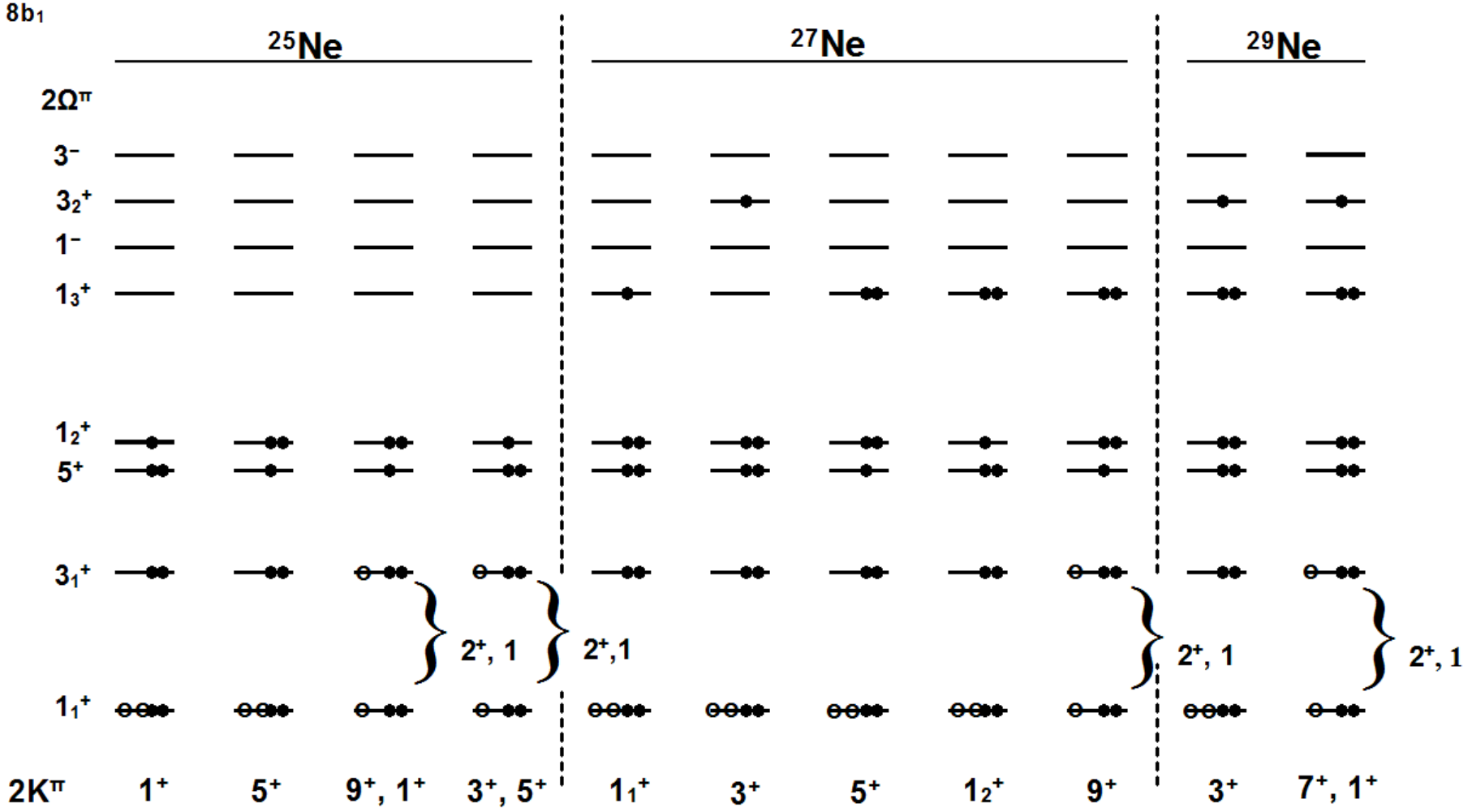
25Ne
27Ne
29Ne
2Ω^π
3^-
3_2^+
1^-
1_3^+
1_2^+
5^+
3_1^+
1_1^+
2^+, 1
2^+,1
2^+, 1
2^+, 1
2K^π
1^+
5^+
9^+, 1^+
3^+, 5^+
1_1^+
3^+
5^+
1_2^+
9^+
3^+
7^+, 1^+

Fig. 8b2

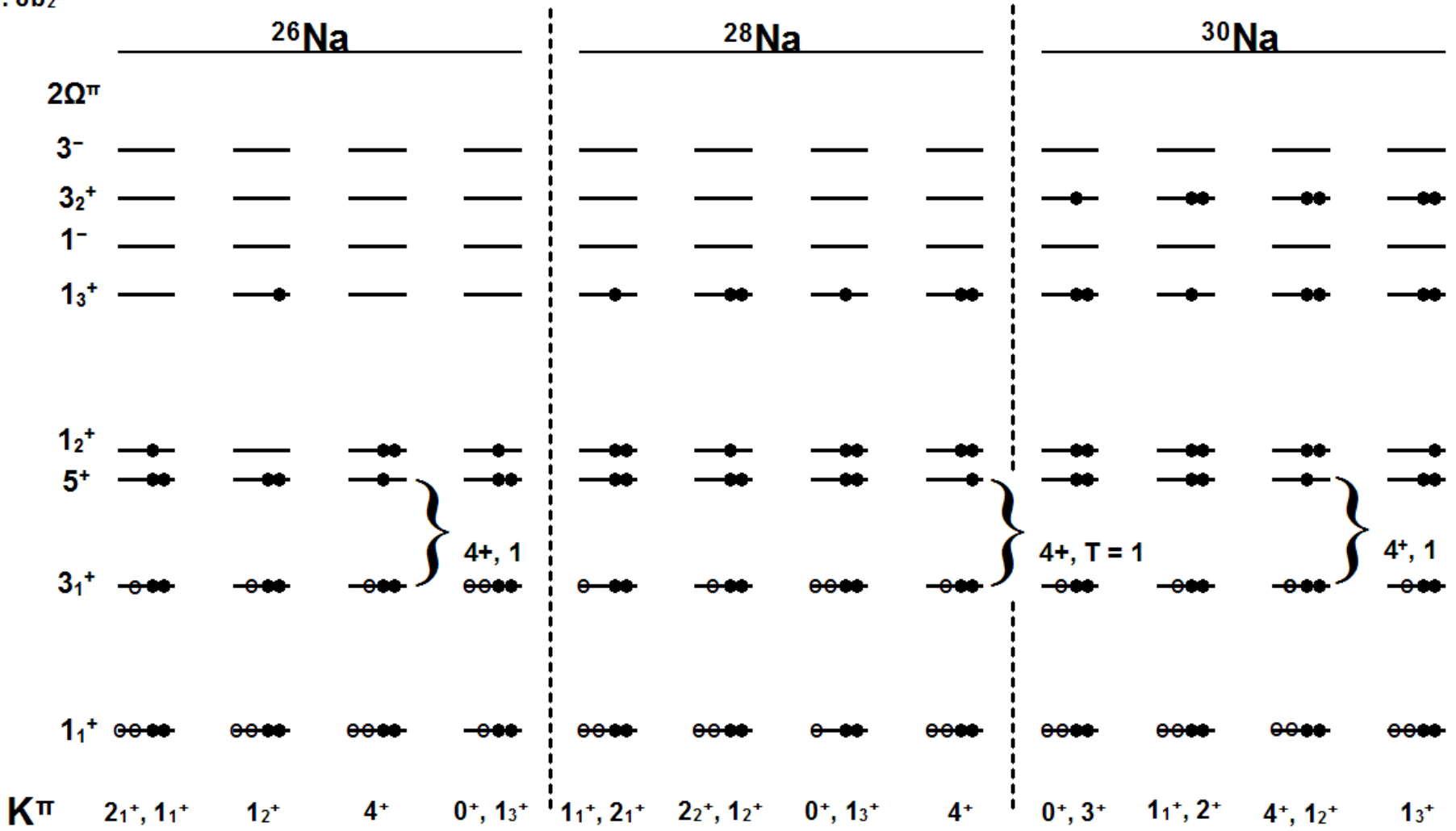
26Na
28Na
30Na
2Ω^π
3^-
3_2^+
1^-
1_3^+
1_2^+
5^+
3_1^+
1_1^+
4+, 1
4+, T = 1
4+, 1
Kπ
2_1^+, 1_1^+
1_2^+
4^+
0^+, 1_3^+
1_1^+, 2_1^+
2_2^+, 1_2^+
0^+, 1_3^+
4^+
0^+, 3^+
1_1^+, 2^+
4^+, 1_2^+
1_3^+

Fig. 8c

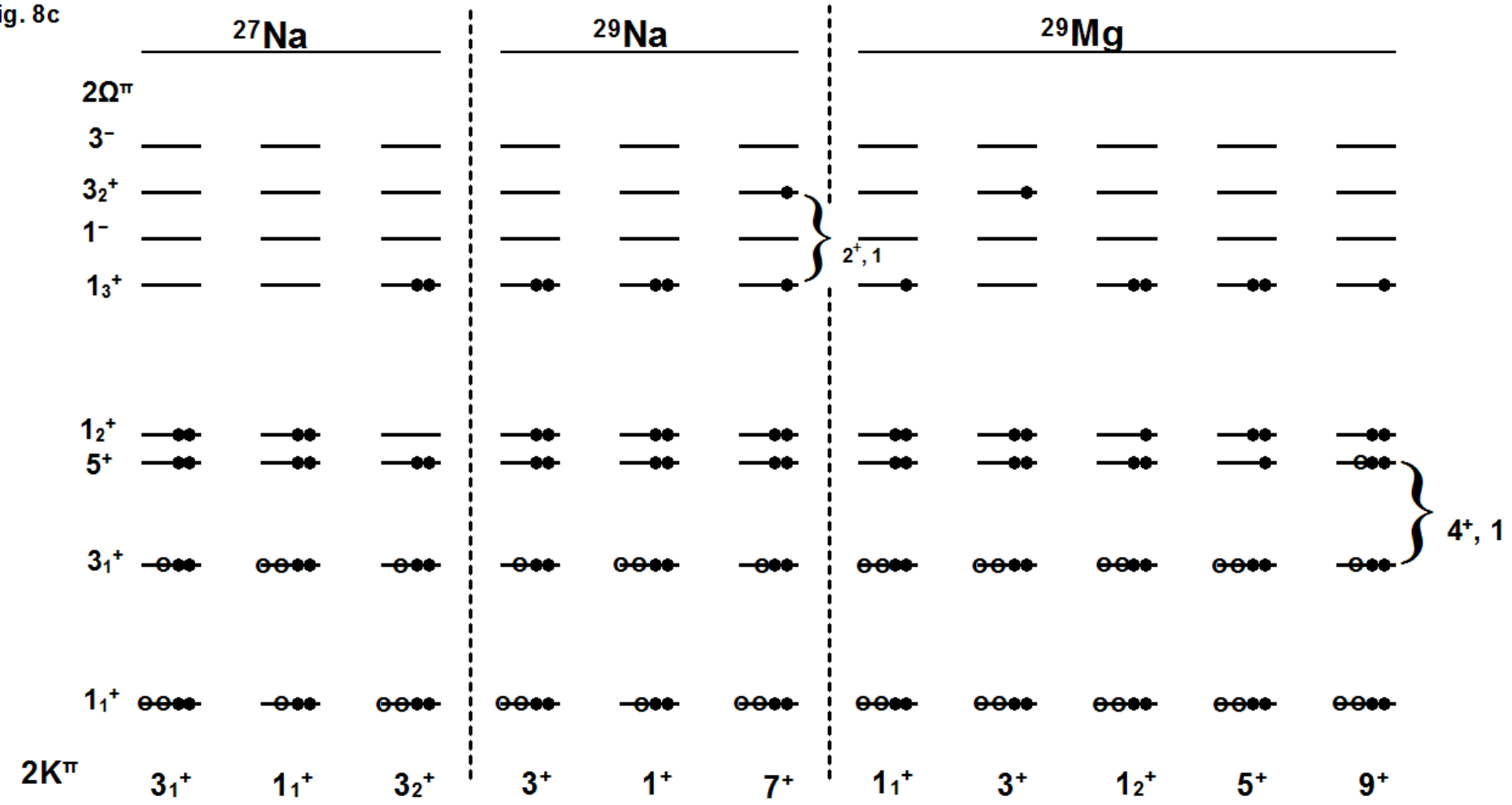
27Na
29Na
29Mg
2Ωπ
3−
3₂+
1−
1₃+
1₂+
5+
3₁+
1₁+
2+, 1
4+, 1
2Kπ
3₁+
1₁+
3₂+
3+
1+
7+
1₁+
3+
1₂+
5+
9+

Fig. 8d

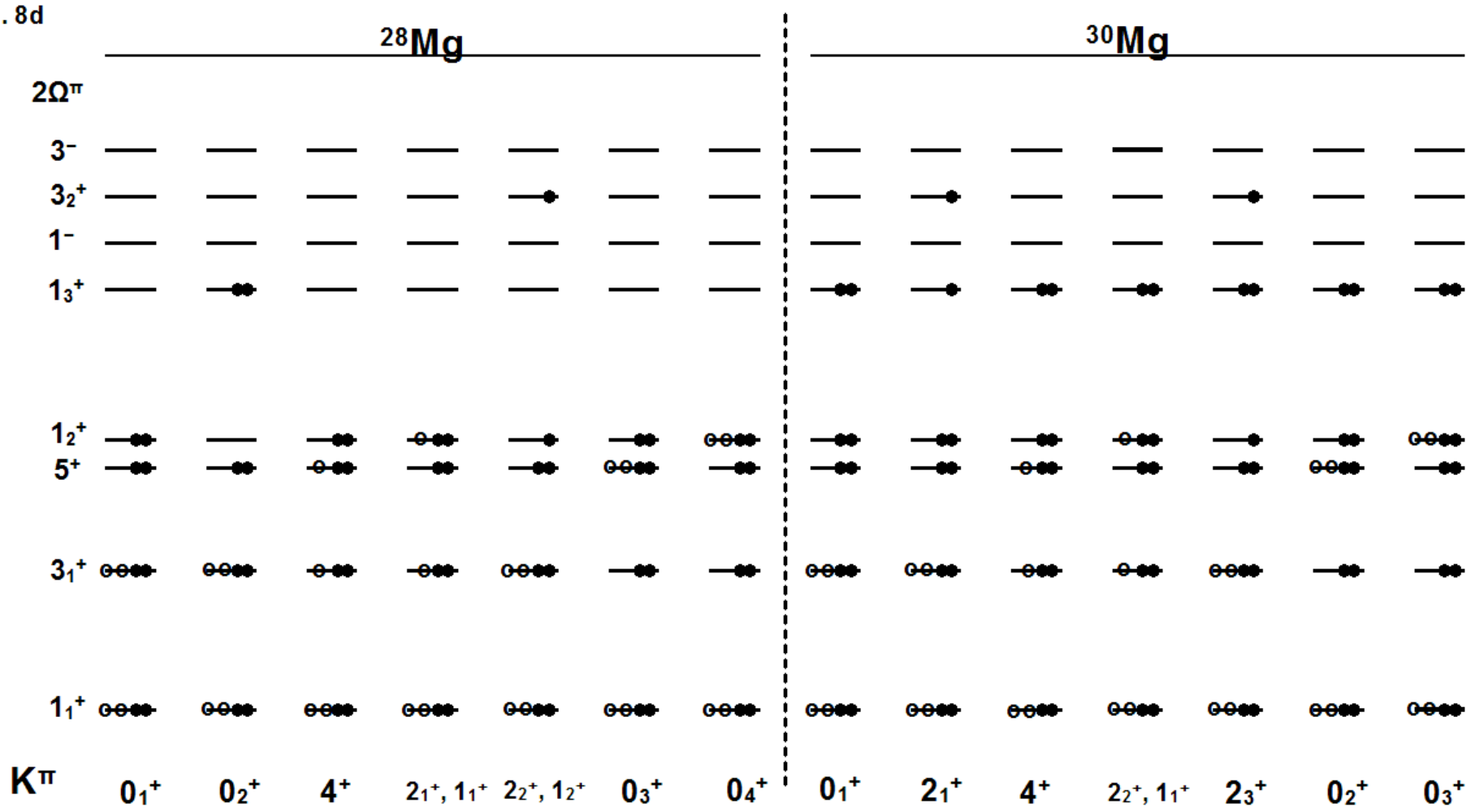
28Mg
30Mg
2Ωπ
3−
3₂+
1−
1₃+
1₂+
5+
3₁+
1₁+
Kπ
0₁+
0₂+
4+
2₁+, 1₁+
2₂+, 1₂+
0₃+
0₄+
0₁+
2₁+
4+
2₂+, 1₁+
2₃+
0₂+
0₃+

About the authors

Hartmut Röpke has been a professor of physics at the University of Freiburg/Germany between 1973 and retirement in 2003. Born 1938 he received his Ph. D. at Freiburg in November 1965 when he decided to enter the field of nuclear spectroscopy. After two years as a postdoc he spent 15 month in the same position at the University of Toronto/Canada with A. E. Litherland as the head and frequent contact to the Chalk River Nuclear Laboratories. On return to Freiburg he became a staff member (Habilitation) in 1969 and in 1973/74 he was on leave of absence at the CERN.
With support of DFG (Deutsche Forschungsgemeinschaft) and availability of a 7 MV Van-de-Graaff accelerator he was able to establish a nuclear-spectroscopy group which has generated many of the experimental data discussed here.

Franz Glatz, born 1949, received his Ph. D. in 1979 with work in nuclear-spectroscopy in the group of Hartmut Röpke. He continued as a research fellow of DFG until 1985 and raised a great deal of the experimental data which are discussed here. After 30 years in industry he was still interested in his old field of research and insisted that meanwhile progress should become available in written. These notes are the result.

Cover of the book version

The level schemes of the A = 16 - 44 nuclei along the line of stability are extended to high excitation energy. This is usually the threshold for particle emission but in the 15 MEV region can be reached for levels with high spin (J = 8-15). A sample of roughly 3000 levels, one third with first spin-parity assignments, is completely explained by the combination of the spherical shell model, the Nilsson model and the model of weak coupling (of particles with holes in a different major shell).
Shell model calculations in the unrestricted basis space of the s - d shell (Wildenthal's USD calculations) reproduce precisely a set of 1300 positive-parity levels in A = 18-38 nuclei, leaving only 170 positive-parity states unaccounted for. These intruders are reproduced, however, in one of the other models.
The nuclides with A = 20-30 are known to have deformed shapes so that the Nilsson model yields an alternative approach. A set of 570 rotational bands is identified here which includes the USD states, the intruders and negative-partity states. Helpful is the inclusion of 270 levels which are reliably predicted by the USD calculations while they are not accessible yet to experiment. The Nilsson model configurations of the intrinsic states are determined by introducing a residual interaction (Brink and Kerman 1959) which contains parameters that must be derived from experimental data. The latter ones exceed the number of parameters by a factor of 6. The model is also used to analyze the structure of the neutron-rich isotopes of Mg. For A = 36-44 shape coexistence of intrinsic states with normal deformation and super deformation is predicted and verified.
In the A = 36-44 region multi-particle excitations (n ħω excitations) from s - d into the f - p shell play a significant role. They can be distinguished from 0 ħω or 1 ħω excitations which have been predicted by shell model calculations (Warburton et al. 1984). Multi-particle excitations lead to deformation of the respective nucleus. Thus a sample of 90 rotational bands can be observed and understood, as in the A = 20-30 region, by the Nilsson model with residual interaction. Here the experimental data do exceed the number of adjustable parameters by a factor of 4.
A special observation is is the presence of four, $K^{\pi} = (0\text{-}3)^{-}$, rotational bands in doubly magic ^{40}Ca, but also in ^{38}Ar. The reason might be the octupole vibration of a $K^{\pi} = 0^{+}$, deformed intrinsic state. There remain 2 ħω and 3 ħω excitations in the A = 38-40 region which do not yet lead to deformation. They find a ready explanation in the weak coupling model which reproduces 40 experimental multiplets or singlets with only two adjustable monopole matrix elements.
The theoretical tools are completely adequate to explain the large body of experimental energy levels in A = 16-44 nuclei. Vice versa they indicate that the experimental situation is done to perfection.